

OXYGEN ISOTOPE STUDIES OF SOME SEDIMENTARY AND METASEDIMENTARY
ROCKS OF THE CENTRAL AND NORTHERN APPALACHIAN MOUNTAINS,
THE COLORADO PLATEAU, AND THE OUACHITA MOUNTAINS.

Thesis by

Emelia Anna Burt

In Partial Fulfillment of the Requirements

for the Degree of

Doctor of Philosophy

California Institute of Technology

Pasadena, California

1993

(Submitted on January 8, 1993)

During the tragic days of the American Civil War an unknown soldier penned these reflections:

*I asked God for strength
that I might achieve,
I was made weak,
that I might learn humbly to obey...*

*I asked for health,
that I might do greater things,
I was given infirmity,
that I might do better things...*

*I asked for riches,
that I might be happy,
I was given poverty,
that I might be wise...*

*I asked for power,
that I might have the praise of men,
I was given weakness,
that I might feel the need of God...*

*I asked for all things,
that I might enjoy all life,
I was given life,
that I might enjoy all things...*

*I got nothing that I asked for...
but everything I had hoped for;
Almost despite myself,
my unspoken prayers were answered.
I am among all men most richly blessed.*

Dedication:

To: Miss Winnie D. Burt

ACKNOWLEDGEMENTS

It is humbling to realize that so many people have considered this scientist a worthwhile investment of their lives during this course of study.

My thesis advisor, Hugh Taylor, suggested that I study the oxygen isotopic variation in sedimentary rocks. His high standards as a scientist and concern for detail have left their mark on this work as well as my approach to stable isotope geochemistry. His energy and hard work during these past months in completing this dissertation have indeed been admirable. This work was supported by a series of National Science Foundation grants OCE-80-19021, EAR-78-16874, EAR-83-13106, EAR-88-16413, and EAR-9019190.

George Rossman, my academic advisor and committee chairman, has taught me much about the process of learning and teaching science. I am grateful to him and to my other committee members Samuel Epstein, Peter Wyllie, and Donald Burnett for their encouragement and guidance during my course of study. Leon Silver provided helpful advice on sediment sources for the Colorado Plateau. Clair Patterson and Dorothy Settle were an encouragement to me through some personal struggles.

My thesis advisor, Hugh Taylor, was kind enough to donate the services of his secretary in revising and formatting the final draft of this manuscript. Mary Mellon devoted many long hours to word processing details, and for her heroic efforts I will always be thankful.

Jan Mayne drafted the maps, and I have appreciated her hard work and good humor. Scott Thornburg made final revisions on the computer-generated figures and tables, and I am grateful for his adeptness and encouragement in the last week of editing.

Eleanor Dent, Mike Carr, and Vic Nenow provided technical advice in the laboratory. Joop Goris performed many of the mass spectrometric analyses. I am thankful to these staff members for both their technical support and their friendship.

Many of my colleagues provided stimulating discussion throughout this research. Among them have been Carey Gazis, Mike Palin, Diane Knott, Greg Holk, Tom Latourette, Lisa Grant, Xiahong Feng, Jen Blank, Pat Dobson, Leslie Sonder, Sally Newman and Theresa Bowers.

My years at Caltech have been enriched by a diversity of scientific interaction and personal relationship that I did not foresee. I am grateful to many friends for a breadth of contribution including their companionship, prayers, listening ears, encouragement, sense of humor, and assistance with the technical details in completing this dissertation. I would particularly like to say thank you to my Mom and Dad, my two brothers, Keith and Joe, my Granny Gillette, Norma Wybenga, Jennifer Chung, Danielle Stoppy, Craig Schlue, Ron McGinnis, Rick Hanson, Ron LeBlanc, Art Allen, Mark Bassett, Chris Catherasoo, Betsy Everett, Sherrie Simek, Randy Sorenson, Kim Leong, Jim Cline, John and Sally McGill, Dan Suzuki, Nancy Weigel, John Breckinridge, Tom Gengler, Ernie Prabhakar, David Groseth, Kimo Yap, Tina Kramer-Garyantes, Jay and Theresa Harn, Mike Kelsey, Craig Larimer, Steve Huffey, Nancy Nakanishi, Sarah Snare, Anna Lynn Lowland, Bill Robison, Wendy Shaw, Lisa Knofel and Jim Wallstrom.

Last, but certainly not least, I would like to thank my Lord Jesus Christ, the unseen presence in every conversation and solitary hour in the laboratory and at study, for making a childhood dream come true. I have indeed been surprised by joy.

Abstract

Terrigenous sedimentary rocks from the Colorado Plateau show a relatively uniform bulk silicate $\delta^{18}\text{O}$ of +14.8 with an SEM of 0.32. Shales and calcilutites in this region have a mean bulk silicate $\delta^{18}\text{O}$ of +17.7 which is significantly heavier than the mean for interbedded sandstones and siltstones. Bulk silicate $\delta^{18}\text{O}$ is decoupled from carbonate $\delta^{18}\text{O}$ due to differences in mode of deposition and diagenetic behavior.

Central Appalachian terrigenous sedimentary rocks show a surprisingly uniform bulk silicate $\delta^{18}\text{O}$ of +14.8 with an SEM of 0.1. The mean bulk silicate $\delta^{18}\text{O}$ for all shales (+15.2) is only 0.3 per mil heavier than the mean for all sandstones and siltstones (+14.9). The oxygen isotope uniformity of Central Appalachian sedimentary rocks is mainly a primary depositional feature that is the result of thorough, grand-scale mixing of terrigenous sediment in the Appalachian geosyncline, probably involving several cycles of sedimentation, uplift, erosion, and reworking extending over hundreds of millions of years during the Paleozoic era. The bulk silicate $\delta^{18}\text{O}$ of siltstones and shales shows a significant ($P < 0.05$) correlation with conodont color alteration index, which is a measure of diagenetic temperature. As a result of isotopic exchange with porewater during diagenesis, the bulk silicate $\delta^{18}\text{O}$ of shales and siltstones can apparently be lowered by as much as 2.5 to 4.0 per mil. These diagenetic effects contributed to the overall homogeneity of these sedimentary rocks because the shales started out at higher $\delta^{18}\text{O}$.

A reconnaissance $^{18}\text{O}/^{16}\text{O}$ study of 14 samples of terrigenous sedimentary rocks from the Ouachita Mountains suggests more inherent isotopic variation in these samples, perhaps in part as a result of greater heterogeneity of source regions. Some of the isotopic variation also seems clearly attributable to diagenetic effects. A significant ($P < 0.05$) correlation was found between mean vitrinite reflectance, also a measure of diagenetic

temperature, and the bulk silicate $\delta^{18}\text{O}$ difference between shale-sandstone pairs in three different sedimentary formations.

Northern Appalachian metasedimentary rocks show a decrease in bulk silicate $\delta^{18}\text{O}$ at garnet grade and higher. The terrigenous facies metamorphic rocks have been depleted in ^{18}O by about two per mil relative to their unmetamorphosed counterparts in the Central Appalachians, except where they are adjacent to carbonate-rich sections. Carbonate facies metasedimentary rocks are 5 to 6 per mil higher than interbedded terrigenous facies rocks, but at the margins of that formation there is a distinct lowering of bulk silicate $\delta^{18}\text{O}$ and carbonate $\delta^{18}\text{O}$ due to influx of metamorphic hydrothermal fluids from the adjacent terrigenous rocks. This is attributed to the involvement of isotopically light fluids during metamorphism. Further work is need to elucidate the differences between metamorphic processes in pelitic and calcareous sediments.

TABLE OF CONTENTS

ACKNOWLEDGEMENTS	iv
ABSTRACT	vi
TABLE OF CONTENTS	viii
LIST OF FIGURES	xii
LIST OF TABLES	xxii
CHAPTER 1	1
Introduction	1
1.1 Purpose of study	1
1.2 Brief review of the geochemistry of sedimentary rocks pertinent to the present study	9
1.2.1 Marine pelagic sediments	9
1.2.2 Sedimentation in offshore deep subsiding basins	14
1.2.3 Geosynclines	16
1.2.4 Evaporite basins	18
1.2.5 Stable continental shelf and craton	19
1.2.6 Euxinic environments	20
1.2.7 Transitional sedimentary environments and marine-nonmarine	21
1.2.7.1 Oscillatory marine-nonmarine basins	21
1.2.7.2 Shore deposits	21
1.2.7.3 Bay and lagoon deposits	22
1.2.7.4 Deltaic complex	22
1.2.7.5 Marsh	22
1.2.8 Terrestrial sedimentary environments	23
1.2.8.1 Volcaniclastic	23
1.2.8.2 Alluvial fan	23
1.2.8.3 River channel and floodplain	23
1.2.8.4 Lacustrine	24
1.2.8.5 Swamp	25
1.2.8.6 Eolian	25
1.2.8.7 Glacial	25
1.3 Brief review of the geochemistry of metasedimentary rocks pertinent to the present study	26
1.3.1 Contact metamorphism	26
1.3.2 Regional metamorphism	28

CHAPTER 1 CONTINUED

1.3.3	Fluid-restricted regional metamorphism	29
1.3.4	Fluid-dominated regional metamorphism	31
CHAPTER 2		35
Analytical Methods and Sample Collection		35
2.1	Analytical methods	35
2.1.1	Oxygen extraction from bulk silicates	35
2.1.2	Carbon and oxygen extraction from carbonates	37
2.1.3	Mass spectrometer analyses	38
2.2	Sample collection	40
2.3	Tabulation of isotopic analyses	42
2.4	Guide to sample inventory spread sheet	43
2.5	Abbreviations used in sample inventory	46
CHAPTER 3		61
Whole Rock Oxygen Isotopic Ratios in Sedimentary Rocks: A Review of the Literature		61
3.1	General overview	61
3.2	Pelagic sediments	62
3.2.1	Metalliferous sediments	62
3.2.2	Siliceous and calcareous sediments	70
3.2.3	Argillites, sandstones, and siltstones	74
3.2.4	Summary	75
3.3	Terrigenous sedimentary rocks	79
3.3.1	Marine samples	79
3.3.2	Transitional and non-marine samples	88
3.4	Summary and conclusions	92
3.5	Inventory of samples in the sedimentary literature review	96
3.5.1	Explanation of Table 3.1	96
3.5.2	Abbreviations used in the sedimentary literature review	100
3.5.3	Abbreviations and list of depositional environments (Column B)	103
CHAPTER 4		114
Oxygen and Carbon Isotopic Compositions of Sedimentary Rocks from Southern Utah, Northwestern Arizona, and the Uinta Mountains, Utah		114

CHAPTER 4 CONTINUED

4.1	Description of the analyzed samples	114
4.2	Overview of bulk $^{18}\text{O}/^{16}\text{O}$ silicate data	119
4.3	Comparison with cherts and carbonates	124
4.4	Geographic and lithological variation in bulk silicate $\delta^{18}\text{O}$	129
4.5	Carbonate carbon and oxygen isotopic trends	140
4.6	Decoupling of carbonate $\delta^{18}\text{O}$ and bulk silicate $\delta^{18}\text{O}$	157
4.7	Conclusions	165
CHAPTER 5		167
Oxygen and Carbon Isotope Studies of Central Appalachian Sedimentary Rocks		167
5.1	Description of the analyzed samples	167
5.2	Overview of bulk silicate oxygen isotope data	171
5.3	Bulk silicate oxygen isotope variation with geographic area	196
5.4	Bulk silicate oxygen isotope variation with geologic age	199
5.5	$^{18}\text{O}/^{16}\text{O}$ Variation with bulk silicate mineralogy	218
5.5.1	Sandstones	218
5.5.2	Shales	227
5.5.3	Siltstones	234
5.5.4	Summary	235
5.6	Oxygen isotopic variations in the source regions	237
5.7	Diagenetic changes in oxygen isotopic composition	240
5.7.1.	General statement	240
5.7.2	Correlation between $\delta^{18}\text{O}$ and conodont alteration index	242
5.7.3	Mineralogical changes during diagenesis	260
5.7.4	Diagenetic pore fluids	267
5.8	Summary	273
CHAPTER 6		277
Oxygen Isotope Studies of Terrigenous Sedimentary Rocks of the Central and Southern Ouachita Mountains		277
6.1	Introduction	277
6.2	Overview of bulk silicate $^{18}\text{O}/^{16}\text{O}$ analyses	277
6.3	Indicators of thermal maturity in the Ouachita Mountains	284
6.4	Correlation of bulk silicate $\delta^{18}\text{O}$ with vitrinite reflectance	287
6.5	Conclusions	298

CHAPTER 7	300
Oxygen Isotope Studies of Sedimentary and Metasedimentary Rocks of the Northern Appalachians	300
7.1 Description of the analyzed samples	300
7.2 Overview of bulk silicate $\delta^{18}\text{O}$ of carbonate- and terrigenous-facies rocks	307
7.3 Oxygen isotope studies of metasedimentary rocks from the St. Johnsbury Quadrangle, Vermont	321
7.4 Oxygen isotope studies of metasedimentary rocks from western Vermont	330
7.5 Relationships between bulk silicate $\delta^{18}\text{O}$ and carbonate $\delta^{18}\text{O}$ in sedimentary and metasedimentary rocks	332
7.6 Conclusions	358
CHAPTER 8	360
Summary and Conclusions	360
REFERENCES	371

LIST OF FIGURES

Figure 1.1	Map of the United States and part of eastern Canada, showing the general areas covered by the $^{18}\text{O}/^{16}\text{O}$ analyses of sedimentary and metasedimentary rocks studied in this work.	5
Figure 3.1	Stack histogram showing distribution of bulk silicate $\delta^{18}\text{O}$ values for all pelagic sediments in the literature survey, based on four subdivisions of these rocks, as indicated in the inset.	63
Figure 3.2	Plot of bulk silicate $\delta^{18}\text{O}$ versus geologic age for all pelagic sediments tabulated in the literature survey	63
Figure 3.3	Stack histogram showing bulk silicate $\delta^{18}\text{O}$ values of all metalliferous sediments in the literature survey, subdivided into three groups as indicated on the inset	67
Figure 3.4	Plot of bulk silicate $\delta^{18}\text{O}$ vs. geologic age for all metalliferous sediments in the literature survey	67
Figure 3.5	Plot of bulk silicate $\delta^{18}\text{O}$ vs. depth below sediment-ocean interface for all metalliferous sediments from the literature survey	71
Figure 3.6	Histogram showing distribution of bulk silicate $\delta^{18}\text{O}$ values for siliceous and calcareous pelagic sediments from the literature review	71
Figure 3.7	Plot of bulk silicate $\delta^{18}\text{O}$ against age for siliceous and calcareous pelagic sediments from the literature review.	76
Figure 3.8	Histogram showing bulk silicate $\delta^{18}\text{O}$ distribution for 39 argillites, a sandstone, a siltstone, and a clay conglomerate from the pelagic suite of rocks in the literature review	76
Figure 3.9	Bulk silicate $\delta^{18}\text{O}$ versus geologic age for pelagic argillites, a sandstone, a siltstone, and a clay conglomerate from the literature review	80

Figure 3.10	Histogram showing bulk silicate $\delta^{18}\text{O}$ distribution for all marine terrigenous sediments from the literature review, subdivided into shales, greywackes, and other types of sandstones	80
Figure 3.11	Bulk silicate $\delta^{18}\text{O}$ vs. stratigraphic depth for the Texas Gulf Coast and Glacier National Park samples listed in Table 3.1	84
Figure 3.12	Carbonate $\delta^{18}\text{O}$ vs bulk silicate $\delta^{18}\text{O}$ for Texas Gulf Coast and Glacier National Park samples of Yeh and Savin (1977) and Eslinger and Savin (1973)	84
Figure 3.13	Five comparative histograms showing bulk silicate $\delta^{18}\text{O}$ values of various categories of terrigenous sedimentary rocks from the literature survey	89
Figure 3.14	Histograms showing bulk silicate $\delta^{18}\text{O}$ distribution of all transitional and nonmarine terrigenous sediments from the literature survey, subdivided into shales and sandstones	89
Figure 3.15	Bulk silicate $\delta^{18}\text{O}$ vs. geologic age for all fine-grained transitional and nonmarine terrigenous sedimentary rocks from the literature survey, subdivided into bentonites and shales	93
Figure 3.16	Eight comparative histograms showing bulk silicate $\delta^{18}\text{O}$ values of various categories of terrigenous sedimentary rocks from the literature survey	93
Figure 3.17	Four comparative histograms showing bulk silicate $\delta^{18}\text{O}$ values of various categories of terrigenous sedimentary rocks from the literature survey	97
Figure 4.1	Map of Utah and Arizona showing sample locations of the sedimentary rocks studied in this work from the Colorado Plateau physiographic province	115
Figure 4.2	Six comparative histograms showing bulk silicate $\delta^{18}\text{O}$ values of terrigenous sedimentary rocks from Utah and Arizona	121
Figure 4.3	Plot of bulk silicate $\delta^{18}\text{O}$ values of Utah/Arizona sedimentary rocks in this study and $\delta^{18}\text{O}$ of marine cherts from the literature vs. geologic age	125

Figure 4.4	Eight comparative histograms showing bulk silicate $\delta^{18}\text{O}$ values of terrigenous sedimentary rocks from Utah and Arizona separated according to 4 geologic age intervals and $\delta^{18}\text{O}$ values of cherts from the literature	125
Figure 4.5	Plot of bulk silicate $\delta^{18}\text{O}$ values of Utah/Arizona terrigenous sedimentary rocks in this study and carbonate $\delta^{18}\text{O}$ values of marine limestones and dolomites from the literature versus geologic age	130
Figure 4.6	Two plots of bulk silicate $\delta^{18}\text{O}$ vs. distance in an east-west direction. Top diagram is for Utah/Arizona shales, calcilutites, and eolian sandstones	130
Figure 4.7	Two plots of bulk silicate $\delta^{18}\text{O}$ vs. distance in a north-south direction	133
Figure 4.8	Two plots of bulk silicate $\delta^{18}\text{O}$ vs. distance for Utah/Arizona siltstones	133
Figure 4.9	Carbonate $\delta^{18}\text{O}$ vs. carbonate $\delta^{13}\text{C}$ for Utah/Arizona terrigenous sedimentary rocks subdivided into shales (and calcilutites), siltstones, and sandstones	141
Figure 4.10	This is the same as Figure 4.9, with the addition of fields delineating non-marine sandstones, siltstones, and shales and calcilutites	141
Figure 4.11	Plot of carbonate $\delta^{18}\text{O}$ versus per cent carbonate for Utah/Arizona sedimentary rocks	146
Figure 4.12	Plot of carbonate $\delta^{13}\text{C}$ versus per cent carbonate for Utah/Arizona terrigenous sedimentary rocks	149
Figure 4.13	Plot of carbonate $\delta^{13}\text{C}$ versus distance in an east-west direction for all Utah/Arizona sedimentary rocks analyzed in this study	151
Figure 4.14	Plot of carbonate $\delta^{18}\text{O}$ versus distance in an east-west direction for all Utah/Arizona terrigenous sedimentary rocks analyzed in this study	151
Figure 4.15	Plot of per cent carbonate versus distance in an east-west direction for the Utah/Arizona terrigenous sedimentary rocks . . .	154

Figure 4.16	Plot of bulk silicate $\delta^{18}\text{O}$ versus per cent carbonate for Utah/Arizona terrigenous sedimentary rocks excluding volcanics	154
Figure 4.17	Plot of $\delta^{13}\text{C}$ of carbonate versus bulk silicate $\delta^{13}\text{C}$ for the Utah/Arizona terrigenous sedimentary rocks	158
Figure 4.18	Plot of carbonate $\delta^{18}\text{O}$ versus bulk silicate $\delta^{18}\text{O}$ for all Utah/Arizona terrigenous sedimentary rocks analyzed in this study	158
Figure 4.19	Plot of oxygen yield in micromoles of oxygen per milligram of sample versus distance in an east-west direction for the Utah/Arizona terrigenous sedimentary rocks analyzed in this study	162
Figure 5.1	Map of southwestern Pennsylvania, western Maryland, eastern West Virginia, and northern Virginia, showing sample localities of most of the samples analyzed in this work from the Central Appalachian Mountains	168
Figure 5.2	Map of the U.S. mid-Atlantic states, showing those sample localities from the Central Appalachians that are not shown in Figure 5.1	168
Figure 5.3	Eight comparative histograms showing the bulk silicate $\delta^{18}\text{O}$ values of various categories of Central Appalachian terrigenous sedimentary rocks	173
Figure 5.4	Two comparative histograms showing the oxygen yields from the bulk silicate material of calcareous and noncalcareous Central Appalachian shales in micromoles per milligram	178
Figure 5.5	Two comparative histograms showing the bulk silicate $\delta^{18}\text{O}$ values for all analyzed marine and nonmarine sedimentary rocks from the Central Appalachians	180
Figure 5.6	Three comparative histograms showing the bulk silicate $\delta^{18}\text{O}$ values of all of the sedimentary rocks from the Central Appalachians subdivided into marine, transitional, and fluvial categories	182

Figure 5.7	Six comparative histograms showing the bulk silicate $\delta^{18}\text{O}$ values of all Central Appalachian sedimentary rocks, subdivided into calcareous and noncalcareous varieties and then further subdivided into marine, transitional, and fluvial environments	185
Figure 5.8	Six comparative histograms showing the bulk silicate $\delta^{18}\text{O}$ values of all calcareous and noncalcareous Central Appalachian shales from marine, transitional, and fluvial environments	187
Figure 5.9	Four comparative histograms showing the bulk silicate $\delta^{18}\text{O}$ values of all Central Appalachian calcareous and noncalcareous siltstones, subdivided into marine, transitional, and fluvial categories	189
Figure 5.10	Six comparative histograms showing bulk silicate $\delta^{18}\text{O}$ values of all Central Appalachian sandstones, subdivided into calcareous and noncalcareous varieties, and further subdivided into marine, transitional, and fluvial categories	191
Figure 5.11	Two comparative histograms showing: (1) all whole-rock $\delta^{18}\text{O}$ values of sedimentary rocks (pelagics excluded) from the literature; and (2) all whole-rock $\delta^{18}\text{O}$ values from this study of Central Appalachian sedimentary rocks	194
Figure 5.12	Map of the Central Appalachian Mountains showing the 5 geographic groupings of samples referred to in the text: Areas I, II, III, IV, and V	197
Figure 5.13	Map of the Central Appalachian area, showing bulk silicate $\delta^{18}\text{O}$ values of noncalcareous shales as a function of sample location	200
Figure 5.14	Map of the Central Appalachian area, showing mean bulk silicate $\delta^{18}\text{O}$ values of siltstones as a function of sample location	202
Figure 5.15	Map of the Central Appalachians showing mean bulk silicate $\delta^{18}\text{O}$ values of noncalcareous shales and noncalcareous siltstones as a function of sample location	204
Figure 5.16	Map of the Central Appalachian area, showing mean bulk silicate $\delta^{18}\text{O}$ values of sandstones as a function of sample location	206

Figure 5.17	Map of the Central Appalachian area, showing mean bulk silicate $\delta^{18}\text{O}$ values of calcareous shales, as a function of sample location	208
Figure 5.18	Plot of bulk silicate $\delta^{18}\text{O}$ versus geologic age for all Central Appalachian sedimentary rocks	210
Figure 5.19	Plot of bulk silicate $\delta^{18}\text{O}$ versus geologic age for all Central Appalachian sandstones, subdivided into calcareous and noncalcareous varieties	210
Figure 5.20	Plot of bulk silicate $\delta^{18}\text{O}$ versus geologic age for all Central Appalachian shales, subdivided into calcareous and noncalcareous varieties	210
Figure 5.21	Plot of bulk silicate $\delta^{18}\text{O}$ versus geologic age for all Central Appalachian siltstones	210
Figure 5.22	Plot of geologic age of Central Appalachian noncalcareous siltstones analyzed in this study versus their interpolated conodont color alteration index	216
Figure 5.23	Map of the Central Appalachians showing the distribution of Paleozoic sandstone samples in this work, separated into categories based on composition and petrographic characteristics	222
Figure 5.24	Four comparative histograms showing bulk silicate $\delta^{18}\text{O}$ values of Central Appalachian sandstones, subdivided into several categories, using the sandstone compositional classification of Pettijohn (1975)	222
Figure 5.25	Plot of bulk silicate $\delta^{18}\text{O}$ versus oxygen yield for Central Appalachian noncalcareous shales	231
Figure 5.26	Plot of bulk silicate $\delta^{18}\text{O}$ versus oxygen yield for noncalcareous shales and siltstones from the Central Appalachians	231
Figure 5.27	Sample location map from Figure 5.1, showing Upper Devonian - Mississippian sample localities, together with the contours of Conodont Alteration Index	245

Figure 5.28	Sample location map from Figure 5.1, showing Silurian - Mid Devonian sample localities, together with the contours of Conodont Alteration Index	245
Figure 5.29	Sample location map from Figure 5.1, showing Ordovician sample localities, together with the contours of Conodont Alteration Index	245
Figure 5.30	Plot of bulk silicate $\delta^{18}\text{O}$ of Central Appalachian noncalcareous sandstones versus conodont alteration index	249
Figure 5.31	Plot of bulk silicate $\delta^{18}\text{O}$ of Central Appalachian calcareous sandstones versus conodont alteration index	249
Figure 5.32	Plot of bulk silicate $\delta^{18}\text{O}$ of Central Appalachian siltstones versus conodont alteration index	253
Figure 5.33	Plot of bulk silicate $\delta^{18}\text{O}$ of Central Appalachian shales versus conodont alteration index	253
Figure 5.34	Plot of bulk silicate $\delta^{18}\text{O}$ versus conodont alteration index (CAI), showing three linear regression lines for (a) noncalcareous siltstones, (b) calcareous shales and the calcareous siltstone, and (c) green noncalcareous shales	257
Figure 5.35	Bulk silicate $\delta^{18}\text{O}$ shift with conodont CAI for shales and siltstones	262
Figure 5.36	Plot of carbonate $\delta^{18}\text{O}$ values from Central Appalachian calcareous shales versus interpolated conodont color alteration index	262
Figure 5.37	Plot of carbonate $\delta^{18}\text{O}$ values from Central Appalachian sandstones versus interpolated conodont color alteration index	262
Figure 5.38	Plot of carbonate $\delta^{18}\text{O}$ values from Central Appalachian sandstones and shales versus bulk silicate $\delta^{18}\text{O}$, showing the lack of a correlation, and indicating that the $\delta^{18}\text{O}$ values of these coexisting materials are effectively decoupled	262
Figure 5.39	The same siltstone $\delta^{18}\text{O}$ and CAI data shown in Figure 5.32, but with the samples separated according to environment of deposition instead of mineralogy and color	270

Figure 5.40	The same shale $\delta^{18}\text{O}$ and CAI data as shown in Figure 5.33, but with the samples separated according to environment of deposition instead of mineralogy and color	270
Figure 6.1	Map of eastern Oklahoma, western Arkansas, and northeastern Texas, showing locations and sample numbers of terrigenous sedimentary rocks from the Ouachita Mountains	278
Figure 6.2	Three comparative histograms showing the bulk silicate $\delta^{18}\text{O}$ values of various categories of terrigenous sedimentary rocks from the Ouachita Mountains	280
Figure 6.3	Three comparative histograms showing the bulk silicate $\delta^{18}\text{O}$ values of several shale and sandstone samples from the Mississippian Stanley Formation of the Ouachita Mountains	288
Figure 6.4	Plot of bulk silicate $\delta^{18}\text{O}$ versus the zone of mean vitrinite reflectance in which the sample was collected	290
Figure 6.5	Three comparative histograms showing the bulk silicate $\delta^{18}\text{O}$ values of several shale and sandstones samples from the Ouachita Mountains, separated according to zones of mean vitrinite reflectance	293
Figure 6.6	Plot of the difference in whole-rock $\delta^{18}\text{O}$ values between adjacent of shale and sandstone from the Ouachita Mountains versus zone of mean vitrinite reflectance	295
Figure 6.7	The same plot shown in Figure 6.6, with the addition of two more data-points from Mississippian Stanley Group	295
Figure 7.1	General locations of Northern Appalachian sample transects in this study	301
Figure 7.2	Simplified geologic map of the St. Johnsbury Quadrangle, Vermont, modified after Hall (1959), showing sample locations studied in this work	304
Figure 7.3	Two comparative histograms showing bulk silicate $\delta^{18}\text{O}$ values for Northern Appalachian samples analyzed in this study	304

Figure 7.4	Eight comparative histograms showing bulk silicate $\delta^{18}\text{O}$ values of various metamorphic grades of terrigenous-facies and carbonate-facies sedimentary rocks of the Northern Appalachians analyzed in this study.	309
Figure 7.5	Bulk silicate $\delta^{18}\text{O}$ versus metamorphic grade for Appalachian sedimentary and metasedimentary rocks analyzed in this study.	309
Figure 7.6	Bulk silicate $\delta^{18}\text{O}$ of terrigenous-facies sedimentary rocks versus metamorphic grade for samples analyzed in this study.	314
Figure 7.7	Bulk silicate $\delta^{18}\text{O}$ versus metamorphic grade for metasedimentary rocks from the Trois Seigneurs Massif in the Pyrenees analyzed by Wickham and Taylor (1985)	314
Figure 7.8	Eight comparative histograms showing oxygen isotopic compositions of carbonate-facies Northern Appalachian samples in this study.	319
Figure 7.9	Three comparative histograms of bulk silicate $\delta^{18}\text{O}$ values determined on metasedimentary rocks in this study for: (a) Waits River Formation, St. Johnsbury Quadrangle, east-central Vermont; (b) Gile Mountain Formation, St. Johnsbury Quadrangle, east-central Vermont, and (c) west-central Vermont samples (mainly from the Lincoln Mountain Quadrangle).	322
Figure 7.10	Plot of bulk silicate $\delta^{18}\text{O}$ versus carbonate $\delta^{18}\text{O}$ for Northern Appalachian metamorphic rocks in this study. The linear regression line shown is for the 16 biotite zone and higher grade samples	333
Figure 7.11	Plot of bulk silicate $\delta^{18}\text{O}$ versus carbonate $\delta^{18}\text{O}$ for Appalachian metamorphic rocks in this study	333
Figure 7.12	Plot of bulk silicate $\delta^{18}\text{O}$ versus carbonate $\delta^{18}\text{O}$ for Northern Appalachian samples in this study and Texas Coastal Plain shales from Yeh and Savin (1977)	337
Figure 7.13	Plot of bulk silicate $\delta^{18}\text{O}$ versus carbonate $\delta^{18}\text{O}$ for sedimentary and metamorphic rocks from the Appalachians (this study) and the Texas Coastal Plain (Yeh and Savin, 1977).	337

Figure 7.14	Plot of bulk silicate $\delta^{18}\text{O}$ versus carbonate $\delta^{18}\text{O}$ for Appalachian metamorphic rocks in this study	341
Figure 7.15	Plot of bulk silicate $\delta^{18}\text{O}$ versus carbonate $\delta^{18}\text{O}$ showing hypothetical trajectories that would be followed during closed-system heating of a sedimentary rock containing variable amounts of carbonate and bulk silicate	344
Figure 7.16	Plot of bulk silicate $\delta^{18}\text{O}$ versus carbonate $\delta^{18}\text{O}$ showing hypothetical trajectories that would be followed during open-system heating of a sedimentary rock containing either variable amounts of carbonate and bulk silicate, or following different paths of metamorphism and aqueous fluid-rock interaction (see text).	346
Figure 7.17	Plot of bulk silicate $\delta^{18}\text{O}$ versus carbonate $\delta^{18}\text{O}$ for the same data shown in Figure 7.10 but delineating two groups of samples, one containing more than 40% carbonate and the other less than 15% carbonate	352
Figure 7.18	Plot of whole rock $\delta^{18}\text{O}$ versus per cent carbonate for Northern Appalachian samples in this study.	352
Figure 7.19	Plot of $\delta^{18}\text{O}$ carbonate versus $\delta^{13}\text{C}$ carbonate for Northern Appalachian metasedimentary rocks in this study.	352
Figure 8.1	Two histograms comparing the bulk silicate $\delta^{18}\text{O}$ of marine and nonmarine samples from the literature and this study	361
Figure 8.2	Two histograms comparing the bulk silicate $\delta^{18}\text{O}$ of all marine samples with all nonmarine samples analyzed in this study	361
Figure 8.3	Two histograms comparing the bulk silicate $\delta^{18}\text{O}$ of greywackes and shales from a eugeosynclinal environment based on analyses by Magaritz and Taylor (1976)	364
Figure 8.4	Two histograms comparing all available bulk silicate $\delta^{18}\text{O}$ values for sandstones and shales in this study and the literature	364

LIST OF TABLES

Table 2.1	Inventory of all samples analyzed in this study	47
Table 3.1	Isotopic compositions and other information on all samples in the sedimentary literature review	104
Table 5.1	Bulk silicate $\delta^{18}\text{O}$ calculations for a hypothetical quartz arenite	220
Table 5.2	Temperature ranges for conodonts for heating durations of 1 million to 500 million years	244

CHAPTER 1

Introduction

1.1 Purpose of study

Oxygen isotope studies of sedimentary rocks have demonstrated utility in determining the paleohydrology and porewater evolution in sedimentary basins, in estimating geothermal gradients and maximum depths of burial, in determining whether carbon dioxide derived from organic matter has been incorporated into carbonates, in understanding sedimentary processes like dolomitization and the formation of chert, and in studying the paleoclimate of the earth. These kinds of oxygen isotopic studies have up to now been concentrated largely on biogenic, authigenic, or diagenetic minerals (*e.g.*, Garlick, 1974; Savin, 1980; Savin and Yeh, 1981; Longstaffe, 1986a, 1986b, 1987a, 1987b). In other words, such studies have focused on minerals either that were deposited from, or that exchanged with, aqueous solutions in nature.

In a like manner, oxygen isotope studies of metamorphosed sedimentary rocks have generally focused on the degree of attainment of oxygen isotopic equilibrium among minerals and their coexisting metamorphic pore fluids (*e.g.*, Taylor *et al.*, 1963; Garlick and Epstein, 1967, Wickham and Taylor, 1985). These studies have proven useful for geothermometry and for constraining the role of fluids in metamorphism. Such studies are particularly useful in determining the amount of water and the source of the water involved in metamorphism.

In spite of the large number of studies of the above problems over the past 30 years, particularly on carbonate sediments, there remain a number of significant gaps in our understanding of $^{18}\text{O}/^{16}\text{O}$ variations of sedimentary rocks in nature and of the role

of fluids in the diagenesis and metamorphism of these sedimentary rocks. Very little work of any kind has been carried out on the whole-rock $^{18}\text{O}/^{16}\text{O}$ variations in the vast bulk of terrigenous sedimentary and metasedimentary rocks in nature, namely the sandstones, siltstones, mudstones, and shales, and their metamorphic equivalents. A critical unanswered question is: what roles do diagenesis and metamorphism play in altering the whole-rock $\delta^{18}\text{O}$ values of large masses of these kinds of terrigenous sedimentary rocks? Another related question is: how homogeneous are the $\delta^{18}\text{O}$ values of these various kinds of terrigenous sedimentary rocks prior to diagenesis and metamorphism, and why?

The above questions are not in general answered by the analysis of authigenic or diagenetic minerals in such sedimentary rocks, because authigenic and diagenetic minerals commonly compose only a small fraction of these kinds of rocks. In the same way, isotopic analyses of mineral separates of metamorphic rocks are not in general the best way of demonstrating bulk shifts in whole-rock $\delta^{18}\text{O}$ with metamorphism, unless all of the minerals in the rock specimen are analyzed and accurate modal abundances are reported. This requires a prodigious amount of work and is a very difficult task at best in fine-grained rocks. Understanding bulk shifts in whole-rock $\delta^{18}\text{O}$ values as a result of diagenesis and metamorphism is clearly an essential link in understanding the large-scale role of aqueous fluids in these two processes. However, in order to understand the effects of these processes on the bulk silicate $\delta^{18}\text{O}$ values of sedimentary rocks, it is important to first characterize and then to understand the range and variation of whole-rock $\delta^{18}\text{O}$ values in sedimentary rocks as a function of such factors as lithology, depositional environment, source region, geologic age, and post-depositional diagenetic changes.

The whole-rock $\delta^{18}\text{O}$ distribution of the sedimentary precursors of regional metamorphic rocks has heretofore been largely a matter of guesswork. One of the purposes of the present research has been to take a major step in rectifying these gaps in our understanding of the variations in whole-rock oxygen isotopic composition of such rocks as slates, phyllites, schists, and gneisses compared to their detrital sedimentary protoliths (sandstones, siltstones, and shales). Given the significant gaps in our understanding of how diagenesis and metamorphism affect the $\delta^{18}\text{O}$ of the bulk silicate (*i.e.*, the non-carbonate portion of such sedimentary rocks), another major focus of this work has been on that problem. The intent has been to gather together a large isotopic data set and thus lay a foundation upon which stable isotope geochemists in the fields of both sedimentary and metamorphic petrology can relate their more detailed studies on individual field areas. Both types of approach are necessary for an understanding of the role of aqueous fluids in the alteration of large masses of the Earth's crust. Without a foundation of this sort, any detailed studies of the role of fluids in the metamorphism and diagenesis of sedimentary rocks are like "not seeing the forest for the trees".

It is important to emphasize that without doing an enormous number of individual isotopic analyses of mineral separates from rocks, one cannot understand large-scale shifts in crustal $\delta^{18}\text{O}$ simply by analyzing coexisting minerals. The isotopic compositions of minerals may vary widely, and selective separation may leave large portions of the rock specimen unanalyzed. How fluids interact with the unanalyzed portion of the rock then becomes a matter of speculation. That is why this study has taken a different approach to oxygen isotopic analysis of sedimentary rocks, namely one which involves analyzing the bulk silicate fraction of a large number of these rocks over

vast geographic areas. Where present, the carbonate fraction is usually analyzed separately, thereby giving us a direct measurement of these important minerals, upon which so much stable isotope research has been done. This approach also allows us then to calculate the overall whole-rock $\delta^{18}\text{O}$ of each rock studied, by combining the appropriate proportion of carbonate and bulk silicate.

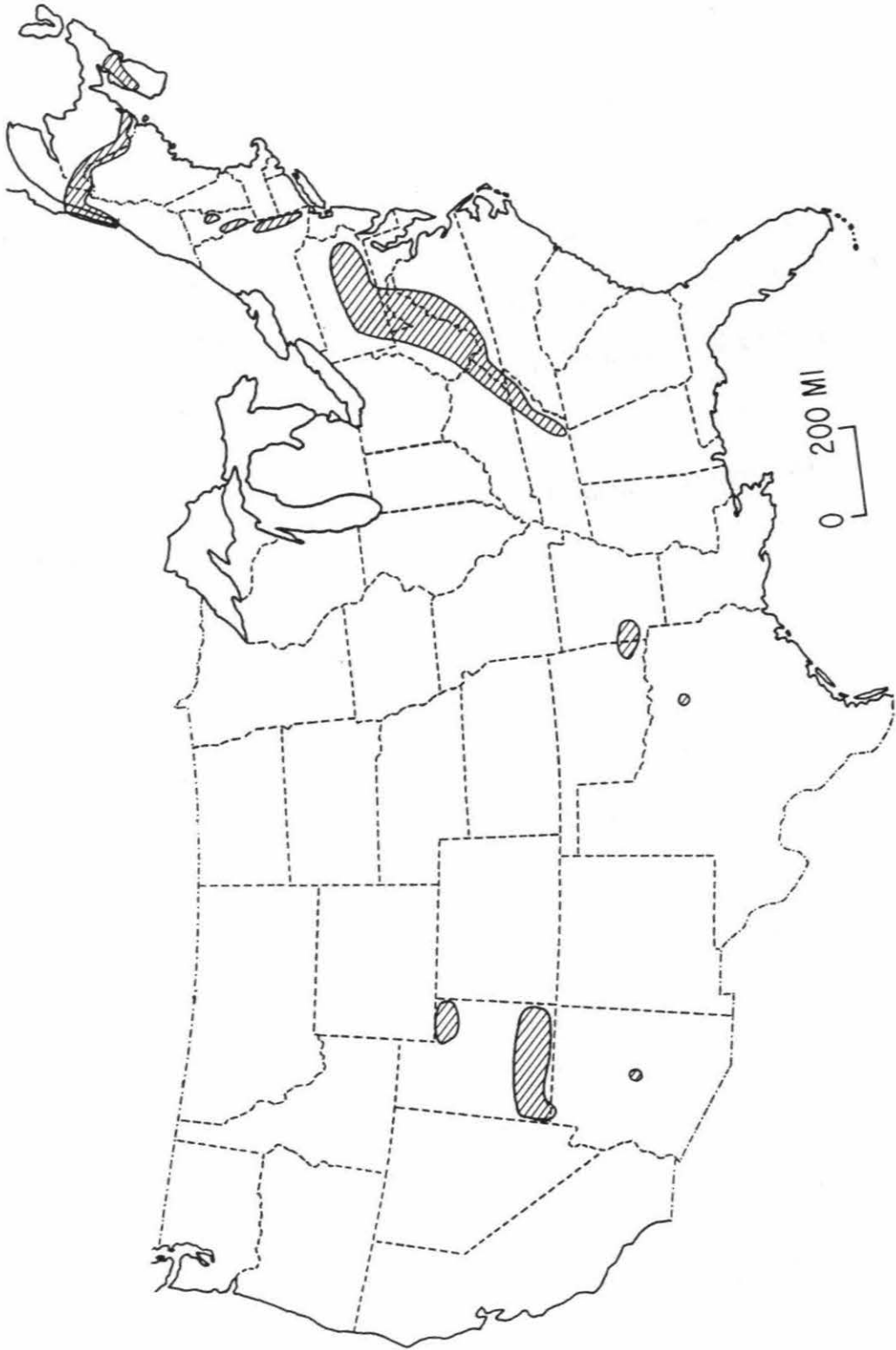
Instead of analyzing a few sedimentary rock samples from many separate regions all around the world, this study focuses on three major regions in the United States: the Appalachian Mountains, the Ouachita Mountains, and the Colorado Plateau. In spite of this restriction, this study constitutes the largest major regional study of the bulk silicate $\delta^{18}\text{O}$ of terrigenous sedimentary rocks yet undertaken. The general areas that were sampled in this study are shown on the map in Figure 1.1.

The approach taken in this thesis was chosen with the view of trying to understand the bulk silicate $\delta^{18}\text{O}$ systematics of detrital sedimentary rocks such as sandstones and shales on a regional scale and over an age range of hundreds of millions of years. It is very important to appreciate the scale of this study and understand the reason for carrying out such a large-scale study. The only previous study of this type is that in an earlier Ph.D. thesis at Caltech by Savin (1967), who made a reconnaissance study of the bulk silicate $\delta^{18}\text{O}$ of sedimentary rocks on a global scale, including samples from the oceanic crust. That work has up to now been the primary reference for metamorphic petrologists studying changes in $\delta^{18}\text{O}$ during metamorphism of sedimentary rocks, but less than fifty whole-rock analyses were done, and they were from samples scattered over the entire globe.

It was the intention of the present study to do more than just add to the

Figure 1.1

Map of the United States and part of eastern Canada, showing the general areas covered by the $^{18}\text{O}/^{16}\text{O}$ analyses of sedimentary and metasedimentary rocks studied in this work (diagonal-lined envelopes). Samples were collected from (1) the Colorado Plateau area of northeastern and southern Utah and part of Arizona; (2) the Ouachita Mountains in western Arkansas and eastern Oklahoma, including a couple of samples in northeastern Texas; and (3) along the entire length of the Appalachian Mountains from Tennessee, Virginia, and West Virginia north to Quebec, New Brunswick, and Nova Scotia in Canada.



relatively small current data base of whole-rock oxygen isotope analyses of terrigenous sedimentary rocks, although that is certainly an important aspect of the problem. Instead, the intent has been to study the regional variation of the bulk silicate $\delta^{18}\text{O}$ of such sedimentary rocks over several hundreds of millions of years in two major Paleozoic geosynclinal areas (the Central Appalachians and the Ouachitas) and in a major stable shelf environment (the Colorado Plateau), in order to better understand the isotopic effects of sedimentation, burial, diagenesis, and regional metamorphism on large segments of the crust formed in these two major types of depositional environments. The present work is significant in large part because it is the first such study to be conducted at this scale. The results to date have proven to be quite promising, and they suggest that this approach could be useful in future work to understand burial diagenesis and regional metamorphism.

Some of the most critical questions currently debated in metamorphic petrology concern the role of fluids in metamorphism (Thompson, 1983; Ferry, 1983, 1984, 1986, 1987, 1988a, 1988b; Valley and O'Neil, 1984; Wickham and Taylor, 1985, 1987, 1990; Valley, 1986; Wood and Walther, 1986; Wood and Graham, 1986; Chamberlain and Rumble, 1988, 1989; Rumble, 1989; McCaig *et al.*, 1990; Valley *et al.*, 1990; Walther, 1990; Baumgartner and Ferry, 1991; Mora and Valley, 1989; Nesbitt and Muehlenbachs, 1989, 1991). Oxygen isotope studies help to constrain the origins and amounts of metamorphic fluids (Gregory and Criss, 1986). One difficulty with this approach however, is that it is difficult to estimate the whole-rock oxygen isotopic ratios of the metamorphic protoliths (Rumble, 1989). As an example of possible applications, the sedimentary rock data set developed in this study will be compared with

a number of measured whole-rock $\delta^{18}\text{O}$ values of psammitic and pelitic metasediments from the Northern Appalachians in Vermont, New England, Nova Scotia, and New Brunswick. The locations of these areas are shown on the map in Figure 1.1.

In summary, this work addresses and attempts to answer some of the following questions:

1. What is the general distribution and range of bulk silicate $\delta^{18}\text{O}$ values in detrital sedimentary rocks such as sandstones, siltstones and shales?
2. More specifically, what is the distribution and range of bulk silicate $\delta^{18}\text{O}$ values in such sedimentary rocks in the Central Appalachian Mountains, the Ouachita Mountains, and the Colorado Plateau ?
3. Are there any differences between the distribution and range of bulk silicate $\delta^{18}\text{O}$ values of all previously analyzed detrital sedimentary rocks in the geochemical literature and those of the Central Appalachians, the Ouachitas, and the Colorado Plateau and, if so, why?
4. What is the relationship, if any, between the bulk silicate $\delta^{18}\text{O}$ of such terrigenous sedimentary rocks with respect to: a) environment of deposition, b) lithology, c) age, d) carbonate content, and e) degree of diagenesis?
5. What is the relationship, if any, between bulk silicate $\delta^{18}\text{O}$ of metasedimentary rocks and carbonate content?
6. Is it possible to delineate any large-scale bulk shifts in $\delta^{18}\text{O}$ that correlate with other geochemical parameters related to the diagenesis of sediments in the Appalachian Mountains, the Ouachita Mountains, and the Colorado

Plateau?

7. What bearing do these isotopic shifts, or lack thereof, have with respect to the role of fluids in the diagenesis of sediments?
8. Is it possible to delineate large-scale bulk shifts in $\delta^{18}\text{O}$ as a result of the metamorphism of analogous sedimentary rocks in the Northern Appalachians, and what bearing, if any, do these isotopic shifts have regarding the general problem of the role of fluids in the metamorphism of sedimentary rocks?

1.2 Brief review of the geochemistry of sedimentary rocks pertinent to the present study

1.2.1 Marine pelagic sediments

The first major contribution to the understanding of the oxygen isotope geochemistry of the pelagic sediments, as well as to the general problem of the $\delta^{18}\text{O}$ variations in the silicate portions of the common types of sedimentary rocks was made by Savin and Epstein (1970a, 1970b). They analyzed 27 core samples of pelagic sediments and about 20 samples of coarse-grained sedimentary rocks.

Most of the silicate component of pelagic sediments is probably of eolian origin (*e.g.*, see Garlick, 1974). For example, Clayton *et al.* (1972b) showed that the $\delta^{18}\text{O}$ values of silt-sized and clay-sized quartz in northern hemisphere Pacific Ocean sediments ranged from +16 to +19 and that of southern hemisphere Pacific Ocean sediments from +12 to +16. These differences are thought to reflect the much greater surface area of continental land mass exposed to weathering (and thus to low-temperature enrichment in ^{18}O) in the northern hemisphere. Both sets of values are much higher than those found

in most igneous rocks (which are typically about +6 to +12). Comparisons with the $\delta^{18}\text{O}$ values of quartz from nearby land masses led these workers to conclude that the source of silt-sized quartz in Pacific Ocean pelagic sediments was atmospheric dust from the continents. The high $\delta^{18}\text{O}$ values observed by Clayton et al. (1972b) require that a major component of relatively low-temperature (*i.e.* authigenic or biogenic) quartz be present in these eolian samples.

Tropospheric transport of clay minerals also contributes a great deal of material to the formation of pelagic sediments. Most of the clay minerals in typical deep sea sediments have $\delta^{18}\text{O}$ values between +11 and +20 (Savin and Epstein, 1970b; Yeh and Savin, 1976). The fact that these values fall within the range reported for clay minerals in soils (Savin and Epstein, 1970a, Lawrence and Taylor, 1971, 1972) and in sediments from the Mississippi River area (Yeh and Savin, 1977) supports the conclusion that a high percentage of the clay minerals in deep-sea sediments could also be of continental origin.

Another process involved in the formation of pelagic sediments is the submarine hydrothermal alteration of basalt. Some of the alteration products include montmorillonite, phillipsite, and metalliferous deposits such as those found on the East Pacific Rise. Clay minerals which form in sea water are typically heavier in ^{18}O than equivalent minerals formed by weathering on the continents. This is because ocean water is higher in ^{18}O than meteoric water, and also because ocean bottom waters are usually very cold. Smectites formed by the submarine alteration of basalt range in $\delta^{18}\text{O}$ from +26 to +34.5 (Savin and Epstein, 1970b; Yeh and Savin, 1976; Lawrence et al., 1979; Hein et al., 1979). This wide range in $\delta^{18}\text{O}$ is thought to be due primarily to the

range of temperatures over which alteration of basalt occurs. Dymond et al. (1973) concluded that the metalliferous deposits of the East Pacific Rise formed by the hydrothermal alteration of basalt and consisted of a mixture of iron-rich montmorillonite and iron and manganese oxides. Iron and manganese oxides which form in ocean water at low temperature have $\delta^{18}\text{O}$ values between +10 and +15, as evidenced by analyses of manganese nodules which precipitate at low temperature on the ocean floor (Dymond et al., 1973). Anderson and Lawrence (1976) found that vein-filling calcite from ocean basalts ranged in $\delta^{18}\text{O}$ from +25 to +32. They concluded that this calcite precipitated from hydrothermal solutions that had been depleted in ^{18}O by closed-system interaction with basalt.

Volcanic eruptions on land contribute tephra to deep-sea sediments. These may take the form of glass shards dispersed throughout the sediment or a consolidated layer composed almost entirely of volcanic debris. Tephra entering the ocean will be subject to low-temperature alteration, forming such products as smectite and zeolites (Friedman and Sanders, 1978).

Biogenic precipitation of calcareous and siliceous tests contributes to the formation of the most widespread of the pelagic deposits: the oozes. Most deep-sea carbonate is produced by foraminifera and coccolithophorids in the upper portions of the water column. Tests of foraminifera from the genus *Globigerina* form the widespread *Globigerina* oozes. *Globigerina* oozes are the main deep-sea sediment found in the Atlantic and also in much of the Pacific and Indian Oceans. Coccolith ooze forms the main deep-sea sediment in the Mediterranean Sea and the Black Sea. Coccolith tests, however, may also comprise up to fifty per cent of the calcareous oozes in the Atlantic,

Pacific, and Indian Oceans (Friedman and Sanders, 1978). Phytoplankton are also a primary source of organic matter to pelagic marine sediments.

The main factors affecting the oxygen isotopic composition of neoformed calcareous tests in pelagic sediments are: biological fractionation of carbonate and degree of attainment of equilibrium, temperature of formation, and the isotopic composition of ocean water. There are several on-going isotopic studies of different marine organisms that continue to refine the original paleotemperature work of Urey *et al.* (1951) as to whether a given species deposits calcite in equilibrium with sea water, or whether there is a biological effect which results in non-equilibrium precipitation. For example, planktonic foraminifera generally secrete calcite at close to isotopic equilibrium while coccolith tests are less likely to be in equilibrium with seawater when secreted. The temperature of formation will affect the isotopic composition of the calcite because the calcite-water fractionation factor is temperature dependent. This means that for foraminifera in the same water column the benthic tests would be expected to be heavier in ^{18}O than the planktonic tests. Douglas and Savin (1973; 1975) found $\delta^{18}\text{O}$ values of about +30 in for a miniferal and nannoplankton tests from warm surface waters, whereas $\delta^{18}\text{O}$ values for benthic cold water foraminiferal tests were about +34.

The oxygen isotopic composition of modern ocean water is fairly well characterized (*e.g.*, see Sheppard, 1986, and the references therein); $\delta^{18}\text{O}$ of sea water ranges from +0.5 to -1.0 with a mean of 0.0, so the $\delta^{18}\text{O}$ of seawater is one of the best constrained of all the variables discussed above. Under special conditions the range in $\delta^{18}\text{O}$ may be greater. For example, the amount of continental ice is the primary factor affecting the mean isotopic composition of the oceans. Local isotopic effects,

particularly in ocean surface waters, may result from evaporation, freezing, precipitation, and mixing processes. While there is some debate about the oxygen isotopic content of ancient ocean water, there is strong evidence, based on high- and low-temperature alteration of basalt at mid-ocean ridges, to support a relatively constant $\delta^{18}\text{O}$ value over time of about -1 to 0 (± 1 per mil) (see Muehlenbachs, 1987, 1986; Muehlenbachs and Clayton, 1976; Gregory and Taylor, 1981).

Siliceous oozes consist of the siliceous skeletons of marine microorganisms. The main contributors are diatoms, which predominate in polar waters, and radiolarians, which are found in most parts of the ocean, except in bottom sediments (Friedman and Sanders, 1978). Such materials are typically very high in $\delta^{18}\text{O}$ (*e.g.*, Knauth, 1973).

Post-depositional alteration of sediments is complex and often not well understood. A brief overview is made here of those processes affecting the oxygen isotopic ratios of sediments. A common diagenetic alteration of calcareous tests is recrystallization and reprecipitation of carbonate overgrowths. Biogenic silica is often altered to form chert according to: opal-A > opal-CT > microcrystalline quartz = chert (Savin, 1980). Both the diagenetic alteration of calcareous tests and biogenic silica can cause re-equilibration of oxygen isotopes, with the final $\delta^{18}\text{O}$ value being sensitive to the temperature of alteration and the isotopic content of the formation waters. Calcite may also precipitate in sediments as a result of the carbon liberated in the oxidation of organic matter by sulfate-reducing bacteria. Burial and compaction of sediments can cause an increase in temperature and entrapment of pore waters. Detrital clay minerals are altered under these conditions. A common transformation which occurs when these sediments reach temperatures above 80°C is the conversion of smectite to illite (Hower *et al.*,

1976). This transformation has been shown to be accompanied by isotopic exchange between the clay mineral and pore water (Yeh and Savin, 1977). The alteration of volcanic material to form clay minerals or zeolites and chert also continues after burial and is thought to be responsible for the increase in $\delta^{18}\text{O}$ in the pore waters of ocean sediments (Egeberg *et al.*, 1990; Lawrence *et al.*, 1979; Aagaard *et al.*, 1989; Vrolijk *et al.*, 1990).

1.2.2 Sedimentation in offshore deep subsiding basins

Many of the processes operating in the formation of pelagic sediments are also important to the formation of sedimentary rocks in offshore marine basins. The main differences between these two environments are: (1) the great thicknesses of sediments in the basins can give rise to potentially deep burial of the latter, thereby producing greater heating and other post-depositional diagenetic changes; (2) the proximity of the marine basin to land masses gives rise to a much wider range of sizes of the terrigenous clastic debris, and it may also have as a consequence the possible introduction of lower- ^{18}O meteoric waters into the rock column as sedimentary pore fluids.

In contrast to the pelagic sediments, the contribution of atmospheric transport of extremely fine-grained silicate material is far outweighed by the fluvial contribution of sedimentary detrital material of a vast range of grain sizes from the adjacent landmass. Clays, rock fragments, feldspars, quartz and other detritus are common components of river sediments. The proximity of the basin sediment to the river mouth is an important factor in determining the detrital mineral content of the sediment. Atmospheric transport, however, can still be important for the deposition of volcanic tephra in such marine basins. As in the deep-sea environment, post-depositional alteration of volcanic debris

to clays and zeolites is an important process. The biogenic formation of carbonate and silica and their subsequent diagenetic alteration is also important, as is the contribution of marine plants and organisms to the organic matter content of basin sediments. Argillaceous sediments may contain a few tenths to a few per cent organic matter (Savin and Yeh, 1981). In addition to organic debris, fish contribute apatite in the form of fish teeth to marine sediments (Savin, 1980).

In the diagenesis of basin sediments, deep burial results in an increase in temperature and de-watering of sediments. Yeh and Savin (1977) found a tendency toward isotopic homogenization for the clay-size fractions of shales from the Texas Gulf Coast. They concluded that this effect was mainly due to the formation of illite from smectite. Mineral transformations, such as the smectite-illite reaction, mineral dissolution, and precipitation are common diagenetic reactions. In sandstones, dissolution and re-precipitation of minerals can form secondary cements, the most common of which are calcite, quartz, and clay minerals. During these reactions the new mineral may be in isotopic equilibrium with the pore water from which it forms. Using this assumption, Yeh and Savin (1977) were able to estimate formation temperatures from the clay-size quartz and illite in their samples of Gulf Coast shales. The literature on the use of diagenetic minerals as geothermometers and as indicators of the paleohydrology of basins is voluminous (Eslinger and Savin, 1973; Yeh and Savin, 1977; Suchecki and Land, 1983; Eslinger and Yeh, 1986; Longstaffe, 1984; Land, 1984; Land and Dutton, 1978; Ayalon and Longstaffe, 1988; Longstaffe, 1986a; Lee *et al.*, 1989; Lundegard and Trevena, 1990; Fisher and Land, 1986; Milliken *et al.*, 1981; Tilley and Longstaffe, 1989; Dutton and Land, 1988; Longstaffe and Ayalon,

1990; Longstaffe and Ayalon, 1987; Land and Fisher, 1987; and other references included in the above papers). In these studies the diagenetic minerals are painstakingly separated from the sedimentary rocks and then analyzed isotopically. Comparatively few whole-rock $\delta^{18}\text{O}$ analyses have been carried out on these samples.

Another factor involved in the diagenesis of sediments in offshore marine basins is the involvement of meteoric water, which will have the effect of lowering the $\delta^{18}\text{O}$ of authigenic minerals formed from such waters, as compared to the values observed in the same materials formed in the presence of undiluted sea water. Meteoric water may enter a still subsiding marine basin through subsurface flow from the adjoining landmass. However, after the basin is tectonically deformed and uplifted, then meteoric water may also enter through the overlying ground surface, contributing to the pore waters present during diagenesis.

1.2.3 Geosynclines

Following Pettijohn (1975), a geosyncline will here be defined as "a linear trough or depression, perhaps divided medially by an anticlinal ridge, that was filled mainly with clastics from the craton, the medial ridge, and (or) most especially from a tectonic border land". Geosynclinal sediments reach great thicknesses, and like the deposits described in the previous section they also form in deep subsiding basins. Therefore, much of the previous discussion applies to the geosynclines as well. However, these geosynclinal basins are distinctive in their great lengths, commonly thousands of kilometers parallel to the edge of the adjacent continental craton.

Geosynclines are conveniently divided into two types of facies, eugeosynclinal and miogeosynclinal (Kay, 1951). The dominant lithologies in the eugeosynclinal

facies are graywacke sandstones and submarine volcanic and volcanoclastic rocks of various types (including pillow lavas). A major isotopic study of whole-rock samples from this type of geosynclinal facies was carried out by Magaritz and Taylor (1976) on Mesozoic rocks from the California Coast Ranges. The eugeosynclinal facies is generally formed in deeper water, typically in a volcanic island environment (island-arc?), whereas the miogeosynclinal facies is formed nearer to the craton and is lithologically transitional to the generally much thinner sections of sediments that form in a stable shelf environment where shallow seas lap onto the craton. The miogeosynclinal facies commonly contains shales, limestones and dolomites, and "cleaner" sandstones and siltstones grading to quartz arenites; volcanic rocks and volcanoclastic debris are rare.

The geosynclines are typically characterized by rapid uplift of the source land followed by erosion and deposition in the adjacent marine trough. Submarine slope and fan deposits are common in such environments. Such sediments are commonly transported as high-density flows from their original place of deposition. Such slump-generated turbidity flows move coarse sediments from shallow water to deep water environments. These turbidite flows can travel long distances, and they are an effective means of transporting clastic material into the deep ocean.

The flysch facies of geosynclines is an interbedded sandstone-shale sequence. Flysch can be thousands of meters in thickness representing continuous deposition of these terrigenous clastic sediments. The sediments are texturally and mineralogically immature, being derived from high-standing, low-grade metamorphic, crystalline, or volcanic terranes. A common sandstone in flysch is graywacke. These rocks are common in Paleozoic and older orogenic belts and are typically absent in undeformed

terrane and shelf environments (Pettijohn 1975). Graywackes are particularly common in the eugeosynclinal facies, and are generally dark grey in appearance and contain lithic fragments, feldspar, and a fine-grained matrix of clays, quartz, and feldspar. They are rich in iron, magnesium, and sodium. Their composition reflects the immaturity of the sediments from which they formed. One-fourth to one-fifth of all sandstones are graywackes (Pettijohn, 1975). As one moves from the eugeosyncline into the miogeosyncline, the sandstones typically contain a lower content of lithic fragments, particularly volcanic debris, and interbedded sequences of carbonate rocks also become more common.

Active volcanism in the eugeosynclinal facies of geosynclines commonly results in pillow basalts interbedded with sediments and water-laid tuffaceous deposits. The pillow basalts are commonly hydrothermally altered to greenstone. These hydrothermal fluids (heated ocean water?) may interact and exchange isotopically with interbedded sediments. After deposition of the thick section of sediments, a geosyncline is typically deformed, uplifted, and subjected to regional metamorphism and diagenesis. Uplift of sediments affords the opportunity for involvement of meteoric water. For example, Magaritz and Taylor (1976) demonstrated the involvement of meteoric water during low-temperature serpentinization of ultramafic bodies in the eugeosynclinal Franciscan Formation of California.

1.2.4 Evaporite basins

Evaporite basins may contain either sea water or meteoric water, but with vastly increased salt content. Evaporation concentrates $\delta^{18}\text{O}$ in the water as well as salts. Carbonates and sulfate salts (gypsum and anhydrite) typically precipitate in these

environments. In contrast to the carbonates, once it is formed the sulfate oxygen generally does not exchange with the oxygen in the adjacent water. This means that the oxygen in sulfate salts is typically not in isotopic equilibrium with its coexisting diagenetic pore water. However, the action of microorganisms can alter the isotopic composition of sulfate, particularly its $\delta^{34}\text{S}$ value. Another concern is the post-depositional exchange of these salts in the presence of hot brines. The dependence of the oxygen isotope fractionation factor on both temperature and salinity must be considered [Truesdell, 1974]. It is important to realize that for a basin receiving limited recharge the $\delta^{18}\text{O}$ of the water is not constant. Highly saline fluids are very reactive and can be expected to exchange very readily with many silicate minerals (particularly clay minerals).

1.2.5 Stable continental shelf and craton

This category includes pericontinental seas, as exemplified by continental shelves, and epicontinental seas which extend over continents to form shallow seas on the craton. Depositional thicknesses of sediments are much less than in subsiding basins, and alternating regression and transgression of the shallow seas is common. Although volcanic contributions can be locally important, sediment is most commonly supplied to these seas through the action of rivers. Limestones, dolomites, mudstones, siltstones, shales, and sandstones (commonly orthoquartzites or quartz arenites) dominate the lithologies of the shelf environment.

The first reliable oxygen isotopic analyses of such rocks, or of silicate rocks in general for that matter, were made by Baertschi and Silverman (1951) and Silverman (1951). Silverman, in an analysis of five sedimentary rocks, all from shelf

environments, found that $\delta^{18}\text{O}$ increased with increasing percentage of authigenic silica. For example, Silverman (1951) compared the $\delta^{18}\text{O}$ values of three orthoquartzites, the Cambrian Potsdam Sandstone (+15.5), the Precambrian Wishart Orthoquartzite (+15.1), and the Ordovician St. Peter Sandstone (+10.9), with the latter being very friable and containing much less authigenic quartz cement compared to the other two samples.

Temperature and precipitation are important factors in the weathering process to supply sediment from the continent. If the shelf sea is tide-dominated, then strong daily bottom currents allow greater transport of sand. In storm-dominated shelf seas sediment transport is limited to winter storms. Reworking of older sediments is also accomplished by these forces. Such continuous reworking can lead to better sorting and mineralogically more homogeneous rocks (*e.g.*, pure quartz sandstones).

Because sea-level transgressions and regressions are commonplace in the shelf environment, these factors are the dominant control on the temporal and spatial distribution of sedimentary facies. Shallow marine organisms contribute organic matter to sediments. Biogenic carbonate and silica are also important in this environment as is the authigenic formation of clay minerals. And again, proximity to a land mass coupled with sea level changes allows for the introduction of meteoric water (Reading, 1978)

1.2.6 Euxinic environments

Euxinic environments are depositional environments where waters are anoxic or, conversely, waters are oxic but the sediments become anoxic a few millimeters below the depositional surface due to the action of bacteria and the slow oxygen replenishment by diffusion. A key ingredient in a euxinic environment is the relationship of abundance of organic matter to oxygen supply. The decomposition of organic matter reduces the

oxygen content in the water which allows for the accumulation of organic-rich sediments. Anoxic conditions allow the growth of anaerobic sulfate-reducing bacteria, producing hydrogen sulfide and leading to the formation of pyrite. The type euxinic environment is the Black Sea, which has become anoxic over a wide area due to restricted circulation of water.

Other euxinic environments can include parts of the open ocean and the continental shelf, both of which typically contain oxic waters but can become anoxic just below the depositional surface (Tourtelot, 1979). Common products of the euxinic environment are the black shales. These rocks are high in organic matter, iron sulfides, and contain minor amounts of carbonate. They are a common pre-flysch deposit and thought to be induced by the emergence of the geosynclinal ridge which restricts circulation in the adjacent waters Pettijohn (1975).

1.2.7 Transitional sedimentary environments and marine-nonmarine oscillations

1.2.7.1 Oscillatory marine-nonmarine basins

These basins are filled with marine or fresh water at different points in their history. The main isotopic effect is the introduction of meteoric waters into the sedimentary pile, which can lead to lower- ^{18}O diagenetic alteration products. Also, any authigenic minerals forming from these meteoric pore waters will be lower in ^{18}O than those formed in sea water.

1.2.7.2 Shore deposits

Shore deposits include beach sand, tidal flat, barrier island, and beach deposits. A major process in this environment is the sorting action of the waves and currents.

Again, transgressive or regressive seas will affect the spatial distribution of these deposits. Accessibility to meteoric water is also important.

1.2.7.3 Bay and lagoon deposits

Lagoons and bays are extremely variable shallow water environments. Sediments accumulating in this environment are often fine-grained and rich in organic matter. During storms, however, sand may be deposited by strong wave action in the adjoining sea. Rivers may bring fresh water to these environments which will mix with marine water resulting in intermediate ^{18}O contents.

1.2.7.4 Deltaic complex

A delta is a cone of sediment deposited at the confluence of a river and a large water body. In the case where that large water body is the ocean, the location of sea level will play an important role in the geometry of the deltaic deposit. The sourceland for river sediment and the degree of weathering of that sediment will have a large influence on the oxygen isotopic content of the deltaic complex. Again, the mixing of fresh water and sea water may result in an intermediate $\delta^{18}\text{O}$ near the river mouth.

1.2.7.5 Marsh

As bays or lagoons are filled with sediment, they are colonized by vegetation and become marshes and swamps. Marsh deposits consist of thinly laminated clays and organic matter. Again, the $\delta^{18}\text{O}$ of the water in the marsh environment is important, because the $\delta^{18}\text{O}$ can be lowered as meteoric waters become dominant over sea water. The $\delta^{18}\text{O}$ values can also vary as water is lost through evaporation and replenished through storms and floods.

1.2.8 Terrestrial sedimentary environments

1.2.8.1 Volcaniclastic

One important factor in the ^{18}O contribution of volcanic debris to sediments is the $\delta^{18}\text{O}$ value of the parent magma from which the rock formed. In the presence of liquid water, the glassy portion of volcanic debris is subject to rapid alteration to form clays and zeolites. The characteristic clays formed in these environments are montmorillonites, and the rocks formed by alteration of such tuffaceous material are termed bentonites. The ^{18}O content of the alteration water and the time and temperature of alteration will control the isotopic compositions of the clays and zeolites. This water may be ocean water, lake water, or other types of meteoric water. Tephra that is newly deposited on steep slopes is susceptible to erosion, particularly by torrential rains. Debris flows may result which eventually become part of stream alluvium and are carried out to sea.

1.2.8.2 Alluvial fan

Alluvial fans form adjacent to mountain ranges or high hills. This environment is characterized by intermittent torrential flow. In alluvial fans clastic material is deposited in close proximity to its source, commonly as mud flows or debris flows. The alluvium is of all sizes up to conglomerates and megabreccias, and is poorly sorted (Pettijohn, 1975). The oxygen isotopic content of these rapidly deposited materials is almost wholly determined by the isotopic composition of the immediate source material.

1.2.8.3 River channel and floodplain

Sediment supply and amount and velocity of water are critical factors related to the deposition of river channel deposits, which are commonly sandstones. The $\delta^{18}\text{O}$

values of the sediments are strongly dependent upon the $\delta^{18}\text{O}$ of the source sediment.

Sediments deposited when a river overflows its banks form floodplain deposits. By their very nature these deposits are episodic. Sediments dry between floods and are often covered with vegetation, in which case soil development occurs. As in the river channel, the velocity of the water is related to the grain size of the deposited sediment. Fine sand, silt, and clay deposits are common, and the sorting action of the fluvial environment can lead to a spectrum of different whole-rock $\delta^{18}\text{O}$ compositions if these different size fractions have inherently different mean $\delta^{18}\text{O}$ values. The $\delta^{18}\text{O}$ of the river water at the time of deposition is only significant in terms of its possible effect during exchange with the clay-size particles in the channel or floodplain deposit.

1.2.8.4 Lacustrine

Lakes are non-marine water bodies that are landlocked. Their waters range in $\delta^{18}\text{O}$ from very low values in glacial meltwater to very high values (perhaps even higher than ocean water) in hypersaline lakes in arid regions. The $\delta^{18}\text{O}$ of lake water may be an important factor in the oxygen isotopic content of its sediments. This is particularly true for minerals formed in the lake water, such as alteration products of tephra, and particularly in such strongly reactive environments as saline lakes (see Section 1.2.4 above). Lakes are often rich in plants and animals which contribute a significant organic component to sediments. Biogenic carbonate is produced on some lake shores. As with other environments, the source of sediments supplied to the lake, along with the wind and water power to erode and sort them, are important factors controlling the $\delta^{18}\text{O}$ content of sediments.

1.2.8.5 Swamp

A swamp is essentially a lacustrine environment with limited terrigenous input compared to the organic input. Plant growth dominates the swamp and its most common deposit is peat.

1.2.8.6 Eolian

When wind blows in a desert area, silt- and clay-size particles are transported for long distances. Sand moves along the ground by saltation and can be formed into dunes by the wind. When the wind carrying the silt and clay fraction is slowed near the steppes it drops its load and forms loess deposits. Wind is the most important factor in sorting both types of deposits. The $\delta^{18}\text{O}$ of the wind-eroded sediment source material will have a dominant influence on the $\delta^{18}\text{O}$ of the eolian deposit. However, because of the strong sorting effects of the wind, any variation in $\delta^{18}\text{O}$ related to the sizes of the mineral grains or rock fragments will be strongly emphasized in the whole-rock $\delta^{18}\text{O}$ analyses of the various kinds of eolian deposits. For example, the sand-size fraction might be dominated by relatively uniform quartz grains having a limited range of $\delta^{18}\text{O}$. Also, the $\delta^{18}\text{O}$ of any secondary cement that may form as a result of burial and diagenesis obviously will be controlled by the temperature and $\delta^{18}\text{O}$ of the circulating ground waters.

1.2.8.7 Glacial

The main geologic agents in a glacial environment are the moving ice itself and melt water produced in glacial outflow areas. $\delta^{18}\text{O}$ of this ice is often unusually low, and when the ice melts, interaction of this very low- ^{18}O water with sediment could cause a lowering of $\delta^{18}\text{O}$ in any fine-grained minerals that undergo exchange, or in newly-

formed authigenic or biogenic minerals. However, the $\delta^{18}\text{O}$ of the rock debris scoured by the glacier and left as unsorted deposits such as till, will in general be wholly determined by the $\delta^{18}\text{O}$ of the source material.

1.3 Brief review of the geochemistry of metasedimentary rocks pertinent to the present study

There are four major factors that control the oxygen isotope variations of metamorphic rocks: (1) the isotopic composition of the original pre-metamorphic protolith; (2) the isotopic changes produced by volatilization reactions such as decarbonation and dehydration; (3) the amount of isotopic exchange with infiltrating fluids and the overall fluid/rock ratios; and (4) the temperatures at which metamorphism and isotopic exchange occur. A brief review of these concepts is given in Valley (1986).

1.3.1 Contact metamorphism

The geologic environment of contact metamorphism is generally much better constrained than that of regional metamorphism, particularly because the lithostatic overburden pressures are more easily reconstructed from geologic mapping. When an igneous body intrudes a section of sedimentary rocks, metamorphism clearly proceeds from high to low grade as one moves away from the heat source. Constant lithostatic pressure can also commonly be assumed at a given structural horizon. Fluid flow is generally related to the igneous contact and may be wholly driven by this "heat engine". However, the most important advantage of the contact metamorphic environment with respect to bulk $^{18}\text{O}/^{16}\text{O}$ studies is that it often allows access to correlative unmetamorphosed sediments whose stable isotope compositions can be directly compared to their metamorphosed equivalents simply by successively sampling at greater distances

from the pluton. An example of such a study is the work of Shieh and Taylor (1969) on several contact aureoles in Nevada.

In their study of several different kinds of granitic plutons and metamorphic aureoles in northern Nevada, Shieh and Taylor (1969) concluded that upward movement of water in the aureole was more important than outward horizontal movement of water into the aureole. They found small-scale oxygen isotopic exchange effects in the country rock within 0.5 to 3 feet of the contact. However, except in these exchange zones, Shieh and Taylor (1969) discovered that the $\delta^{18}\text{O}$ values of the metamorphic rocks were not different from their unmetamorphosed equivalents, even in the cordierite and sillimanite grades. They concluded that large influxes of water did not occur during in the formation of these contact aureoles, even the ones which formed under conditions of relatively high $P_{\text{H}_2\text{O}}$.

In another interesting isotopic study of contact metamorphism, Nabelek et al. (1984) concluded that carbon isotopic ratios of argillites surrounding the Notch Peak stock in Utah were lowered through Rayleigh decarbonation reactions. However, enough CO_2 was not lost to explain the low $\delta^{18}\text{O}$ values of the argillites. Nabelek et al. (1984) thus postulated that the extensive decarbonation reactions near the igneous contact enhanced permeability, allowing infiltration of magmatic water which reacted with the high grade argillites and lowered the $\delta^{18}\text{O}$.

Valley (1986) made a comparison of sixteen metamorphic aureoles, and demonstrated a coupled trend of decreasing $\delta^{18}\text{O}$ and $\delta^{13}\text{C}$ in the metamorphosed carbonate rocks. In the past, many of these trends were attributed to decarbonation

reactions by invoking unusual fractionation factors or reaction mechanisms. Valley (1986) contends that large-scale isotopic shifts require other explanations such as fluid infiltration or polythermal effects.

Metamorphosed sediments which show a coupled trend of decreasing $\delta^{18}\text{O}$ and $\delta^{13}\text{C}$ may also form in hydrothermal systems in which the temperature of exchange is variable. Examples of such hydrothermal systems have been shown for the lead-zinc deposits at Providencia, Zacatecas, Mexico (Rye, 1966) and for the base metal sulfide deposits at McArthur River, Northern Territory, Australia (Rye and Williams, 1981). These polythermal effects should be addressed when evaluating C-O trends in contact metamorphic aureoles, as a cooling igneous body would be expected to generate temperature differentials. Nabelek (1991) has recently written a detailed review of $^{18}\text{O}/^{16}\text{O}$ relationships in contact metamorphic environments.

1.3.2 Regional metamorphism

The role of fluids in regional metamorphism has been the subject of much controversy in the past decade. Two major schools of thought exist which will here be termed "fluid-restricted" and "fluid-dominated" regional metamorphism. Fluid-restricted metamorphism is that in which substantial fluid flow is limited to local cracks, fissures, or channels which develop in the rock, and where fluid-rock isotopic exchange occurs on a limited basis through diffusion and recrystallization. Isotopic heterogeneity is common. In fluid-dominated regional metamorphism, metasediments are pervasively infiltrated by fluids, resulting in large-scale isotopic changes in the bulk rocks. This type of metamorphism is commonly accompanied by local isotopic homogenization of the metasediments and an overall lowering of $\delta^{18}\text{O}$, and it almost certainly requires some

kind of advective circulation of fluids. It is fluid-dominated because there is generally a lack of isotopic, chemical, and thermal equilibrium between the initially infiltrating fluid and the mineral assemblages with which it comes into contact. This lack of equilibrium is thought to be a primary cause of the prograde metamorphic reactions in many cases.

1.3.3 Fluid-restricted regional metamorphism

In a study of metasediments of the Clough Formation, Black Mountain, New Hampshire, Rumble (1978) found that mineral assemblages reached chemical equilibrium on the scale of single sedimentary beds up to one meter thick. He concluded that an aqueous metamorphic fluid was present which varied in isotopic composition and in abundance from bed to bed. Rumble (1978) attributes local heterogeneity in ^{18}O to premetamorphic heterogeneity in the sedimentary rocks. Water/rock ratios were not high enough to homogenize these heterogeneities. Sheppard and Schwarcz (1970) found that the carbon and oxygen isotopic compositions of four samples of biotite-zone marbles from South Dorset, Vermont showed more variation across 10 centimeters perpendicular to bedding than in 31 meters parallel to bedding. They concluded that this lack of isotopic equilibrium, in an area where thermal equilibrium was closely attained, was due to the lack of an efficient communicating fluid. Both of these studies demonstrate the need to constrain the isotopic composition and heterogeneity of protolith sediments.

Rye *et al.* (1976) in a study of the regional metamorphic complex at Naxos, Greece found that low-grade marbles had only exchanged oxygen at the margins while some marbles at higher grade had lighter $\delta^{18}\text{O}$ values in the interiors of the units. No large-scale homogenization of the marbles was found, even above the 540°C isograd.

On the other hand, the schist-rich zones at Naxos showed evidence of pervasive exchange with large amount of fluid. This study demonstrates the important role that lithology and its consequent porosity and permeability play in the involvement of fluids in metamorphism, particularly the fact that relatively pure limestone and dolomite units tend to be very impermeable during regional metamorphism.

Extensive studies of granulite-facies metamorphism in the Adirondack Mountains (Valley and O'Neil, 1984; Valley *et al.*, 1990, Taylor, 1969) suggest deep-crustal, fluid-absent metamorphism in carbonate-rich areas, but are controversial regarding aqueous fluid exchange in the plutonic meta-igneous rocks. Taylor (1969) presented evidence for bulk changes in $\delta^{18}\text{O}$ in large volumes of the Adirondack anorthosites and syenites during the extensive series of regional metamorphic events that affected this area, but these effects may have occurred during pre-granulite facies or post-granulite facies metamorphism, rather than during the peak event.

Samples of metasediments in the Adirondacks locally preserve a steep isotopic gradient of 8 per mil over 25 meters, and Valley and O'Neil (1984) believe that this isotopic heterogeneity is pre-metamorphic and that fluid-absent granulite-facies metamorphism has preserved the composition of the protolith. A comparison of granulite-facies carbonates with unmetamorphosed or lower grade limestones showed no major isotopic shifts with metamorphism, again indicative of fluid-absent metamorphism in the relatively pure limestones and dolomites.

Barnett and Chamberlain (1991) in a study of metamorphosed sediments in east-central Vermont concluded that the observed differences in metamorphic grade between anticlines and synclines were due to the higher temperature of formation reached

in the synclines. The differences in metamorphic grade within synclines, however, were attributed to fluid infiltration. The dolomite-out isograd represented the boundary of reaction progress with the fluid and this conclusion was supported by stable isotope data. Fluid flow was apparently limited, as heterogeneities occurred over distances of hundreds of meters. Barnett and Chamberlain (1991) calculated that the amount of fluid necessary for metamorphism could be derived from adjacent pelitic schists and amphibolites. No externally derived fluids were required. They hypothesized that the lack of exotic fluids in this terrane was due to the great depth at which metamorphism occurred (20 km). Similarly, Wickham and Taylor (1987) concluded that infiltrating fluids were largely absent in the deeper zones of metamorphism in the Pyrenees (including the granulite-facies rocks).

1.3.4 Fluid-dominated regional metamorphism

Garlick and Epstein (1967) in a study of 58 metamorphic rocks from New York, Vermont, Connecticut, and Idaho found a trend toward decreasing $\delta^{18}\text{O}$ with increasing metamorphic grade in some areas. Local isotopic homogeneity of particular minerals in adjacent dissimilar rocks was also found in some areas. This led them to conclude that bulk isotopic exchange between the rocks and the coexisting pore fluids had occurred during regional metamorphism. Taylor *et al.* (1963) sampled three mineralogically distinct assemblages from the chloritoid-kyanite zone in central Vermont which were up to 200 meters apart. Within analytic reproducibility the $\delta^{18}\text{O}$ of the quartz from the samples was identical. Taylor *et al.* (1963) therefore conclude that this homogeneity was the result of metamorphism involving the pervasive infiltration of aqueous fluids.

Wickham and Taylor (1985, 1987, 1990) present strong evidence for the large-scale infiltration of marine pore waters during metamorphism in the Trois Seigneurs Massif, Pyrenees, France. Paleozoic samples above the "andalusite in" isograd are lighter in $\delta^{18}\text{O}$ by 2 to 3 per mil and are relatively homogeneous in $\delta^{18}\text{O}$. They argue that metamorphism and anatexis of the metasediments occurred in an extensional tectonic setting at depths of 6 to 12 kilometers. The significance of their work is the recognition that such pervasive deep penetration of surface-derived waters can occur during rift-related regional metamorphism. A major question raised by the work of Wickham and Taylor is how common is this deep pervasive involvement of fluids in metamorphism and why?

Fleck and Criss (1985) found that the whole-rock $\delta^{18}\text{O}$ values of metasediments surrounding the Idaho Batholith decreased with increasing metamorphic grade. They attributed this trend to exchange with fluids which were convectively driven by heat from the cooling batholith. One significant aspect of their work was that they documented this effect up to 50 kilometers from the batholith margin. This requires extensive and pervasive involvement of aqueous fluids.

In a study of pelitic schists from the Waterville Formation in south-central Maine, Ferry (1984) concluded that the biotite isograd delineated the front of a decarbonation reaction moving through the metamorphic terrane, and that this decarbonation reaction was driven by the pervasive infiltration of at least 1 to 2 rock volumes of water and the addition of heat. Decarbonation resulted in the conversion of meta-shales containing 6 to 10 per cent carbonate to carbonate-free pelitic schists. Ferry (1984) proposed that these kinds of decarbonation reactions, in which the formation of

pelitic schists occurs during pervasive infiltration of heated aqueous fluids, may in fact be an important worldwide process during regional metamorphism.

In a companion study of metamorphosed sandstones of the Vassalboro Formation in south-central Maine, Ferry (1988a) found fluid flow to be pervasive at biotite through sillimanite grades. This contrasted with fluid flow in the argillaceous carbonate rocks of the Waterville Formation which was channelized in the biotite and garnet zones. These channels recorded fluid-rock ratios which were 50 to 60 times greater than the surrounding beds. In the sillimanite zone, however, fluid flow was pervasive as in the Vassalboro Formation. These two formations experienced the same metamorphic event.

The important contribution of this work, then, is to demonstrate the effect of lithology on fluid flow during regional metamorphism, particularly the fact that argillaceous marbles undergoing decarbonation can be quite permeable to regional metamorphic pore fluids. Recently, Baumgartner and Ferry (1991) applied their model for coupled fluid flow and devolatilization reactions to the Waterville formation. They found that fluid flow was channelized along and within lithologic layers, that the direction of flow was from low to high temperature within the metamorphic terrane, and that enormous quantities of fluid flowed through all parts of the argillaceous limestone unit.

The amount of open-system fluid-rock $^{18}\text{O}/^{16}\text{O}$ exchange during regional metamorphism is clearly strongly dependent on the permeabilities of the rocks at the time of deformation and metamorphism. There is now considerable agreement that these permeabilities overall tend to decrease at the highest pressures and greatest depths of

metamorphism, which is no great surprise. Another general conclusion that now has wide acceptance among isotope geochemists and metamorphic petrologists is that relatively pure limestones and dolomites undergoing ductile deformation are extremely impermeable to aqueous pore fluids during metamorphism. However, much higher permeabilities may be observed in adjacent interbedded metasedimentary rocks that are more rigid and which undergo brittle fracture rather than ductile flow. Also, "dirty" siliceous and argillaceous limestones and dolomites may have their porosity and permeability markedly increased during the volume changes that accompany large-scale decarbonation reactions. Because the stratified nature of metasedimentary rocks can lead to abrupt lithological and tectonic differences across bedding planes, it is likely that the flow of metamorphic pore fluid is strongly focused along certain stratigraphic horizons that have high fracture permeability. However, metamorphic terranes with large concentrations of cross-cutting veins may also be very permeable.

From the above discussion it is evident that aqueous fluid flow during regional metamorphism is highly variable and has only just begun to be understood. Both the amounts of waters and the timing of the oxygen isotopic exchange are poorly known. It is also important to continue to gather information on the source of the aqueous fluids. Oxygen isotope studies are one of the prime ways of pursuing such studies.

CHAPTER 2

Analytical Methods and Sample Collection

2.1 Analytical methods

2.1.1 Oxygen extraction from bulk silicates

Oxygen was extracted from whole-rock or bulk silicate material and quantitatively converted to carbon dioxide using the same procedure and apparatus described by Solomon (1989). "Bulk silicate" as here defined refers to the non-carbonate fraction of a sedimentary or metasedimentary rock. The method used for the analysis of $\delta^{18}\text{O}$ in bulk silicate samples follows that outlined by Taylor and Epstein (1962a), with the exception that HF is no longer employed. Samples were prepared for oxygen extraction by crushing a representative portion of the rock, 4 to 5 cm diameter, down to <2 mm-sized material, being careful not to lose any of the crushed rock. Most of the analyzed samples are fine- to medium-grained sedimentary rocks, and grain size was generally not a problem in obtaining a representative sample of these rocks. Coarser-grained samples were handled in a special way, utilizing a significantly larger initial rock specimen.

In each extraction procedure, five whole-rock powder separates were weighed to between 20 and 30 mg, and together with a sample of the Caltech Rose Quartz standard material, were each placed into a separate nickel reaction vessel. The whole-rock powders had previously been checked for carbonate content and any carbonate originally present had already been removed by acid treatment (see below). The loading into nickel reaction vessels was carried out after drying for at least 24 hours in a dry-box with zero humidity, maintained by dry P_2O_5 . The reaction vessels were then attached

to the metal portion of a vacuum system, similar to the one described in Taylor and Epstein (1962a).

Before evacuating the reaction vessels, about 1/6 of an atmosphere of F_2 gas was introduced into the metal sections outside the vessels, and heated by torch to react any possible contaminating atmospheric H_2O introduced during the previous procedures. This reacted fluorine was then expelled from the system by reacting it with hot (about $120^\circ C$) KBr pellets, and trapping the resultant Br gas in cold traps. Following this, the system was evacuated to a vacuum of about 10 microns (including the reaction vessels).

Approximately 0.8 atmospheres of F_2 gas were then introduced and sealed into the reaction vessels, and the vessels were heated for at least 12 hours at about $525^\circ C$ by external furnaces. During the 12-hour period, F_2 reacted with each silicate sample to liberate 100% of its oxygen as O_2 . Following reaction, the gases in a single reaction vessel were allowed to expand through several liquid N_2 traps and a heated KBr trap in the metal portion of the vacuum system. This removed the excess F_2 and all condensable gases, leaving only O_2 (and a negligible amount of N_2 contaminant from the original F_2). The resultant O_2 gas was then combusted with a spectrographic-grade, resistance-heated carbon rod to produce CO_2 , which was simultaneously frozen away from the rod by a liquid N_2 trap. To insure that no CO was inadvertently formed during this procedure, an aliquot of fresh O_2 was always introduced into the carbon-rod chamber at the end of the first combustion; this procedure is known to result in complete conversion to CO_2 (Taylor and Epstein, 1962a). After measuring the amount of CO_2 produced in a calibrated Hg manometer, and calculating the yield of oxygen in micromoles per milligram of sample, the gas was further purified by reacting it with hot Hg vapor before

trapping it in a glass sample container for transport to the mass spectrometer.

For the 117 analyzed samples that contained no discernible carbonates, the bulk silicate oxygen also represents the whole-rock oxygen. For the 76 samples that do contain carbonate, as determined by noting effervescence of the powdered sample upon addition of dilute hydrochloric acid, the carbonates were removed prior to the analysis for silicate oxygen. This was done by adding approximately 50 ml of cold dilute hydrochloric acid to one gram of powdered sample for one hour. The sample and dilute acid were then centrifuged for 10 minutes at about 1200 rpm and the supernatant decanted. The sample was then centrifuge-washed twice with distilled water and placed in a 60°C oven to dry. The loss of finer particles in the sample powder was minimized through the use of centrifugation before decanting the supernatant. However, because of this relatively complex procedure, $^{18}\text{O}/^{16}\text{O}$ reproducibility on these kinds of acid-treated bulk silicate samples is probably no better than ± 0.5 per mil.

2.1.2 Carbon and oxygen extraction from carbonates

Carbon dioxide was extracted from carbonate-bearing samples at 25°C using the phosphoric acid dissolution technique of McCrea (1950). This procedure was also performed a total of three times on samples of Harding Iceland Spar, which acted as a standard for the analysis. Results for the standard analyses were identical and did not vary from the Harding Iceland Spar reference gas in the mass spectrometer within analytic error (see below). A fractionation factor of 1.01008 was employed, following Sharma and Clayton (1965). The fractionation factor varies with the composition of the carbonate (*e.g.*, dolomite vs. calcite). However, based on the work of Sharma and Clayton (1965), this is not expected to shift the $\delta^{18}\text{O}$ values more than one per mil. It

was neither desirable nor practical in the broad scope of this work to perform detailed mineralogical analyses of individual carbonate-rich samples.

2.1.3 Mass spectrometer analyses

A McKinney-Nier, 60° sector double-collecting mass spectrometer was employed for isotopic analysis of samples. The standard δ notation is employed as described by

O'Neil (1986):
$$\delta_x = \left(\frac{R_x - R_{std}}{R_{std}} \right) 10^3$$

where $R_x = (^{18}\text{O}/^{16}\text{O})_x$ or $(^{13}\text{C}/^{12}\text{C})_x$ and R_{std} is the appropriate ratio in an arbitrary standard. For oxygen analyses the accepted standard is Standard Mean Ocean Water (SMOW) as defined by Craig (1961). For carbon analyses the standard is PDB, a Cretaceous belemnite, *Belemnitella americana*, from the Peedee formation of South Carolina. For practical purposes carbon dioxide samples were analyzed relative to a working standard, CO₂ from Harding Iceland Spar (HIS), instead of carbon dioxide prepared directly from PDB or SMOW. The fluorinated silicate oxygen analyses were corrected to the SMOW standard using the following equation:

$$\delta^{18}\text{O}(\text{SMOW})_x = \{ \delta^{18}\text{O}(\text{HIS})_x - \delta^{18}\text{O}(\text{HIS})_{rs} \} \{ A \} + B$$

where rs = Rose Quartz standard carbon dioxide measured relative to the HIS standard gas, $A = (1.02162) (1 + \text{Background}/2520)$ and $B = +8.45$. Parameter A contains the fractionation factor between HIS and SMOW (1.02162) and a correction factor for background carbon dioxide signal and for leakage across the sample and standard gas inlet valves. This instrument correction factor was usually around 1.022. A precision of about ± 0.2 was typically obtained for the average sample. Parameter B represents the $\delta^{18}\text{O}$ of the Caltech Rose Quartz standard relative to SMOW. A Rose Quartz standard

was analyzed with virtually every batch of five samples and typically had a value of $\delta^{18}\text{O}$ (HIS)_{rs} = -13.2.

The carbonate analyses were corrected to the appropriate standards using the following equations:

$$\delta^{13}\text{C}(\text{PDB})_x = \delta^{13}\text{C}(\text{HIS})_x \{D\} - \delta^{18}\text{O}(\text{HIS})_x \{E\} + F$$

where $D = (1.0624) (1 + \text{Background}/2520)$ and $E = (0.0334) (1 + \text{Background}/2520)$.

The constant terms in D and E represent corrections for the $^{12}\text{C}^{16}\text{O}^{17}\text{O}$ contribution to the mass 45 beam (Craig, 1957), and the instrument corrections are as before. The value of F is -4.56 which is the $\delta^{13}\text{C}$ of Harding Iceland Spar relative to PDB.

The $\delta^{18}\text{O}$ of carbonates were calculated relative to the SMOW standard in order to facilitate comparison with bulk silicate data. The carbonate data were converted to the SMOW scale using the following correction factors:

$$\delta^{18}\text{O}(\text{SMOW})_x = \delta^{18}\text{O}(\text{HIS})_x \{G\} + \delta^{13}\text{C}(\text{HIS})_x \{H\} + J$$

where $G = (1.02162) (1 + \text{background}/2520)$; $H = (.0094) (1 + \text{background}/2520)$; $J = 11.59$. The first term in G is the fractionation factor between Harding Iceland Spar, the working standard, and SMOW. The second term in G and in H are the standard instrument corrections described above. The first term in H is the correction factor for the $^{13}\text{C}^{16}\text{O}^{17}\text{O}$ contribution to the mass 46 beam (Craig, 1957). The value of J is 11.59 and represents $\{\delta^{18}\text{O}(\text{HIS})_{\text{SMOW}} - a\}$ where a is the fractionation between carbonate and carbon dioxide at 25°C during the phosphoric acid extraction process and is equal to ten per mil (Sharma and Clayton, 1965). Craig's (1957) correction for ^{17}O was not employed in either of the $\delta^{18}\text{O}(\text{SMOW})_x$ equations because its effect on analytical results was negligible.

Laboratory analyses were recorded in three laboratory notebooks which have been left with Dr. Hugh P. Taylor, Jr. at the Division of Geological and Planetary Sciences, California Institute of Technology. Mass spectrometric records kept by the Caltech laboratory are located in the basement of the North Mudd building and are keyed to the laboratory notebooks.

2.2 Sample collection

The objectives in sample collection were to sample across large segments of the mid-Atlantic Appalachian Mountains, the Ouachita Mountains in Oklahoma and Arkansas, and the Colorado Plateau in Utah and Arizona, in order to characterize the oxygen isotopic compositions of terrigenous sedimentary rocks in these three widely separated areas (Figure 1.1). Samples were collected from fresh road cuts throughout the areas of study. The intent was to procure essentially a random sampling of the various kinds of terrigenous sedimentary rocks in the area under study, which would give us a representative set of oxygen isotopic analyses of those rocks.

Sedimentary rocks in the Appalachian Mountains span most of the Paleozoic Era and provide an opportunity to study any isotopic variation that may occur in these geosynclinal environments over a very long time period from about 500 Ma to 200 Ma. A substantial data set was obtained from this area (75 samples). Mesozoic and Paleozoic continental shelf samples from Utah and Arizona (38 samples) and Paleozoic geosynclinal sediments from Oklahoma and Arkansas (14 samples) were collected for comparison with the data from the Appalachian geosyncline. After characterizing the isotopic compositions of the sedimentary rocks of the Central Appalachians, a limited number of new isotopic analyses were also obtained on Northern Appalachian metamorphosed

sedimentary rocks (Figure 1.1); it was hoped that the protoliths of these metamorphic rocks might be similar to the Central Appalachian sedimentary rocks, thereby enabling us to monitor any changes in bulk silicate $\delta^{18}\text{O}$ that occurred during metamorphism.

Samples were collected from three major traverses across the Central Appalachian Mountains: across Pennsylvania; across Maryland, West Virginia, and easternmost Kentucky; and across Virginia and easternmost Tennessee. Locations of all samples were plotted on road maps and on state geologic maps at a scale of 1:250,000. About 90,000 square kilometers of crust were sampled on a relatively dense scale in central Pennsylvania, western Maryland, eastern West Virginia, and the western part of Virginia. In addition, reconnaissance samples were collected from eastern Kentucky, western West Virginia, and eastern Tennessee; their inclusion in this survey effectively doubles the sample area, but at the cost that this wider area is much more poorly characterized isotopically. Most of the analyzed samples were collected by the author. However, a few samples were collected by Dr. Hugh P. Taylor, mainly from Virginia and Tennessee.

Mesozoic and Paleozoic sedimentary rocks were collected by the author from about a 60,000 square kilometer area of the Colorado Plateau spanning much of southern Utah. A few samples from northeastern Utah were collected by Dr. Hugh P. Taylor for comparison purposes. The samples of terrigenous sedimentary rocks from the Ouachita Mountains of western Arkansas and eastern Oklahoma were collected from fresh road cuts by Dr. Hugh P. Taylor.

A number of metasedimentary rocks were collected from west-central Vermont by the author; most of these are from the Lincoln Mountain Quadrangle. Dr. Hugh P.

Taylor collected the metasedimentary rocks from the St. Johnsbury Quadrangle in northeastern Vermont, and also those from New York, Nova Scotia, New Brunswick, and Quebec.

The metasedimentary rocks were collected in a manner similar to that described for the sedimentary rocks, usually from fresh road cuts. In all cases, care was taken to collect samples with a minimum of chemical weathering, as evidenced by examination with a hand lens and the 'ringing' sound resulting from a blow with a geologist's hammer. Sampling from fresh blasted road cuts greatly facilitated this.

2.3 Tabulation of isotopic analyses

Table 2.1 is a complete sample inventory of the 189 samples analyzed in this study, arranged as follows:

- (1) Samples 2-40 are flat-lying, essentially undeformed terrigenous sedimentary rocks, mostly of Permian and Mesozoic age from the Colorado Plateau area of Arizona and Utah; these were deposited in a marine shelf and/or terrestrial environment. The Paleozoic section of the Colorado Plateau lies uncomfortably upon Proterozoic sedimentary rocks or upon the crystalline rocks of the Precambrian craton. Three samples of these Proterozoic sedimentary rocks are also included in this data set (samples 32, 33, and 34).
- (2) Samples 42-58 are moderately folded and deformed terrigenous sedimentary rocks of Paleozoic age, mainly from the Ouachita Mountains of western Arkansas and eastern Oklahoma; these were deposited in a miogeosynclinal environment. This set also includes two essentially undeformed samples from Texas (samples 57 and 58).

- (3) Samples 62-146 are terrigenous sedimentary rocks from the Central Appalachian Mountains of Pennsylvania, West Virginia, Maryland, Virginia, eastern Tennessee and eastern Kentucky. These samples were collected from the Appalachian miogeosyncline, mainly from the strongly folded and deformed Valley and Ridge Province, although a few samples are from the moderately folded Appalachian Plateau Province. This set also includes two samples of low-grade metasedimentary rocks from Maryland, samples 118 and 119.
- (4) Samples 148-186 are from the northern Appalachians of Vermont and New York. The metamorphic grade of these rocks varies from chlorite and biotite grade to staurolite and garnet grade. One sample was analyzed from the sillimanite grade (166).
- (5) Samples 188-207 are a variety of terrigenous sedimentary rocks and low-grade metasedimentary rocks from the northern Appalachians of Quebec, Nova Scotia, and New Brunswick in Canada.

2.4 Guide to sample inventory spread sheet

In the 14-page sample inventory in Table 2.1, each group of samples occupies two sheets of papers, linked by the numbers in the column on the far left-hand side of each page. The pages are organized by geographic area, and the column on the left-hand side of each page contains the sample numbers referred to in all maps, in numerical order from 2 to 207. Column A contains the actual sample reference number marked on the rock specimen; these samples are all described in field notebooks and archived in a set of sample storage cabinets kept by Dr. Hugh P. Taylor at the California Institute of Technology. The sample reference numbers usually contain letters that refer to the state

or province in which the sample was collected (*e.g.*, A-Arizona, U-Utah, Q-Quebec, etc.). Further descriptions of sample localities are given in Columns C and N, and in addition the locations of the samples are shown on maps in Figures 4.1, 5.1, 6.1, and 7.1, each in various chapters of this thesis.

An abbreviated description of each sample's lithology, based on a hand-specimen identification, is given in Column B. Samples are first described according to color and then to a textural description modified from Folk, Andrews, and Lewis (1970); finally, they are classified using a compositional description modified from Pettijohn (1975). The textural description includes a description of the degree of induration, a sorting term, and a grain size term, and these are commonly abbreviated, as indicated on the list given below. The compositional description follows the textural description, and it is separated from the textural description by a colon. The compositional description includes the type of cement, prominent accessory minerals, and the lithologic name. The rock color (*e.g.*, brown, red, etc.) is described first, just before the textural description. In addition, other descriptive terms which do not easily fit into the above categories of color, degree of induration, sorting, grain size, and composition are added between the color description and the textural description (*e.g.*, laminated, mottled).

If a long string of abbreviations is used in column B, then each of these terms is separated by a slash, in the following order: Color/Induration/Sorting/Grain Size: Mineralogy and Cement, Lithologic Name. For example, sample number 20 is a wh/ind/f-lam/si-bi-mg-fg: qc quartz arenite. These abbreviations mean that it is a white, indurated, finely-laminated, silty, bimodal, medium-to-fine-grained, quartz-cemented, quartz sandstone.

The rest of Table 2.1 is largely self-explanatory. Columns D, E, and G give, respectively, the stratigraphic unit from which the sample was collected, the accepted map abbreviation of that unit, and the generally accepted age of that stratigraphic unit. Column F classifies the sample according to depositional environment as described in Chapter 1. Column I gives the metamorphic grade of the metamorphosed samples. Column J gives the measured bulk silicate $\delta^{18}\text{O}$ value, and columns K, L, and M give, respectively, the weight per cent, $\delta^{13}\text{C}$, and $\delta^{18}\text{O}$ of the coexisting carbonate, if any was present in the sample. Column N gives the detailed position of the sample locality based on road distances in miles, keyed to a numbered U.S. or state highway (Rt = Route), a highway intersection (Jct = Junction), or a landmark of some kind (e.g., a town or a mountain).

2.5 Abbreviations used in sample inventory

Color

b	brown
bl	black
dk	dark
g	grey
gn	green
l	light
o	orange
pk	pink
prp	purple
r	red
wh	white
y	yellow

Induration

fr	friable
ind	indurated

General adjectives

h	heavily
mod	moderately
p	poorly
v	very
ml	metalithic

Sorting and Grain Size

bi	bimodal
cg	coarse-grained
cs	cross-stratified
f-lam	finely laminated
fg	fine-grained
lam	laminated
mas	massive
mg	medium-grained
ms	moderately well sorted
mu	muddy
peb	pebbly
ps	poorly sorted
rip-lam	ripple laminated
s	sorted
si	silty
th-lam	thickly laminated
vfg	very fine grained
ws	well sorted

Mineralogy and Cement

bt	biotite
c	cemented
ca	carbonate
cac	carbonate cemented
f	feldspathic
feldsp	feldspathic
fos	fossiliferous
m	micaceous
q	quartz
qc	quartz cemented
qcac	quartz and carbonate cemented
tuff	tuffaceous

Table 2.1 Sample Inventory

	A	B	C	D	E	F	G
1	Sample	Description	Location	Stratigraphic Unit	Abbrev.	Dep. Env.	Stratigraphic Age
2	A1f	l-g/h-ind/mod-ws/cg:qcac, quartz arenite	Virgin Rl. Gorge, AZ	Undifferentiated Dev,Ord,Camb(1)	DOE	Marine Shelf(1)	Dev,Ordovician, Cambrian(1)
3	A1e	Green grey shale	Virgin Rl. Gorge, AZ	Undifferentiated Dev,Ord,Camb(1)	DOE	Marine Shelf(1)	Dev,Ordovician, Cambrian(1)
4	A2	r/mod-w-ind/ws/fg:qc,m, quartz arenite	Virgin Rl. Gorge, AZ	Queantowep SS,Supai Group (2)	PIPs	Eolian/Marine(2)	Permian (2)
5	Sedona	r/w-ind/rp-lam/ws/fg:qc,quartz arenite	Sedona, AZ	Bell Rock Mbr,Schneibly Hill Fm (3,4,5)	PIP	Marine Shelf (3,4)	Lower Permian (3)
6	U1	rp-ind/mod ws/mu-fg:qcac,m,feldsp arenite	ST. George, UT	Kayenta Formation (6)	JTrk	Fluvial (7)	Lower Jurassic (7)
7	U2B	o/ind/ws/fg: qc quartz arenite	Hurricane, UT	Shinarump Mbr,Chinle Formation(8)	Trs	Fluvial (8)	Upper Triassic (7)
8	U3A	b/ind/ws/fg: qc,m, feldsp arenite	Hurricane, UT	Moenkopi Formation	Trm	Fluvial (9,7)	Lower to Middle Triassic (7)
9	U7	b-r,m, fine sandy siltstone	Grafton, UT	Moenkopi Formation	Trm	Fluvial (9,7)	Lower to Middle Triassic (7)
10	U 10	b/ind/ws/fg: qcac, feldsp arenite	Alton, UT	Wahweap Sandstone	Kwa	Fluvial (10)	Upper Cretaceous(10)
11	U14A	g-r/mottled/laminated/shaly calcilutite	Escalante, UT	Carmel Fm, San Rafael Group (11, 7)	Je	Marginal Marine (11, 17)	Middle Jurassic (7)
12	U 16 A	y-r/ind/cs/ws/fg:qc quartz arenite	Escalante Rl., UT	Navajo Sandstone, Glen Canyon Gr	JTrn	Eolian (7)	Lower Jurassic (7)
13	U16 b	y-r/ind/cs/ws/fg:qc quartz arenite	Escalante Rl., UT	Navajo Sandstone, Glen Canyon Gr	JTrn	Eolian (7)	Lower Jurassic (7)
14	U 17	b/ind/ws/fg: qc quartz arenite	Escalante Rl., UT	Navajo Sandstone, Glen Canyon Gr	JTrn	Eolian (7)	Lower Jurassic (7)
15	U 20	o,ind,ws,fg: qc quartz arenite	Henry Mtns., UT	Wingate (12)	Trw	Eolian (12)	U. Triassic/L. Jurassic (7)
16	U 21	b/ind/ws/mg:qcac,m, feldsp arenite	Henry Mtns., UT	Church Rock Mbr, Chinle F. (8)	Trcc	Fluvial (13)	Upper Triassic (13)
17	U22	Dark red shale	Hite, UT	Moenkopi Formation	Trm	Laugustrine (9)	Lower to Middle Triassic (7)
18	U 23 b	Deep red, laminated, silty shale	Hite, UT	Hoskinnini Mbr,L. Moenkopi F.	Trm	Laugustrine (9)	Lower to Middle Triassic (7)
19	U 23 d	l-b to prp/h-ind/ws/fg:qc feldspathic arenite	Hite, UT	Hoskinnini Mbr,L. Moenkopi F.	Trm	Laugustrine (9)	Lower to Middle Triassic (7)
20	U 23 f	w/ind/f-lam/sl-bl-mg-fg: qc quartz arenite	Hite, UT	Organ Rock Tongue Mbr, Cutler F. (3)	Pco	Fluvial/Tidal (3)	L. Permian (3)
21	U 26	o-b/ind/lam/sl-bl-mg-fg:qc quartz arenite	Hite, UT	Organ Rock Tongue Mbr, Cutler F. (3)	Pco	Fluvial/Tidal (3)	L. Permian (3)
22	U 27	pk-b/ind/ws/vfg: qc quartz arenite	Hite, UT	Cedar Mesa SS Mbr, Cutler F. (14)	Pcc	Coastal (14)	L. Permian (7)
23	U 33 A	brown-red micaceous siltstone	Mexican Hat, UT	Cedar Mesa SS Mbr, Cutler F. (14)	Pcc	Coastal (14)	L. Permian (7)
24	U 35	l-b/ind/ws/fg: qc quartz arenite	Mexican Hat, UT	Cedar Mesa SS Mbr, Cutler F. (14)	Pcc	Coastal (14)	L. Permian (7)
25	U 36	l-b/ind/ws/fg: qcac quartz arenite	Mexican Hat, UT	Cedar Mesa SS Mbr, Cutler F. (14)	Pcc	Coastal (14)	L. Permian (7)
26	U 39	y-b/ind/ws/fg: qcac quartz arenite	Mexican Hat, UT	Cedar Mesa SS Mbr, Cutler F. (14)	Pcc	Coastal (14)	L. Permian (7)
27	U 41	r/lam/m shaley calcilutite	Mexican Hat, UT	Holgaito Tongue Mbr, Cutler F.	Pch	Fluvial/Tidal Flat (7)	L. Permian (7)
28	U 42	r/ca/m sandy siltstone	Mexican Hat, UT	Holgaito Tongue Mbr, Cutler F.	Pch	Fluvial/Tidal Flat (7)	L. Permian (7)
29	U 43	o-b/ind/ws/sl-vfg:qcac,m,quartz arenite	Mexican Hat, UT	Holgaito Tongue Mbr, Cutler F.	Pch	Fluvial/Tidal Flat (7)	L. Permian (7)
30							
31	Hu 1	g/r/h-ind/ws/mu-vfg: qcac,bl,tuff arenite	Uinta Basin, UT	Uinta Formation	T3	Fluvial/Laugustrine (15)	Eocene
32	Hu 2	g-r/h-ind/ps/peb-bl-og-fg:qc lithic arkose	Uinta Mts, UT	Uinta Mountain Group	PE	Fluvial (16)	1.65 billion years
33	Hu 3	g-r/h-ind/ws/mg:qc quartz arenite	Uinta Mts, UT	Uinta Mountain Group	PE	Shallow Marine (16)	1.65 billion years
34	Hu 4	g-r/h-ind/th-lam/ws/cg: qc quartz arenite	Uinta Mts, UT	Uinta Mountain Group	PE	Deltaic (16)	1.65 billion years
35	Hu 5	b/ind/ws/mg:qc quartz arenite	Uinta Mts, UT	Weber Sandstone	IP	Eolian (4)	U Penn-L Permian (7)
36	Hu 6	o/lam/ca/sandy siltstone	Uinta Mts, UT	Moenkopi Formation	Tr	Fluvial (9)	Lower to Middle Triassic (7)
37	Hu 7	l-b/ind/cs/ws/fg: qc quartz arenite	Uinta Mts, UT	Navajo Sandstone	JTr	Eolian (7)	Lower Jurassic (7)
38	Hu 8	g/h-ind/mod-ws/peb-mg: qc,m,lithic arenite	Uinta Mts, UT	Morrison Formation	J2	Fluvial/Laugustrine (7,17)	Upper Jurassic (7)
39	Hu 9	l-b/h-ind/ws/fg:qc quartz arenite	Uinta Mts, UT	Dakota Sandstone	K1	Fluvial (7)	Upper Cretaceous (7)
40	Hu 10	gn/lam/fossiliferous shale	Uinta Mts, UT	Mowry Shale	K2	Marine/Deltaic(15)	Lower Cretaceous (7)

Table 2.1 Sample Inventory

	H	I	J	K	L	M	N
1	Sample	Metamorphic Grade	Delta 18 (O)	% carb.	$\delta^{13}C$	$\delta^{18}O$	Notes
2	A1f		15.4	26.2	3.1	27.9	Fresh roadcut halfway through Gorge at prominent contact with overlying red Supai Formation .on I-15
3	A1e		17.9	17.6	1.9	28.1	On I-15; 5 mi NE Site A1, 10 mi S of Black Rock Rd
4	A2		13.7	0.1			7 miles South of Sedona on Rt 179
5	Sedona		15.8				
6	U1		15.2	26.1	-2.4	17.0	I-15 at St. George, upper strata in basalt capped ridge
7	U2B		14.4				5.65 mi N of jct I-15&St. George Blvd on I-15
8	U3A		16.2				8.5 mi N of jct I-15&St. George Blvd on I-15
9	U7		14.2	2.8	-1.3	23.2	18.8 mi E jct 59&9 on HWY 9, near Zion
10	U10		15.9	43.3	0.0	16.3	14.5 mi N of Mt. Carmel Jct. on HWY 89
11	U14A		18.5	69.6	2.8	23.4	8.7 mi E of Escalante on HWY 12
12	U 16 A		13.5				0.6 mi SW of Escalante Riv. on HWY 12
13	U16 b		13.8				250 from U16A, same road cut
14	U 17		12.9				1.9 mi N Escalante River on HWY 12
15	U 20		13.5	0.6	-3.2	21.7	6.8 mi S jct 95&276 on HWY 95
16	U 21		14.8	8.8	-5.7	18.8	10 mi S jct 95&276 on HWY 95
17	U 22		16.7		-4.6		11.6 mi S jct 95&276 on HWY 95
18	U 23 b		16.2	9.5	0.8	28.0	HWY 95; prominent exposure at very large bend in road just west of intersection with Dirty Devil River
19	U 23 d		15.3	13.2	-2.3	24.2	
20	U 23 f		13.0	tr.			
21	U 26		13.9	4.1		31.1	1.1 mi W of CO Riv. on HWY 95
22	U 27		12.9				0.3 mi W of CO Riv. on HWY 95
23	U 33 A		14.3	34.8	-2.9	24.5	2.7 mi S jct 261&95 on HWY 261
24	U 35		13.2	4.5	-0.7	21.0	8.5 mi N jct 261&163 on HWY 261
25	U 36		13.3	17.4	-1.2	22.1	8.3 mi N jct 261&163 on HWY 261
26	U 39		13.4	15.3	0.4	22.9	7.5 mi N jct 261&163 on HWY 261
27	U 41		16.7	58.5	1.3	27.7	6.7 mi N jct 261&163 on HWY 261
28	U 42		15.2	17.2	-0.1	31.0	6.6 mi N jct 261&163 on HWY 261
29	U 43		14.3	36.4	-1.5	20.9	6.5 mi N jct 261&163 on HWY 261
30							
31	Hu 1		14.6	10.7	-2.7	16.4	9.2 mi W of Red Creek on I40
32	Hu 2		12.7				North side of Flamingo Gorge Dam
33	Hu 3		13.7				3.6 mi N of Jct 44&91 on Rt 91
34	Hu 4		13.2				1.9 mi S of Jct w/Rt 191 & 44 on Rt191
35	Hu 5		12.4				17.3 mi S of Jct Rt 191&44 on Rt 191
36	Hu 6		13.2	16.6	-2.4	25.6	24.15 mi S of Jct Rt 191&44 on Rt 191
37	Hu 7		12.3				24.95 mi S of Jct Rt 191&44 on Rt 191
38	Hu 8		20.6	0.8	-2.2	21.8	30.9 mi S of Jct Rt 191&44 on Rt 191
39	Hu 9		14.9				5.5 mi N of Vernal on RT 191
40	Hu 10		20.0				5.3 mi N of Vernal on RT 191

Table 2.1 Sample Inventory

A	B	C	D	E	F	G
Sample	Description	Location	Stratigraphic Unit	Abbrev.	Dep. Env.	Stratigraphic Age
41						
42	black, carbonaceous, pyritic slate	Ouachita Mts, AR	Polk Creek Shale	Umo	Deep Marine	L. Ordovician
43	grey, finely laminated shale	Ouachita Mts, AR	Jackforth Group	LIPj	Deep Marine Fan	Lower PA (Morrowan)
44	g/h-ind/massive/ws.qc quartz arenite	Ouachita Mts, AR	Jackforth Group	LIPj	Deep Marine Fan	Lower PA (Morrowan)
45	g-gr/h-ind/mas/ws/fg.qc, sub-meta-lithic arenite	Ouachita Mts, AR	Jackforth Group	LIPj	Deep Marine Fan	Lower PA (Morrowan)
46	black shale	Ouachita Mts, AR	Stanley Group	Ms	Deep Marine Fan	Mississippian
47						
48	green shale	Ouachita Mts, OK	Jackforth Group	LIPj	Deep Marine Fan	Lower PA (Morrowan)
49	gn/h-ind/mas/ws/fg.qc, m.f, sub-meta-lithic arenite	Ouachita Mts, OK	Jackforth Group	LIPj	Deep Marine Fan	Lower PA (Morrowan)
50	gn/h-ind/mas/ws/fg.qc, meta-lithic quartz arenite	Ouachita Mts, OK	Jackforth Group	LIPj	Deep Marine Fan	Lower PA (Morrowan)
51	black micaceous shale	Ouachita Mts, OK	Stanley Group	Ms	Deep Marine Fan	Mississippian
52	dark grey green shale	Ouachita Mts, OK	Stanley Group	Ms	Deep Marine Fan	Mississippian
53	bl/nt/ws/fg.m quartz arenite	Ouachita Mts, OK	Stanley Group	Ms	Deep Marine Fan	Mississippian
54	gn-b fissile silty shale	Ouachita Mts, OK	Blaylock Sandstone	Op	Submarine Fan Channel	Silurian
55	gn-b/h-ind/ws/si-vfg.qc quartz arenite	Ouachita Mts, OK	Blaylock Sandstone	Op	Submarine Fan Channel	Silurian
56	gn/h-ind/ws/fg.qc, m quartz arenite	Ouachita Mts, OK	Blaylock Sandstone	Op	Submarine Fan Channel	Silurian
57						
58	gn-b micaceous siltstone	Ft. Worth Basin, TX	Strawn Group	IPd	Fluvial-Deltaic	M. Pennsylvanian
59	bl/nd/ws/mu-vfg.qc, m, meta-lithic, f, idsp. arenite	Ft. Worth Basin, TX	Strawn Group	IPd	Fluvial-Deltaic	M. Pennsylvanian
60						

Table 2.1 Sample Inventory

	H	I	J	K	L	M	N
	Sample	Metamorphic Grade	Delta 18 (O)	% carb.	$\delta^{13}C$	$\delta^{18}O$	Notes
41	AR 115	High grade diagenesis	15.9	20.2	0.0	16.8	1.25 mi N of Mt Ida on Rt 270
42	AR 117 A	High grade diagenesis	16.7				2.65 mi S of Jct Rt 71 on Rt 270
43	AR 117 B	High grade diagenesis	15.9				2.65 mi S of Jct Rt 71 on Rt 270
44	AR 118	High grade diagenesis	15.4				0.4 mi S of Jct Rt 71 and Rt 70 on Rt 71
45	AR 119	High grade diagenesis	14.3				0.4 mi N of 2nd Jct Rt 270 & 71 on Rt 71
46							
47							
48	OK 123 A	Chlorite	15.9				5.0 mi S of Big Cedar on Rt 259
49	OK 123 B	Chlorite	14.6				5.0 mi S of Big Cedar on Rt 259
50	OK 123 C	Chlorite	14.3				5 mi S of Big Cedar on Rt 259
51	OK 124	Chlorite	13.7				0.3 mi S of Jct w/ Rt 4 on Rt 259
52	OK 125 A	Chlorite	13.6				52 mi S of Jct w/Rt 4 on Rt 259
53	OK 125 B	Chlorite	13.4				52 mi S of Jct w/Rt 4 on Rt 259
54	OK 126 A	Chlorite	14.2				Summit of Carter Mtn on Rt 259
55	OK 126 B	Chlorite	16.6				Summit of Carter Mtn on Rt 259
56	OK 126 C	Chlorite	16.9				Summit of Carter Mtn on Rt 259
57							
58	TX 150 A		15.7				55 mi W of Ft Worth on I-20
59	TX 150 B		15.8				55 mi W of Ft Worth on I-20
60							

Table 2.1 Sample Inventory

A	B	C	D	E	F	G
Sample	Description	Location	Stratigraphic Unit	Abbrev.	Dep. Env.	Stratigraphic Age
61						
62	g/ind/mod-ws/mg; qc,sub-shaley-chloritic-arenite	Clarion, PA	Pottsville Group	IPp	Fluvial	Lower Pennsylvanian
63	l-g/ind/lam/mod-ws/fg; qcac,metalithic, quartz arenite	Phillipsburg,PA	Mauch Chunk	Mimc	Nearshore Marine	Mississippian
64	dk-olive/h-ind/lam/foe/ws/si-vg; qcac,m,sub-mi arenite	Phillipsburg,PA	Mauch Chunk	Mimc	Nearshore Marine	Mississippian
65	gn/ws/vfg,qc sub-metalithic arenite	Phillipsburg,PA	Mauch Chunk	Mimc	Nearshore Marine	Mississippian
66	gn/h-ind/lam/ws/fg;qcac,metalithic, quartz arenite	Phillipsburg,PA	Mauch Chunk	Mimc	Nearshore Marine	Mississippian
67	r/ind/ws/fg;qc sublithic arenite	Port Matilda,PA	Catskill Formation	Dck	Fluvial	Upper Devonian
68	red siltstone	Port Matilda,PA	Catskill Formation	Dck	Fluvial	Upper Devonian
69	gn/h-ind/ws/vfg,qc,m metalithic arenite	Port Matilda,PA	Catskill Formation	Dck	Shallow Marine	Upper Devonian
70	gn/h-ind/ws/vfg; qc,m metalithic arenite	Port Matilda,PA	Catskill Formation	Dck	Shallow Marine	Upper Devonian
71	g/ind/ws/fg;qc metalithic arenite	State College,PA	Wills Creek Formation	Dskm	Marginal Marine Basin	Devonian Silurian
72	gn,laminated,clayey shale	Mifflintown,PA	Bloomsburg Formation	Dskm	Marginal Marine Basin	Devonian-Silurian
73	black calcareous shale	Thompsonstown,PA	Old Port Formation	Doo	Shallow Marine	Lower Devonian
74	l-gn/ind/lam/ws/vfg; qc,m,ml arenite	Thompsonstown,PA	Old Port Formation	Doo	Shallow Marine	Lower Devonian
75	r/h-ind/lam/ws/vfg; qc,m,f sublithic arenite	Millertown,PA	Duncannon Member	Dcd	Fluvial	Upper Devonian
76	r/h-ind/ws/fg;qc,m,f sublithic arenite	Sunbury,PA	Irish Valley Member	DclV	Fluvial	Upper Devonian
77	green clayey shale	Sellingsgrove,PA	Hamilton Group	Dh	Marine Transitional	Middle Devonian
78	red micaceous shale	Sellingsgrove,PA	Irish Valley Member	DclV	Fluvial	Upper Devonian
79	grey-green, finely laminated micaceous shale	Millersburg,PA	Wills Creek Formation	Dskm	Marginal Marine Basin	Devonian Silurian
80	grey-red,finely laminated, micaceous shale	Millersburg,PA	Hamilton Group	Dh	Marine Transitional	Middle Devonian
81	g/h-ind/ws/mg; qc quartz arenite	Millersburg,PA	Pocono Formation	Mp	Fluvial	Mississippian
82	white/h-ind/mg;qc quartz arenite	McConnellsburg,PA	Tuscarora Formation	St	marine/shell/sand/wave	Lower Silurian
83	g-r/h-ind/ps/peb-mu-fg; qc,m,lithic arenite	McConnellsburg,PA	Juniata/Bald Eagle	Ojbe	Fluvial	U. Ordovician
84	white/r/ws/mg;qc quartz arenite	McConnellsburg,PA	Tuscarora Formation	St	marine/shell/sand/wave	Lower Silurian
85	g-r/h-ind/f-lam/ws/vfg; m sublithic greywacke	McConnellsburg,PA	Juniata/Bald Eagle	Ojbe	Fluvial	U. Ordovician
86	grey-green shale	Mill Creek,PA	Reedsville Formation	Or	Marine basin	Ordovician
87	gn/h-ind/ps/peb-cg;qc lithic arenite	Mill Creek,PA	Bald Eagle Formation	Obe	Fluvial	U. Ordovician
88	g-gn/h-ind/ws/fg,qc,m lithic arenite	Mill Creek,PA	Reedsville Formation	Or	Marine basin	Ordovician
89	g-r/h-ind/ws/fg; m quartz wacke	Mill Creek,PA	Juniata Formation	Oj	Fluvial	U. Ordovician
90	grey-green calcareous shale	Huntington,PA	Wills Creek Formation	Swc	Marginal marine basin	Devonian
91	red siltstone	Bedford,PA	Bloomsburg Formation	Sbm	Marine;platform	Devonian
92	wh/h-ind/ws/mg; qc quartz arenite	Bedford,Pa	Tuscarora Formation	St	marine/shell/sand/wave	Lower Silurian
93	g-r/h-ind/ws/fg; m sublithic greywacke	Everett,PA	Catskill Formation	Dck	Fluvial	Upper Devonian

Table 2.1 Sample Inventory

H	I	J	K	L	M	N
Sample	Metamorphic Grade	Delta 18 (O)	% carb.	$\delta^{13}C$	$\delta^{18}O_c$	Notes
61						
62	Pa 2 a	15.3				2.1 mi W of Jct I-80 & 322 on I-80
63	Pa 5a 1	13.6	12.2	-5.6	18.5	5.9 mi SE of Jct 322 & 53 on Rt 322
64	Pa 5b 3	14.8	3.7	-6.6	21.0	100 ft South of Pa5a1
65	Pa 5b 2	14.5				100 ft South of Pa5a1
66	Pa 5c 2	14.4	24.2	-5.2	19.6	100 ft South of Pa5b2
67	Pa 7a	15.4				9.7 mi SE of Jct 322 and 53 on Rt 322
68	Pa 7f	13.7				200 ft NW of Pa7a
69	Pa 8 a	15.4				10.5 mi SE of Jct 322 & 53 on Rt 322
70	Pa 8 d	15.3				0.2 mi NW of Pa8a
71	Pa 14 b	14.8				0.5 mi NW of Jct 322 & 550 on Rt 322
72	Pa 28 A	14.8				16.9 mi S of Jct 655 & 322 on Rt 322
73	Pa 31 a	16.1	0.8	-5.5	19.7	27.4 mi S of Jct 655 & 322 on Rt 322
74	Pa 31 b	16.2				27.4 mi S of Jct 655 & 322 on Rt 322
75	Pa 32 a	15.3	1.2	-8.9	22.0	36.1 mi S of Jct 655 & 322 on Rt 322
76	Pa 36 b	14.8				13.4 mi S of Jct 15 & 80 on Rt 15
77	Pa 38 b	13.4				22.6 mi S of Jct 15 & 80 on Rt 15
78	Pa 40 a	13.2				23.9 mi S of Jct 655 & 322 on Rt 322
79	Pa 41 c	14.7				35.75 mi S of Jct 655 & 322 on Rt 322
80	Pa 42 a	14.8				36.15 mi S of Jct 655 & 322 on Rt 322
81	Pa 43	14.6				40.5 mi S of Jct 655 & 322 on Rt 322
82	Pa 48 A	15.7				2.6 mi E of Tuscarora Summit
83	Pa 49	14.1				2.1 mi E of Tuscarora Summit
84	Pa 50	13.7				0.6 mi E of Tuscarora Summit
85	Pa 51	14.4				0.5 mi W of Tuscarora Summit
86	Pa 55	15.0				2.4 mi NW of Jct 522 & 22 on Rt 22
87	Pa 55.5	13.6				2.4 mi NW of Jct 522 & 22 on Rt 22
88	Pa 55.8	15.6				2.4 mi NW of Jct 522 & 22 on Rt 22
89	Pa 56	13.9				2.9 mi NW of Jct 522 & 22 on Rt 22
90	Pa 57	15.1	35.2	0.0	23.3	17.5 mi NW of Jct 522 & 22 on Rt 22
91	Pa 60	14.3				1.6 mi E Jct 30 & 220 on HWY 30
92	Pa 61	14.6				2.0 mi E Jct 30 & 220 on HWY 30
93	Pa 63.6	13.7				4.1 mi E of Jct 26 & 30 on HWY 30

Table 2.1 Sample Inventory

	A	B	C	D	E	F	G
	Sample	Description	Location	Stratigraphic Unit	Abbrev.	Dep. Env.	Stratigraphic Age
94							
95	Wva 3	g-r/h-ind/lam/ws/fg: m sublithic greywacke	Keyser, WV	Hampshire Formation	Dhs	Fluvial	Upper Devonian
96	Wva 5	g/h-ind/ws/fg: qc sublithic arenite	Keyser, WV	Mauch Chunk	Mmc	Fluvial	Upper Mississippian
97	Wva 5 a	g/h-ind/ws/fg: qc sublithic arenite	Keyser, WV	Mauch Chunk	Mmc	Fluvial	Upper Mississippian
98	Wva 10	red, micaceous, fine-sandy siltstone	Aurora, WV	Hampshire Formation	Dhs	Fluvial	Upper Devonian
99	WVA 11	r-g/ind/ws/vfg: qc feldsp sublithic arenite	Aurora, WV	Hampshire Formation	Dhs	Fluvial	Upper Devonian
100	WVA 14	g-r/h-ind/ws/vfg: m, f sublithic greywacke	Macomber, WV	Hampshire Formation	Dhs	Fluvial	Upper Devonian
101	WVA 15	gn-b, laminated, micaceous siltstone	Macomber, WV	Mauch Chunk	Mmc	Fluvial	Upper Mississippian
102	WVA 20	gn-gr/h-ind/mod-ws/mg/qcac, m metalithic arenite	Clarksburg, WV	Monongahela Group	IPm	Deltaic	Upper Pennsylvanian
103	WVA 24	o-g/ind/ws/fg: qc lithic quartz arenite	Buckhannon, WV	Pottsville Group	IPPV	Fluvial	Pennsylvanian
104	WVA 26	wh/ind/ws/mg: qc m quartz arenite	Buckhannon, WV	Pottsville Group	IPPV	Fluvial	Pennsylvanian
105	WVA 28 c	gn/h-ind/ws/fg: m sublithic arenite	Elkins, WV	Allegheny Formation	IPa	Deltaic	Pennsylvanian
106	WVA 33 A	dk g-gn, micaceous siltstone	Elkins, WV	Hampshire Formation	Dhs	Deltaic	Upper Devonian
107	WVA 33 B	grey-black micaceous siltstone	Elkins, WV	Hampshire Formation	Dhs	Deltaic	Upper Devonian
108	WVA 33 c	dark grey-green laminated siltstone	Elkins, WV	Hampshire Formation	Dhs	Deltaic	Upper Devonian
109	WVA 35	gn/h-ind/ws/vfg: qc sublithic arenite	Elkins, WV	Mauch Chunk	Mmc	Fluvial	Upper Mississippian
110	WVA 39	olive green, micaceous siltstone	Harmon, WV	Chemung Group	Dch	Marine	Upper Devonian
111	WVA 40	b/ind/ws/fg: qc, m, feldspathic arenite	Harmon, WV	Chemung Group	Dch	Marine	Upper Devonian
112	WVA 41	r/h-ind/lam/ws/fg: qcac quartz arenite	Harmon, WV	Mauch Chunk Group	Mh	Fluvial	Mississippian
113	WVA 46	r/h-ind/ws/vfg: qc quartz arenite	Seneca Rocks, WV	Hampshire Formation	Dhs	Fluvial	Upper Devonian
114	WVA 52	r/h-ind/ws/vfg: qc quartz arenite	Seneca Rocks, WV	?Tuscarora Formation	St	marine/shell/sand/wave	Lower Silurian
115	WVA 64 b	green-grey calcareous shale	Alderson, WV	Bluefield Formation	Mbf	Shallow marine	Mississippian
116	WVA 77 c	gn-g/ind/ws/mg: qc metalithic arenite	Charleston, WV	Kanawha Formation	lpk	Deltaic	Penns/Permian
117							
118	MD 1 A	Phyllite, green, pyrite	Frederick, MD	ijamsville Formation	lf	Eugeosyncline	Late PreCambrian
119	MD 1 B	Phyllite, green	Frederick, MD	ijamsville Formation	lf	Eugeosyncline	Late Pre-Cambrian
120							
121	Md 3 C	gn/h-ind/ws/fg: qc sublithic arenite	Hancock, MD	Chemung Formation	Dch	Marine	Upper Devonian
122	Md 5	red micaceous siltstone	Hancock, MD	Hampshire Formation	Dh	Deltaic	Upper Devonian
123	Md 9 D	olive/h-ind/ws/mg: qc, m lithic arenite	Hancock, MD	Hampshire Formation	Dh	Deltaic	Upper Devonian
124	Md 9 K	olive/h-ind/ws/mg: qc, m lithic arenite	Hancock, MD	Hampshire Formation	Dh	Deltaic	Upper Devonian
125	Md 9 P	olive/h-ind/ws/mg: qc, m lithic arenite	Hancock, MD	Hampshire Formation	Dh	Deltaic	Upper Devonian
126	Md 10	red micaceous siltstone	Hancock, MD	Hampshire Formation	Dh	Deltaic	Upper Devonian
127	Md 15	olive/h-ind/ws/mg: qc, m lithic arenite	Cumberland, MD	Wills Creek Formation	Swc	Marginal marine basin	Devonian
128	Md 22	green shale	Keyser, WV	Harrel Shale		Marine: shallow	Upper Devonian
129							

Table 2.1 Sample Inventory

	H	I	J	K	L	M	N
	Sample	Metamorphic Grade	Delta 18 (O)	% carb.	$\delta^{13}C$	$\delta^{18}O_c$	Notes
94							
95	WVA 3		14.8				2.5 mi W of Jct 93 & 50 on HWY 50
96	WVA 5		15.9				4.5 mi W of Jct 93 & 50 on HWY 50
97	WVA 5 a		15.4				4.5 mi W of Jct 93 & 50 on HWY 50
98	WVA 10		14.8				5.3 mi W of Jct 24 & 50 on HWY 50
99	WVA 11		15.1				5.5 mi W of Jct 24 & 50 on HWY 50
100	WVA 14		15.0				2.5 mi W of Jct 72 & 50 on HWY 50
101	WVA 15		15.0				3.4 mi W of Jct 72 & 50 on HWY 50
102	WVA 20		14.9	6.2	-10.7	17.8	5.65 mi W of Harrison Co. Line on Rt 50
103	WVA 24		14.5				4.65 mi E of Buckhannon Ri. on HWY 33
104	WVA 26		14.4				6.0 mi E of Buckhannon Ri. on HWY 33
105	WVA 28 c		14.7				.25 mi W of Jct 33 & 250.92 on HWY 33
106	WVA 33 A		15.4				6.55 mi E of Jct 33 & 219 on HWY 33
107	WVA 33 B		15.2				6.55 mi E of Jct 33 & 219 on HWY 33
108	WVA 33 c		14.1				6.55 mi E of Jct 33 & 219 on HWY 33
109	WVA 35		15.0				8.55 mi E of Jct 33 & 219 on HWY 33
110	WVA 39		14.7				7.6 mi W of 32 & 33 on HWY 32
111	WVA 40		15.0				7.2 mi W of 32 & 33 on HWY 32
112	WVA 41		15.9	10.4	-5.0	17.9	4.35 mi W of 32 & 33 on HWY 32
113	WVA 46		13.9				5.3 mi W of Jct 28 & 33 on HWY 33
114	WVA 52		15.8				8.65 mi W of Jct 28 & 33 on HWY 33
115	WVA 64 b		17.3	13.4	-0.6	24.0	3.25 mi SW of Jct 12 & 63 on HWY 12
116	WVA 77 c		14.1				0.9 mi SW of Jct I-79 & I-79 on I-79
117							
118	MD 1 A	Chlorite	11.9				1.3 mi E of Jct I-70 & 144 on I-70
119	MD 1 B	Chlorite	13.1				200 ft W of MD1A
120							
121	Md 3 C		16.3				2.45 mi E of Jct 615 & I-70 on I-70
122	Md 5		14.5				0.1 mi E of Jct 144 & 70 on I-70
123	Md 9 D		14.8				0.2 mi E of Allegheny Co. Line on Rt 40
124	Md 9 K		14.6				0.2 mi E of Allegheny Co. Line on Rt 40
125	Md 9 P		14.9				0.2 mi E of Allegheny Co. Line on Rt 40
126	Md 10		13.9	nd			7.2 mi W of Allegheny Co. Line on Rt 40
127	Md 15		15.6	16.5	-2.2	19.4	7.65 mi E of Jct 220 & 40 on Rt 40
128	Md 22		15.0				0.1 mi N of Jct 220 & 135 on HWY 220
129							

Table 2.1 Sample Inventory

A	B	C	D	E	F	G
Sample	Description	Location	Stratigraphic Unit	Abbrev.	Dep. Env.	Stratigraphic Age
130						
131	grey-green, f-lam, micaceous siltstone	Grayson, KY	Lower Breathitt Formation	lPhl	Deltaic	Lower-mid Penns.
132	light green, laminated siltstone	Olive Hill, KY	Borden Formation	Mb	Deltaic	Lower Miss.
133						
134	Before 95T					
135	black, finely laminated, calcareous shale	Kingsport, TN	Sevier Shale	Osv	Deep Marine	Ordovician
136	green calcareous shale	Harrison, TN	Pond Spring F. Chickamauga Supergrp	Ops	Deep Marine	M. Ordovician
137	green siltstone	Harrison, TN	Pond Spring F. Chickamauga Supergrp	Ops	Deep Marine	M. Ordovician
137	blue-green shale	Lookout Mtn., TN	Pennington Formation	Mp	Transitional	U. Mississippian
138	blue-grey, massive, calcilitite	Lookout Mtn., TN	Pennington Formation	Mp	Transitional	U. Mississippian
139						
140	b&wh./nd/th-lam/ws/fg:qc quartz arenite	Gothen, VA	Clinton Formation	Stc	Fluvial	Silurian
141	l-prp/ind/ws/mg:qc quartz arenite	Gothen, VA	Cuyuga Group	Scy	Marine- platform	Silurian
142	black, laminated shale	Gothen, VA	Brallier Formation	Db	Fluvial	Devonian
143	black, finely laminated slate	Milboro, VA	Brallier Formation	Db	Fluvial	Devonian
144	black, thickly laminated shale	Milboro, VA	Brallier Formation	Db	Fluvial	Devonian
145	green, laminated shale	Fincastle, VA	Athens Shale	Oa	Marine	Ordovician
146	green/h-ld/ws/fg: qcac, m metallithic arenite	Fincastle, VA	Athens Shale	Oa	Marine	Ordovician

Table 2.1 Sample Inventory

H	I	J	K	L	M	N
Sample	Metamorphic Grade	Delta 18 (O)	% carb.	$\delta^{13}C$	$\delta^{18}O$	Notes
130		15.7				2.7 mi W of Jct 60 and 7&1 on HWY 60
131		16.3				14.5 mi W of Jct 60 and 7&1 on HWY 60
132						
133						
134	Before 95T	16.6	3.0	-1.7	18.7	Jct Alt Rt 58 and I-88
135	T 102 A	14.7	3.6	-1.2	24.8	Jct I-75 and Rt 11 near Ootlewa, TN
136	T 102 B	16.0	23.8	-1.0	26.8	Jct I-75 and Rt 11 near Ootlewa, TN
137	T 103 A	17.6				from Lookout Mtn, along Hwy 148
138	T 103 B	21.7	92.6	0.6	25.2	from Lookout Mtn, along Hwy 148
139						
140	VA 70	15.1				8.25 mi SE of Goshen on Rt 39
141	VA 76	14.3				2.65 mi SE of Goshen on Rt 39
142	VA 79 a	15.6	11.4			0.3 mi NW of Goshen on Rt 39
143	VA 81 A	13.8				1.1 mi E of Millboro Springs on Rt 39
144	VA 81 B	15.8				1.1 mi E of Millboro Springs on Rt 39
145	VA 87 A	14.5	0.8	-5.0	17.7	1.4 mi N of Fincastle on Rt 220
146	VA 87 B	14.6	5.1	-1.7	18.7	1.4 mi N of Fincastle on Rt 220

Table 2.1 Sample Inventory

A	B	C	D	E	F	G
147	Sample	Location	Stratigraphic Unit	Abbrev.	Dep. Env.	Stratigraphic Age
148	J 7 B	St. Johns. Quad, VT	Waits River Formation	Dwr	Geosyncline	Siluro-Devonian
149	J 4	St. Johns. Quad, VT	Waits River Formation	Dwr	Geosyncline	Siluro-Devonian
150	J 2	St. Johns. Quad, VT	Waits River Formation	Dwr	Geosyncline	Siluro-Devonian
151	J 7 A	St. Johns. Quad, VT	Waits River Formation	Dwr	Geosyncline	Siluro-Devonian
152	J 7 D	St. Johns. Quad, VT	Waits River Formation	Dwr	Geosyncline	Siluro-Devonian
153	J 15	St. Johns. Quad, VT	Waits River Formation	Dwr	Geosyncline	Siluro-Devonian
154	J 22 A	St. Johns. Quad, VT	Waits River Formation	Dwr	Geosyncline	Siluro-Devonian
155	J 22 B	St. Johns. Quad, VT	Waits River Formation	Dwr	Geosyncline	Siluro-Devonian
156	J 3 B	St. Johns. Quad, VT	Waits River Formation	Dwr	Geosyncline	Siluro-Devonian
157	J 3 A	St. Johns. Quad, VT	Waits River Formation	Dwr	Geosyncline	Siluro-Devonian
158	J 5	St. Johns. Quad, VT	Dwr near Dgm	Dwr	Geosyncline	Siluro-Devonian
159	J 6	St. Johns. Quad, VT	Dwr near Dgm	Dwr	Geosyncline	Siluro-Devonian
160	J 6 A	St. Johns. Quad, VT	Dwr near Dgm	Dwr	Geosyncline	Siluro-Devonian
161	J 6 B	St. Johns. Quad, VT	Dwr near Dgm	Dwr	Geosyncline	Siluro-Devonian
162	P 7 A	Plainfield Quad, VT	near Dgm ?		Geosyncline	
163	J 16	St. Johns. Quad, VT	Gile Mtn. Formation	Dgm	Geosyncline	Siluro-Devonian
164	J 8	St. Johns. Quad, VT	Gile Mtn. Formation	Dgm	Geosyncline	Siluro-Devonian
165	J 20	St. Johns. Quad, VT	Gile Mtn. Formation	Dgm	Geosyncline	Siluro-Devonian
166	J 9	St. Johns. Quad, VT	Gile Mtn. Formation	Dgm	Geosyncline	Siluro-Devonian
167	Vt 1 c	Bemington, VT	Monkton Formation	Em	Miogeosyncline	Lower Cambrian
168	Vt 3 d	Arlington, VT	Cheshire Quartzite	Ec	Miogeosyncline	Lower Cambrian
169	Vt 4 D 2	Arlington, VT	Moosalamoo Phyllite	Emo	Eugeosyncline	Lower Cambrian
170	Vt 14	Poultney, VT	St. Catherine's Formation	Esc	Mio-Eugeosyncline	Lower Cambrian
171	Vt 16	Poultney, VT	Pawlett Formation	Opa	Mio-Eugeosyncline	Middle Ordovician
172	Vt 18 a	Rutland, VT	Dunham dolomite	Ed	Miogeosyncline	Lower Cambrian
173	Vt 20 B	Bristol, VT	Dunham dolomite	Ed	Miogeosyncline	Lower Cambrian
174	Vt 24	Lincoln Mt Quad, VT	Cheshire Quartzite	Ec	Miogeosyncline	Lower Cambrian
175	Vt 26 A	Lincoln Mt Quad, VT	Pinnacle Formation	Ep	Eugeosyncline	Cambrian
176	Vt 27	Lincoln Mt Quad, VT	Underhill Formation	Eu	Eugeosyncline	Lower Cambrian
177	Vt 48	Lincoln Mt Quad, VT	Underhill formation	Eug	Eugeosyncline	Lower Cambrian
178	Vt 52	Lincoln Mt Quad, VT	Underhill Formation	Eu	Eugeosyncline	Lower Cambrian
179	Vt 54	Lincoln Mt Quad, VT	Underhill Formation	Eu	Eugeosyncline	Lower Cambrian
180	Vt 55	Lincoln Mt Quad, VT	Underhill Formation	Eu	Eugeosyncline	Lower Cambrian
181	Vt 56	Lincoln Mt Quad, VT	Underhill Formation	Eu	Eugeosyncline	Lower Cambrian
182	Vt 58	Lincoln Mt Quad, VT	Underhill Formation	Eu	Eugeosyncline	Lower Cambrian
183	NY 2 E	Hoosic, NY	Poultney Formation	Op	Eugeosyncline	Lower Cambrian
184	NY 62	Chatham, NY	Elizabethville Formation	OCe	Eugeosyncline	Cambrian-Ordovician
185	NY 67	Kingston, NY	Trenton Grp. Austen Glen F	Oag	Eugeosyncline	Cambrian-Ordovician
186	NY 68	Newburgh, NY	Austen Glen Formation	Oag	Eugeosyncline	Ordovician

Table 2.1 Sample Inventory

	H	I	J	K	L	M	N
	Sample	Metamorphic Grade	Delta 18 (O)	% carb.	$\delta^{13}C$	$\delta^{18}O$	Notes
147							
148	J 7 B	Garnet	16.3				See Map
149	J 4	Staurolite	20.0	48.2	-0.3	20.4	See Map
150	J 2	Garnet	18.2	84.5	-4.9	21.1	See Map
151	J 7 A	Garnet	16.9	12.6	-2.4	15.8	See Map
152	J 7 D	Garnet	15.3	0.7	-4.3	15.6	See Map
153	J 15	Staurolite	17.4	4.4	-4.1	18.8	See Map
154	J 22 A	Garnet	17.1				See Map
155	J 22 B	Garnet	18.7	9.6	-1.3	17.9	See Map
156	J 3 B	Garnet	17.7	8.0	0.6	21.2	See Map
157	J 3 A	Garnet	19.5	8.0	-4.8	19.4	See Map
158	J 5	Garnet	18.5	61.0	-4.8	18.2	See Map
159	J 6	Garnet	18.2	45.4	-2.1	18.3	See Map
160	J 6 A	Garnet	16.0	tr.			See Map
161	J 6 B	Garnet	17.4	51.3	-2.2	18.6	See Map
162	P 7 A	Staurolite or Garnet	18.3	50.6	-2.7	19.6	See Map
163	J 16	Staurolite	13.5				See Map
164	J 8	Garnet	11.8				See Map
165	J 20	Garnet	13.3				See Map
166	J 9	Sillimanite	17.0				See Map
167	Vt 1 c	Biotite	18.1	64.2	-3.4	20.9	1.6 mi N of Jct 7 & 9 on Rt 7N
168	Vt 3 d	Biotite	13.1	tr.			0.8 mi E of Jct 7 & 7A on Rt 7
169	Vt 4 D 2	Biotite	20.5				3.2 mi N of Jct 7 & 7A on Rt 7A
170	Vt 14	Chlorite	13.9				0.9 mi S of Jct 30 & 140 on HWY 30
171	Vt 16	Chlorite	17.9	20.9	-4.4	16.8	2.8 mi N of Jct 30 & 140 on HWY 30
172	Vt 18 a	Biotite	20.4	59.8	0.3	24.0	4.75 mi N of Jct 4 & 7 on HWY 7
173	Vt 20 B	Biotite	21.3	42.9	-0.5	23.5	0.2 mi W of W Jct 116&17E on Rt 17E
174	Vt 24	Biotite	13.2				0.05 mi E of E Jct 116&17E on Rt 17E
175	Vt 26 A	Biotite	13.7				3.8 mi E of E Jct 116&17E on Rt 17E
176	Vt 27	Chloritoid-Kyanite	13.3				7.3 mi E of W Jct 116&17E on Rt 17E
177	Vt 48	Chloritoid-Kyanite	7.1				5.1 mi W of JCT 100&17W on 17W
178	Vt 52	Garnet	12.4	tr.			7.2 mi W of JCT 100&17W on 17W
179	Vt 54	Garnet	12.8				0.1 mi W of VT 52
180	Vt 55	Garnet	14.4	5.3	-8.8	13.2	0.1 mi W of VT 54
181	Vt 56	Chl. Kyanite/ Garnet	11.4				0.05 mi W of VT 54
182	Vt 58	Chl. Kyanite/ Garnet	13.0				6.65 mi W of Jct 17W&100 on 17W
183	NY 2 E	Biotite	13.4				1.45 mi W of Jct 7 & 22 on Rt 7
184	NY 62	Chlorite	14.3				4.3 mi S of Jct 66&90 on Rt 66
185	NY 67	Chlorite	15.8				2.45 mi W of Jct 9W and 199 on Rt 199
186	NY 68	Chlorite	14.4				0.9 mi N of Jct 184 and 9D on Rt 9D

Table 2.1 Sample Inventory

A	B	C	D	E	F	G
Sample	Description	Location	Stratigraphic Unit	Abbrev.	Dep. Env.	Stratigraphic Age
187						
188	black calcilitite w/fossils	Portneuf,Q	Utica Group	76	Miogeosyncline	M-U Ordovician
189	grey shale	Isle d'Orleans ,Q	Cambro-Ord and older seds	57	Eugeosyncline	Camb-Ord and older
190	grey phyllite	N. Dame du Lac,Q	Temiscouata Formation	67	Miogeosyncline	Lower Devonian
191						
192	grn mica-phyllite	Waverly, NS	Meguma Gp:Goldenville F.	EOg	Eugeosyncline	Cambrian
193	green slate	Waverly, NS	Meguma Gp:Goldenville F.	EOg	Eugeosyncline	Cambrian
194	green schist	Waverly, NS	Meguma Group: Halifax F.	EOh	Eugeosyncline	Cambrian-Ordovician
195	green schist	Sackville, NS	Meguma Gp:Goldenville F.	EOg	Eugeosyncline	Cambrian
196	grey phyllite	Sackville, NS	Meguma Group: Halifax F.	EOh	Eugeosyncline	Cambrian-Ordovician
197	grn/lam/m shale phyllite	Annapolis Royal,NS	Meguma Group: Halifax F.	EOh	Eugeosyncline	Cambrian-Ordovician
198						
199	g-grn/lam shale	Edmonston, NB	Metapeda Belt	D1	Eugeosyncline	Devonian
200	grey shale w/calcite veins	Siegas, NB	Cary's Mills Formation	Os1	Miogeosyncline	Ordovician-Silurian
201	grey/lam calcilitite	Perth-Ancover, NB	Cary's Mills Formation	Os1	Miogeosyncline	U Ord-L Silurian
202	g/f-lam shale	Bristol, NB	Cary's Mills Formation	Os1	Miogeosyncline	U Ord-L Silurian
203	g-grn /lam calcilitite w/calcite veins	Bristol, NB	Cary's Mills Formation	Os1	Miogeosyncline	U Ord-L Silurian
204	grey/lam siltstone	Hartland, NB	Cary's Mills Formation	Os1	Miogeosyncline	U Ord-L Silurian
205	green & brown shale	Meductic, NB	Fredericton Belt	O1	Eugeosyncline	Ordovician
206	green phyllite	Kingsclear,NB	Fredericton Belt	S	Eugeosyncline	Silurian
207	g/f-lam shale	Kingsclear,NB	Fredericton Belt	S	Eugeosyncline	Silurian

Table 2.1 Sample Inventory

H	I	J	K	L	M	N
Sample	Metamorphic Grade	Delta 18 (O)	% carb.	$\delta^{13}C$	$\delta^{18}O$	Notes
187	High Grade Diagenesis	20.4	56.2	0.8	23.3	3.0 mi E of Port Neuf on Hwy 138
188	High Grade Diagenesis	14.2	16.9	-2.8	21.3	SE corner St Michel's Isle on Hwy 138
189	High Grade Diagenesis	16.1	2.5	-8.9	18.1	Hwy 185 at Notre Dame du Lac
190						
191						
192	Biotite	12.1				4.9 mi N of Jct 118&102 on Rt 102
193	Biotite	10.8				4.9 mi N of Jct 118&102 on Rt 102
194	Biotite	13.0				6.8 mi N of Jct 118&102 on Rt 102
195	Biotite	12.6				7.25 mi N of Jct 101 and 102 on Rt 101
196	Biotite	13.3				2.25 mi N of Jct 101 and 102 on Rt 101
197	Chlorite	13.7				3.7 mi N of Jct 101 and 10 on RT 101
198						
199	High Grade Diagenesis	14.1				4.5 mi S of Edmunston on Hwy 2
200	High Grade Diagenesis	16.2	13.3	0.3	19.1	23.3 mi S of Edmunston on Hwy 2
201	High Grade Diagenesis	20.7	59.9	-0.6	20.5	4.05 mi N of Jct 109 and 190 on Hwy 2
202	Chlorite	19.9	10.4	0.7	22.0	4.45 mi N of Bridge at St. J. R on Hwy 2
203	Chlorite	19.4	78.3	0.3	21.2	4.45 mi N of bridge at St. J. R on Hwy 2 near Bristol
204	Chlorite	17.7	27.4	0.7	19.6	4.7 mi S of bridge at St. J. R on Hwy 2 near Hartland
205	Chlorite	12.5	nd			1.4 mi S of Meductic on Hwy 2
206	High Grade Diagenesis	12.5	2.2	2.6	9.5	2.0 mi N of Jct Hwy 2 and 3 on Hwy 2
207	High Grade Diagenesis	13.2				2.0 mi N of Jct Hwy 2 and 3 on Hwy 2

CHAPTER 3

**Whole Rock Oxygen Isotopic Ratios in Sedimentary Rocks:
A Review of the Literature****3.1 General overview**

Published whole-rock or bulk silicate oxygen isotope analyses of 240 samples of terrigenous and pelagic sedimentary rocks are compiled in Table 3.1. Limestones, dolomites and cherts are not considered in this compilation. "Bulk silicate $\delta^{18}\text{O}$ " is here defined as the oxygen isotope composition of the non-carbonate fraction of the rock samples, either; (a) measured directly, in the case of samples with little or no carbonate, or for those samples where the carbonate could be readily removed by acid treatment; or (b) by material-balance calculation from analyses of different minerals or size fractions from the rock.

The 240 samples listed in Table 3.1 are categorized by depositional environment, in order to assess the impact of any environment-specific factors on the $\delta^{18}\text{O}$ values of these sedimentary rocks. This compilation is limited essentially to sedimentary rocks that are unmetamorphosed, namely those that have undergone no greater post-depositional alteration than that of high-grade diagenesis. Thus, Table 3.1 includes only the following four categories of samples: (1) those showing no petrographic evidence of metamorphism; (2) those formed at lower grade than the biotite-in isograd; (3) those collected from locations where temperatures of metamorphism are reported to be less than 300°C; and (4) those that have not been subjected to any obvious hydrothermal alteration effects. Sedimentary rocks that are known to have been altered in $\delta^{18}\text{O}$ through interaction with meteoric-hydrothermal systems were specifically not considered. From the available data set, there are 9 analyses of evaporite deposits, 94 analyses of pelagic marine sediments, 57 analyses of non-pelagic marine

sedimentary rocks, 50 analyses of terrestrial and non-marine sedimentary rocks, and 31 other samples either unclassified as to environment of deposition, or whose bulk silicate $\delta^{18}\text{O}$ value could not be accurately calculated.

3.2 Pelagic sediments

Of the three major divisions of depositional environments considered, the pelagic sediments show by far the greatest range in bulk silicate $\delta^{18}\text{O}$ (Figure 3.1). Figure 3.2 shows that for all pelagic sediments there is no significant correlation between bulk silicate $\delta^{18}\text{O}$ and geologic age. For ease of discussion the pelagic sediments have been divided into three compositional groups based on the dominant mineralogy of each sample. While certain of the processes of formation are unique to each group, it must be remembered that the sediments themselves commonly form a continuum of materials that overlap the various compositional groups.

3.2.1 Metalliferous sediments

Metalliferous sediments form from iron and manganese hydroxides which precipitate from hydrothermal plumes at spreading centers. Biogenic silica reacts with the iron oxides to form nontronite. Metalliferous sediments therefore represent a mixing line between iron and manganese hydroxides of varying degrees of crystallinity and nontronite (Dymond *et al.*, 1973).

The metalliferous sediments as a whole have the widest range in $\delta^{18}\text{O}$ of all sediments (Figure 3.3). The lightest sample of the 38 plotted samples is a gelatinous mud containing iron and manganese oxides. Other things being equal, iron-bearing minerals tend to have lower equilibrium $\delta^{18}\text{O}$ values than their magnesium- and aluminum-rich counterparts.

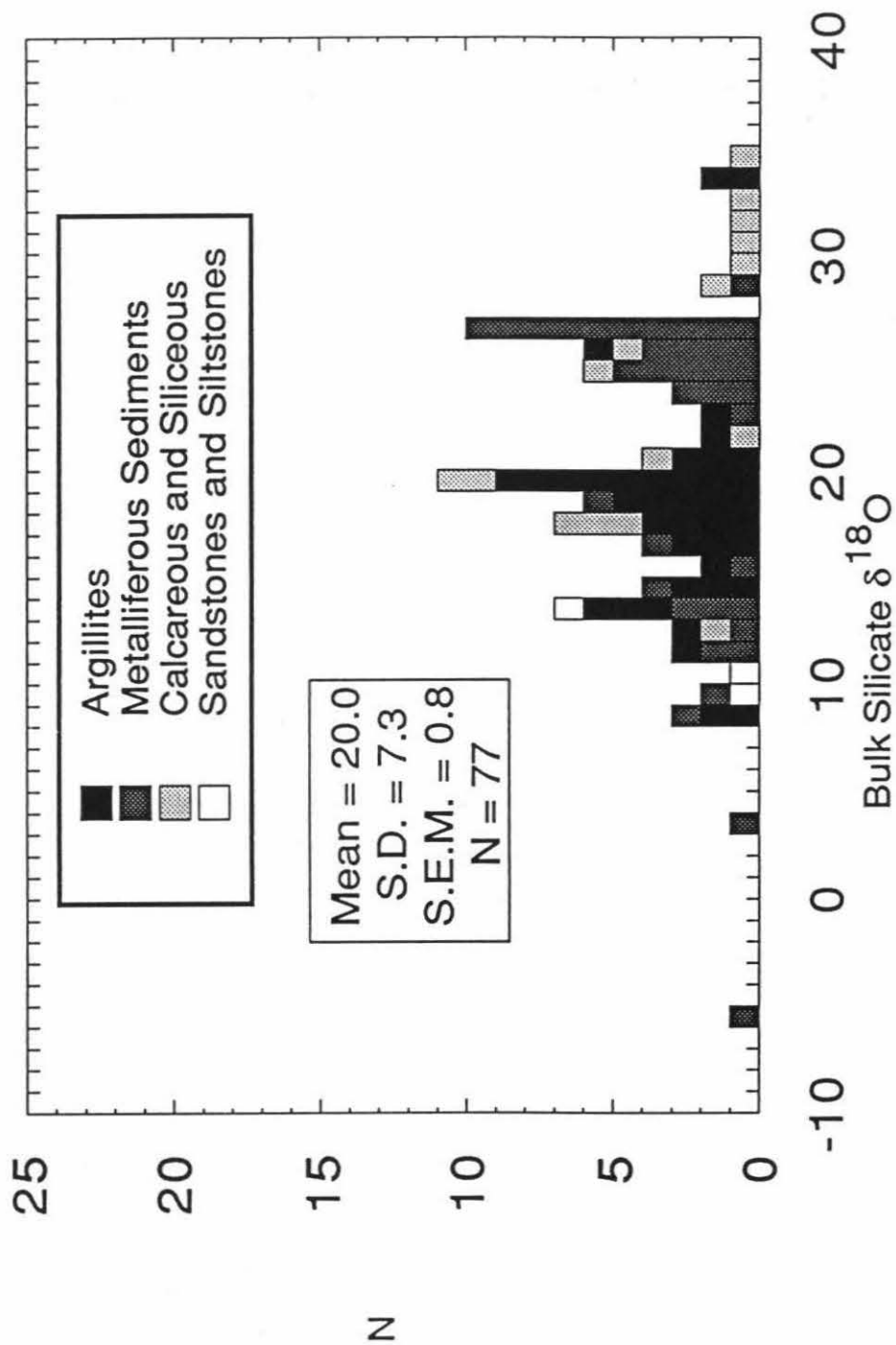
Figure 3.1

Stack histogram showing distribution of bulk silicate $\delta^{18}\text{O}$ values for all pelagic sediments in the literature survey, based on four subdivisions of these rocks, as indicated in the inset. S.D. is standard deviation. S.E.M. is standard deviation of the mean. N is number of samples (Fisher et al., 1970).

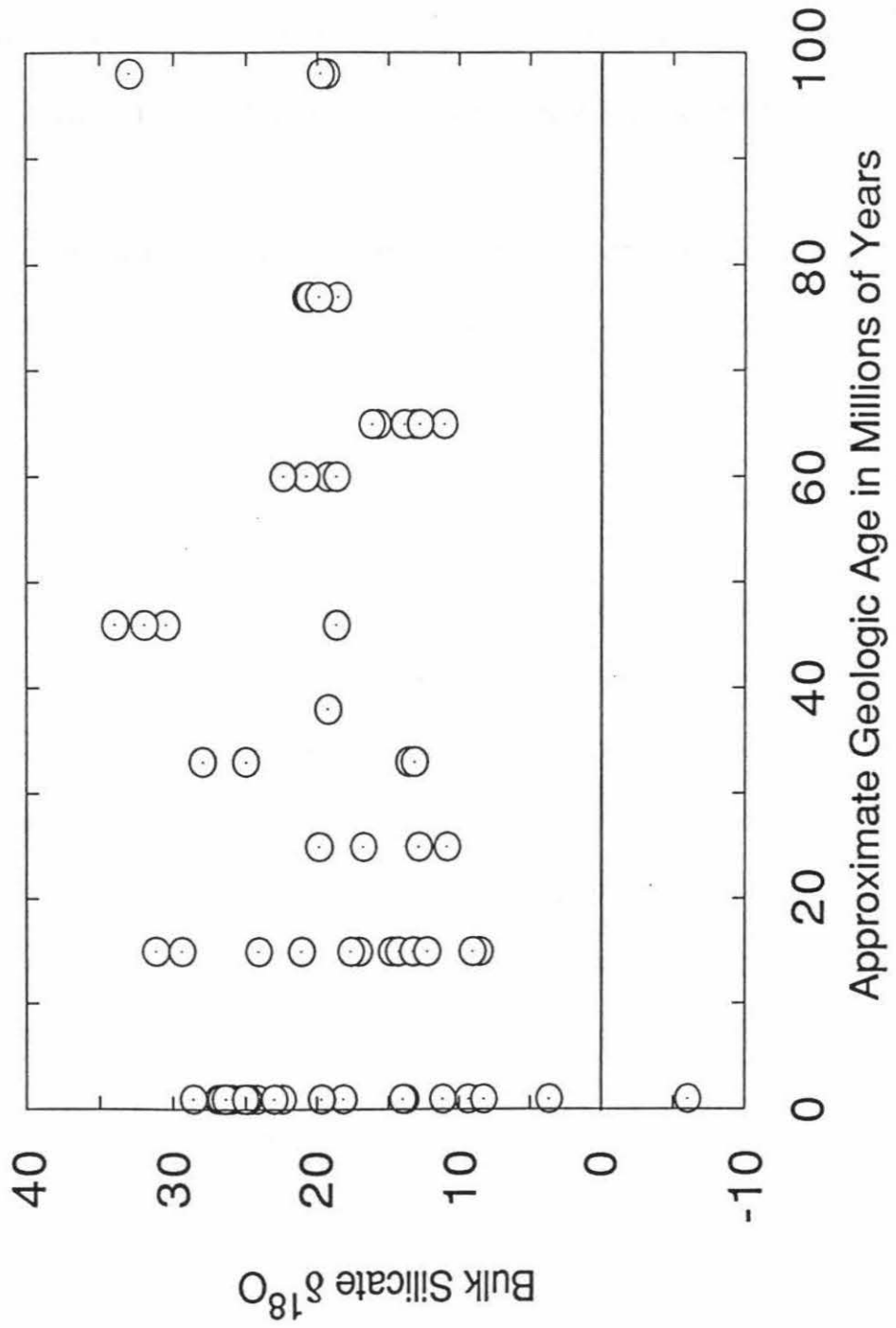
Figure 3.2

Plot of bulk silicate $\delta^{18}\text{O}$ versus geologic age for all pelagic sediments tabulated in the literature survey.

Bulk Silicate $\delta^{18}\text{O}$ Distribution of all Pelagic Sediments



Bulk Silicate $\delta^{18}\text{O}$ vs Age: All Pelagic Sediments



Thus, the metal-oxide $^{18}\text{O}/^{16}\text{O}$ fractionation factor and the lack of crystallinity both probably contribute to the unusually low $\delta^{18}\text{O}$ of -6 in this sample. The heaviest sample is a Galapagos Mound granular nontronite with a $\delta^{18}\text{O}$ of $+28.6$ which is interpreted to have formed at the relatively low temperature of 9°C .

Figure 3.4 is a plot of bulk silicate $\delta^{18}\text{O}$ for metalliferous sediments as a function of geologic age. The Pleistocene sediments show a much greater range in bulk silicate $\delta^{18}\text{O}$ (from -6 to $+28.6$) than do the Cretaceous-Tertiary sediments ($+11.1$ to $+16.2$). While the number of Cretaceous-Tertiary samples is much smaller, the observed dramatic decrease in the range of bulk silicate $\delta^{18}\text{O}$ from about 35 per mil to about 5 per mil over 65 million years suggests that diagenetic processes perhaps can be responsible for large changes in bulk silicate oxygen isotopic compositions of metalliferous samples with time. More data are needed, however, to quantify this hypothesis.

Bulk silicate $\delta^{18}\text{O}$ values for the 38 metalliferous sediments are plotted against depth below the sediment surface in Figure 3.5. The wide range in $\delta^{18}\text{O}$ for the sediments as a whole is apparent. Three general groupings of $\delta^{18}\text{O}$ can be distinguished: the iron and manganese oxides, the nontronites, and the smectite-metal oxide mixtures. Many of the differences in $\delta^{18}\text{O}$ among the metalliferous sediments can be attributed to differences between the equilibrium oxygen isotopic fractionation factors for iron and manganese oxides as compared to the fractionation factors for various kinds of nontronite. Using a smectite isotopic geothermometer, Barrett *et al.* (1983, 1988) calculated the formation temperatures for Galapagos Mounds nontronites. Most nontronites formed at temperatures below 36°C . One exception was a granular nontronite that gave a formation temperature of 137°C . Dymond *et al.* (1973) showed that metalliferous sediments that were high in iron and manganese oxides had $\delta^{18}\text{O}$ values

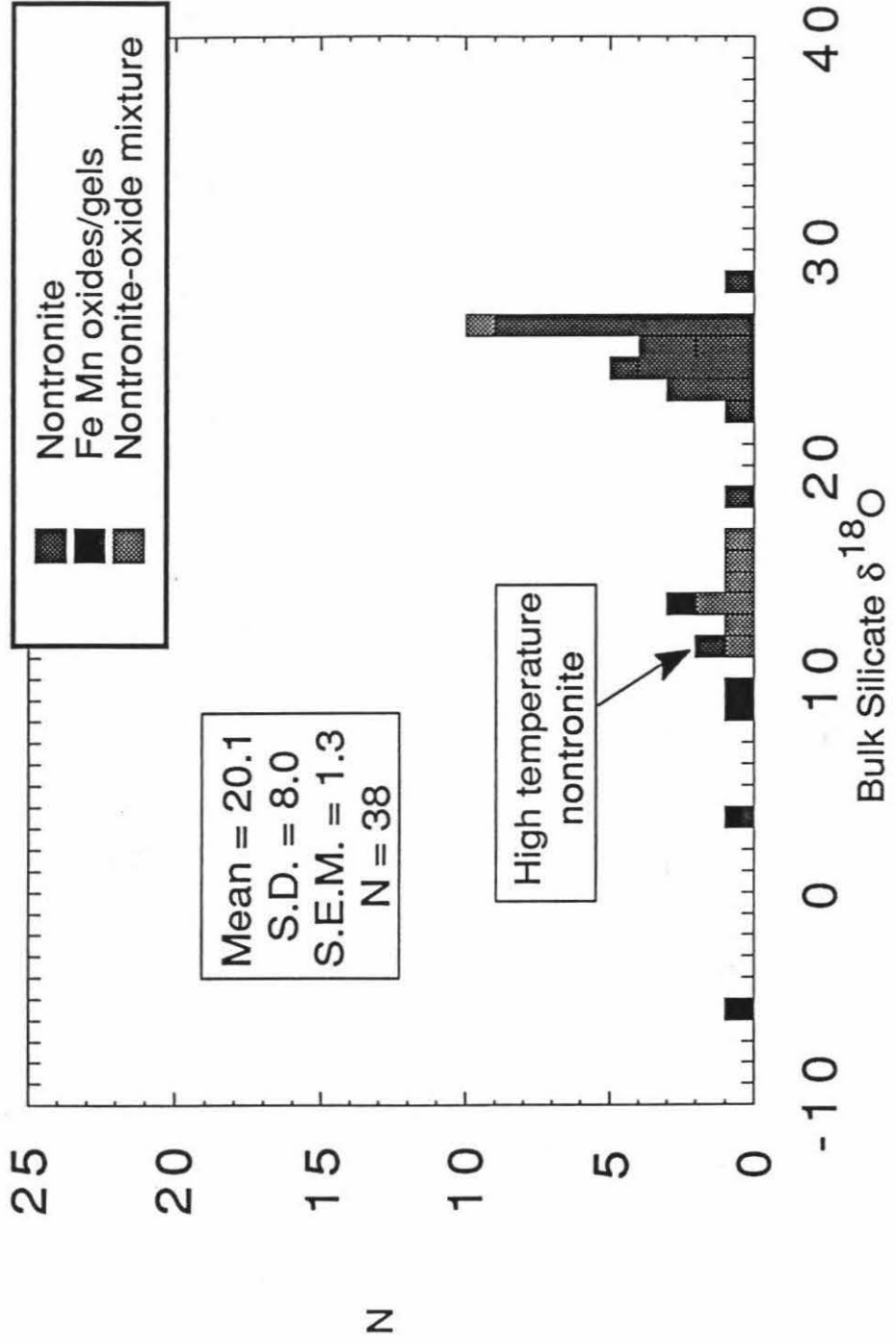
Figure 3.3

Stack histogram showing bulk silicate $\delta^{18}\text{O}$ values of all metalliferous sediments in the literature survey, subdivided into three groups as indicated on the inset. The high temperature nontronite is a special sample discussed in the text.

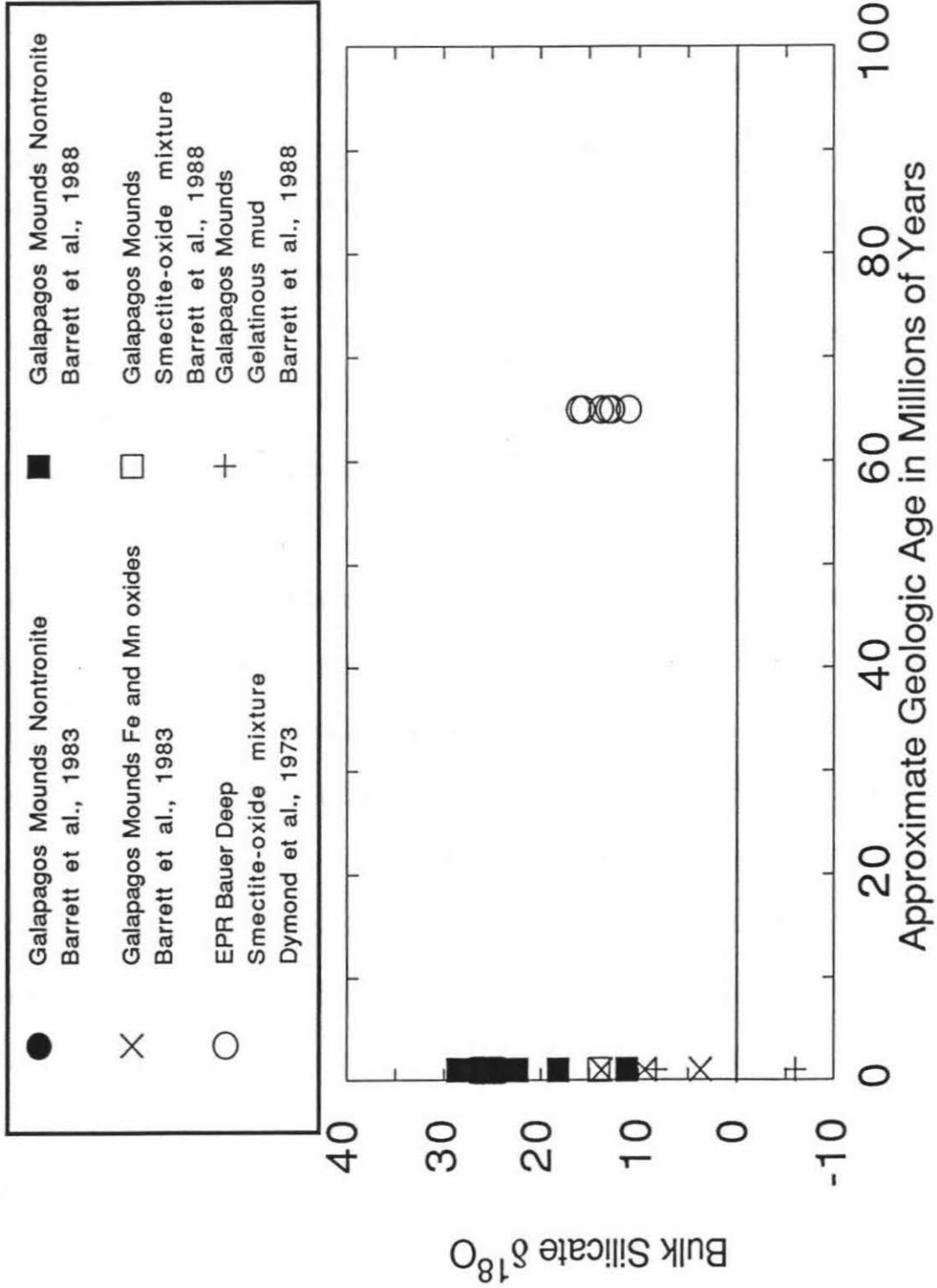
Figure 3.4

Plot of bulk silicate $\delta^{18}\text{O}$ vs. geologic age for all metalliferous sediments in the literature survey.

Bulk Silicate $\delta^{18}\text{O}$ Distribution Metalliferous Sediments



Bulk Silicate $\delta^{18}\text{O}$ vs Age: Metalliferous Sediments



similar to those of manganese nodules which presumably formed at low temperature on the ocean floor. It can be seen from Figure 3.5 that there are no significant changes in $\delta^{18}\text{O}$ with depth within each of the three compositional groupings of metalliferous sediments. The one distinction that can be made in the Galapagos Mounds is that iron and manganese crusts and gelatinous muds are not present below 5 meters. This is presumably because they have all reacted with silica to form nontronite.

3.2.2 Siliceous and calcareous sediments

Oxygen isotopic data for the non-carbonate portion of 17 silica and carbonate-bearing pelagic sediments are shown in Figures 3.6 and 3.7. The highest- ^{18}O sediments are from the Venezuela Basin, DSDP Site 149 (Lawrence, 1973). The older sediments are enriched in $\delta^{18}\text{O}$, most likely as a result of increased silica content. This siliceous material (chert?) formed as an alteration product of volcanic ash and also as a result of recrystallization of biogenic silica. Another factor that causes $\delta^{18}\text{O}$ to increase with age in these sediments is the increasing ratio of biogenic silica to detrital or terrigenous material with depth. The detrital silicates in general have a much lower $\delta^{18}\text{O}$ than biogenic marine silica.

The other data points in Figures 3.6 and 3.7 are from DSDP Sites 322 and 323 in the Bellinghausen Abyssal Plain (BAP) and from Site 325 in the Central Continental Rise in the southeastern Pacific Ocean on the Antarctic Plate (Anderson and Lawrence, 1976; Lawrence *et al.*, 1979). There is no clear-cut trend of $\delta^{18}\text{O}$ in these samples with age. At about 400 to 500 m depth at Site 323 there is a silica-indurated zone caused by solution and reprecipitation of silica. This zone corresponds to a peak in the bulk silicate $\delta^{18}\text{O}$ values, and is preceded in the directly overlying part of the stratigraphic column by a $\delta^{18}\text{O}$ minimum. This suggests that silica from upper zones is mobilized and deposited in lower units. The amount of silica deposition

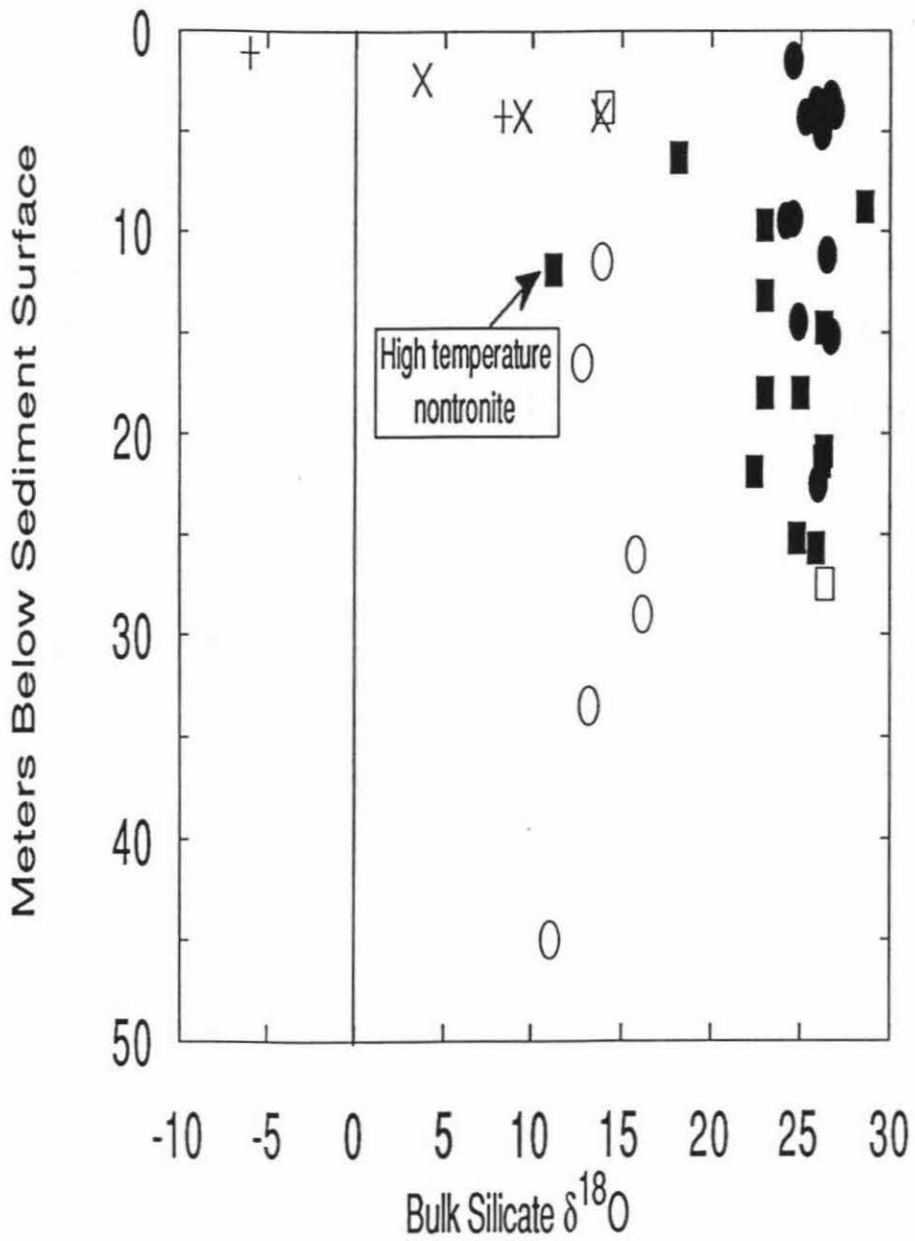
Figure 3.5

Plot of bulk silicate $\delta^{18}\text{O}$ vs. depth below sediment-ocean interface for all metalliferous sediments from the literature survey. Filled ovals and filled rectangles are nontronites from Barrett *et. al.* (1983) and Barrett *et. al.* (1988), respectively. Unfilled ovals are smectite-oxide mixtures from Dymond *et. al.* (1973) and unfilled rectangles are smectite-oxide mixtures from Barrett *et. al.* (1988). Crosses are iron and manganese oxides from Barrett *et. al.* (1983) and pluses are gelatinous mud from Barrett *et. al.* (1983). A high temperature nontronite from Barrett *et. al.* (1983) has an unusually low bulk silicate $\delta^{18}\text{O}$ compared to the other nontronites. Most nontronites have high bulk silicate $\delta^{18}\text{O}$ while gelatinous muds and oxides tend to be low. Smectite-oxide mixtures typically show intermediate $\delta^{18}\text{O}$ values.

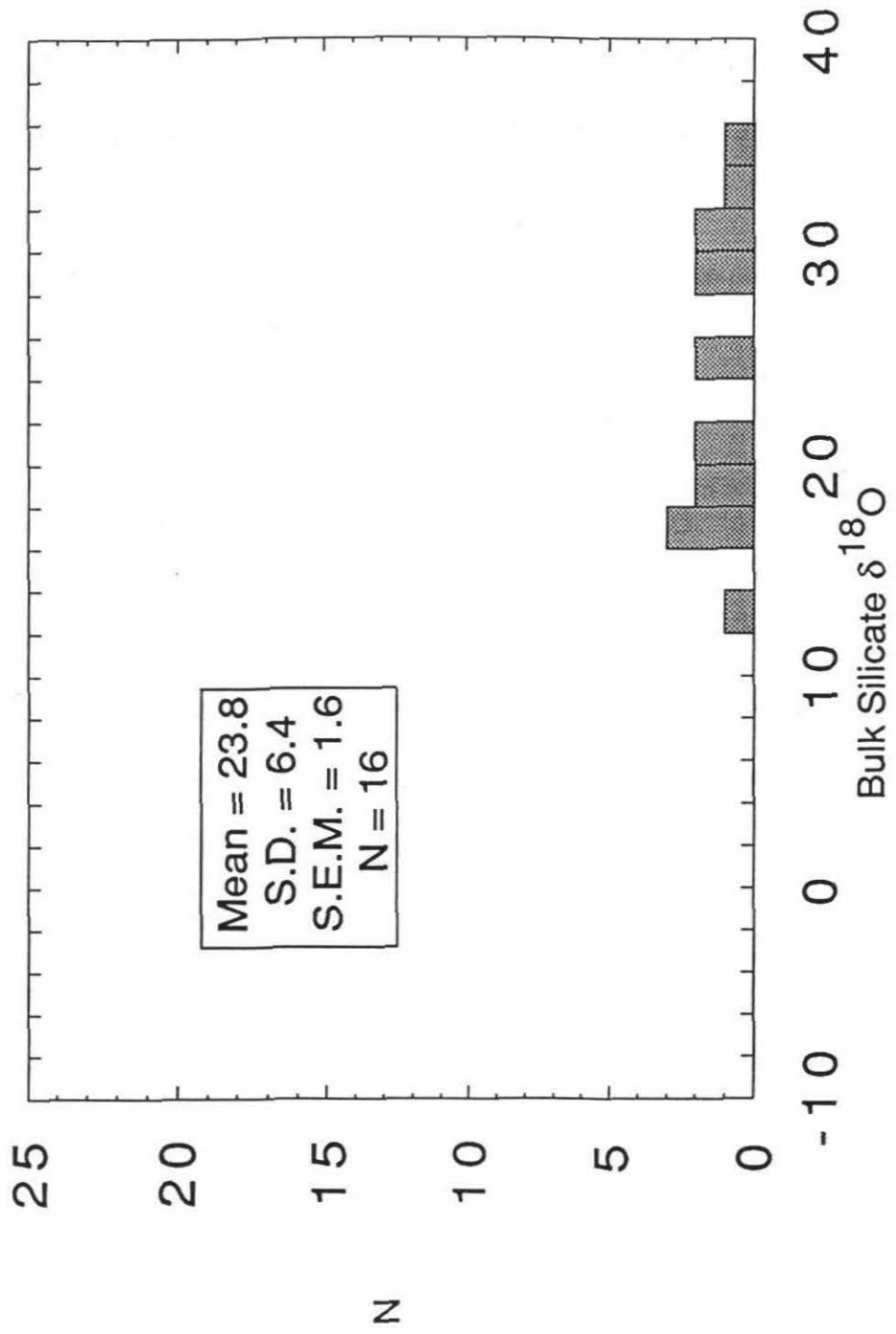
Figure 3.6

Histogram showing distribution of bulk silicate $\delta^{18}\text{O}$ values for siliceous and calcareous pelagic sediments from the literature review.

Depth vs $\delta^{18}\text{O}$ for all Metalliferous Sediments



Bulk Silicate $\delta^{18}\text{O}$ Distribution of all Siliceous and Calcareous Sediments



peaks at about 400 m and then decreases with depth to 500 m. The general trend is the removal of biogenic silica from the upper sediments, leaving behind lower- $\delta^{18}\text{O}$ detrital materials, and the deposition of silica as chert deeper in the stratigraphic column.

Two similarities between the Antarctic samples and the Venezuela Basin samples are the predominance of altered volcanic material at the base of the stratigraphic column and the predominance of detrital materials in the upper parts of the sediment column. Solution and reprecipitation of silica appear to play an important role in the increase in $\delta^{18}\text{O}$ with depth in both areas. In the Antarctic, this increase in $\delta^{18}\text{O}$ is followed by a decrease due to progressively lower rates of silica precipitation with depth.

Summing up, silica- and carbonate-bearing pelagic sediments range in $\delta^{18}\text{O}$ from +12.3 to +34.0. The highest- $\delta^{18}\text{O}$ sediments are from the Venezuela Basin and contain chert which formed as an alteration product of volcanic ash and recrystallization of biogenic silica. The lowest- $\delta^{18}\text{O}$ sediments are from just above a silica-indurated zone in the Antarctic Ocean; these represent a zone of biogenic silica removal through dissolution by pore waters, leaving behind lower- $\delta^{18}\text{O}$ terrigenous sediments. There is a positive correlation of bulk silicate $\delta^{18}\text{O}$ with approximate geologic age for the siliceous and calcareous sediments ($r = 0.71$). This correlation is significant at the 0.01 probability level.

3.2.3 Argillites, sandstones, and siltstones

Bulk silicate $\delta^{18}\text{O}$ analyses are reported for one sandstone and one clayey siltstone from the Bellinghausen Abyssal Plain (BAP). The $\delta^{18}\text{O}$ values of +10.9 and +13.3 respectively, imply that these sediments are probably mainly composed of terrigenous material (Anderson and Lawrence, 1976) These $\delta^{18}\text{O}$ values are within the range of those reported for marine sandstones and shales (see below).

Bulk silicate oxygen isotopic analyses of 37 pelagic argillites are shown in Figure 3.8. These sediments range in $\delta^{18}\text{O}$ from +8.6 to +33.0. The frequency distribution shows a peak around $\delta^{18}\text{O} = +20$. The two lowest $\delta^{18}\text{O}$ values are from the Central Continental Rise (CCR) off the coast of Antarctica. The bulk silicate $\delta^{18}\text{O}$ of these two argillites may be depressed because the terrigenous clays in these argillites originally formed in the presence of isotopically light meteoric waters. The two highest $\delta^{18}\text{O}$ values are for sediments that consist of a large percentage of altered volcanic material. It would be expected that argillites containing predominantly authigenic clay versus terrigenous clay would be significantly richer in $\delta^{18}\text{O}$ (Savin and Epstein, 1970a).

Figure 3.9 shows the relationship of bulk silicate $\delta^{18}\text{O}$ to approximate geologic age for argillites from the BAP and CCR in the southeastern Pacific. The correlation is significant at the 0.01 probability level. The trend toward heavier $\delta^{18}\text{O}$ values with increasing age is largely explained by the predominance of altered volcanic materials in the older sediments and of terrigenous material in the younger sediments. Also, the advection of seawater through the basal sediments could have contributed to the $\delta^{18}\text{O}$ gradient within the altered volcanic materials.

3.2.4 Summary

Pelagic sediments show a wide range in oxygen isotope compositions. This can be attributed to the diversity of materials in the sediments and to the diversity of diagenetic processes operating on them, but mainly to the fact that authigenic and biogenic materials deposited from ocean waters at very low temperatures tend to be extremely ^{18}O -rich. Processes which have a large effect on whole-rock $\delta^{18}\text{O}$ are: formation and transport of low- $\delta^{18}\text{O}$ iron and manganese oxides by hydrothermal fluids at spreading centers; formation of high- $\delta^{18}\text{O}$ authigenic clay minerals; solution, transport, and re-precipitation of silica as a high- $\delta^{18}\text{O}$ phase;

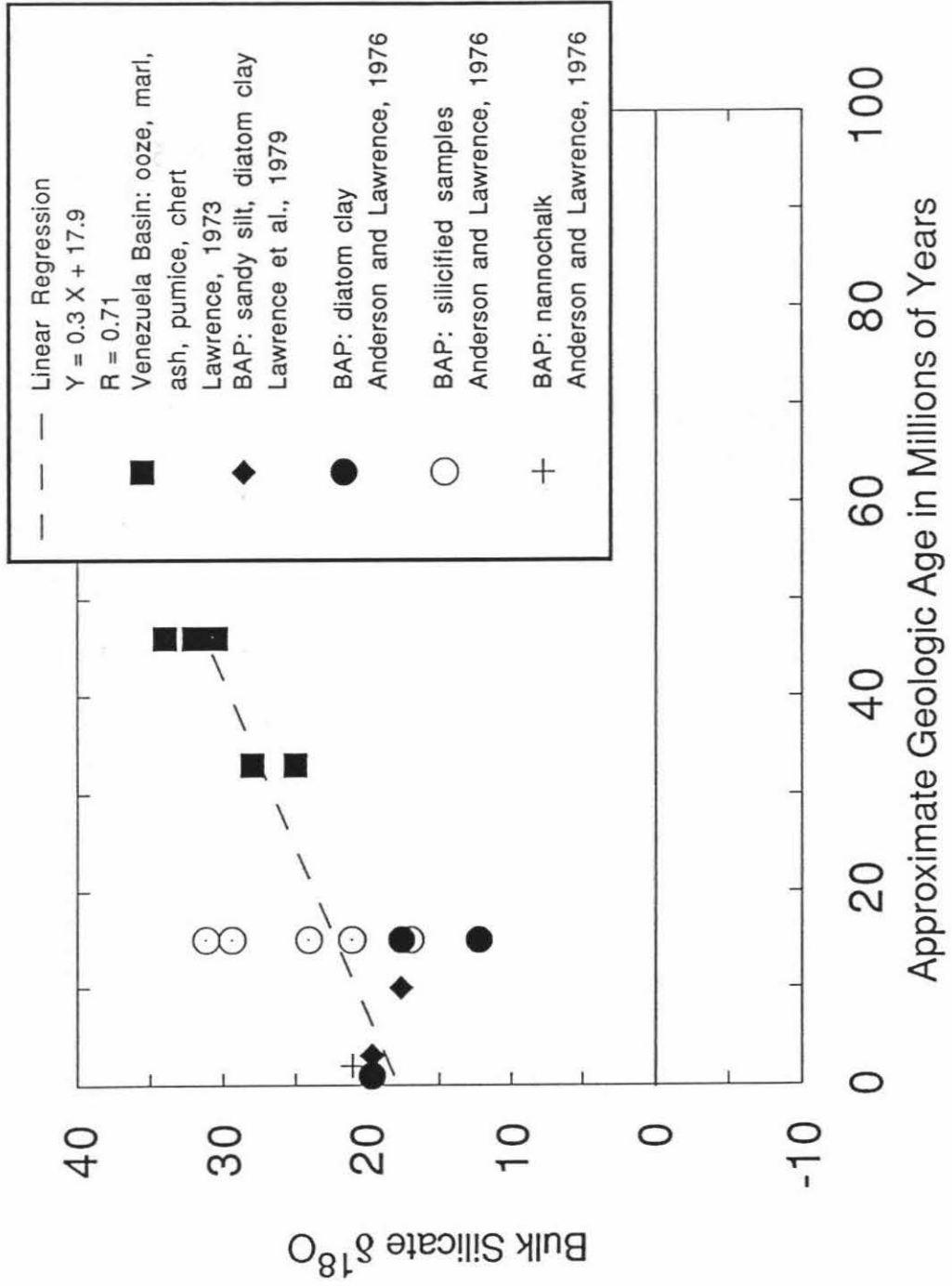
Figure 3.7

Plot of bulk silicate $\delta^{18}\text{O}$ against age for siliceous and calcareous pelagic sediments from the literature review. Simple linear regression calculated according to Fisher et al. (1970). R is the correlation coefficient.

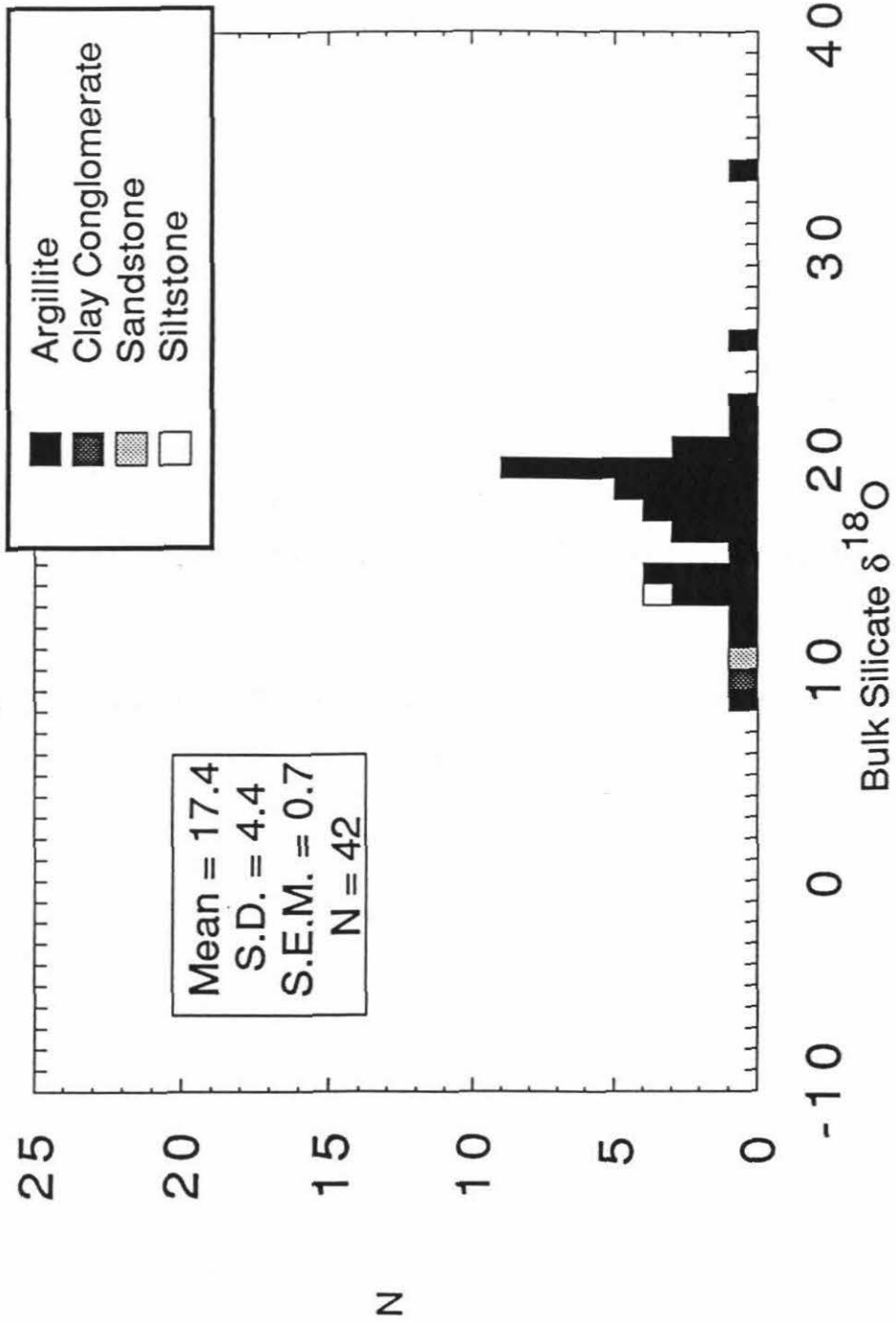
Figure 3.8

Histogram showing bulk silicate $\delta^{18}\text{O}$ distribution for 39 argillites, a sandstone, a siltstone, and a clay conglomerate from the pelagic suite of rocks in the literature review.

Bulk Silicate $\delta^{18}\text{O}$ vs Age: Siliceous and Calcareous Sediments



Bulk Silicate $\delta^{18}\text{O}$ Distribution Pelagic argillites, sandstone, siltstone, and clay conglomerate



the addition of relatively low- ^{18}O volcanic and terrigenous materials; and the addition of very high- ^{18}O biogenic carbonate and silica.

Argillites and the bulk silicate fraction of siliceous and calcareous sediments show a significant correlation of $\delta^{18}\text{O}$ with geologic age. The oxygen isotopic compositions of metalliferous sediments may become more homogeneous with age as a result of diagenesis. More data, however, is needed to support this hypothesis. One conclusion that is clear from this survey is that there is no one $\delta^{18}\text{O}$ value that can be used to adequately represent pelagic sediments as a whole.

3.3 Terrigenous sedimentary rocks

3.3.1 Marine samples

Published data on the bulk silicate oxygen isotopic compositions of marine terrigenous sedimentary rocks form a distinctly bimodal population (Figure 3.10). This bimodality is due to the shale distribution; the shales show one local maximum at about $\delta^{18}\text{O} = +18$ and another at around $+13$. No correlation is found for bulk silicate $\delta^{18}\text{O}$ of marine terrigenous sedimentary rocks with geologic age.

The bulk silicate $\delta^{18}\text{O}$ values of marine shales are the result of a complex interplay of factors. In a study by Yeh and Savin (1977) on Lower Miocene and Upper Oligocene argillaceous sediments from the Gulf Coast of the United States, the high bulk silicate $\delta^{18}\text{O}$ of $+18$ to $+20$ can be attributed largely to the original isotopic composition of sediment deposited from the Mississippi River drainage systems. In Eslinger and Savin's (1973) study of diagenetic burial metamorphism of the very thick section of sedimentary rocks from the Precambrian Belt Supergroup in Montana, the whole-rock $\delta^{18}\text{O}$ values appear to have undergone sizeable ^{18}O -shifts after deposition, as a result of diagenetic factors. This inference is based on the

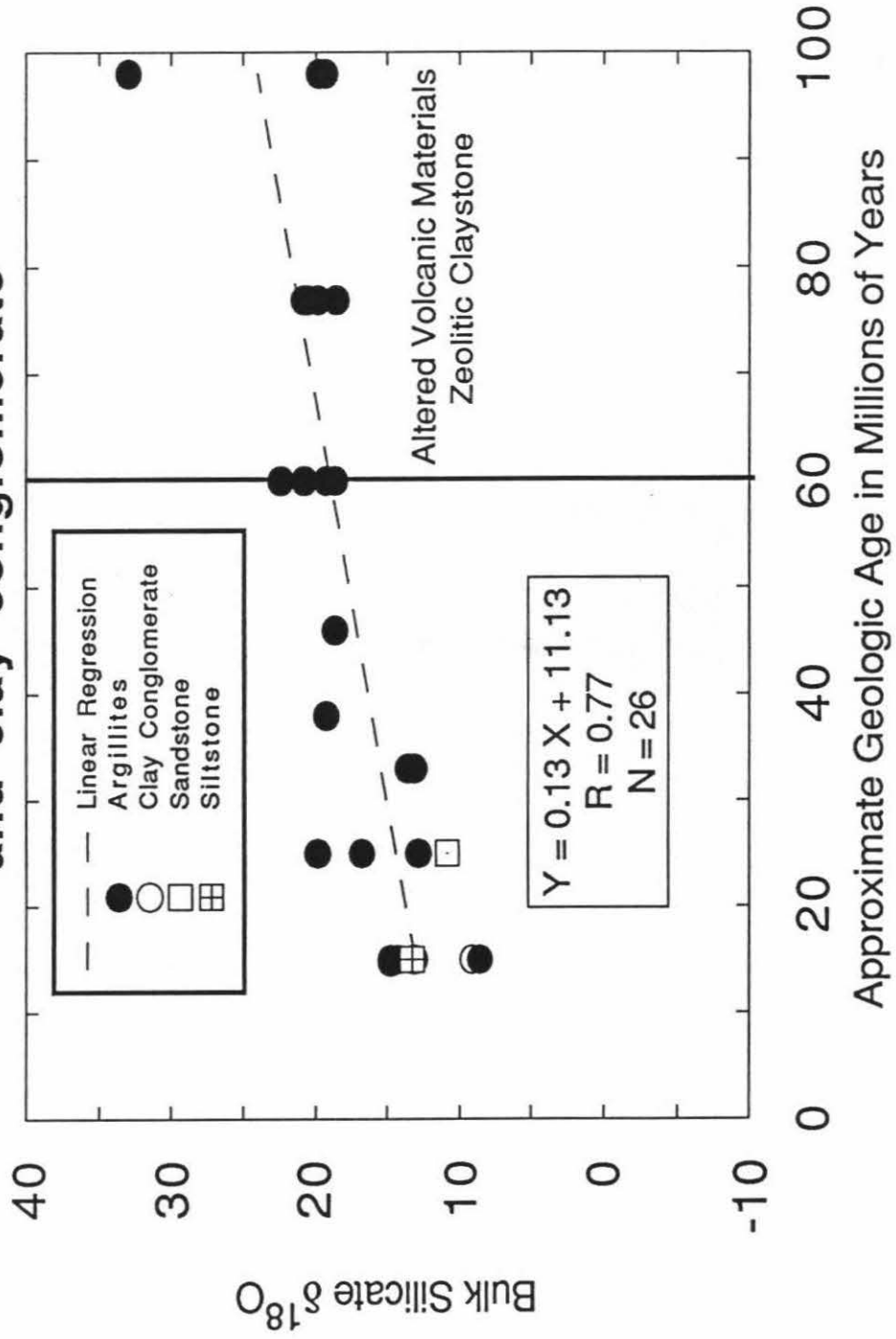
Figure 3.9

Bulk silicate $\delta^{18}\text{O}$ versus geologic age for pelagic argillites, a sandstone, a siltstone, and a clay conglomerate from the literature review. A simple linear regression was calculated for these data points (Fisher *et al.*, 1970).

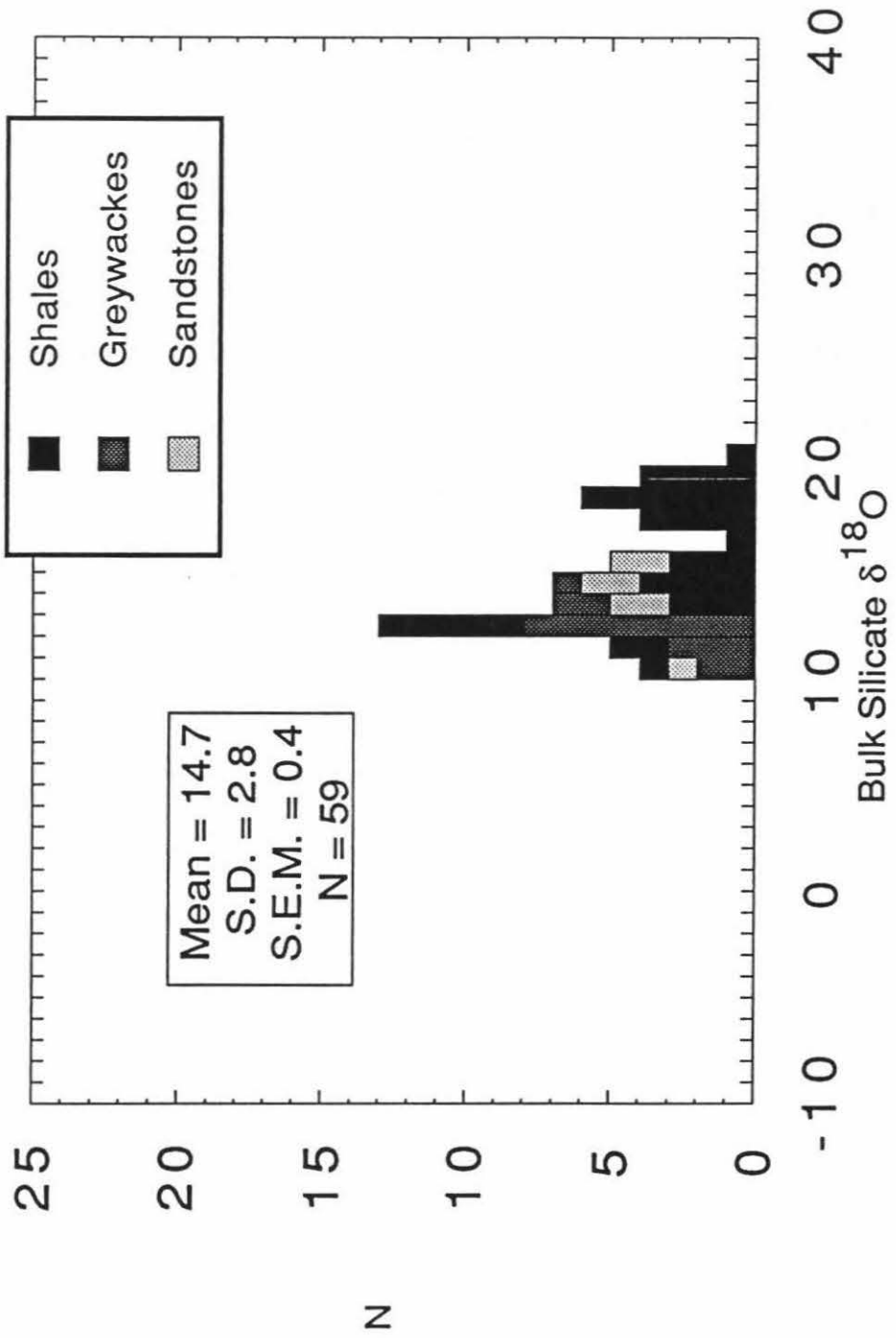
Figure 3.10

Histogram showing bulk silicate $\delta^{18}\text{O}$ distribution for all marine terrigenous sediments from the literature review, subdivided into shales, greywackes, and other types of sandstones.

Bulk Silicate $\delta^{18}\text{O}$ vs Age: Pelagic argillites, sandstone, siltstone, and clay conglomerate



Bulk Silicate $\delta^{18}\text{O}$ Distribution Marine Sediments



observation that there is little variation in the mineralogy of the samples showing these whole-rock $\delta^{18}\text{O}$ variations. In addition, mineral separates of quartz, feldspar, and clay show similar trends in $\delta^{18}\text{O}$ variation to those of the bulk sample.

Three important differences between terrigenous sedimentary rocks of the Texas Gulf Coast and the Belt Supergroup in Montana are: (1) the much greater age of the Belt Supergroup; (2) the greater depth of burial of the Belt Supergroup; and (3) the much higher temperatures of diagenesis of the Belt Supergroup as estimated by quartz-illite geothermometry. A comparison of bulk silicate $\delta^{18}\text{O}$ with stratigraphic depth for the Belt Supergroup and the Texas Gulf Coast sediments (Figure 3.11) shows a general trend of decreasing $\delta^{18}\text{O}$ with depth. This trend could be interpreted to be simply the result of the diagenetic conversion of smectite to illite if (1) the original sediments were of similar mineralogy and bulk silicate $\delta^{18}\text{O}$, and (2) the original pore waters were of similar $\delta^{18}\text{O}$.

A comparison of $\delta^{18}\text{O}_{\text{bulk silicate}}$ with $\delta^{18}\text{O}_{\text{carbonate}}$ for the carbonate-bearing terrigenous sediments from the Texas Gulf Coast and from the Belt Supergroup shows a positive correlation of these two parameters (Figure 3.12, $r = 0.94$). This suggests that $\delta^{18}\text{O}_{\text{calcite}}$, like $\delta^{18}\text{O}_{\text{bulk silicate}}$, is lowered during diagenesis. In the Belt Supergroup study, the $\delta^{18}\text{O}_{\text{bulk silicate}}$ also increases with proximity to the two limestone formations in the stratigraphic section. This raises the question as to what extent the $\delta^{18}\text{O}_{\text{bulk silicate}}$ is influenced by $\delta^{18}\text{O}_{\text{carbonate}}$ during diagenesis of fine-grained sediments.

The few quartz-rich marine sandstones that have been analyzed range in bulk silicate $\delta^{18}\text{O}$ from +10.9 to +15.5. This range in $\delta^{18}\text{O}$ may be due to differences in the isotopic composition of the original quartz grains, or due to the amount and composition of secondary cement in the sample. The low $\delta^{18}\text{O}$ value is for a specimen of St. Peter Sandstone (Silverman,

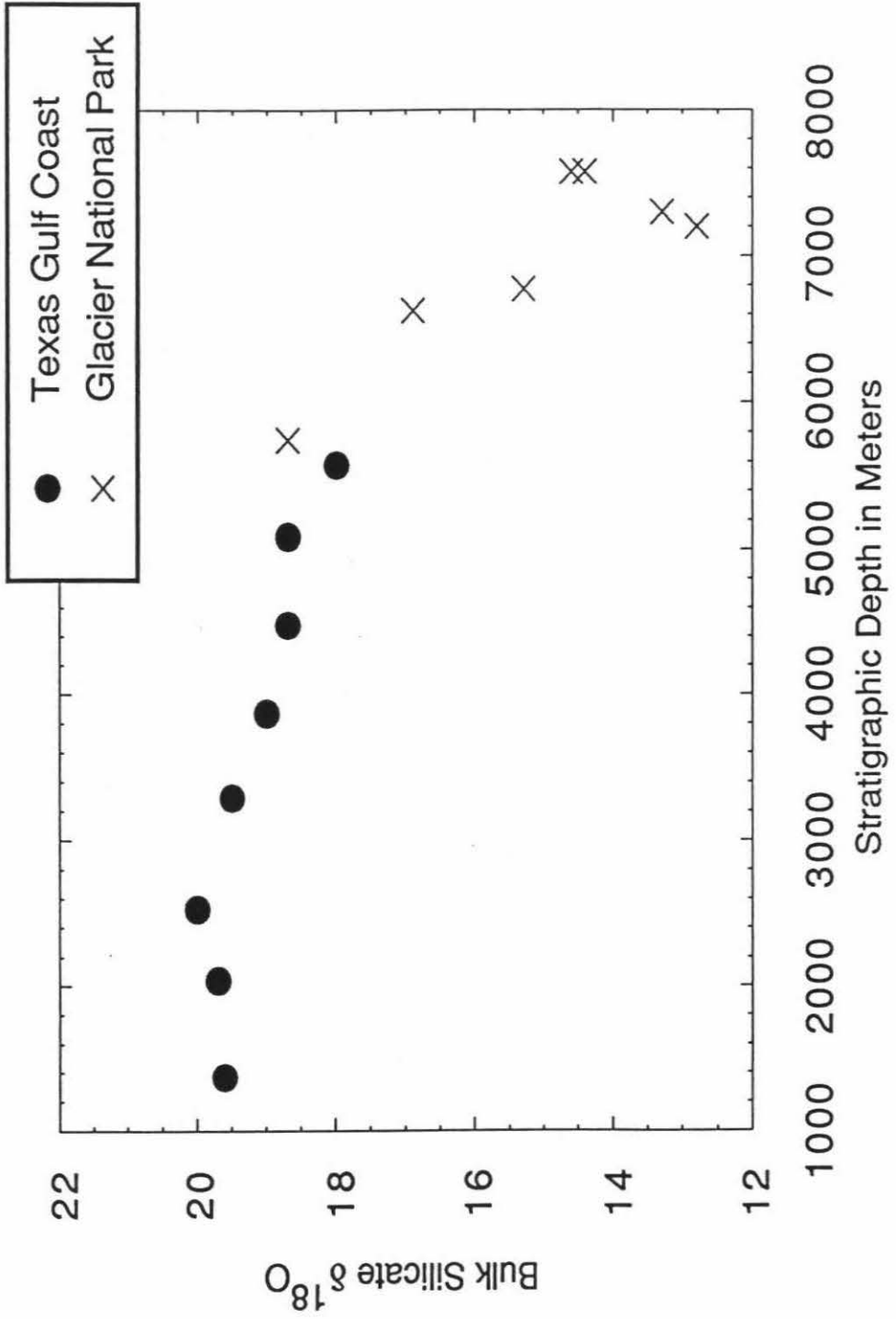
Figure 3.11

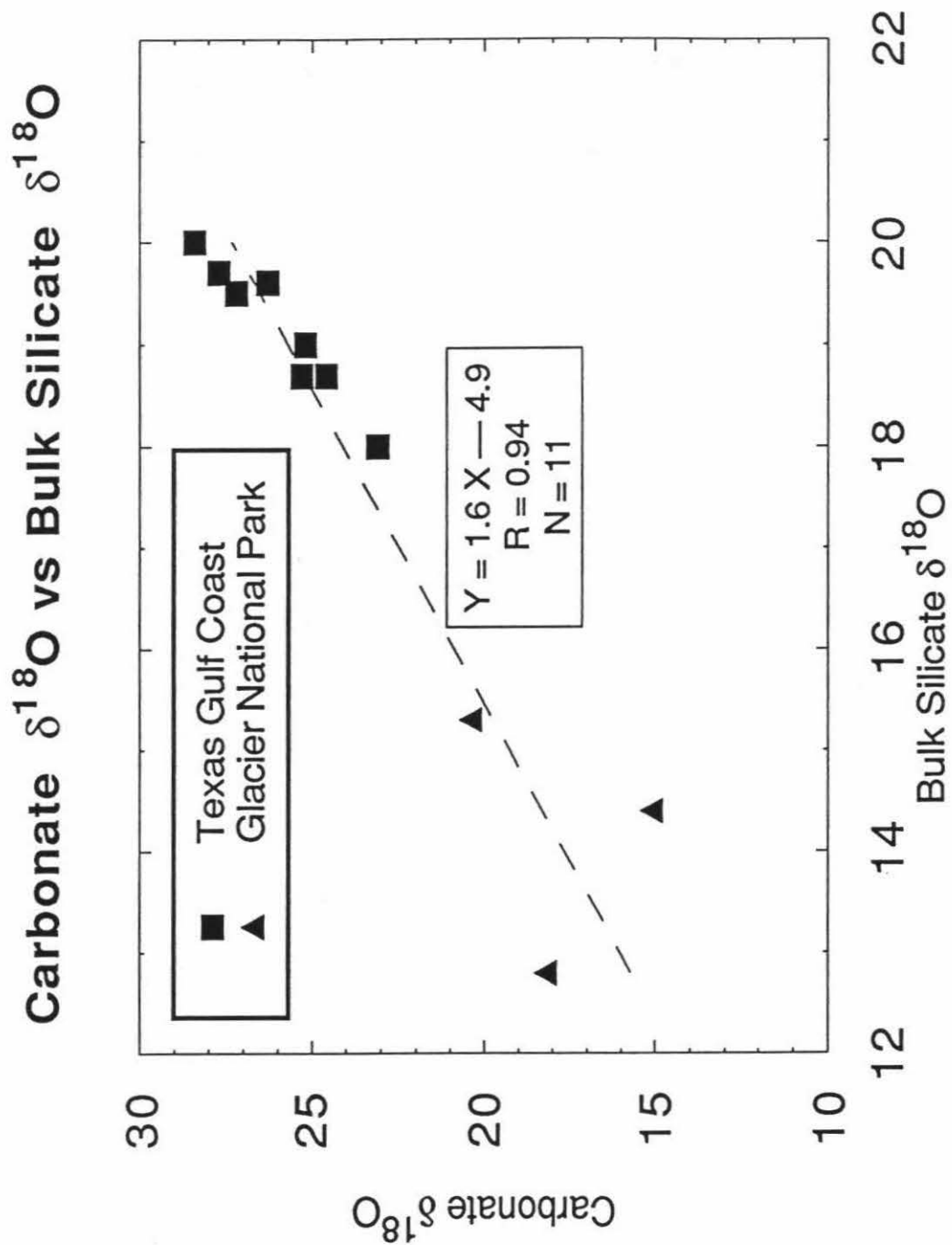
Bulk silicate $\delta^{18}\text{O}$ vs. stratigraphic depth for the Texas Gulf Coast and Glacier National Park samples listed in Table 3.1 (data from Yeh and Savin, 1977, and Eslinger and Savin, 1973).

Figure 3.12

Carbonate $\delta^{18}\text{O}$ vs bulk silicate $\delta^{18}\text{O}$ for Texas Gulf Coast and Glacier National Park samples of Yeh and Savin (1977) and Eslinger and Savin (1973). The simple linear regression (Fisher et al., 1970) displays a very high correlation coefficient of 0.94.

Bulk silicate $\delta^{18}\text{O}$ vs Stratigraphic Depth





1951), which has very little secondary cement. This value is within the range reported for igneous quartz (Taylor and Epstein, 1962b). The high $\delta^{18}\text{O}$ value is for a sample of Potsdam Sandstone and could be due to secondary silica cement or to primary quartz clasts of metamorphic origin.

Greywackes from the Franciscan Formation range in $\delta^{18}\text{O}$ from +10.3 to +14.0 (Magaritz and Taylor, 1976). These are the lowest- ^{18}O marine sandstones reported in the literature, with the exception of uncemented orthoquartzites like the aforementioned St. Peter Sandstone. The lower $\delta^{18}\text{O}$ values of greywackes can largely be explained by the difference in their mineralogic composition. The greywackes analyzed by Magaritz and Taylor (1976) consisted primarily of quartz, feldspar, and volcanoclastic and metamorphic rock fragments. The quartz in these rocks had a $\delta^{18}\text{O}$ only slightly higher than that of quartz in average igneous rocks. On the other hand, plagioclase in the greywackes typically had a $\delta^{18}\text{O}$ that would be expected for feldspar in isotopic equilibrium with higher- ^{18}O vein quartz; thus, the plagioclase was not in isotopic equilibrium with its coexisting quartz. This suggests that there has been some diagenetic alteration of the isotopic composition of the feldspar by the same fluids which deposited the vein quartz, but that these fluids did not isotopically equilibrate with the coexisting greywacke quartz. This is consistent with the well known observation that quartz is much more resistant than feldspar to exchange with aqueous fluids in hydrothermal systems (*e.g.*, see Magaritz and Taylor, 1986).

Figure 3.13 compares the bulk silicate $\delta^{18}\text{O}$ values of various groups of marine shales. One important observation is that Franciscan shales, Franciscan greywackes, and non-greywacke sandstones have a similar range in bulk silicate $\delta^{18}\text{O}$. This is an important observation in terms of understanding sedimentary precursors to metamorphic rocks. The non-eugeosynclinal marine

shales have a heavier bulk silicate $\delta^{18}\text{O}$ than Franciscan shales, Franciscan greywackes, and non-greywacke marine shales. One explanation for this is that the non-eugeosynclinal shales have less isotopically light feldspar and more isotopically heavy clay minerals than these other sediments. The eugeosynclinal shales may also have undergone more interaction with isotopically light meteoric waters such as those involved in the alteration of the greywackes. However, it would be useful to study some eugeosynclinal sediments other than those of the Franciscan Formation for comparison purposes.

3.3.2 Transitional and non-marine samples

The distribution of $\delta^{18}\text{O}$ for transitional and non-marine sediments (Figure 3.14) shows a $\delta^{18}\text{O}$ maximum around +15 and a range from +9.0 to +19.7. The lowest values reported are for bentonites from the Disturbed Belt, Montana (Eslinger and Yeh, 1986). These rocks are low in ^{18}O due to the presence of isotopically light volcanic quartz and feldspar. The other low $\delta^{18}\text{O}$ values are for the Athabasca Sandstone, a quartz-rich fluvial sandstone from Saskatchewan, Canada (Bray *et. al* , 1988). Again, this may be attributed to a large component of isotopically unaltered igneous quartz.

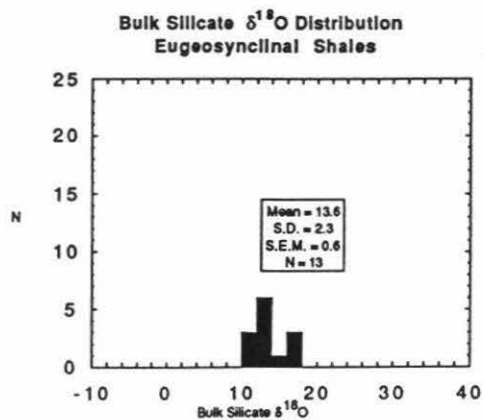
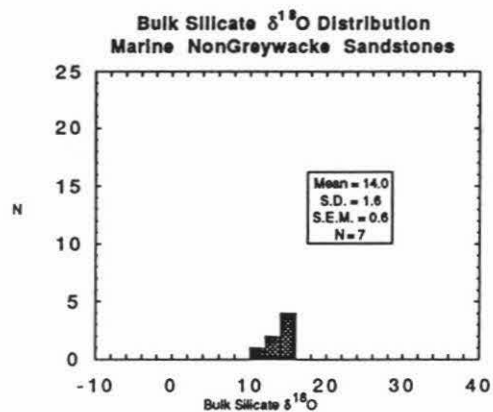
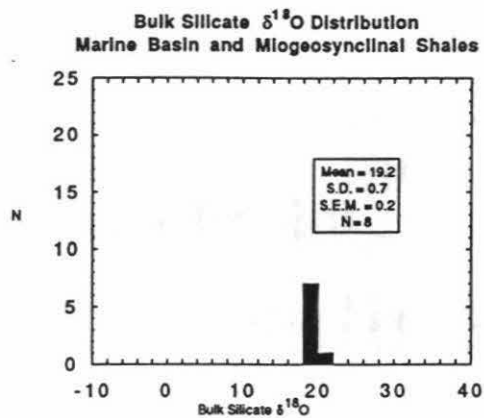
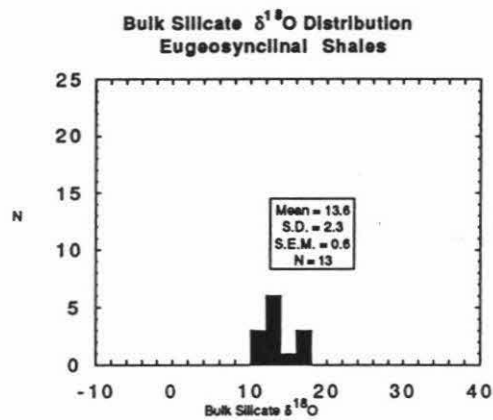
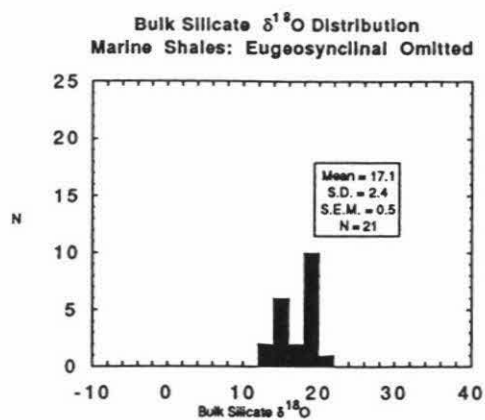
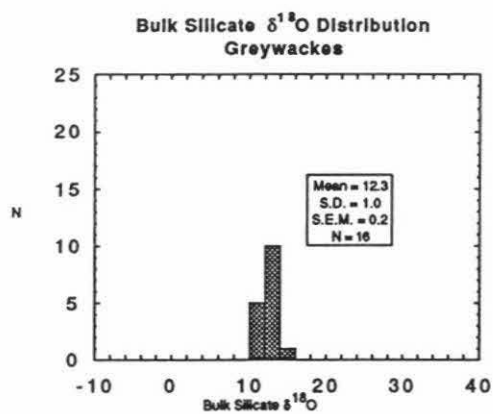
A comparison of $\delta^{18}\text{O}$ and geologic age for transitional and non-marine shales and bentonites (Figure 3.15) shows a trend toward homogenization of $\delta^{18}\text{O}$ with time. This is consistent with the observations of Eslinger and Yeh (1986) in the Disturbed Belt that there was an increasing homogenization of $\delta^{18}\text{O}$ among quartz and clay fractions with increasing diagenetic grade of shales and bentonites. This trend in transitional and non-marine sediments could also be the result of mineralogic differences or an artifact of the limited number of analyses for

Figure 3.13

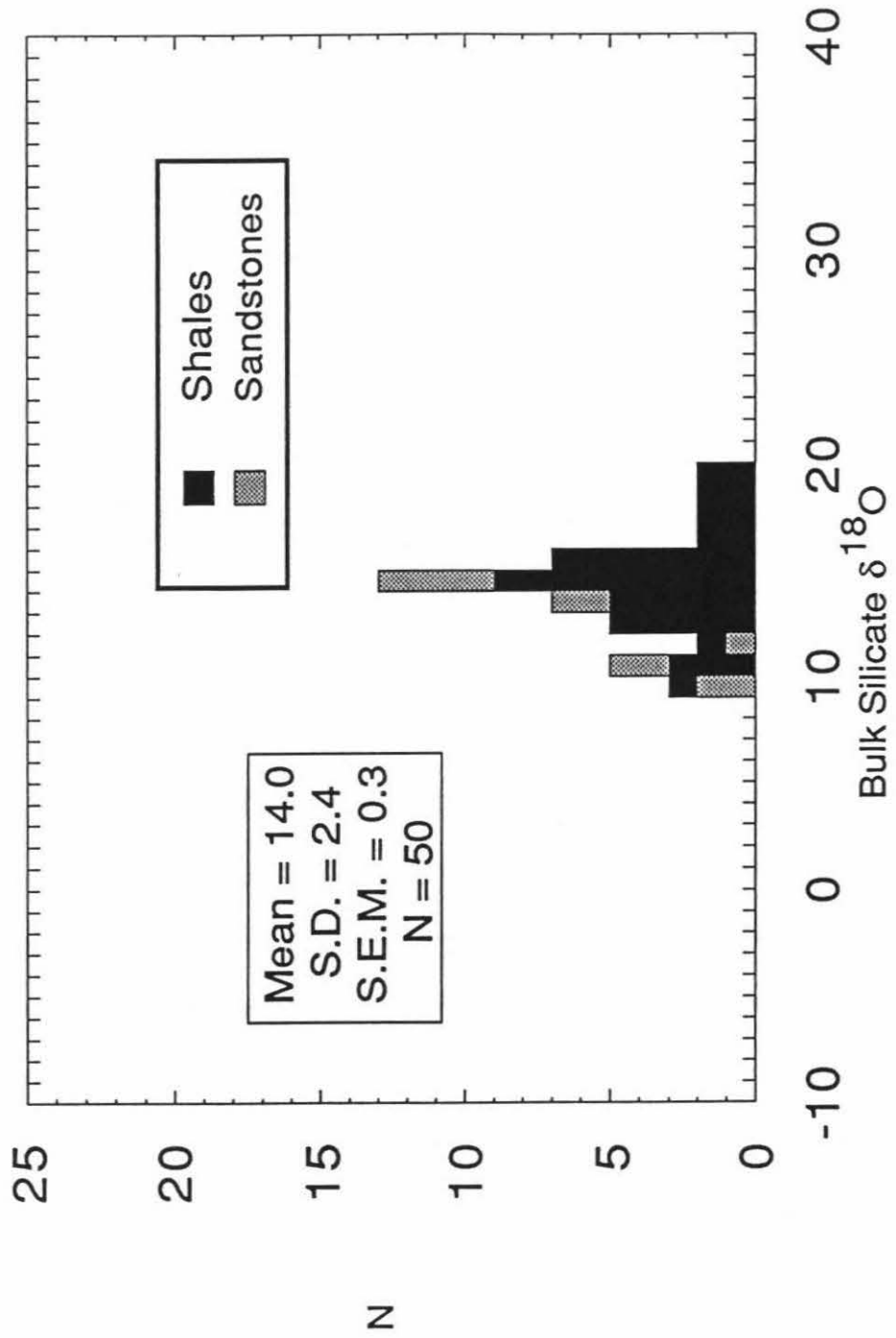
Five comparative histograms showing bulk silicate $\delta^{18}\text{O}$ values of various categories of terrigenous sedimentary rocks from the literature survey. The plotted categories include: (a) greywackes, (b) all marine shales with eugeosynclinal shales omitted, (c) all eugeosynclinal shales, (d) marine basin and miogeosynclinal shales, and (e) all marine sandstones exclusive of greywackes. The histogram for all eugeosynclinal shales is repeated in both columns for purposes of comparison.

Figure 3.14

Histograms showing bulk silicate $\delta^{18}\text{O}$ distribution of all transitional and nonmarine terrigenous sediments from the literature survey, subdivided into shales and sandstones.



Bulk Silicate $\delta^{18}\text{O}$ Distribution Transitional and Nonmarine Sediments



sedimentary rocks older than the Jurassic.

3.4 Summary and conclusions

The whole rock $\delta^{18}\text{O}$ of marine (excluding pelagic), non-marine, and transitional terrigenous sediments is summarized in Figure 3.16. The $\delta^{18}\text{O}$ distribution ranges from +9 to +21 with a maximum at +15. The bimodal marine shale $\delta^{18}\text{O}$ distribution has a distinct influence on the $\delta^{18}\text{O}$ distribution of the entire population. The $\delta^{18}\text{O}$ values of marine, pelagic, and non-marine shales are shown in Figure 3.16 and the corresponding sandstone distribution is also shown in Figure 3.16. The sandstones range from $\delta^{18}\text{O}$ from +10 to +17, while the shales range in $\delta^{18}\text{O}$ from +8 to +33. This difference may be due to discrepancies in the number of analyses reported for the two rock types: 35 sandstones as compared to 73 shales. There is a notable gap in the shale $\delta^{18}\text{O}$ values between +15 and +16 that is unexplained. This gap is all the more remarkable because, as will be shown below, the results of the present study show a marked concentration of $\delta^{18}\text{O}$ values in this particular range. From Figure 3.16 it can be seen that the mean $\delta^{18}\text{O}$ for all sandstones is significantly different than the mean $\delta^{18}\text{O}$ for all non-pelagic shales ($P < 0.01$). Marine, transitional and nonmarine sandstones are not significantly different in bulk silicate $\delta^{18}\text{O}$, but this is decidedly not the case for the shales reported in the literature. Pelagic shales are significantly heavier than marine terrigenous shales ($P < 0.025$), which are significantly different than transitional and nonmarine terrigenous shales ($P < 0.05$). The effect of low-temperature hydrothermal alteration by seawater is most likely responsible for the heavier bulk silicate $\delta^{18}\text{O}$ of pelagic argillites. The influence of lower- ^{18}O meteoric waters during diagenesis may be responsible for the lower bulk silicate $\delta^{18}\text{O}$ values observed in transitional and nonmarine sediments. The difference in mean $\delta^{18}\text{O}$ values between marine shales and transitional and nonmarine shales could also be in part a function of selective sampling.

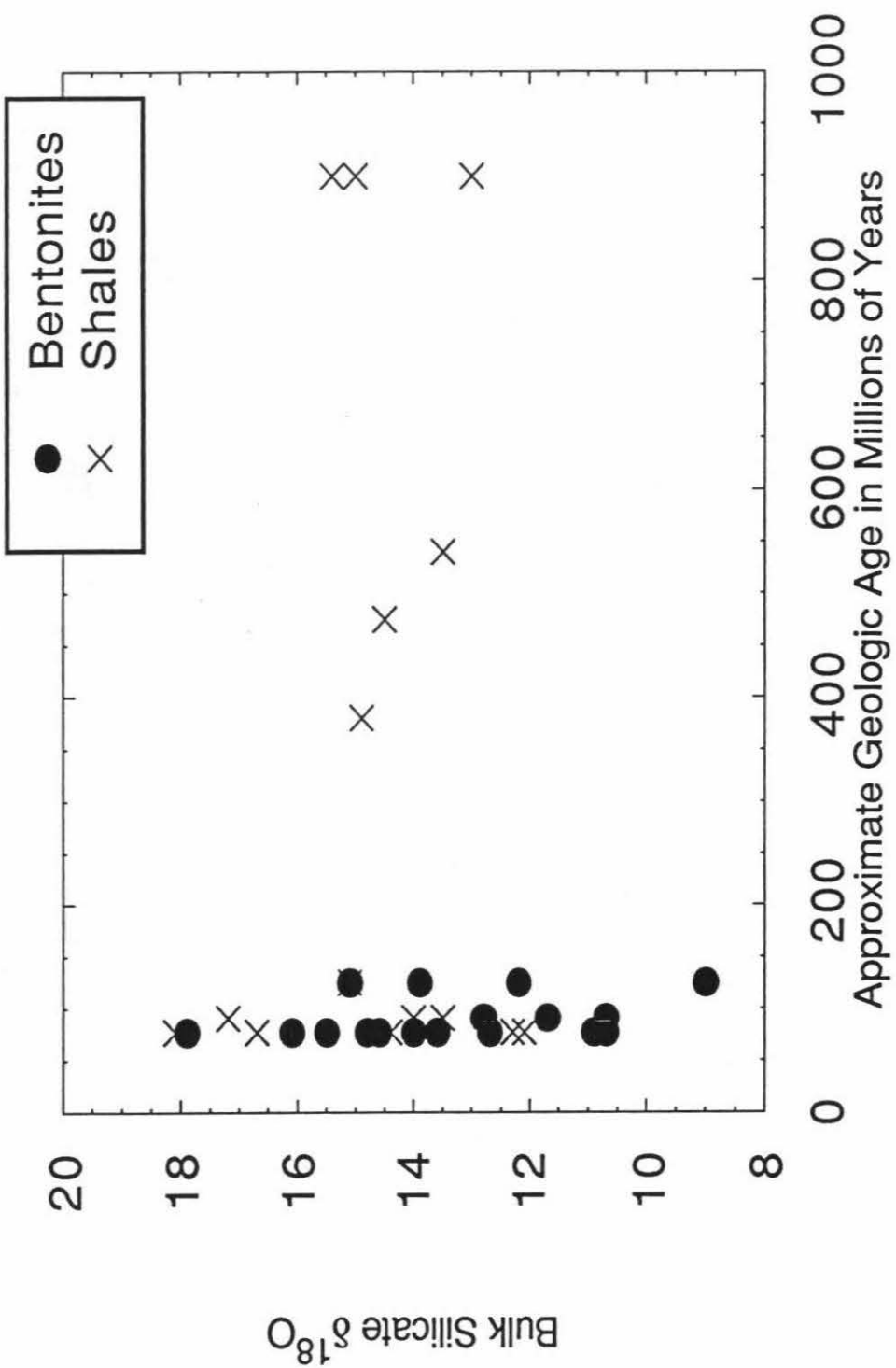
Figure 3.15

Bulk silicate $\delta^{18}\text{O}$ vs. geologic age for all fine-grained transitional and nonmarine terrigenous sedimentary rocks from the literature survey, subdivided into bentonites and shales.

Figure 3.16

Eight comparative histograms showing bulk silicate $\delta^{18}\text{O}$ values of various categories of terrigenous sedimentary rocks from the literature survey. The plotted categories include: (a) all marine, transitional, and nonmarine clastic sediments, (b) all marine, transitional, and nonmarine shales, (c) all sandstones, (d) all pelagic shales, (e) all marine sandstones, (f) all marine shales, (g) all transitional and nonmarine sandstones, and (h) all transitional and nonmarine shales.

Bulk Silicate $\delta^{18}\text{O}$ vs Age: Transitional and Nonmarine Sedimentary Rocks



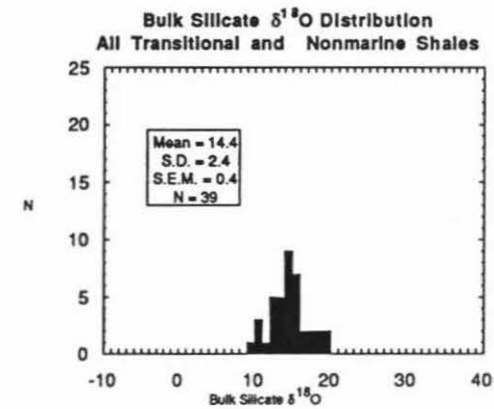
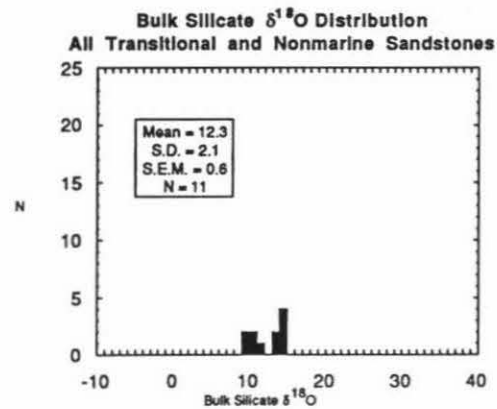
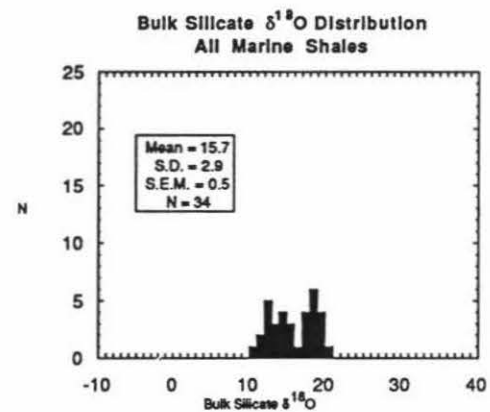
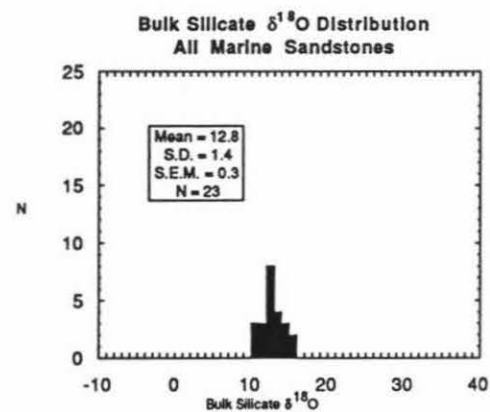
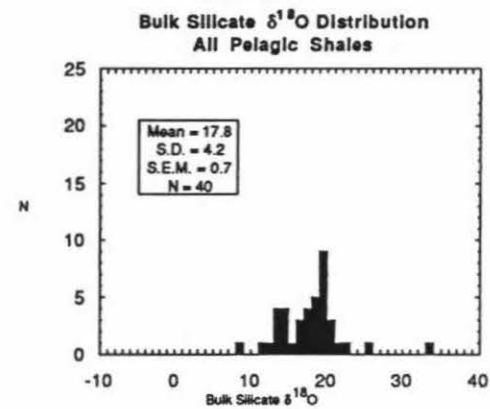
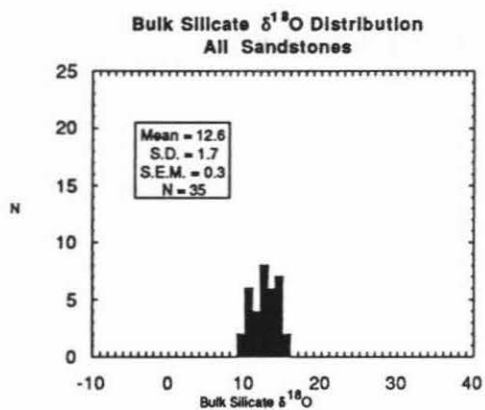
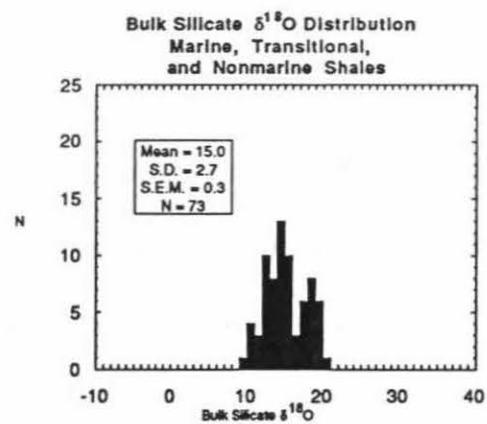
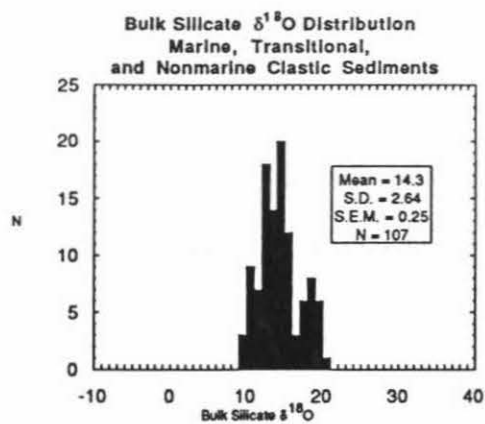


Figure 3.17 compares bulk silicate $\delta^{18}\text{O}$ distributions for sedimentary rocks from 4 different environmental groupings: eugeosynclinal; non-eugeosynclinal; volcanic and volcanoclastic bentonites and eugeosynclinal sediments; and non-volcanically influenced sediments. The volcanically-influenced sedimentary rocks show a narrower range in bulk silicate $\delta^{18}\text{O}$ than do those which do not contain a significant volcanic component. The mean $\delta^{18}\text{O}$ for the bentonite-eugeosynclinal group (+13.0) is significantly different from that of the non-eugeosynclinal and non-bentonite group (+15.1). Similarly, the mean $\delta^{18}\text{O}$ for the eugeosynclinal sedimentary rocks is significantly lower than that of the non-eugeosynclinal sedimentary rocks ($P < 0.01$), +12.9 vs. +14.8.

The processes responsible for the whole-rock $\delta^{18}\text{O}$ values of sedimentary rocks are many and complex. Overall, there is no significant correlation between bulk silicate $\delta^{18}\text{O}$ and geologic age for the terrigenous sedimentary rocks in the literature. This is distinctly not the case for siliceous- and carbonate-rich sediments (see Chapter 4 below). In general, the source rocks (provenance), mineralogic content, relative proportions of authigenic, biogenic, and terrigenous material, and extent of diagenetic alteration (which is somewhat related to the depth of burial) seem to be the most important factors in determining the $\delta^{18}\text{O}$ of terrigenous sedimentary rocks.

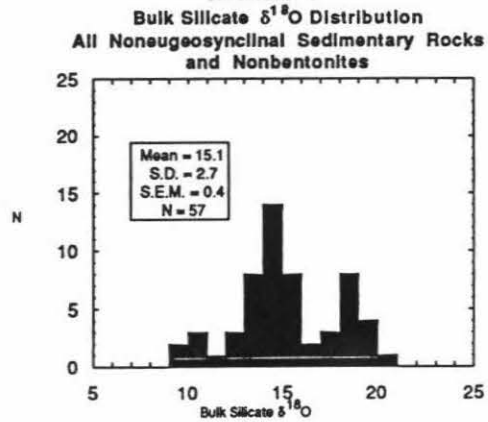
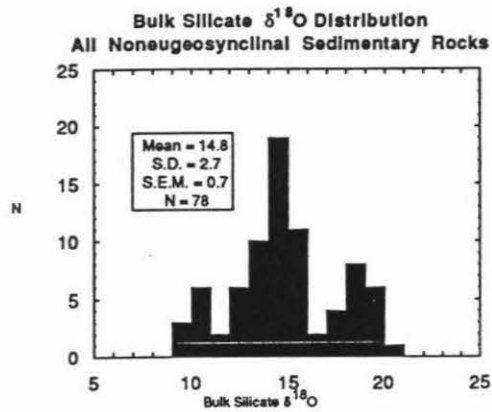
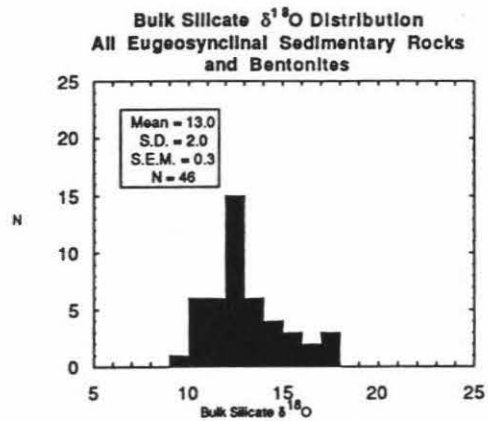
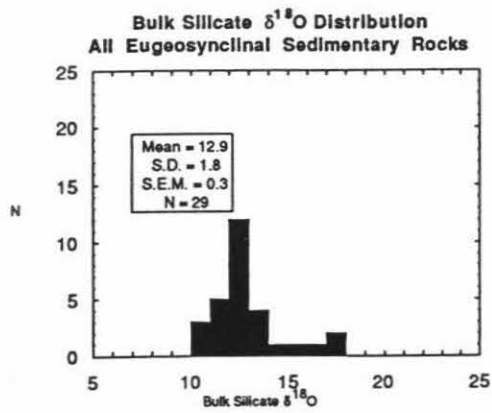
3.5 Inventory of samples in the sedimentary literature review

3.5.1. Explanation of Table 3.1

In Table 3.1 are tabulated most of the readily available oxygen isotope data on unmetamorphosed sedimentary rocks from the literature that were available to the author during the writing of this Ph.D. thesis. The data for each group of samples in Table 3.1 are arranged on two adjacent pages, with the arbitrary sample numbers from 6 to 365 listed in the column on

Figure 3.17

Four comparative histograms showing bulk silicate $\delta^{18}\text{O}$ values of various categories of terrigenous sedimentary rocks from the literature survey. The plotted categories include: (a) all eugeosynclinal sedimentary rocks, (b) all eugeosynclinal sedimentary rocks and bentonites, (c) all sedimentary rocks except those having eugeosynclinal affinities, and (d) all sedimentary rocks except those that typically contain a volcanic component, namely the eugeosynclinal rocks and the bentonites.



the far-left-hand side of each page. These sample numbers link the tabulated data on the two pages. They should not be confused with the actual sample numbers in the published papers, which are given in Column A.

The columns of information and data are arranged as follows:

Column A:	Sample identification number used by the authors of the paper from which the data were taken.
Column B:	Depositional environment of the sample (see list of abbreviations below).
Column C:	Estimated maximum temperature of diagenesis based on data given in the original references or in other data from the literature.
Column D:	Location of sample (see list of abbreviations below).
Column E:	Stratigraphic unit from which the sample was collected.
Column F:	Lithology of the sample, including mineralogy where available (see list of abbreviations below).
Column G:	Stratigraphic age of the sample.
Column H:	Percent carbonate in the sample (cc = calcite, do = dolomite).
Column I:	Whole-rock or bulk-silicate $\delta^{18}\text{O}$ value.
Column J:	Quartz size fraction analyzed (see list of abbreviations below).
Column K:	$\delta^{18}\text{O}$ of quartz separate.
Column L:	Clay size fraction analyzed.
Column M:	$\delta^{18}\text{O}$ of clay.
Column N:	$\delta^{18}\text{O}$ of carbonate.
Column O:	$\delta^{13}\text{C}$ of carbonate.
Column P:	$\delta^{18}\text{O}$ of any other minerals analyzed, plus additional remarks.

3.5.2 Abbreviations used in the sedimentary literature review

information not given	-
samples collected from same outcrop	<
uncertain	?
abundant	ab
arkose	AK
amphibolite facies	Amph
argillite	AR
Archean	Ar
Australia	AU
subsiding deep basin	ba
British Columbia	BC
bentonite	BE
carbonates	C
California	CA
calculated	calc
Cambrian	Cam
calcite	cc
chert	CH
chlorite	chl
Churchill Province	Church
clay minerals	cl
Canada	CN
Colorado	CO
Cretaceous	Cret
calcsilicate	CS
Connecticut	CT
diatomaceous earth	DE
depositional environment	Dep. Env.
Devonian	Dev.
dolomite	do
England	EN
eocene	Eoc
formation	F
feldspar	fsp
garnet	g
Geochimica et Cosmochimica Acta	GCA
glaucinite	gl
Glacier National Park	Glac. Nat.
glaucophane	gp
Grenville Province	Gren
greenschist	Grnschst
geosyncline	gs

Geological Society of America Bulletin	GSA Bulletin
greywacke	GW
gypsum	gy
high grade	HG
Holocene	Hol
Iowa	IA
illite	ill
Indiana	IN
interbedded	intbd
jadeitej
Jurassic	Jur.
kaolinite	k
lower	L
Labrador	LR
lawsonitelw
middle	m
marine	m
metamorphic fragment	m
Montana	MA
Maine	ME
Miocene	Mio
Mississippi River bottom sediment	Miss. Riv. Btm. sed.
Mississippian	Miss.
Minnesota	MN
Missouri	MO
Montana	MT
mountains	Mts.
muscovite	Musc.
nonmarine	mn
Nova Scotia	NS
Nevada	NV
New York	NY
chert	o
Oligocene	Olig.
Ordovician	Ord.
Pennsylvania	PA
Paleocene	Pal
Paleocene	Paleo
phyllite	PH
plagioclasepl
Pleistocene	Pleis
Pliocene	Plio
prehnite-pumpellyitePp
Proterozoic	Prot.
phyllitepy

pyrite	.py
pyroxene	pyx
Quaternary	Q
quartz	q
quartz arenite	QA
quartzite	QZ
river channel	rc
stable continental shelf/craton	sc
South Dakota	SD
southeast	SE
sericite	ser
serpentine	serp
shale	SH
siltstone	si
Silurian	Sil.
slate	SL
smectite	sm
sandstone	SS
schist	ST
superior Province	Sup
southwest	SW
Tertiary	Tert.
trace	tr.
Triassic	Trias.
Texas	TX
Upper Cretaceous Series	U. Cret. Ser.
upper	U
micron	u
Utah	UT
volcanic	v
Wisconsin	WI
bulk silicate	WR
zeolite	.z
zeolite facies	zeol
samples collected from same outcrop	{

3.5.3 Abbreviations and list of depositional environments (Column B)

Nonmarine Environments:	NM
Alluvial Fan:	af
River Channel:	rc
Floodplain:	fp
Lacustrine:	lc
Swamp:	sw
Volcanic:	v
Eolian (not volcanic):	eo
Glacial:	gl
Transitional Environments and Marine-Nonmarine	
Oscillations:	T
Oscillatory Marine-Nonmarine Basin:	ba
Shore Deposits:	
beach sand, tidal flat, barrier island and beach:	sd
Deltaic Complex:	dc
Bay, Lagoon:	bl
Marsh:	ms
Volcanic:	v
Marine Environments:	M
Stable continental shelf/craton:	sc
Offshore subsiding deep basin:	ba
Geosyncline:	gs
Miogeosyncline:	mg
Eugeosyncline:	eg
Evaporite Basins:	ev
Submarine slope and fan deposits:	sf
Ocean Floor, Pelagic:	pg
Euxinic, black shale anoxic:	eu
Volcanic:	v

Table 3.1 Sedimentary Literature Review

	A	B	C	D	E	F	G
1	Sample I.D	Dep. Env.	Tmax (est.)	Location	Stratigraphic Unit	Lithology	Age
2							
3	Yeh,H.W. and S.M. Savin. 1977. GSA Bull. 88:1321-1330.						
4							
5							
6	YS1977-1341	M: ba	44°C	TX : coastal plain	Anahuac F.	SH: clay mostly ill-sm	L. Mio.
7	"	"	"	"	"	"	"
8	"	"	"	"	"	"	"
9	"	"	"	"	"	"	"
10	YS1977-2012	M: ba	58°C	TX : coastal plain	Anahuac F.	SH: clay mostly ill-sm	L. Mio.
11	"	"	"	"	"	"	"
12	"	"	"	"	"	"	"
13	"	"	"	"	"	"	"
14	YS1977-2500	M: ba	68°C	TX : coastal plain	Frio F.	SH: clay mostly ill-sm	U. Olig.
15	"	"	"	"	"	"	"
16	"	"	"	"	"	"	"
17	"	"	"	"	"	"	"
18	YS1977-3232	M: ba	84°C	TX : coastal plain	Frio F.	SH: clay mostly ill-sm	U. Olig.
19	"	"	"	"	"	"	"
20	"	"	"	"	"	"	"
21	"	"	"	"	"	"	"
22	YS1977-3841	M: ba	104°C	TX : coastal plain	Frio F.	SH: clay mostly ill-sm	U. Olig.
23	"	"	"	"	"	"	"
24	"	"	"	"	"	"	"
25	"	"	"	"	"	"	"
26	YS1977-4451	M: ba	130°C	TX : coastal plain	Frio F.	SH: clay mostly ill-sm	U. Olig.
27	"	"	"	"	"	"	"
28	"	"	"	"	"	"	"
29	"	"	"	"	"	"	"
30	YS1977-5061	M: ba	155°C	TX : coastal plain	Frio F.	SH: clay mostly ill-sm	U. Olig.
31	"	"	"	"	"	"	"
32	"	"	"	"	"	"	"
33	"	"	"	"	"	"	"
34	YS1977-5549	M: ba	169° C	TX : coastal plain	Frio F.	SH: clay mostly ill-sm	U. Olig.
35	"	"	"	"	"	"	"
36	"	"	"	"	"	"	"
37	"	"	"	"	"	"	"
38	YS1977-MISS	NM: rc	—	MO: Miss. River	—	Miss. Riv. btm. sed. .q-ill-sm	—
39	"	"	—	"	—	"	—
40	"	"	—	"	—	"	—
41	"	"	—	"	—	"	—
42							
43							
44	Estlinger, Eric V. and Hsueh-Wen Yeh.1986. GCA 50:59-68.						
45							
46	EY1985-1	T: ba-v	160min-250max	MT: Sweetgrass Arch	Blackleaf F.	BE: cl 95	L. Cret.
47	EY1985-4	T: ba-v	160min-250max	MT: Disturbed Belt	Marias River Shale F.	BE: q 30, cl 65, cc 5	U. Cret.
48	EY1985-10B	T: ba-v	160min-250max	MT: Disturbed Belt	Marias River Shale F.	BE: cl 55, cc 20,pl 10	U. Cret.
49	{EY1985-15	T: ba-v	160min-250max	MT: Disturbed Belt	Marias River Shale F.	SH: q 30, cl 50,cc 5, do 5	U. Cret.
50	{EY1985-14	T: ba-v	160min-250max	MT: Disturbed Belt	Marias River Shale F.	BE: pl 10, cl 10, cc 80	U. Cret.
51	EY1985-21	T: ba-v	160min-250max	MT: Disturbed Belt	Blackleaf F.	BE: q 15,pl 15,cl 70	L. Cret.
52	"	T: ba-v	160min-250max	MT: Disturbed Belt	"	"	"
53	{EY1985-25	T: ba-v	160min-250max	MT: Disturbed Belt	Blackleaf F.	SH: q 30,pl 15,cl 60	L. Cret.
54	{EY1985-24	T: ba-v	160min-250max	MT: Disturbed Belt	Blackleaf F.	BE: cl 95	L. Cret.
55	EY1985-31	T: ba-v	160min-250max	MT: Disturbed Belt	Blackleaf F.	BE: q 5, pl 20,cl 75	L. Cret.
56	<EY1985-43	T: ba-v	160min-250max	MT: Sweetgrass Arch	Marias River Shale F.	SH: q 30, pl 15, cl 55	U. Cret.
57	<EY1985-42	T: ba-v	160min-250max	MT: Sweetgrass Arch	Marias River Shale F.	BE: cl 95	U. Cret.
58	"	T: ba-v	160min-250max	MT: Sweetgrass Arch	Marias River Shale F.	"	"
59	{EY1985-52	T: ba-v	160min-250max	MT: Disturbed Belt	Marias River Shale F.	SH: q 30,cl 60,do 5,py 5	U. Cret.
60	{EY1985-51	T: ba-v	160min-250max	MT: Disturbed Belt	Marias River Shale F.	BE: pl 5,cl 90	U. Cret.
61	<EY1985-72	T: ba-v	160min-250max	MT: Disturbed Belt	Two Medicine F.	SH: q 30, pl 30,cl 40	U. Cret.
62	<EY1985-69C	T: ba-v	160min-250max	MT: Disturbed Belt	Two Medicine F.	BE: q 5,pl 15, cl 80	U. Cret.
63	EY1985-73	T: ba-v	160min-250max	MT: Disturbed Belt	Two Medicine F.	BE: pl 5, cl 25, cc 70	U. Cret.
64	EY1985-85	T: ba-v	160min-250max	MT: Disturbed Belt	Marias River Shale F.	BE: q 20, cl 80	U. Cret.
65	{EY1985-95	T: ba-v	160min-250max	MT: Disturbed Belt	Marias River Shale F.	SH: q 35,cl 55	U. Cret.
66	{EY1985-93A	T: ba-v	160min-250max	MT: Disturbed Belt	Marias River Shale F.	BE: q 5,pl 75,cl 20	U. Cret.
67	EY1985-96A	T: ba-v	160min-250max	MT: Disturbed Belt	Marias River Shale F.	BE: pl 90,cl 10	U. Cret.
68	<EY1985-110	T: ba-v	160min-250max	MT: Disturbed Belt	U.Cret. Ser.	SH : q 30,pl 5,cl 50,cc 10,do 5	U. Cret.
69	<EY1985-109	T: ba-v	160min-250max	MT: Disturbed Belt	U.Cret. Ser.	BE: q 10,,cl 90	U. Cret.
70	"	T: ba-v	160min-250max	MT: Disturbed Belt	"	"	"
71	"	T: ba-v	160min-250max	MT: Disturbed Belt	"	"	"
72	"	T: ba-v	160min-250max	MT: Disturbed Belt	"	"	"
73	{EY1985-129	T: ba-v	160min-250max	MT: Disturbed Belt	Marias River Shale F.	SH q 30,pl 10,cl 60,	U. Cret.
74	{EY1985-128	T: ba-v	160min-250max	MT: Disturbed Belt	Marias River Shale F.	BE: q 10,pl 40,cl 45,cc 5	U. Cret.
75	"	T: ba-v	160min-250max	MT: Disturbed Belt	Marias River Shale F.	"	"
76	EY1985-139A	T: ba-v	160min-250max	MT: Sweetgrass Arch	Two Medicine F.	BE: cl 95	U. Cret.
77	<EY1985-159	T: ba-v	160min-250max	MT: Disturbed Belt	Telegraph Creek F.	SH: q 20,pl 10,cl 75	U. Cret.

Table 3.1 Sedimentary Literature Review

1	H	I	J	K	L	M	N	O	P
2	% Co or Do	∅ 18 O:W R	Quartz fraction	∅ 18 O:Quartz	Clay fraction	∅ 18 O: Clay	∅ 18 O: C	∅ 13 C: C	∅ 18 O: Misc.
3									
4									
5									
6	—	19.6	>2u	16.1	2-1u	17.6	26.3	—	—
7	—	*	2-1u	17.9	1-0.5u	19.6	*	—	—
8	—	*	1-0.5u	24.1	0.5-0.1u	19.6	*	—	—
9	—	*	0.5-0.1u	25.9	<0.1u	22.4	*	—	—
10	—	19.7	>2u	17.8	2-1u	8.4	27.7	—	—
11	—	*	2-1u	23.7	1-0.5u	20.7	*	—	—
12	—	*	1-0.5u	24.6	0.5-0.1u	22.1	*	—	—
13	—	*	0.5-1u	26.1	<0.1u	21.7	*	—	—
14	—	20.0	>2u	16.4	2-1u	18.3	28.4	—	Zoned qtz
15	—	*	2-1u	20.8	1-0.5u	20.9	*	—	—
16	—	*	1-0.5u	27.4	0.5-0.1u	22.2	*	—	—
17	—	*	0.5-0.1u	25.6	<0.1u	20.9	*	—	—
18	—	19.5	>2u	18.7	2-1u	20.7	27.2	—	—
19	—	*	2-1u	23.6	1-0.5u	19.3	*	—	—
20	—	*	1-0.5u	26.3	0.5-0.1u	18.7	*	—	—
21	—	*	0.5-0.1u	26.9	<0.1u	20.8	*	—	—
22	—	19.0	>2u	18.9	2-1u	18.7	25.2	—	—
23	—	*	2-1u	23.8	1-0.5u	19.6	*	—	—
24	—	*	1-0.5u	26.0	0.5-0.1u	18.4	*	—	—
25	—	*	0.5-0.1u	27.0	<0.1u	19.8	*	—	—
26	—	18.7	>2u	19.8	2-1u	20.1	25.3	—	Zoned qtz
27	—	*	2-1u	25.7	1-0.5u	19.3	*	—	—
28	—	*	1-0.5u	26.5	0.5-0.1u	19.2	*	—	—
29	—	*	0.5-0.1u	26.4	<0.1u	18.6	*	—	—
30	—	18.7	>2u	18.6	2-1u	19.0	24.6	—	—
31	—	*	2-1u	23.6	1-0.5u	19.4	*	—	—
32	—	*	1-0.5u	25.7	0.5-0.1u	19.0	*	—	—
33	—	*	0.5-0.1u	26.0	<0.1u	19.6	*	—	—
34	—	18.0	>2u	18.9	2-1u	18.6	23.1	—	—
35	—	*	2-1u	25.2	1-0.5u	18.1	*	—	—
36	—	*	1-0.5u	25.4	0.5-0.1u	18.2	*	—	—
37	—	*	0.5-0.1u	22.8	<0.1u	17.7	*	—	—
38	—	2-1 u: 16.2	—	—	—	—	—	—	—
39	—	1-0.5u: 16.1	—	—	—	—	—	—	—
40	—	0.5-0.1u: 16.8	—	—	—	—	—	—	—
41	—	<0.1u: 20.0	—	—	—	—	—	—	—
42									
43									
44									
45									
46	0	9.0	—	—	<0.1u	12.3	—	—	—
47	5 cc	16.1	<1u	8.0	<0.1u	16.9	—	—	—
48	20 cc	—	1-2u	17.9	<0.1u	14.7	—	—	—
49	5 cc, 5 do	—	0.1-0.5u	24.8	<0.1u	13.7	—	—	—
50	80 cc	13.6	0.1-1u	21.2	<0.1u	16.1	—	—	—
51	0	15.1	0.1-1u	20.5	<0.1u	16.1	—	—	—
52	*	*	>2u	19.6	<0.1u	16.1	—	—	—
53	0	15.1	0.1-0.5u	20.6	<0.1u	13.9	—	—	—
54	0	12.2	0.1-1u	20.3	<0.1u	15.0	—	—	—
55	0	13.9	—	—	<0.1u	11.4	—	—	—
56	0	16.7	0.1-0.5u	23.0	<0.1u	17.3	—	—	—
57	0	17.9	0.1-1u	22.8	<0.1u	20.2	—	—	—
58	*	*	1-2u	22.2	<0.1u	20.2	—	—	—
59	5 do	—	0.1-0.5u	24.6	<0.1u	15.3	—	—	—
60	tr. cc	12.7	—	—	<0.1u	15.4	—	—	—
61	0	12.3	0.1-0.5u	18.8	<0.1u	13.0	—	—	—
62	0	14.0	>2u	16.7	<0.1u	16.1	—	—	—
63	70 cc	—	>2u	11.1	<0.1u	13.4	—	—	—
64	0	—	—	—	<0.1u	15.7	—	—	—
65	0	—	0.1-0.5u	23.9	<0.1u	15.2	—	—	—
66	0	14.6	<1u	19.5	<0.1u	18.8	—	—	—
67	0	10.7	—	—	<0.1u	17.2	—	—	—
68	10 cc, 5 do	18.1	0.1-0.5u	23.0	<0.1u	17.0	—	—	—
69	tr do	—	0.1-0.5u	23.1	<0.1u	17.1	—	—	—
70	*	—	0.5-1u	22.7	<0.1u	17.1	—	—	—
71	*	—	1-2u	22.8	<0.1u	17.1	—	—	—
72	*	—	>2u	21.0	<0.1u	17.1	—	—	—
73	0	—	0.1-0.5u	22.2	<0.1u	17.5	—	—	—
74	5 cc	14.8	0.5-1u	19.7	<0.1u	19.9	—	—	—
75	*	*	>2u	18.8	<0.1u	19.9	—	—	—
76	0	15.5	0.1-1u	15.4	<0.1u	18.0	—	—	—
77	0	12.1	0.1-0.5u	16.7	<0.1u	10.7	—	—	—

Table 3.1 Sedimentary Literature Review

	A	B	C	D	E	F	G
1	Sample I.D	Dep. Env.	Tmax (est.)	Location	Stratigraphic Unit	Lithology	Age
2							
78	<EY1985-158	T: ba-v	160min-250max	MT: Disturbed Belt	Telegraph Creek F.	BE: cl 95	U. Cret.
79	"	T: ba-v	160min-250max	MT: Disturbed Belt	"	"	"
80	"	T: ba-v	160min-250max	MT: Disturbed Belt	"	"	"
81	[EY1985-163	T: ba-v	160min-250max	MT: Disturbed Belt	Marias River Shale F.	SH: q 35, pl 5, cl 60	U. Cret.
82	[EY1985-162	T: ba-v	160min-250max	MT: Disturbed Belt	Marias River Shale F.	BE: pl 25, cl 65, cc 5	U. Cret.
83	<EY1985-179	T: ba-v	160min-250max	MT: Disturbed Belt	Colorado Group	SH: q 35, cl 60	Cret.
84							
85	<EY1985-178	T: ba-v	160min-250max	MT: Disturbed Belt	Colorado Group	BE: q 5, pl 40, cl 55	Cret.
86	[EY1985-E2	T: ba-v	160min-250max	MT: Sweetgrass Arch	Colorado Group	SH: q 30, cl 40, py10, gy	Cret.
87	[EY1985-E1	T: ba-v	160min-250max	MT: Sweetgrass Arch	Colorado Group	BE: q 15, pl 45, cl 35, gy	Cret.
88	"	T: ba-v	160min-250max	MT: Sweetgrass Arch	"	"	"
89	<EY1985-E22	T: ba-v	160min-250max	MT: Disturbed Belt	Colorado Group	SH: q 25, pl 5, cl 70	Cret.
90	<EY1985-E21	T: ba-v	160min-250max	MT: Disturbed Belt	Colorado Group	BE: pl 5, cl 95	Cret.
91	[EY1985-E24	T: ba-v	160min-250max	MT: Disturbed Belt	Colorado Group	SH: q 24, pl 5, cl 70	Cret.
92	[EY1985-E23	T: ba-v	160min-250max	MT: Disturbed Belt	Colorado Group	BE: q 10, cl 60, cc 30	Cret.
93	"	"	160min-250max	MT: Disturbed Belt	"	"	"
94	"	"	160min-250max	MT: Disturbed Belt	"	"	"
95							
96							
97	Silverman, Sol R. 1951. The isotope geology of oxygen. GCA 2:26-42.						
98							
99	S1951-2	—	—	EN: Dover Cliffs	—	flint nodule	—
100	S1951-9	—	—	IA: Belleview	Maquoketa Shale	SH	U. Ord.
101	S1951-13	—	—	CA: Santa Barbara Co.	—	DE	—
102	S1951-46	M: sc	—	MN: St. Paul	St. Peter ss	QA, little cement	—
103	S1951-2698	—	—	CT: New Haven	—	AK	Trias.
104	S1951-F-75	—	—	LR: Gasson Lake	Wishart oq	QA, 20% authigenic silica	L. Prot.
105	S1951-2039	M: sc	—	WI: Sauk Co.	Potsdam ss	QA	—
106							
107							
108	Eslinger, Eric V. and Samuel M. Savin. 1973. GSA Bul. 84:2549-2560.						
109							
110	ES1973-28	M: gs	—	MT: Glac. Nat. Park	Siyeh Limestone?	DO: q27, ill+ch148, fsp5, do 20	M-U Prot.
111	ES1973-1	M: gs	225°C	MT: Glac. Nat. Park	Siyeh Limestone	DO: q20, ill+ch166, fsp11, cc 3	M-U Prot.
112	ES1973-4	M: gs	—	MT: Glac. Nat. Park	Siyeh Limestone	DO: q ab, cc 10, do 17	M-U Prot.
113	ES1973-25	M: gs	—	MT: Glac. Nat. Park	Siyeh Limestone	DO: q25, ill+ch161, fsp8, do6	M-U Prot.
114	ES1973-17	M: gs	245°C	MT: Glac. Nat. Park	Grinnell Argillite	AR: q24, ill+ch167, fsp8	M-U Prot.
115	ES1973-19	M: gs	260°C	MT: Glac. Nat. Park	Grinnell Argillite	AR: q22, ill+ch170, fsp8	M-U Prot.
116	ES1973-21	M: gs	245°C	MT: Glac. Nat. Park	Grinnell Argillite	AR: q25, ill+ch163, fsp12	M-U Prot.
117	ES1973-23	M: gs	310°C	MT: Glac. Nat. Park	Appekuny Argillite	AR+QZ: q22, ill+ch166, fsp12	M-U Prot.
118	ES1973-10	M: gs	—	MT: Glac. Nat. Park	Appekuny Argillite	AR+QZ: q ab, fsp ab	M-U Prot.
119							
120							
121	Taylor, H.P., Jr., and Epstein, S., 1962, J.G.R. 67: 4485-4490.						
122							
123	TEK1962-47	M	—	PA: Lanesboro	New Milford Shale	SH	Dev.
124	TEK1962-27	M	—	NY: Lewistown	Queenston Shale	SH	Ord.
125	TEK1962-GR	M	—	NY: Rochester	Sodus Shale	SH	Sil.
126	TEK1962-53	M	—	IN: Crawfordsville	Keokuk Shale	SH	Miss.
127	TEK1962-CG	M	—	CA: Santa Ana Mts.	—	CG: shale-chip w/arkosic matrix	Cret.
128							
129							
130	Savin, S.M., 1967, Ph.D. Thesis.						
131							
132	SE1970c-E14	M	—	AU: Gulf of Carpenteria	Crawford Formation	SS: gl., Fe oxides, >95% Q	M. Prot.
133	SE1970c-E15	M	—	AU: Gulf of Carpenteria	Crawford Formation	SS: gl., Fe oxides, >95% Q	M. Prot.
134	SE1970c-E16	M	—	AU: Gulf of Carpenteria	Crawford Formation	SS: gl., Fe oxides, >95% Q	M. Prot.
135	SE1970c-E18	M	—	AU: Gulf of Carpenteria	Crawford Formation	SS: gl., Fe oxides, >95% Q	M. Prot.
136	SE1970c-E19	M	—	AU: Gulf of Carpenteria	Crawford Formation	SS: gl., Fe oxides, >95% Q	M. Prot.
137							
138							
139	Savin, S.M. and Epstein, S., 1970b, GCA 34: 43-63.						
140							
141	SE1970b-J4	M, pg	—	Ocean cores	—	AR: sm, ill, k, chl, <14% Q	—
142	SE1970b-J11	M, pg	—	Ocean cores	—	AR: sm, ill, k, chl, <14% Q	—
143	SE1970b-J20	M, pg	—	Ocean cores	—	AR: sm, ill, k, chl, <14% Q	—
144	SE1970b-J11b	M, pg	—	Ocean cores	—	AR: sm, ill, k, chl, <14% Q	—
145	SE1970b-L159	M, pg	—	Ocean cores	—	AR: sm, ill, k, chl, <14% Q	—
146	SE1970b-L163	M, pg	—	Ocean cores	—	AR: sm, ill, k, chl, <14% Q	—
147	SE1970b-L183	M, pg	—	Ocean cores	—	AR: sm, ill, k, chl, <14% Q	—
148	SE1970b-L212	M, pg	—	Ocean cores	—	AR: sm, ill, k, chl, <14% Q	—
149	SE1970b-L217	M, pg	—	Ocean cores	—	AR: sm, ill, k, chl, <14% Q	—
150	SE1970b-L223	M, pg	—	Ocean cores	—	AR: sm, ill, k, chl, <14% Q	—
151	S1970b-M121	M, pg	—	Ocean cores	—	AR: sm, ill, k, chl, <14% Q	—
152	S1970b-R56	M, pg	—	Ocean cores	—	AR: sm, ill, k, chl, <14% Q	—

Table 3.1 Sedimentary Literature Review

1	H	I	J	K	L	M	N	O	P
	% Cc or Do	∅ 18 O:W R	Quartz fraction	∅18 O:Quartz	Clay fraction	∅ 18 O: Clay	∅18O: C	∅13C : C	∅ 18 O : Misc.
2									
78	0	10.9	0.1-1u	15.5	<0.1 u	14.3	—	—	—
79	*	*	1-2u	15.7	<0.1 u	14.3	—	—	—
80	*	*	>2u	12.3	<0.1 u	14.3	—	—	—
81	0	—	0.1-0.5u	21.0	<0.1 u	14.8	—	—	—
82	0	—	>2u	12.6	<0.1 u	16.6	—	—	—
83	—	—	0.1-0.5u	18.5	<0.1 u	15.5	—	—	—
84									
85	—	—	1-2 u	17.1	<0.1 u	17.8	—	—	—
86	tr. do.	17.2	0.1-0.5u	24.1	<0.1 u	15.0	—	—	—
87	0	11.7	0.1-1u	23.6	<0.1 u	18.8	—	—	—
88	*	*	1-2u	23.0	<0.1 u	18.8	—	—	—
89	0	14.0	0.1-0.5u	22.7	<0.1 u	13.5	—	—	—
90	0	12.8	>2u	13.1	<0.1 u	14.1	—	—	—
91	0	13.5	0.1-0.5u	19.9	<0.1 u	13.8	—	—	—
92	30 cc	10.7	0.1-0.5	19.0	<0.1 u	14.6	—	—	—
93	*	*	1-2u	18.9	<0.1 u	14.6	—	—	—
94	*	*	>2u	18.6	<0.1 u	14.6	—	—	—
95									
96									
97									
98									
99	—	29.3	—	—	—	—	—	—	—
100	—	15.5	—	—	—	—	—	—	—
101	—	30.3	—	—	—	—	—	—	—
102	—	10.9	—	—	—	—	—	—	—
103	—	11.4	—	—	—	—	—	—	—
104	—	15.1	—	—	—	—	—	—	—
105	—	15.5	—	—	—	—	—	—	—
106									
107									
108									
109									
110	20 do	—	—	17.8	—	—	21.0	-2.3	fsp: 14.3
111	3 cc	18.7 no cc	—	21.5	—	16.6	18.4	0.5	fsp 19.3
112	10 cc, 17 do	—	—	—	—	—	18.8cc	-0.6	—
113	6 do	16.9 no cc	—	19.6	—	16.8	19.9	-1.2	fsp: 18.7
114	<1 do	15.3	—	18.3	—	13.8	20.4	-1.8	fsp: 16.8
115	<1 do	12.8	—	16.3	—	12.0	18.2	-2.0	fsp: 12.3
116	0	13.3	—	16.8	—	12.4	—	—	fsp: 13.1
117	0	14.6	—	17.5	—	13.8	—	—	fsp: 14.7
118	3 cc	14.4	—	16.7	—	—	15.1	-7.6	—
119									
120									
121									
122									
123	—	14.2	—	—	—	—	—	—	—
124	—	17.6	—	—	—	—	—	—	—
125	—	14.8	—	—	—	—	—	—	—
126	—	15.3	—	—	—	—	—	—	—
127	—	"18.2"	data for shale clast	—	—	—	—	—	12.6 (matrix)
128									
129									
130									
131									
132	0	13.7	—	13.9	—	gl 14.6	—	—	—
133	0	13.7	—	12.8	—	gl 13.7	—	—	—
134	0	14.4	—	14.5	—	gl 18.5	—	—	—
135	0	14.8	—	15.0	—	gl 17.0	—	—	12.0 mica
136	0	15.3	—	16.2	—	gl 16.4	—	—	12.9 mica
137									
138									
139									
140									
141	—	17.0	—	—	—	—	—	—	—
142	—	17.5	—	—	—	—	—	—	—
143	—	16.1	—	—	—	—	—	—	—
144	—	15.7	—	—	—	—	—	—	—
145	—	17.0	—	—	—	—	—	—	—
146	—	18.2	—	—	—	—	—	—	—
147	—	18.3	—	—	—	—	—	—	—
148	—	19.7	—	—	—	—	—	—	—
149	—	19.9	—	—	—	—	—	—	—
150	—	19.2	—	—	—	—	—	—	—
151	—	17.3	—	—	—	—	—	—	—
152	—	21.2	—	—	—	—	—	—	—

Table 3.1 Sedimentary Literature Review

	A	B	C	D	E	F	G
1	Sample I.D	Dep. Env.	Tmax (est.)	Location	Stratigraphic Unit	Lithology	Age
2							
153	S1970b-R69	M.pg	—	Ocean cores	—	AR: sm,ill,k,chl, <14% Q	—
154	S1970b-R80	M.pg	—	Ocean cores	—	AR: sm,ill,k,chl, <14% Q	—
155	S1970b-V75a	M.pg	—	Ocean cores	—	AR: sm,ill,k,chl, <14% Q	—
156	S1970b-V75b	M.pg	—	Ocean cores	—	AR: sm,ill,k,chl, <14% Q	—
157	S1970b-GR6	NM	—	WY: Green River	Green River F.	SH	—
158	S1970b-GR7	NM	—	WY: Green River	Green River F.	SH	—
159							
160	Lawrence, J.R., 1970, Ph. D. Thesis.						
161							
162	L1970-C871	T ?	—	N.W. United States	Claggett Shale	SH: q 15, cl 60, fsp 4	—
163	L1970-C872	T ?	—	N.W. United States	Claggett Shale	SH: q 18, cl 60, fsp 3	—
164	L1970-C885	T ?	—	SD: Stanley Co.	Pierre Shale	SH: q 19, cl 75, fsp 1	—
165	L1970-Jef-1	T ?	—	CO: Jefferson Co.	Pierre Shale Equivalent	SH: q 35, fsp 10, mont 40, chl 15	—
166	L1970-Mis-1	T ?	—	MT: Missoula Co.	Belt Series	SH	PreC
167							
168	L1970-Cal-5	T ?	—	CA: Inyo, White Mts	—	SH: q20,ill40,chl10,C25	Ord
169	L1970-BC-1	T ?	—	BC: Cranbrook	Eager Argillite	SH: q20,ill40,chl40	Camb
170	L1970-BC-3	T ?	—	BC: Cranbrook	Siyeh Formation	SH: q40,ill45,chl15	M-UProt
171	L1970-IN-1	T ?	—	IN: Shelby	Waldron Shale	SH: q20,ill10,chl10,C60	Sil
172	L1970-MT-3	T ?	—	MT: Missoula	Belt Series	SH: q20, fsp10, ill35, chl35	M-U Prot
173	L1970-MT-4	T ?	—	MT: Missoula	Belt Series	SH: q30, fsp15, ill40, chl15	M-U Prot
174	L1970-MT-7	T ?	—	MT	Blackleaf Formation	SH: q20, fsp10, ill50, chl20	U Cret
175	L1970-NY-1	T ?	—	NY: Livingstone	Moscow Shale	SH: q20, ill20, chl20, C40	Dev
176	L1970-NY-2	T ?	—	NY: Rochester	Vernon Shale	SH: q45, ill10, C45	Sil
177	L1970-OH-1	T ?	—	OH: Hamilton	Eden Shale	SH	U Ord
178							
179							
180	Longstaffe, F.J., 1986, J. Sed. Pet. 56:78-88						
181							
182	L1986-3	T:dc	75-90° C	CN:w-central Alberta	Basal Belly River F.	SS:q20, fsp16, o 46, m, si, v	U-Cret
183	L1986-4	T:dc	75-90° C	CN:w-central Alberta	Basal Belly River F.	SS:q20, fsp16, o 46, m, si, v	U-Cret
184	L1986-5	T:dc	75-90° C	CN:w-central Alberta	Basal Belly River F.	SS:q20, fsp16, o 46, m, si, v	U-Cret
185	L1986-18	T:dc	75-90° C	CN:w-central Alberta	Basal Belly River F.	Sl:	U-Cret
186	L1986-19	T:dc	75-90° C	CN:w-central Alberta	Basal Belly River F.	SS:q20, fsp16, o 46, m, si, v	U-Cret
187	L1986-22	T:dc	75-90° C	CN:w-central Alberta	Basal Belly River F.	SS:q20, fsp16, o 46, m, si, v	U-Cret
188							
189							
190	Magaritz, M. and Taylor, H.P., Jr., 1976, GCA 40: 215-234.						
191							
192	MT1976-10A	M: eg	100-300° C	CA: San Luis Obispo	Franciscan Formation	SH: q, fsp, chl, mica	M-U Jur
193	MT1976-10B	M: eg	100-300° C	CA: San Luis Obispo	Franciscan Formation	SH: q, fsp, mica	M-U Jur
194	MT1976-48	M: eg	100-300° C	CA: San Luis Obispo	Franciscan Formation	SH: q, fsp, mica	M-U Jur
195	MT1976-50	M: eg	U:100-300° C	CA: San Luis Obispo	Great Valley Sequence	GW: q, fsp, chl, mica	M-U Jur
196	MT1976-51A	M: eg	U:100-300° C	CA: San Luis Obispo	Great Valley Sequence	GW: q, mica	M-U Jur
197	MT1976-51B	M: eg	100-300° C	CA: San Luis Obispo	Great Valley Sequence	SH: q, fsp, chl (chip)	M-U Jur
198	MT1976-51C	M: eg	U:100-300° C	CA: San Luis Obispo	Great Valley Sequence	GW: q, fsp, mica (host rock)	M-U Jur
199	MT1976-52	M: eg	100-300° C	CA: San Luis Obispo	Franciscan Formation	SH: q, fsp, chl	M-U Jur
200	MT1976-54	M: eg	100-300° C	CA: San Luis Obispo	Franciscan Formation	SH: q, fsp, mica	M-U Jur
201	MT1976-56A	M: eg	100-300° C	CA: Sur	Franciscan Formation	GW: q, fsp, chl, lw	M-U Jur
202	MT1976-B	M: eg	100-300° C	CA: Sur	Franciscan Formation	SH: q, fsp, chl	M-U Jur
203	MT1976-57	M: eg	I:100-300° C	CA: Sur	Franciscan Formation	GW: q, fsp, mica, lw	M-U Jur
204	MT1976-58	M: eg	100-300° C	CA: Sur	Franciscan Formation	SH: q, mica, chl	M-U Jur
205	MT1976-60	M: eg	100-300° C	CA: Sur	Franciscan Formation	SH: q, cc, mica, chl	M-U Jur
206	MT1976-62B	M: eg	U:100-300° C	CA: Sur	Franciscan Formation	GW: q, fsp, do (host rock)	M-U Jur
207	MT1976-62A	M: eg	100-300° C	CA: Sur	Franciscan Formation	SH: q, fsp, mica, do (chip)	M-U Jur
208	MT1976-63	M: eg	100-300° C	CA: Sur	Franciscan Formation	GW: q, fsp, chl	M-U Jur
209	MT1976-65A	M: eg	I:100-300° C	CA: Mt. Hamilton	Franciscan Formation	GW: q, fsp, chl	M-U Jur
210	MT1976-65B	M: eg	I:100-300° C	CA: Mt. Hamilton	Franciscan Formation	GW: q, fsp, chl	M-U Jur
211	MT1976-67	M: eg	100-300° C	CA: Mt. Hamilton	Franciscan Formation	SH: q, fsp, chl	M-U Jur
212	MT1976-FR47	M: eg	U:100-300° C	CA: Fort Ross	Franciscan Formation	GW: q, fsp, mica	M-U Jur
213	MT1976-T45	M: eg	U:100-300° C	CA: Trinity	Franciscan Formation	GW: q, fsp, chl	M-U Jur
214	MT1976-T46A	M: eg	U:100-300° C	CA: Trinity	Franciscan Formation	GW: q, fsp, chl (host rock)	M-U Jur
215	MT1976-46B	M: eg	100-300° C	CA: Trinity	Franciscan Formation	SH: mica, chl, q, fsp (chip)	M-U Jur
216	MT1976-T37	M: eg	100-300° C	CA: Trinity	Franciscan Formation	SH: q, chl, mica	M-U Jur
217	MT1976-LN19	M: eg	U:100-300° C	CA:Laytonville-Newville	Franciscan Formation	GW: q, fsp, chl	M-U Jur
218	MT1976-LN21	M: eg	U:100-300° C	CA:Laytonville-Newville	Franciscan Formation	GW: q, fsp, chl	M-U Jur
219	MT1976-LN23	M: eg	I:100-300° C	CA:Laytonville-Newville	Franciscan Formation	GW: q, fsp, chl	M-U Jur
220	MT1976-24	M: eg	I:100-300° C	CA:Laytonville-Newville	Franciscan Formation	GW: q, chl, fsp	M-U Jur
221							
222							
223	Nabelek et al., 1984, Cont. Min. Pet. 86: 25-34.						
224							
225	NE1984-11H5	M: mg	—	UT: Notch Peak	Orr Formation *	AR: q, cc, fsp, mica, cl	U-Camb
226	NE1984-12H3	M: mg	—	UT: Notch Peak	Orr Formation	AR: q, cc, fsp, mica, cl	U-Camb
227	NE1984-11H7	M: mg	—	UT: Notch Peak	Orr Formation	AR: q, cc, fsp, mica, cl	U-Camb

Table 3.1 Sedimentary Literature Review

1	H	I	J	K	L	M	N	O	P
	% Cc or Do	∑ 18 O:W R	Quartz fraction	∑ 18 O:Quartz	Clay fraction	∑ 18 O: Clay	∑ 18O: C	∑ 13C: C	∑ 18 O: Misc.
2									
153	—	16.4	—	—	—	—	—	—	—
154	—	25.9	—	—	—	—	—	—	—
155	—	11.5	—	—	—	—	—	—	—
156	—	14.1	—	—	—	—	—	—	—
157	—	18.1	—	—	—	—	—	—	—
158	—	19.1	—	—	—	—	—	—	—
159									
160									
161									
162	—	14.6	—	—	ill 20, mont 20j-m 48	—	—	—	—
163	—	14.6	—	—	ill 17, mont 20j-m 53	—	—	—	—
164	—	19.7	—	—	ill 18, mont 33, i-m 44	—	—	—	—
165	—	15.3	—	—	—	—	—	—	—
166	—	15.0	—	—	—	—	—	—	—
167									
168	25	14.5	C not removed ?	—	—	—	16.7	—	—
169	0	13.5	—	—	—	—	—	—	—
170	0	13.0	—	—	—	—	—	—	—
171	60	—	—	—	—	—	28.1	—	—
172	0	15.4	—	—	—	—	—	—	—
173	0	15.0	—	—	—	—	—	—	—
174	0	14.4	—	—	—	—	—	—	—
175	40	14.9	C not removed ?	—	—	—	24.0	—	—
176	45	—	—	—	—	—	22.3	—	—
177	—	—	—	—	—	—	24.5	—	—
178									
179									
180									
181									
182	cc: tr	14.6	—	—	<2u: k62, ill16, ch121	11.3	—	—	—
183	cc: 15	13.7	—	—	<2u: k54, ill24, ch119	11.1	—	—	—
184	0	14.0	—	—	<2u: k19, ill12, ch69	6.8	—	—	—
185	—	14.2	—	—	<2u: k21, sm45, ill24, ch110	13.4	—	—	—
186	cc: tr	13.5	—	—	<2u: k59, chl 30	9.2	14.7cc	-5.6	do22.1,-1.7
187	cc: 1	14.5	—	—	<2u: k 42, chl 38	9.1	11.8cc	-5.1	—
188									
189									
190									
191									
192	—	15.6	—	17.3	—	—	—	—	—
193	—	16.3	—	16.6	—	—	—	—	—
194	—	17.3	—	—	—	—	—	—	—
195	—	10.7	—	10.9	—	—	—	—	7.8 mica
196	—	10.3	—	10.7	—	—	—	—	6.6 mica/9.7 f
197	—	12.0	—	—	—	—	—	—	—
198	—	12.1	—	—	—	—	—	—	—
199	—	13.4	—	—	—	—	—	—	—
200	—	17.3	—	—	—	—	—	—	—
201	—	12.7	—	—	—	—	—	—	—
202	—	12.7	—	—	—	—	—	—	—
203	—	12.6	—	13.2	—	—	—	—	—
204	—	10.8	—	—	—	—	—	—	—
205	cc	12.2	—	—	—	—	—	—	—
206	do	11.2	—	13.3	—	—	21.8	-4.3	—
207	do	11.2	—	—	—	—	25.0	-2.6	—
208	—	12.7	—	—	—	—	—	—	—
209	—	12.3	—	—	—	—	—	—	—
210	—	12.4	—	—	—	—	—	—	—
211	—	11.8	—	—	—	—	—	—	—
212	—	11.9	—	11.7	—	—	—	—	—
213	—	13.6	—	—	—	—	—	—	—
214	—	12.5	—	—	—	—	—	—	—
215	—	13.1	—	—	—	—	—	—	—
216	—	12.8	—	—	—	—	—	—	—
217	—	11.6	—	—	—	—	—	—	—
218	—	12.1	—	12.4	—	—	—	—	—
219	—	13.5	—	—	—	—	—	—	—
220	—	14.0	—	—	—	—	—	—	—
221									
222									
223									
224									
225	73	18.8	—	—	—	—	—	0.5	—
226	38	18.8	—	—	—	—	—	1.4	—
227	30	17.3	—	—	—	—	—	0.3	—

Table 3.1 Sedimentary Literature Review

	A	B	C	D	E	F	G
1	Sample I.D	Dep. Env.	Tmax (est.)	Location	Stratigraphic Unit	Lithology	Age
2							
228							
229	Barrett et al., 1983, Init. Repts. DSDP, 70.						
230							
231	B1983-1	M: pg	20-30° C	Galapagos Mounds	metalliferous sediments	Nontronite	U-Pleis
232	B1983-21	M: pg	20-30° C	Galapagos Mounds	metalliferous sediments	Nontronite	U-Pleis
233	B1983-3	M: pg	20-30° C	Galapagos Mounds	metalliferous sediments	Nontronite	U-Pleis
234	B1983-5	M: pg	20-30° C	Galapagos Mounds	metalliferous sediments	Nontronite	U-Pleis
235	B1983-22	M: pg	20-30° C	Galapagos Mounds	metalliferous sediments	Nontronite	U-Pleis
236	B1983-12	M: pg	20-30° C	Galapagos Mounds	metalliferous sediments	Nontronite	U-Pleis
237	B1983-23	M: pg	20-30° C	Galapagos Mounds	metalliferous sediments	Nontronite	U-Pleis
238	B1983-17	M: pg	20-30° C	Galapagos Mounds	metalliferous sediments	Nontronite	U-Pleis
239	B1983-24	M: pg	20-30° C	Galapagos Mounds	metalliferous sediments	Nontronite	U-Pleis
240	B1983-25	M: pg	20-30° C	Galapagos Mounds	metalliferous sediments	Nontronite	U-Pleis
241	B1983-26	M: pg	20-30° C	Galapagos Mounds	metalliferous sediments	Nontronite	U-Pleis
242	B1983-20	M: pg	20-30° C	Galapagos Mounds	metalliferous sediments	Nontronite	U-Pleis
243	B1983-15	M: pg	—	Galapagos Mounds	metalliferous sediments	Mn-oxide crust	U-Pleis
244	B1983-18	M: pg	—	Galapagos Mounds	metalliferous sediments	Mn-Fe-oxide mud	U-Pleis
245	B1983-10	M: pg	—	Galapagos Mounds	metalliferous sediments	Mn-oxide crust	U-Pleis
246	B1983-5	M: pg	10-7° C	Galapagos Mounds	pelagic ooze	5-10%cl, <10% Si fossils	U-Pleis
247	B1983-6	M: pg	10-7° C	Galapagos Mounds	pelagic ooze	5-10%cl, <10% Si fossils	U-Pleis
248	B1983-8	M: pg	10-7° C	Galapagos Mounds	pelagic ooze	5-10%cl, <10% Si fossils	U-Pleis
249	B1983-9	M: pg	10-7° C	Galapagos Mounds	pelagic ooze	5-10%cl, <10% Si fossils	U-Pleis
250							
251							
252							
253	Dymond, J., et al., 1973, GSA Bul. 84: 3355-3372.						
254							
255	D1973-37-3	M:pg	Low T	Central North Pacific	metalliferous sediments	Fe-sm, Fe-Mn oxides	Tert-Cret
256	D1973-37-5	M:pg	Low T	Central North Pacific	metalliferous sediments	Fe-sm, Fe-Mn oxides	Tert-Cret
257	D1973-38-3	M:pg	Low T	Central North Pacific	metalliferous sediments	Fe-sm, Fe-Mn oxides	Tert-Cret
258	D1973-38-4	M:pg	Low T	Central North Pacific	metalliferous sediments	Fe-sm, Fe-Mn oxides	Tert-Cret
259	D1973-39-3	M:pg	Low T	Central North Pacific	metalliferous sediments	Fe-sm, Fe-Mn oxides	Tert-Cret
260	D1973-39-5	M:pg	Low T	Central North Pacific	metalliferous sediments	Fe-sm, Fe-Mn oxides	Tert-Cret
261							
262							
263	Lawrence, J.R., 1973, Initial Reports of DSDP, v. 20.						
264							
265	L1973-240	M: pg	10-20° C	Venezuela Basin	—	Radiolarian marl, volcanic debris	Olig
266	L1973-260	M:pg	10-20° C	Venezuela Basin	—	Radiolarian marl, volcanic debris	Olig
267	L1973-340	M:pg	10-20° C	Venezuela Basin	—	ooze, marl, ash, pumice, chert	Eoc
268	L1973-375	M:pg	10-20° C	Venezuela Basin	—	ooze, marl, ash, pumice, chert	Eoc
269	L1973-380	M:pg	10-20° C	Venezuela Basin	—	Chert horizon: opal nodule	Eoc
270							
271							
272	Lawrence, J.R., 1974, Initial Reports of DSDP, v. 23.						
273							
274	L1974-6	M: ev	<70° C	Red Sea	—	silty oozes, chalks, calcareous silt	U-Pleis
275	L1974-85	M: ev	<70° C	Red Sea	—	silty oozes, chalks, calcareous silt	U-Plio
276	L1974-194	M: ev	<70° C	Red Sea	—	evaporites	U-Mio
277	L1974-260	M: ev	<70° C	Red Sea	—	evaporites	Mio
278	L1974-307	M: ev	<70° C	Red Sea	—	evaporites	L-Mio
279							
280							
281	Anderson, T.F. and Lawrence, J.R., 1976, Initial Reports of DSDP, v. 35.						
282							
283	AL1976-322a	M: pg	<40° C	SE Pacific Basin	—	SS: fine grained	Mio-Olig
284	AL1976-322b	M: pg	<40° C	SE Pacific Basin	—	AR: silty claystone	Mio-Olig
285	AL1976-322c	M: pg	<40° C	SE Pacific Basin	—	AR: claystone	Mio-Olig
286	AL1976-322d	M: pg	<40° C	SE Pacific Basin	—	AR: claystone 10 cm from basalt	Mio-Olig
287	AL1976-322a	M: pg	<40° C	SE Pacific Basin	—	Clayey diatom ooze	Hol-Mio
288	AL1976-322b	M: pg	<40° C	SE Pacific Basin	—	Diatom-rich clay	Mio
289	AL1976-322c	M: pg	<40° C	SE Pacific Basin	—	Diatom-rich clay and q clayey silt	Mio
290	AL1976-322d	M: pg	<40° C	SE Pacific Basin	—	CH: silicified claystone	Mio
291	AL1976-322e	M: pg	<40° C	SE Pacific Basin	—	Partly silicified claystone	Mio
292	AL1976-322f	M: pg	<40° C	SE Pacific Basin	—	CH	Mio
293	AL1976-322g	M: pg	<40° C	SE Pacific Basin	—	AR: claystone	Mio
294	AL1976-322h	M: pg	<40° C	SE Pacific Basin	—	CH	Mio
295	AL1976-322i	M: pg	<40° C	SE Pacific Basin	—	AR: Claystone	Mio
296	AL1976-322j	M: pg	<40° C	SE Pacific Basin	—	CH	Mio
297	AL1976-322k	M: pg	<40° C	SE Pacific Basin	—	AR: q silty claystone	Mio
298	AL1976-322l	M: pg	<40° C	SE Pacific Basin	—	SI: clayey siltstone	Mio
299	AL1976-322m	M: pg	<40° C	SE Pacific Basin	—	Fe- claystone	Paleo
300	AL1976-322n	M: pg	<40° C	SE Pacific Basin	—	Fe- claystone	Paleo
301	AL1976-322o	M: pg	<40° C	SE Pacific Basin	—	AR: claystone	U-Cret
302	AL1976-322p	M: pg	<40° C	SE Pacific Basin	—	AR: claystone	U-Cret

Table 3.1 Sedimentary Literature Review

	H	I	J	K	L	M	N	O	P
1	% Cc or Do	∅ 18 O:W R	Quartz fraction	∅18 O:Quartz	Clay fraction	∅ 18 O: Clay	∅18O: C	∅13C : C	∅ 18 O : Misc.
2									
228									
229									
230									
231	—	25.9	—	—	—	—	—	—	—
232	—	25.3	—	—	—	—	—	—	—
233	—	26.5	—	—	—	—	—	—	—
234	—	26.0	—	—	—	—	—	—	—
235	—	24.9	—	—	—	—	—	—	—
236	—	24.6	—	—	—	—	—	—	—
237	—	26.9	—	—	—	—	—	—	—
238	—	26.7	—	—	—	—	—	—	—
239	—	26.2	—	—	—	—	—	—	—
240	—	24.6	—	—	—	—	—	—	—
241	—	24.2	—	—	—	—	—	—	—
242	—	26.7	—	—	—	—	—	—	—
243	—	3.7	—	—	—	—	—	—	—
244	—	13.8	—	—	—	—	—	—	—
245	—	9.4	—	—	—	—	—	—	—
246	>80% cc	—	—	—	—	—	31.8	1.5	—
247	>80% cc	—	—	—	—	—	32.3	1.8	—
248	>80% cc	—	—	—	—	—	31.7	0.6	—
249	>80% cc	—	—	—	—	—	32.6	1.9	—
250									
251									
252									
253									
254									
255	—	15.8	—	—	—	—	—	—	—
256	—	16.2	—	—	—	—	—	—	—
257	—	13.2	—	—	—	—	—	—	—
258	cc	11.1	—	—	—	—	—	—	—
259	—	13.9	—	—	—	—	—	—	—
260	—	12.8	—	—	—	—	—	—	—
261									
262									
263									
264									
265	—	25.0	—	—	—	—	29.0	—	—
266	—	28.0	—	—	—	—	29.1	—	—
267	—	30.5	—	—	—	—	28.7	—	—
268	—	32.0	—	—	—	—	28.5	—	—
269	—	34.0	—	—	—	—	28.2	—	—
270									
271									
272									
273									
274	30-65%	18.1	—	—	—	—	35.0	0.8	—
275	30-65%	12.6	—	—	—	—	30.9	0.8	—
276	<25 %	11.7	—	—	—	—	30.0	0.0	—
277	<25 %	10.5	—	—	—	—	—	—	—
278	<25 %	15.3	—	—	—	—	—	—	—
279									
280									
281									
282									
283	—	10.9	—	—	—	—	—	—	—
284	—	12.9	—	—	—	—	—	—	—
285	—	19.9	—	—	—	—	—	—	—
286	—	16.8	—	—	—	—	—	—	—
287	—	19.7	—	—	—	—	—	—	—
288	—	17.7	—	—	—	—	—	—	—
289	—	12.3	—	—	—	—	—	—	—
290	—	31.2	—	—	—	—	—	—	—
291	—	17.1	—	—	—	—	—	—	—
292	—	29.4	—	—	—	—	—	—	—
293	—	14.8	—	—	—	—	—	—	—
294	—	24.1	—	—	—	—	—	—	—
295	—	13.2	—	—	—	—	—	—	—
296	—	21.1	—	—	—	—	—	—	—
297	—	14.3	—	—	—	—	—	—	—
298	—	13.3	—	—	—	—	—	—	—
299	—	19.3	—	—	—	—	—	—	—
300	—	18.7	—	—	—	—	—	—	—
301	—	20.8	—	—	—	—	—	—	—
302	—	20.6	—	—	—	—	—	—	—

Table 3.1 Sedimentary Literature Review

	A	B	C	D	E	F	G
1	Sample I.D	Dep. Env.	Tmax (est.)	Location	Stratigraphic Unit	Lithology	Age
2							
303	AL1976-323q	M: pg	<40° C	SE Pacific Basin	—	AR: claystone	U-Cret
304	AL1976-323r	M: pg	<40° C	SE Pacific Basin	—	AR: zeolitic claystone	U-Cret
305	AL1976-325a	M: pg	<40° C	SE Pacific Basin	—	Non-C in nannochalk	Mio-Q
306	AL1976-325b	M: pg	<40° C	SE Pacific Basin	—	AR: claystone	Mio
307	AL1976-325c	M: pg	<40° C	SE Pacific Basin	—	CG: clay conglomerate	Mio
308							
309							
310	Lawrence, J.R., et al, 1979, GCA 43: 573-588.*						
311							
312	L1979-82	M:pg	<40° C	SE Pacific Basin	—	Sandy silt, diatomclay : il-sm	Q
313	L1979-260	M:pg	<40° C	SE Pacific Basin	—	Sandy silt, diatomclay : il-sm	Mio
314	L1979-550	M:pg	<40° C	SE Pacific Basin	—	AR: claystone, sm	Olig
315	L1979-626	M:pg	<40° C	SE Pacific Basin	—	AR: claystone, sm	Olig
316	L1979-638	M:pg	<40° C	SE Pacific Basin	—	AR: claystone, sm	Olig-Eoc
317	L1979-655	M:pg	<40° C	SE Pacific Basin	—	AR: iron-rich claystone, sm	Eoc
318	L1979-670	M:pg	<40° C	SE Pacific Basin	—	AR: zeolitic claystone, sm	Paleo
319	L1979-683	M:pg	<40° C	SE Pacific Basin	—	AR: zeolitic claystone, sm	Paleo
320	L1979-696	M:pg	<40° C	SE Pacific Basin	—	AR: zeolitic claystone, sm	Cret
321	L1979-697	M:pg	<40° C	SE Pacific Basin	—	AR: zeolitic claystone, sm	Cret
322	L1979-700	M:pg	<40° C	SE Pacific Basin	—	AR: zeolitic claystone, sm *	Cret
323							
324							
325	Barrett, T.J. et al., 1988, Canadian Mineralogist 26: 841-848.						
326							
327	B1988-25	M:pg	27°C *	Galapagos Mounds	—	slightly granular notronite	Pleis
328	B1988-67	M:pg	21°C	Galapagos Mounds	—	granular notronite	Pleis
329	B1988-36	M:pg	—	Galapagos Mounds	—	notronite with Fe-Mn oxide mud	Pleis
330	B1988-102	M:pg	137°C	Galapagos Mounds	—	granular notronite	Pleis
331	B1988-93	M:pg	19°C	Galapagos Mounds	—	slightly granular notronite	Pleis
332	B1988-80	M:pg	—	Galapagos Mounds	—	transitional notronite	Pleis
333							
334	B1988-96	M:pg	19°C	Galapagos Mounds	—	granular notronite	Pleis
335	B1988-132	M:pg	19°C	Galapagos Mounds	—	granular notronite	Pleis
336	B1988-31	M:pg	—	Galapagos Mounds	—	transitional notronite	Pleis
337	B1988-113	M:pg	—	Galapagos Mounds	—	gelatinous mud:oxides	Pleis
338	B1988-125	M:pg	21°C	Galapagos Mounds	—	granular notronite:oxides	Pleis
339	B1988-120	M:pg	—	Galapagos Mounds	—	gelatinous mud:oxides	Pleis
340	B1988-144	M:pg	9°C	Galapagos Mounds	—	granular notronite	Pleis
341	B1988-59	M:pg	—	Galapagos Mounds	—	transitional notronite	Pleis
342	B1988-142	M:pg	—	Galapagos Mounds	—	transitional notronite	Pleis
343	B1988-30	M:pg	36°C	Galapagos Mounds	—	Notronitic mottle	Pleis
344	B1988-30b	M:pg	26°C	Galapagos Mounds	—	Subsample	Pleis
345							
346							
347	Bray, C.J. et al., 1988, Can. Miner. 26: 249-268.						
348							
349	B1988-2038	M-NM: ba	—	CN: Saskatchewan	Athabasca Sandstone	SS: quartz; fluvial	M-Prot
350	B1988-1004	M-NM: ba	—	CN: Saskatchewan	Athabasca Sandstone	SS: quartz; fluvial	M-Prot
351	B1988-1186	M-NM: ba	—	CN: Saskatchewan	Athabasca Sandstone	SS: quartz; fluvial	M-Prot
352	B1988-1001	M-NM: ba	—	CN: Saskatchewan	Athabasca Sandstone	SS: quartz; fluvial	M-Prot
353	B1988-331	M-NM: ba	—	CN: Saskatchewan	Athabasca Sandstone	SS: quartz; fluvial	M-Prot
354							
355							
356	Matthews, A. and Kolodny, Y., 1978, E.P.S.L. 39: 179-192.						
357							
358	MK1978-SG57	M: ev	—	Israel	—	marl: clay, carbonates	UCret(Ter)
359	MK1978-549B	M: ev	—	Israel	Ghareb F.	phosphatic chalk: clay, ca	U-Cret
360	MK1978-167S	M: ev	—	Israel	Taqiya F.	SH: clay, carbonates	Paleo
361	MK1978-170S	M: ev	—	Israel	Taqiya F.	SH: clay, carbonates	Paleo

Table 3.1 Sedimentary Literature Review

1	H	I	J	K	L	M	N	O	P
	% Ce or Do	$\delta^{18} \text{O:W R}$	Quartz fraction	$\delta^{18} \text{O:Quartz}$	Clay fraction	$\delta^{18} \text{O:Clay}$	$\delta^{18}\text{O: C}$	$\delta^{13}\text{C: C}$	$\delta^{18} \text{O: Misc.}$
2									
303	—	18.6	—	—	—	—	—	—	—
304	—	19.9	—	—	—	—	—	—	—
305	—	20.0	—	—	—	—	—	—	—
306	—	8.6	—	—	—	—	—	—	—
307	—	9.1	—	—	—	—	24.3 *	-21.2	—
308									
309									
310									
311									
312	—	19.7	—	—	—	—	—	—	—
313	—	17.7	—	—	—	—	—	—	—
314	—	13.6	—	—	—	—	—	—	—
315	—	13.2	—	—	—	—	—	—	—
316	—	19.3	—	—	—	—	—	—	—
317	—	18.7	—	—	—	—	—	—	—
318	—	20.8	—	—	—	—	—	—	—
319	—	22.4	—	—	—	—	—	—	—
320	—	19.4	—	—	—	—	—	—	—
321	—	33.0	—	—	—	—	—	—	—
322	—	19.6	—	—	—	—	—	—	—
323									
324									
325									
326									
327	—	24.8	—	—	—	—	—	—	—
328	—	25.9	—	—	—	—	—	—	—
329	—	14.0	—	—	—	—	—	—	—
330	—	11.2	—	—	—	—	—	—	—
331	—	26.3	—	—	—	—	—	—	—
332	C	18.2	—	—	—	—	—	—	—
333									
334	—	26.3	—	—	—	—	—	—	—
335	—	26.2	—	—	—	—	—	—	—
336	—	22.4	—	—	—	—	—	—	—
337	—	-6.0	—	—	—	—	—	—	—
338	C	26.4	—	—	—	—	—	—	—
339	—	8.3	—	—	—	—	—	—	—
340	—	28.6	—	—	—	—	—	—	—
341	—	23.0	—	—	—	—	—	—	—
342	—	23.0	—	—	—	—	—	—	—
343	C	23.0	—	—	—	—	—	—	—
344	—	25.0	—	—	—	—	—	—	—
345									
346									
347									
348									
349	—	9.9	—	—	—	—	—	—	—
350	—	10.0	—	—	—	—	—	—	—
351	—	11.4	—	—	—	—	—	—	—
352	—	10.0	—	—	—	—	—	—	—
353	—	9.7	—	—	—	—	—	—	—
354									
355									
356									
357									
358	abundant	17.6	—	—	—	—	27.3	1.5	—
359	abundant	18.3	—	—	—	—	28.3	-0.5	—
360	abundant	19.6	—	—	—	—	28.5	1.9	—
361	abundant	16.8	—	—	—	—	28.4	1.9	—

CHAPTER 4

**Oxygen and Carbon Isotopic Compositions of Sedimentary
Rocks from Southern Utah, Northwestern Arizona,
and the Uinta Mountains, Utah****4.1 Description of the analyzed samples**

Thirty-eight samples of sedimentary rocks from the Colorado Plateau were analyzed for $\delta^{18}\text{O}$ (Table 2-1). The locations of the samples are shown in Figure 4.1. They cover a range of ages of lithologies from shale to sandstone and a range of ages of deposition from late Precambrian (Uinta Mountain Group - 3 samples) to Eocene (Uinta Formation - 1 sample), but most of the samples were deposited in the Permian (13 samples), the Triassic (8 samples), the Jurassic (8 samples), or the Cretaceous (3 samples). Only two Lower Paleozoic samples were analyzed.

The oldest analyzed samples are three Proterozoic sandstones from the Uinta Mountains deposited more than 1.5 billion years ago. These samples are well indurated and free of carbonate, and have uniformly low bulk silicate $\delta^{18}\text{O}$ values of +12.7 to +13.7.

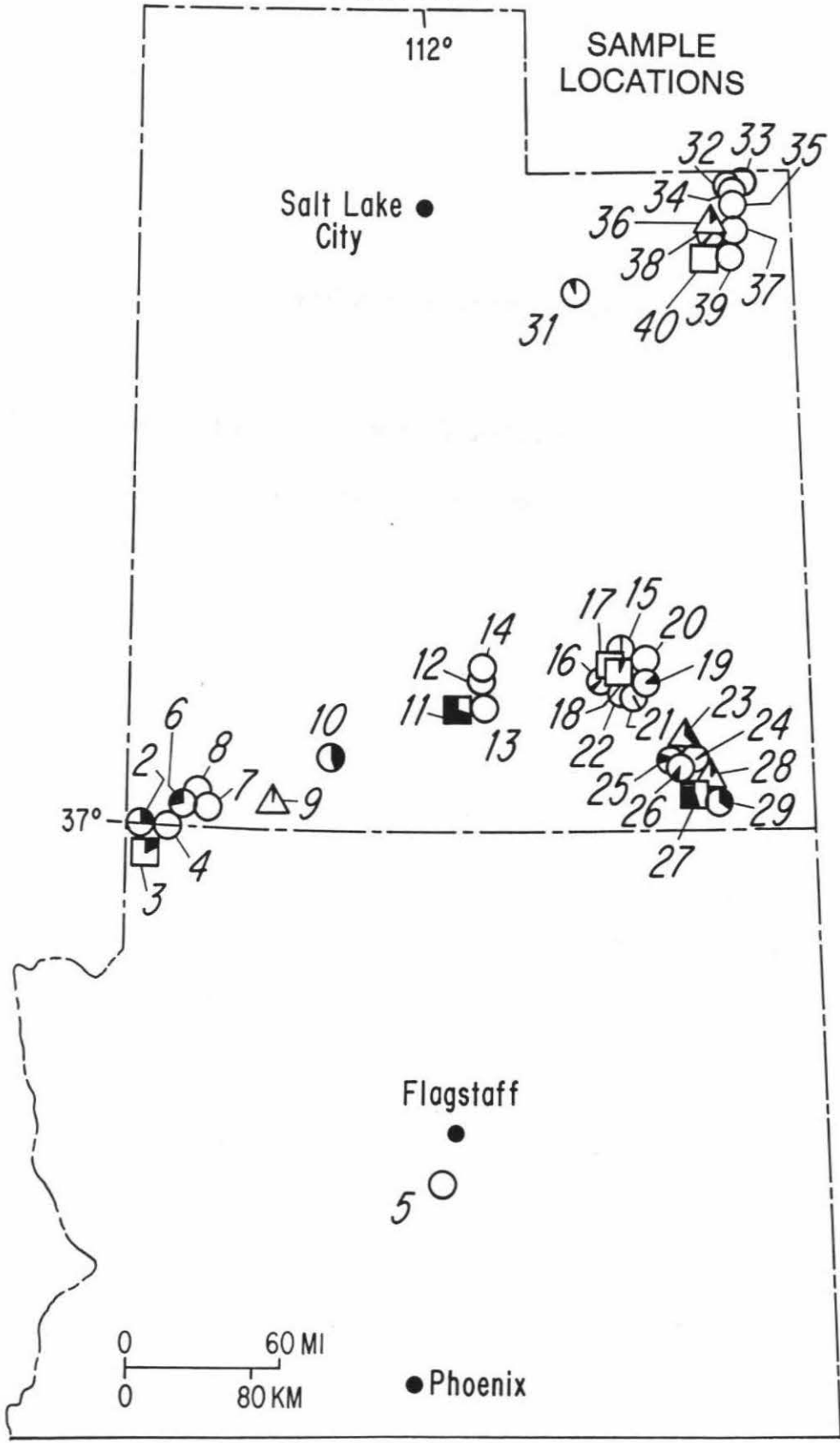
The two Lower Paleozoic samples are both marine deposits from the Virgin River Gorge in Arizona, and include a sandstone (bulk silicate $\delta^{18}\text{O} = +15.4$) and a shale ($\delta^{18}\text{O} = +17.9$); both samples contain large amounts of carbonate with $\delta^{18}\text{O} = +27.9$ to +28.1. Such high $\delta^{18}\text{O}$ values for the carbonates are indicative that these marine samples are well preserved, and only minimally shifted from their primary $\delta^{18}\text{O}$ values. These two samples also display relatively high $\delta^{13}\text{C} = +1.9$ to +3.1, typical of marine limestones.

The analyzed Upper Paleozoic samples are all of Permian age and include 10 samples of the Lower Permian Cutler Formation from Mexican Hat and Hite in Utah,

Figure 4.1

Map of Utah and Arizona showing sample locations of the sedimentary rocks studied in this work from the Colorado Plateau physiographic provinces. The symbols are as follows: circles = sandstones, triangles = siltstones, and squares = shales. The percent blackened area in each symbol indicates the weight per cent carbonate in the sample.

UTAH - ARIZONA



2 samples of red beds from Arizona, and the Weber Sandstone from the Uinta Mountains in northern Utah. The latter is a carbonate-free eolian quartz sandstone that has the lowest bulk silicate $\delta^{18}\text{O}$ of any of the Permian samples (+12.4). The two red sandstones from Arizona are also free of carbonate and have bulk silicate $\delta^{18}\text{O} = +13.7$ and +15.8. Several of the samples from the Cutler Formation, which formed in a transitional or oscillating marine/nonmarine environment, contain large amounts of carbonate (Table 2-1), commonly 15-60%. The 6 carbonate-rich Cutler samples include one shale, 2 siltstones, and 3 sandstones. The shale sample is a calcilutite with bulk silicate $\delta^{18}\text{O} = +16.7$, higher than any other Permian sample in the data set. The 2 siltstones have intermediate bulk silicate $\delta^{18}\text{O} = +14.3$ and +15.2, and the 3 sandstones have somewhat lower bulk silicate $\delta^{18}\text{O} = +13.3$ to +14.3. The 4 Cutler samples with less than 5% carbonate are also all quartz sandstones, and they display still lower bulk silicate $\delta^{18}\text{O} = +12.9$ to +13.9.

The carbonate $\delta^{18}\text{O}$ values of these samples of the Cutler Formation range from +20.9 to +31.1, and form a bimodal population, six (fresh water? and/or exchanged?) samples with $\delta^{18}\text{O} = +21.0$ to +24.5 and $\delta^{13}\text{C} = -2.9$ to +0.4, and three (marine? and/or more pristine?) samples with $\delta^{18}\text{O} = +27.7$ to +31.1 and $\delta^{13}\text{C} = -0.1$ to +1.3.

The analyzed Triassic samples are mainly from the Moenkopi Formation, which is a widespread fluvial and lacustrine unit found all across the Colorado Plateau. Two fluvial sandstone samples were also analyzed from the Upper Triassic Chinle Formation; these have bulk silicate $\delta^{18}\text{O} = +14.4$ and +14.8. One contains 8.8% carbonate with a very low $\delta^{18}\text{O} = +18.8$ and a very low $\delta^{13}\text{C} = -5.7$, probably indicative of

deposition in a fresh-water environment. The six Moenkopi samples range in bulk silicate $\delta^{18}\text{O}$ from a low of +13.2 in a carbonate-rich siltstone from northern Utah to a high of +16.2 and +16.7 in two red shales from southern Utah. Intermediate $\delta^{18}\text{O}$ values of +14.2, +15.3, and +16.2 are observed in the Moenkopi siltstones and sandstones from southern Utah. Most of these Moenkopi samples are relatively low in carbonate (0-13%), except in the aforementioned siltstone from northern Utah which contains 16.6% carbonate. The Moenkopi carbonates show a $\delta^{18}\text{O}$ range from +23.2 to +28.0 and $\delta^{13}\text{C}$ from -4.6 to +0.8. These relatively low isotopic values are typical of relatively unexchanged primary depositional values in carbonates formed in fresh-water environments.

Half of the 8 Jurassic samples were collected from a single formation, the Lower Jurassic Navajo Sandstone, which forms massive cliffs of eolian quartz sandstone over much of Utah. These Navajo Sandstone samples have relatively uniform whole-rock $\delta^{18}\text{O}$ values of +12.3 to +13.8; the lower $\delta^{18}\text{O}$ value is from the northernmost outcrop sampled. Other analyzed Jurassic samples include: (1) an eolian quartz sandstone (bulk silicate $\delta^{18}\text{O} = +13.5$) from the Lowermost Jurassic Wingate Formation that is petrographically and isotopically similar to the Navajo Sandstone samples, except that it contains a trace of carbonate ($\delta^{18}\text{O} = +21.7$ and $\delta^{13}\text{C} = +2.8$); (2) a carbonate-rich, feldspathic red sandstone from the Lower Jurassic fluvial Kayenta Formation, which has a bulk silicate $\delta^{18}\text{O} = +15.2$ and contains 26.1% carbonate with $\delta^{18}\text{O} = +17.0$ and $\delta^{13}\text{C} = -2.4$; (3) an extremely carbonate-rich sample of shaly calcilutite from the Middle Jurassic marine Carmel Formation, which has a very high bulk silicate $\delta^{18}\text{O} = +18.5$ and which contains 69.6% carbonate with $\delta^{18}\text{O} = +23.4$ and $\delta^{13}\text{C} = +2.8$; and

(4) a lithic bentonitic sandstone from the Upper Jurassic Morrison Formation that has the highest bulk silicate $\delta^{18}\text{O}$ value of any sample from the Colorado Plateau data set, +20.6.

The three Cretaceous samples include the marine Lower Cretaceous Mowry Shale, which has the second highest bulk silicate $\delta^{18}\text{O}$ value of these Colorado Plateau samples, +20.0. The other two samples are Upper Cretaceous fluvial sandstones, the Dakota and Wahweap. The carbonate-free Dakota Sandstone has whole rock $\delta^{18}\text{O} = +14.9$, while the carbonate-rich Wahweap Sandstone has a bulk silicate $\delta^{18}\text{O} = +15.9$ and 43.4% carbonate with $\delta^{18}\text{O} = +16.3$ and $\delta^{18}\text{O} = 0.0$.

The youngest sample studied is a tuffaceous sandstone from the Eocene Uinta Formation. This fluvial/lacustrine sandstone has a bulk silicate $\delta^{18}\text{O} = +14.6$ and contains 10.7% carbonate with $\delta^{18}\text{O} = +16.4$ and $\delta^{13}\text{C} -2.7$. This sample and the slightly older Wahweap Sandstone described above have the lowest calcite $\delta^{18}\text{O}$ values in this Colorado Plateau data set. The extremely low $\delta^{18}\text{O}$ values of these calcites are undoubtedly attributable to deposition from, or exchange with, low- $\delta^{18}\text{O}$ meteoric waters, probably during diagenesis.

4.2 Overview of bulk $^{18}\text{O}/^{16}\text{O}$ silicate data

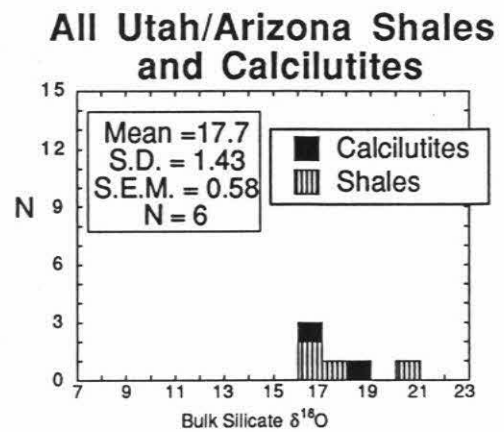
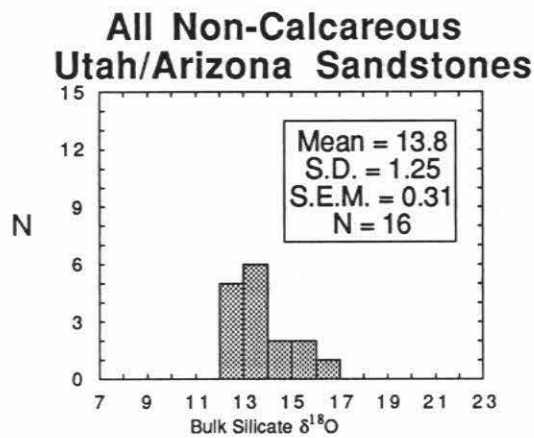
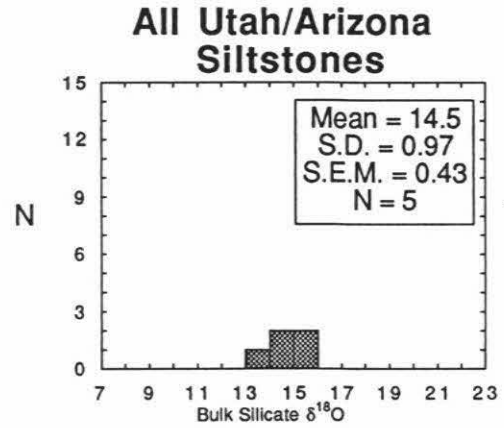
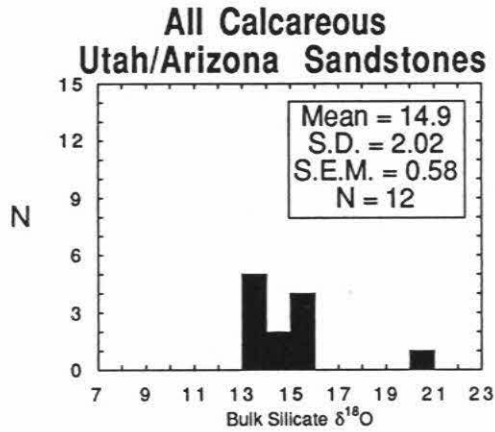
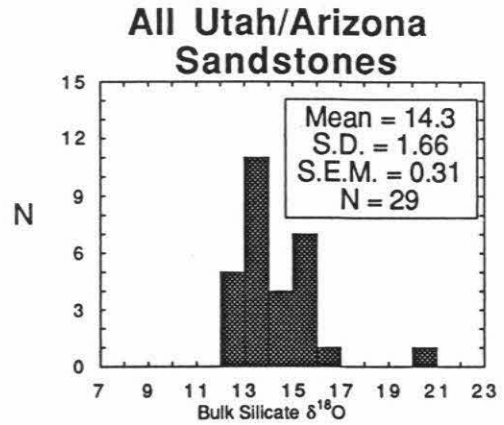
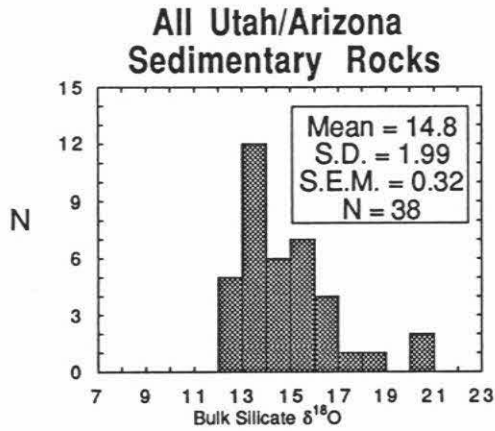
The Colorado Plateau sedimentary rocks from the localities shown in Figure 4.1 have a fairly uniform mean bulk silicate $\delta^{18}\text{O}$ of +14.8 and a standard error of the mean (SEM) of 0.32 per mil. An analysis of variance followed by a 5% Student-Neuman-Keuls multiple range test indicates that the group containing calcilutites and shales, with a mean bulk silicate $\delta^{18}\text{O} = +17.7$, has a significantly higher bulk silicate $\delta^{18}\text{O}$ than the calcareous sandstones (+14.9), the noncalcareous sandstones

(+13.8), or the siltstones (+14.5). However, the calcareous sandstones, the noncalcareous sandstones, and the siltstones are statistically not significantly different from one another in bulk silicate $\delta^{18}\text{O}$, particularly if the anomalously ^{18}O -rich calcareous sandstone sample from the Morrison Formation is deleted from the population (Figure 4.2). Nonetheless, even excluding this sandstone sample with $\delta^{18}\text{O} = +20.6$, there is some tendency for the calcareous sandstones to be slightly higher in ^{18}O than their non-calcareous counterparts (mean bulk silicate $\delta^{18}\text{O} = +14.4$ vs. +13.8). The 29 sandstones lumped together have a mean bulk silicate $\delta^{18}\text{O}$ of +14.3 and a SEM of 0.31 per mil, indistinguishable from the 5 siltstones, which have a mean bulk silicate $\delta^{18}\text{O}$ of +14.5 and a SEM of 0.43 per mil.

The six shale and calcilutite samples were collected from widely separated localities in the Uinta Mountains, northern Utah; Mexican Hat, Hite, and Escalante, southern Utah; and the Virgin River Gorge, northwestern Arizona. They have a relatively uniform mean bulk silicate $\delta^{18}\text{O}$ of +17.7 with a SEM of 0.58, in spite of the fact that they were formed in a great variety of depositional environments, including marine, tidal flat, fluvial, and deltaic. One possible reason for the heavier $\delta^{18}\text{O}$ value of the calcilutite might be the presence of high- ^{18}O chert formed during diagenesis of this sample. Chert is a common product of diagenesis in calcilutites (Pettijohn, 1975; Degens and Epstein, 1962; Wilson, 1966). Another possibility is that the bulk silicate fractions of the calcilutites contain a large component of clay minerals, which would also be high in $\delta^{18}\text{O}$. Still another possibility is that the $\delta^{18}\text{O}$ was increased during diagenetic exchange between very fine-grained, high- ^{18}O carbonate material and the co-existing fine-grained bulk silicate material in the presence of a small amount of aqueous

Figure 4.2

Six comparative histograms showing bulk silicate $\delta^{18}\text{O}$ values of terrigenous sedimentary rocks from Utah and Arizona. The plotted categories include: (a) all sedimentary rocks, (b) all sandstones (c) all calcareous sandstones, (d) all siltstones, (e) all non-calcareous sandstones, and (f) all shales and calcilutites. S.D. is standard deviation. S.E.M. is standard error of the mean. N is sample number. Statistics after Fisher et al. (1970).



pore fluid (see Chapters 5 and 7 for a more general discussion of this third possibility).

The two Utah/Arizona samples in the present data set which have bulk silicate $\delta^{18}\text{O}$ values of +20 or greater both probably contain altered volcanic debris. One is a sample of the Mowry Shale, which is reported by Hummel (1969) to be bentonitic in the region sampled. Bentonite typically has a very high $\delta^{18}\text{O}$ value because the dominantly montmorillonitic clays in such samples were usually formed by alteration of volcanic ash at very low temperatures (Savin and Epstein, 1970a, Eslinger and Yeh, 1986). Churchman *et al.* (1976) found that a sample of the Mowry Shale from Wyoming with an almost identical whole-rock $\delta^{18}\text{O} = +21.2$ contained 45 weight per cent quartz, and that this quartz had a $\delta^{18}\text{O}$ value of +23.2. Churchman *et al.* (1976) attributed the heavy $\delta^{18}\text{O}$ value of the quartz to its formation as chert or biogenic silica. The other sample with a high $\delta^{18}\text{O}$ value is a sample of a lithic arenite from the Morrison Formation in the Uinta Mountains, already referred to above. The Morrison Formation is described by Craig and Shawe (1975) as containing large amounts of sediments derived from volcanic detritus. Bentonitic clays and chalcedony are common low-temperature alteration products of volcanic glass and would be high in ^{18}O (Savin and Epstein, 1970a). Bentonitic mudstone is in fact, a dominant lithology of the Morrison Formation, and extensive reworking of volcanic material could have separated isotopically heavy volcanic glass from isotopically light volcanic phenocrysts. However, more detailed work is required to establish any possible relationship between volcanic detritus and $\delta^{18}\text{O}$ in this particular ^{18}O -rich sample of lithic arenite.

4.3 Comparison with cherts and carbonates

A number of samples of coexisting carbonate were analyzed in this study of the terrigenous sedimentary rocks of the Colorado Plateau (Table 2.1), and it is instructive to compare these new data with data from the literature. Also, even though they have markedly different origins than the terrigenous sedimentary rocks, it is useful to compare the $\delta^{18}\text{O}$ values of the two major kinds of biogenic-authigenic sedimentary rocks of the shelf environment (*e.g.*, limestones and cherts) with the $\delta^{18}\text{O}$ values obtained in the present study. Figure 4.3 is a comparison of marine chert $\delta^{18}\text{O}$ values from the literature with bulk silicate $\delta^{18}\text{O}$ values of the Utah/Arizona sedimentary rocks. Marine cherts show a range in $\delta^{18}\text{O}$ of more than 25 per mil, from values of about +10 to +35. This is in striking contrast to the much smaller range of bulk silicate $\delta^{18}\text{O}$ values of the terrigenous sedimentary rocks from the terrestrial and marine shelf environments in this study, which display a range of only 8.3 per mil. Chert $\delta^{18}\text{O}$ values show a distinct negative correlation with geologic age (Figure 4.3); the correlation coefficient ($r = 0.65$) is significant at the 0.01 probability level. The bulk silicate $\delta^{18}\text{O}$ values of the Utah/Arizona rocks in this study also have a slightly negative correlation with geologic age, but the correlation coefficient ($r = 0.25$) is not statistically significant (Figure 4.3).

Figure 4.4 is a set of comparative histograms compiled from the same data set shown in Figure 4.3. These histograms show that the Utah/Arizona sedimentary rocks in this study have relatively uniform $\delta^{18}\text{O}$ values over geologic time. Marine cherts typically show a broad scatter of $\delta^{18}\text{O}$ within each geologic time period, in addition to a shift of the mean $\delta^{18}\text{O}$ to much lower values in successively older geologic eras. Knauth and Lowe (1978) interpret the scatter in marine chert $\delta^{18}\text{O}$ within the same

Figure 4.3

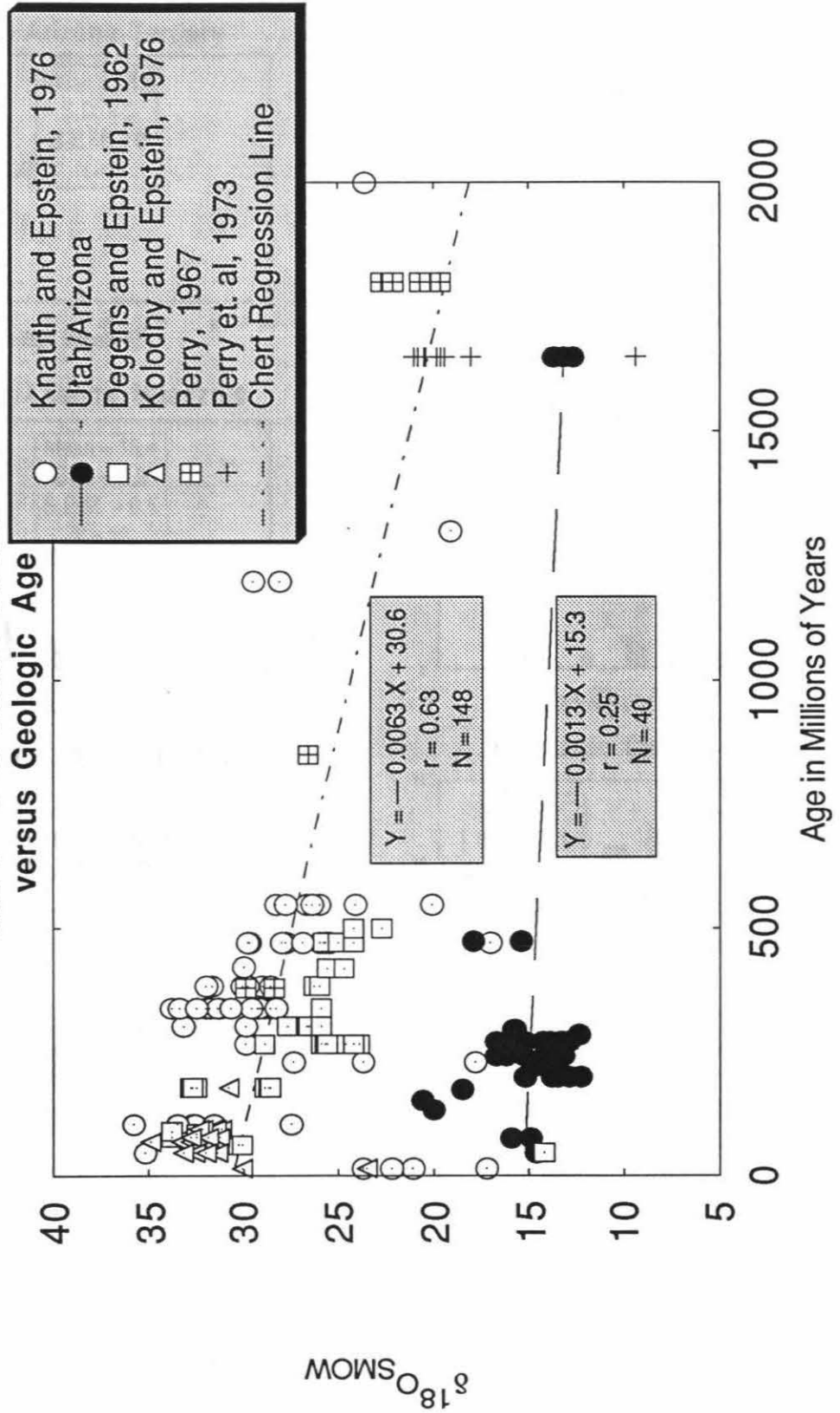
Plot of bulk silicate $\delta^{18}\text{O}$ values of Utah/Arizona sedimentary rocks in this study and $\delta^{18}\text{O}$ of marine cherts from the literature vs. geologic age. Simple linear regression calculated according to Fisher et al. (1970). r is the correlation coefficient.

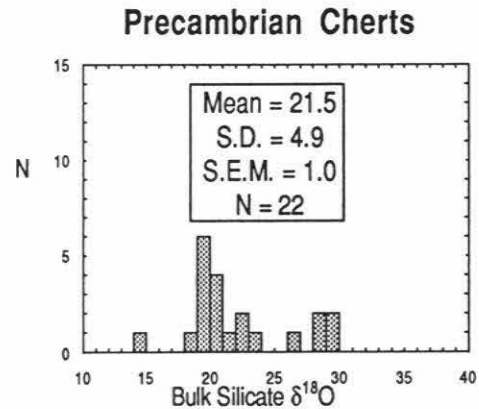
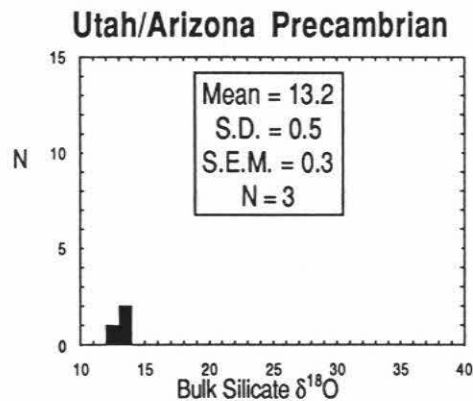
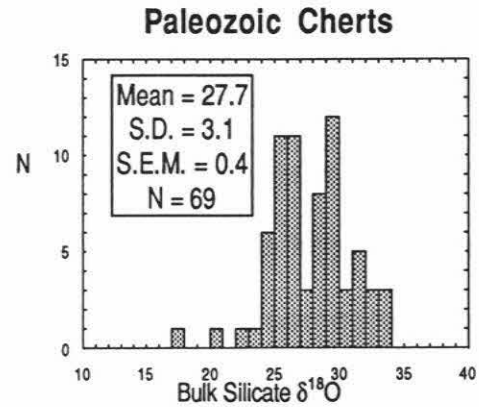
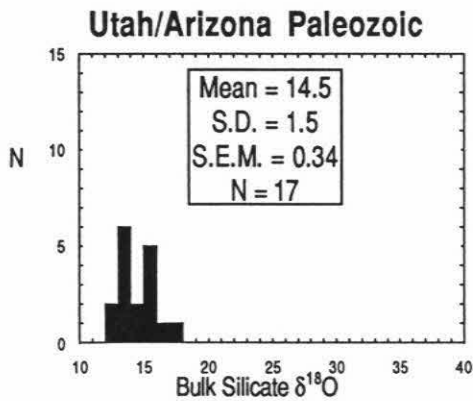
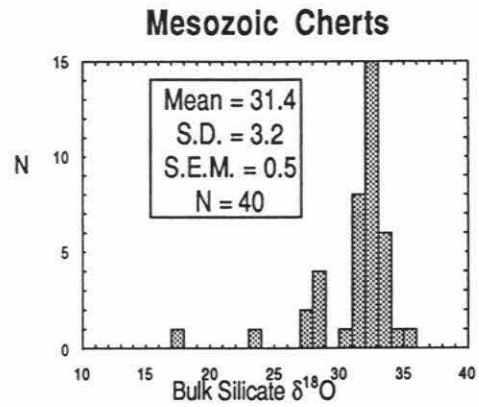
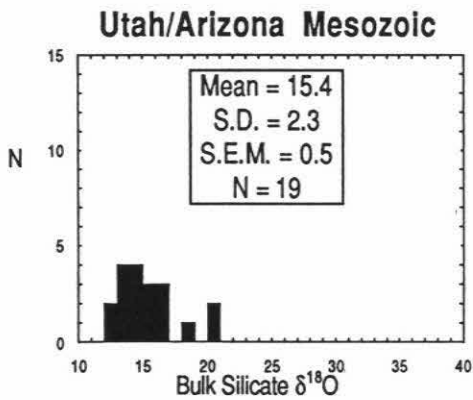
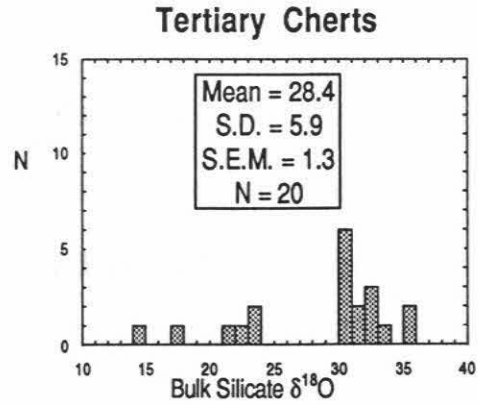
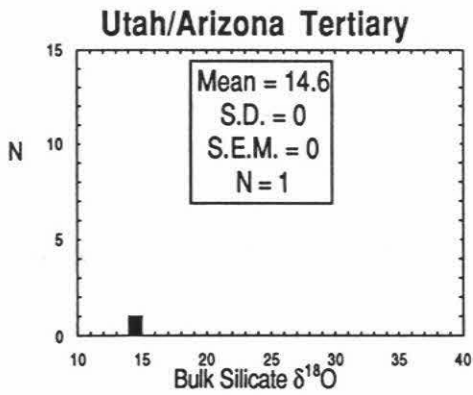
Figure 4.4

Eight comparative histograms showing bulk silicate $\delta^{18}\text{O}$ values of terrigenous sedimentary rocks from Utah and Arizona separated according to 4 geologic age intervals (left column) and $\delta^{18}\text{O}$ values of cherts from the literature, also separated according to geologic age (right column).

Bulk Silicate $\delta^{18}\text{O}$ of Utah/Arizona Sedimentary Rocks in this Study

and $\delta^{18}\text{O}$ of Marine Cherts versus Geologic Age





geologic age interval to be mainly the result of alteration by early diagenetic meteoric waters, because variable degrees of exchange with such low- ^{18}O waters will shift the $\delta^{18}\text{O}$ of the chert to a range of values below those of the original marine chert. In this interpretation, the highest- ^{18}O marine cherts in any geologic period would represent the least diagenetically altered samples. Knauth and Lowe (1978) interpret the $\delta^{18}\text{O}$ variation of the isotopically heaviest cherts in any particular geologic epoch to be mainly the result of variation in Earth's surface temperature over geologic time. In contrast, Perry and Tan (1972) argue that the observed change in $\delta^{18}\text{O}$ of marine cherts over geologic time is the result of variations in the $\delta^{18}\text{O}$ of the oceans over geologic time.

For the purposes of this study the important point is not the cause of the $\delta^{18}\text{O}$ variation in cherts, but that the bulk silicate $\delta^{18}\text{O}$ values of the Utah/Arizona terrigenous sedimentary rocks are relatively homogeneous by comparison. Obviously, different processes are responsible for the formation of cherts and the Utah/Arizona sedimentary rocks. Chert generally forms at low temperatures and, if it forms in the presence of sea water, is initially very high in $\delta^{18}\text{O}$. The quartz component of the Utah/Arizona sedimentary rocks is clearly much lower in ^{18}O and more complex in its provenance, as it is in general a mixture of detrital quartz of both high- and moderate-temperature origin, in addition to diagenetically formed quartz such as the authigenic quartz cement in some of the sandstones.

Veizer and Hoefs (1976) in a study of 169 sedimentary carbonate rocks of various ages from all over the world found that, like the cherts, there was a trend toward lighter carbonate $\delta^{18}\text{O}$ with increasing geologic age. This trend was attributed to diagenetic alteration involving isotopically light meteoric waters, a conclusion similar to that

reached by earlier workers, including Degens and Epstein (1962). Again, other investigators (Perry, 1967; Perry and Tan, 1972) have interpreted these types of variations to be the result of a change in the isotopic composition of the oceans over time.

Figure 4.5 is a plot of the data of Veizer and Hoef (1976) for marine carbonates, showing a linear regression of carbonate $\delta^{18}\text{O}$ vs. geologic age that is significant at the 0.01 probability level. These data are compared to the bulk silicate $\delta^{18}\text{O}$ values of Utah/Arizona sedimentary rocks in this study. The weak linear correlation displayed by the bulk silicate $\delta^{18}\text{O}$ of Utah/Arizona sedimentary rocks vs. geologic age is not statistically significant. It is clear that diagenetic alteration of carbonates occurs under different conditions and at vastly different rates than diagenetic alteration of siliclastic material, and the comparison in Figure 4.5 is useful in showing that bulk silicate $\delta^{18}\text{O}$ values of the terrigenous sedimentary rocks of the Colorado Plateau reflect this geochemical difference.

4.4 Geographic and lithological variation in bulk silicate $\delta^{18}\text{O}$

The terrigenous sedimentary rocks of the Colorado Plateau show some interesting variations of $\delta^{18}\text{O}$ with sample location in an east-west direction. These variations show up as a correlation of bulk silicate $\delta^{18}\text{O}$ with distance east of the eastern Nevada state border (Figure 4.6). For example, the eolian sandstones, non-eolian sandstones, and the shales all tend to decrease in $\delta^{18}\text{O}$ eastward. The correlation coefficients for all three groups of rocks are about 0.7, which is significant at the 0.10 probability level. Similar correlations are also observed with distance north of the Utah-Arizona state line (Figures 4.7 and 4.8); in these north-south trends the eolian sandstones still show a statistically

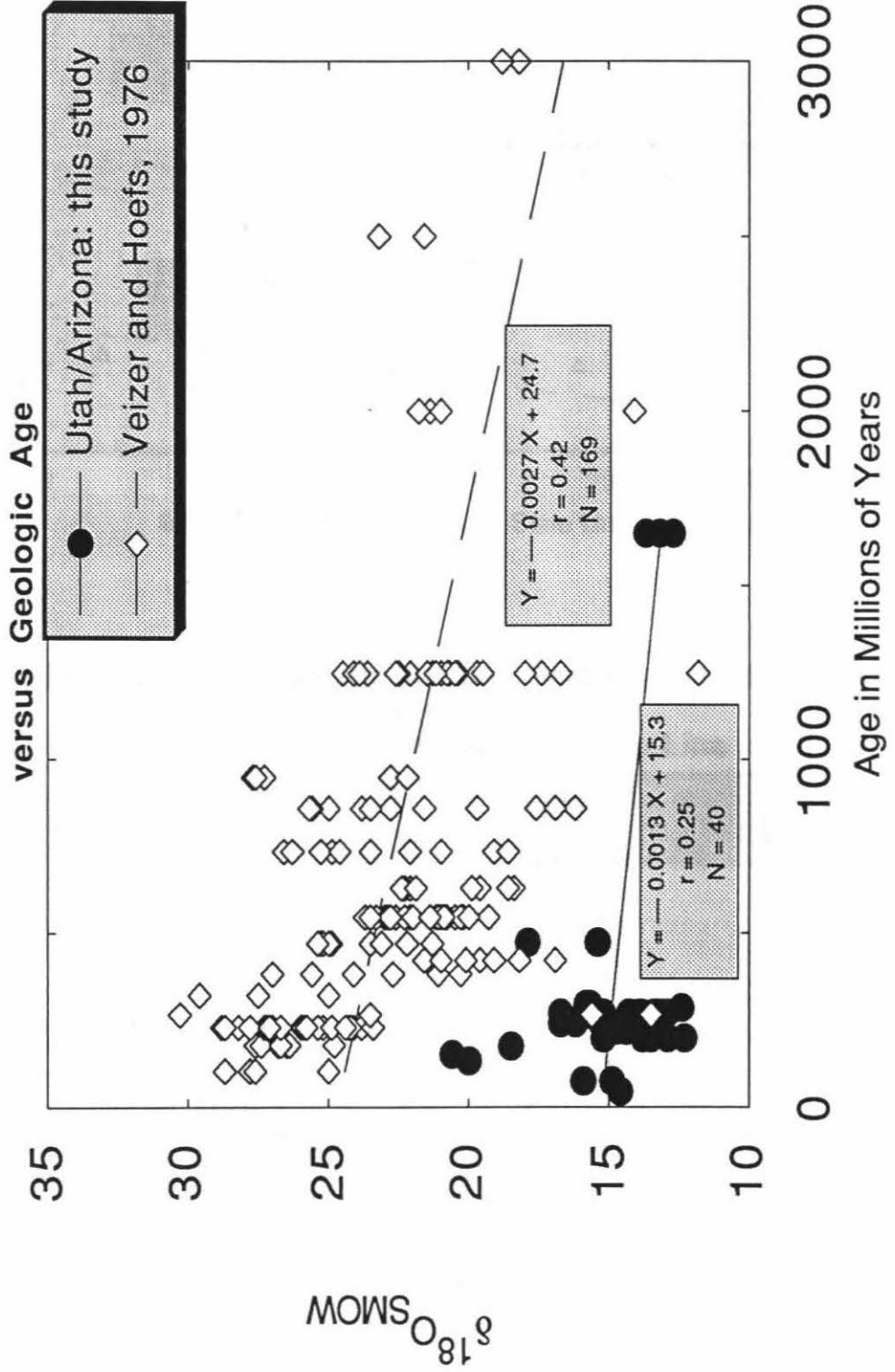
Figure 4.5

Plot of bulk silicate $\delta^{18}\text{O}$ values of Utah/Arizona terrigenous sedimentary rocks in this study and carbonate $\delta^{18}\text{O}$ values of marine limestones and dolomites from the literature versus geologic age.

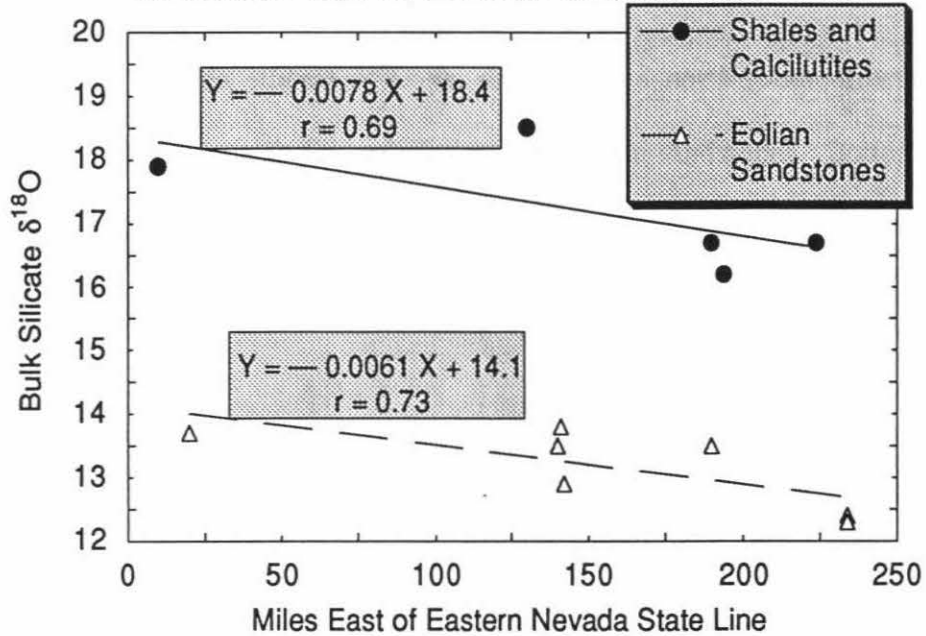
Figure 4.6

Two plots of bulk silicate $\delta^{18}\text{O}$ vs. distance in an east-west direction. Top diagram is for Utah/Arizona shales, calcilutites, and eolian sandstones. Bottom diagram is for Utah/Arizona non-eolian sandstones. Regression lines and correlation coefficients (r) calculated according to Fisher *et al.* (1970).

Bulk Silicate $\delta^{18}\text{O}_{\text{SMOW}}$ of Utah/Arizona Sedimentary Rocks in this study and Carbonate $\delta^{18}\text{O}_{\text{SMOW}}$ of Marine Limestones and Dolomites versus Geologic Age



**Bulk Silicate $\delta^{18}\text{O}$ of Utah and Arizona Sedimentary Rocks
versus
Distance East of Eastern Nevada State Line**



**Bulk Silicate $\delta^{18}\text{O}$ of Utah and Arizona Sedimentary Rocks
versus
Distance East of Eastern Nevada State Line**

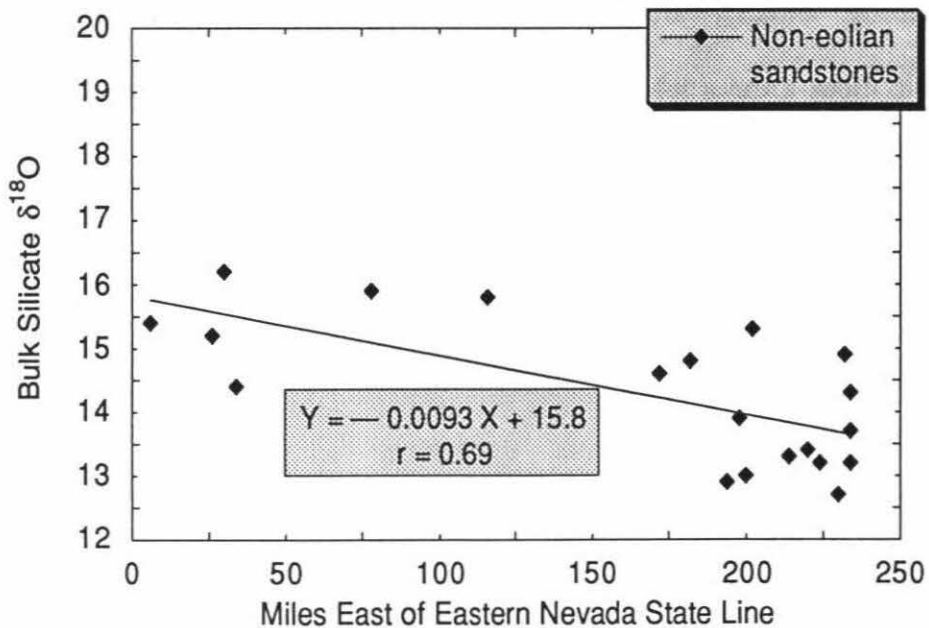


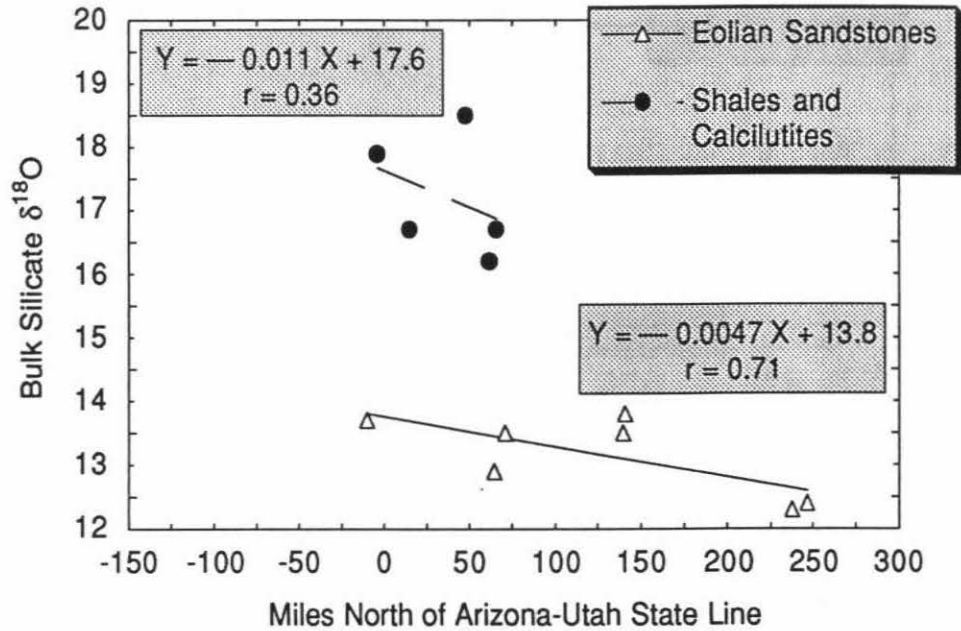
Figure 4.7

Two plots of bulk silicate $\delta^{18}\text{O}$ vs. distance in a north-south direction. Top diagram is for Utah/Arizona shales, calcilutites, and eolian sandstones. Bottom diagram is for Utah/Arizona non-eolian sandstones.

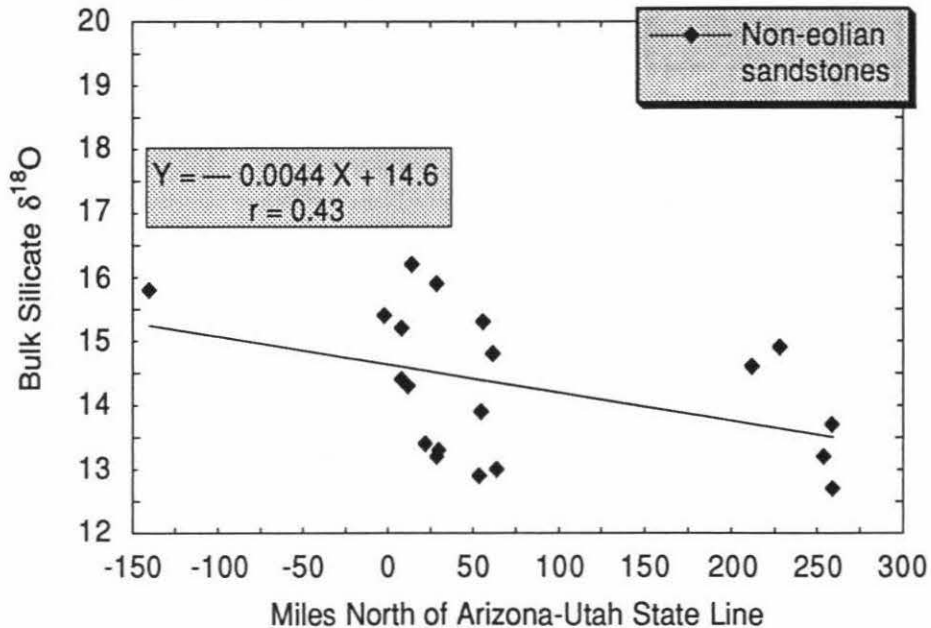
Figure 4.8

Two plots of bulk silicate $\delta^{18}\text{O}$ vs. distance for Utah/Arizona siltstones. Top diagram is for an east-west direction. Bottom diagram is for a north-south direction.

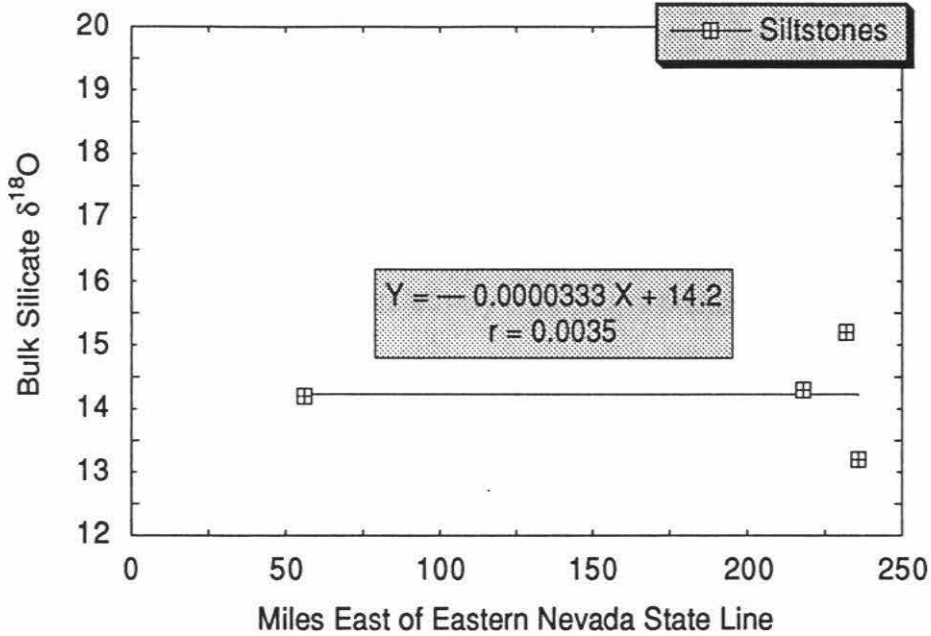
**Bulk Silicate $\delta^{18}\text{O}$ of Utah and Arizona Sedimentary Rocks
versus
Distance North of Arizona-Utah State Line**



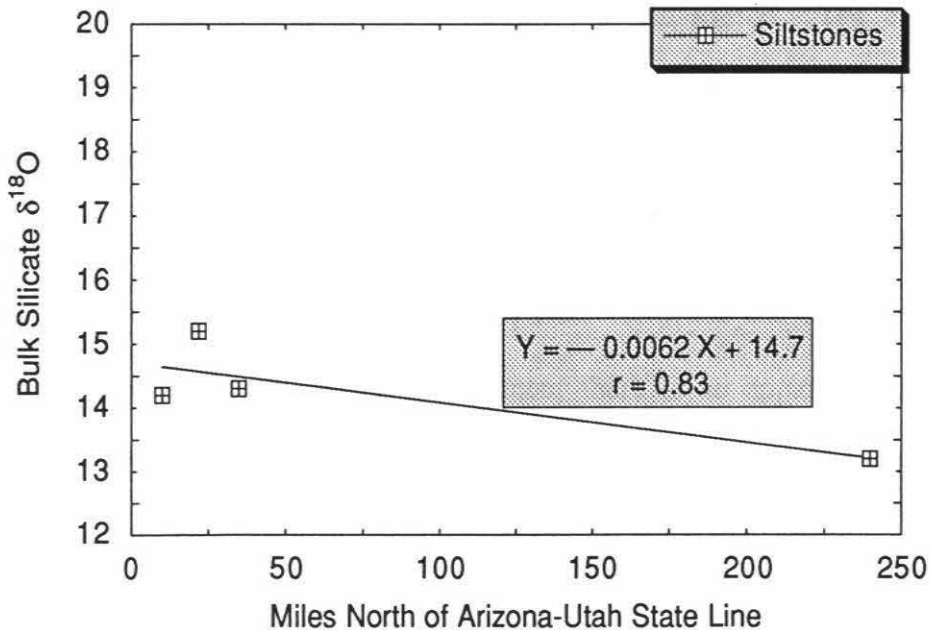
**Bulk Silicate $\delta^{18}\text{O}$ of Utah and Arizona Sedimentary Rocks
versus
Distance North of Arizona- Utah State Line**



**Bulk Silicate $\delta^{18}\text{O}$ of Utah and Arizona Sedimentary Rocks
versus
Distance East of Eastern Nevada State Line**



**Bulk Silicate $\delta^{18}\text{O}$ of Utah and Arizona Sedimentary Rocks
versus
Distance North of Arizona - Utah State Line**



significant correlation coefficient of 0.7, but for the non-eolian sandstones and the shales the correlation coefficients are poorer, 0.43 and 0.36. The eolian sandstones, which are Permian to Jurassic in age, also have a significantly different ($P < .025$) bulk silicate $\delta^{18}\text{O}$ mean than the non-eolian sandstones, which cover a much broader age span. The eolian sandstones display a mean $\delta^{18}\text{O}$ of +13.2, with a SEM of 0.2 per mil, whereas the non-eolian sandstones have a mean of +14.3 with a SEM of 0.25 per mil. The eolian sandstones in this study are all relatively pure quartz arenites, while the non-eolian sandstones contain other minerals such as feldspar (Table 2.1), which may account for their generally lower mean bulk silicate $\delta^{18}\text{O}$ values.

Even though the correlations are not so clear-cut as for the eolian sandstones, it is worthy of discussion that the shales and non-eolian sandstones also show similar correlations of bulk silicate $\delta^{18}\text{O}$ with distance in an east-west direction. These isotopic variations are orthogonal to the general north-south tectonic trends of the Cordilleran orogenic belt, suggesting the possibility that the $\delta^{18}\text{O}$ variation with distance might be due to mixing between an eastern and a western isotopic source. The $\delta^{18}\text{O}$ values decrease eastward, toward the craton and away from the Cordilleran miogeosyncline. However, because there is no correlation between geologic age and $\delta^{18}\text{O}$, this would suggest that either the source areas remained generally similar over a significant range of geologic time, or perhaps that the sediments were reworked and therefore recycled over geologic time (or both). In hand specimen, there is no apparent difference in cementation between eastern and western eolian samples, so it is unlikely that these $^{18}\text{O}/^{16}\text{O}$ differences are a result of post-depositional diagenetic processes.

It is interesting that Solomon and Taylor (1989) observed a similar oxygen isotope trend in the Mesozoic plutonic igneous rocks of this broad region, with the granitic samples from central Nevada having whole-rock $\delta^{18}\text{O} > +11$ and those from the craton of Colorado and Utah having whole-rock $\delta^{18}\text{O} < +9$. The coexisting quartz in these granitic plutons is characteristically about 1 per mil higher in ^{18}O than the whole rock. Thus, the common quartz eroded from the Mesozoic igneous rocks of Nevada is typically very ^{18}O rich ($\delta^{18}\text{O} = +12$ to $+14$), whereas quartz eroded from analogous rocks in Utah and Colorado usually has a lower $\delta^{18}\text{O} = +8$ to $+10$. Some of these different types of igneous quartz grains have undoubtedly been incorporated in certain of the sedimentary rocks of the Colorado Plateau.

Johansen (1988) discussed possible sources for the quartzose sandstones of the American southwest and concluded that the major primary source was the northwest flank of the Transcontinental Arch. Fluvial systems would have drained the Transcontinental Arch and deposited sediment in the western Cordilleran miogeosyncline during the Paleozoic. Large volumes of Pennsylvanian and Permian quartz-rich sandstone in the Canadian portion of the miogeosyncline perhaps reflect the output of these cratonically-derived fluvial systems. The orientation and location of the continent was such that trade winds would have driven coastal current and wind current systems southward, parallel to the hinge of the miogeosyncline. This hingeline curved westward in Utah where the southward-blowing trade winds would have blown reworked sands onto the craton. Johansen (1988) also suggested that another locally important source of sediment was the Ancestral Rockies. In contrast, Marzolf (1988) held that the major source of sand for Upper Paleozoic sandstones was the Ancestral Rockies. He

considered the source for the Mesozoic eolian sandstones to be cratonically derived from the east and southeast.

The oxygen isotope data of this study thus suggest that there was a mixing of sediment from at least two provenances, one dominantly from western Utah and Nevada, and another from eastern Utah, Colorado and Wyoming. The eastern source was most likely the Ancestral Rockies, a relatively low- ^{18}O cratonal source dominated by Precambrian crystalline basement and the sediments derived therefrom. The western source was composed of sands from various sources that were reworked and well mixed in the high- ^{18}O Late Precambrian and Paleozoic miogeosyncline and the craton-margin basins of the early Jurassic. Eolian and fluvial reworking of sediments and marine transgressions or storms may have helped to mix sands from the high- ^{18}O western and the low- ^{18}O eastern sources during the formation of the Mesozoic eolian sandstones.

The limited number of eolian samples prevents us from examining a significant " $\delta^{18}\text{O}$ -time slice". However, it is worth trying to see whether the types of correlations described above also hold up for a specific geologic epoch. In this connection, note that the Pennsylvanian-Permian Weber Sandstone sample is isotopically lighter and also lies to the east of the Permian Quantoweap Sandstone. A comparison of the four analyzed Lower Jurassic Navajo Sandstone samples with the Triassic-Jurassic Wingate Sandstone also shows the trend of lighter $\delta^{18}\text{O}$ to the east and north. This supports the hypothesis that the conjectured mixing of sand-size particles occurred across Utah during at least two separate geologic time periods.

We also need to discuss the possibility that these differences in $\delta^{18}\text{O}$ are attributable to an increasing amount of high- ^{18}O authigenic quartz overgrowth toward the

west. It is also possible that the quartz overgrowths precipitated from waters that varied in $\delta^{18}\text{O}$ in an east-west direction. Given the variations in depth of burial due to tectonic activity over geologic time, which would be reflected in variations in the temperature and fluid pressure during diagenesis, as well as the probably significant variations in pore water $\delta^{18}\text{O}$ due to the large number of marine transgressions and regressions, it is unlikely that a regional trend that is not in some way correlated with geologic age would be established through diagenesis. Also, in hand specimen, there are no obvious regional trends in cementation in the samples studied. However, given samples from such divergent environments of deposition and burial, it is reasonable to expect that diagenetic effects will be responsible for some of the finer-scale variations in $\delta^{18}\text{O}$.

Non-eolian sandstones show a wider variety in composition and cementation than the eolian sandstones (Table 2.1). Nevertheless, the former also show a significant correlation ($P < 0.01$) of bulk silicate $\delta^{18}\text{O}$ with distance east of the eastern Nevada state line (Figure 4.6). However, the limited number of siltstones analyzed show no variation in bulk silicate $\delta^{18}\text{O}$ in the east-west direction (Figure 4.8). In Figure 4.6, it is interesting to note that the regression lines for marine and fluvial sandstones have the steepest slope, the regression line for water-deposited shales and calcilutites has an intermediate slope, and the regression line for the eolian sandstones has the shallowest slope. One might hypothesize that the latter effect is due to the greater efficiency of the eolian mixing processes in the east to west direction.

Eolian sandstones, non-eolian sandstones, siltstones, and shales and calcilutites all show a trend of decreasing bulk silicate $\delta^{18}\text{O}$ toward the north (Figures 4.7 and 4.8). The correlation coefficients for both the eolian sandstones and the non-eolian sandstones

are significant at the 0.10 probability level. However, the correlation coefficients for the siltstones and the shale-calculutite group are not statistically significant, perhaps due to their small sample sizes. While these correlations are weaker than the east to west correlations, "miles north" in these plots corresponds to the direction of the Ancestral Rockies of Wyoming and Montana just as "miles east" does toward the Ancestral Rockies of Colorado and New Mexico in the east-west plots. The bulk silicate oxygen isotopic evidence from Utah and Arizona suggests that the cratonic sedimentary rocks analyzed from this study are a mixture of silicate material from at least two different sources that had distinct $^{18}\text{O}/^{16}\text{O}$ ratios. One source was the region of the Ancestral Rockies, especially the Uncompahgre Highlands. The other source was perhaps a mixture of sources from the Cordilleran miogeosyncline to the west and south. This second source or sources contributed materials that were at least 1.5 to 2.0 per mil higher in bulk silicate $\delta^{18}\text{O}$ than the cratonic Ancestral Rockies source.

4.5 Carbonate carbon and oxygen isotopic trends

A vast literature exists on oxygen and carbon isotope variations in carbonate rocks (*e.g.*, Keith and Weber, 1964), and such data are commonly plotted on $\delta^{18}\text{O} - \delta^{13}\text{C}$ diagrams like that of Figure 4.9. A simple linear correlation of carbonate $\delta^{18}\text{O}$ and $\delta^{13}\text{C}$ for all Utah/Arizona samples is significant at the 0.01 probability level (Figure 4.9). The correlation coefficient is 0.5.

In general, on such $\delta^{18}\text{O} - \delta^{13}\text{C}$ diagrams, unexchanged marine carbonates typically plot near $\delta^{18}\text{O} = +28$ to $+31$ and $\delta^{13}\text{C} = -1$ to $+2$, and most diagenetically altered marine carbonates or unexchanged fresh-water carbonates plot down and to the left at lower values of $\delta^{13}\text{C}$ and $\delta^{18}\text{O}$. This also is characteristic of the present data set

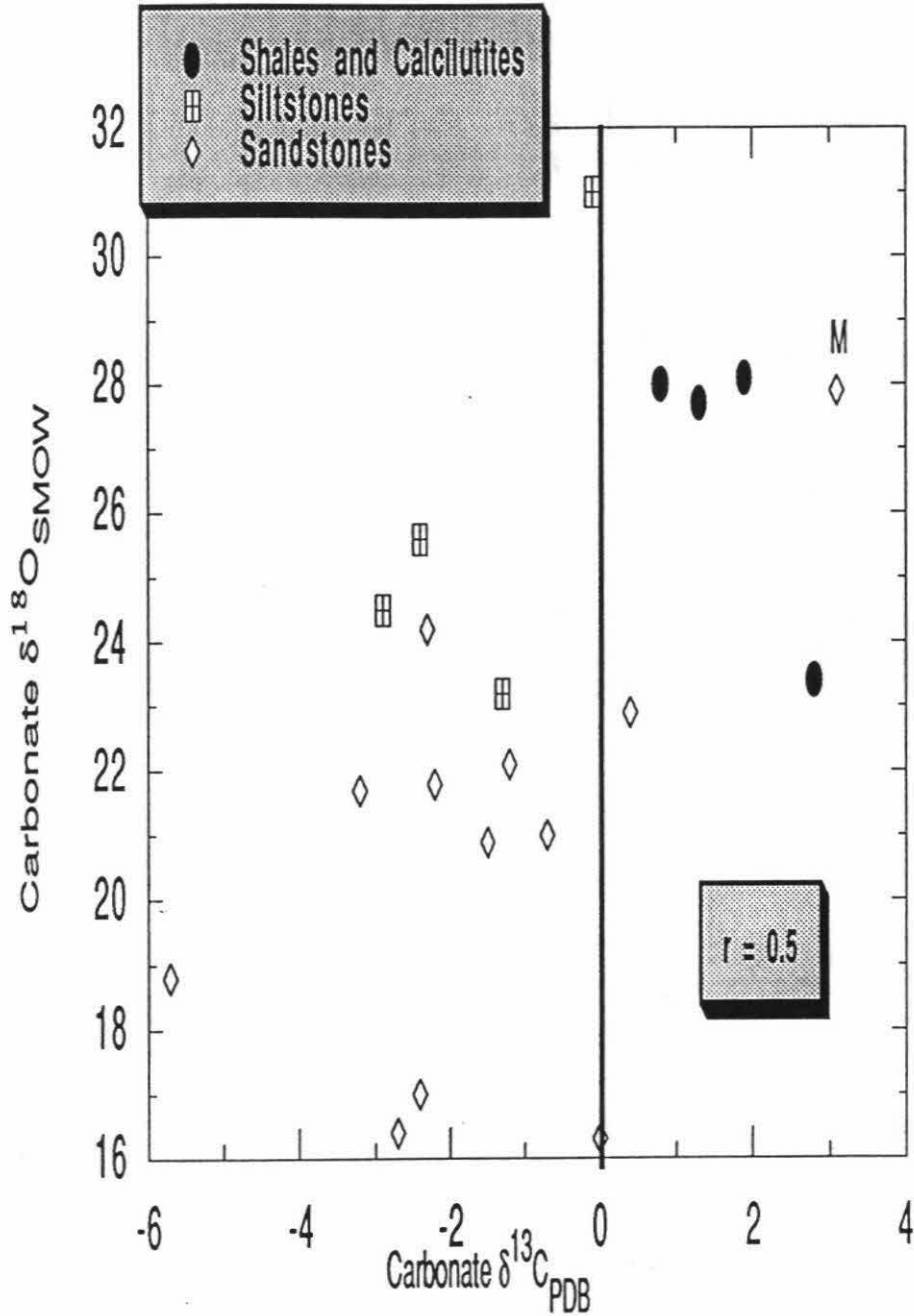
Figure 4.9

Carbonate $\delta^{18}\text{O}$ vs. carbonate $\delta^{13}\text{C}$ for Utah/Arizona terrigenous sedimentary rocks subdivided into shales (and calcilutites), siltstones, and sandstones. The "M" marks the single marine sandstone analyzed. These data points display a very weak correlation ($r = 0.5$).

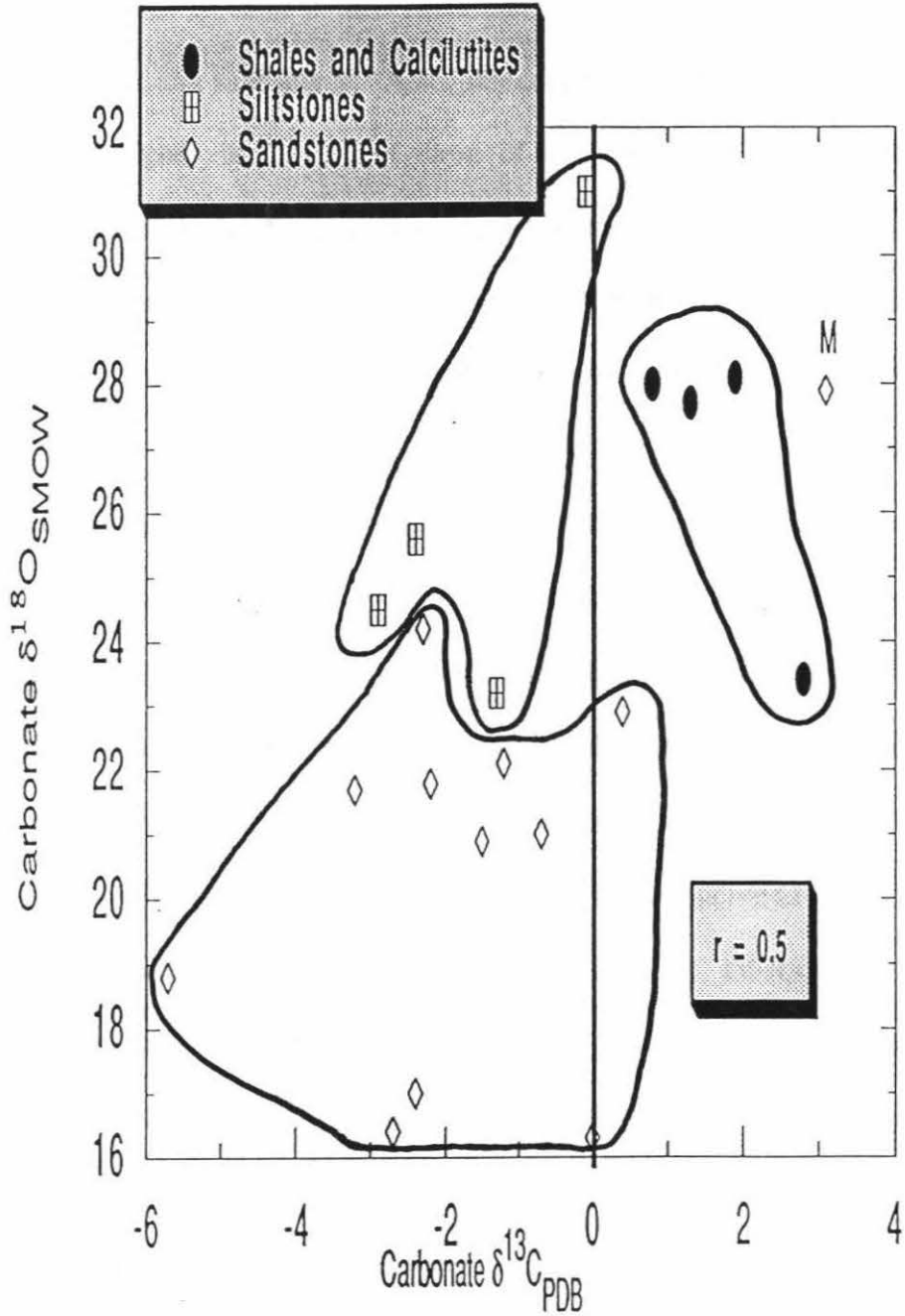
Figure 4.10

This is the same as Figure 4.9, with the addition of fields delineating non-marine sandstones, siltstones, and shales and calcilutites.

Carbonate $\delta^{18}\text{O}_{\text{SMOW}}$ vs Carbonate $\delta^{13}\text{C}_{\text{PDB}}$ for Utah/Arizona Sedimentary Rocks



Carbonate $\delta^{18}\text{O}_{\text{SMOW}}$ vs Carbonate $\delta^{13}\text{C}_{\text{PDB}}$
for Utah/Arizona Sedimentary Rocks



shown in Figure 4.9. If the single marine sandstone sample in the data set of Figure 4.9 is excluded, the other sandstones, siltstones, and shales and calcilutites fall into three non-overlapping fields on the $\delta^{18}\text{O}$ - $\delta^{13}\text{C}$ plot (Figure 4.10). In Figure 4.10 the shales and calcilutites are seen to contain carbonates that are distinctly heavier in $\delta^{13}\text{C}$ than those of the siltstones and sandstones. Also, the carbonates in the shales, calcilutites, and siltstones are higher in $\delta^{18}\text{O}$ than those of the sandstones, all of which are non-marine. The carbonates of the siltstones and sandstones are generally negative in $\delta^{13}\text{C}$, suggesting the influence of terrestrial carbon from fresh-water sources; together, all these carbonates form an almost continuous $\delta^{18}\text{O}$ array between +31 and +16.

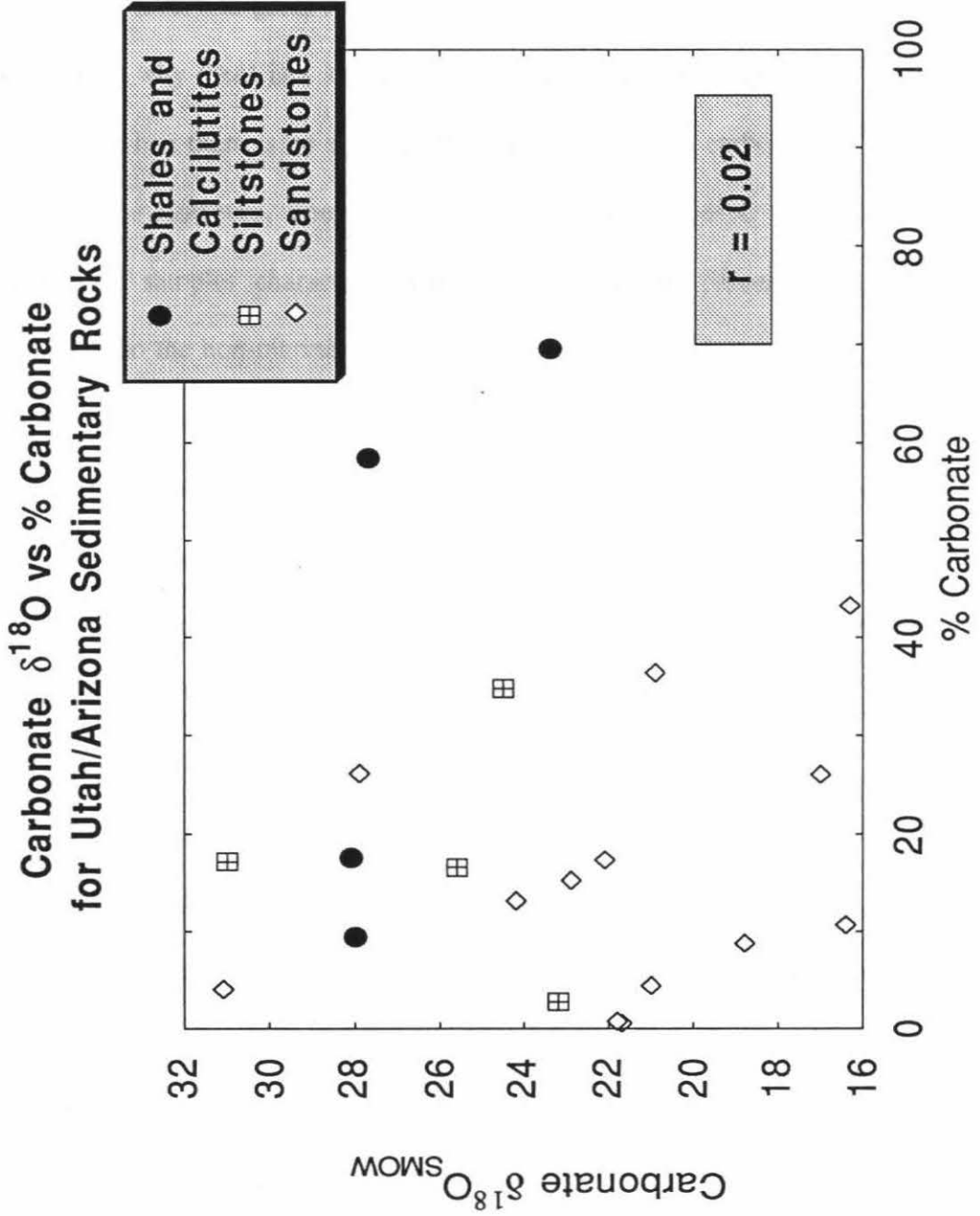
The probable explanation for the trends on Figure 4.10 is the dominant involvement of meteoric water containing isotopically light oxygen and carbon in the formation or alteration of the carbonate minerals in sandstones and siltstones. Following this line of reasoning, it is apparent that the carbonates of the sandstones in general show isotopic evidence of more complete exchange with such meteoric waters than do the siltstones or shales. From general clast size considerations, it would be expected that the initial porosity and permeability of the sandstones would be conducive to greater flow of ground waters than in the case of the siltstones or shales. Also, most of the calcite in the sandstones would have been deposited as authigenic calcite directly from these low- ^{18}O (heated?) groundwaters, whereas much of the carbonate in the finer-grained rocks may have been originally deposited with the coexisting terrigenous silt and clay at lower temperatures, either in a marine or lacustrine environment, or in some cases from transitional marine-meteoric intertidal waters. Although these carbonates undoubtedly also exchanged with ground waters during diagenesis, the exchange may not have been

so complete as in the case of the calcite cements of the sandstones. According to this model, some isotopic exchange of the coexisting carbonate fraction of each sample could proceed without concomitant isotopic exchange of the existing silicate fraction, particularly if relatively low temperatures prevailed during diagenesis. Again, however, it is not possible from this data set to constrain the amount of biogenic versus diagenetic or authigenic carbonate in each sample.

A plot of carbonate $\delta^{18}\text{O}$ vs. per cent carbonate shows no significant correlation between these two variables (Figure 4.11). The siltstones and shales are distinctly heavier in carbonate $\delta^{18}\text{O}$ than the majority of sandstones even though all these rocks span the same wide range of per cent carbonate content from 0 to 40%. If the shales and siltstones had consistently higher carbonate contents than the sandstones, it perhaps could have been argued from mass-balance considerations that the reason the sandstone carbonates were lower in ^{18}O was because their smaller amounts of carbonate made them more susceptible to depletion in ^{18}O , other things being equal (*e.g.*, water/rock ratios, $\delta^{18}\text{O}$ of the waters, degree of isotopic exchange, etc.). The fact that there is not a significant correlation between carbonate $\delta^{18}\text{O}$ and per cent carbonate, and that the sandstones are uniformly more ^{18}O depleted than the other rocks, supports the argument that the carbonate $\delta^{18}\text{O}$ values are lithologically controlled. In combination with Figure 4.10, these data suggest that there was greater involvement of isotopically light meteoric water with the carbonates from the sandstones of the Colorado Plateau than with the carbonates in the siltstones or shales. Again, this is probably because the carbonate in the sandstones is largely authigenic cement directly deposited from circulating ground waters during diagenesis rather than being partially exchanged carbonate originally

Figure 4.11

Plot of carbonate $\delta^{18}\text{O}$ versus per cent carbonate for Utah/Arizona sedimentary rocks.



deposited with the coexisting terrigenous clay and silt in a marine, lacustrine, or transitional environment.

A simple linear correlation of $\delta^{13}\text{C}$ with per cent carbonate is significant at the 0.05 probability level and gives a correlation coefficient of 0.5 (Figure 4.12). It is not readily apparent why there is a significant correlation between carbonate $\delta^{13}\text{C}$ and per cent carbonate when there is no significant correlation between carbonate $\delta^{18}\text{O}$ and per cent carbonate. However, one possibility is that the high- $\delta^{13}\text{C}$ marine or mixed marine/meteoric samples characteristically contain a higher percentage of biogenic carbonate than do the non-marine samples, which tend to have lower $\delta^{13}\text{C}$. Also, it is well known that during diagenesis it is more difficult in general to shift the $\delta^{13}\text{C}$ values of carbonate-rich samples than it is to change the $\delta^{18}\text{O}$ of the carbonate, again because of mass-balance effects (the diagenetic waters are large reservoirs of oxygen but not of carbon, while the reverse is true for the carbonates). Note that without the very carbonate-rich and ^{13}C -rich shales and calcilutites, the correlation between $\delta^{13}\text{C}$ and per cent carbonate shown on Figure 4.12 would not be statistically significant.

Figures 4.13, 4.14 and 4.15 show that there are no correlations among the variables per cent carbonate, carbonate $\delta^{18}\text{O}$, or carbonate $\delta^{13}\text{C}$, and distance in an east-west direction. This is in contrast with the bulk silicate $\delta^{18}\text{O}$ which does show a correlation with distance east of the Nevada-Utah border. This clearly substantiates that the processes responsible for these carbonate $\delta^{18}\text{O}$ and $\delta^{13}\text{C}$ values are different than the processes responsible for the bulk silicate $\delta^{18}\text{O}$ values.

There are also no correlations between per cent carbonate, carbonate $\delta^{18}\text{O}$, carbonate $\delta^{13}\text{C}$ and distance in a north-south direction (these plots are not included in this

Figure 4.12

Plot of carbonate $\delta^{13}\text{C}$ versus per cent carbonate for Utah/Arizona terrigenous sedimentary rocks.

Carbonate $\delta^{13}\text{C}$ vs Per Cent Carbonate for Utah/Arizona Sedimentary Rocks

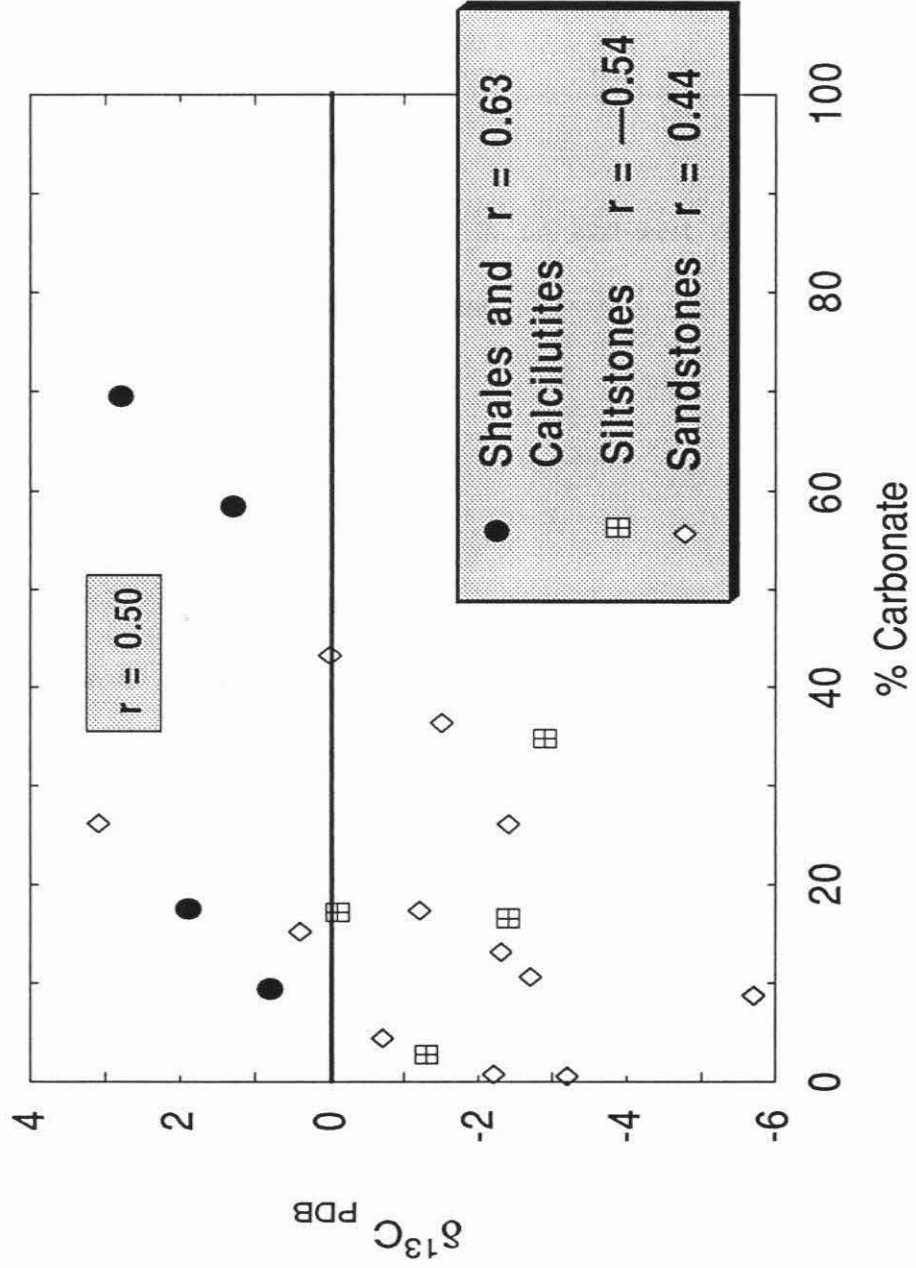
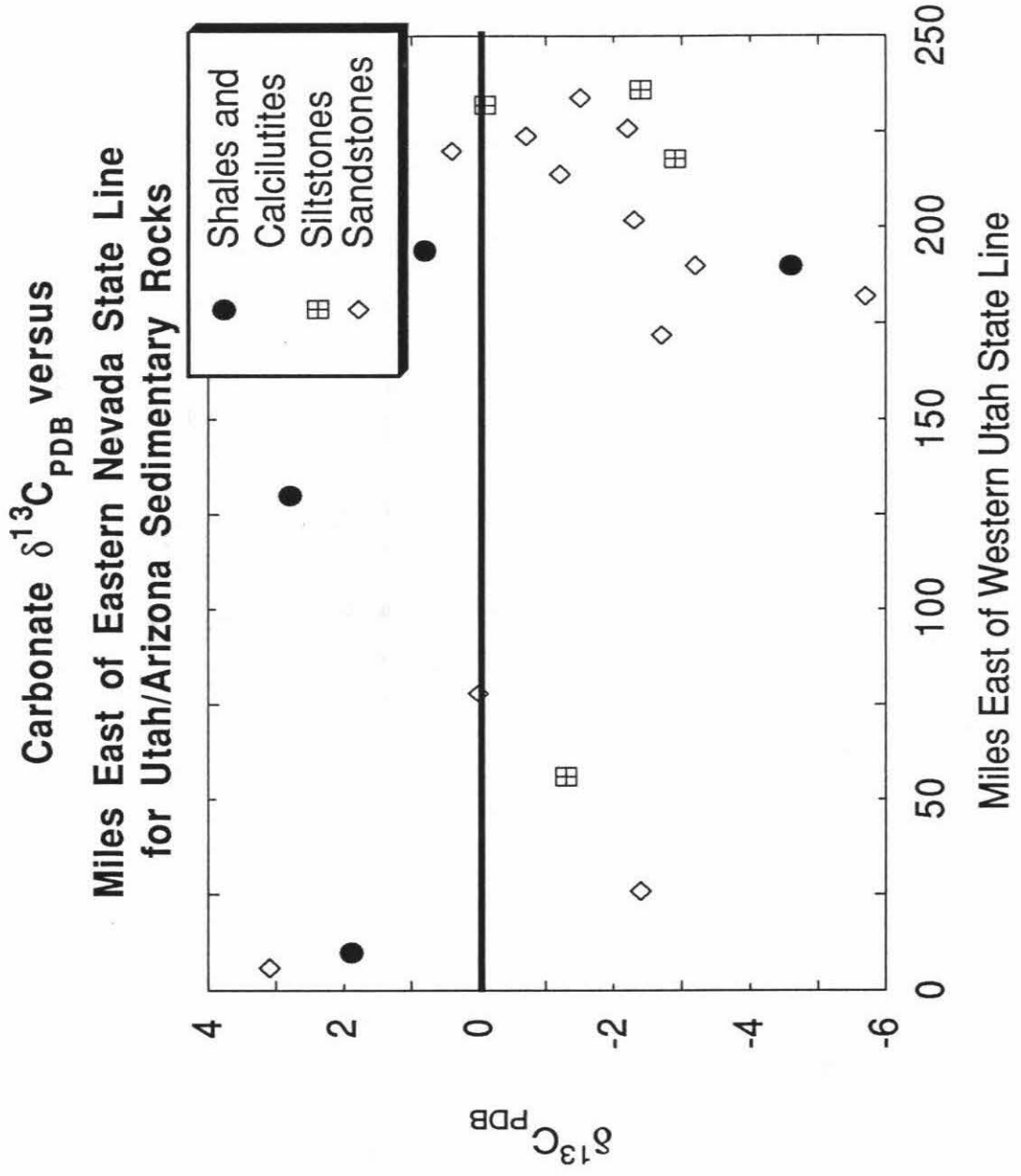


Figure 4.13

Plot of carbonate $\delta^{13}\text{C}$ versus distance in an east-west direction for all Utah/Arizona sedimentary rocks analyzed in this study.

Figure 4.14

Plot of carbonate $\delta^{18}\text{O}$ versus distance in an east-west direction for all Utah/Arizona terrigenous sedimentary rocks analyzed in this study.



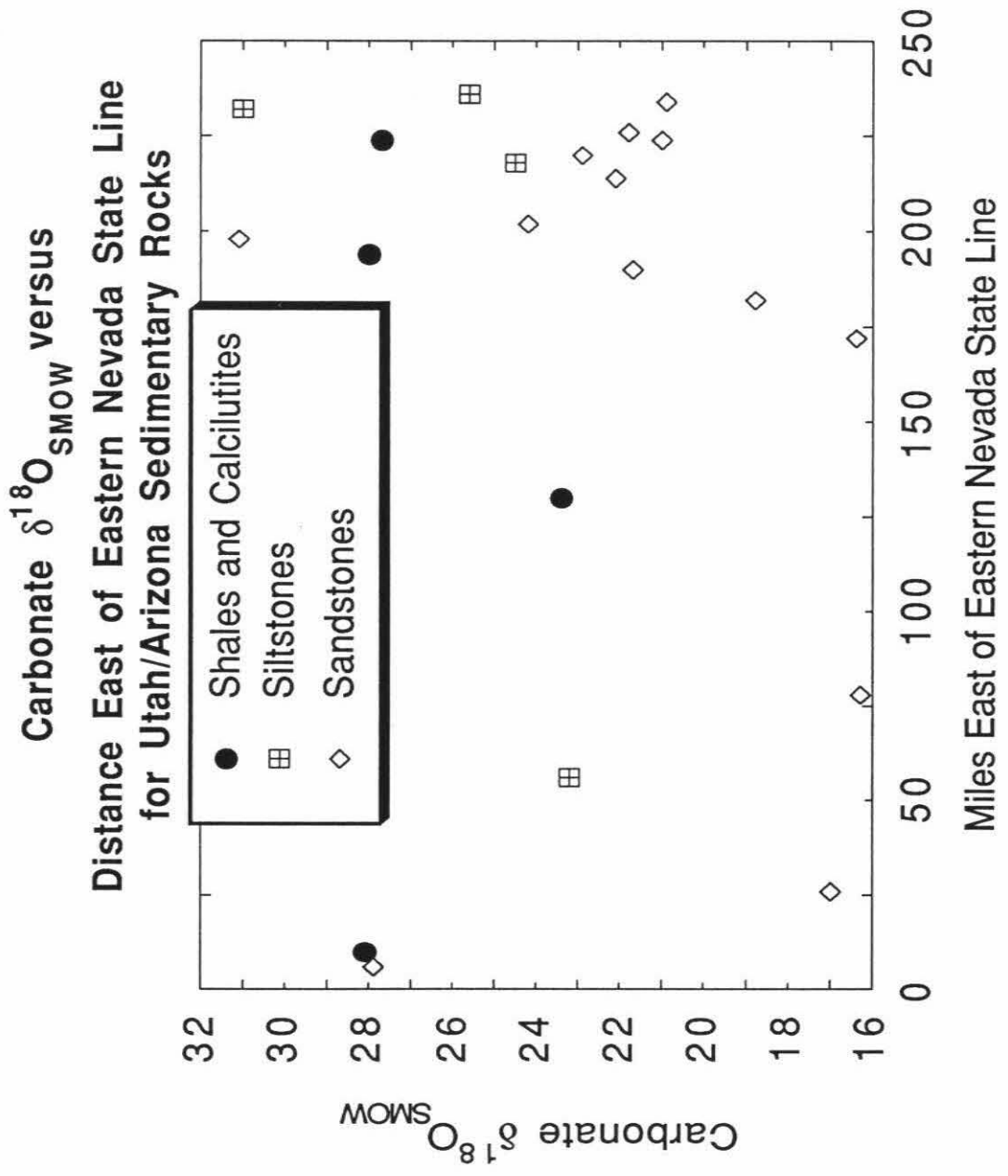


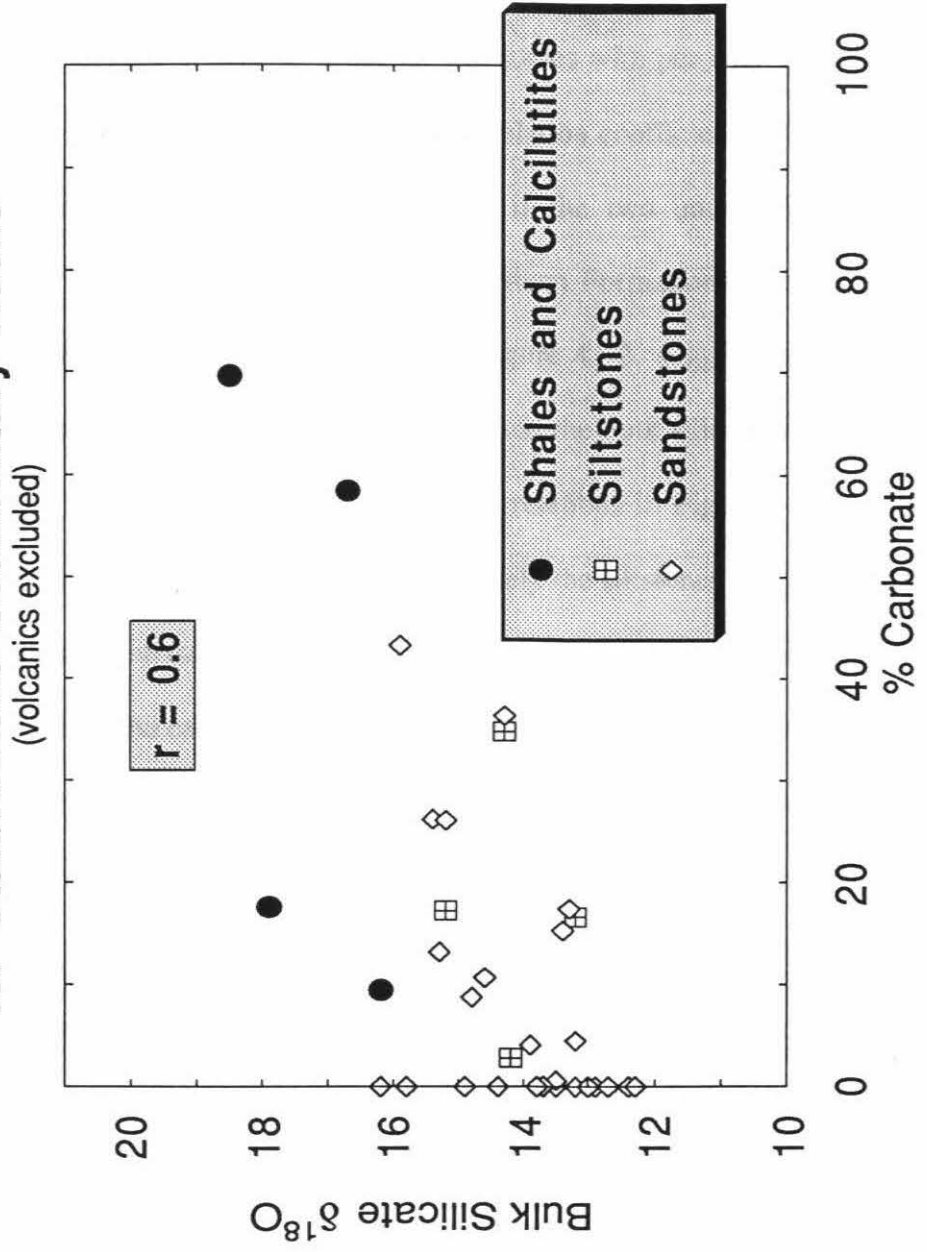
Figure 4.15

Plot of per cent carbonate versus distance in an east-west direction for the Utah/Arizona terrigenous sedimentary rocks.

Figure 4.16

Plot of bulk silicate $\delta^{18}\text{O}$ versus per cent carbonate for Utah/Arizona terrigenous sedimentary rocks excluding volcanics. These samples show a weak correlation ($r = 0.6$).

Per Cent Carbonate vs Bulk Silicate $\delta^{18}\text{O}$ for Utah/Arizona Sedimentary Rocks (volcanics excluded)



thesis, however). Again, this is in contrast to the bulk silicate $\delta^{18}\text{O}$ which does show a correlation with distance north of the Utah-Arizona border (Figures 4.7 and 4.8), further demonstrating that the processes responsible for the carbonate isotopic compositions are decoupled from the processes responsible for the bulk silicate $\delta^{18}\text{O}$.

A correlation of bulk silicate $\delta^{18}\text{O}$ for all lithologies with per cent carbonate is significant at the 0.01 probability level and gives a correlation coefficient of 0.6 (Figure 4.16). However, this correlation is not significant if the two unusually high- ^{18}O bentonitic samples from the Mowry Shale and the Morrison Formation are included.

Figure 4.16 bears a striking resemblance to Figure 4.12, suggesting that there might be a correlation between $\delta^{13}\text{C}$ of the carbonates and the bulk silicate $\delta^{18}\text{O}$. This is indeed the case as shown in Figure 4.17. These correlations in Figures 4.12, 4.16, and 4.17 are dominated by the finer-grained rocks, namely the siltstones and shales, and they are not so evident in the data set as a whole. The correlations are probably a result of the fact that the shales and calcilutites, which tend to have relatively high bulk silicate $\delta^{18}\text{O}$ values, are dominantly marine with characteristically high $\delta^{13}\text{C}$ values, whereas the sandstones and siltstones, which have lower bulk silicate $\delta^{18}\text{O}$, are dominantly non-marine and have the low $\delta^{13}\text{C}$ values characteristic of such rocks. There is clearly a coupling of some type between the three variables per cent carbonate, carbonate $\delta^{13}\text{C}$, and bulk silicate $\delta^{18}\text{O}$ for these sedimentary rocks from the Colorado Plateau.

4.6 Decoupling of carbonate $\delta^{18}\text{O}$ and bulk silicate $\delta^{18}\text{O}$

Carbonate $\delta^{18}\text{O}$ values for the Utah/Arizona samples range from +16.3 to +31.1, a variation of about 15 per mil. This is in distinct contrast to bulk silicate $\delta^{18}\text{O}$ values, which range only from +12.3 to +20.6 (Figure 4.18; also compare Figures

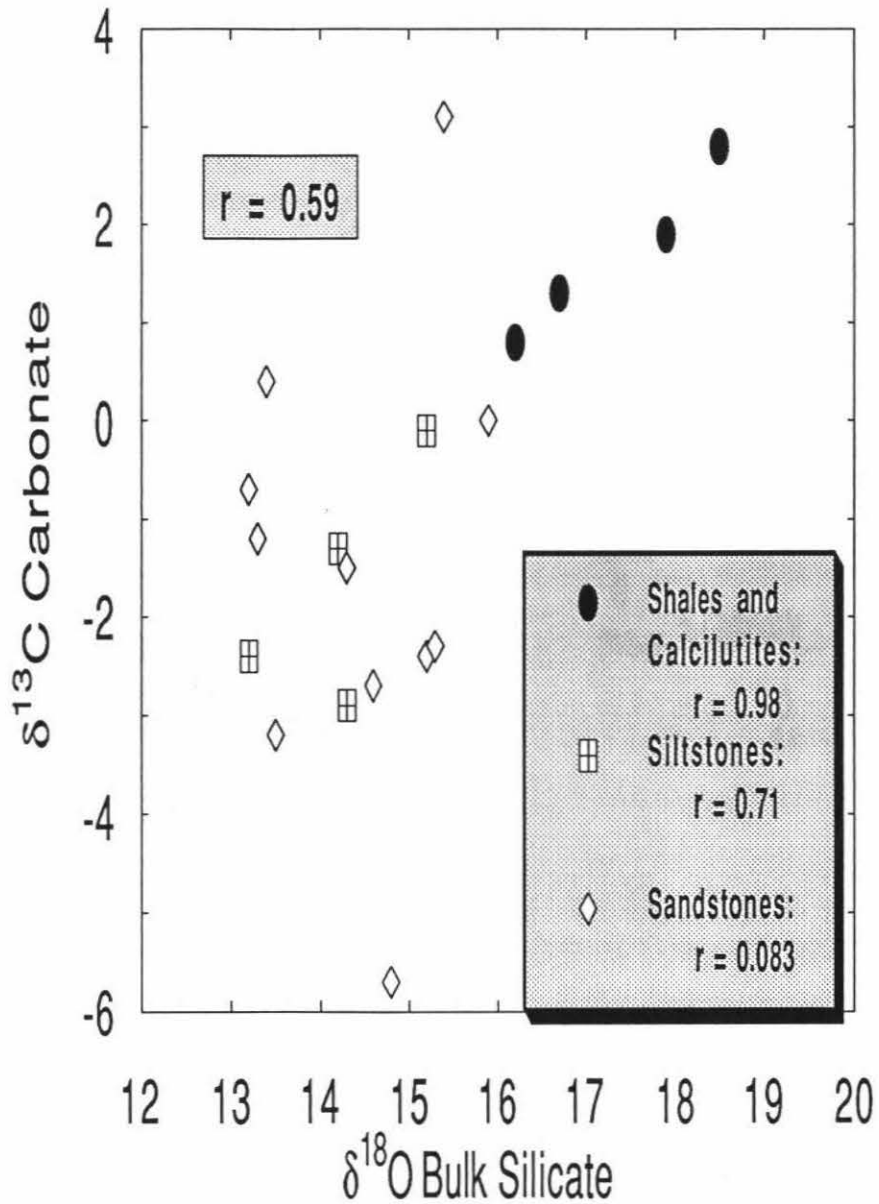
Figure 4.17

Plot of $\delta^{13}\text{C}$ of carbonate versus bulk silicate $\delta^{13}\text{C}$ for the Utah/Arizona terrigenous sedimentary rocks. These samples show a correlation coefficient of 0.59. The shales, calcilutites, and siltstones are better correlated ($r = 0.98$ and 0.71). Although the sandstones data-points are not correlated ($r = 0.08$), the bulk of the sandstones plot on the shale-siltstone trend.

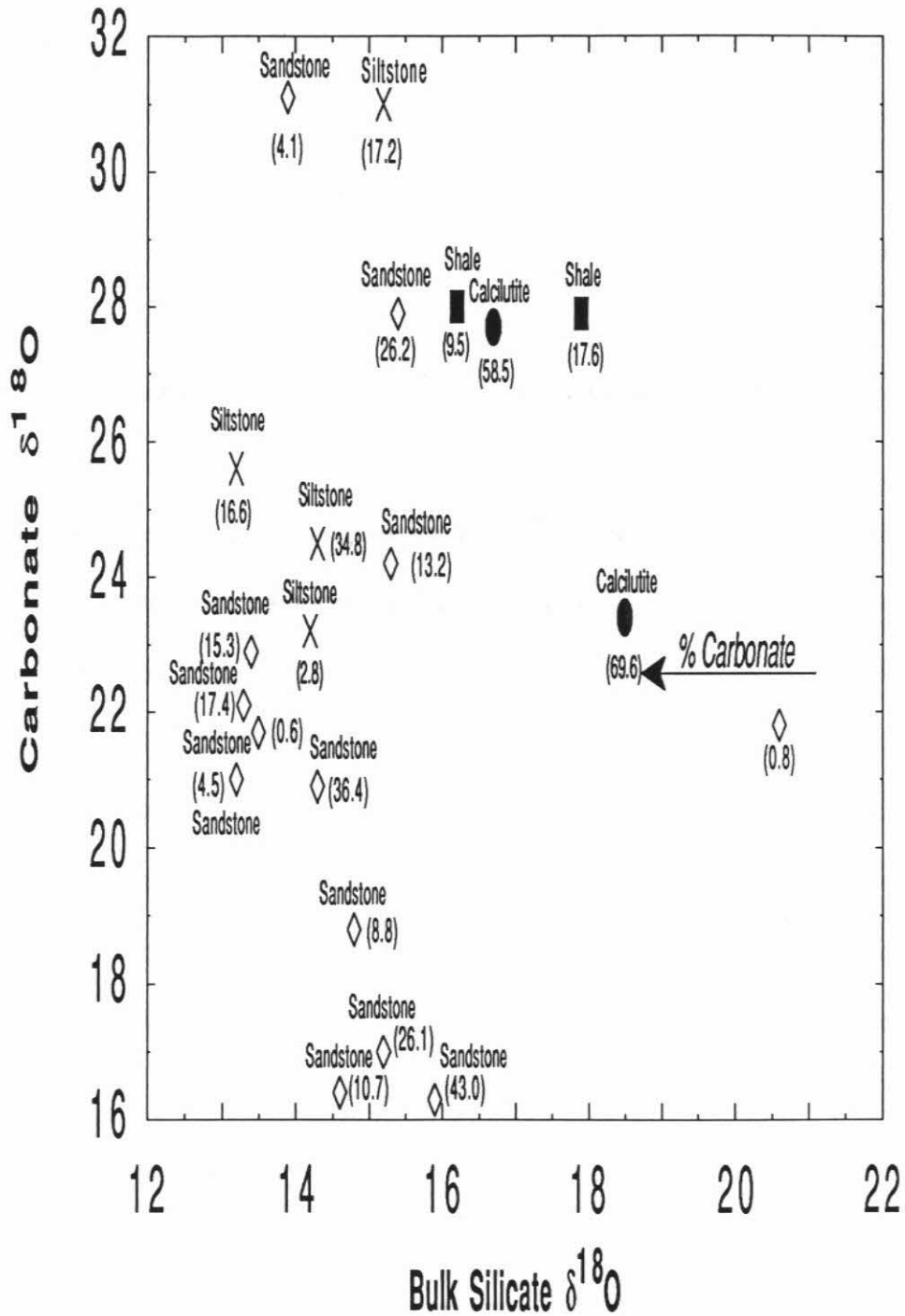
Figure 4.18

Plot of carbonate $\delta^{18}\text{O}$ versus bulk silicate $\delta^{18}\text{O}$ for all Utah/Arizona terrigenous sedimentary rocks analyzed in this study.

$\delta^{13}\text{C}$ Carbonate vs. $\delta^{18}\text{O}$ Bulk Silicate Utah/Arizona Sedimentary Rocks



All Colorado Plateau Sedimentary Rocks:

Carbonate $\delta^{18}\text{O}$ vs Bulk Silicate $\delta^{18}\text{O}$ 

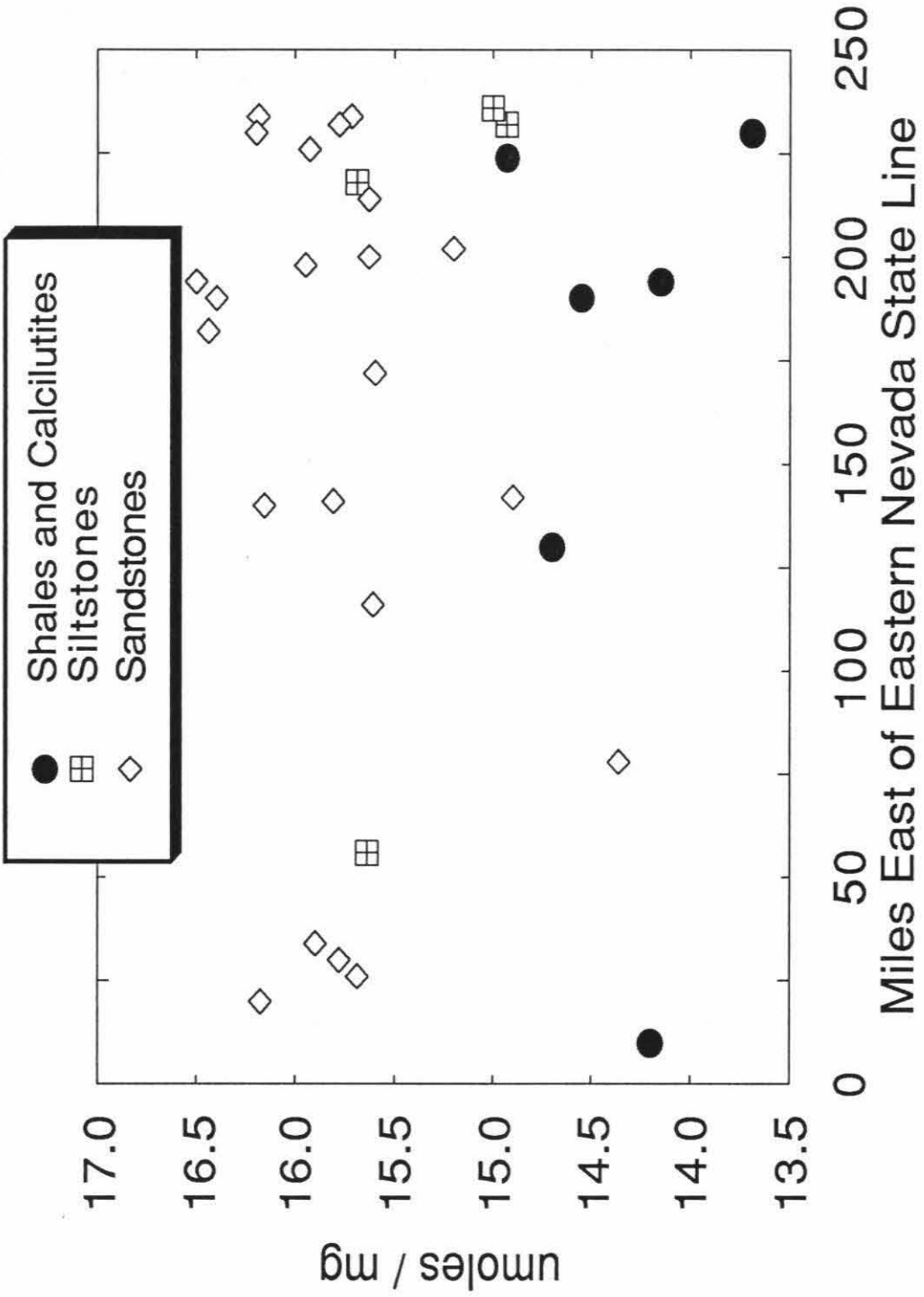
4.10 and 4.2). If the bulk silicate $\delta^{18}\text{O}$ values from the two high- ^{18}O bentonitic samples are excluded, then the range of bulk silicate $\delta^{18}\text{O}$ is +12.3 to +17.9. If 4 high- ^{18}O shales and calcilutites are excluded in addition to the 2 bentonitic samples, then the range for bulk silicate $\delta^{18}\text{O}$ is further reduced to only +12.3 to +16.2, a variation of less than 4 per mil compared to the range of 15 per mil for the $\delta^{18}\text{O}$ of the coexisting carbonate from the same samples. The isotopic data in Figure 4.18 thus again make it clear that the processes responsible for the relatively homogeneous bulk silicate $\delta^{18}\text{O}$ values are drastically different than the processes responsible for the comparatively heterogeneous carbonate $\delta^{18}\text{O}$ values. This is in fact no great surprise, given our knowledge of the contrasting behavior of carbonate minerals and silicate minerals in sedimentary geochemistry.

Figure 4.19 shows a plot of oxygen yields per milligram of sample, as obtained during the bulk silicate fluorination analyses of the samples studied in this work. There is no significant correlation of oxygen yield with distance east of the Nevada-Utah border for shales and calcilutites, siltstones, and sandstones. However, this plot is convenient to show that there is a statistically significant difference in the means of oxygen liberated per milligram of sample between the shale-calcilutite group and the siltstones, and between the shale-calcilutite group and the sandstones. There is no significant difference between the oxygen yields of the sandstones and the siltstones. This difference in oxygen yields for the bulk silicate (*i.e.*, non-carbonate) fraction in the shale-calcilutite group is attributable to compositional and mineralogical differences. The sandstones and siltstones are certainly as a group more quartz-rich and less clay-rich than the shales and calcilutites. Therefore, a higher oxygen yield would be expected for these quartz-rich

Figure 4.19

Plot of oxygen yield in micromoles of oxygen per milligram of sample versus distance in an east-west direction for that Utah/Arizona terrigenous sedimentary rocks analyzed in this study. Note that the shales display consistently lower oxygen yields than the sandstones, and the siltstones tend to have intermediate oxygen yields.

Utah and Arizona: Oxygen Yield vs Miles East of Eastern Nevada State Line



lithologies than for the clay-rich lithologies, as quartz has the highest oxygen yield of any of the common rock-forming silicate minerals (16.67 moles per milligram; see Chapter 2).

The main point of Figure 4.19 is again the confirmation that the carbonate $\delta^{18}\text{O}$ and bulk silicate $\delta^{18}\text{O}$ values are effectively decoupled from one another. This decoupling is clearly due to differences in original primary depositional isotopic compositions of these materials, as well as to differing effects of diagenesis on the carbonate and bulk silicate fractions of these terrigenous sedimentary rocks. The carbonate and bulk silicate fractions were apparently not in isotopic equilibrium with each other at anytime during their depositional and diagenetic history. The carbonate fraction bears the clear signature of deposition from a variety of marine and non-marine waters as well as evidence of extensive post-depositional exchange and alteration; this has produced a carbonate component in these sedimentary rocks of the Colorado Plateau that is isotopically extremely non-homogeneous compared to the bulk silicate material.

The carbonate $\delta^{18}\text{O}$ values for the Utah/Arizona samples are within the range reported by Keith and Weber (1964) for unaltered marine and freshwater limestones from the Permian, Triassic, and Jurassic periods. The three carbonate $\delta^{18}\text{O}$ values below +17 are near the low end of this range, however. It is not possible to tell without further detailed study how much of the carbonate in the Utah/Arizona sedimentary rocks is primary marine, primary fresh-water, or diagenetic, nor how much is reworked detrital material. It is possible, however, to say conclusively that the oxygen isotopic trends of the carbonate have been decoupled from those of the bulk silicate oxygen.

To summarize so far, there are two factors responsible for variance in bulk

silicate $\delta^{18}\text{O}$. One factor is provenance. This factor is responsible for the increase in $\delta^{18}\text{O}$ to the west and south within a given lithology. Another postulated factor is a diagenetic fluid which inhibits the deposition of secondary silica while increasing carbonate cement. This diagenetic fluid may be limited in its effect by primary porosity of the sediment. Primary porosity of the sediment may be related to the original carbonate content of the sediment.

4.7 Conclusions

1. Terrigenous sedimentary rocks from a variety of depositional environments in the Colorado Plateau of Utah/Arizona are relatively uniform in bulk silicate $\delta^{18}\text{O}$ over geologic time, especially when compared to sedimentary cherts and carbonates from other areas throughout the world. The bulk silicate $\delta^{18}\text{O}$ values of these rocks range only from +12.4 to +20.6, even though they include marine, transitional marine/nonmarine, fluvial, and eolian samples that differ in age by more than 1.5 billion years.
2. In spite of the overall general uniformity of $^{18}\text{O}/^{16}\text{O}$, the Utah/Arizona shales and calcilutites can be singled out as having significantly higher bulk silicate $\delta^{18}\text{O}$ values than the interbedded sandstones and siltstones. This is undoubtedly because of the greater abundance of high- ^{18}O clay minerals and/or chert in these fine-grained samples.
3. Bulk silicate $\delta^{18}\text{O}$ decreases to the east and north in the sedimentary rocks of the study area in essentially all lithologies, particularly the sandstones. This suggests the presence of a long-lived, relatively low- ^{18}O source in the vicinity of the Ancestral Rockies of Wyoming and Colorado and a similarly long-lived, higher- ^{18}O source

in the Cordilleran miogeosyncline to the west.

4. The above correlation is parallel to the variation in $\delta^{18}\text{O}$ in the Mesozoic and early Cenozoic plutonic granitic rocks in this broad region, wherein granitic plutons emplaced within the Cordilleran geosyncline are typically 2 to 4 per mil higher in ^{18}O than analogous plutons from the craton of Colorado and eastern Utah (Solomon and Taylor, 1989). The $\delta^{18}\text{O}$ values of the granitic plutons are thought to be controlled by the $\delta^{18}\text{O}$ values of their country rocks at depth (Taylor and Silver, 1978), thus confirming the existence of a large area of high- ^{18}O source rocks to the west of the Colorado Plateau and a large area of lower- ^{18}O source rocks to the east and north.
5. Bulk silicate $\delta^{18}\text{O}$ and carbonate $\delta^{18}\text{O}$ are thoroughly decoupled in Utah/Arizona sedimentary rocks, clearly as a result of: (a) differences in mode of primary deposition of the carbonates and silicates; and (b) differences in the behavior of the carbonate minerals and silicate minerals during diagenesis. Further work is necessary to quantify the details of this decoupling.
6. Bulk silicate $\delta^{18}\text{O}$, carbonate $\delta^{13}\text{C}$, and % carbonate together show a weak correlation, probably mainly because the siltstones and shales analyzed are dominantly marine or transitional, and also richer in high- ^{18}O biogenic carbonate, whereas the coarser-grained samples are dominantly non-marine and typically contain smaller quantities of calcite (as authigenic cement deposited from circulating meteoric waters). More than half the sandstones contain no discernible calcite whatsoever.

CHAPTER 5

Oxygen and Carbon Isotope Studies of Central Appalachian Sedimentary Rocks

5.1 Description of the analyzed samples

The sample localities of 75 Paleozoic terrigenous sedimentary rocks from the central Appalachian Mountains are plotted on Figures 5.1 and 5.2. The location of Figure 5.1 is shown as an inset in the upper right corner of Figure 5.2. Eight of the 75 sample localities are shown on Figure 5.2, and all the others are plotted on Figure 5.1, including two metamorphic rocks from Maryland.

The sample localities are mainly from the folded and deformed Valley and Ridge Province of the Appalachians, but a few samples collected farther to the west are from the Appalachian Plateau Province. The two metasedimentary rocks are from the Piedmont Province. The samples are mainly sandstones (60%), but a number of siltstones (17%) and shales (23%) were also analyzed. These cover an age range from Ordovician to Carboniferous; only the lowermost and uppermost Paleozoic are missing from the data set. The distribution of samples is as follows: Ordovician (11), Silurian and Siluro-Devonian (9), Devonian (35), Mississippian (13), Pennsylvanian and Pennsylvanian-Permian (7). Thus, about half of the samples are Devonian in age, and more than three quarters come from central Pennsylvania, western Maryland, and eastern West Virginia. In spite of this slight age and geographic bias, it is felt that this data set should give a reasonably good, statistically valid, sample collection of the Paleozoic terrigenous sedimentary rocks of the Central Appalachians. Note that more sandstones are represented in the collection than shales simply because the former are in fact more

abundant than the latter in the sampled sections.

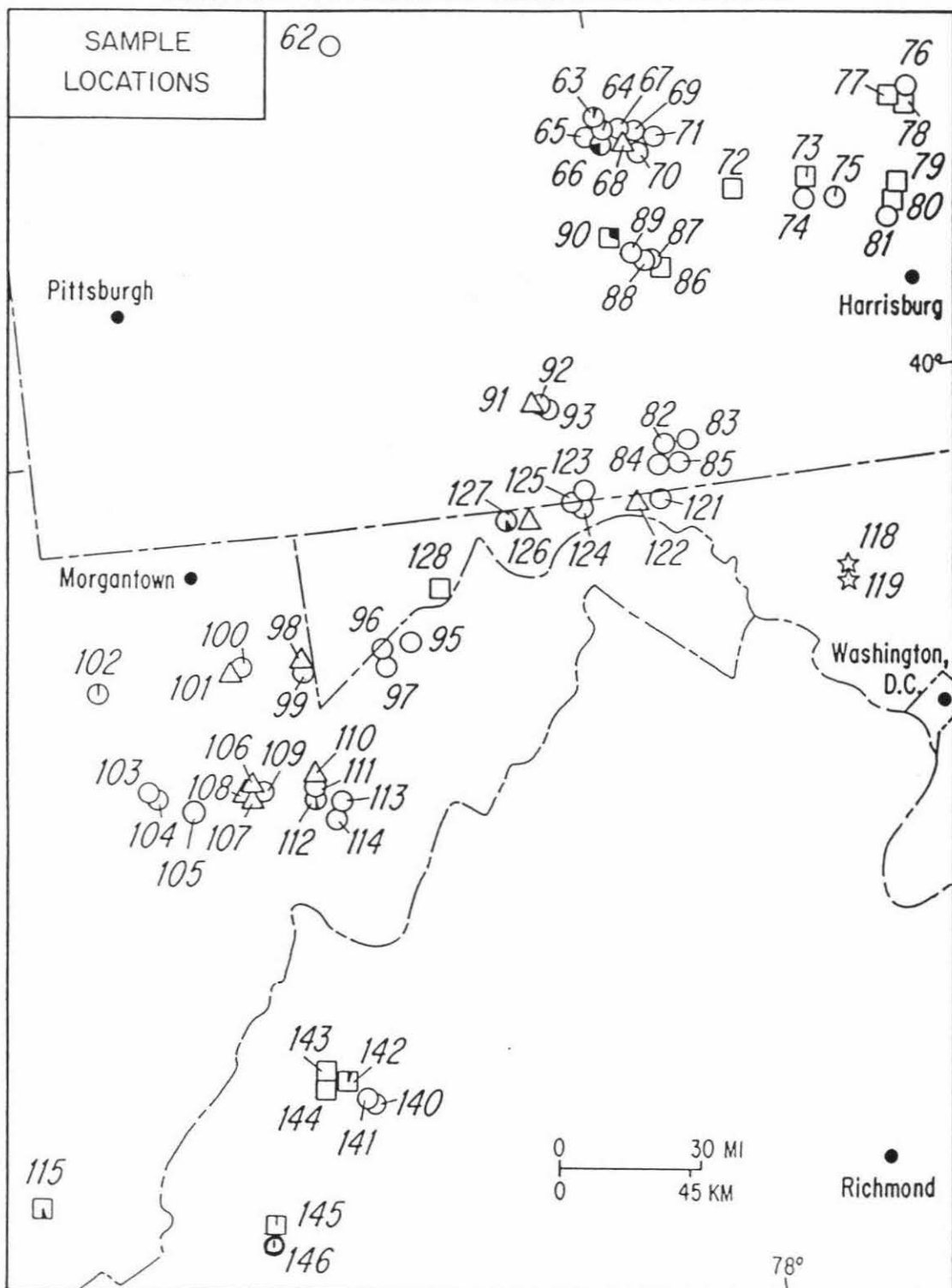
Figure 5.1

Map of southwestern Pennsylvania, western Maryland, eastern West Virginia, and northern Virginia, showing sample localities of most of the samples analyzed in this work from the Central Appalachian Mountains. The sample numbers are keyed to Table 2.1. Sample symbols are as follows: circles = sandstones; squares = shales; triangles = siltstones; stars = metamorphic rocks. The percent blackened area within each symbol indicates the percent carbonate in the sample.

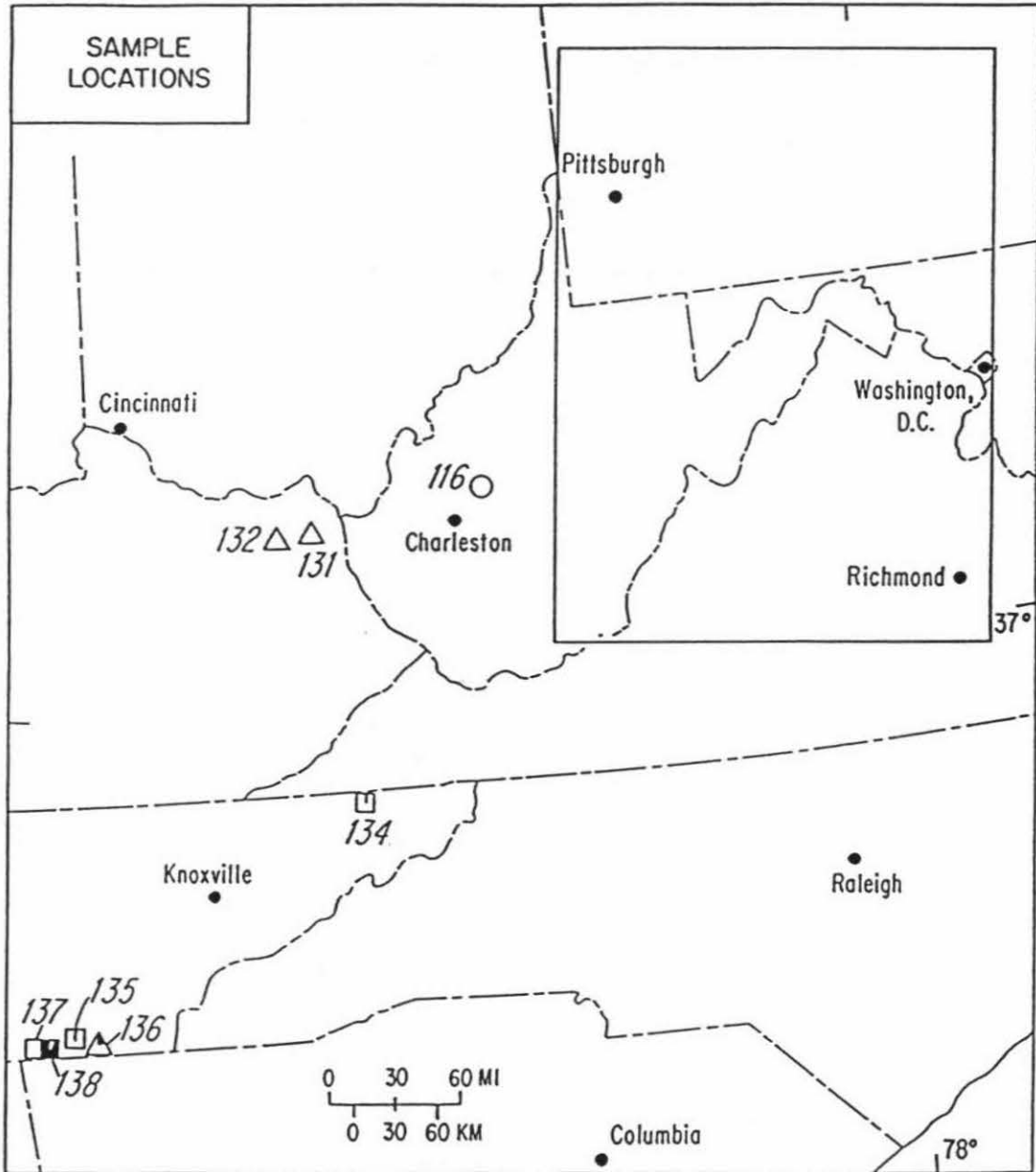
Figure 5.2

Map of the U.S. mid-Atlantic states, showing those sample localities from the Central Appalachians that are not shown in Figure 5.1. Figure 5.1 is shown as an inset in the upper right corner of this figure. Explanation of symbols is the same as for Figure 5.1.

CENTRAL APPALACHIAN SEDIMENTARY ROCKS:



CENTRAL APPALACHIAN SEDIMENTARY ROCKS:



The 75 samples cover a wide range of depositional environments, including marine, transitional, and non-marine (Table 2.1). Most are free of carbonate, but 17 have measurable carbonate contents, including 5 Ordovician ($\delta^{18}\text{O} = +17.7$ to $+26.8$), 5 Devonian ($\delta^{18}\text{O} = +19.4$ to $+23.3$), 6 Mississippian ($\delta^{18}\text{O} = +17.9$ to $+25.2$), and 1 Pennsylvanian ($\delta^{18}\text{O} = +17.8$). One of these samples (138) is a Mississippian calcilutite from Tennessee containing 93% carbonate and only a tiny amount of terrigenous material; this sample is treated separately in much of the discussion that follows. The $\delta^{13}\text{C}$ values of the carbonate-bearing rocks range from a low of -10.7 in an Upper Pennsylvanian sandstone sample (102) to a high of $+0.6$ in the aforementioned calcilutite.

The carbon isotope ratios of the carbonates from these terrigenous sedimentary rocks form a distinctly bimodal population, with half the samples having $\delta^{13}\text{C} = -2.2$ to $+0.6$ and the other half having $\delta^{13}\text{C} = -10.7$ to -5.0 . The mean $\delta^{18}\text{O}$ value of the 8 carbonates in the high- $\delta^{13}\text{C}$ group is $+22.6$ whereas the mean $\delta^{18}\text{O}$ of the 8 low- $\delta^{13}\text{C}$ carbonates is more than 3 per mil lower at $+19.3$. The low- $\delta^{13}\text{C}$, low- $\delta^{18}\text{O}$ group is made up of fresh-water or near-shore marine deposits, whereas the high- $\delta^{13}\text{C}$, high- $\delta^{18}\text{O}$ group is dominantly marine (Table 2.1). These carbonate isotope data thus fit the available information on environment of deposition of these samples pretty well, because relatively low $\delta^{13}\text{C}$ and low $\delta^{18}\text{O}$ values are typical of carbonate deposited in terrestrial fresh-water or brackish-water environments.

5.2 Overview of bulk silicate oxygen isotope data

The bulk silicate $\delta^{18}\text{O}$ values of the 75 Central Appalachian terrigenous sedimentary rocks from the Appalachian miogeosyncline are strikingly uniform, with a

mean of +14.8 and a standard error of the mean (SEM) of 0.1 (Figure 5.3). Again, recall that for the purposes of this work, "bulk silicate" means either (1) the entire whole-rock oxygen of samples that contain less than 0.1% carbonate, or (2) the residual whole-rock remaining after acid treatment has extracted the carbonate fraction (see Chapter 2). Also "Central Appalachians" refers to outcrops in the states of Pennsylvania, Maryland, West Virginia, Virginia, Eastern Kentucky and Eastern Tennessee.

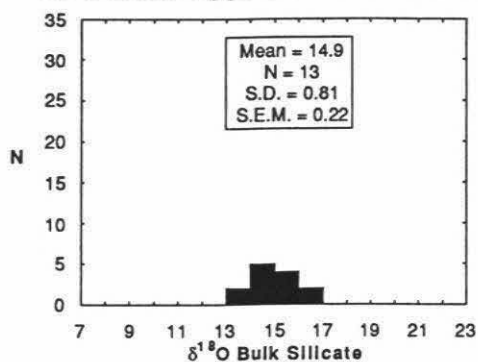
Comparison of Figure 5.3 with the data in Figure 3.17 of Chapter 3 demonstrates that Central Appalachian sedimentary rocks are much more uniform in $^{18}\text{O}/^{16}\text{O}$ than previously studied non-eugeosynclinal sedimentary rocks in the geochemical literature (also see Figure 5.11 below). Central Appalachian sedimentary rocks also have a significantly higher mean bulk silicate $\delta^{18}\text{O}$ than that reported for previously analyzed eugeosynclinal sedimentary rocks in the literature. It must be remembered, however, that the only major earlier study of eugeosynclinal rocks is that of Magaritz and Taylor (1976) on the Franciscan Formation of the California Coast Ranges.

Of the various groupings of Appalachian sedimentary rocks based on grain size, sandstones show the most uniform bulk silicate $\delta^{18}\text{O}$, with a mean of +14.9 and a SEM of 0.09. Of the analyzed sandstones, 80% have $\delta^{18}\text{O}$ values within two per mil of each other, lying between $\delta^{18}\text{O} = +14$ and +16. Calcareous and noncalcareous sandstones have essentially the same mean bulk silicate $\delta^{18}\text{O}$ (+14.9 vs. +14.8), although the noncalcareous varieties are far more abundant. Bulk silicate $\delta^{18}\text{O}$ values of 8 calcareous sandstones show slightly more dispersion than do those of the 37 noncalcareous sandstones (SEM of 0.3 vs. 0.10). Siltstones display the same mean bulk silicate $\delta^{18}\text{O}$

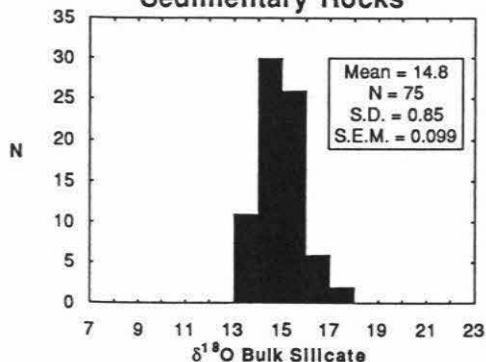
Figure 5.3

Eight comparative histograms showing the bulk silicate $\delta^{18}\text{O}$ values of various categories of Central Appalachian terrigenous sedimentary rocks. The analyzed samples are subdivided on the basis of clast size and grain size, as well as upon the presence or absence of carbonate as detected by reacting the samples with ten weight per cent hydrochloric acid (see Chapter 2). The plotted categories include: all 75 rocks of all lithologies; all 45 sandstones; all 17 shales; and all 13 siltstones; in addition, the sandstones and shales are further subdivided into calcareous and noncalcareous varieties. Only one calcareous siltstone was analyzed; it had a bulk silicate $\delta^{18}\text{O}$ of +16.0 and was included with the noncalcareous siltstones in the histogram for all siltstones. The bulk silicate $\delta^{18}\text{O}$ value for the only limestone analyzed, a calcilutite, is depicted in the histogram for the Central Appalachian calcareous shales. This calcilutite bulk silicate $\delta^{18}\text{O}$ is not, however, included in the calculation of the mean for the calcareous shales.

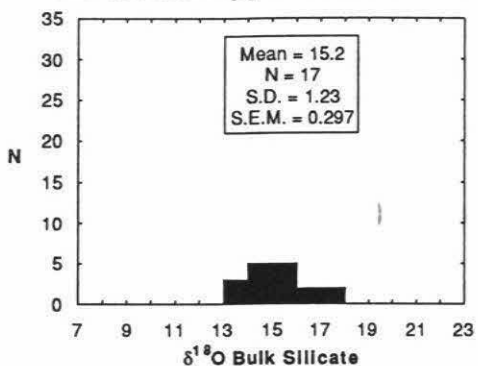
All Central Appalachian Siltstones



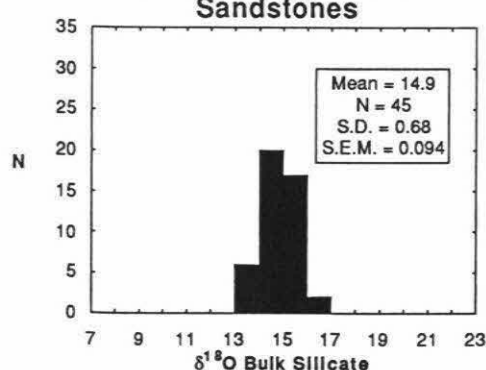
All Central Appalachian Sedimentary Rocks



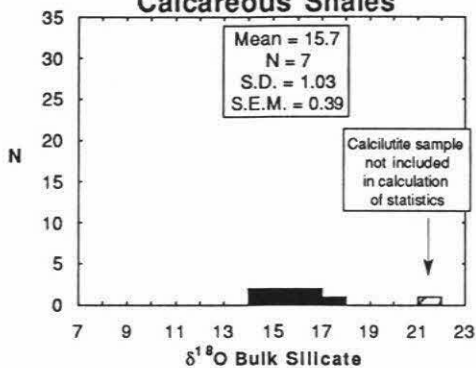
All Central Appalachian Shales



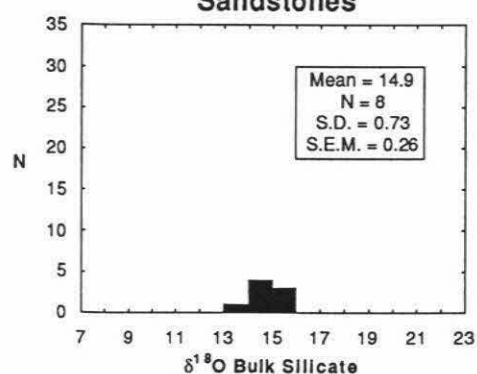
All Central Appalachian Sandstones



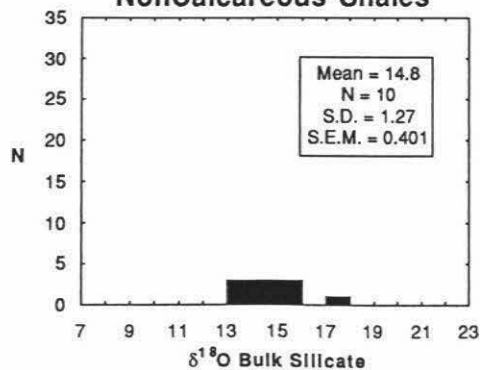
Central Appalachian Calcareous Shales



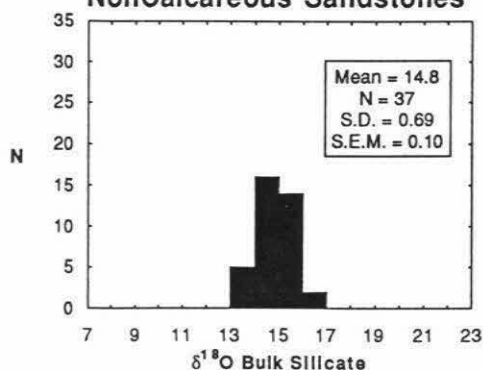
Central Appalachian Calcareous Sandstones



Central Appalachian NonCalcareous Shales



Central Appalachian NonCalcareous Sandstones



as sandstones, but show slightly greater dispersion (SEM of 0.2 vs. 0.1). Shales have a somewhat greater mean bulk silicate $\delta^{18}\text{O}$ than siltstones and sandstones (+15.2 vs. +14.9) and a slightly greater dispersion (SEM of 0.3). It is interesting that dispersion increases with decreasing median grain size among the three lithologic groups from 0.1 to 0.2 to 0.3 in the sequence: sandstone, siltstone, and shale. This observation is in agreement with the hypothesis to be advanced below that post-depositional isotopic exchange has contributed to the bulk silicate $\delta^{18}\text{O}$ variation in these terrigenous sediments as a result of more extreme isotopic exchange effects produced during diagenesis among the more reactive, higher-surface-area (*i.e.*, finer-grain size) particles.

The mean bulk silicate $\delta^{18}\text{O}$ for seven calcareous shales is +15.7. Calculation of this mean does not include the unusually heavy $\delta^{18}\text{O}$ value obtained for the single analyzed limestone, a calcilutite from the Pennington Formation in Tennessee, which is +21.7. Thus, the mean bulk silicate $\delta^{18}\text{O}$ for calcareous shales is 0.9 per mil heavier than the mean for non-calcareous shales. While these means are not markedly different, the small difference may be a real effect, and it does raise interesting questions about the possible influence of carbonates in producing differences in isotopic exchange behavior between aqueous fluids and shales.

Why is there essentially no difference in bulk silicate $\delta^{18}\text{O}$ between calcareous and noncalcareous sandstones while there is a difference of 0.9 per mil between calcareous and noncalcareous shales? Below, we discuss three possible reasons for this effect. One possibility is that oxygen isotopic exchange has taken place between the high- ^{18}O carbonate component and the lower- ^{18}O , fine-grained, bulk-silicate shale component during diagenesis, whereas such exchange is either limited or non-existent for

these same components in the coarser-grained sandstones. Any such isotopic exchange effects obviously would have to be mediated by aqueous fluids, because of prohibitively slow solid-state diffusion coefficients at low temperatures. Another possibility is the formation of large amounts of isotopically heavy authigenic or biogenic silica in the calcareous units. Still another possibility is an original compositional difference between calcareous and noncalcareous shales. Such compositional differences might include: (1) a higher proportion of isotopically heavy clay minerals in the calcareous shales; or (2) primary isotopic differences related to a difference in provenance (*e.g.*, source area) for the calcareous and noncalcareous shales.

The two major sources of sediment for the Paleozoic sedimentary rocks of the Appalachian Mountains were a cratonic source to the west and north, and a tectonic source to the east and south (Meckel, 1970). However, all formations in this study, except the Devonian black shales, are described as representing portions of several large westward-verging tongues of terrigenous clastic material whose source is dominantly to the east and south. Therefore, a tectonic versus cratonic source would not explain differences in bulk silicate $\delta^{18}\text{O}$ for calcareous versus noncalcareous shales. There remains the possibility that differences in bulk silicate $\delta^{18}\text{O}$ along strike in the tectonic source would be responsible for these effects. However, the isotopic homogeneity of the sandstones for considerable distances along the NE-SW tectonic grain of the Appalachians argues against this.

The oxygen yield per milligram of sample as measured during the fluorine extraction process should give a rough estimate of the quartz content of the shales, other things being equal. This is because of the relatively low atomic weight of silicon, giving

quartz the highest oxygen yield per milligram of any sample of the major terrigenous rock-forming silicate minerals. Figure 5.4 compares oxygen yields for the bulk silicate fractions of the calcareous and noncalcareous shales. Neither the mean nor the standard deviation from the mean are significantly different for the two groups, suggesting that the amounts of quartz in calcareous and noncalcareous shales are not in fact significantly different. This could be more conclusively determined through detailed x-ray diffraction analysis, which was not done in this work. Still unconstrained are the isotopic compositions of the quartz in each shale sample and the degree of isotopic exchange of the bulk silicate material with the coexisting carbonate component.

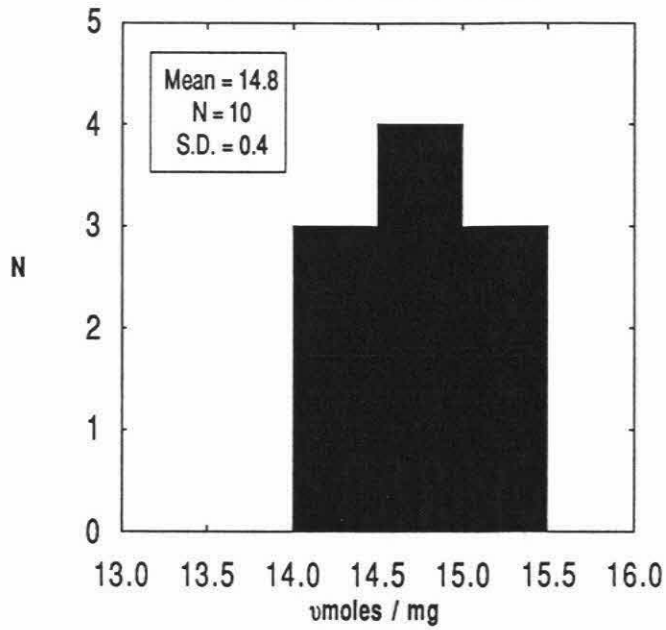
Figures 5.5 to 5.10 are a series of comparative histograms of bulk silicate $\delta^{18}\text{O}$ in Central Appalachian sedimentary rocks, based on depositional environment, lithology, and carbonate content. The calcilutite sample is not included. Figure 5.5 compares the two categories of marine vs. nonmarine terrigenous sedimentary rocks. The means of the marine and nonmarine rocks are +15.3 and +14.7, respectively, which is significantly different at the 0.025 probability level. One reason the nonmarine rocks might *a priori* be expected to be isotopically lighter than the marine rocks could be the increased opportunity for meteoric water interaction in nonmarine environments. Meteoric waters in such environments during the Paleozoic would probably be at least 3 to 5 per mil lower in ^{18}O than the corresponding marine waters.

Figure 5.6 subdivides the nonmarine bulk silicate $\delta^{18}\text{O}$ of the Appalachian sedimentary rocks values into two categories, fluvial and transitional, and compares these data with the samples from all the various marine environments. This figure shows that there is no significant difference between the isotopic means for the transitional and

Figure 5.4

Two comparative histograms showing the oxygen yields from the bulk silicate material of calcareous and noncalcareous Central Appalachian shales in micromoles per milligram. The oxygen yield from the calcilutite sample is included in the histogram for calcareous shales. The number of micromoles of oxygen liberated by reaction with fluorine for each sample was measured with a mercury manometer before the sample was collected for mass spectrometric analysis. To obtain the oxygen yield in micromoles per milligram, the number of micromoles of gas collected for each sample was divided by the weight of the sample measured before loading into the nickel reaction vessel. A sample which was pure quartz and gave a 100 per cent yield would have a yield of 16.64 micromoles per milligram.

Oxygen Yields for Noncalcareous Shales



Oxygen Yields for Calcareous Shales

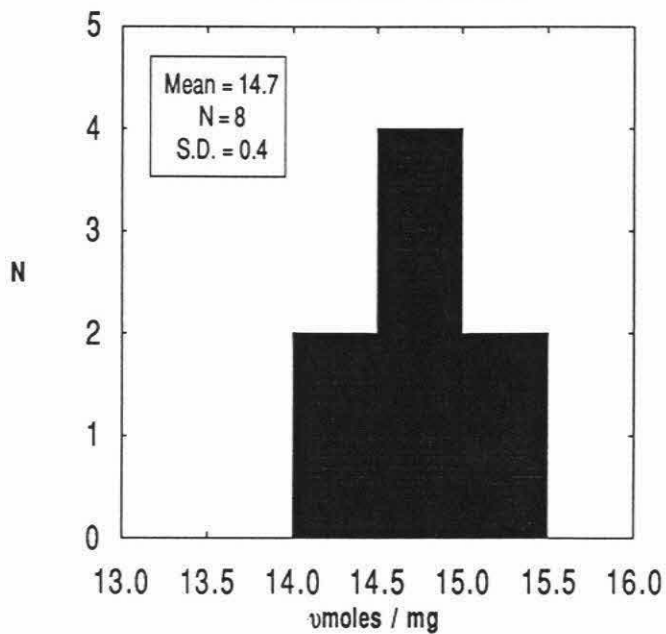
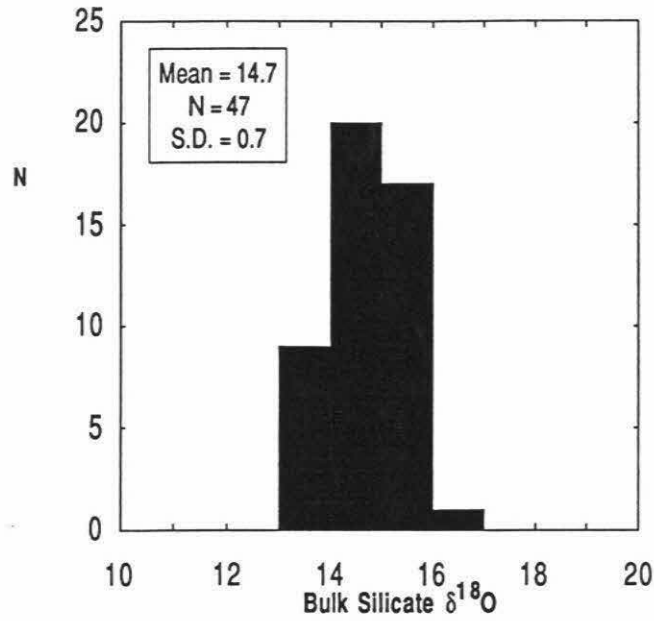


Figure 5.5

Two comparative histograms showing the bulk silicate $\delta^{18}\text{O}$ values for all analyzed marine and nonmarine sedimentary rocks from the Central Appalachians. Results of a two-way analysis of variance showed that the means of the marine and nonmarine groups are significantly different at the 0.025 probability level. The marine samples also show greater dispersion than the nonmarine samples.

**All Central Appalachian
Nonmarine Sedimentary Rocks**



**All Central Appalachian
Marine Sedimentary Rocks**

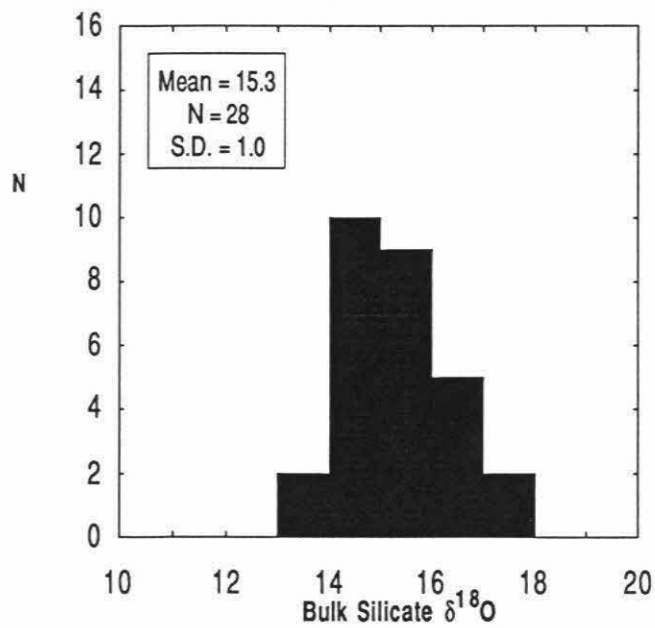
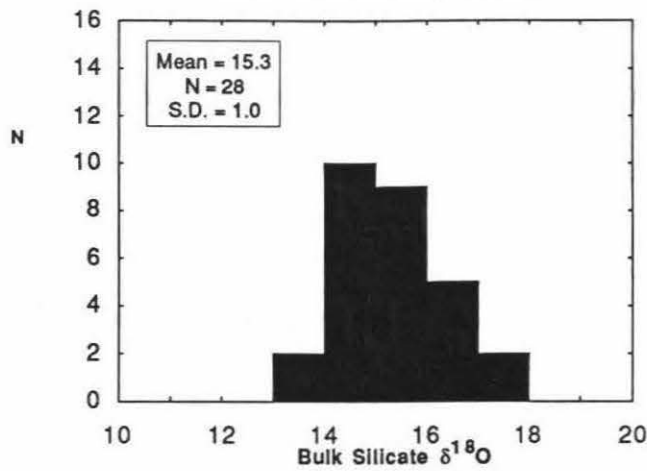


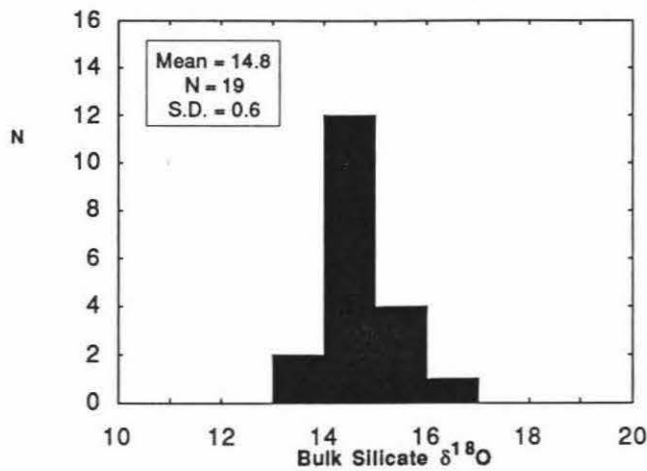
Figure 5.6

Three comparative histograms showing the bulk silicate $\delta^{18}\text{O}$ values of all of the sedimentary rocks from the Central Appalachians subdivided into marine, transitional, and fluvial categories. The transitional and fluvial samples are the same samples lumped together as nonmarine in Figure 5.5; these two nonmarine categories both display similar mean bulk silicate $\delta^{18}\text{O}$, as well as a similar dispersion in bulk silicate $\delta^{18}\text{O}$ values. One reason why the bulk silicate $\delta^{18}\text{O}$ values for transitional and fluvial sedimentary rocks may be lighter than those of marine sedimentary rocks is the increased opportunity for the fluvial and transitional samples to have interacted with isotopically light meteoric waters during diagenesis.

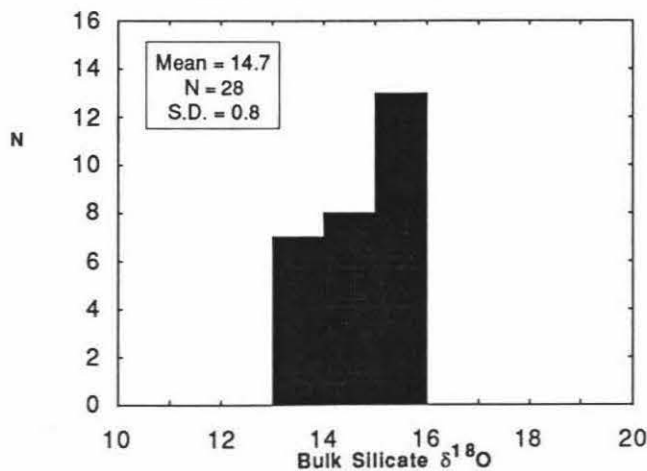
**All Central Appalachian
Marine Sedimentary Rocks**



**All Central Appalachian
Transitional Sedimentary Rocks**



**All Central Appalachian
Fluvial Sedimentary Rocks**



fluvial environments ($\delta^{18}\text{O} = +14.8$ and $+14.7$, respectively), but that both of these non-marine groupings have lower mean $\delta^{18}\text{O}$ than that of the marine data set.

Figure 5.7 compares the bulk silicate $\delta^{18}\text{O}$ of calcareous and noncalcareous samples from the three different depositional environments. Although the number of calcareous samples in the nonmarine categories is very small, there is a definite tendency toward heavier bulk silicate $\delta^{18}\text{O}$ values in the calcareous samples compared to the noncalcareous samples from all three aqueous environments.

In Figures 5.8, 5.9, and 5.10, these data are further subdivided into shales, siltstones and sandstones, but in general, the sample size is so small with this number of subdivisions of the data that it is not prudent to draw substantial conclusions from any of the variations displayed in these figures, other than the fact that the mean $\delta^{18}\text{O}$ values of all of the subdivisions are so uniform. Note that the sixteen different subdivisions of the isotopic data set in Figures 5.8, 5.9, and 5.10 give a range of mean $\delta^{18}\text{O}$ values from only $+14.3$ to $+16.0$! In spite of this remarkable uniformity of the 16 tabulated mean $\delta^{18}\text{O}$ values, there are some consistent relationships among these means: (1) The calcareous categories consistently have slightly higher mean $\delta^{18}\text{O}$ values than the analogous noncalcareous categories; the only exception to this rule is the group of marine sandstones, where the calcareous samples are overall 0.6 per mil lower than the noncalcareous samples (Figure 5.10). (2) The marine categories are consistently higher in ^{18}O than the non-marine categories; the only exceptions are in the cases where the sample population in a given category involves only one or two samples (Figures 5.9 and 5.10). These diagrams may be helpful in raising questions to address in future more detailed investigations.

Figure 5.7

Six comparative histograms showing the bulk silicate $\delta^{18}\text{O}$ values of all Central Appalachian sedimentary rocks, subdivided into calcareous and noncalcareous varieties (columns), and then further subdivided into marine, transitional, and fluvial environments (rows). Though the sample size is small for the calcareous rocks, for each environment the mean calcareous bulk silicate $\delta^{18}\text{O}$ value is heavier than the corresponding noncalcareous bulk silicate $\delta^{18}\text{O}$ value. Also, for the calcareous samples, the mean bulk silicate $\delta^{18}\text{O}$ is distinctly heavier for samples from the marine environment than from the transitional and fluvial environments. For noncalcareous samples, the mean bulk silicate $\delta^{18}\text{O}$ is also higher for marine samples than for the fluvial or transitional samples.

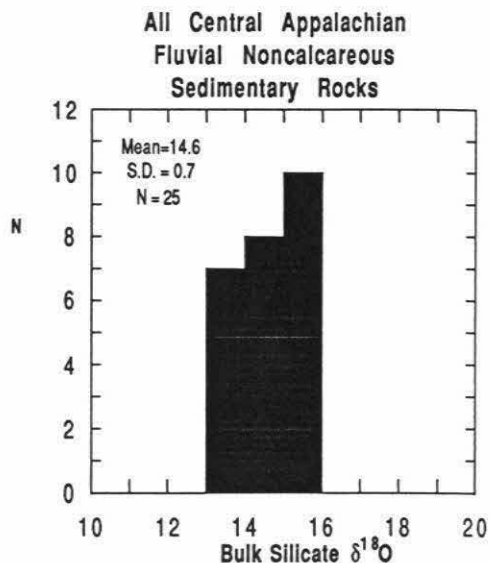
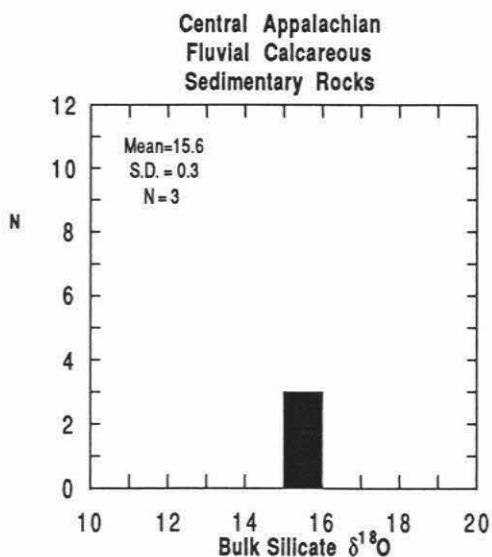
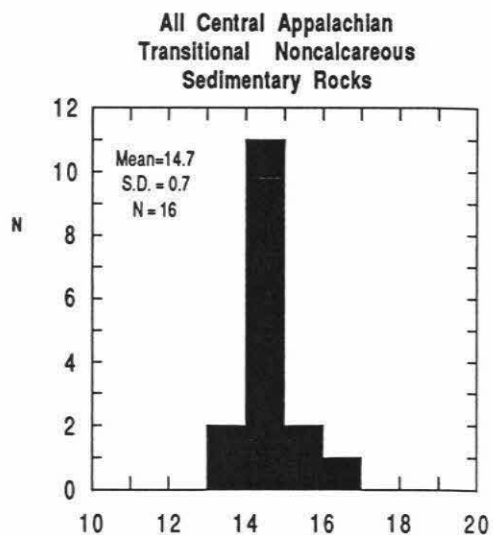
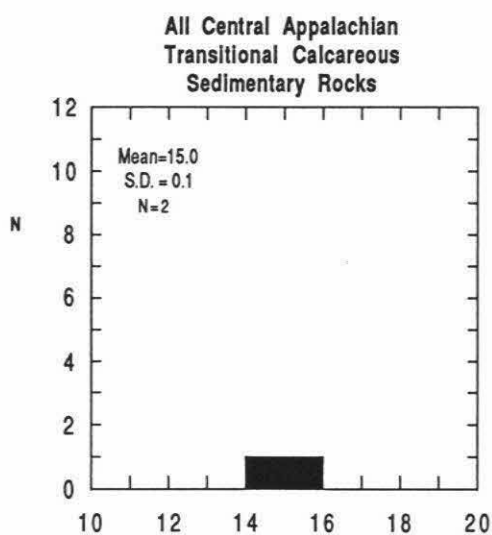
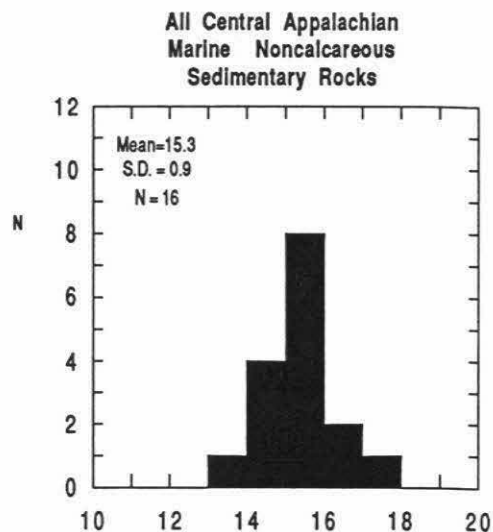
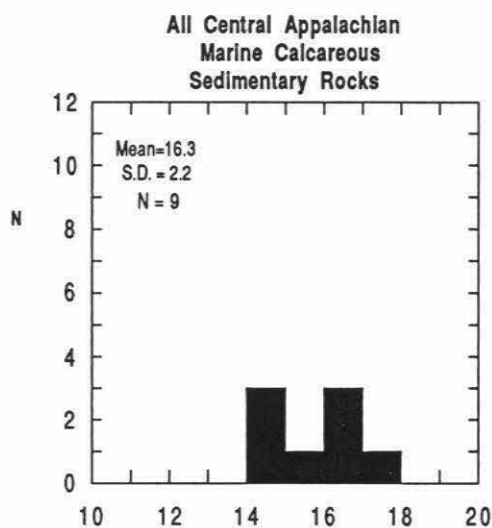


Figure 5.8

Six comparative histograms showing the bulk silicate $\delta^{18}\text{O}$ values of all calcareous and noncalcareous Central Appalachian shales from marine, transitional, and fluvial environments.

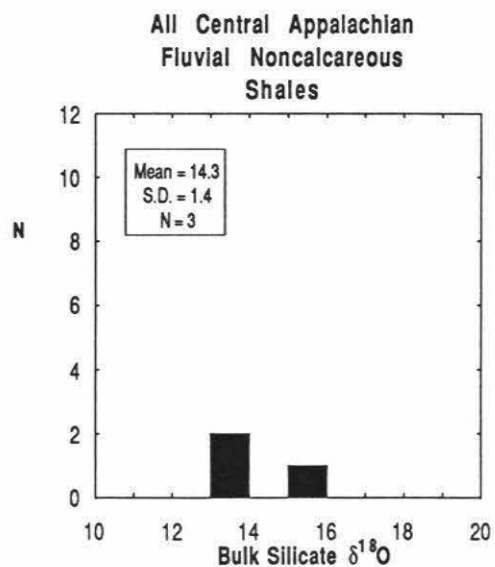
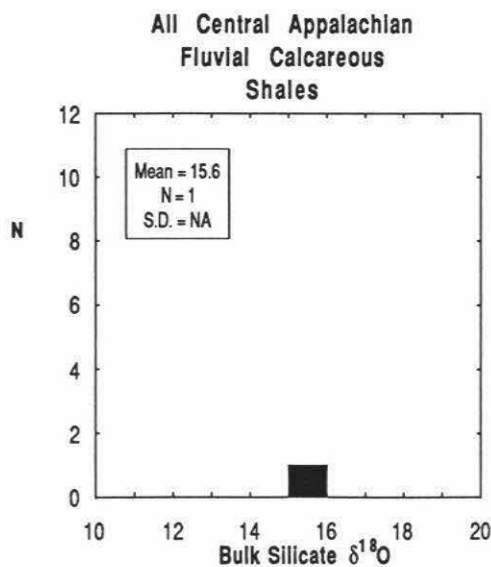
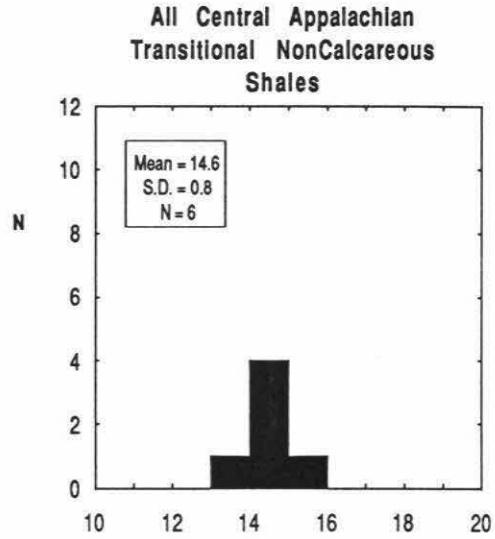
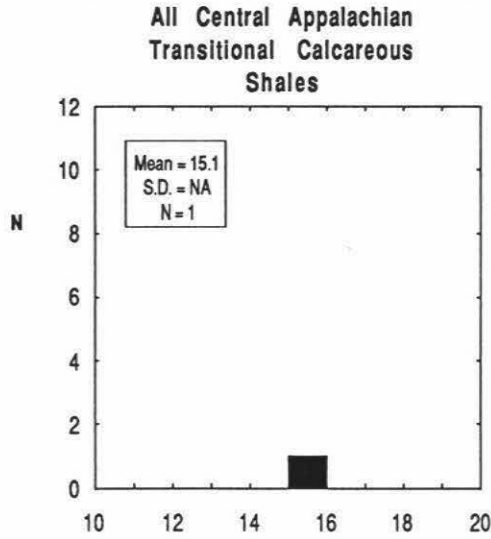
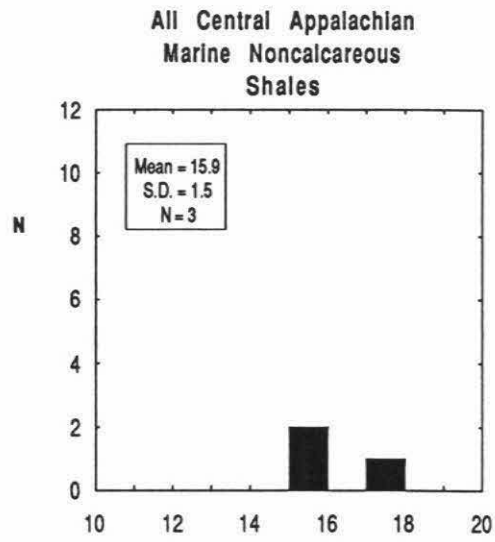
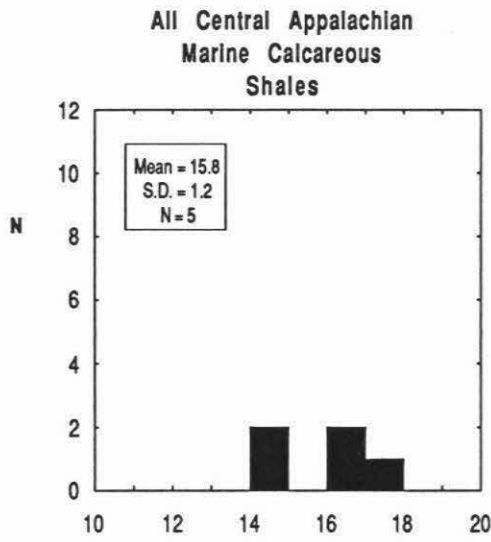


Figure 5.9

Four comparative histograms showing the bulk silicate $\delta^{18}\text{O}$ values of all Central Appalachian calcareous and noncalcareous siltstones, subdivided into marine, transitional, and fluvial categories. However, note that only one calcareous siltstone was analyzed, and it is a marine sample. The noncalcareous siltstones from the marine, fluvial, and transitional environments have mean bulk silicate $\delta^{18}\text{O}$ values that are 0.9 to 1.5 per mil lower than this marine calcareous siltstone.

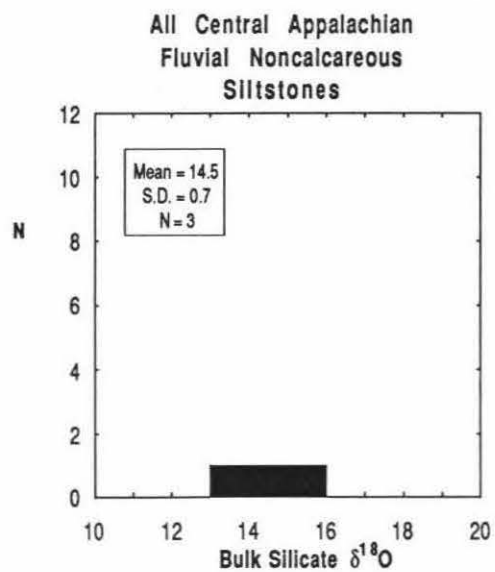
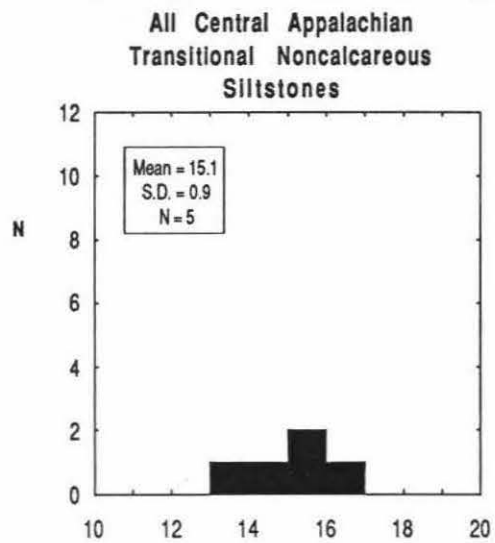
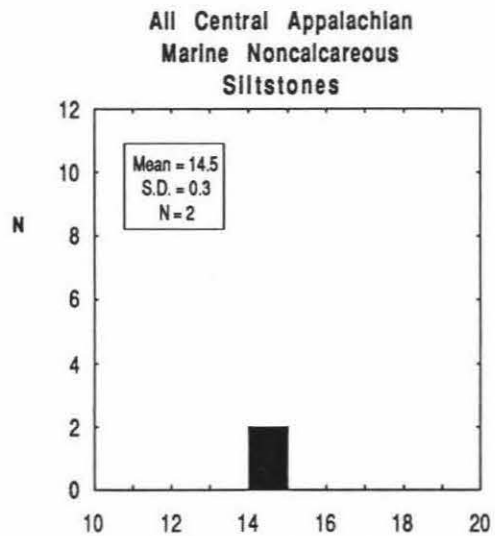
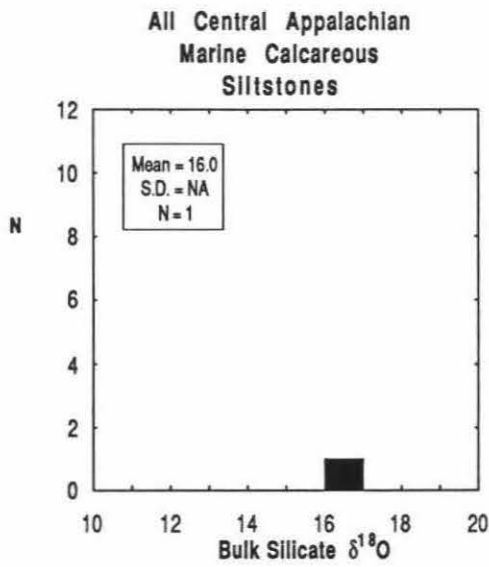
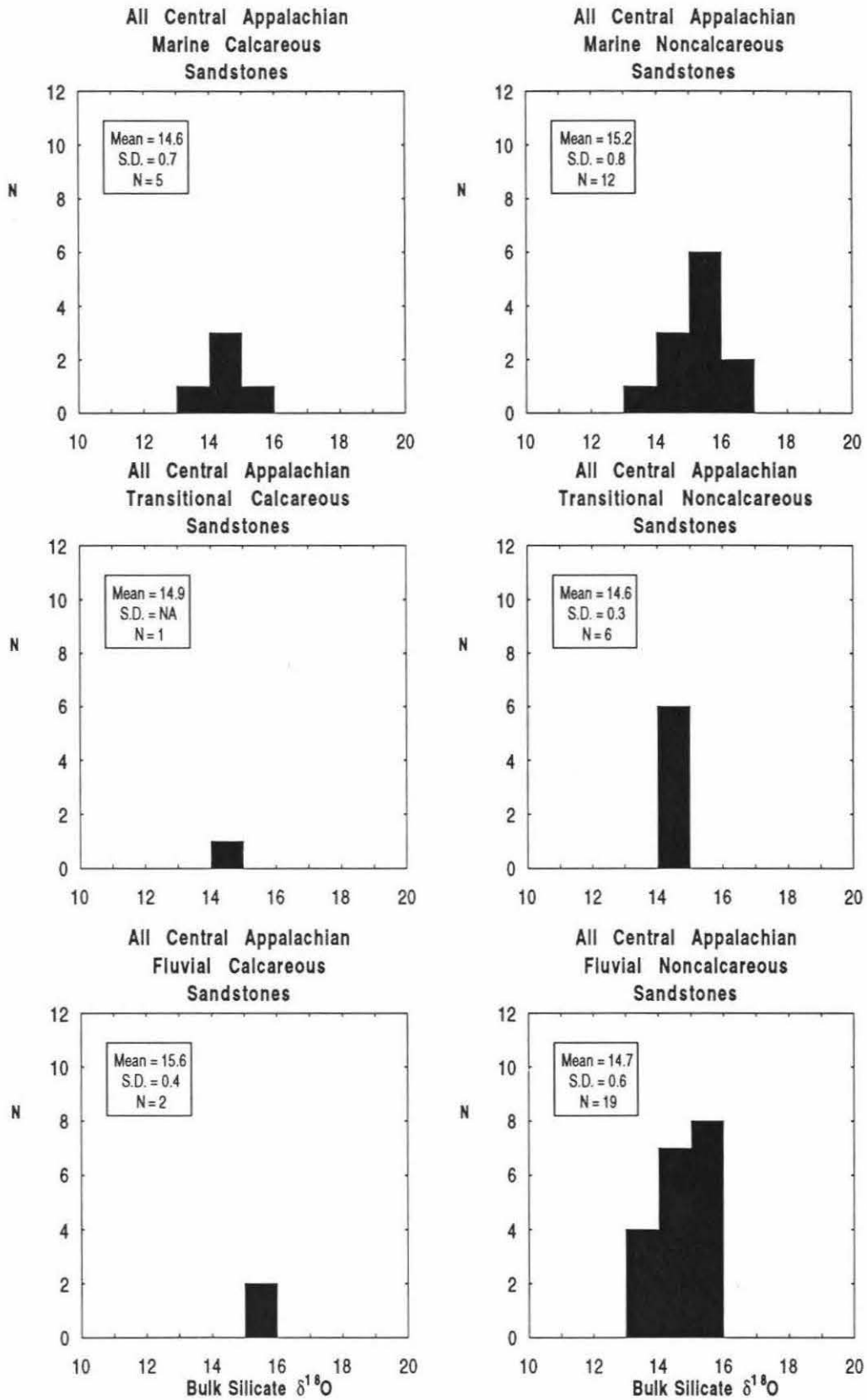


Figure 5.10

Six comparative histograms showing bulk silicate $\delta^{18}\text{O}$ values of all Central Appalachian sandstones, subdivided into calcareous and noncalcareous varieties (columns), and further subdivided into marine, transitional, and fluvial categories (rows). The mean bulk silicate $\delta^{18}\text{O}$ value of the marine calcareous sandstones is 0.3 to 1.0 per mil lighter than the three analyzed samples of fluvial and transitional calcareous sandstones. This trend is the opposite of that generally observed for the shales and siltstones, where the mean bulk silicate $\delta^{18}\text{O}$ of the various categories of calcareous samples are usually heavier than the means of the analogous noncalcareous samples (Figures 5.8 and 5.9). This suggests the possibility that during diagenesis there may have been some oxygen isotopic exchange between carbonate and bulk silicate oxygen for the smaller diameter silt and shale particles, but that this effect was limited or non-existent for the much coarser grained sandstones (see text). Further work would be necessary to prove this hypothesis.



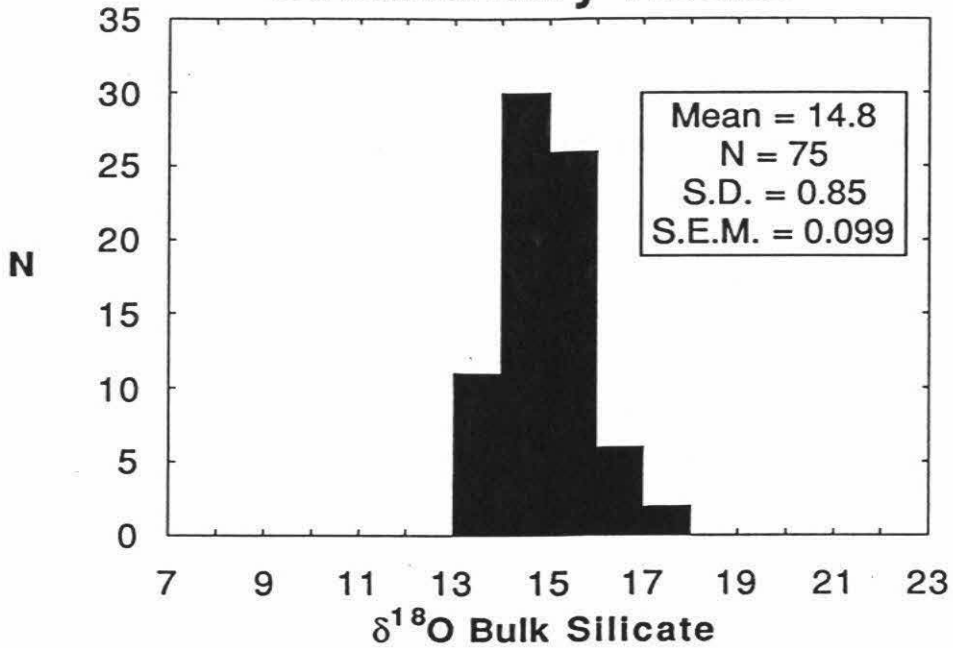
While much of the following discussion will indeed focus on the relatively small differences in bulk silicate $\delta^{18}\text{O}$ between different sedimentary lithologies in the Appalachians, it must be emphasized that the most striking aspect of the bulk silicate $\delta^{18}\text{O}$ data presented in Figures 5.3 to 5.10 is that the $\delta^{18}\text{O}$ values are so uniformly similar in such a great variety of sandstones, siltstones, and shales from an enormous area of about 200,000 km² across six states. These remarkable similarities are also seen across depositional ages that differ by more than 200 million years (from the Ordovician through the Pennsylvanian geologic periods), as well as spanning over 1000 km along the SW-NE strike of the Appalachian Mountains.

It is useful to compare the Appalachian data set with a compilation of whole-rock $\delta^{18}\text{O}$ values from the geochemical literature for all marine, transitional, and nonmarine terrigenous sedimentary rocks (see Chapter 3). The latter display a range of more than 11 per mil (Figure 5.11). In this literature compilation, we have excluded all samples of pelagic sediments, as well as all those from areas that have suffered complex post-depositional geologic histories of hydrothermal alteration, strong metamorphism or intense tectonic shearing. Also, all sedimentary samples that are dominantly biogenic or authigenic are excluded. Otherwise, the $^{18}\text{O}/^{16}\text{O}$ range of the sediments from the literature would be vastly greater than the reported 11 per mil. The bulk silicate $\delta^{18}\text{O}$ values for all Central Appalachian sedimentary rocks from marine, transitional, and nonmarine samples (excluding the single calcilutite) display a range of only 4.4 per mil, less than half the range of the whole-rock $^{18}\text{O}/^{16}\text{O}$ data from the literature. (Note that if true whole-rock $\delta^{18}\text{O}$ values are calculated for Central Appalachian samples by adding the various carbonate contributions, then the range increases from 4.4 to 5.4 per mil.

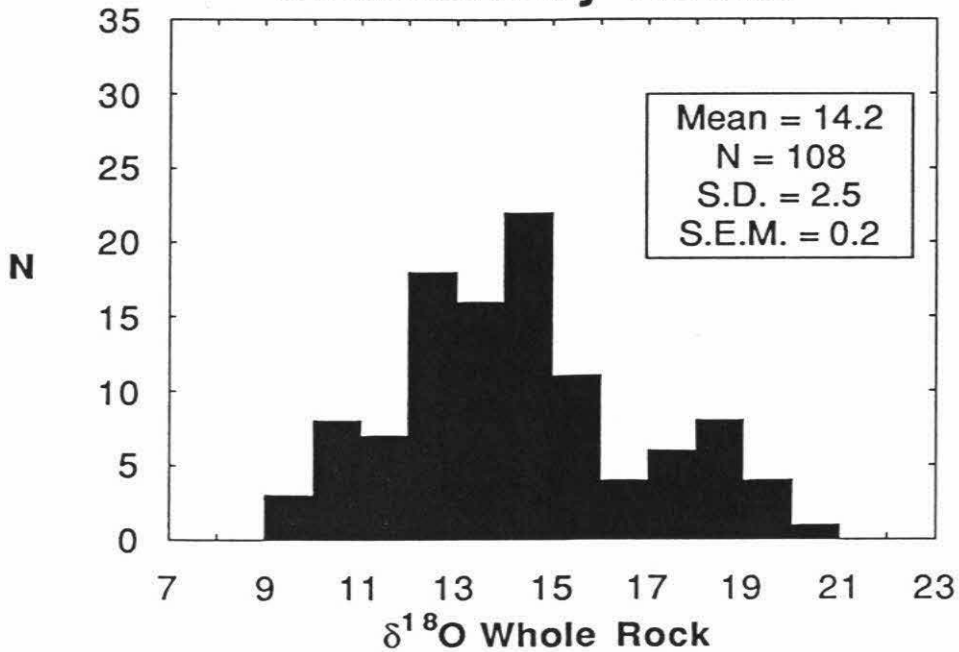
Figure 5.11

Two comparative histograms showing: (1) all whole-rock $\delta^{18}\text{O}$ values of sedimentary rocks (pelagics excluded) from the literature; and (2) all whole-rock $\delta^{18}\text{O}$ values from this study of Central Appalachian sedimentary rocks (calcilutite excluded). This figure clearly shows that the Central Appalachian sedimentary rocks are much more uniform in whole-rock $\delta^{18}\text{O}$ than previously analyzed samples from a wide variety of areas. Note that these are whole-rock $\delta^{18}\text{O}$ values, not bulk silicate $\delta^{18}\text{O}$ values. In cases where carbonates are present, the whole-rock $\delta^{18}\text{O}$ values were calculated by material balance from the measured bulk silicate and carbonate $\delta^{18}\text{O}$ values.

All Central Appalachian Sedimentary Rocks



All Literature Nonpelagic Sedimentary Rocks



However, this is still less than half the range of whole-rock values from the literature.)

Why are the bulk silicate $\delta^{18}\text{O}$ values of sedimentary rocks from the Central Appalachians so uniform and homogeneous? Possible answers include oxygen isotopic homogeneity of the original sediments, homogenization through post-depositional oxygen isotopic alteration of the original sediments, or some combination of these two possibilities. It will be shown below that it may be possible to answer the bulk silicate $\delta^{18}\text{O}$ homogeneity question through detailed study of the relatively small systematic differences in bulk silicate $\delta^{18}\text{O}$ between different lithologies and between different locations along the SW-NE strike of the Central Appalachian Mountains.

5.3 Bulk silicate oxygen isotope variation with geographic area

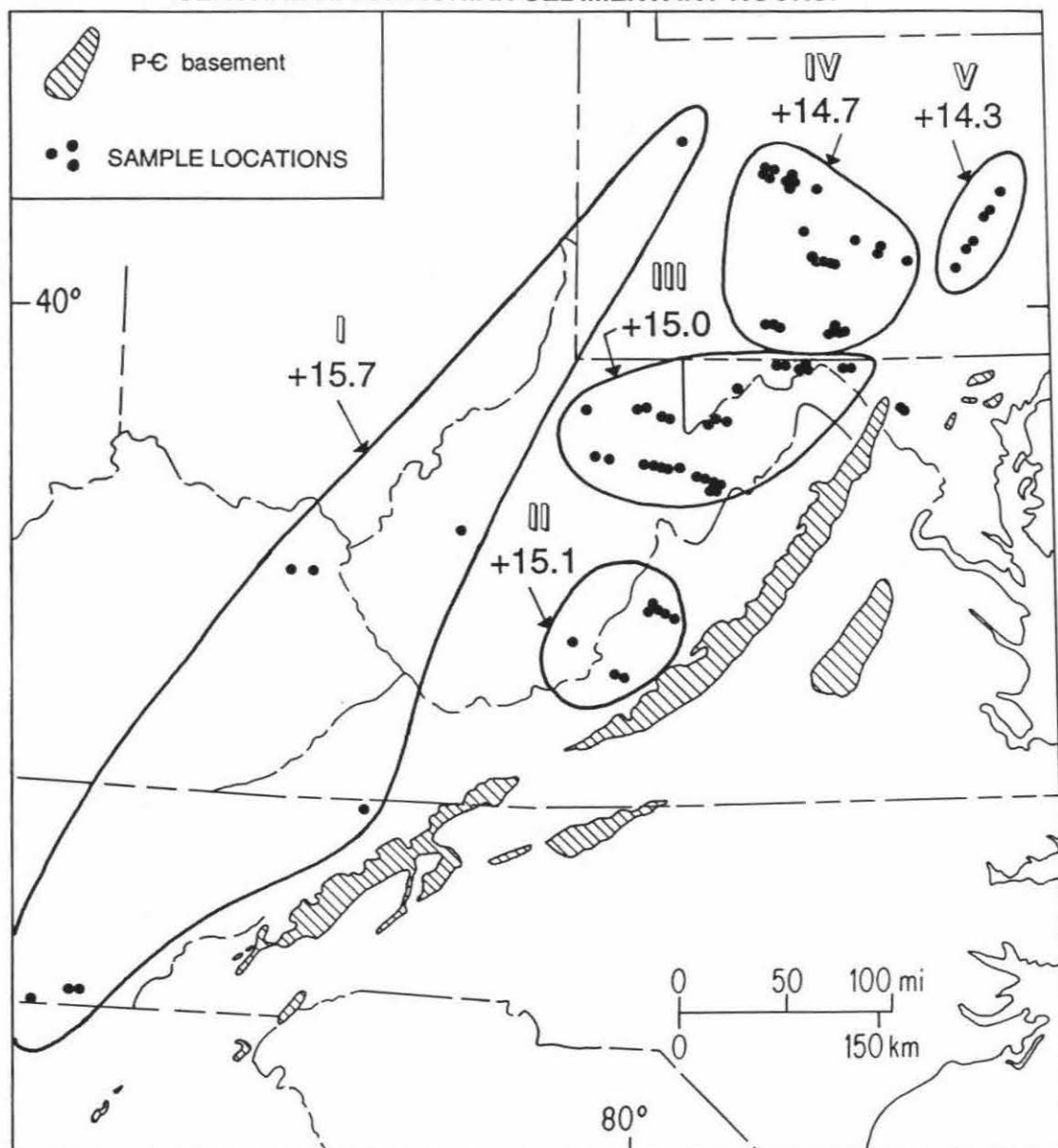
For purposes of discussion, the Central Appalachian samples studied in this work are subdivided into 5 geographic areas, as shown in Figure 5.12: Area I is farthest west and represents the Appalachian Plateau physiographic province; it includes eastern Tennessee, eastern Kentucky and the western parts of Pennsylvania and West Virginia. Moving eastward perpendicular to the tectonic grain, we move into the Valley and Ridge Province, where most of the isotopic data were obtained. This zone is divided into 3 areas arrayed from southwest to northeast along the tectonic grain of the Appalachians, as follows: Area II straddling the Virginia-West Virginia border; Area III in the vicinity of western Maryland and the northeastern part of West Virginia; and Area IV in central Pennsylvania. Finally, Area V is farthest east, in the vicinity of the strongly deformed anthracite coal region of eastern-central Pennsylvania.

The mean bulk silicate $\delta^{18}\text{O}$ values of these groupings of sedimentary rocks vary from a high of +15.7 in Area I of the West-Central Appalachians to a low of +14.3 in

Figure 5.12

Map of the Central Appalachian Mountains showing the 5 geographic groupings of samples referred to in the text: Areas I, II, III, IV, and V with mean bulk silicate $\delta^{18}\text{O}$ values of +15.7, +15.1, +15.0, +14.7, and +14.3, respectively.

CENTRAL APPALACHIAN SEDIMENTARY ROCKS:



Area V of the East-Central Appalachians (Figure 5.12). Areas II, III, and IV display remarkably uniform intermediate mean $\delta^{18}\text{O}$ values that decrease very slightly to the northeast: +15.1, +15.0 and +14.7, respectively.

An analysis of bulk silicate $\delta^{18}\text{O}$ by lithology shows that most of the above-described west-to-east shift in bulk silicate $\delta^{18}\text{O}$ across the tectonic grain of the Appalachians is attributable to the noncalcareous shales and noncalcareous siltstones (Figures 5.13, 5.14, 5.15). The sandstones and the calcareous shales do not show any significant variation in bulk silicate $\delta^{18}\text{O}$ with geographic area (Figures 5.16, 5.17); these lithologies are effectively "isotopic" noise in the geographic variation. The mean $\delta^{18}\text{O}$ values of the few analyzed calcareous shales from Areas I, II, and IV are relatively high at +15.4, +15.9, and +15.6. The sandstones have remarkably uniform mean $\delta^{18}\text{O}$ values over the entire sampling region, with Areas I, II, IV, and V identical at $\delta^{18}\text{O} = +14.7$ and only Area II slightly different at +15.1 (Figure 5.16). Patterned against the very homogeneous bulk silicate $\delta^{18}\text{O}$ values of the sandstones, the 2.5 per mil west-to-east shift in noncalcareous shales and noncalcareous siltstones is particularly striking.

5.4 Bulk silicate oxygen isotope variation with geologic age

Sedimentary rocks in the Central Appalachians generally increase in geologic age to the east. Is the eastward change in bulk silicate $\delta^{18}\text{O}$ described above thus attributable to a correlation with geologic age? The answer seems to be negative, based on the data in Figures 5.18, 5.19, 5.20, and 5.21. Figure 5.18 shows that for the overall Central Appalachian rock suite there is no significant correlation of bulk silicate mineralogy with geologic age, and Figure 5.19 shows that there is no significant correlation of sandstone bulk silicate $\delta^{18}\text{O}$ with geologic age. Although the data in Figure 5.20 display greater

Figure 5.13

Map of the Central Appalachian area, showing bulk silicate $\delta^{18}\text{O}$ values of noncalcareous shales as a function of sample location. The $\delta^{18}\text{O}$ values of these carbonate-free shales increase from west to east perpendicular to the tectonic grain of the Appalachians: from a high $\delta^{18}\text{O} = +16.7$ in Area I (2 samples), to $+14.8$ (2 samples), $+14.6$ (2 samples), and $+14.9$ (2 samples) in Areas II, III, and IV, to a low of $\delta^{18}\text{O} = +14.0$ (4 samples) in Area V (compare with Figure 5.12). The per cent blackened area inside each sample symbol denotes the per cent carbonate in each sample (this is zero for all the samples on this figure).

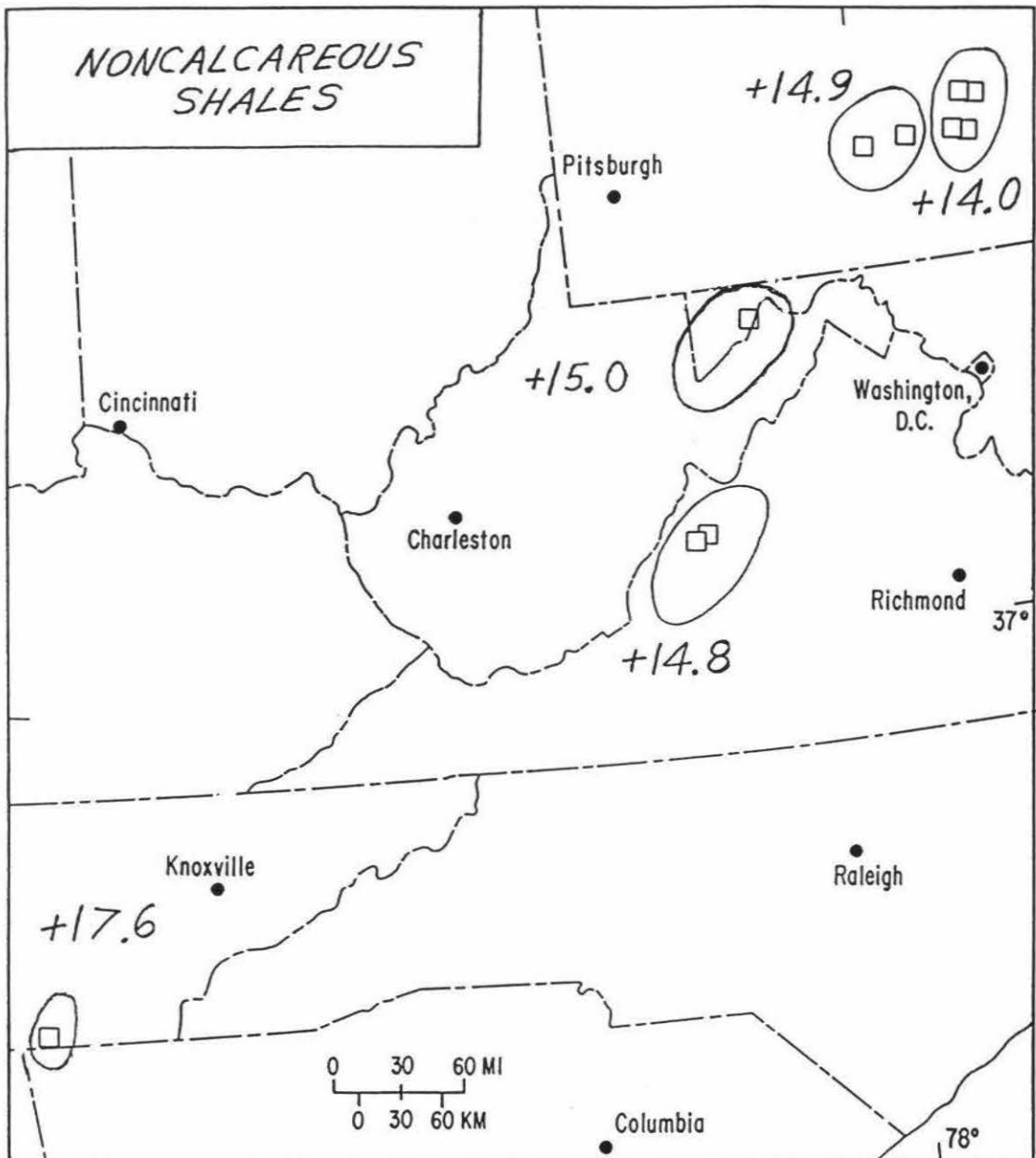


Figure 5.14

Map of the Central Appalachain area, showing mean bulk silicate $\delta^{18}\text{O}$ values of siltstones as a function of sample location. The $\delta^{18}\text{O}$ values of the siltstones increase from west to east across the Appalachians from $\delta^{18}\text{O} = +16.2$ in Area I (2 samples), to $+14.8$ in Area II (7 samples), to a low of $+14.0$ in Area IV (2 samples). The per cent blackened area inside each sample symbol denotes the per cent carbonate in each sample (this happens to be zero for all these samples except the single calcareous siltstone from Tennessee).

CENTRAL APPALACHIAN SEDIMENTARY ROCKS:

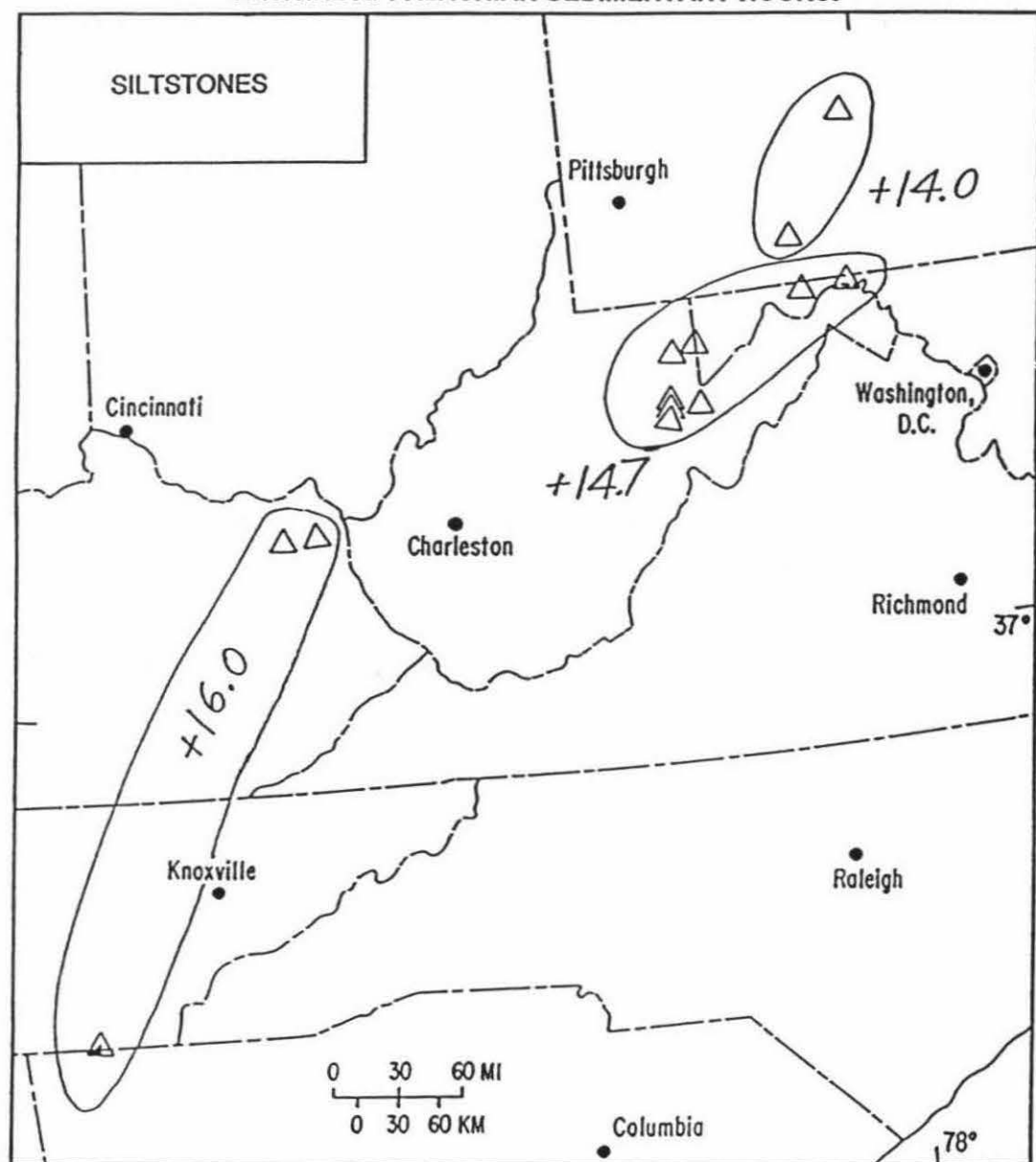


Figure 5.15

Map of the Central Appalachians showing mean bulk silicate $\delta^{18}\text{O}$ values of noncalcareous shales and noncalcareous siltstones as a function of sample location. Squares represent shales. Triangles represent siltstones. This figure combines the samples from the maps of Figures 5.13 and 5.14, except for the deletion of the single calcareous siltstone from Area I in Tennessee. The $\delta^{18}\text{O}$ values of these carbonate-free shales and siltstones increase from west to east perpendicular to the tectonic grain of the Appalachians: from a high $\delta^{18}\text{O} = +16.5$ (3 samples) in Area I, to $+14.8$ (2 samples), $+14.4$ (9 samples), and $+14.5$ (4 samples) in Areas II, III, and IV, to a low of $\delta^{18}\text{O} = +14.0$ (4 samples) in Area I. If the single calcareous siltstone had been added to the group of Area I samples, the mean $\delta^{18}\text{O}$ of those 4 Area I shales and siltstones would be $+16.4$. The per cent blackened area inside each sample symbol denotes the per cent carbonate in each sample (this is zero for all of the samples plotted on this figure).

CENTRAL APPALACHIAN SEDIMENTARY ROCKS:

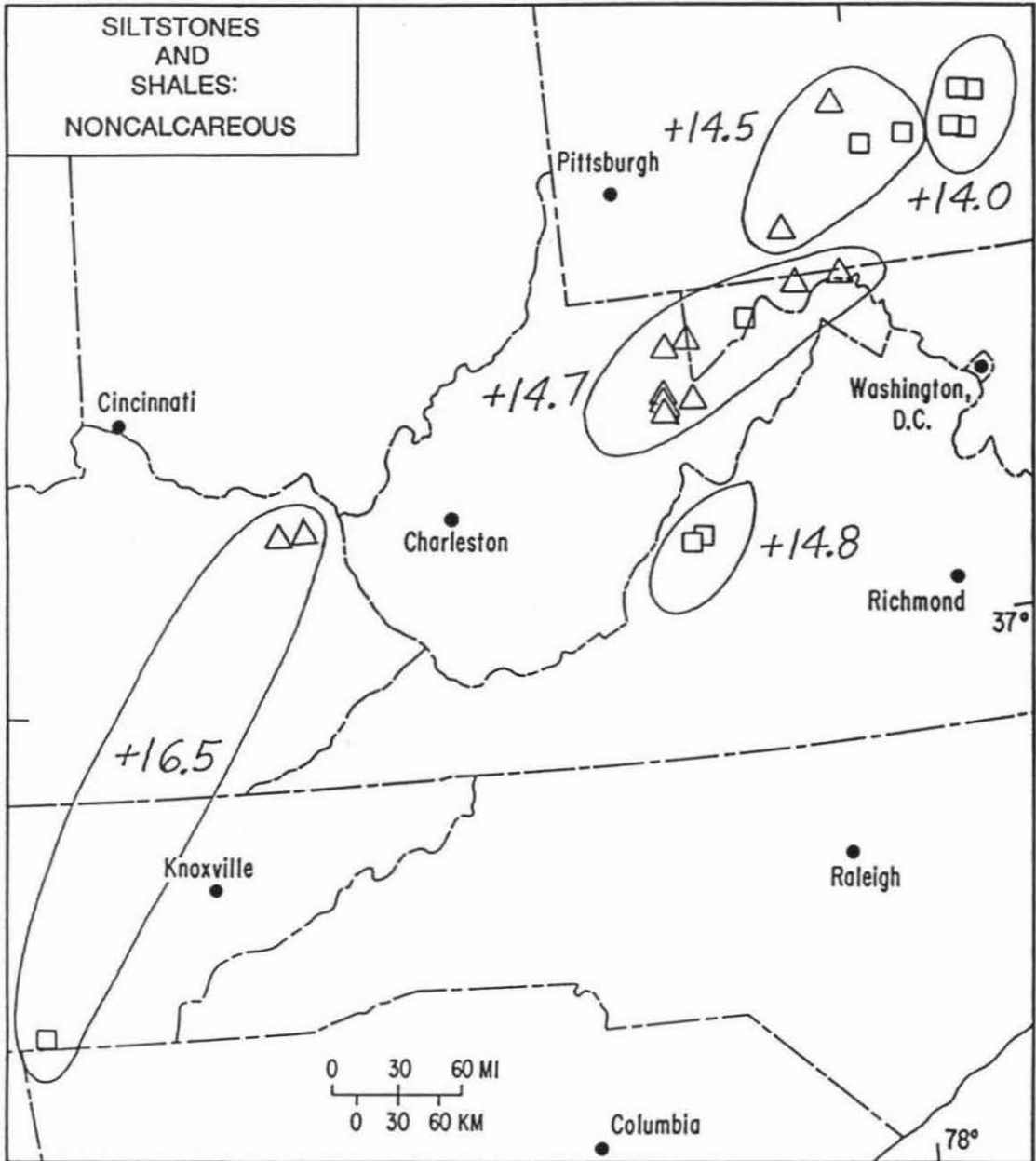


Figure 5.16

Map of the Central Appalachian area, showing mean bulk silicate $\delta^{18}\text{O}$ values of sandstones as a function of sample location. The bulk silicate $\delta^{18}\text{O}$ values of the sandstones are very uniform in all these regions: Area I (+14.7, 2 samples), Area IV (+14.7, 16 samples), and Area V (+14.7, 4 samples) from west to east in Pennsylvania; Area III (+15.1, 18 samples) in western Maryland and eastern West Virginia, and Area II (+14.7, 3 samples) in Virginia at the southernmost part of the map. The per cent blackened area inside each sample symbol denotes the per cent carbonate in each sample.

CENTRAL APPALACHIAN SEDIMENTARY ROCKS:

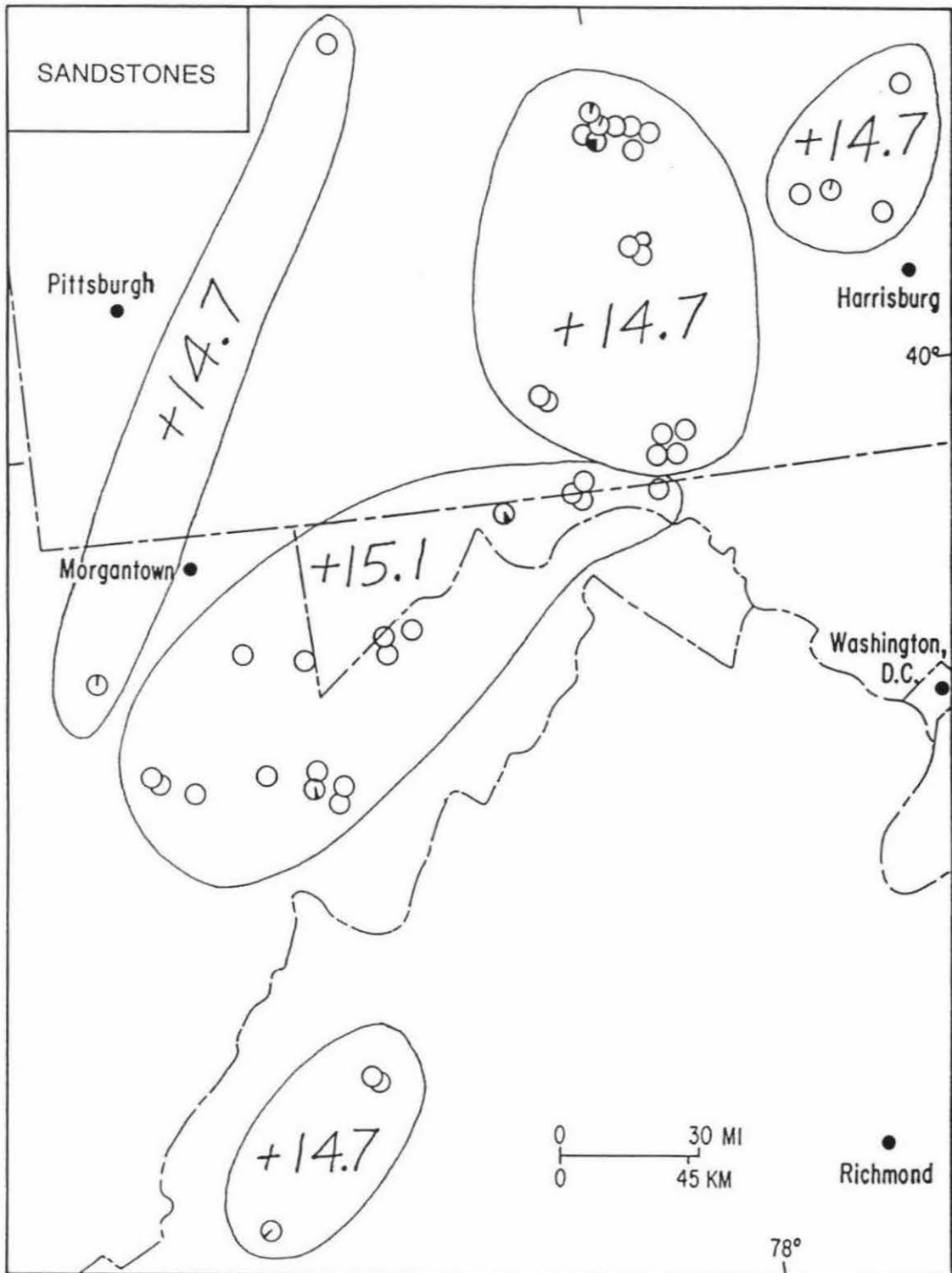


Figure 5.17

Map of the Central Appalachian area, showing mean bulk silicate $\delta^{18}\text{O}$ values of calcareous shales, as a function of sample location. The per cent blackened area inside each sample symbol denotes the per cent carbonate in each sample. The bulk silicate $\delta^{18}\text{O}$ values of the calcareous shales do not show much variation across the Appalachians: $\delta^{18}\text{O} = +15.4$ in Area I (2 samples), $\delta^{18}\text{O} = +15.9$ in Area II (3 samples) and $\delta^{18}\text{O} = +15.6$ in Area IV (2 samples). If the bulk silicate $\delta^{18}\text{O}$ of the calcilutite (sample 138) had been plotted in Area I, the mean $\delta^{18}\text{O}$ of the three samples would be raised to +17.7 (see text).

CENTRAL APPALACHIAN SEDIMENTARY ROCKS:

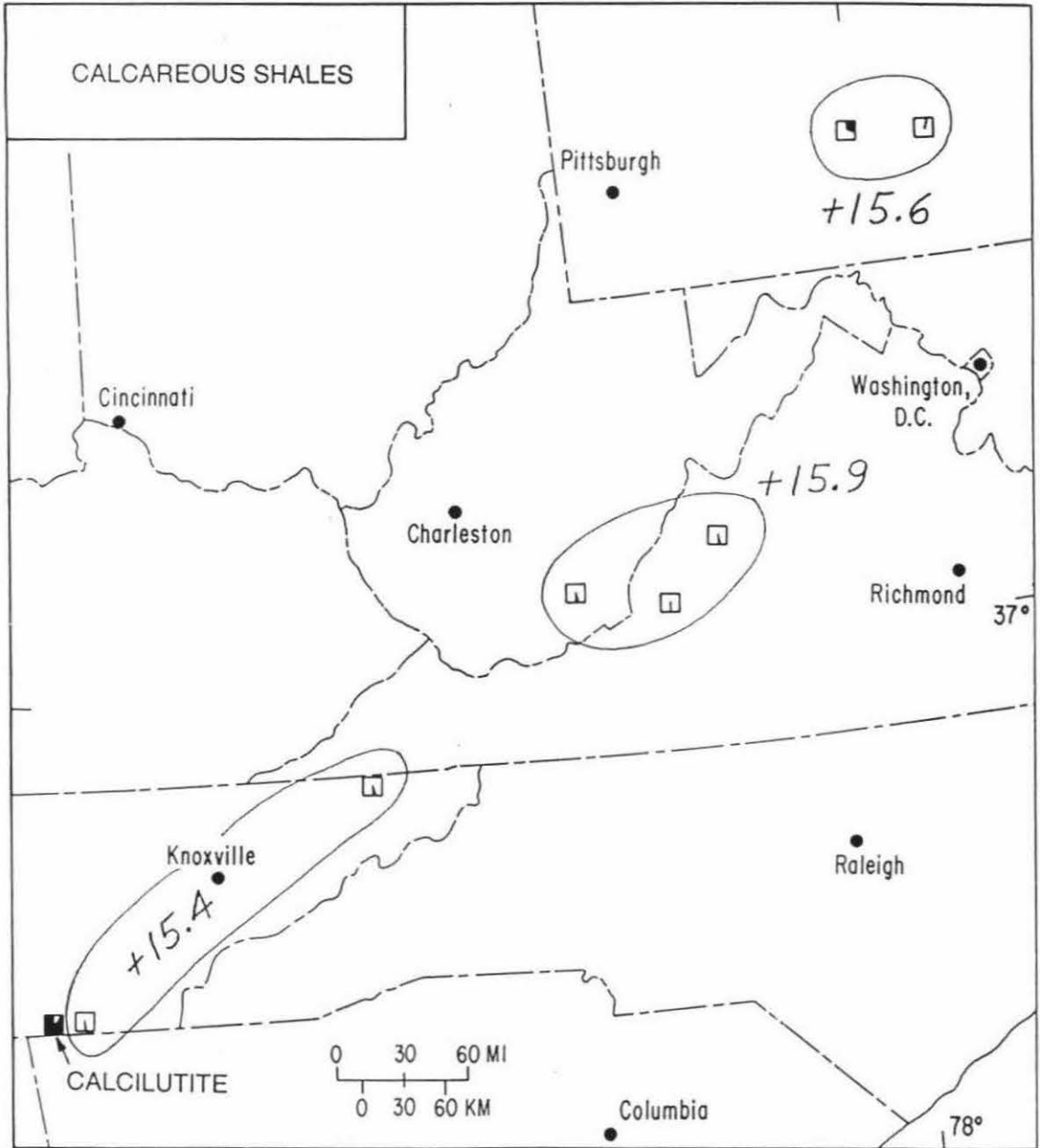


Figure 5.18

Plot of bulk silicate $\delta^{18}\text{O}$ versus geologic age for all Central Appalachian sedimentary rocks (calcilutite excluded).

Figure 5.19

Plot of bulk silicate $\delta^{18}\text{O}$ versus geologic age for all Central Appalachian sandstones, subdivided into calcareous and noncalcareous varieties.

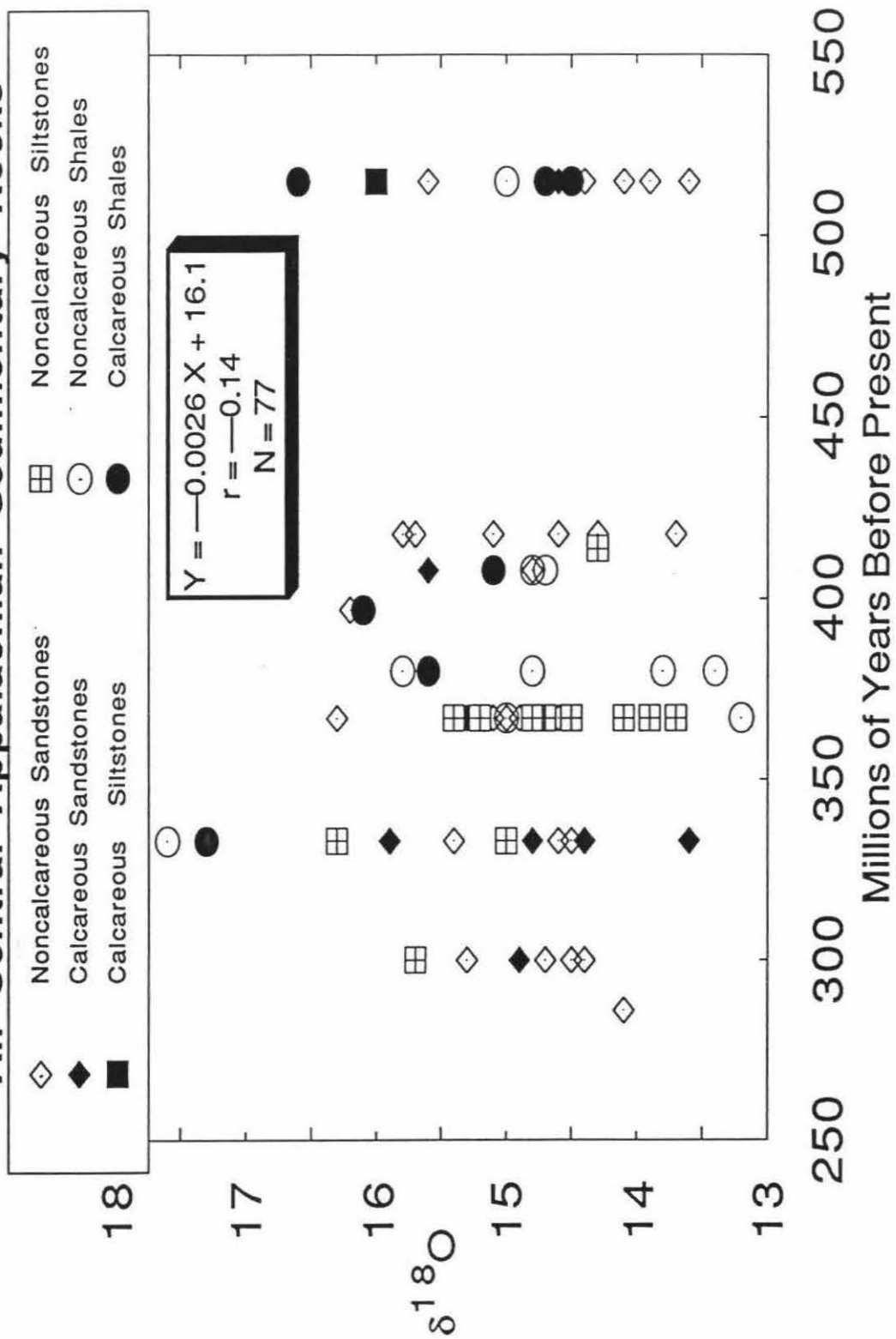
Figure 5.20

Plot of bulk silicate $\delta^{18}\text{O}$ versus geologic age for all Central Appalachian shales, subdivided into calcareous and noncalcareous varieties.

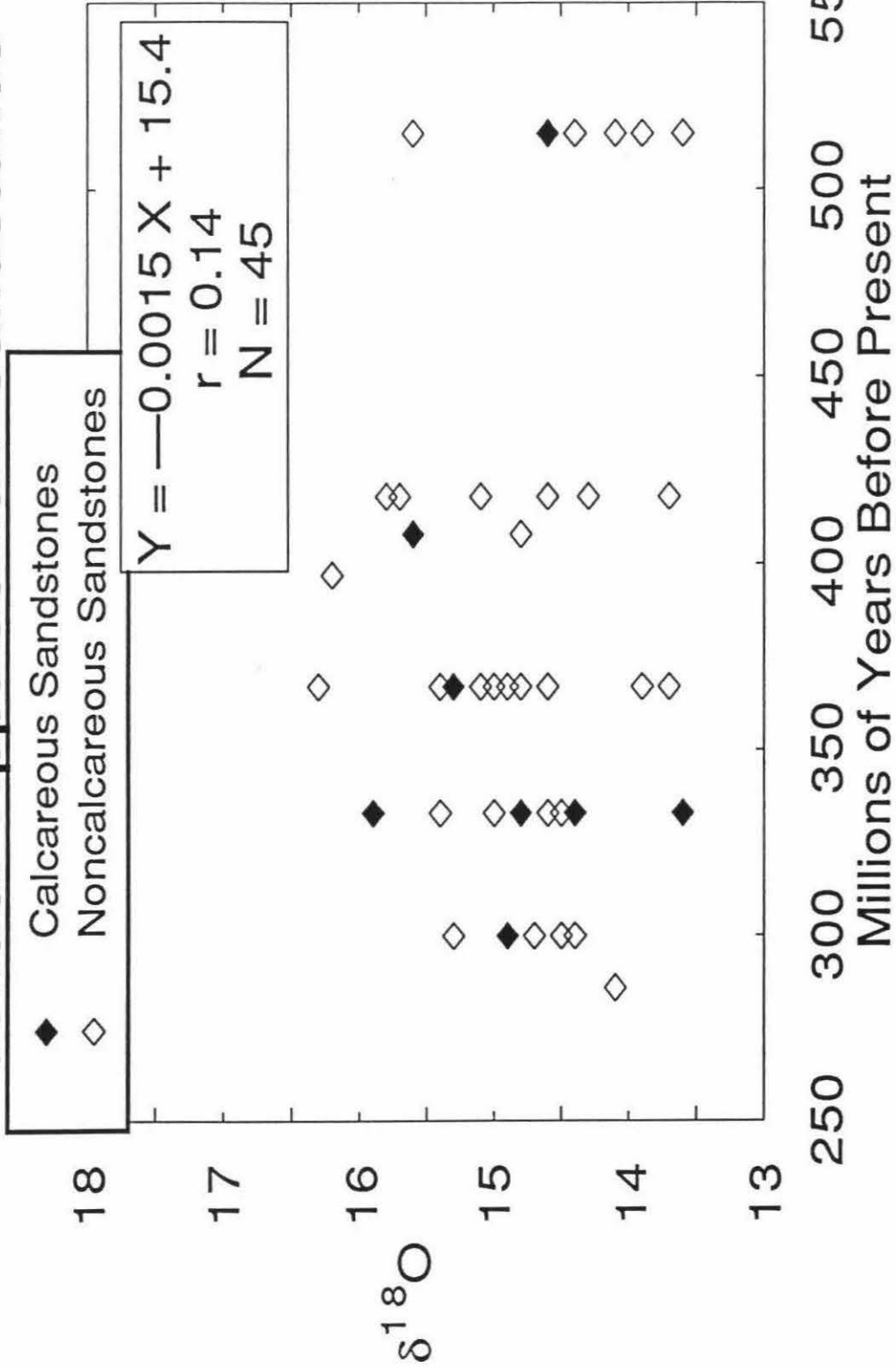
Figure 5.21

Plot of bulk silicate $\delta^{18}\text{O}$ versus geologic age for all Central Appalachian siltstones. For the noncalcareous siltstones, the correlation coefficient with geologic age is 0.61, which is significant at the 0.05 probability level.

Bulk Silicate $\delta^{18}\text{O}$ vs Geologic Age: All Central Appalachian Sedimentary Rocks



Bulk Silicate $\delta^{18}\text{O}$ vs Geologic Age: Central Appalachian Sandstones



scatter, there is still no significant correlation of shale bulk silicate $\delta^{18}\text{O}$ with geologic age; however, the relationships on this diagram are obscured because most of the data points are confined to a small age range between 360 and 410 Ma.

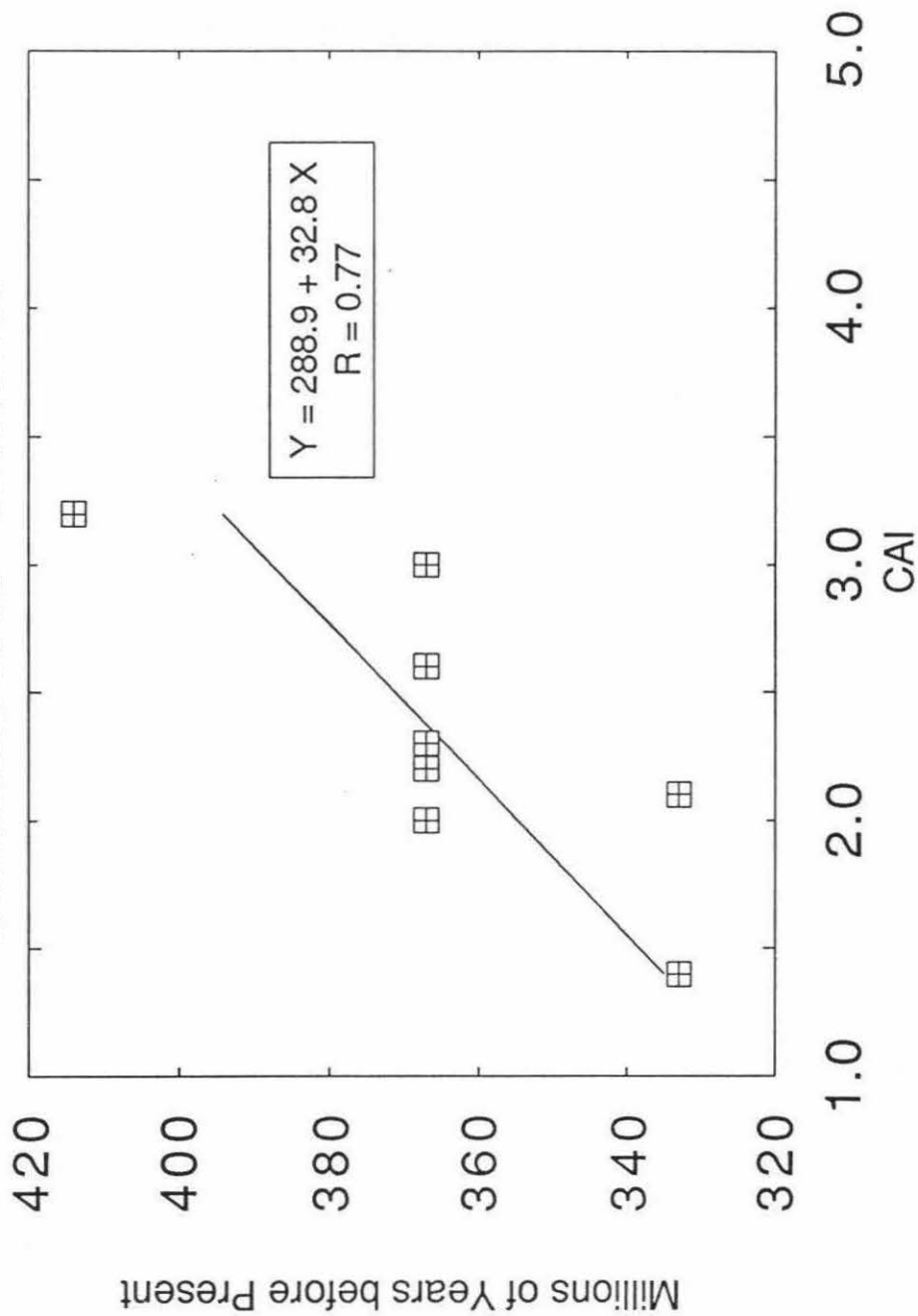
The data in Figure 5.21 also show that there is no significant correlation of overall siltstone bulk silicate $\delta^{18}\text{O}$ values with geologic age. However, if the single analysis of a calcareous siltstone of Cambrian age is deleted, and only the 12 noncalcareous siltstones (with depositional ages of 300 to 410 Ma) are considered, there is a distinct trend toward lighter $\delta^{18}\text{O}$ with increasing age; the correlation coefficient (r) is 0.61 and is significant at the 0.05 probability level. Nonetheless, it will be shown below that the bulk silicate $\delta^{18}\text{O}$ values of both shales and siltstones correlate even better with conodont color alteration index, which is a measure of the intensity of low-grade metamorphism that takes place during diagenesis. Thus, we believe that the correlation between $\delta^{18}\text{O}$ and age for the noncalcareous siltstones is a secondary correlation produced by the fact that, for the sample locations chosen in this work, the conodont color alteration index also correlates with geologic age (Figure 5.22). This is discussed in more detail below.

To summarize, with the possible exception of the noncalcareous siltstones, there is no significant correlation of bulk silicate $\delta^{18}\text{O}$ with geologic age for any of the terrigenous sedimentary rocks of the Appalachian Mountains. Therefore, we conclude that during the entire 300-million-year history of deposition in the Appalachian geosyncline there was no major change in the $\delta^{18}\text{O}$ of the source regions of this detritus. Also, during this age span there does not appear to have been any major change in the post-depositional processes that have affected the bulk silicate $\delta^{18}\text{O}$ values of such rocks.

Figure 5.22

Plot of geologic age of Central Appalachian noncalcareous siltstones analyzed in this study versus their interpolated conodont color alteration index (CAI, see text). The correlation is significant at the 0.05 probability level and is thought to be due to choice of sample locations. In other words, in this particular sampling scheme, the ages of the siltstones fortuitously correlate with conodont color alteration index because of the general west-to-east increase in the ages of the sedimentary rocks in this part of the Appalachians.

Geologic Age vs Conodont CAI: Central Appalachian Noncalcareous Siltstones



5.5 $^{18}\text{O}/^{16}\text{O}$ Variation with bulk silicate mineralogy

5.5.1 Sandstones

Figure 5.23 is a map of Central Appalachian sandstone samples by sandstone composition, showing that each sandstone lithology is fairly well distributed throughout the sample area. The exception to this is the lack of sandstone samples in Kentucky and Tennessee. There is also a lack of wacke samples in Virginia. Nevertheless, there is clearly sufficient geographic coverage of the different types of sandstones to warrant trying to relate $\delta^{18}\text{O}$ value with bulk mineralogy.

Figure 5.24 is a set of comparative histograms of sandstones differentiated by mineralogical composition. There are small differences in the means between the 4 sandstone types, but none of the means differ by more than 0.8 per mil. The wackes display the lowest mean $\delta^{18}\text{O}$ value (+14.4), but the sample size for the wackes is relatively small ($N=5$), which makes it difficult to draw conclusions about these Central Appalachian wackes. These would be a very interesting group of sandstones for further detailed isotopic studies. One reason the sandstones from different compositional classifications might have similar bulk silicate $\delta^{18}\text{O}$ could be the relative isotopic homogeneity of the primary quartz, which is a major component of all these rocks. For example, lithic arenites contain up to 75 per cent quartz, sublithic arenites contain up to 95 per cent quartz, and quartz arenites (orthoquartzites) contain greater than 95 per cent quartz (Pettijohn, 1975).

Detailed petrographic data on Central Appalachian sandstones are sparse. A survey of the literature indicates that an estimated composition of 50 per cent or more quartz is reasonable for most of these sandstones. Lithic fragments of such sandstones

are typically relatively unweathered and less than 10 per cent chert is reported. In addition, there is generally a dearth of silt- and clay-sized particles in non-wacke sandstones. If the bulk quartz separates from these sandstones were isotopically relatively uniform and the lithic fragments were well-mixed, this could account for the isotopic homogeneity of the sandstones, even if the quartz grains and lithic fragments themselves are isotopically nonhomogeneous on a microscopic scale, as seems likely (see below).

The primary cementing agent in these sandstones is quartz (Folk, 1960; Hoque, 1968; Yeakel, 1962; Pelletier, 1958; Pettijohn, 1963). Siever (1959) made a study of 120 quartz-cemented sandstones from the Eastern Interior, Midcontinent, Michigan, and Appalachian basins, and found that the distribution of silica cement was not related in any simple manner to structural position, stratigraphic horizon, or depth of burial. Although detailed information on the amount of quartz cement in Appalachian sandstones is not available, a reasonable estimate would be about 10 to 30% quartz cement (Pettijohn, 1975; Pelletier, 1958).

No attempt was made in this study to analyze the quartz cement from any of the sandstones, nor to examine the isotopic homogeneity of the quartz grains themselves. However, other workers have studied this problem, and going back to Silverman (1951) the workers have generally concluded that the authigenic quartz cements are relatively ^{18}O -rich, as would be expected during deposition from low-temperature waters, even if such waters were meteoric in origin (*e.g.*, see Lee and Savin, 1985). Table 5.1 was prepared purely for discussion purposes. It gives calculated bulk silicate $\delta^{18}\text{O}$ values for hypothetical quartz arenites containing 0 to 50% quartz cement, an average primary

Table 5.1

Table 5.1 Bulk Silicate $\delta^{18}\text{O}$ Calculations for a Hypothetical Quartz Arenite

Per Cent Primary Quartz	$\delta^{18}\text{O}$ Primary Quartz	Per Cent Secondary Quartz	$\delta^{18}\text{O}$ Secondary Quartz	$\delta^{18}\text{O}$ Bulk Silicate
90	12.0	10	22.0	13.0
80	12.0	20	22.0	14.0
70	12.0	30	22.0	15.0
60	12.0	40	22.0	16.0
50	12.0	50	22.0	17.0

quartz $\delta^{18}\text{O}$ value of +12, and an average authigenic quartz cement $\delta^{18}\text{O}$ value of +22 (Lee and Savin, 1985).

These assumed $\delta^{18}\text{O}$ values are probably close to the extreme end-member values that might be encountered in the Appalachians, as most primary igneous and metamorphic quartz on Earth exhibits $\delta^{18}\text{O}$ values of about +9 to +16, and some of the primary quartz grains in these rocks will also have been re-worked from previous-cycle sandstones with $\delta^{18}\text{O}$ values that were very likely about +14 to +16. Most authigenic silica in these rocks probably has $\delta^{18}\text{O} = +15$ to +25, with the higher $\delta^{18}\text{O}$ values having formed at lower temperatures and/or from higher- ^{18}O waters. While numerous variations of per cent cement, primary $\delta^{18}\text{O}$, and quartz cement $\delta^{18}\text{O}$ are imaginable, the simple calculations in Table 5.1 reasonably reproduce the range of bulk silicate $\delta^{18}\text{O}$ in all Central Appalachian sandstones, siltstones and shales, as well as in the quartz arenites. Table 5.1 shows that even for the relatively extreme end-member $\delta^{18}\text{O}$ values utilized, a wide variation from 20 to 40% authigenic silica produces a $\delta^{18}\text{O}$ change of only +14 to +16 in the hypothetical whole-rock sample. This simple calculation shows why the quartz arenites and thus probably the quartzose component of all the other sandstones (and siltstones?) might overall be similar to the rest of the terrigenous clastic material that makes up these geosynclinal sedimentary rocks. Namely, all the sandstones ultimately represent a mixture of a relatively high- ^{18}O quartz (authigenic cement plus minor chert) with a relatively low- ^{18}O quartz derived mainly from primary quartz grains that once resided in crystalline igneous and metamorphic rocks. Such mixing processes will always reduce the overall $\delta^{18}\text{O}$ variation, giving some value between the two extremes.

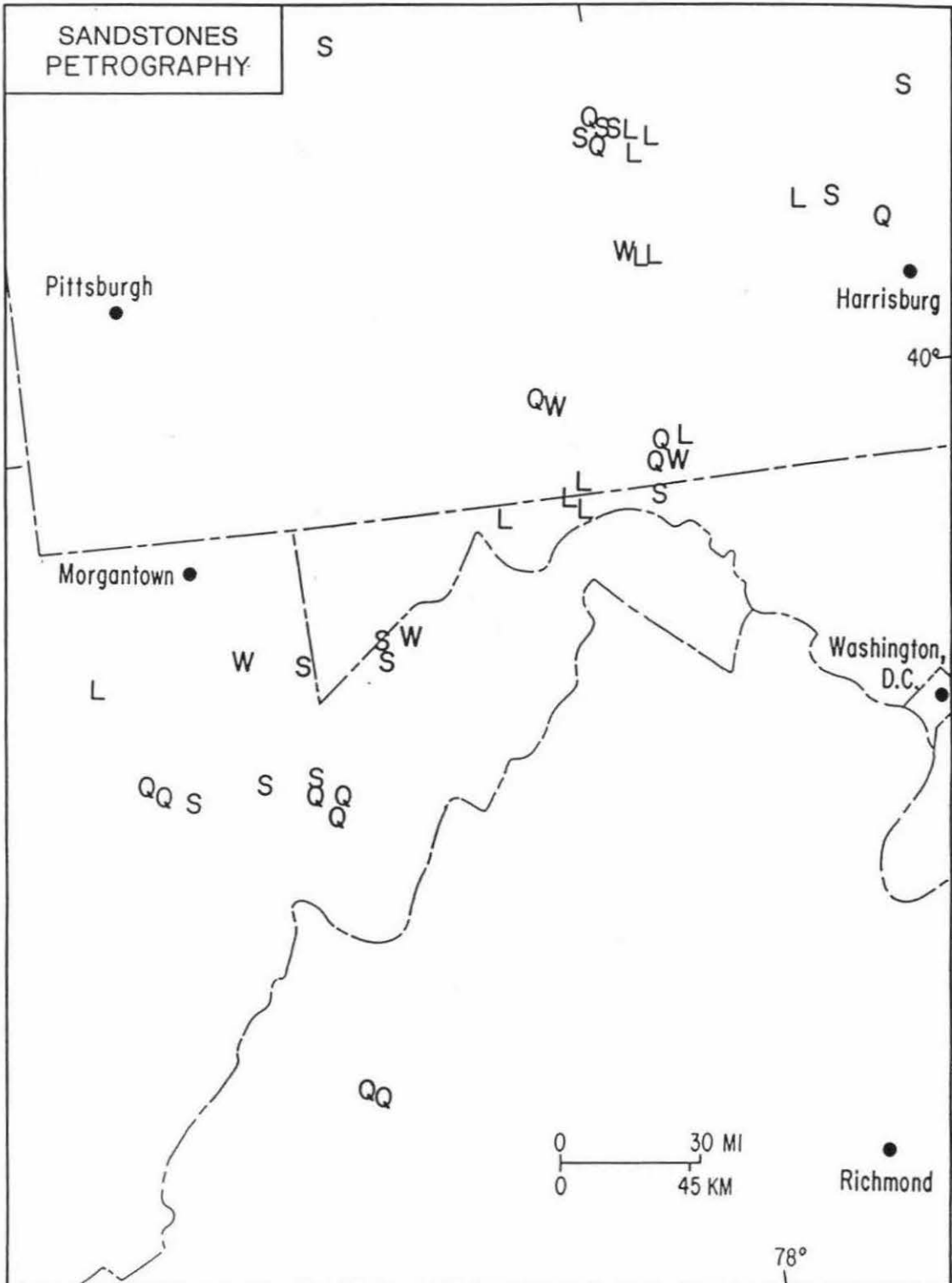
Figure 5.23

Map of the Central Appalachians showing the distribution of Paleozoic sandstone samples (*i.e.*, arenites) in this work, separated into categories based on composition and petrographic characteristics. S = sublithic arenites; Q = quartz arenites; L = lithic arenites; W = wackes.

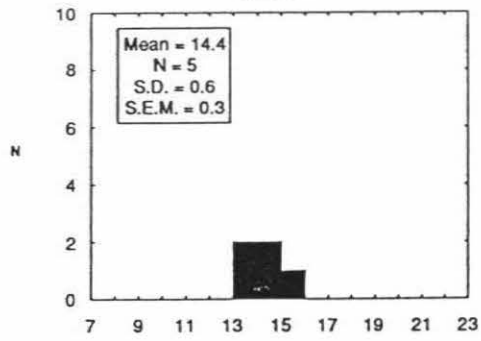
Figure 5.24

Four comparative histograms showing bulk silicate $\delta^{18}\text{O}$ values of Central Appalachian sandstones, subdivided into several categories, using the sandstone compositional classification of Pettijohn (1975). All sandstone compositional categories display relatively uniform bulk silicate $\delta^{18}\text{O}$ values. The wackes have somewhat lower and more variable $\delta^{18}\text{O}$ values than the other kinds of sandstone, but the sample size is too small to draw any clear-cut distinctions among the $\delta^{18}\text{O}$ values of the various sandstone compositional classes.

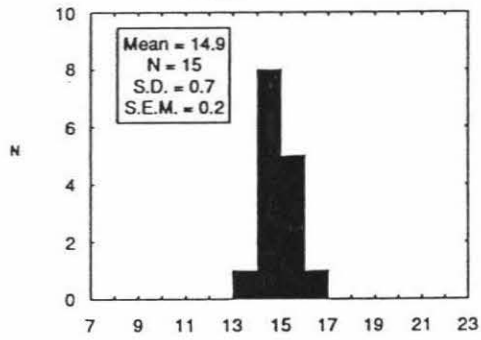
CENTRAL APPALACHIAN SEDIMENTARY ROCKS:



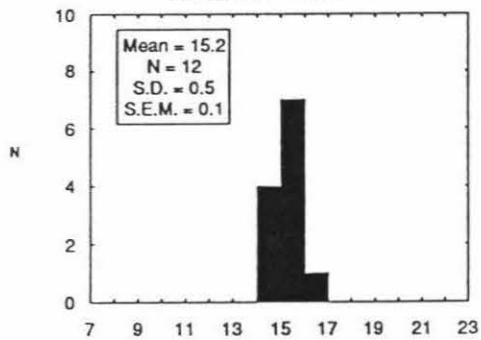
Central Appalachians:
Wackes



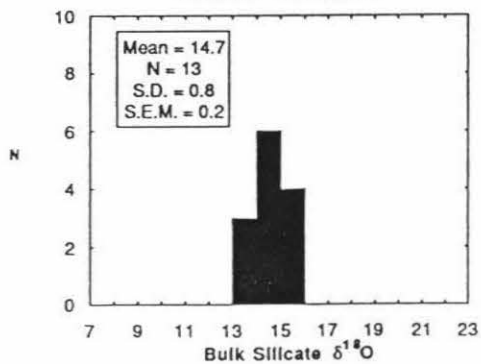
Central Appalachians:
Lithic Arenites



Central Appalachians:
Sublithic Arenites



Central Appalachians:
Quartz Arenites



The $\delta^{18}\text{O}$ values of the quartz grains in a sandstone that had been derived from a second (or third) cycle of sedimentation would include lithic fragments and quartz grains from sedimentary rocks, as well as primary quartz grains from igneous and metamorphic rocks. These quartz grains would be nonhomogeneous mixtures of primary igneous and metamorphic quartz together with authigenic cement. Such isotopically inhomogeneous grains of quartz would thus be overall higher in $\delta^{18}\text{O}$ than the primary quartz grains from the first cycle of erosion of the crystalline complex. These higher- ^{18}O , non-homogeneous quartz grains would then be recemented by even higher- ^{18}O authigenic cement during diagenesis, and the whole cycle would be repeated. The $\delta^{18}\text{O}$ values of recycled quartz grains could conceivably get higher and higher until they reach some steady-state value intermediate between the $\delta^{18}\text{O}$ of the primary igneous and metamorphic quartz and the authigenic cement.

Pettijohn (1975) describes wackes as those sandstones containing more than 15 per cent by volume of silt-size or finer particles, which are termed "matrix". If part of the variation in bulk silicate $\delta^{18}\text{O}$ is due to diagenetic alteration of finer particles, then the matrix of wackes may also be subject to this alteration. If that were the case, then a larger standard error of the mean, closer to that for shales, might be expected. Again, though the sample size is small, this seems to be the case for the wackes. The wackes have the lowest mean bulk silicate $\delta^{18}\text{O}$ of all the various kinds of sandstones (or the shales). If the wackes were dominantly a mixture of two end member compositions -- one characteristic of the shales and the other of the non-wacke sandstones -- the bulk silicate $\delta^{18}\text{O}$ might be expected to be intermediate between the mean bulk silicate $\delta^{18}\text{O}$ for non-wacke sandstones and that for shales. However, this is not the case. Instead,

the mean $\delta^{18}\text{O}$ for wackes is lower than that for either non-wacke sandstones or for shales. Two hypotheses that would fit this observation are: (1) that the $\delta^{18}\text{O}$ of the wackes has been lowered below that of the non-wacke sandstones by diagenetic reactions of the wacke matrix with larger volumes of water; or (2) that the wacke matrix is in fact not like that of the fine-grained material in the shales, but is dominated to a greater degree by lower- ^{18}O rock fragments and minerals such as chlorite. One plausible reason why hypothesis (1) might be important to consider is that sandstones and shales are known to have vastly different permeabilities to ground-water flow. For example, the water involved in the diagenetic reactions perhaps had greater access to the fine-grained matrix material in the wackes than to the analogous material in the shales, because of the increased porosity and permeability of the sandstones compared to the shales; sandstones are known to typically form aquifers while the shales tend to form aquitards. This is one of the aspects of the Central Appalachian wackes that makes them an interesting prospect for further study.

To summarize, the isotopic homogeneity of the Appalachian sandstones is in large part most likely the result of a grand-scale mixing process involving three main components. The most important component is a relatively low- ^{18}O quartz derived from crystalline igneous and metamorphic rocks in the tectonic source lands. This component would form many of the new quartz grains derived from such sources during each cycle of erosion, but this component would also be found in the cores and other portions of quartz grains derived from earlier-cycle sandstones that had been through a similar diagenetic event. A lesser component is the relatively high- ^{18}O authigenic silica cement that is ubiquitous in these sandstones. The $\delta^{18}\text{O}$ value of this authigenic silica is strongly

dependent on the temperature and $\delta^{18}\text{O}$ of the aqueous fluids from which it was deposited. Many of the sandstones in this study probably contain authigenic silica with relatively low $\delta^{18}\text{O} = +16$ to $+20$, based on the great depth and temperature to which they were subjected. Together, these two components make up a large component of well-mixed, isotopically-heterogeneous quartz which has a relatively uniform mean $\delta^{18}\text{O}$ value of about $+14$ to $+16$, even though this siliceous component is itself probably made up of materials with $\delta^{18}\text{O}$ values that vary by as much as 10 per mil. This composite quartz component is present in each of the different sandstone compositional types, and some of this material is also undoubtedly reworked composite quartz from earlier-cycle sandstones and conglomerates in the Appalachians. A third contribution is the presence of smaller amounts of relatively unweathered, fine-grained, well-mixed lithic fragments and matrix, which are particularly important in the wackes. This component also seems to have had a relatively uniform intermediate $\delta^{18}\text{O}$ value somewhat similar to that of the shales and siltstones, as well as to that of the composite quartz component. The wackes, though not significantly isotopically anomalous, are indeed somewhat lower in ^{18}O than the other sandstones, and they also show greater dispersion in bulk silicate $\delta^{18}\text{O}$ than the other sandstone types (Figure 5.24). Another factor that probably contributes to the overall $^{18}\text{O}/^{16}\text{O}$ homogeneity of these rocks is the relatively low abundance of such anomalously high- $\delta^{18}\text{O}$ material as chert and such anomalously low- $\delta^{18}\text{O}$ material as hydrothermally altered volcanic rocks. Those kinds of materials are far more common in the eugeosynclinal facies than in the miogeosynclinal facies.

5.5.2 Shales

The bulk silicate mineralogy of the shales is much more difficult to constrain than

that of the sandstones. One of the most thorough compilations of clay mineral compositional data has been assembled by Weaver (1989). What follows is primarily a summary of Weaver's pertinent work as related to the Paleozoic shales of the Appalachians.

Tidal flat carbonates were the major rock type deposited adjacent to the craton in the Lower Ordovician. The carbonate rocks are characterized by a mixed-layer chlorite-smectite component. This chlorite-smectite component is thought to be derived from mafic and intermediate volcanic material formed in a volcanic arc on the eastern margin of North America. In the Central and Southern Appalachians this volcanic material was delivered mainly in the form of volcanic ash. In the Middle Ordovician, deformation and metamorphism of the eastern flank of Laurentia began, followed by uplift and erosion in the Late Ordovician. As uplift progressed, the relative amount of igneous material decreased, but a rich supply of chloritic material continued. During the Ordovician, the Canadian Shield and Transcontinental Arch were a northern and western source of illite and illite-smectite. Thus, from the Early Ordovician a two-source system developed in the Appalachian Basin. The phyllosilicate suite in the Central and Southern Appalachians tended to be homogenized by the presence of metamorphic rocks in both source areas.

The Silurian pattern is similar to the Upper and Middle Ordovician. Oolitic ironstone is found in the Silurian Clinton Group. Illite and varying amounts of chlorite are the only phyllosilicates found in Appalachian Basin Silurian sedimentary rocks.

The Acadian Orogeny extended from Middle Devonian through Early Mississippian. As in the Ordovician, orogenic activity was preceded by the deposition

of volcanic ash beds. These ash beds contain illite-smectite and some kaolinite. Three ash beds have been altered to K-bentonite and occur throughout much of the Appalachian Basin. The primary clay mineral in Early and Middle Devonian shales is illite. The Catskill Delta, a thick wedge of continental sediments, was deposited in the Upper Devonian. In the New York-Pennsylvania area west and southwest of the Catskill Delta, black shales were deposited in a large epicontinental sea which covered much of the eastern United States. These shales decrease in thickness and increase in organic content from east to west. Hosterman and Whitlow (1983), in an analysis of over 2,000 Devonian shale samples from Tennessee to Central New York, found that most shales contained 60 to 75% clay minerals and 20 to 30% quartz.

The dominant clay mineral in Lower Mississippian rocks is illite. Upper Mississippian shales of the Illinois Basin (Kentucky, Illinois, and Indiana) contain illite-smectite as the dominant phyllosilicate. In the Cumberland Plateau region, chlorite-smectite is the dominant clay mineral. Clay mineral assemblages are complex, changing over short intervals. This change in clay mineral assemblage in the Upper Mississippian is attributed to volcanic activity preceding the collision of Gondwana and Laurussia. Bentonitic beds are absent, suggesting that volcanic material was deposited on emergent land masses and transported by water to depositional basins.

The Allegheny Orogeny (Mississippian-Permian) resulted from the collision of Laurussia and Gondwana to form Pangaea. Pennsylvanian sedimentary rocks contain a relatively consistent, complex, and fairly distinctive clay mineral assemblage. The primary phyllosilicate is illite. Illite-smectite, kaolinite, and chlorite occur in varying amounts. There is scattered occurrence of vermiculite and/or chlorite-smectite. This

clay mineral suite was the result of uplift and erosion of older sedimentary and metamorphic rocks along the eastern and southeastern margin of the North American craton. Most of the Pennsylvanian rocks were exposed to burial temperatures less than 150°C and have not been strongly altered by burial metamorphism.

Weaver's phyllosilicate history of the Appalachians suggests that shales from the Lower Ordovician, Devonian, and Upper Mississippian may contain volcanic ash from pre-orogenic volcanic arcs. How would the isotopic composition of the volcanically derived clay minerals differ from that of nonvolcanic clay minerals? Since the isotopic fractionation between clay minerals and water is significantly greater at lower temperatures, volcanic ash altered in sea water at earth surface temperatures would be isotopically heavy compared to clay minerals formed at diagenetic or metamorphic temperatures. For this reason shales containing clay minerals from the Lower Ordovician, Devonian, and Upper Mississippian might be initially heavier in bulk silicate $\delta^{18}\text{O}$ due to a difference in primary clay mineralogy.

Varying proportions of isotopically heavy chert formed at low temperature could also be a source of isotopic heterogeneity within shales. The formations sampled in this study, however, are not reported to contain appreciable chert in the areas sampled. Large differences in the amount of quartz in shales might be reflected by differences in oxygen yield when the samples are reacted with fluorine. Quartz gives a total oxygen yield of 16.64 micromoles per milligram, while yields for chlorite and illite are significantly lower (8 to 13 micromoles per milligram). Figure 5.25 is a plot of bulk silicate $\delta^{18}\text{O}$ versus oxygen yield for noncalcareous shales. In this figure it can be seen that the shale sample with bulk silicate $\delta^{18}\text{O}$ greater than +17 has a lower oxygen yield

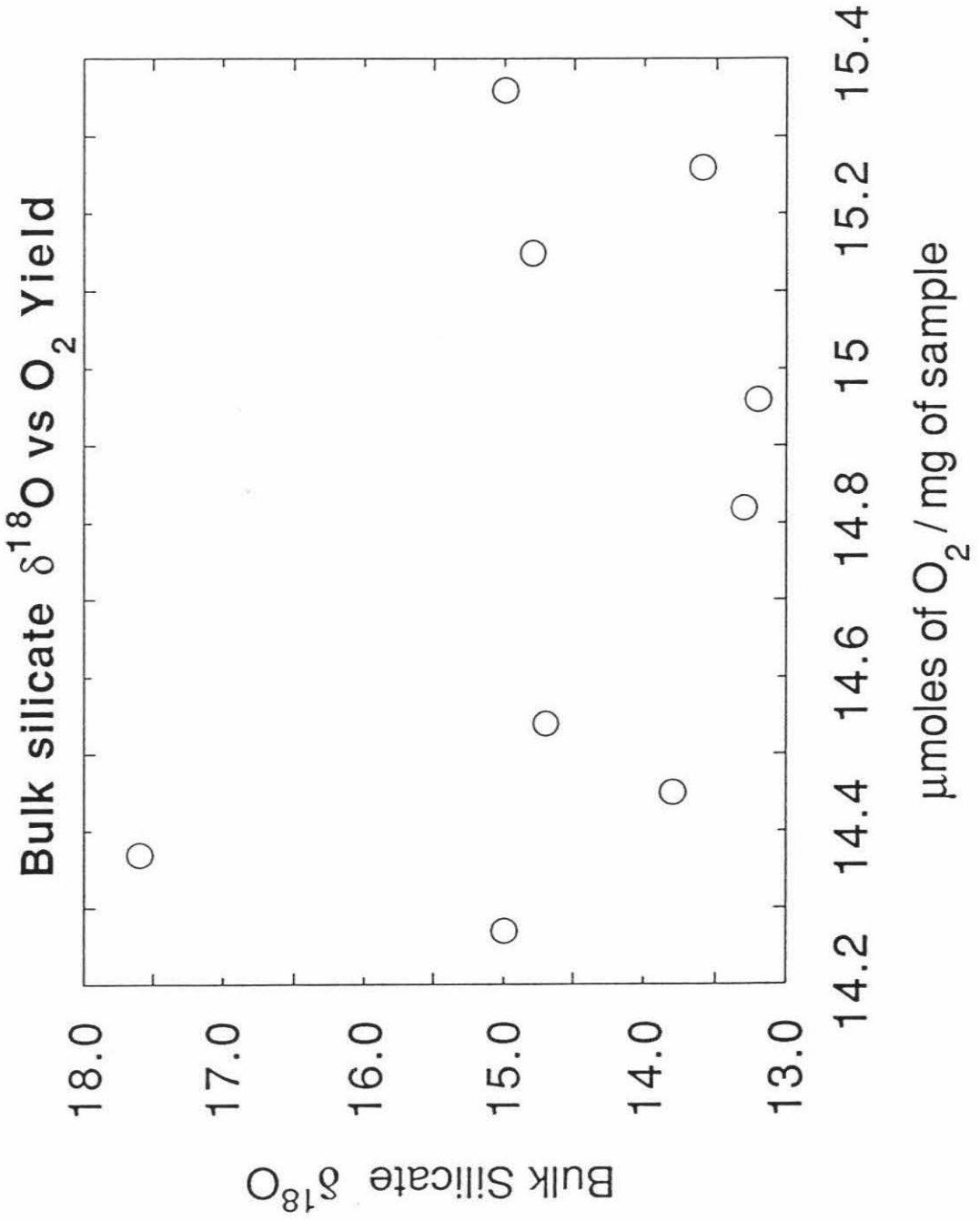
Figure 5.25

Plot of bulk silicate $\delta^{18}\text{O}$ versus oxygen yield for Central Appalachian noncalcareous shales. The shale with a bulk silicate $\delta^{18}\text{O}$ greater than +17 has a very low oxygen yield, and is therefore suspected of having a high clay mineral content, which would explain its high $\delta^{18}\text{O}$. This sample is also Upper Mississippian and may contain altered volcanic ash. The other noncalcareous shales show no significant correlation between bulk silicate $\delta^{18}\text{O}$ and oxygen yield.

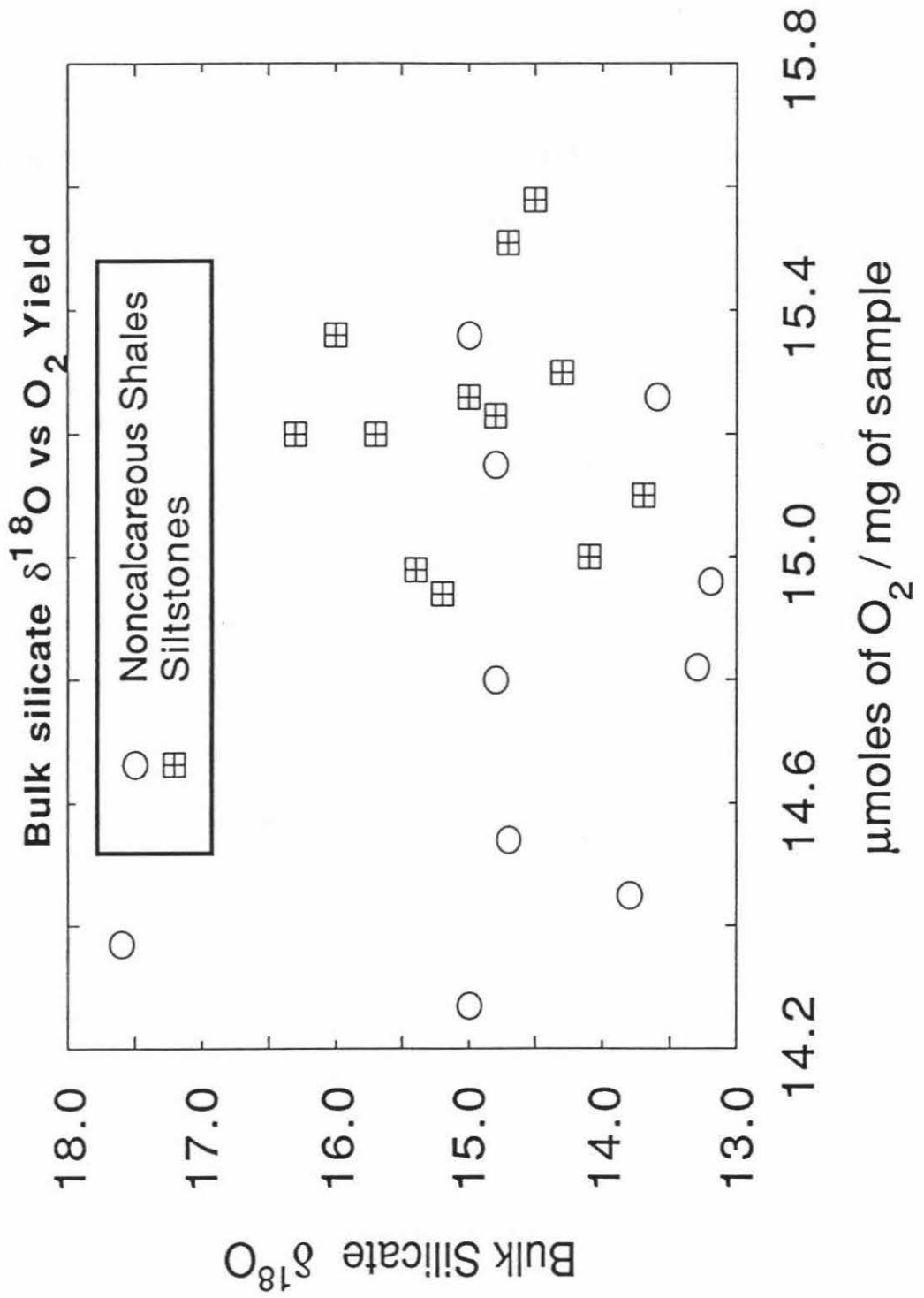
Figure 5.26

Plot of bulk silicate $\delta^{18}\text{O}$ versus oxygen yield for noncalcareous shales and siltstones from the Central Appalachians.

Noncalcareous Central Appalachian Shales:



Central Appalachian
Siltstones and Noncalcareous Shales:



than the other noncalcareous shales. It is thus possible that this sample is heavier in $\delta^{18}\text{O}$ due to a high clay mineral content.

Work by Yeh and Savin (1977) on Mississippi River mud suggests that the unaltered clay minerals from the Mississippi River Basin have a $\delta^{18}\text{O}$ of about +17.6. If Appalachian shale quartz was primarily of high temperature origin it might have a $\delta^{18}\text{O}$ of about +14.7 (average of Central Appalachian quartz arenites). If this were the case, and if Central Appalachian shales were largely a mixture of quartz and clay similar to Mississippi River mud, then samples with a high unaltered clay content would be expected to be heavier in bulk silicate $\delta^{18}\text{O}$. While this is true for the heaviest noncalcareous shale, it is not true for the remaining noncalcareous shales. This suggests that a factor other than the amount of quartz and clay minerals is responsible for $\delta^{18}\text{O}$ variation in the noncalcareous shales that have $\delta^{18}\text{O}$ lower than +17. If the bulk silicate $\delta^{18}\text{O}$ of quartz arenites is taken as an indication of the uniformity of the mean $\delta^{18}\text{O}$ of primary shale quartz, then the isotopic heterogeneity of shales would be due to the heterogeneity in the isotopic composition of the clay minerals and any diagenetically formed quartz.

5.5.3 Siltstones

Little information is available concerning the mineralogic content of siltstones. However, the bulk of these rocks are probably just very fine-grained sandstones transitional to shales and mudstones. Thus, one might *a priori* predict that the siltstones would have $\delta^{18}\text{O}$ values intermediate between the sandstones and shales. The bulk silicate $\delta^{18}\text{O}$ values of the siltstones are in fact very similar to the bulk silicate $\delta^{18}\text{O}$ values of Central Appalachian sandstones and noncalcareous shales, which are themselves

isotopically similar; this indeed suggests some similarities in mineralogy. Figure 5.26 is a graph of bulk silicate $\delta^{18}\text{O}$ of siltstones versus oxygen yield. Noncalcareous shales are included for comparison. Siltstones have only a slightly higher average oxygen yield (14.9 versus 14.8 micromoles per milligram) and show no general trend of bulk silicate $\delta^{18}\text{O}$ with oxygen yield. Siltstones show less variation in oxygen yield than noncalcareous shales. Perhaps the analyzed siltstones have even more uniform quartz contents than the analyzed noncalcareous shales.

5.5.4 Summary

To summarize the relationships between bulk silicate $\delta^{18}\text{O}$ and mineralogy, it is again most important to emphasize how remarkably little effect large variations in mineralogy and lithology seem to have on the $\delta^{18}\text{O}$ values of these miogeosynclinal sedimentary rocks. The source material for most of these formations was eroded from mountains to the east. None of the formations sampled are reported to contain significant amounts of chert. The Central Appalachian non-wacke sandstones contain a large percentage of quartz and little weathered minerals. If this quartz was well mixed, it would account for much of the homogeneity in sandstone bulk silicate $\delta^{18}\text{O}$ over wide areas.

Shales are largely mixtures of quartz and clay. Some volcanic ash which was altered to clay minerals was deposited in formations from the Devonian, Upper Mississippian and Lower Ordovician. There is no significant correlation between bulk silicate $\delta^{18}\text{O}$ and oxygen yield for noncalcareous shales. This suggests, but does not prove, that the variation in bulk silicate $\delta^{18}\text{O}$ is due to a factor other than variation in the proportion of quartz in each shale. Central Appalachian siltstone bulk mineralogy is

poorly constrained. There is no significant correlation between bulk silicate $\delta^{18}\text{O}$ and oxygen yield for siltstones, suggesting that for siltstones also there is a factor other than the proportion of quartz responsible for the minor geographic variation in bulk silicate $\delta^{18}\text{O}$. While the average oxygen yield for siltstones and noncalcareous shales is similar, the variation in oxygen yield is less for siltstones. This suggests that the siltstones may overall display a smaller variation in proportions of clay and quartz than the noncalcareous shales.

It should also be noted what is not being said about the bulk silicate $\delta^{18}\text{O}$ values and the mineralogy of these sandstones, siltstones, and shales. It is not being said that these rocks are homogeneous in $^{18}\text{O}/^{16}\text{O}$, nor that they are all the same mineralogically. Nor is it being said that there is no variation in quartz content. What is being said is that all of these rocks probably contain a large component of well-mixed, albeit isotopically heterogeneous quartz. This major, very well-mixed siliceous component may to a large degree be derived by several cycles of re-working of earlier-deposited sedimentary rocks during the 300 million years of Appalachian sedimentation and orogeny. Note that there is no statistically significant correlation between bulk silicate $\delta^{18}\text{O}$ and quartz content, as inferred from oxygen yields, within a given lithology. The presence of such a dominant, well-mixed siliceous component in all these rocks would tend to make the bulk silicate $\delta^{18}\text{O}$ values of sandstones, siltstones, and shales much more uniform than would otherwise be the case.

5.6 Oxygen isotopic variations in the source regions

Could the geographic variation of bulk silicate $\delta^{18}\text{O}$ be the result of isotopic variations in the various source regions of the Appalachian sediments? The probable contribution of volcanic ash has been discussed above. Meckel (1970) describes the two major sources in the Appalachians as a tectonic borderland (Appalachia) to the southeast and the stable craton to the northwest. Virtually all of the terrigenous clastic material was supplied by the tectonic borderland. The Devonian black shales are the exception. The sourceland in this case was the craton.

What type of petrologic (and $\delta^{18}\text{O}$) variation existed in this tectonic borderland? A study of Late Paleozoic crustal composition by Davis and Ehrlich (1974) found that sediment composition varied in the two major Carboniferous basins in the southeastern United States. Immature sandstones from the Black Warrior Basin in Alabama indicated erosion of a greenschist terrane which contained extrusive and intrusive volcanics. The Carboniferous Pocahontas Basin of West Virginia is located primarily on the Appalachian Plateau. Thin section studies of continuous cores from this basin indicated not only the erosion of sedimentary-volcanic cover and a low-grade metamorphic terrane, but also the unroofing and erosion of a localized plutonic complex. Plagioclase, muscovite, chlorite, volcanic fragments, and schistose fragments were ubiquitous. It was the minor localized presence of minerals such as microcline, sedimentary fragments, perthitic K-feldspar, and biotite with non-perthitic twinned feldspar that allowed Davis and Ehrlich to construct their pre-erosional crustal model for the Pocahontas source region.

Two aspects of this study are relevant to the question of oxygen isotopic variation in the source region of the Appalachians. First, by Carboniferous time the region that

now constitutes northern Alabama was at least somewhat isolated from the Pocahontas Basin in West Virginia, such that localized source terranes were important in sediment composition. Detailed petrographic work in the Black Warrior Basin indicates that the source terrane was to the south, probably part of the Ouachita trend. Erosion of the Ouachita source never penetrated a localized pluton. The uplift of the Pocahontas source continued until a wide spectrum of rock types was eroded. It is important to keep in mind that this southern Ouachita source is not reported to be the source for any of the formations sampled in the present study, which are all located to the north of the Black Warrior Basin. Due to the isolation of the Black Warrior Basin and the large influx of clastics from the Alleghenian Orogeny, it is unlikely that the heterogeneity of sources between these two Carboniferous basins described by Davis and Ehrlich (1974) would affect the isotopic heterogeneity of samples in the present work. Second, and most importantly, the mineralogical heterogeneity described within the Pocahontas Basin is mainly attributable to accessory minerals. Unless these minerals were highly weathered or present in abundance, and they were not, they would not be expected to cause significant variation in bulk silicate $\delta^{18}\text{O}$.

The work of Beaumont, Quinlan, and Hamilton (1988) indicates that at different periods during the Paleozoic, the amount of erosion from the Appalachian source areas varied along strike. It is possible that the depth of erosion would cause isotopic heterogeneity if the source region varied with depth. Petrographic data from the Taconic clastic wedge in Quebec, the Martinsburg wedge in Pennsylvania, and the Blount wedge in Tennessee and Georgia indicate that these sandstones are almost identical on a QFL (quartz-feldspar-lithics) diagram, with the exception of a lower percentage of quartz in

some Martinsburg samples (Mack, 1985). Most of these sandstones contain greater than 60 per cent quartz, but vary somewhat in type of lithic fragment. The Blount sandstones contain quartzofeldspathic rock fragments while the Taconic and Martinsburg sandstones contain volcanic rock fragments. Depending on the type of volcanic rock fragment, feldspar phenocrysts or volcanic glass, this might cause variation in bulk silicate $\delta^{18}\text{O}$. These volcanic fragments constitute less than 30 per cent of the Martinsburg and Taconic sandstones.

Finally, work by Dulong and Cecil (1989) on the mineralogy of Pennsylvanian coal underclays from eastern Kentucky to southwestern Pennsylvania shows variations of clay mineralogy with paleoclimate. Samples from the Middle and Upper Pennsylvanian contain poorly crystalline kaolinite and illite interpreted to form as the result of *in situ* alteration. The paleoclimate during this period was dry seasonal. Samples from the Lower and lower Middle Pennsylvanian contain well-crystallized illite and kaolinite, indicating little alteration from precursor shales. The paleoclimate during this period was ever-wet tropical. Due to the large difference in the clay-water fractionation factor, significant differences in $\delta^{18}\text{O}$ would be expected from clay minerals formed as a result of weathering and those formed at higher temperature.

To summarize so far, there is no doubt that it is possible to obtain a variation in bulk silicate $\delta^{18}\text{O}$ through a difference in primary mineralogy. However, at least in the case of the Appalachian geosyncline, arguing strongly against this is the striking isotopic homogeneity of the Appalachian sandstones, over wide regions and over hundreds of millions of years of depositional history. Also arguing against it is the lack of correlation between oxygen yield and bulk silicate $\delta^{18}\text{O}$; nonetheless, we cannot exclude this

possibility from consideration. Another difficulty is that no systematic variation in mineralogy which persists throughout most of the Paleozoic has been described in the Central Appalachians, which would be essential to explain the lack of any correlation between $\delta^{18}\text{O}$ and geologic age.

Samples for the present study were collected in essentially a random fashion, without regard to geologic age, lithology, or depositional environment. This is because we wanted to avoid sampling bias toward any single factor involved in sedimentation. While complete randomness was limited by accessible outcrop, it is probable that the sampling method would average out limited differences in primary mineralogy. Note that because sampling was almost wholly done in road cuts and not on eroded outcrops (see Chapter 2), it is unlikely that the more resistant units such as the sandstones were inadvertently oversampled to any significant degree compared to the shales. Thus, while it remains possible that some of the geographic $\delta^{18}\text{O}$ differences observed across the Appalachians are due to variations in average bulk silicate $\delta^{18}\text{O}$ of the source areas, no systematic correlation has been found with respect to the geologic history of the region or with any variation in primary mineralogy.

5.7 Diagenetic changes in oxygen isotopic composition

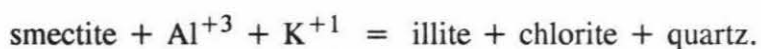
5.7.1. General statement

What evidence is there that the variation in oxygen isotopic composition of the Central Appalachian sedimentary rocks is due to diagenetic alteration of the primary oxygen isotopic composition of the sediments? First, there is the isotopic homogeneity of the sandstones. This suggests isotopic homogeneity of source region and/or effective mixing of sediments from heterogeneous source regions. Second, there is the slightly greater oxygen isotopic heterogeneity of shales, siltstones, and wackes. These lithologies

contain finer-grained particles which would be more susceptible to oxygen isotope exchange in view of their greater reactive surface area. Third, there is the increased crystallinity of illite and the increase in products of diagenesis in Devonian shales of the Appalachian Basin, both of which correlate well with a regional increase in thickness of Devonian rocks and with the conodont alteration index (Hosterman and Whitlow, 1983). Fourth, there is the correlation of bulk silicate $\delta^{18}\text{O}$ of shales and siltstones and the carbonate $\delta^{18}\text{O}$ of shales from this study with conodont alteration index in the Central Appalachians. And fifth, there is the correlation of $\delta^{18}\text{O}$ in fine-grained quartz of the southern Appalachians, presumably formed during diagenesis, with conodont alteration index (Weaver, Eslinger, and Yeh, 1984). The first two lines of evidence have been discussed. The remaining four will be explored below.

Hosterman and Whitlow (1983) analyzed over 2000 samples of Devonian black shales in the Appalachian Basin from southern New York to Alabama. They found that illite, recrystallized during diagenesis, was uniformly present in the shales. Illite crystallinity increased with regional thickness of Devonian rocks. Chlorite, which formed during low-grade metamorphism, was least abundant in the younger shales and most abundant in the older shales. Illite-smectite, the metamorphic precursor to chlorite, was most abundant in the younger shales and least abundant in the older shales. The Marcellus Shale was the only shale unit sampled that did not show an increase in chlorite in older units. This was attributed to the higher calcite component of the Marcellus Shale (average of 25%) which was thought to inhibit chlorite formation. Kaolinite was the only unaltered clay mineral identified and it was found in 25 to 30 per cent of the samples. Hosterman and Whitlow (1983) interpreted the source of the Devonian shales

to be to the northeast and east of the Appalachian Basin. Three volcanic ash beds were recognized in the Middle and Upper Devonian rocks by Hosterman and Whitlow (1983). The composition of the ash beds differed from that of the black shales in that the ash beds had a lower quartz content and that the dominant clay mineral was illite-smectite as opposed to illite. It was impossible to accurately determine the primary mineral suite of the shales because they had all been altered by diagenesis and low-grade metamorphism. Quartz and some kaolinite were thought to be the only unaltered minerals in the shales. Quartz was ubiquitous and showed no depositional pattern. The authors speculate that the present clay mineral suite was probably derived from smectite by the reaction :



Smectite is a common alteration product of volcanic ash. Lastly, the regional change in illite crystallinity, which corresponds closely to the regional increase in thickness of Devonian rocks, also corresponds closely to the conodont color alteration index (index described below).

5.7.2 Correlation between $\delta^{18}\text{O}$ and conodont alteration index

The conodont alteration index is an index of organic metamorphism developed and exploited by Epstein, Epstein, and Harris (1977). Detailed field and laboratory experiments showed that color alteration of conodonts was time and temperature dependent. Irreversible, progressive color changes from pale yellow to black have been discriminated. Epstein *et al.* (1977) calculated an Arrhenius plot showing the temperature-time dependence of conodont alteration data as experimentally determined with open-air heating runs. The experimentally determined time-temperature relationship

proved to be compatible with their field geologic data. The color alteration index (CAI) correlated with isopach data, fixed carbon, vitrinite reflectance, and palynomorph translucency data. Table 5.2 gives temperature ranges for the CAI as determined from the experimental Arrhenius plot of Epstein et al. (1977) representing heating durations of 1 million to 500 million years (lower temperature is for the 500 m.y. value). Epstein et al. (1977) developed maps showing CAI isograds for the entire Appalachian basin. These maps were compared by the authors with isopach maps of the Appalachian Basin, and the CAI isograds were found to correlate with the amount of overburden. The isograds were also found to correlate with thermal cutoffs for oil and gas generation.

The maps of CAI isograds are shown for three different ages of sedimentary rocks in the Appalachian Mountains. The analogous localities of samples of similar age from this oxygen isotope study are plotted on the same maps (Figures 5.27, 5.28 and 5.29).

The detailed mapping of CAI isograds in the Appalachian Basin permits the assignment of a CAI number to each sample analyzed for $\delta^{18}\text{O}$ in the present study, based on interpolations between the CAI contours of each of the 3 maps shown in Figures 5.27, 5.28, and 5.29. These assignments were made, and Figure 5.30 is a plot of the bulk silicate $\delta^{18}\text{O}$ values of noncalcareous sandstones against those conodont CAI values. Figure 5.31 is a similar plot of bulk silicate $\delta^{18}\text{O}$ against conodont CAI for calcareous sandstones. In both Figure 5.30 and Figure 5.31 there is no significant correlation between bulk silicate $\delta^{18}\text{O}$ and conodont CAI. Also, in Figure 5.30, it can be seen that even if the noncalcareous sandstones are broken into separate groups based on grain size, there is no correlation with CAI. For noncalcareous siltstones (Figure 5.32) there is a definite correlation. The correlation coefficient for noncalcareous

Table 5.2

Table 5.2 Temperature ranges for conodonts for heating durations of 1 million to 500 million years

CAI	°C Temperature
1	<50-80
1.5	50-90
2	60-140
3	110-200
4	190-300
5	300-400

(Epstein, et al., 1977)

Figure 5.27

Sample location map from Figure 5.1, showing Upper Devonian - Mississippian sample localities, together with the contours of Conodont Alteration Index (CAI) from Epstein et al. (1977) at values of 2.0, 2.5, and 3.0 for this same age range of rocks (see text). Values of CAI were assigned to each sample from the oxygen isotope data set by interpolation between the contours shown on this map.

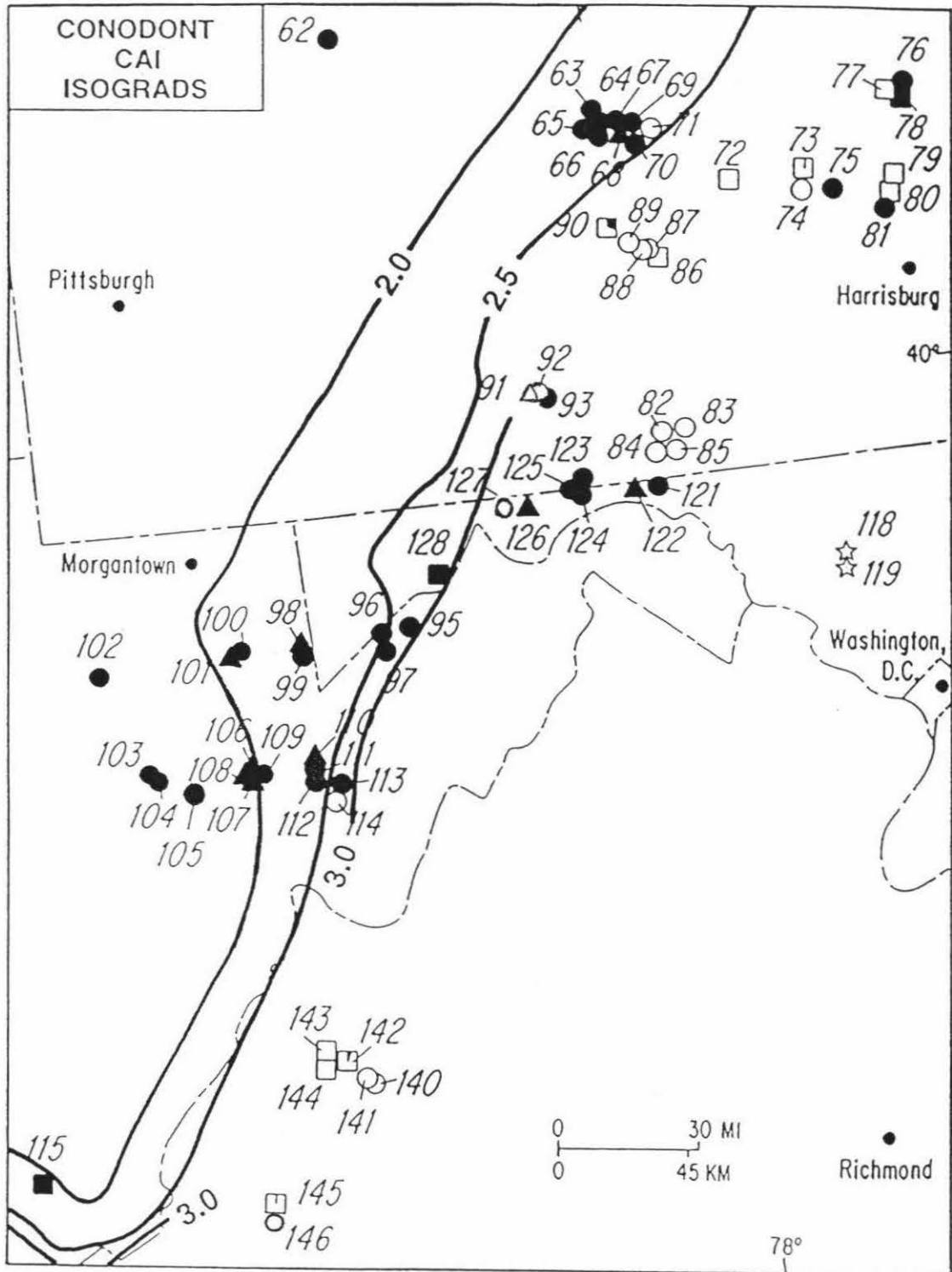
Figure 5.28

Sample location map from Figure 5.1, showing Silurian - Mid Devonian sample localities, together with the contours of Conodont Alteration Index (CAI) from Epstein et al. (1977) at values of 2.5, 3.0, 3.5, and 4.0 for this same age range of rocks (see text). Values of CAI were assigned to each sample from the oxygen isotope data set by interpolation between the contours shown on this map.

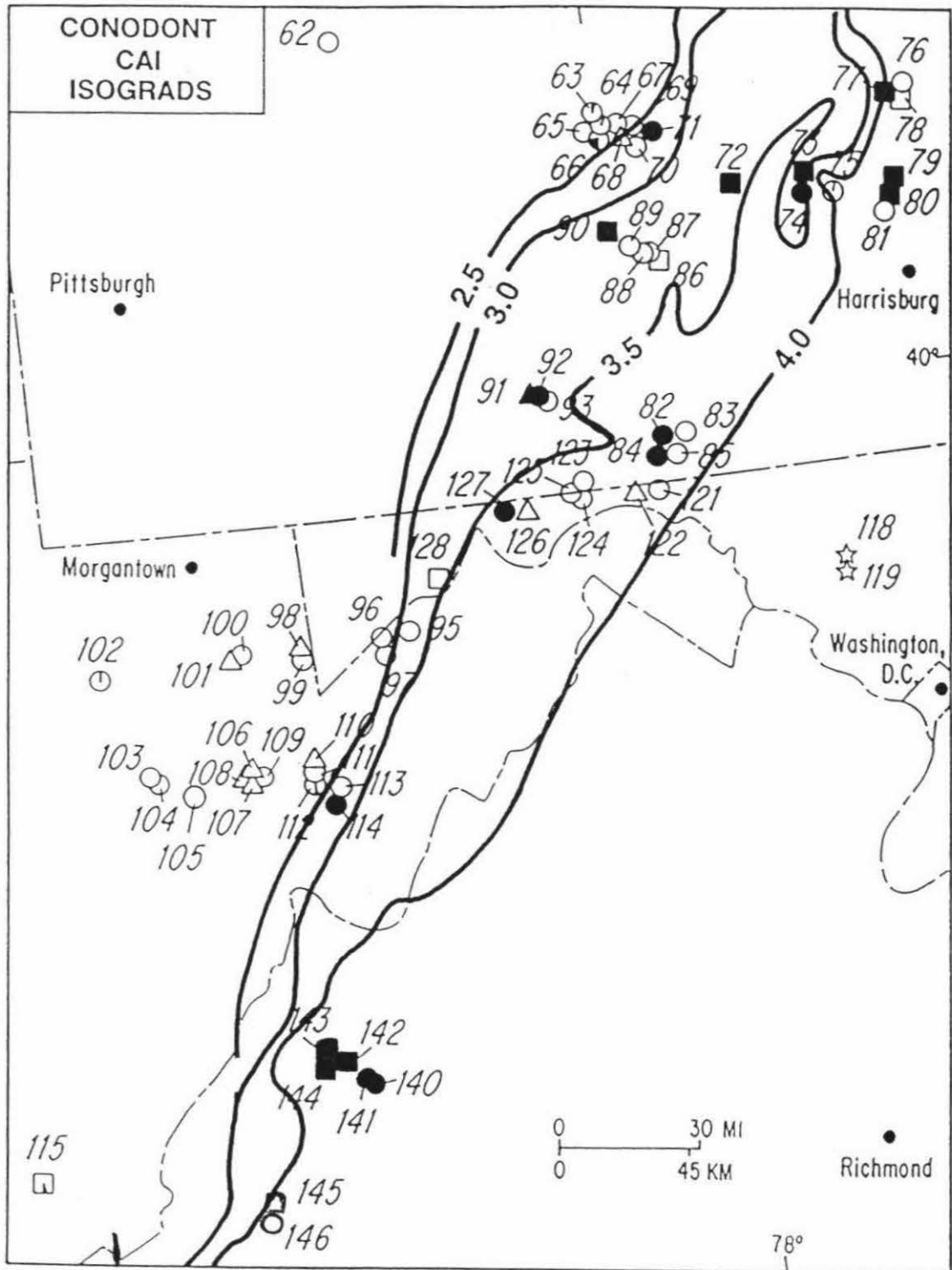
Figure 5.29

Sample location map from Figure 5.1, showing Ordovician sample localities, together with the contours of Conodont Alteration Index (CAI) from Epstein et al. (1977) at values of 3.5, 4.0, 4.5, and 5.0 for this same age range of rocks (see text). Values of CAI were assigned to each sample from the oxygen isotope data set by interpolation between the contours shown on this map.

UPPER DEVONIAN - MISSISSIPPIAN



SILURIAN - MID DEVONIAN



ORDOVICIAN

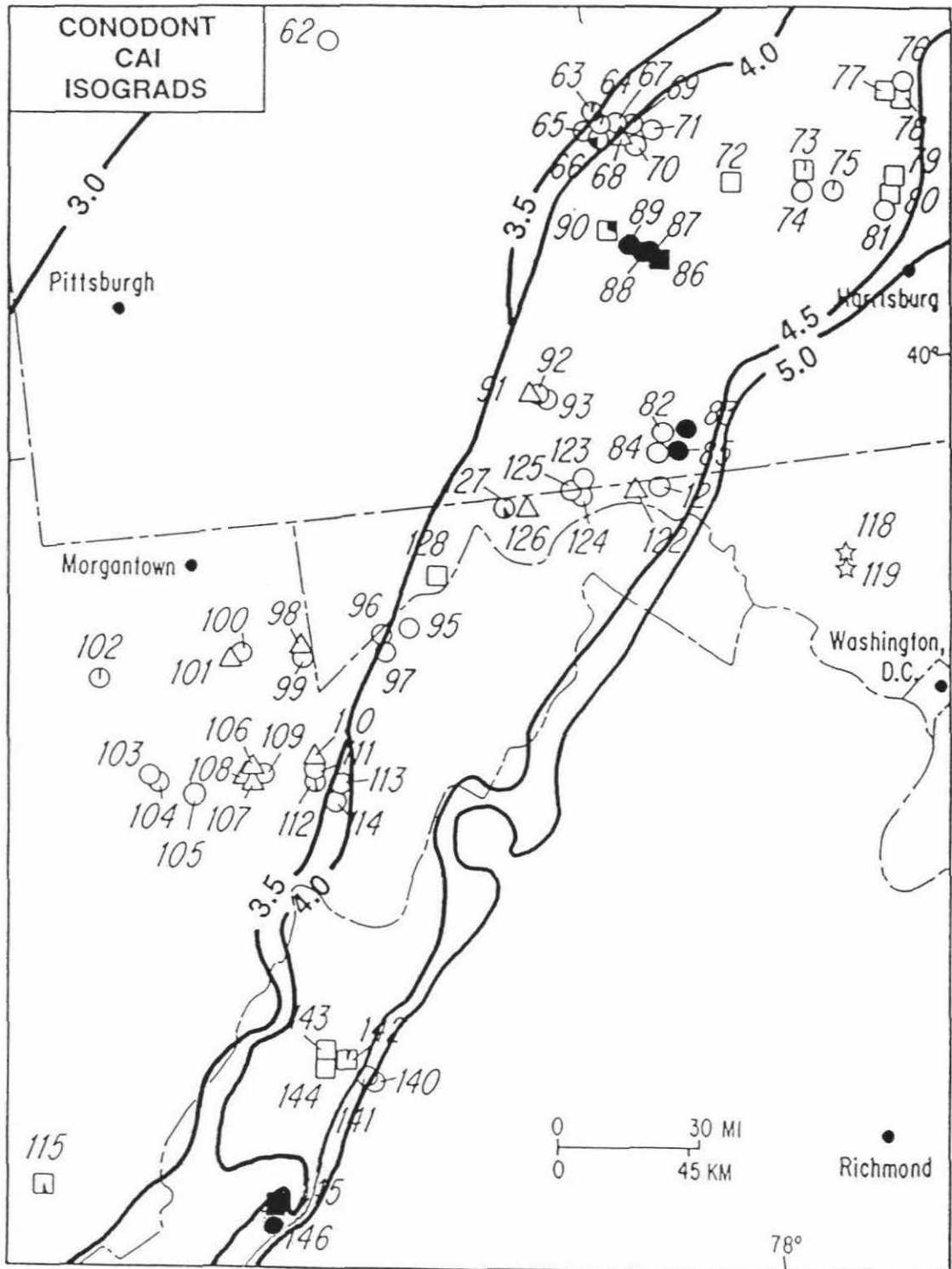


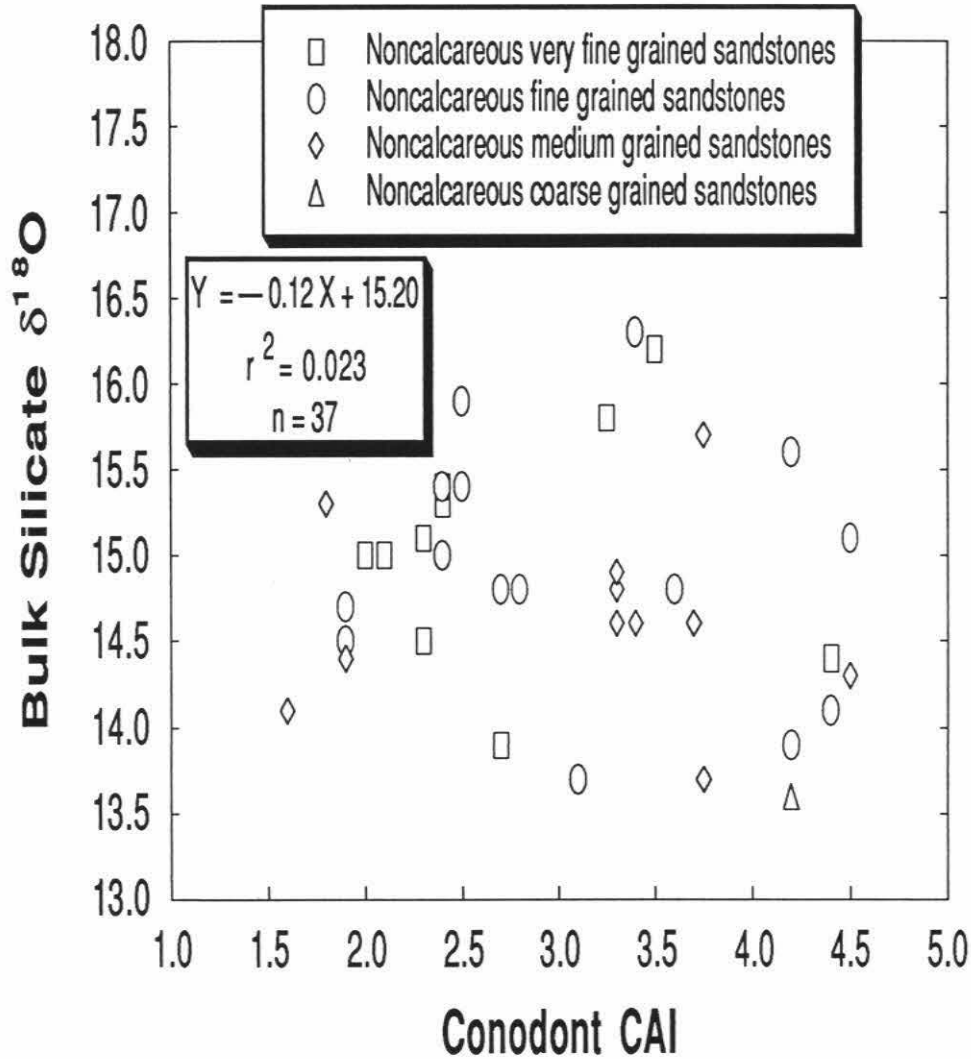
Figure 5.30

Plot of bulk silicate $\delta^{18}\text{O}$ of Central Appalachian noncalcareous sandstones versus conodont alteration index (CAI). There is no significant correlation.

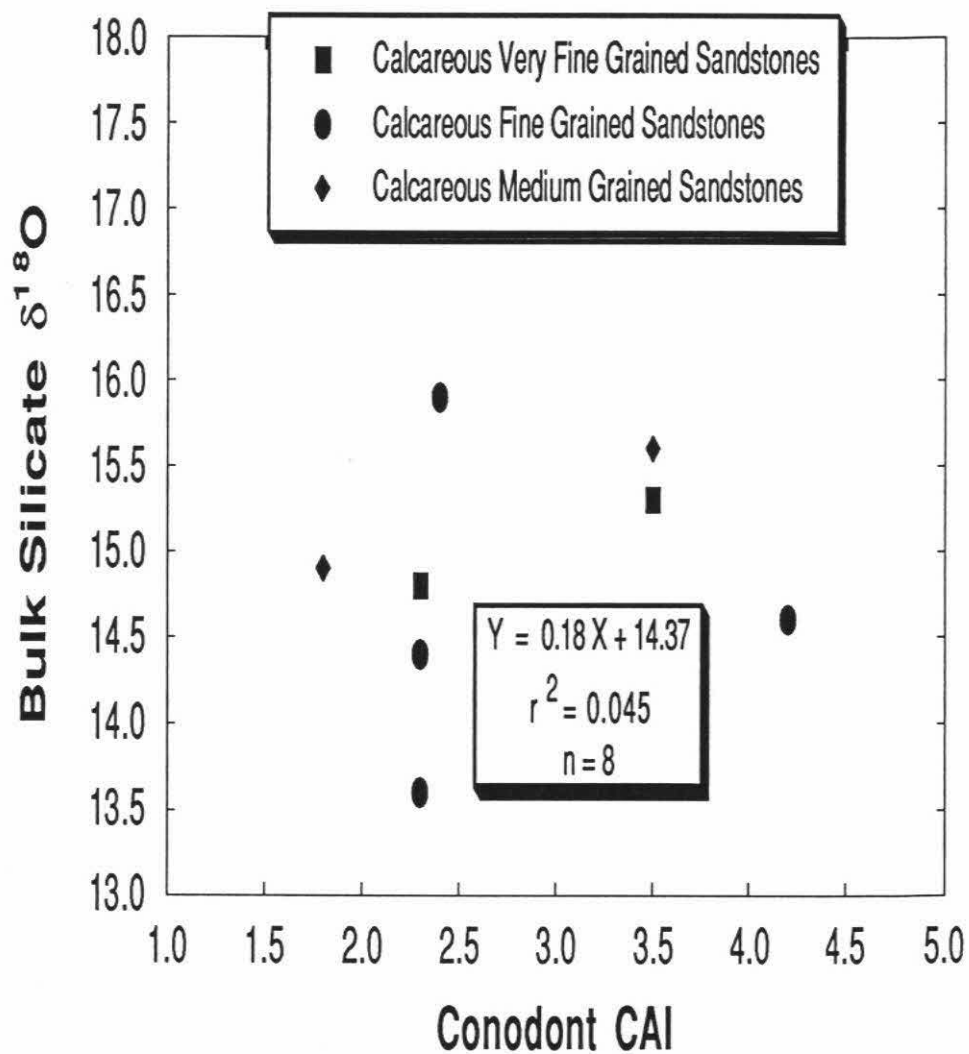
Figure 5.31

Plot of bulk silicate $\delta^{18}\text{O}$ of Central Appalachian calcareous sandstones versus conodont alteration index (CAI). There is no significant correlation.

Bulk Silicate $\delta^{18}\text{O}$ vs Conodont CAI for Central Appalachian Noncalcareous Sandstones



Bulk Silicate $\delta^{18}\text{O}$ vs Conodont CAI for Central Appalachian Calcareous Sandstones



siltstones is 0.715, which is significant at the 0.01 probability level. However, it should be noted that this correlation is dominated by the fact that the 5 distinguishable red siltstones tend to be both low in $\delta^{18}\text{O}$ and high in conodont CAI, whereas the reverse is true for the population of 7 green siltstones.

Figure 5.33 is a plot of bulk silicate $\delta^{18}\text{O}$ against conodont CAI for shales. The correlation coefficient for the 12 green and red shales is significant at the 0.05 probability level. The 5 black shales are excluded from this correlation, primarily because work by Hosterman and Whitlow (1983) suggest a different source for Devonian black shales, and because it is possible that diagenetic reactions proceed differently in the presence of organic matter. Weaver (1989) found that organic acids released during the process of thermal maturation complexed with aluminum and other ions, slowing diagenetic clay mineral transformations. If this were the case for the Devonian black shales, it would be expected that the $\delta^{18}\text{O}$ of the organic shale would be higher at a given CAI than that of the nonorganic shales, as is the case with this data set.

As with the red siltstones, it is interesting that the red shale samples also tend to have similarly low $\delta^{18}\text{O}$ values as well as high conodont CAI values. However, the CAI values of the red shales are significantly higher (3.5 to 4.5) than those of the red siltstones (2.0 to 3.5). The green shale samples show a much wider $\delta^{18}\text{O}$ variation (and also a much wider conodont CAI variation) than the green siltstones. If the shale groups are broken down into 3 separate sub-groupings based on color and carbonate content, the green calcareous shales, the green noncalcareous shales, and the black shales each display a negative correlation between bulk silicate $\delta^{18}\text{O}$ and CAI (Figure 5.33).

Figure 5.34 is a combination of Figure 5.31 and Figure 5.32 (black shales excluded), and on this figure three regression lines are drawn. The calcareous shales and

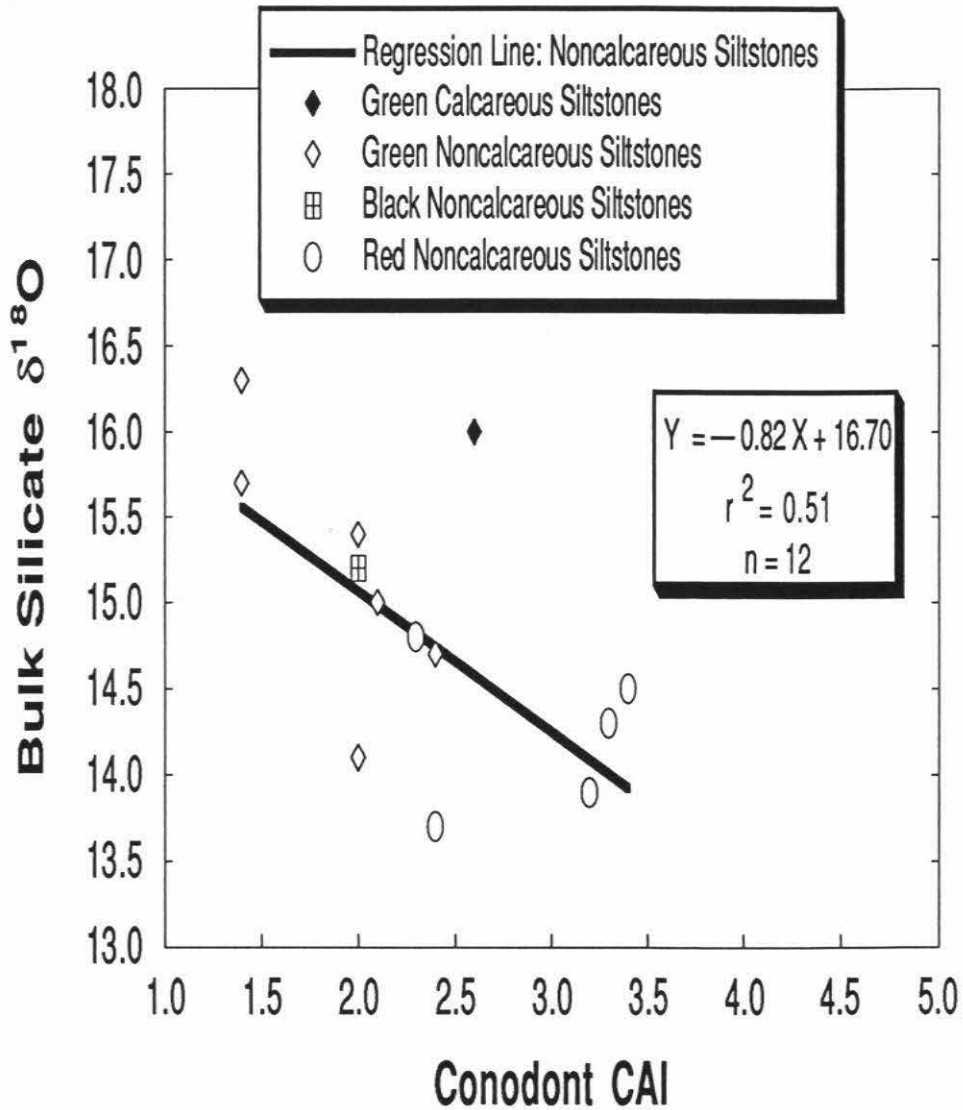
Figure 5.32

Plot of bulk silicate $\delta^{18}\text{O}$ of Central Appalachian siltstones versus conodont alteration index (CAI). The correlation is significant at the 0.01 probability level. The single calcareous siltstone is not included in the correlation.

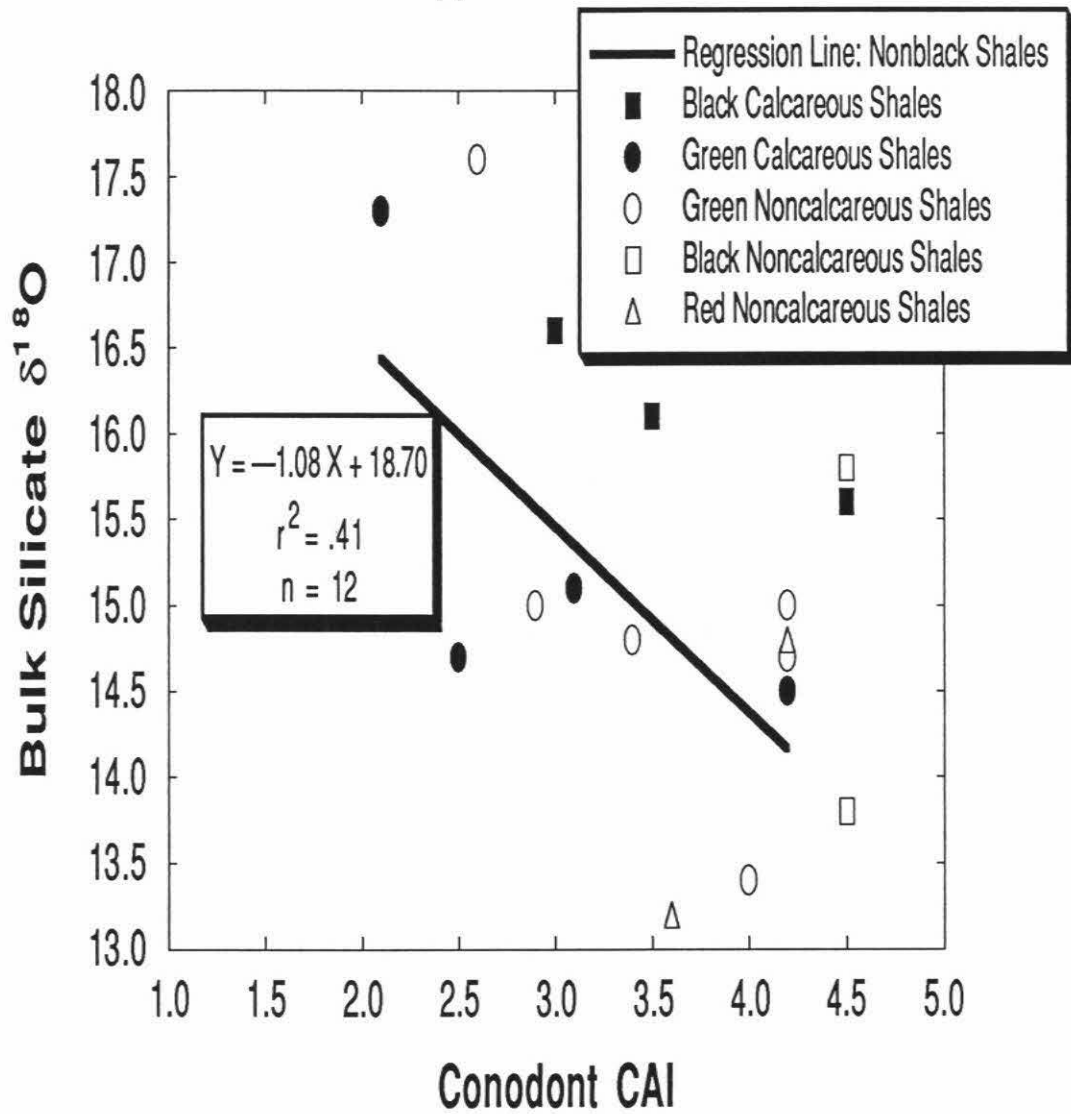
Figure 5.33

Plot of bulk silicate $\delta^{18}\text{O}$ of Central Appalachian shales versus conodont alteration index (CAI). The black shales are thought to be higher in ^{18}O than the rest of the population, possibly as a result of the influence of organic matter on clay mineral transformations. The black shale at $\delta^{18}\text{O} = +13.8$ is actually a slate, and probably should be considered to be somewhat metamorphosed. Because of their unusual petrographic and isotopic characteristics, the black shales are omitted from the regression line, which is significant at the 0.05 probability level. A regression line for all 17 shales (not plotted) has a slope of -0.81 and an intercept of 18.09 , with $r^2 = 0.26$ (significant at $P < 0.05$). A regression line for the 5 black shales alone has a slope of -1.025 and an intercept of 19.68 , with $r^2 = 0.46$.

Bulk Silicate $\delta^{18}\text{O}$ vs Conodont CAI for Central Appalachian Siltstones



Bulk Silicate $\delta^{18}\text{O}$ vs Conodont CAI for Central Appalachian Shales



the calcareous siltstone are grouped together. The thinking here is that fine-grained calcareous rocks may behave differently than noncalcareous rocks. The more easily exchanged carbonate may act as a buffer, limiting the amount of bulk silicate isotopic exchange. Also, calcium ions are strongly adsorbed by clay minerals, which may affect clay-mineral transformations responsible for changes in bulk silicate $\delta^{18}\text{O}$. Figure 5.35 is a graph of the regression lines only from Figure 5.34. The shift in bulk silicate $\delta^{18}\text{O}$ expected for a change in CAI from 1 to 4 is calculated in the accompanying table. By definition the lowest possible CAI number is 1. From these regression lines the expected shift in bulk silicate $\delta^{18}\text{O}$ in going from a CAI of 1.0 to a CAI of 4.0 is 2.5 per mil for noncalcareous siltstones and 4.2 per mil for noncalcareous shales (Figure 5.35). The calcareous fine-grained sediments give intermediate values. What this means is that these shifts in bulk silicate $\delta^{18}\text{O}$ could be due to diagenesis at temperatures well below 300°C, and that a 2.5 to 4.2 per mil lowering of bulk silicate $\delta^{18}\text{O}$ could occur without these sediments having been subjected to high-temperature metamorphism.

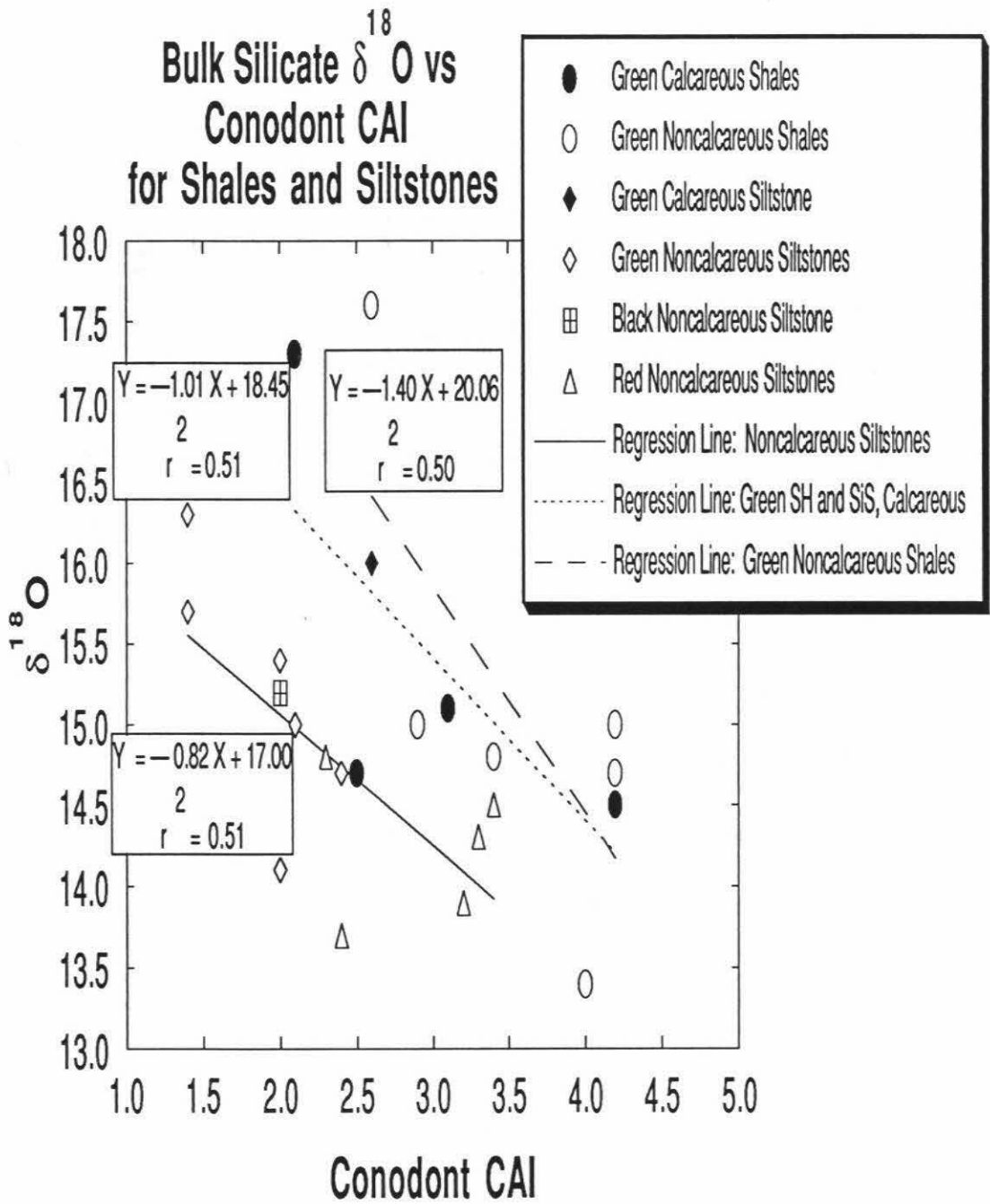
Inasmuch as CAI is a direct index of organic diagenesis, its correlation with bulk silicate $\delta^{18}\text{O}$ suggests a diagenetic origin for the $\delta^{18}\text{O}$ shifts in the shales and the siltstones. It is particularly important that there is a significant correlation of CAI with $\delta^{18}\text{O}$ for the shales, and the siltstones, but not for the sandstones. The reaction of smectite with potassium ions to form illite, chlorite, and quartz, which was proposed for Devonian shales (Hosterman and Whitlow, 1983) may have application here, driving the bulk silicate $\delta^{18}\text{O}$ value toward lower $\delta^{18}\text{O}$ values as the temperature increases and the illite and chlorite contents increase.

Figure 5.34

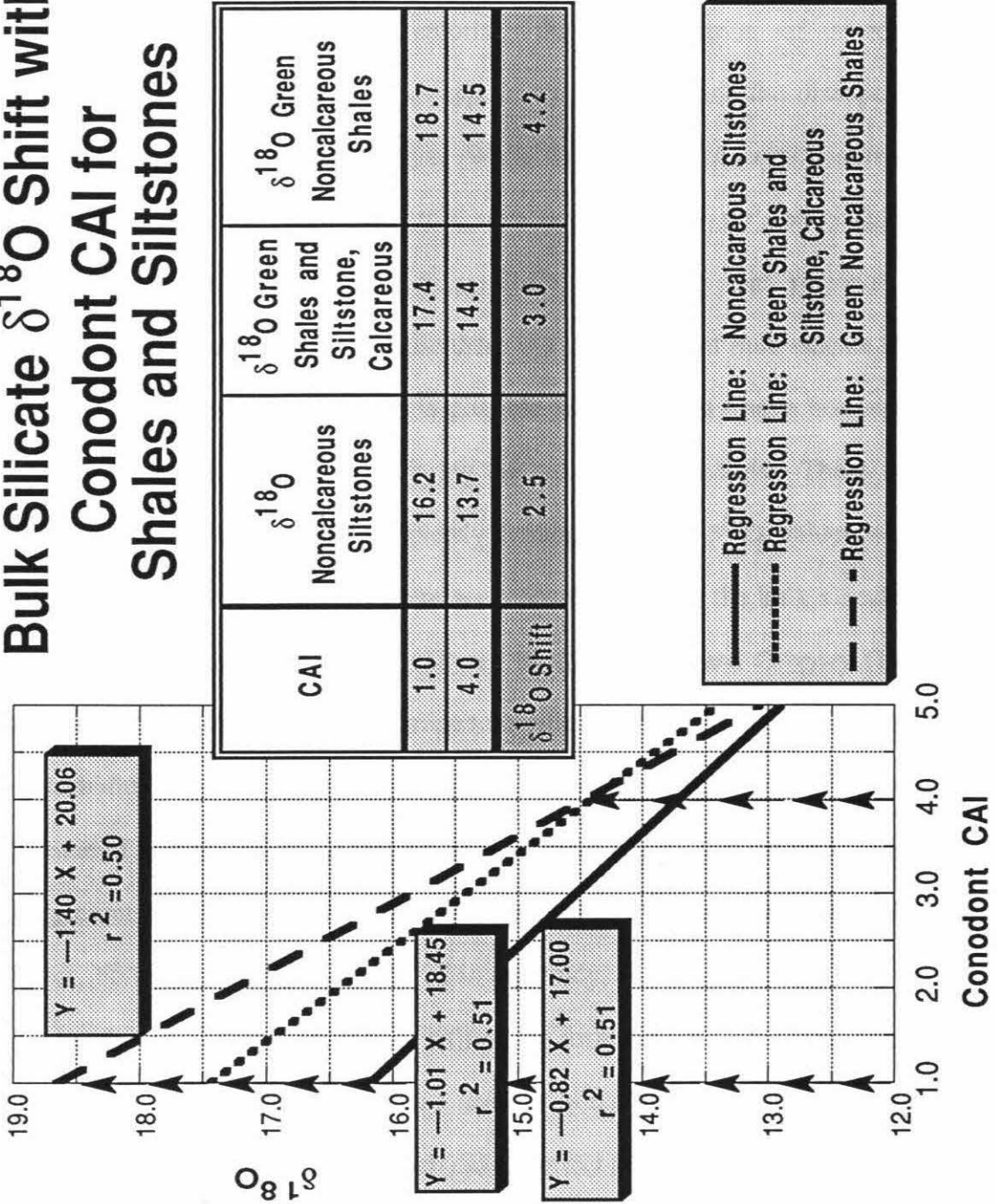
Plot of bulk silicate $\delta^{18}\text{O}$ versus conodont alteration index (CAI), showing three linear regression lines for (a) noncalcareous siltstones, (b) calcareous shales and the calcareous siltstone (excluding the black shales), and (c) green noncalcareous shales. The r^2 values of these regression lines (0.51, 0.51, 0.50) are all similar, but because of the small sample populations, the only line that is truly statistically significant is the siltstone correlation.

Figure 5.35

Bulk silicate $\delta^{18}\text{O}$ shift with conodont CAI for shales and siltstones. The rectangular box (inset) shows how the $\delta^{18}\text{O}$ values would shift from one regression line to another if one increases the $\delta^{18}\text{O}$ value at a constant value of CAI equal to a low value of 1.0 (upward pointing arrows along the ordinate line) or a high value of 4.0 (upward pointing arrows at CAI = 4.0). For example, at a CAI of 1.0 (low-temperature diagenesis) the expected mean $\delta^{18}\text{O}$ values for the different lithological groupings would be: noncalcareous siltstones (+16.2), green calcareous shales and siltstone (+17.4), and green noncalcareous shales (+18.7). At a CAI of 4.0 (high-temperature diagenesis), these lithologies would be expected to have much different mean $\delta^{18}\text{O}$ values, +13.7, +14.4, and +14.5, respectively.



Bulk Silicate $\delta^{18}\text{O}$ Shift with Conodont CAI for Shales and Siltstones



— Regression Line: Noncalcareous Siltstones
 Regression Line: Green Shales and Siltstone, Calcareous
 - - - Regression Line: Green Noncalcareous Shales

5.7.3 Mineralogical changes during diagenesis

Weaver, Eslinger, and Yeh (1984) found that the $\delta^{18}\text{O}$ of clay-sized quartz from the Cambrian Conasauga Shale in Georgia decreased with increasing CAI. Careful X-ray diffraction and electron microscopy work on the Conasauga Shale have documented the formation of quartz, illite, and chlorite, the disappearance of smectite, the recrystallization of illite and mica, the appearance of biotite and the disappearance of chlorite with increasing CAI in Georgia. While there was an observable correlation of clay-sized quartz $\delta^{18}\text{O}$ with CAI, this was not the case for the <0.2 micron illite-smectite fraction of the Conasauga Shale, suggesting that regional isotopic homogenization did not occur. Because there is a correlation of bulk silicate $\delta^{18}\text{O}$ with CAI in the Central Appalachians, it is possible that there may have been an overall higher water/rock ratio in this area during the period of diagenesis. There was not a high enough flux of water to completely homogenize the $\delta^{18}\text{O}$ values of Central Appalachian shales, but apparently there was enough water for the bulk silicate $\delta^{18}\text{O}$ to reflect increases in temperature as monitored by CAI. Grey and Gregory (1991) in a study of quartz veins in Eastern Australian turbidities suggested that the water/rock ratio in the turbidities was so low that quartz $\delta^{18}\text{O}$ was insensitive to changes in temperature or the time of crystallization. However, because there is a correlation of $\delta^{18}\text{O}$ with CAI in the present work, this does not appear to be the case in the Central Appalachians. However, no quartz veins were analyzed in our study.

Work by Elliot and Aronson (1990) on the formation of illite in the Appalachian Basin supports the formation of illite as a result of burial diagenesis. These authors also suggest a Mesozoic fluid overprint which did not affect the K-Ar systematics of the illite.

Studies by Schedl *et al.* (1992) on dolomite cement suggest that the fluid involved in a late Paleozoic diagenetic event in the Appalachians was metamorphic and basin-derived, not meteoric. Schedl *et al.* (1992) found that quartz and dolomite were not in oxygen isotopic equilibrium in the Upper Knox dolomite. They attributed this to a higher temperature for quartz formation and, based on fluid inclusion studies, the formation of quartz and dolomite from fluids of different salinities. They found that the $\delta^{18}\text{O}$ of dolomite cement formed during this late Paleozoic diagenetic event increased toward the craton in the Valley and Ridge Province of the Central Appalachians. This increase in $\delta^{18}\text{O}$ was attributed to higher temperatures of dolomite formation closer to the Pulaski thrust fault. Schedl *et al.* (1992) believed that sediments buried below the Blue Ridge-Piedmont Detachment Fault were the source of hot fluids which cooled with distance from the fault. An increase in $\delta^{18}\text{O}$ of dolomite cement was reported from a minimum of +18 near the Pulaski thrust fault to a maximum of +23.5, 18.6 miles from the Pulaski thrust fault.

The bulk silicate $\delta^{18}\text{O}$ shifts reported in the present study occur up to 150 km from the Pulaski thrust fault and were formed by a different process than the dolomite cements described by Schedl *et al.* (1992). In addition to the bulk silicate $\delta^{18}\text{O}$ decrease with decreasing CAI number, an even more significant correlation ($P < 0.01$) is observed in the present study for shale carbonate $\delta^{18}\text{O}$ and CAI (Figure 5.36). This decrease of carbonate $\delta^{18}\text{O}$ from +25 to +18 over a distance of 40 km is of the same magnitude as that found by Schedl *et al.* (1992) over a distance of about 30 km. It is possible that the carbonate in these shales recorded the same late Paleozoic diagenetic event as the dolomite cements of Schedl *et al.* (1992). Again, it is important to note that sandstone carbonate $\delta^{18}\text{O}$ does not show a similar decrease in with CAI (Figure 5.37).

Figure 5.36

Plot of carbonate $\delta^{18}\text{O}$ values from Central Appalachian calcareous shales versus interpolated conodont color alteration index (CAI), showing that the $\delta^{18}\text{O}$ of the carbonate decreases sharply from about +25 to +15 as CAI goes up from a value of 2.0 to a value of 4.5. Both features are considered to be correlated with increasing temperatures of diagenesis.

Figure 5.37

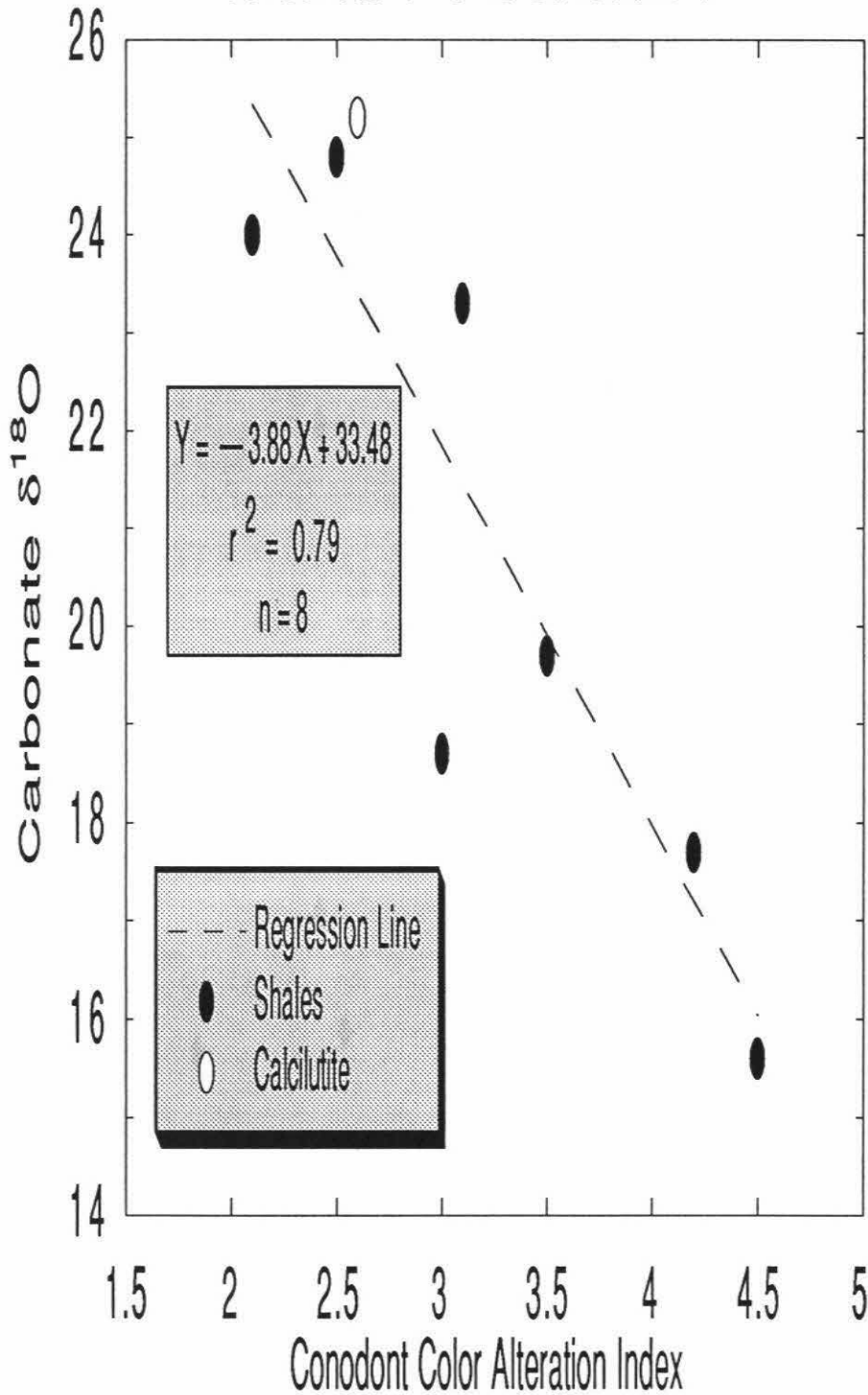
Plot of carbonate $\delta^{18}\text{O}$ values from Central Appalachian sandstones versus interpolated conodont color alteration index (CAI). There is no obvious correlation between CAI and the carbonate $\delta^{18}\text{O}$ values.

Figure 5.38

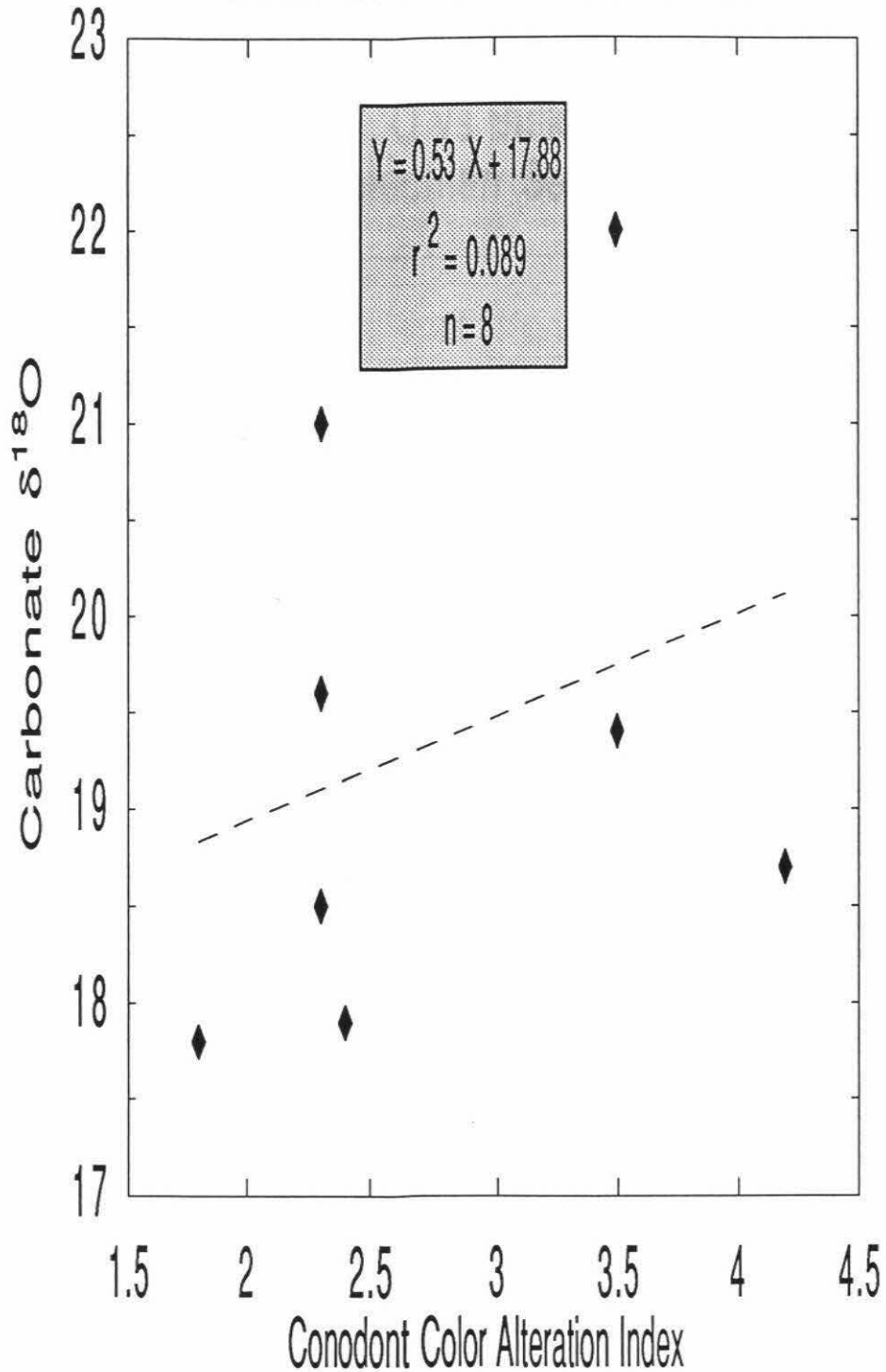
Plot of carbonate $\delta^{18}\text{O}$ values from Central Appalachian sandstones (filled diamonds) and shales (open circles) versus bulk silicate $\delta^{18}\text{O}$, showing the lack of a correlation, and indicating that the $\delta^{18}\text{O}$ values of these coexisting materials are effectively decoupled.

Central Appalachian Calcareous Shales and Calcilutite:

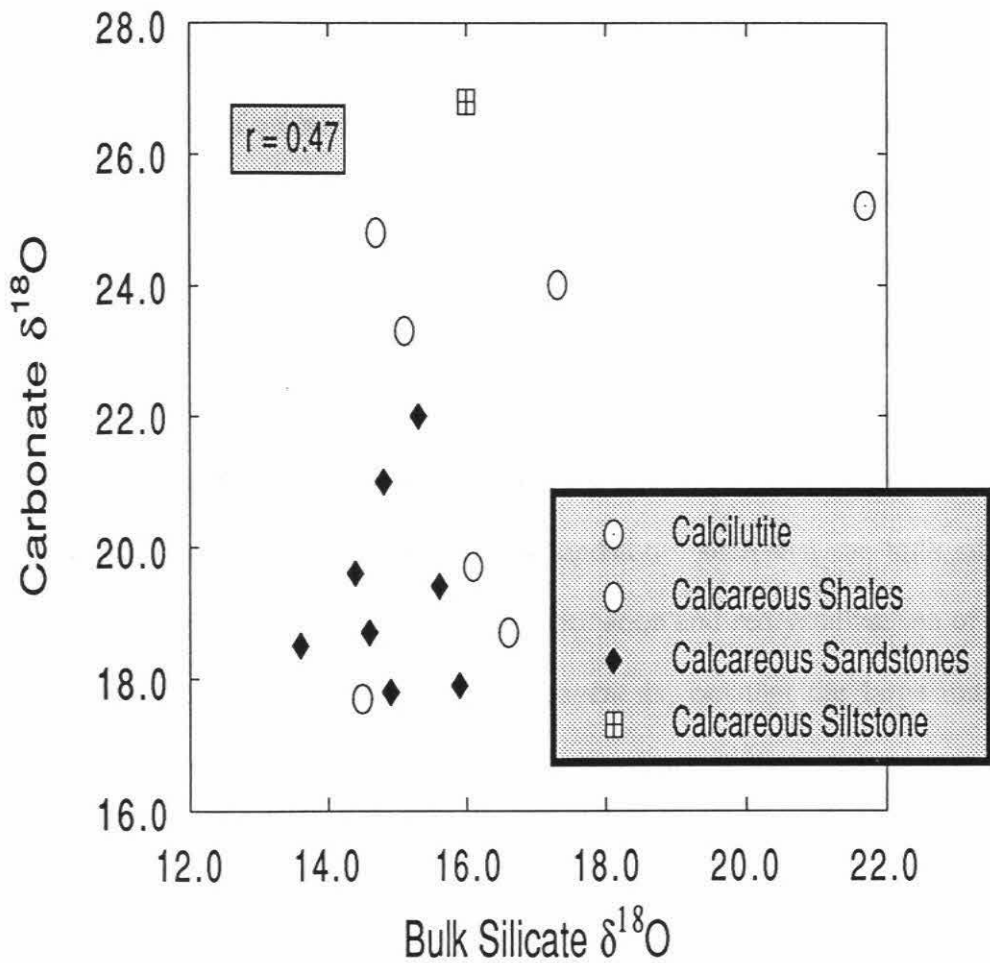
Carbonate $\delta^{18}\text{O}$ vs Conodont CAI



Central Appalachian Calcareous Sandstones:

Carbonate $\delta^{18}\text{O}$ vs Conodont CAI

Carbonate $\delta^{18}\text{O}$ vs Bulk Silicate $\delta^{18}\text{O}$ for Central Appalachian Sedimentary Rocks



The following scenario is proposed for the bulk silicate $\delta^{18}\text{O}$ evolution of the terrigenous sedimentary rocks of the Central Appalachians in this study. Clastic sediments were eroded dominantly from a tectonic sourceland to the southeast. Devonian black shales are the exception, having a cratonic sourceland to the north and northwest (Meckel, 1970; Hosterman and Whitlow, 1983). The sandstone to shale ratio decreased to the west, away from the tectonic sourceland (Meckel, 1970). It is not unlikely that diagenetic reactions similar to those documented for the Conasauga Shale occurred in other Paleozoic Appalachian shales. These reactions included the formation of chlorite, illite, and small amounts of quartz from smectite, the alteration of detrital biotite to white mica and phengite, the recrystallization of illite and mica, and the dissolution of feldspar and quartz (Weaver, 1989). Some diagenetic quartz precipitated in the shales. Much of the silica dissolved in interstitial waters was transported into Paleozoic sandstones elsewhere in the section, where it was deposited as quartz cement. The sandstone to shale ratio was high in much of the study area and the dissolved silica was deposited as small quantities of cement over a large mass of sandstone, such that the bulk silicate $\delta^{18}\text{O}$ of the shales was significantly decreased by formation and recrystallization of illite and micas at increasing temperatures of burial diagenesis, but that the large mass of sandstone did not show significant large shifts in bulk silicate $\delta^{18}\text{O}$.

Weaver, Eslinger, and Yeh (1984) concluded from studies of carbonate rocks in the Conasauga Shale that the thrusting action of faults had a greater effect on the micaceous components of carbonate rocks than on those of noncalcareous shales. This conclusion was based on the observation of higher crystallinity of the acid insoluble residue of carbonate rocks compared to equivalent noncalcareous shales. It is thus possible that this increased crystallinity of the acid insoluble residue of carbonate-rich

shales is due to a higher water/rock ratio during diagenesis. This hypothesis is supported by Figures 5.33 and 5.34 which show that at the same CAI the non-black calcareous shales tend to have a slightly lower bulk silicate $\delta^{18}\text{O}$ than the analogous noncalcareous shales. This could possibly be due to further progression of diagenetic reactions within calcareous shales at the same temperature due to an increased water/rock ratio. At higher CAI the bulk silicate $\delta^{18}\text{O}$ values for calcareous and noncalcareous shales might be expected to converge, as in fact they seem to do, as shown in Figures 5.34 and 5.35.

Schedl *et al.* (1992) distinguished six different diagenetic events in the Knox carbonates. The Zone 3 and 4 cements that were discussed in their paper differ from the early syndepositional dolomite in that they apparently formed from strontium-enriched fluids. Authigenic feldspars and illites that presumably formed from these same fluids display K-Ar ages and Ar/Ar ages between 270 and 320 Ma. While the oxygen isotopic signature of the carbonates in the present study may reflect the diagenetic event described by Schedl *et al.* (1992), it is doubtful that the bulk silicate $\delta^{18}\text{O}$ reflects this event. One possible reason is that the carbonate and bulk silicate $\delta^{18}\text{O}$ are decoupled (Figure 5.38). Another reason is the correlation of bulk silicate $\delta^{18}\text{O}$ with CAI. The Alleghenian event of Schedl *et al.* (1992) was relatively brief and presumably would not affect the CAI. This event did not affect the $\delta^{18}\text{O}$ of the entire Knox carbonate, and therefore it could not be expected to affect the bulk silicate $\delta^{18}\text{O}$ of shales and siltstones, which are much less easily exchanged (*e.g.*, see Yeh and Savin, 1977).

5.7.4 Diagenetic pore fluids

Finally, the question must be addressed: What type of fluid was involved in the bulk silicate $\delta^{18}\text{O}$ alteration of shales, siltstones, and to a much lesser extent the sandstones in this study? The most likely explanation would be a diagenetic pore fluid.

Using the illite-water $^{18}\text{O}/^{16}\text{O}$ fractionation equation of Eslinger and Savin (1973) and assuming that the illite formed has a $\delta^{18}\text{O}$ of about +13, the $\delta^{18}\text{O}$ of the diagenetic fluid can be conservatively estimated to be between 0 and +13, which is within the range expected for most sedimentary formation waters. For example, this range is remarkably similar to the $\delta^{18}\text{O}$ range of -2 to +11 found by Yeh and Savin (1977) and by Clayton *et al.* (1966) for Gulf Coast formation waters. Also, if the quartz-water fractionation equation of Clayton *et al.* (1972a) is applied to clay-sized quartz fractions of the Conasauga Shale, the calculated $\delta^{18}\text{O}$ range of pore waters is -5 to +10.

Yeh and Savin (1977) found that bulk silicate $\delta^{18}\text{O}$ decreased for Gulf Coast shales with increasing depth of burial, progress of diagenetic reactions, and increasing temperature measured in the well. They found that the $\delta^{18}\text{O}$ of different size fractions of clay homogenized with increasing depth. This is somewhat similar to the trend of bulk silicate $\delta^{18}\text{O}$ in the Appalachian shales and siltstones with increasing temperature, as reflected by the conodont CAI. Compare their Figure 1 with Figure 5.34 in this study. An important aspect of this process that has yet to be adequately addressed is the heterogeneity in $\delta^{18}\text{O}$ reported by Weaver, Eslinger, and Yeh (1984), Schedl *et al.* (1992), Yeh and Savin (1977), Eslinger and Yeh (1986), and the present study.

The question arises as to whether variations in the $\delta^{18}\text{O}$ of these diagenetic pore fluids might be more important in controlling the final bulk silicate $\delta^{18}\text{O}$ values of the Central Appalachian shales than other variables such as temperature (*e.g.*, as reflected in the CAI values). For example, such an interpretation would have to be strongly entertained if the fresh-water shales consistently had lower $\delta^{18}\text{O}$ values than the marine shales. Such an interpretation would also be suggested if the shales from the high- ^{18}O Area I in Figure 5.12 were dominantly marine compared to their counterparts elsewhere

in the Appalachians, particularly if the shales from the low- ^{18}O Area V (Figure 5.12) were also mostly from fresh-water deposits.

Figures 5.39 and 5.40 were prepared in order to address the above questions. Figure 5.39 shows that the siltstones from transitional or oscillating marine-nonmarine environments cover the entire spectrum of CAI and $\delta^{18}\text{O}$ values, and in particular that the marine siltstones as a group are not higher in ^{18}O than the fresh-water fluvial samples. Similarly, on Figure 5.40 it is seen that the marine and transitional shales cover the entire range of $\delta^{18}\text{O}$ and CAI values plotted on the diagram. However, it is true that all 4 fluvial shales do plot at CAI > 3.5 and they also have relatively low $\delta^{18}\text{O}$ values of +13.2 to +15.8; because of the small number of samples this may not be statistically meaningful. In addition, comparison of Table 2.1 with Figures 5.1, 5.2 and 5.12 shows that all but one of the noncalcareous shales and siltstones from both high- ^{18}O Area I and low- ^{18}O Area V are from transitional environments. Thus, there is no consistent marine versus fresh-water bias in the sampling that can explain the variation in $\delta^{18}\text{O}$ of the fine-grained sedimentary rocks of the central Appalachians. We therefore conclude that the $\delta^{18}\text{O}$ variations of these rocks are most likely brought about mainly by diagenetic temperature variations, modified by other variables such as degree of recrystallization, mineralogy, and $\delta^{18}\text{O}$ of the pore fluid. This suggests that the diagenetic pore fluids migrated across formation boundaries and that ground waters of fresh-water origin did not remain confined to the fluvial strata, nor did marine pore waters necessarily remain confined to the marine sedimentary layers. It is likely that the diagenetic pore fluids were of mixed origins and isotopic compositions, just as is found to be the case today in several sedimentary basins across the North American continent *e.g.*, Gulf Coast, Illinois, Michigan, and Alberta basins: see Clayton *et al.*, 1966).

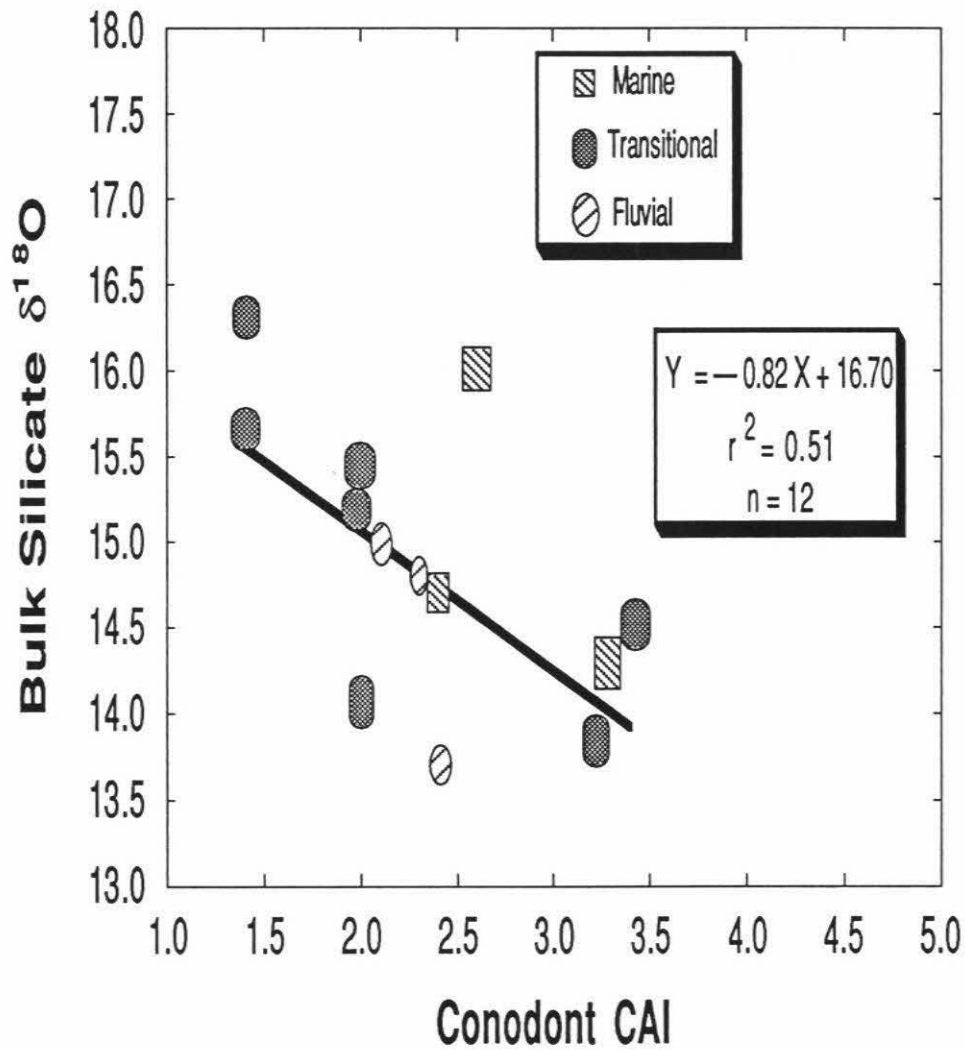
Figure 5.39

The same siltstone $\delta^{18}\text{O}$ and CAI data shown in Figure 5.32, but with the samples separated according to environment of deposition (marine, transitional and oscillating marine-nonmarine, or fresh-water fluvial) instead of mineralogy and color.

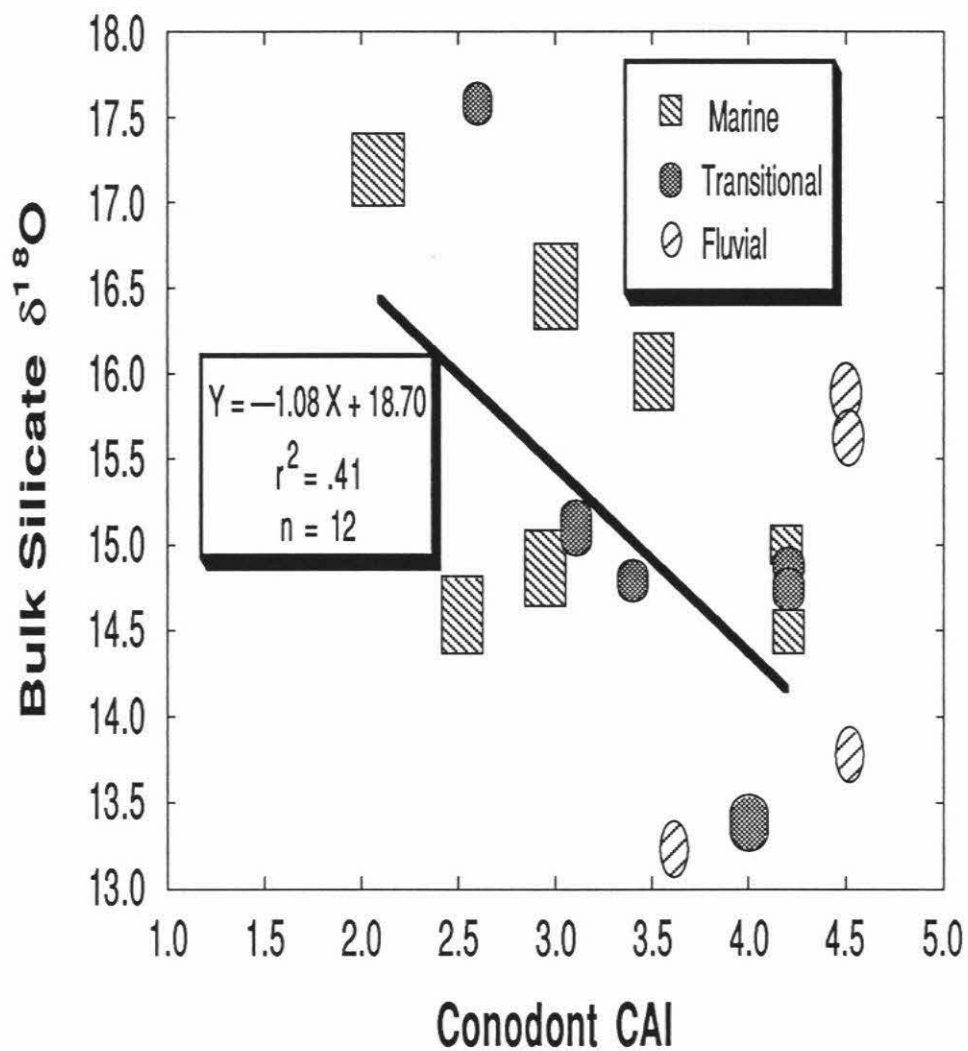
Figure 5.40

The same shale $\delta^{18}\text{O}$ and CAI data as shown in Figure 5.33, but with the samples separated according to environment of deposition (marine, transitional and oscillating marine-nonmarine, or fresh-water fluvial) instead of mineralogy and color.

Bulk Silicate $\delta^{18}\text{O}$ vs Conodont CAI for Central Appalachian Siltstones



Bulk Silicate $\delta^{18}\text{O}$ vs Conodont CAI for Central Appalachian Shales



5.8 Summary

In conclusion, the best explanation for the small geographic variation observed in bulk silicate $\delta^{18}\text{O}$ in shales and siltstones in this study is the very efficient series of mixing processes that operated prior to and during the sediment deposition, modified by the involvement of pore waters in the recrystallization of clay minerals during burial diagenesis. These diagenetic reactions are postulated to be similar to those described by Weaver (1989) for the Conasauga Shale in the southern Appalachians and by Hosterman and Whitlow (1983) for Devonian black shales throughout the Central Appalachians. The higher bulk silicate $\delta^{18}\text{O}$ of black shales in this study as compared to nonblack shales with equivalent CAI, may be due to the complexing of ions by organic matter and the slowing of diagenetic clay-mineral transformations. Nonetheless, the black shales as a group also display a decrease of bulk $\delta^{18}\text{O}$ with increasing temperature of diagenesis.

The illitization of montmorillonite, a major diagenetic reaction proposed by both Weaver (1989) and Hosterman and Whitlow (1983), has been documented in shales throughout the world, including the U.S. Gulf Coast, Oklahoma, France, Ciscaucasia, New Guinea, British Columbia, Germany, and the North Sea (Weaver, 1989). The Gulf Coast sediments are probably the most thoroughly studied. In addition to diagenesis, variations in primary mineralogy and in diagenetic processes account for much of the random isotopic heterogeneity in siltstones and shales. As a result of isotopic exchange with porewater during diagenesis, the bulk silicate $\delta^{18}\text{O}$ values of shales and siltstones apparently can be lowered by as much as 2.5 to 4.2 per mil. The $\delta^{18}\text{O}$ values of both calcareous and noncalcareous shales were found to decrease with increasing CAI. This effect is most likely attributable to simple burial diagenesis, but also possibly to fluid-rock exchange during tectonic activity, as exemplified by the Paleozoic thrusting event

recorded in the dolomite cement of the Knox Formation reported by Schedl *et al.* (1992). Calcareous shales have slightly lower bulk silicate $\delta^{18}\text{O}$ than noncalcareous shales at equivalent CAI. It is postulated that this might be due to a higher water/rock ratio in the calcareous shales or to differences in the rates of clay mineral transformations and recrystallization due to the high concentration of calcium and or magnesium ions in the pore water. No correlation of carbonate $\delta^{18}\text{O}$ with CAI or of bulk silicate $\delta^{18}\text{O}$ with CAI was found for calcareous sandstones. Further work is needed to understand how the water/rock interactions of calcareous sediments may differ from those of noncalcareous sediments.

The very small degree of isotopic variation displayed by the sandstones remains an interesting problem, particularly because the authigenic cement typically has a higher $\delta^{18}\text{O}$ than the sand grains themselves. This $^{18}\text{O}/^{16}\text{O}$ uniformity probably can be explained in part by the fact that, except for deposition of cementing materials, these coarser-grained rocks were much less susceptible to diagenetic changes in bulk $\delta^{18}\text{O}$ than were the shales. In contrast to the shales and siltstones, no correlations between bulk silicate $\delta^{18}\text{O}$ and CAI were observed for the sandstones. Much of the silica for the authigenic cement in the sandstones actually may have been supplied by the diagenetic reactions that lowered the $\delta^{18}\text{O}$ values of the interbedded shales. Weaver (1989) presents evidence for decreasing $\text{SiO}_2/\text{Al}_2\text{O}_3$ ratios in the Conasauga Shale with increasing burial diagenesis and low-grade metamorphism, which he attributes to the loss of silica through solution. That silica could then be deposited in sandstone interstices or as quartz veins. If this mechanism has general applicability, the $\delta^{18}\text{O}$ values of the Appalachian sandstones should have undergone a slight upward shift of $\delta^{18}\text{O}$, even though no such shift can be perceived in our limited data set. Note, however, that sandstones are far

more abundant than shales in the geosynclinal sections studied in this work in the Appalachians. The data set contains 60% sandstones, 17% siltstones and 23% shales, so by material balance we would expect the shales to be shifted downward in $\delta^{18}\text{O}$ to a greater extent than would the sandstones be shifted upward in ^{18}O . Further complicating this picture, however, is the role of the interbedded limestones and dolomites, which also are probably undergoing a downward shift in ^{18}O . Further, very detailed, mineralogic and radiometric studies, including mass-balance studies, are needed to constrain the mechanisms and timing of the diagenetic processes responsible for these shifts in bulk silicate $\delta^{18}\text{O}$, both the ^{18}O -depletions that we have documented for the shales, and the slight ^{18}O -enrichments postulated for the sandstones.

The profound oxygen isotopic homogeneity of the bulk silicate material in sedimentary rocks in the Central Appalachians, particularly in the case of the sandstones, is the most remarkable and potentially the most far-reaching result obtained in the present study. This astonishing uniformity in bulk silicate $\delta^{18}\text{O}$ was not anticipated when this study was initially undertaken, based on limited data obtained in earlier studies, and also because sandstones in general are known to be made up of isotopically heterogeneous grains from many different primary source rocks (volcanic, plutonic, metamorphic, and earlier-cycle sedimentary); they are also known to contain widely variable amounts of ^{18}O -rich silica cement. While local diagenetic changes in bulk silicate $\delta^{18}\text{O}$ of the sandstones certainly must have occurred (slight upward shifts in $\delta^{18}\text{O}$?), it is clear that the observed $\delta^{18}\text{O}$ homogenization of these sandstones on a regional scale cannot be attributed to diagenesis of the Paleozoic geosynclinal sediments in the Central Appalachians. Another mechanism must be sought. The isotopic homogeneity of these Paleozoic sandstones is most likely attributable mainly to the fact that processes involving

several cycles of sedimentation, orogeny, and erosion are one of the better ways (perhaps the best way!) to homogenize large portions of the Earth's crust. Such processes would obviously also tend to homogenize $^{18}\text{O}/^{16}\text{O}$ ratios.

Although less homogeneous in $\delta^{18}\text{O}$ than the sandstones, the shales and siltstones also show a remarkable uniformity in $\delta^{18}\text{O}$. However, on a smaller scale, we also know that, like the sandstones, the minerals that make up the shales are not isotopically homogeneous. For example, analyses of Mississippi River mud reveal considerable isotopic heterogeneity in various size fractions of clays. Also, of Gulf Coast shales display considerable isotopic heterogeneity in different fractions of quartz (Yeh and Savin, 1977). Most earlier studies have concluded that argillaceous sedimentary rocks typically have higher $\delta^{18}\text{O}$ values than sandstones, although considerable overlap in $\delta^{18}\text{O}$ is observed (see Chapter 3). Our own data from the Colorado Plateau Province confirm this general relationship (Chapter 4). Thus, another factor that seems to have contributed to the overall uniformity in $\delta^{18}\text{O}$ of the terrigenous sedimentary rocks of the Appalachians is this diagenetic ^{18}O depletion of the shales, bringing them isotopically closer to the interbedded sandstones.

Summing up, the oxygen isotopic uniformity of the Central Appalachian sedimentary rocks is basically a primary depositional feature that is a result of a thorough, grand-scale mixing of the terrigenous sediment in the Appalachian geosyncline, probably involving several cycles of sedimentation, uplift, erosion, and reworking, extending over hundreds of millions of years during the Paleozoic Era. Perhaps adding to this remarkable $^{18}\text{O}/^{16}\text{O}$ uniformity is the relatively minor post-depositional depletion in ^{18}O that took place during diagenesis of the finer-grained sedimentary rocks such as the shales, bringing them even closer to the $\delta^{18}\text{O}$ values of the sandstones.

CHAPTER 6**Oxygen Isotope Studies of Terrigenous Sedimentary Rocks of the Central and Southern Ouachita Mountains****6.1 Introduction**

A reconnaissance $^{18}\text{O}/^{16}\text{O}$ study of Paleozoic sedimentary rocks from the Ouachita Mountains was undertaken. Fourteen whole-rock samples from southeastern Oklahoma and western Arkansas were analyzed for oxygen isotopic composition. The results supplement and to a certain extent complement the isotopic data obtained from analogous samples from the Appalachian Mountains referred to above. They suggest that the Ouachita Mountains would be a promising area for a future more detailed study.

6.2 Overview of bulk silicate $^{18}\text{O}/^{16}\text{O}$ analyses

The fourteen samples from the Ouachita Mountains span an area of more than 10,000 square kilometers (Figure 6.1). Five samples are from western Arkansas and nine samples are from southeastern Oklahoma. Only one of these samples, a pyritic slate, contained carbonate. Six other shales were analyzed in addition to the pyritic slate.

Five quartz arenites and two lithic arenites were analyzed, for a total of seven sandstones. The age distribution of samples is as follows: one Ordovician, three Silurian, four Mississippian, and six Lower Pennsylvanian.

The distribution of bulk silicate $\delta^{18}\text{O}$ analyses for the Ouachita Mountain samples is shown in Figure 6.2. The mean bulk silicate $\delta^{18}\text{O}$ for all Ouachita Mountain samples is +15.1, which is only 0.3 per mil heavier than the mean for Central Appalachian detrital sedimentary rocks and 0.3 per mil heavier than the mean for all Utah/Arizona detrital sedimentary rocks. The standard deviation (SD) is 1.2 per mil for all Ouachita Mountain samples, which 0.8 per mil less than the SD for all Utah/Arizona

Figure 6.1

Map of eastern Oklahoma, western Arkansas, and northeastern Texas, showing locations and sample numbers of terrigenous sedimentary rocks studied in this work from the Ouachita Mountains (see Table 2.1. for descriptions and isotopic analyses of these samples). The circles represent sandstones and the squares represent shales. The per cent blackened area inside a sample symbol denotes the per cent carbonate in that sample. Samples 55 and 56 are Blaylock Sandstone samples from the southern limb of the Broken Bow Uplift, an area of very high diagenetic temperatures (see text).

OUACHITA MOUNTAINS - CENTRAL AND SOUTHERN

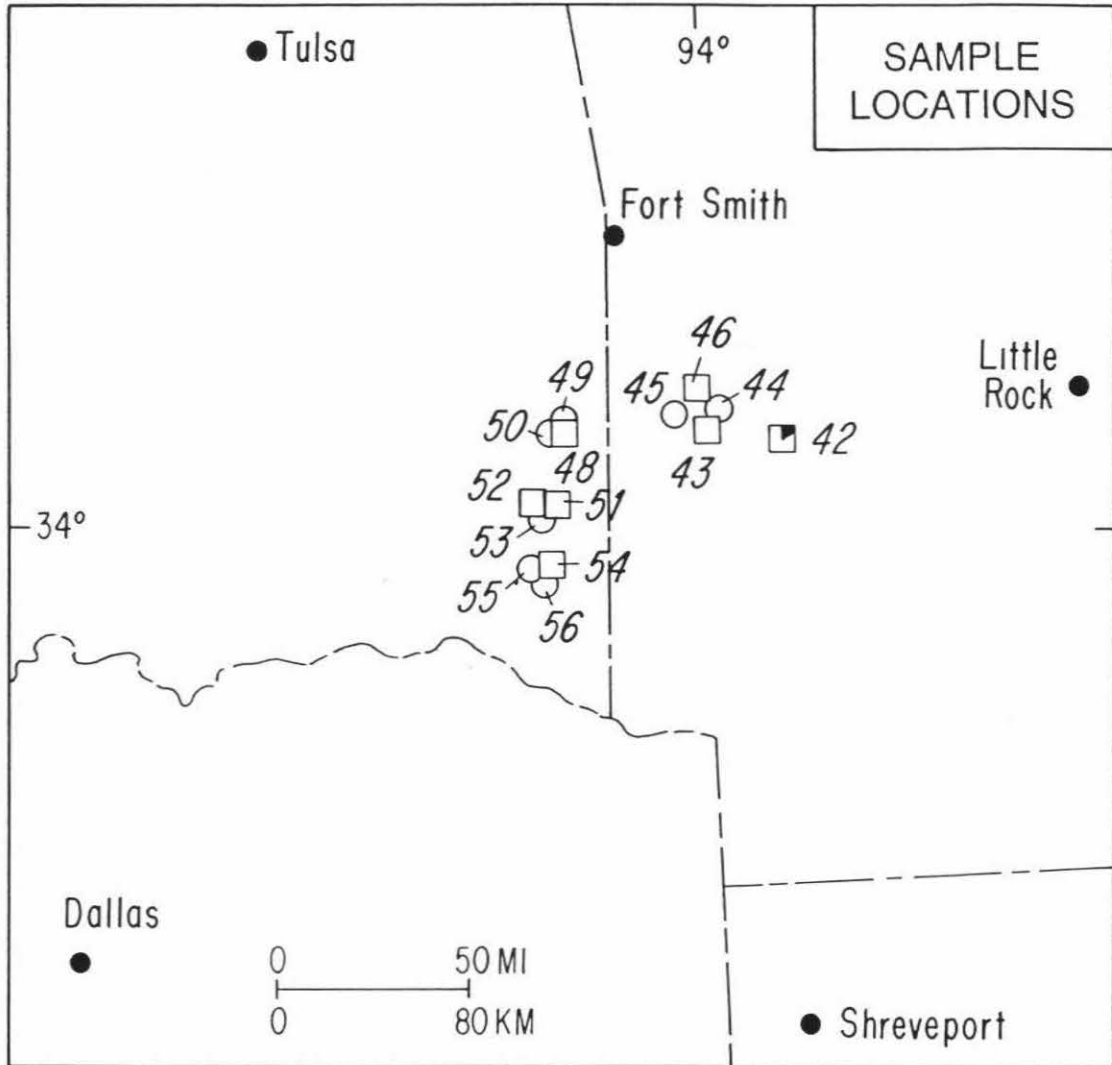
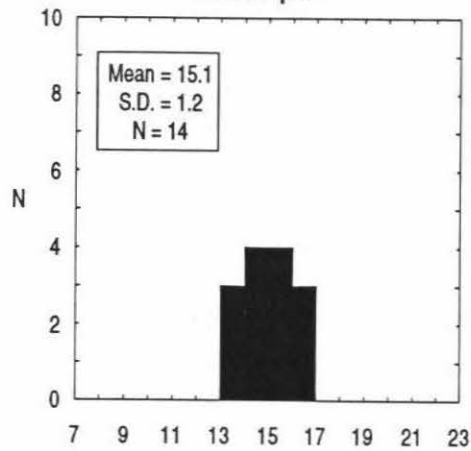


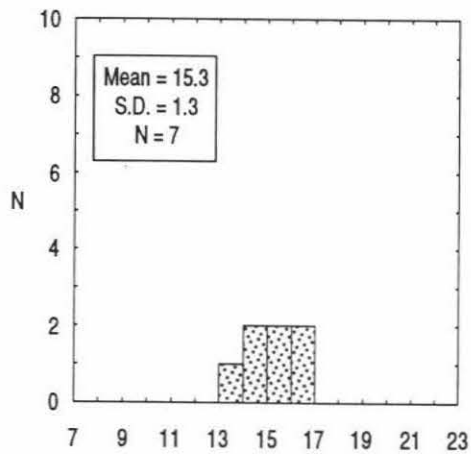
Figure 6.2

Three comparative histograms showing the bulk silicate $\delta^{18}\text{O}$ values of various categories of terrigenous sedimentary rocks from the Ouachita Mountains. The plotted categories include: all 14 rocks of all lithologies; all 7 sandstones of all types; and all 7 shales, subdivided into calcareous and noncalcareous varieties. The mean bulk silicate $\delta^{18}\text{O}$ values of each of the three categories are virtually identical, with the sandstones being very slightly higher in $\delta^{18}\text{O}$ than the shales. These histograms should be compared with similar histograms for the Central Appalachians (Figure 5.3) and the Colorado Plateau (Figure 4.2).

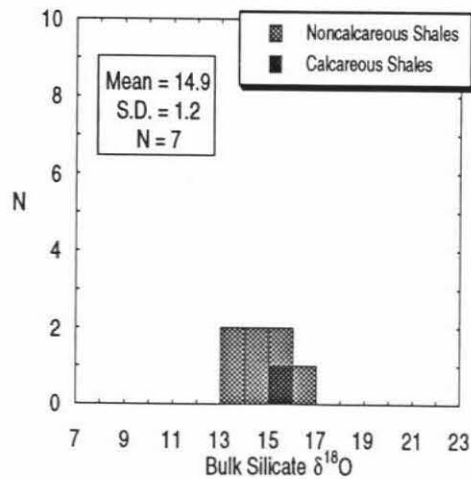
Ouachita Mountains
All Samples



Ouachita Mountains
Sandstones



Ouachita Mountains
Shales



sedimentary rocks and 0.4 per mil greater than the SD for Central Appalachian sedimentary rocks. The mean bulk silicate $\delta^{18}\text{O}$ of all Ouachita Mountain sandstones is +15.3, which is 1.0 per mil heavier than the mean for Utah/Arizona sedimentary rocks and 0.3 per mil heavier than the mean for Central Appalachian sedimentary rocks. The SD for bulk silicate $\delta^{18}\text{O}$ of Ouachita Mountain sandstones is 1.3 per mil as compared to 1.7 per mil for Utah/Arizona sandstones, and only 0.7 per mil for Central Appalachian sandstones. The mean bulk silicate $\delta^{18}\text{O}$ for Ouachita Mountain shales is +14.9, which is 0.3 per mil lighter than the mean for Central Appalachian shales and 2.8 per mil lighter than the mean for Utah/Arizona shales and calcilutites. The SD for Ouachita Mountain shales is 1.2 per mil as compared to 1.2 per mil for Central Appalachian shales and 1.4 per mil for Utah/Arizona shales and calcilutites.

As described in Chapter 5, the Central Appalachian sedimentary rocks analyzed in this study were derived primarily from an eastern tectonic source, and in addition there was an appreciable amount of sediment-mixing on a regional scale within the Appalachian basin. We concluded above that this extensive mixing and homogeneity of source material are the most likely causes of the low SD for bulk silicate $\delta^{18}\text{O}$ in the Central Appalachian sedimentary rocks, especially for the sandstones. In Chapter 4, we showed that the Utah/Arizona sedimentary rocks had $\delta^{18}\text{O}$ values that changed with geographic position; these were interpreted to be a mixture of at least two sources of sediment which were not completely homogenized, accounting for the higher SD for bulk silicate $\delta^{18}\text{O}$ for the Utah/Arizona sedimentary rocks, again especially for the sandstones. In comparison to the above areas, the sediment sources for the Ouachita Mountain samples appear to have been numerous, and they also seem to have varied in contribution

throughout geologic time. Thus, even though the Ouachita Mountain sediments are comprised of great thicknesses of geosynclinal material much more analogous to the Appalachians than to the shelf environments of Utah/Arizona, the sediment sources were apparently not as homogeneous as in the Appalachian clastic wedges. For example, the north-south variation in the Jackforth Group in the Ouachitas has been attributed to the mixing of two different dispersal or fan systems (Hatcher *et al.*, 1989). This heterogeneity of source sediment may in part account for the higher SD for bulk silicate $\delta^{18}\text{O}$ of Ouachita Mountain sandstones.

One consequence of the $\delta^{18}\text{O}$ heterogeneity of source sediment in the Ouachita Mountains is that it may be difficult to distinguish changes in bulk silicate $\delta^{18}\text{O}$ that are the result of differences in temperature of diagenesis or degree of aqueous fluid-rock interaction. For example, two sandstones from the Jackforth Group in Arkansas have an average bulk silicate $\delta^{18}\text{O}$ of +15.7, whereas sandstones collected 50-70 kilometers farther west from the Jackforth Group in Oklahoma have an average bulk silicate $\delta^{18}\text{O}$ of +14.5. This difference in $\delta^{18}\text{O}$ of the sandstones of a single sedimentary formation of Lower Pennsylvanian age in the Ouachitas is in striking contrast to the sandstones of the Central Appalachians, which have remarkably similar bulk silicate $\delta^{18}\text{O}$ values over widely different geographic areas, and regardless of age. Within the same geographic area in the Ouachitas, sandstones of different formations also display different average bulk silicate $\delta^{18}\text{O}$ values. For example, along a 70-km-long, south-to-north traverse in eastern Oklahoma, two Blaylock Sandstone samples have an average bulk silicate $\delta^{18}\text{O}$ of +16.8, a sandstone of the Stanley Group has a bulk silicate $\delta^{18}\text{O}$ of +13.4, and two sandstones of the Jackforth Group have an average bulk silicate $\delta^{18}\text{O}$ of +14.5.

An attempt to surmount the above-described ambiguity can perhaps be made through a comparison of bulk silicate $\delta^{18}\text{O}$ values of shale-sandstone pairs in the Ouachita Mountains. Where a shale-sandstone pair is not directly available for comparison, the unpaired shale is compared with a nearby sandstone of the same formation. These types of comparisons will indicate whether significant correlations exist between the differences in bulk silicate $\delta^{18}\text{O}$ values of shale-sandstone pairs and other independent indicators of thermal maturity in the Ouachita Mountains. First, however, a brief explanation of indicators of thermal maturity in the Ouachita Mountains will be presented.

6.3 Indicators of thermal maturity in the Ouachita Mountains

Houseknecht and Matthews (1985) studied the thermal maturity of Lower Paleozoic and Carboniferous strata in the Ouachita Mountains. They found that in the western two-thirds of the Ouachita Mountains, thermal maturity contours generally parallel structural grain. The major influences on thermal maturation were interpreted to be the depths of sedimentary and tectonic burial.

Houseknecht and Matthews (1985) used vitrinite reflectance as an indicator of thermal maturity. This technique is commonly used in the coal industry to estimate the degree of metamorphism of coal. Houseknecht and Matthews (1985) concentrated organic matter from shales by dissolving shale samples in hydrochloric acid followed by hydrofluoric acid. They mounted the insoluble residues on glass slides, which were then polished. Vitrinite reflectance was measured in oil using a photometer system calibrated with glass standards.

Vitrinite reflectance can be described by the Beer equation:

$$R = \frac{(n-n_o)^2 + n^2K^2}{(n+n_o)^2 + n^2K^2}$$

where n is the refractive index of vitrinite, n_o is the refractive index of the immersion oil, and K is the adsorption index of vitrinite. Refractive index is a function of atomic density. As organic metamorphism progresses, the degree of aromatization of organic matter increases and the index of refraction of vitrinite increases. The adsorption index (K) is a function of the number of delocalized electrons. This is because electron mobility facilitates the absorption of electromagnetic waves. As organic matter increases in aromatization the adsorption index also increases. As a result, vitrinite reflectance increases with degree of organic metamorphism (Teichmuller, 1987). The values of vitrinite reflectance range from less than one to greater than three in the Ouachita Mountains (Houseknecht and Matthews, 1985).

In a study using the samples from Houseknecht and Matthews (1985), Guthrie et al. (1986) showed that illite crystallinity was significantly related to vitrinite reflectance in the Ouachita Mountains. Two different measurements of illite crystallinity were correlated with vitrinite reflectance. Weaver's sharpness ratio is the ratio of the 001 illite-mica peak at 10.0 Angstroms on an X-ray diffraction pattern to the height of the peak at 10.5 Angstroms (Weaver et al., 1984). The sharpness ratio increases with increasing crystallinity and degree of metamorphism. The Kubler Index is the width at half-height of the 10.0 Angstrom illite-mica peak. The Kubler Index decreases with increasing crystallinity and degree of metamorphism (Kubler, 1968). Guthrie et al. (1986) suggest that illite crystallinity can be used in the absence of vitrinite to

quantitatively estimate thermal maturity.

Keller *et al.* (1985) made a scanning electron micrograph study of chert and novaculite textures in the Ouachita Mountains, and they found that mean apparent crystal diameter of quartz followed trends similar to those shown by the vitrinite reflectance and the illite crystallinity data of Houseknecht and Matthews (1985) and Guthrie *et al.* (1986). An area of significantly larger quartz crystals, indicating the most extensive recrystallization, was found near the south of the Broken Bow uplift, also in agreement with the studies cited above. Oxygen isotopic and petrographic studies of the Arkansas Novaculite in Arkansas and Oklahoma also support these broad regional trends in thermal maturity (Jones and Knauth, 1979).

In general, the above studies conclude that rocks in the Benton-Broken Bow uplifts have been subjected to temperatures from 100°C to 315°C. A study of conodont color alteration index indicates temperatures from 150°C to 250°C. The higher temperatures in these thermal maturation studies, such as those near the southern portion of the Broken Bow uplift, are indicative of lower greenschist-facies metamorphism (Hatcher *et al.*, 1989)

There is still some controversy concerning the tectonic history of the Ouachita Mountains (see Babaei and Veile, 1992). It is important to recognize, however, that all of the above cited studies of thermal maturity in the Ouachita Mountains are in general agreement as to the trends and degree of metamorphism in the Broken Bow-Benton Uplifts. The most detailed resolution of thermal variation is provided by the vitrinite reflectance data. Bulk silicate $\delta^{18}\text{O}$ from the present study will therefore be compared with this parameter in the discussion below. However, it should be noted that the

general geographic and stratigraphic features of the vitrinite reflectance data are also corroborated very well by illite crystallinity, chert crystallinity, conodont color alteration index, and chert oxygen isotope data.

6.4 Correlation of bulk silicate $\delta^{18}\text{O}$ with vitrinite reflectance

Figure 6.3 compares bulk silicate $\delta^{18}\text{O}$ of Stanley Group samples grouped by mean vitrinite reflectance as determined from the work of Guthrie *et al.* (1986) on the organic matter of shales sampled from surface outcrop in the study area. Reflectance increases with increasing temperature of organic metamorphism and is not reversible. Reflectance values are used in this study as a measure of comparative temperatures of diagenesis. Figure 6.4 shows the relationship between bulk silicate $\delta^{18}\text{O}$ of Stanley Group shales and mean vitrinite reflectance determined by Guthrie *et al.* (1986) on organic matter in surface outcrop shales at the same or a nearby location where each Stanley Group shale was sampled for $^{18}\text{O}/^{16}\text{O}$ analysis. Where necessary, vitrinite reflectance values were interpolated from the contour map of Guthrie *et al.* (1986). Even though there are only three Stanley Group shales, the correlation coefficient ($r=0.998$) is significant at the 0.05 probability level. Bulk silicate $\delta^{18}\text{O}$ becomes lighter with increasing mean vitrinite reflectance. This is the trend that would be expected if shale $\delta^{18}\text{O}$ was lowered with increasing temperature of diagenesis.

Figure 6.5 is a comparative histogram of $^{18}\text{O}/^{16}\text{O}$ data on Blaylock Sandstone and Jackforth Group samples by mean vitrinite reflectance. In the Jackforth Group, at mean vitrinite reflectance values of 1.7 and 0.9, the shales have higher bulk silicate $\delta^{18}\text{O}$ values than the sandstones. This is similar to the relationship found for the lower-grade Stanley Group shales and sandstones with mean vitrinite reflectance less than or equal to 2. The number of samples is limited, but each of the Stanley Group shales has a

Figure 6.3

Three comparative histograms showing the bulk silicate $\delta^{18}\text{O}$ values of several shale and sandstone samples from the Mississippian Stanley Formation of the Ouachita Mountains, separated according to zones of mean vitrinite reflectance at values of 2.0 (top), 1.9 (middle), and 1.5 (bottom), in order of decreasing temperature. The bottom histogram contains data on low-temperature sample 46, a black shale from western Arkansas. The other three samples were collected near one another from a higher-temperature diagenetic environment in eastern Oklahoma.

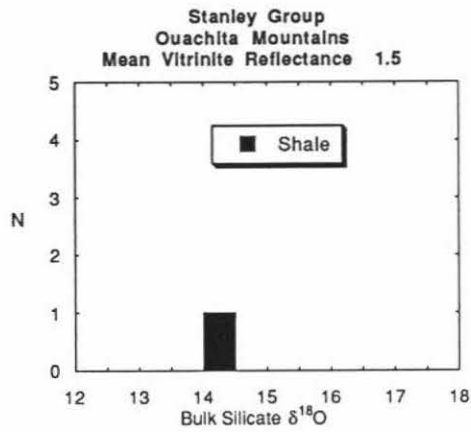
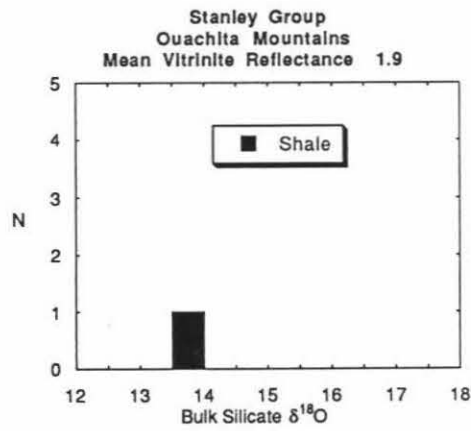
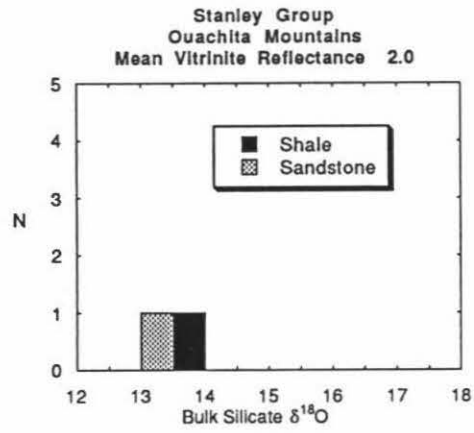
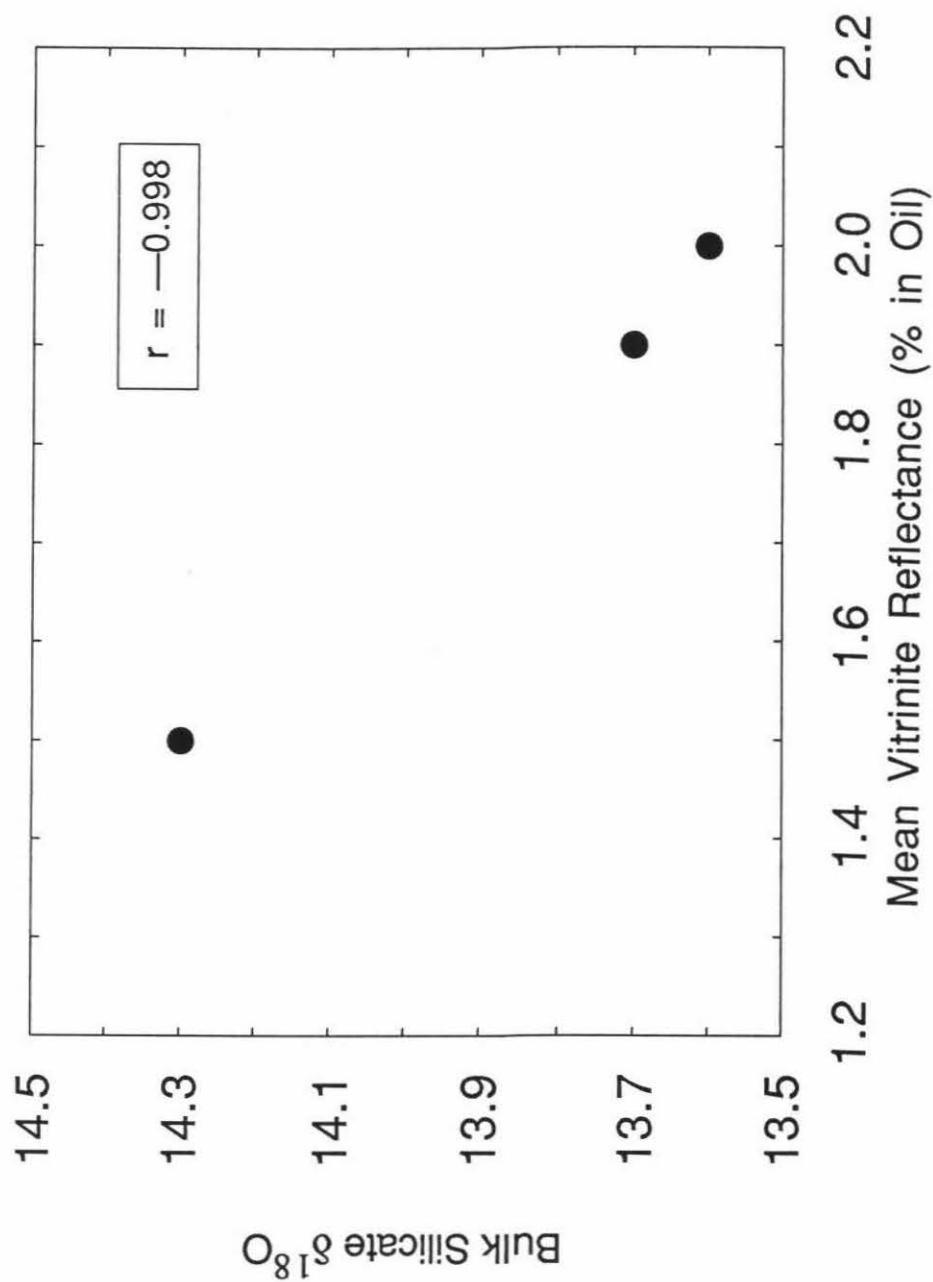


Figure 6.4

Plot of bulk silicate $\delta^{18}\text{O}$ versus the zone of mean vitrinite reflectance in which the sample was collected. These are the same three Stanley Group shales described in Figure 6.3.

Stanley Group Shales Ouachita Mountains



heavier bulk silicate $\delta^{18}\text{O}$ than the one Stanley Group sandstone that was analyzed.

Samples of the Blaylock Sandstone were taken from the southern region of the Broken Bow uplift where, according to thermal maturity indicators, temperatures of diagenesis were the highest in the area of this isotopic study (Figure 6.1). In this high-grade area, the bulk silicate $\delta^{18}\text{O}$ of the shale is lighter than the bulk silicate $\delta^{18}\text{O}$ of adjacent sandstones, in sharp contrast to the bulk silicate $\delta^{18}\text{O}$ values of shales and sandstones at lower mean vitrinite reflectance values. This situation would be expected if, as discussed in Chapter 5 for the Central Appalachians, the bulk silicate $\delta^{18}\text{O}$ values of shales were shifted to lower values to a greater degree than the bulk silicate $\delta^{18}\text{O}$ values of sandstones as a result of fluid-rock oxygen isotopic exchange during diagenesis.

From Figure 6.5 it can be seen that the bulk silicate $\delta^{18}\text{O}$ values of sandstones from areas with a mean vitrinite reflectance of 1.7 are heavier than the bulk silicate $\delta^{18}\text{O}$ values of sandstones from areas with a mean vitrinite reflectance of 0.9. Mean vitrinite reflectance is measured on organic matter in shales and is not directly applicable to sandstones. It is used here only as a general indicator of the thermal maturity of the entire stratigraphic section in each outcrop area under study. The Arkansas Jackforth Group samples are all from an area with mean vitrinite reflectance of 1.7, whereas the Oklahoma Jackforth Group samples are from an area with a mean vitrinite reflectance of 0.9. As discussed above, there is significant geographic variation in the source characteristics of the Jackforth Group, and this may have affected the bulk silicate $\delta^{18}\text{O}$.

Again, sample size is too small to establish the above results conclusively. However, one way is to look for shifts in bulk silicate $\delta^{18}\text{O}$ caused by diagenetic processes, while at the same time minimizing the differences in bulk silicate $\delta^{18}\text{O}$ due to variation

Figure 6.5

Three comparative histograms showing the bulk silicate $\delta^{18}\text{O}$ values of several shale and sandstones samples from the Ouachita Mountains, separated according to zones of mean vitrinite reflectance; (a) the Silurian Blaylock Sandstone of Oklahoma (MVR >3, samples 54, 55, and 56; top diagram); (b) the Lower Pennsylvanian Jackforth Group of western Arkansas (MVR = 1.7, samples 43, 44, and 45; middle diagram); and (c) the Jackforth Group of eastern Oklahoma (MVR = 0.9, samples 48, 49, and 50; bottom diagram). The diagenetic temperatures are presumed to decrease from the top diagram to the bottom diagram.

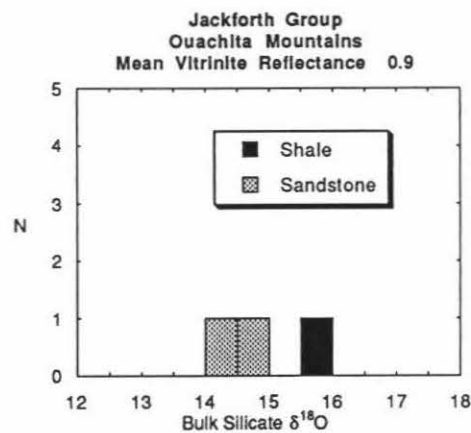
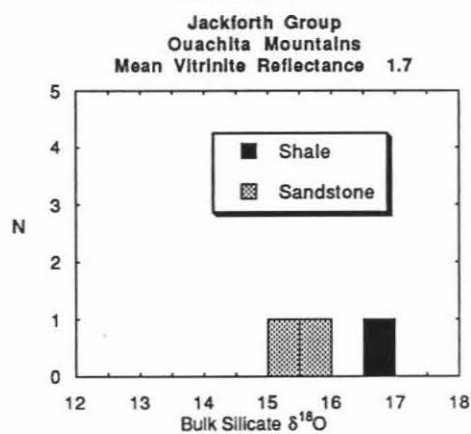
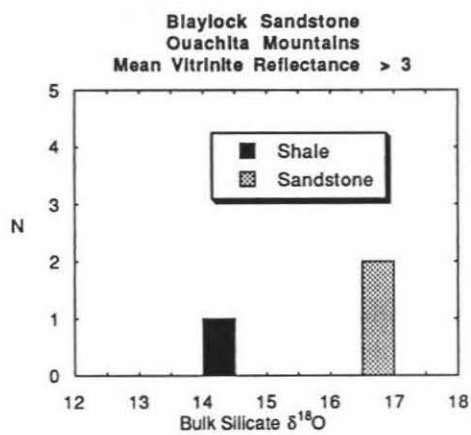
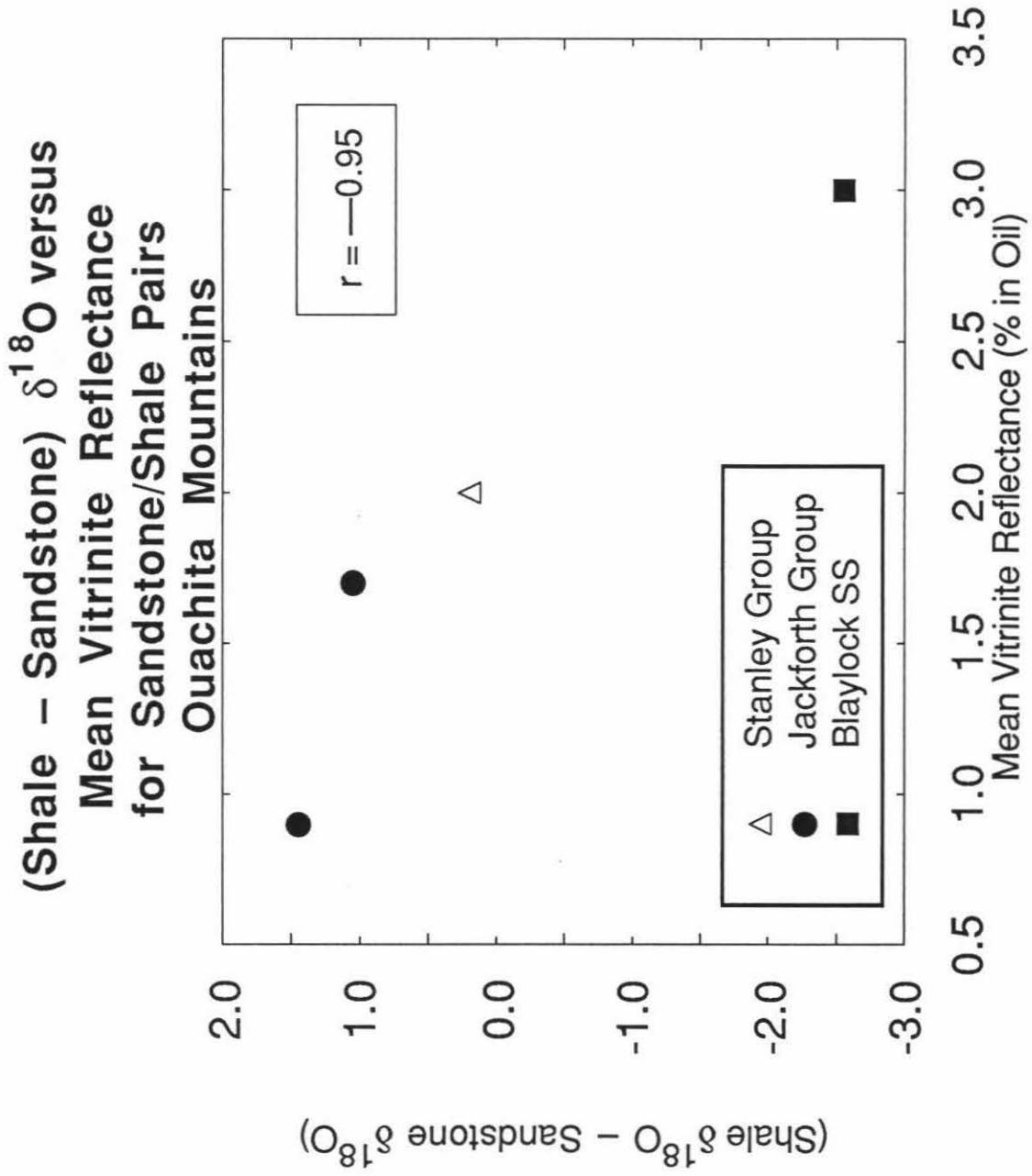


Figure 6.6

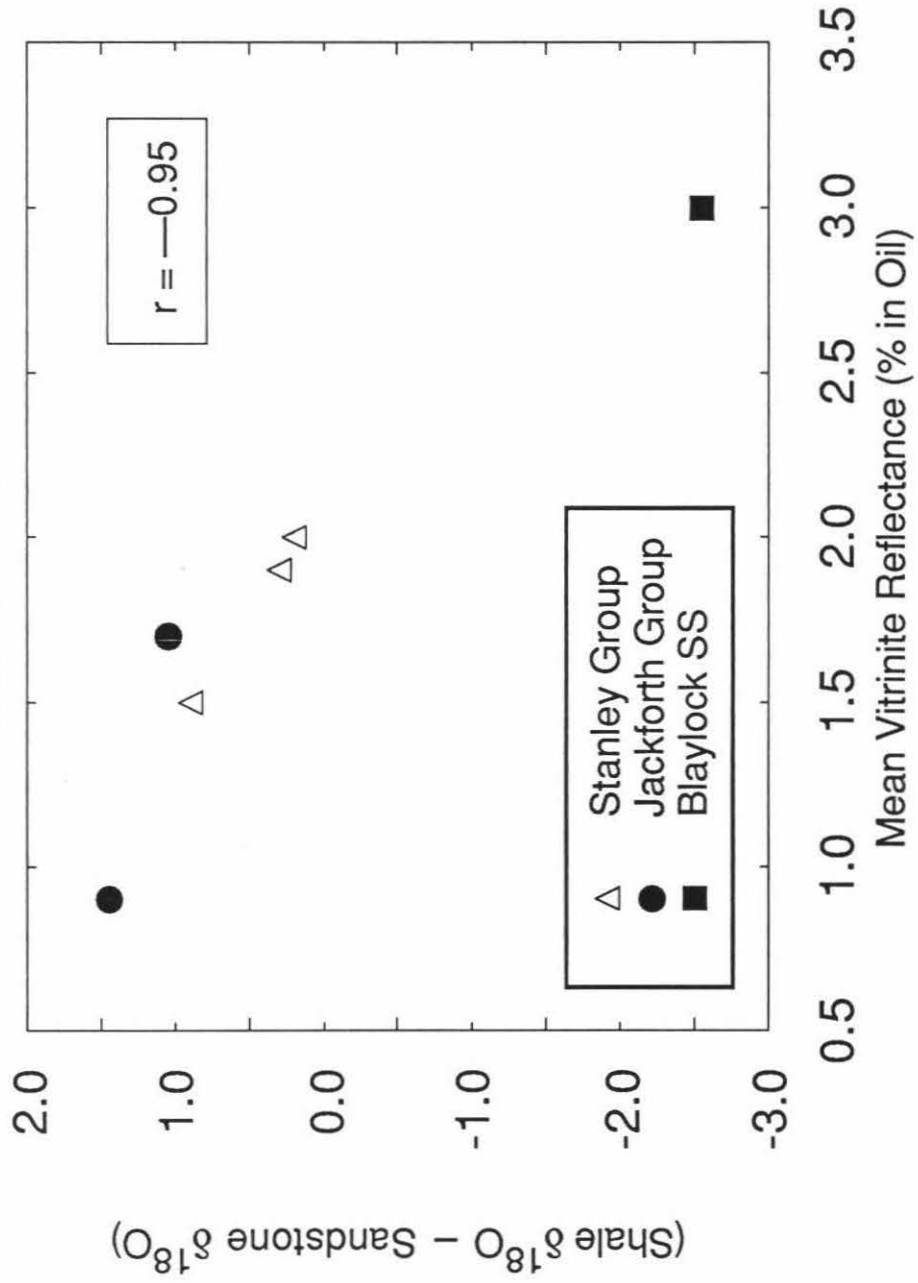
Plot of the difference in whole-rock $\delta^{18}\text{O}$ values between adjacent of shale and sandstone from the Ouachita Mountains versus zone of mean vitrinite reflectance. Positive numbers on the ordinate indicate the shale sample is higher in ^{18}O than the sandstone sample with which it is paired. The plotted shale sandstone "pair" from the Silurian Blaylock Sandstone of Oklahoma is actually three samples (2 sandstones and one shale), and it shows the highest diagenetic temperature (MVR = 3), and a dramatic reversal from the "normal" $\delta^{18}\text{O}$ relationship, with the two sandstones being 2.4 to 2.7 per mil higher than the "coexisting" shale sample from the same outcrop.

Figure 6.7

The same plot shown in Figure 6.6, with the addition of two more data-points from Mississippian Stanley Group. These three data points from the Stanley Group are based on three shale $\delta^{18}\text{O}$ analyses paired with a single sandstone $\delta^{18}\text{O}$ analysis (see text).



(Shale - Sandstone) $\delta^{18}\text{O}$
 versus Mean Vitrinite Reflectance
 Ouachita Mountains



in source material. This is best done by comparing the differences in bulk silicate $\delta^{18}\text{O}$ for sandstone-shale pairs from the same outcrop. A number of such sandstone-shale pairs were collected from a given outcrop for such studies. Figure 6.6 is a plot of differences in bulk silicate $\delta^{18}\text{O}$ for such sandstone-shale pairs against mean vitrinite reflectance for the same area of outcrop. Although there are only four data points, the correlation is surprisingly good. Figure 6.7 is the same as Figure 6.6, except that two data points from the Stanley Group samples have been added. This plot is complicated by the fact that bulk silicate $\delta^{18}\text{O}$ was determined on three Stanley Group shale samples, but only one Stanley Group sandstone. Nevertheless, if the $\delta^{18}\text{O}$ differences between all three Stanley Group shales and the one Stanley Group sandstone are plotted on the same diagram, the comparison agrees favorably with the differences for actual shale-sandstone pairs from outcrops of the other formations. The correlation in Figure 6.7 is significant at the 0.05 probability level.

6.5 Conclusions

This reconnaissance $^{18}\text{O}/^{16}\text{O}$ study of 14 samples of terrigenous sedimentary rocks from the central and southern Ouachita Mountains suggests that there is more inherent isotopic variation in these samples than in the Central Appalachian samples, perhaps in part as a result of a greater heterogeneity of source regions. However, some of the isotopic variation also seems to be clearly attributable to diagenetic effects analogous to the correlations with conodont index observed in the Central Appalachians. A significant ($P < 0.05$) correlation was found between mean vitrinite reflectance and the difference between shale and sandstone bulk silicate $\delta^{18}\text{O}$ for shale-sandstone pairs from three different formations, as well as for three shales from the Stanley Formation

compared with the one available sandstone analyzed from that formation. The difference in bulk silicate $\delta^{18}\text{O}$ between shale and sandstone decreases and then reverses with increasing mean vitrinite reflectance. This would be expected if bulk silicate $\delta^{18}\text{O}$ values of the fine-grained shales were shifted downward more than those of the sandstones with increasing temperature of diagenesis. The correlation of mean vitrinite reflectance with bulk silicate $\delta^{18}\text{O}$ differences between shale-sandstone pairs suggests that the Ouachita Mountains would be a promising area for future detailed oxygen isotope studies of diagenesis of sedimentary rocks, particularly in the light of all the earlier geochemical studies of diagenesis in this broad region.

CHAPTER 7

Oxygen Isotope Studies of Sedimentary and Metasedimentary Rocks of the Northern Appalachians**7.1 Description of the analyzed samples**

Fifty-seven samples of sedimentary and metasedimentary rocks of varying degrees of diagenesis and metamorphic grade were analyzed from the Northern Appalachian Mountains in eastern New York (4 samples), Vermont (35 samples), Quebec (3 samples), Nova Scotia (6 samples), and New Brunswick (9 samples). The general area sampled is shown in Figure 7.1, and the data are tabulated in Table 2.1 (samples 148 to 207). These Northern Appalachian samples were analyzed mainly in order to compare the data from unmetamorphosed sedimentary rocks from the Central Appalachians (Chapter 5) with a set of possibly analogous samples that have been subjected to metamorphism at a variety of metamorphic grades. This is obviously no more than a reconnaissance study, but it was felt that it might lay the groundwork for more detailed studies in the future.

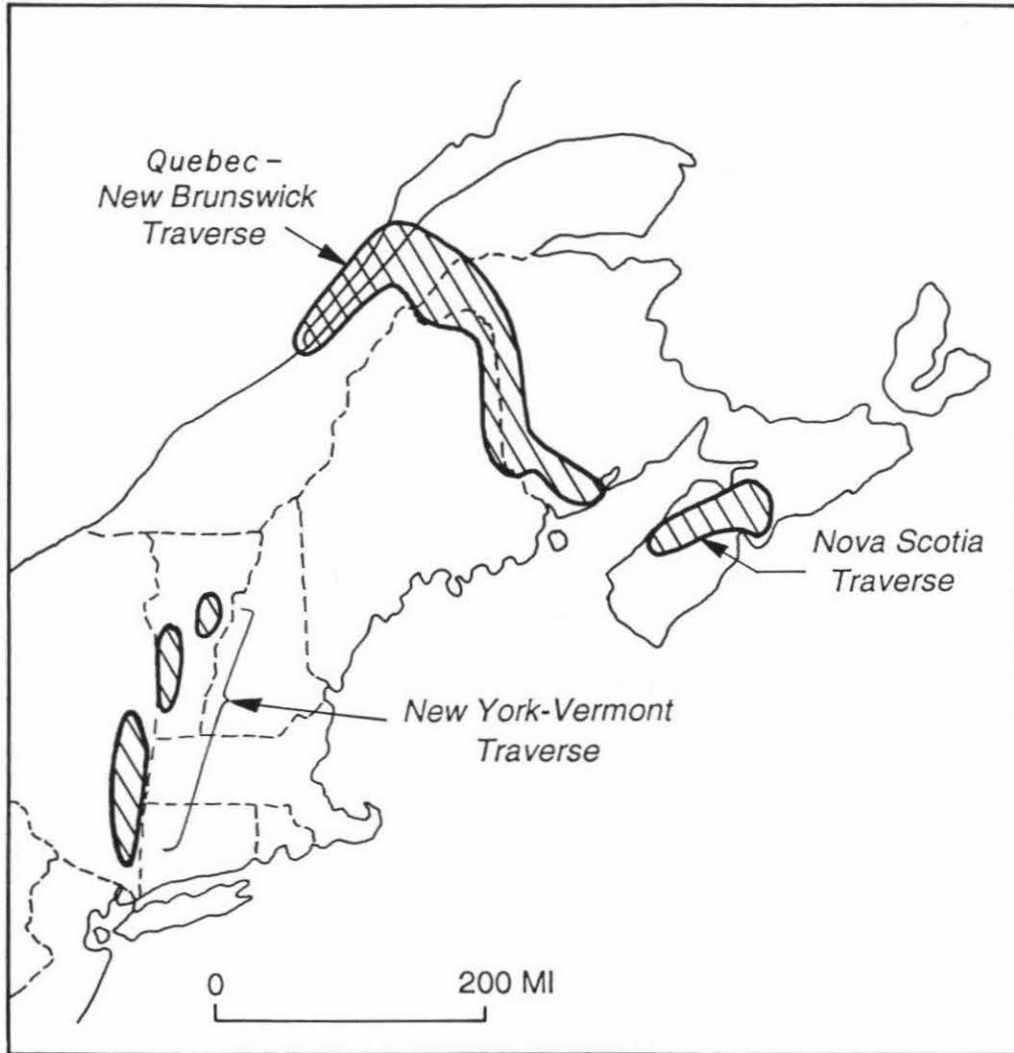
Most of the Vermont samples are strongly metamorphosed sandstones and shales that vary in metamorphic grade from chloritoid-kyanite to garnet to staurolite. One sample is of sillimanite grade, two are of chlorite grade and 7 are of biotite grade (Table 2.1). The 3 samples from Quebec are essentially unmetamorphosed shales. The 6 samples from Nova Scotia are low-grade metamorphosed phyllites (originally shales and siltstones?), mostly of biotite grade, but with one chlorite-grade sample. The 9 New Brunswick samples are made up of 4 essentially unmetamorphosed shales and calcilutites and 5 chlorite-grade slates and phyllites.

Almost half of the analyzed samples contain carbonate in amounts varying from 1 to 85% (Table 2.1), and for these samples the $\delta^{18}\text{O}$ (and $\delta^{13}\text{C}$) of both the coexisting

Figure 7.1

General locations of Northern Appalachian sample transects in this study (diagonal-striped areas).

NORTH APPALACHIAN SAMPLE AREAS



carbonate and the bulk silicate were analyzed. The carbonate-bearing samples from Vermont can be conveniently divided into two groups, those with more than 25% carbonate and those with less than 25% carbonate. The 9 carbonate-rich samples tend to be relatively ^{18}O rich with a mean $\delta^{18}\text{O}$ carbonate of +20.5, while the mean $\delta^{18}\text{O}$ carbonate of the 7 carbonate-poor samples (excluding Vt55, see below) is 2.6 per mil lower at +17.9. The mean $\delta^{13}\text{C}$ values of the two groups are not significantly different, -2.3 versus -3.0, respectively. One of the Vermont samples (Vt55) is somewhat peculiar, with a $\delta^{13}\text{C} = -8.8$ and a $\delta^{18}\text{O} = +13.2$. If Vt55 had been included with the above groupings, it would have lowered the mean $\delta^{18}\text{O}$ of the carbonate-poor samples from +17.9 to +17.3 and the mean $\delta^{13}\text{C}$ from -3.0 to -3.7.

The carbonate-bearing samples from Quebec and New Brunswick are of much lower grade than the Vermont samples and show no particular relationship between $\delta^{18}\text{O}$ and per cent carbonate. The $\delta^{18}\text{O}$ values of the 3 essentially unmetamorphosed Quebec samples vary from +18.1 to +23.3, whereas 5 of the samples from New Brunswick vary from +19.1 to +22.0; most of these samples have $\delta^{13}\text{C} = -2.8$ to +0.8. None of the above isotope values are particularly unusual for such relatively low-grade or unmetamorphosed samples. However, the $\delta^{13}\text{C}$ values do tend to be somewhat higher than in the Vermont samples. Two samples from this group of Canadian samples are unique: phyllite sample 19Q has a very low $\delta^{13}\text{C} = -8.9$, and sample 32NB-a has a very low carbonate $\delta^{18}\text{O} = +9.5$.

The oxygen isotopic difference, or fractionation, between the coexisting carbonate and the coexisting bulk silicate of these samples is of some interest. At equilibrium at high temperatures those two $\delta^{18}\text{O}$ values should be very similar to one another, with the

Figure 7.2

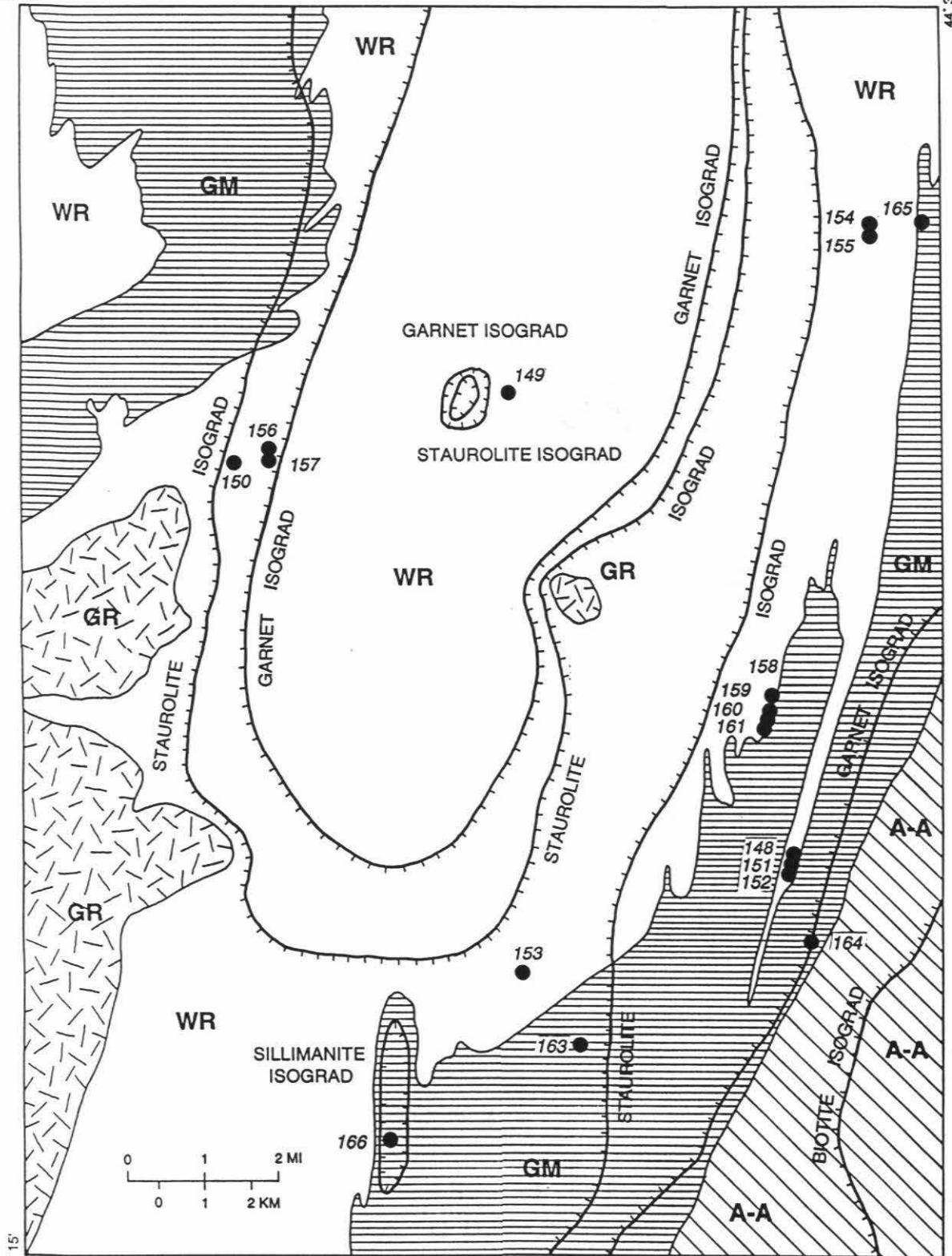
Simplified geologic map of the St. Johnsbury Quadrangle, Vermont, modified after Hall (1959), showing sample locations studied in this work, and metamorphic isograds based on pelitic mineral assemblages. The isograds are hatchured on the high-grade side. The staurolite isograd delineates a high-grade staurolite-kyanite zone (roughly equivalent to the calc-silicate diopside zone of Ferry, 1992) that wraps around the granitic pluton and along the eastern outcrops of the Waits River formation. G is the Gile Mountain Formation. WR is the Waits River Formation. A-A is undifferentiated Ammonoosuc Volcanics, Meetinghouse Slate, and Albee Formation. GR is the Knox Mountain granitic pluton.

Figure 7.3

Two comparative histograms showing bulk silicate $\delta^{18}\text{O}$ values for Northern Appalachian samples analyzed in this study, excluding two calcilutite samples. The top histogram is for Northern Appalachian carbonate facies. The bottom histogram is for Northern Appalachian terrigenous facies. S.D. is standard deviation. S.E.M. is standard error of the mean. N is the number of samples. Statistics calculated after Fisher *et al.* (1970).

72° 15'

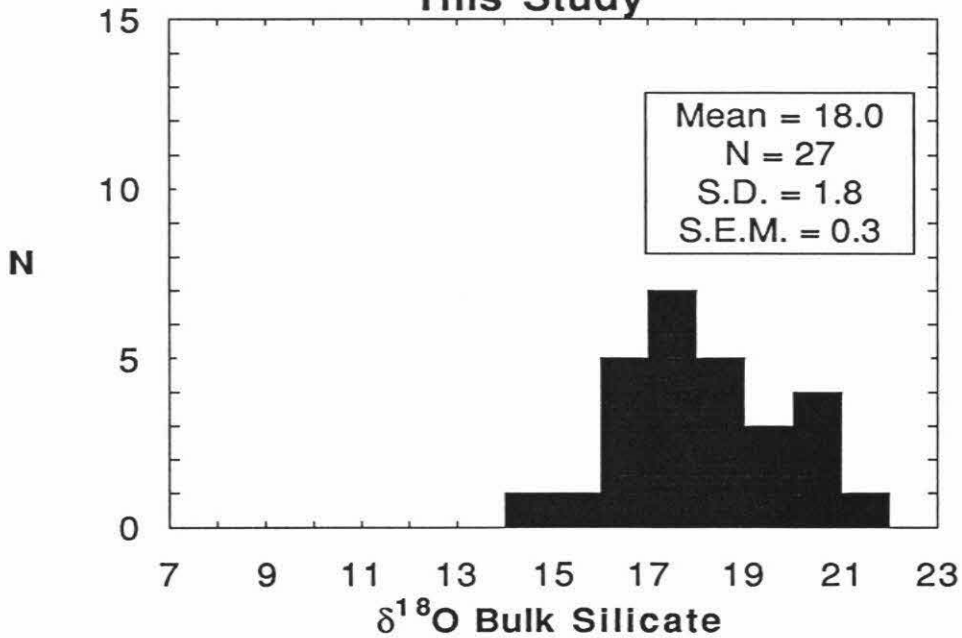
44° 30'



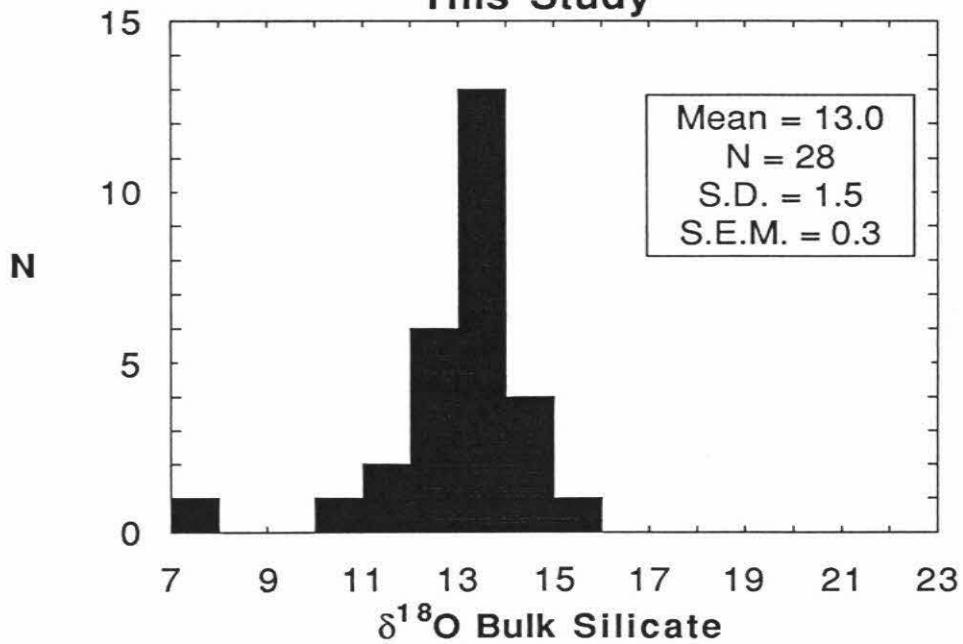
44° 15'

72° 00'

**All Northern Appalachian
Carbonate Facies Rocks:
This Study**



**All Northern Appalachian
Terrigenous Facies Rocks:
This Study**



carbonate generally being lower in ^{18}O than the coexisting bulk silicate in the case of quartz-rich samples and the reverse being true of quartz-free or quartz-poor samples. In most of the analyzed samples these measured fractionations clearly do not represent isotopic equilibrium in the mineral assemblages at the peak temperature of metamorphism or diagenesis. For example, in the Vermont samples these fractionations range from +3.6 per mil to -1.2 per mil (with the bulk silicate $\delta^{18}\text{O}$ subtracted from the carbonate $\delta^{18}\text{O}$); 11 samples show positive values and 6 show negative values. There is a weak correlation with per cent carbonate; all but one of the negative fractionations are for carbonate-poor samples, and most of the positive fractionations are from the carbonate-rich samples. Similar ranges of values are observed for 7 of the Canadian samples, from +2.9 to -0.2 per mil. However, two of the Canadian samples are peculiar, sample 16Q with a very unusual fractionation of +7.1 per mil, and sample 32NM-a with a fractionation of -3.0 per mil (this sample was already singled out above for having such a low $\delta^{18}\text{O}$ carbonate value).

7.2 Overview of bulk silicate $\delta^{18}\text{O}$ of carbonate- and terrigenous-facies rocks

Fifty-seven samples of sedimentary and metasedimentary rocks from the Northern Appalachians were analyzed for bulk silicate $\delta^{18}\text{O}$ (Table 2.1). The general locations of the sample traverses are shown in Figure 7.1 and the detailed locations of the samples from the St. Johnsbury Quadrangle in Vermont are shown in Figure 7.2. Rocks from carbonate-bearing formations such as the Waits River Formation in eastern Vermont (carbonate facies) have a mean bulk silicate $\delta^{18}\text{O}$ of +18.0 (27 samples). The 28 samples from formations containing dominantly detrital material rather than carbonate (terrigenous facies) have a mean bulk silicate $\delta^{18}\text{O}$ of +13.0 (Figure 7.3). The

terrigenous-facies samples show a strong peak in the histogram at $\delta^{18}\text{O} = +12$ to $+14$, whereas the carbonate-facies rocks show a much less well defined peak at bulk silicate $\delta^{18}\text{O} = +16$ to $+21$. There is very little overlap in $\delta^{18}\text{O}$ of the two groups of samples on Figure 7.3.

In Figure 7.4 the analyzed samples from the carbonate facies and the terrigenous facies are further delineated by metamorphic grade. There is a trend toward lighter bulk silicate $\delta^{18}\text{O}$ with increasing metamorphic grade for the terrigenous facies. Isotopic trends for the carbonate-facies rocks with metamorphic grade are not as apparent, but there is no doubt that the bulk silicate $\delta^{18}\text{O}$ values of the carbonate-facies metamorphic rocks are higher than the terrigenous-facies rocks at all metamorphic grades (Figure 7.4).

Figure 7.5 compares the bulk silicate $\delta^{18}\text{O}$ values of the unmetamorphosed terrigenous sedimentary rocks from the Central Appalachians with the $\delta^{18}\text{O}$ values of analogous metamorphosed samples from the Northern Appalachians. The two analyzed limestones (calcilutites) are excluded from this compilation. The 6 samples in Table 2.1 that contain more than 50% carbonate were also omitted from this graph (samples 150, 158, 161, 162, 167 and 172), even though plotting them would in no way change any of the relationships on Figure 7.5. The bulk silicate $\delta^{18}\text{O}$ values of these 6 samples range from $+17.4$ to $+18.5$ (garnet zone) and $+18.1$ to $+20.4$ (biotite zone), so plotting these data points on Figure 7.5 would in fact strengthen the observation that the carbonate-facies rocks have distinctly higher bulk silicate $\delta^{18}\text{O}$ values than the terrigenous-facies values at all metamorphic grades. However, it was felt that it would be unfair to plot such samples because none of the unmetamorphosed samples plotted on the left side of the diagram are from such carbonate-rich environments (the single calcilutite analyzed

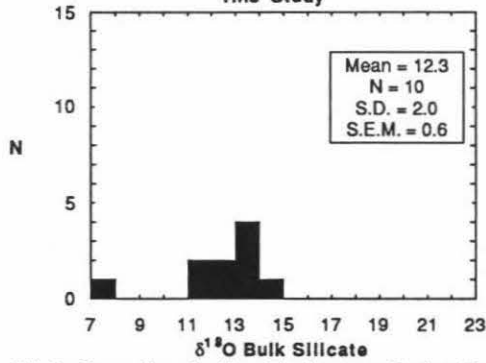
Figure 7.4

Eight comparative histograms showing bulk silicate $\delta^{18}\text{O}$ values of various metamorphic grades of terrigenous-facies and carbonate-facies sedimentary rocks of the Northern Appalachians analyzed in this study. The plotted terrigenous-facies and carbonate-facies categories (left-hand and right-hand columns, respectively) include: (a) garnet grade and higher; (b) biotite grade; (c) chlorite grade, and (d) high-grade diagenesis (non-metamorphic).

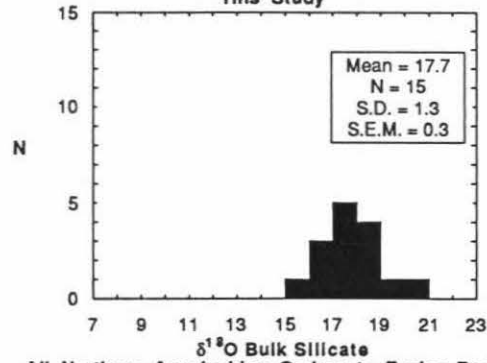
Figure 7.5

Bulk silicate $\delta^{18}\text{O}$ versus metamorphic grade for Appalachian sedimentary and metasedimentary rocks analyzed in this study. Unmetamorphosed Central Appalachian sedimentary samples (open diamonds) are included on the left for comparison with the metamorphic rocks. Open circles are terrigenous-facies metasedimentary rocks. Filled diamonds are carbonate-facies metasedimentary rocks. Plus signs in each box represent the average of the $\delta^{18}\text{O}$ values enclosed in that box. Dia is samples affected only by diagenesis. Ch is chlorite grade. Bi is biotite grade. $\geq G$ is garnet grade and higher. Samples containing more than 50 per cent carbonate have been omitted from this graph (see text).

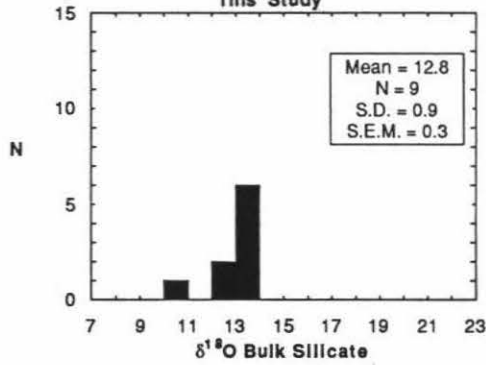
All Northern Appalachian Terrigenous Facies:
Garnet Grade and Higher Samples
This Study



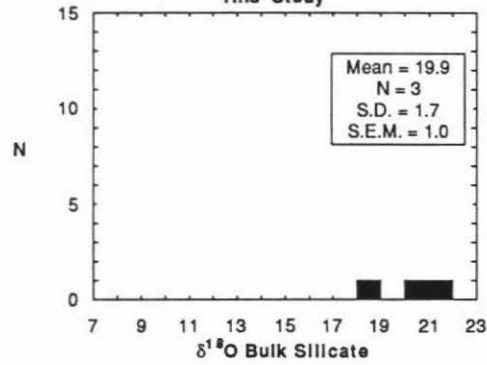
All Northern Appalachian Carbonate Facies Rocks:
Garnet Grade and Higher
This Study



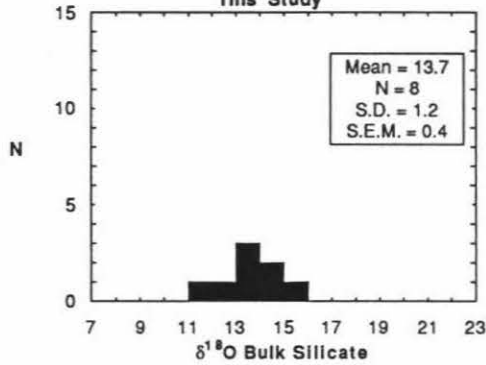
All Northern Appalachian Terrigenous Facies Rocks:
Biotite Grade Samples
This Study



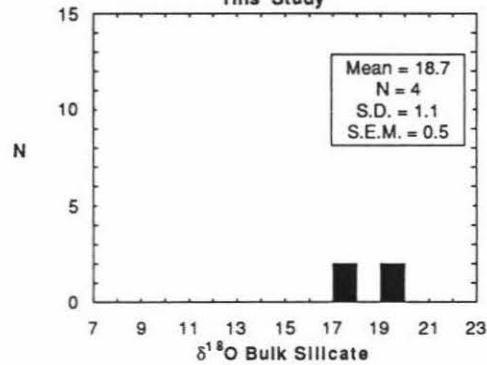
All Northern Appalachian Carbonate Facies Rocks:
Biotite Grade Samples
This Study



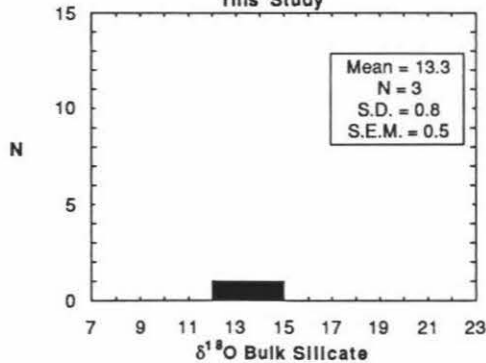
All Appalachian Terrigenous Facies Rocks
Chlorite Grade Samples:
This Study



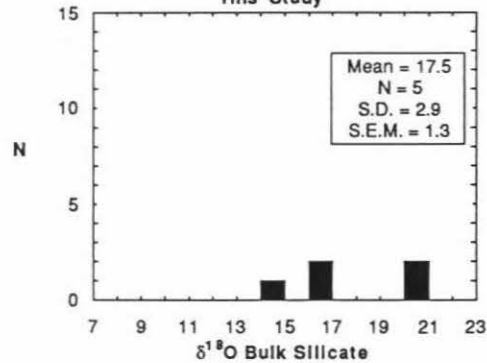
All Northern Appalachian Carbonate Facies Rocks:
Chlorite Grade Samples
This Study



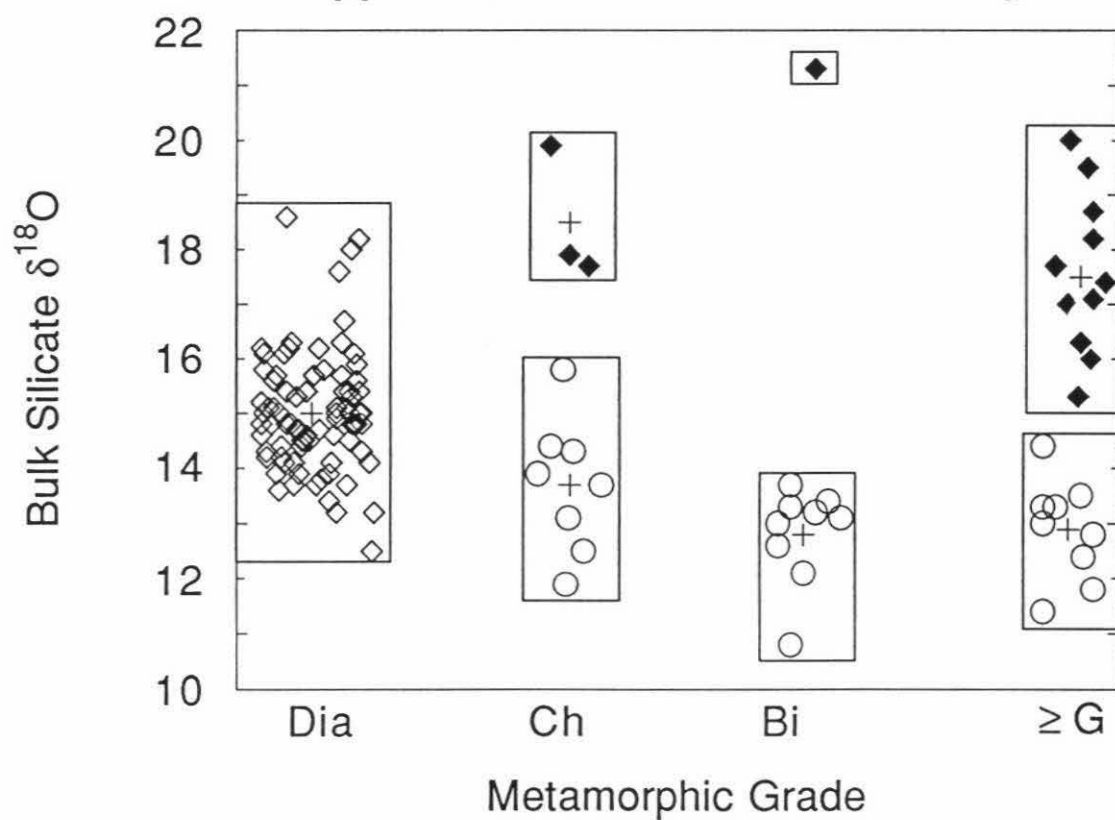
All Northern Appalachian Terrigenous Facies Rocks:
High Grade Diagenesis Samples
This Study



All Northern Appalachian Carbonate Facies Rocks:
Diagenetic Samples
This Study



**Bulk Silicate $\delta^{18}\text{O}$ vs.
Metamorphic Grade:
Appalachian Rocks in this Study**



from the central Appalachians is excluded from that data set).

On Figure 7.5, terrigenous samples show a trend toward decreasing bulk silicate $\delta^{18}\text{O}$ with increasing metamorphic grade. The trend of the carbonate-bearing facies is less clear-cut, but the means for the carbonate-bearing facies rocks at all metamorphic grades are distinctly higher than the mean $\delta^{18}\text{O}$ values of the Central Appalachian sedimentary rocks. The limited sample size at lower grades makes it difficult to know if there is an initial trend toward heavier bulk silicate $\delta^{18}\text{O}$ followed by a decrease in bulk silicate $\delta^{18}\text{O}$ at the higher grades. What is clear is that the bulk silicate $\delta^{18}\text{O}$ values of the highest-grade, carbonate-facies metamorphic rocks are an average of 2.5 per mil heavier than the mean bulk silicate $\delta^{18}\text{O}$ value of the Central Appalachian sedimentary rocks. Also, the mean bulk silicate $\delta^{18}\text{O}$ values of the highest-grade, terrigenous-facies metamorphic rocks are about 2 per mil lighter than unmetamorphosed Central Appalachian sedimentary samples. This indicates that there is an average difference of 4.5 per mil between the highest-grade calcareous-facies and terrigenous-facies metasedimentary rocks, and that this difference is essentially independent of grade of metamorphism.

What process is responsible for these differences in bulk silicate $\delta^{18}\text{O}$ in these different kinds of metamorphic rocks? Interaction with large volumes of a pervasive H_2O -rich fluid at progressively higher temperatures would produce the lowering of bulk silicate $\delta^{18}\text{O}$ with increasing metamorphic grade that is observed for the terrigenous facies. This process has been invoked by many workers over the years as an explanation of a general decrease in whole-rock $\delta^{18}\text{O}$ of metasediments with increasing metamorphic grade (*e.g.*, Garlick and Epstein, 1967). However, it has never been adequately

quantified as a major geochemical process.

Figure 7.6 and Figure 7.7 represent two separate comparisons of bulk silicate $\delta^{18}\text{O}$ with increasing metamorphic grade for terrigenous-facies metasedimentary rocks from the Northern Appalachians in this study and from similar studies in the Pyrenees by Wickham and Taylor (1985); both data sets are compared to the data obtained in the present study on unmetamorphosed sedimentary rocks from the Central Appalachians. The Pyrenees data set is just one of many such examples that could be taken from previous work in the literature, but it is one of the better examples of its type. Studies by Wickham and Taylor (1985), Wickham and Taylor (1987), Bickel *et al.* (1988), and McCaig *et al.* (1990) have demonstrated that the bulk silicate $\delta^{18}\text{O}$ values of metasedimentary rocks in the Trois Seigneurs Massif, Pyrenees, France were lowered by massive fluid infiltration during regional metamorphism.

The low-grade metasedimentary rocks analyzed by Wickham and Taylor (1985) are similar in general characteristics and in bulk silicate $\delta^{18}\text{O}$ to the Central Appalachian geosynclinal sediments. It is reasonable to infer that sediments similar in bulk silicate $\delta^{18}\text{O}$ to those of the Central Appalachians were the metamorphic precursors to the metasedimentary rocks in both the Pyrenees and the Northern Appalachians, implying that in both areas there was a distinct decrease in bulk silicate $\delta^{18}\text{O}$ with increasing metamorphic grade, at least up to and including the biotite zone. At higher metamorphic grades there was apparently very little further shift in whole-rock $\delta^{18}\text{O}$ in either the Northern Appalachians or the Pyrenees. Note that two phyllites from Maryland in the Central Appalachians mentioned in Chapter 5 (samples 118 and 119 with $\delta^{18}\text{O} = +11.9$ and $+13.1$) could be added to the chlorite-zone box in Figure 7.6 without changing its

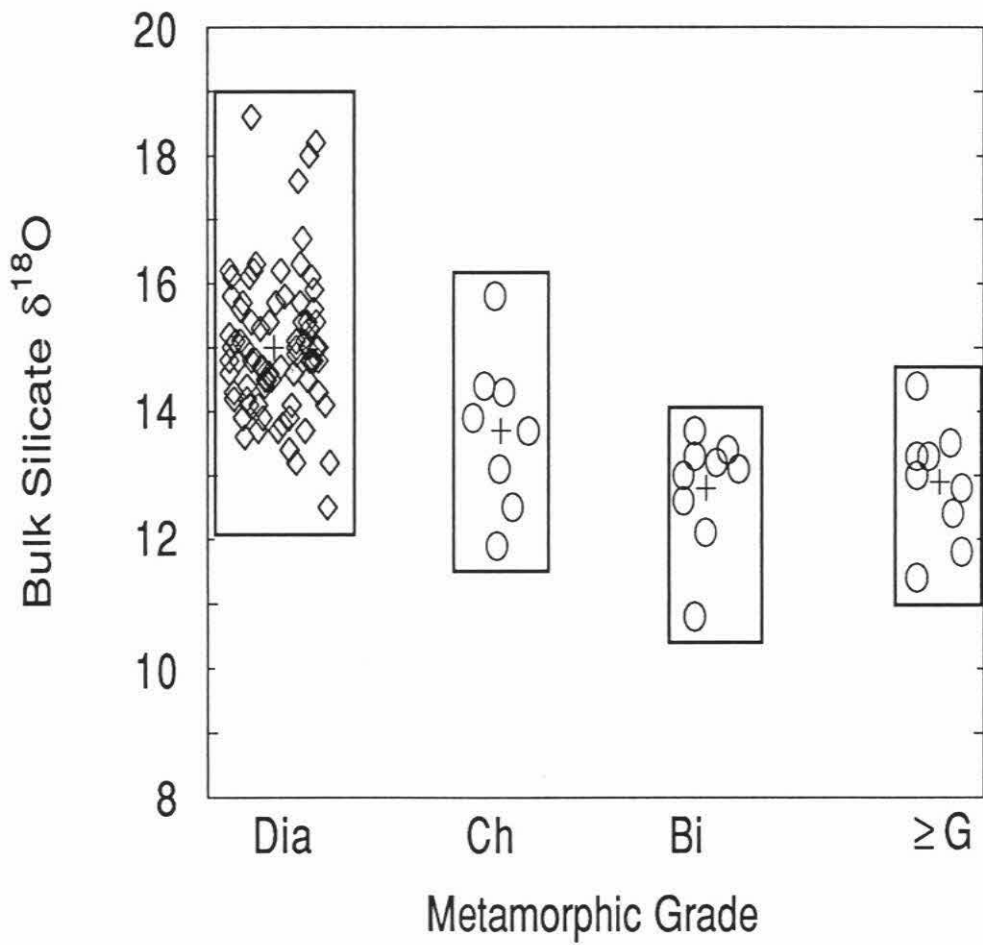
Figure 7.6

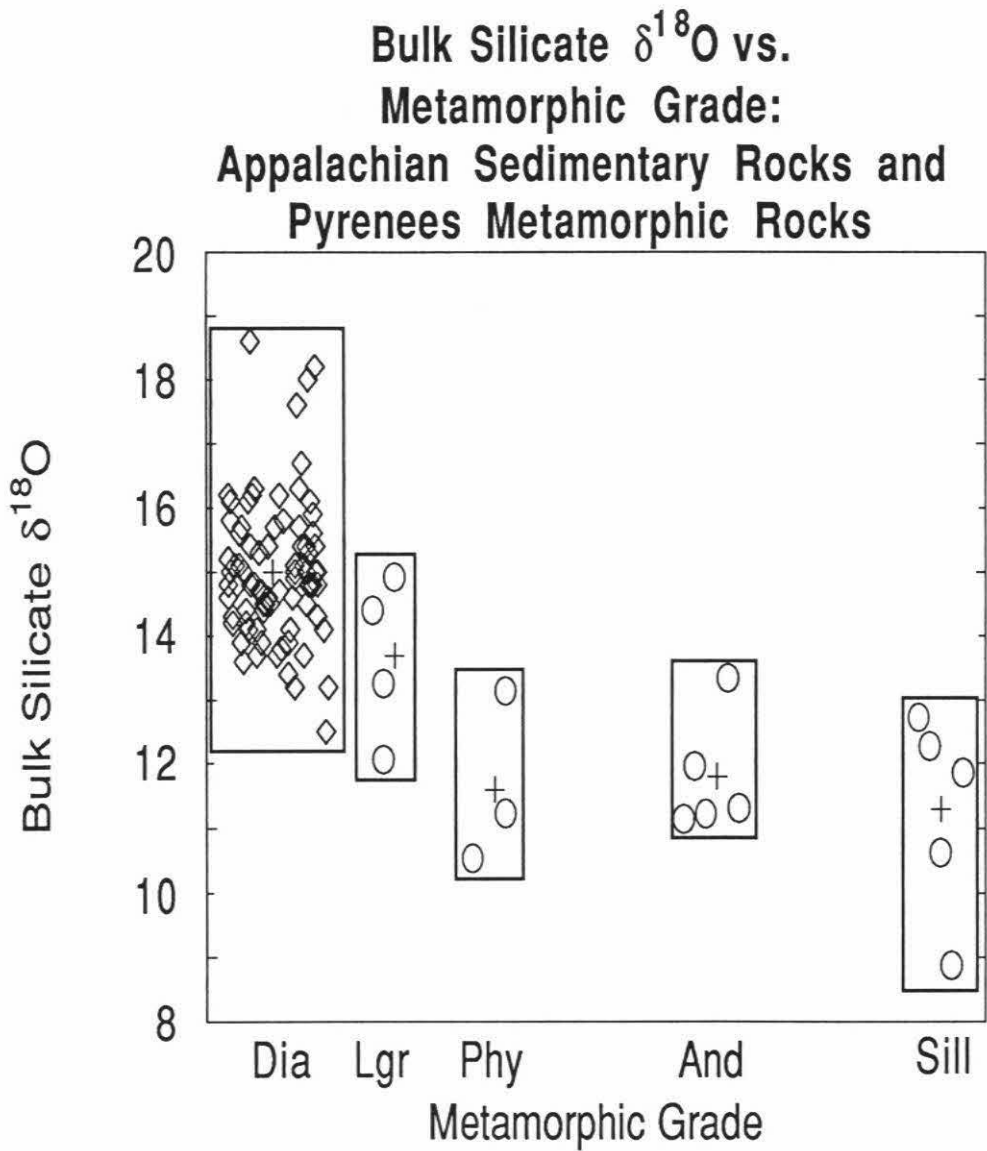
Bulk silicate $\delta^{18}\text{O}$ of terrigenous-facies sedimentary rocks versus metamorphic grade for samples analyzed in this study. Symbols are the same as for Figure 7.5. These are the same data shown in figure 7.5, except that the carbonate-facies data-points have been omitted.

Figure 7.7

Bulk silicate $\delta^{18}\text{O}$ versus metamorphic grade for metasedimentary rocks from the Trois Seigneurs Massif in the Pyrenees analyzed by Wickham and Taylor (1985). Symbols are the same as Figure 7.5. Lgr is low grade metasediments. Phy is phyllites. And represents all samples between the Andalusite-In Isograd and the Sillimanite-In Isograd. Sill represents all samples between the Sillimanite-In Isograd and the zone of anatexis where melting begins. Data from Central Appalachian geosynclinal sedimentary rocks from this work are included for comparison (open diamonds).

**Bulk Silicate $\delta^{18}\text{O}$ vs.
Metamorphic Grade:
Appalachian Rocks in this Study**





dimensions. If we use the Central Appalachian data set as a best estimate of the $\delta^{18}\text{O}$ of the sedimentary precursors for both the Pyrenees and the Appalachians, then a decrease in bulk silicate $\delta^{18}\text{O}$ during metamorphism of at least 2 per mil and 2.5 per mil is indicated for the Northern and Central Appalachians, respectively; a decrease of about 3.5 per mil is inferred for the Pyrenees samples.

Note that the Pyrenees metasedimentary rocks contain less than 5% interbedded carbonate layers (Wickham and Taylor, 1985), and the two chlorite-zone phyllites from Maryland are also from an essentially carbonate-free environment. Interbedded carbonates are also rare in the Gile Mountain Formation (Figure 7.2) and the other terrigenous-facies metamorphic rocks of the Northern Appalachians. This rarity or absence of interbedded sedimentary carbonates may help to explain why bulk silicate $\delta^{18}\text{O}$ decreases with increasing degree of metamorphism in such terrigenous-facies rocks. These isotopic data are in striking contrast to the data obtained for carbonate-rich metamorphic units such as the Waits River Formation of the Northern Appalachians, which show a distinctly higher bulk silicate $\delta^{18}\text{O}$ during regional metamorphism. It seems certain that this increase in $\delta^{18}\text{O}$ is due to the exchange of silicate oxygen with the immediately adjacent reservoir of isotopically heavy carbonate oxygen during metamorphism, mediated by the presence of an H_2O -rich or CO_2 -rich fluid. Limestones always start out with much higher $\delta^{18}\text{O}$ values (up to +29 to +30) than interbedded terrigenous sediments, and this original $\delta^{18}\text{O}$ difference is invariably lessened during diagenesis and metamorphism, with the carbonate $\delta^{18}\text{O}$ values typically ending up at about +16 to +24. By material-balance, some other materials must become ^{18}O -enriched, and it is plausible that in many instances these materials are the nearby

terrigenous sedimentary and metasedimentary rocks. Such an increase in bulk silicate $\delta^{18}\text{O}$ could not happen in the terrigenous-facies metamorphic environments, because in such cases there is no large adjacent reservoir of higher- ^{18}O carbonate rocks.

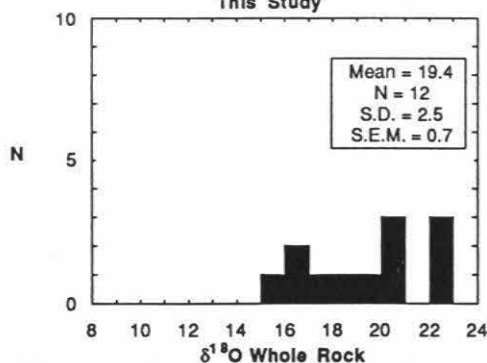
Figure 7.8 is a series of comparative histograms from the Northern Appalachian calcareous-facies sedimentary and metasedimentary rocks. The column of histograms on the right-hand side of the page is for garnet-grade and higher calcareous metasediments. The column of histograms on the left-hand side of the page is for biotite-grade and lower calcareous sediments and metasediments. The mean bulk silicate $\delta^{18}\text{O}$, the mean carbonate $\delta^{18}\text{O}$, and the mean whole-rock $\delta^{18}\text{O}$ for the garnet-grade and higher calcareous sediments are all consistently lower than the respective means for their biotite-grade and lower counterparts. These differences in mean $\delta^{18}\text{O}$ vary from 1.6 per mil (whole-rock) to 1.4 per mil (carbonate) to 0.9 per mil (bulk silicate). These data suggest that there has been a net loss of isotopically heavy oxygen from the higher-grade metasediments during the increase in metamorphic grade from the biotite and chlorite zones to the garnet zone.

The bottom row of Figure 7.8 compares the difference between the $\delta^{18}\text{O}$ value of the bulk silicate and the $\delta^{18}\text{O}$ of the coexisting carbonate fraction of each sample (bulk silicate value subtracted from carbonate value). The mean difference between the carbonate and silicate fractions for the garnet-grade and higher metasediments is +0.7 as compared with +2.3 for the biotite-grade and lower sediments. This represents a three-fold reduction of the difference between carbonate and silicate $\delta^{18}\text{O}$ values at the higher grades of metamorphism. This shift is compatible with the carbonate and silicate fractions of the metasediments more closely approaching isotopic equilibrium at the

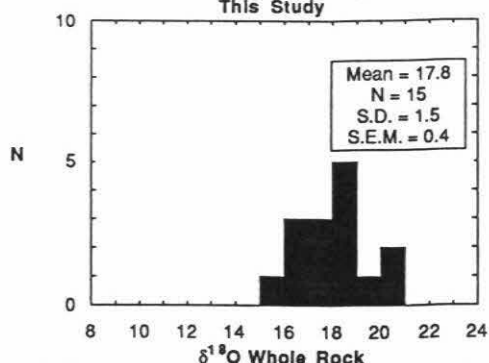
Figure 7.8

Eight comparative histograms showing oxygen isotopic compositions of carbonate-facies Northern Appalachian samples in this study. Samples metamorphosed at the garnet grade and higher are plotted in the right-hand column, and samples metamorphosed at the biotite grade and lower are plotted in the left-hand column. The plotted categories include: (a) whole rock $\delta^{18}\text{O}$; (b) carbonate $\delta^{18}\text{O}$; (c) bulk silicate $\delta^{18}\text{O}$; and (d) the difference between the $\delta^{18}\text{O}$ of the carbonate fraction of a sample and the $\delta^{18}\text{O}$ of the coexisting bulk silicate fraction of the same sample.

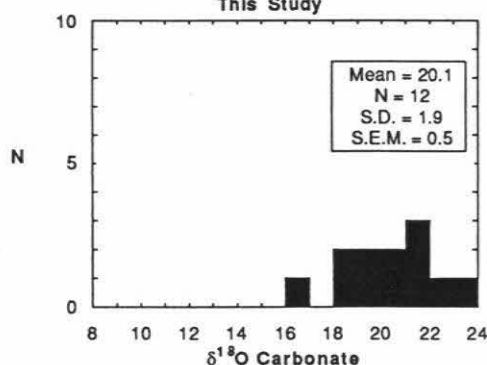
All Northern Appalachian Carbonate Facies Rocks:
Biotite Grade and Lower
This Study



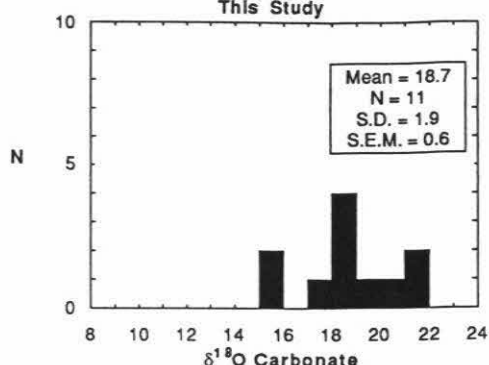
All Northern Appalachian Carbonate Facies Rocks:
Garnet Grade and Higher
This Study



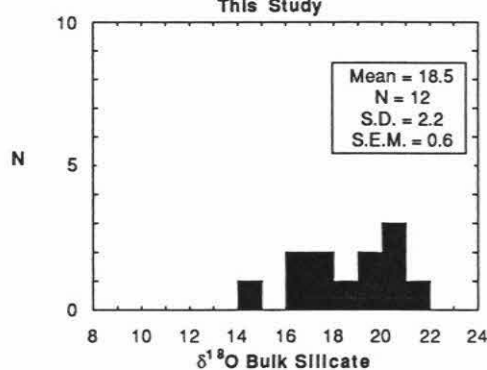
All Northern Appalachian Carbonate Facies Rocks:
Biotite Grade and Lower
This Study



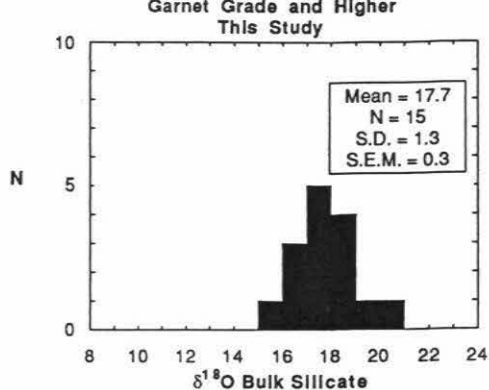
All Northern Appalachian Carbonate Facies Rocks:
Garnet Grade and Higher
This Study



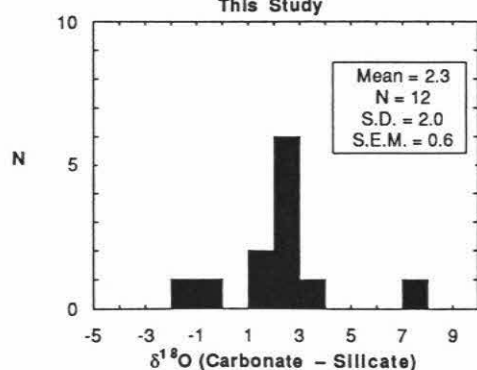
All Northern Appalachian Carbonate Facies Rocks:
Biotite Grade and Lower
This Study



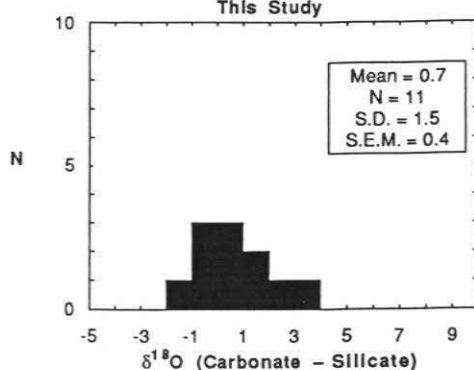
All Northern Appalachian Carbonate Facies Rocks:
Garnet Grade and Higher
This Study



All Northern Appalachian Carbonate Facies Rocks:
Biotite Grade and Lower
This Study



All Northern Appalachian Carbonate Facies Rocks:
Garnet Grade and Higher
This Study



higher grades of metamorphism in an open system, because, by analogy with the simpler systems feldspar-calcite or quartz-calcite, at higher temperatures a reduction in the difference between the equilibrium isotopic compositions of the bulk silicate and carbonate fractions would be expected.

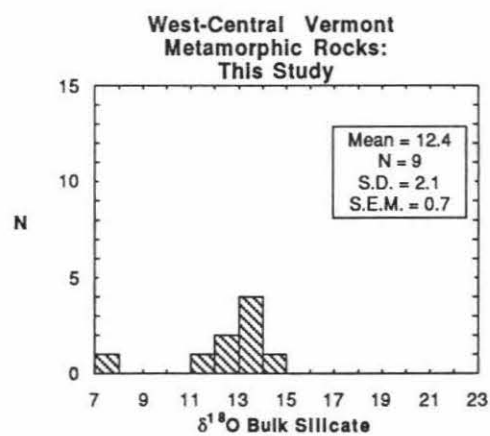
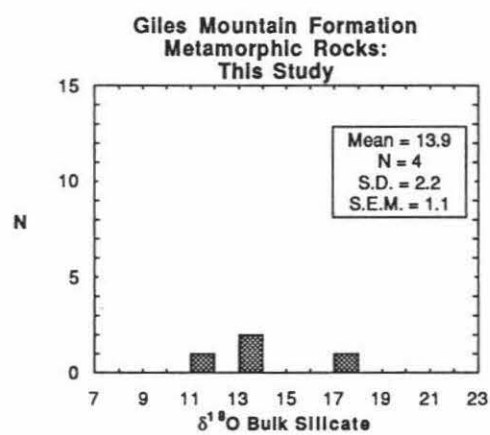
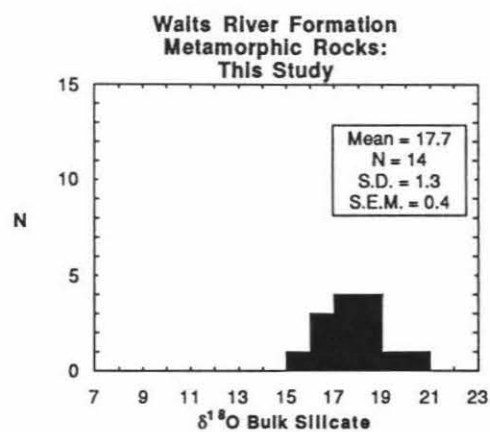
7.3 Oxygen isotope studies of metasedimentary rocks from the St. Johnsbury Quadrangle, Vermont

Eighteen samples of metasedimentary rocks from the St. Johnsbury Quadrangle and one sample from the adjacent Plainfield Quadrangle in east-central Vermont were analyzed for bulk silicate oxygen isotopic composition (Figure 7.9). Fourteen samples are from the Waits River Formation, which contains abundant carbonates and metamorphosed calcareous rocks (Hall, 1959). The Waits River Formation is composed of micaceous limestones and calcareous shales and their metamorphic equivalents. The thickness of individual beds is highly variable, but commonly about 10-100 cm. Regionally the proportion of carbonate rock varies from 50-80% in the vicinity of the St. Johnsbury Quadrangle to 30-50% to the west (Hatch 1988a). The Waits River Formation lies in sedimentary contact beneath the Gile Mountain Formation to the east (Fisher and Karabinos, 1980) and the Northfield Formation to the west. The contacts between the Northfield and Gile Mountain Formations and older Cambro-Ordovician rocks traditionally have been considered unconformities (Doll, 1961), but recent work suggests that they may be faults (Hatch, 1988a, 1988b).

The stratigraphic age of the Waits River Formation is a matter of debate. Doll (1961) concluded it was Devonian. Based on discovery of plant fossils in the Gile Mountain Formation, Hueber *et al.* (1990), assigned an unequivocal Devonian age to part

Figure 7.9

Three comparative histograms of bulk silicate $\delta^{18}\text{O}$ values determined on metasedimentary rocks in this study for: (a) Waits River Formation, St. Johnsbury Quadrangle, east-central Vermont; (b) Gile Mountain formation, St. Johnsbury Quadrangle, east-central Vermont; and (c) west-central Vermont samples (from the Lincoln Mountain Quadrangle).



of the formation, and concluded that field, paleontologic, and radiometric data are most consistent with a Silurian-early Devonian age for both the Waits River and Gile Mountain Formations.

The Waits River Formation was folded into recumbent folds and structural domes, intruded by synmetamorphic granitic plutons, and regionally metamorphosed during the Devonian Acadian Orogeny (Thompson *et al.*, 1968; Thompson and Norton, 1968; Osberg *et al.*, 1989). The Knox Mountain pluton, which crops out along the western edge of the map in Figure 7.2, lies along the axis of the Willoughby-Chester antiform (Strafford-Willoughby arch of Doll, 1961), which extends northward into Canada. This antiform is a regional structural feature about 200 km in length. With respect to minerals in pelitic schists (metamorphosed shales), the Waits River Formation was regionally metamorphosed to conditions corresponding to the biotite, garnet, and staurolite-kyanite zones (Figure 7.2). The axis of the antiform is coincident with a metamorphic high defined by the staurolite isograd and coincident with the Knox Mountain pluton. Garnet, staurolite, and kyanite porphyroblasts grow across foliation associated with the earliest recumbent folds. The peak of regional metamorphism occurred after the recumbent folding and was contemporaneous with or slightly pre-dated development of the domes and antiforms. Radiometric dates from hornblendes collected in and near the domes are 350-397 Ma (Spear and Harrison, 1989), and regional metamorphism is unequivocally Acadian in age.

Work by Ferry (1992) and Stern *et al.* (in press) shows evidence of a very large-scale metamorphic-hydrothermal system in this region. According to Ferry (1992), the lithostatic pressure (calculated from mineral equilibria) was fairly uniform in the area,

7 ± 1.5 kb. The calculated temperatures increase from $\sim 480^\circ\text{C}$ at the lowest grades in the area to $\sim 575^\circ\text{C}$ in the highest grade areas. Calculated X_{CO_2} of the equilibrium metamorphic fluid increases from <0.03 at the lowest grades to ~ 0.2 and finally to ~ 0.07 at the highest grades. Thus these metamorphic pore fluids were dominantly H_2O ($>80\text{-}90\%$) at all metamorphic grades. Time-integrated fluid fluxes calculated by Ferry (1992) increase with increasing metamorphic grade, from $1 \times 10^4 \text{ cm}^3/\text{cm}^2$ at low grades to 7×10^5 at the highest grades in the vicinity of the plutons. Ferry (1992) believes that at about 25 km depth aqueous fluid flowed subhorizontally perpendicular to the axis of the antiforms from their low-temperature flanks toward their hot axial regions, driving prograde decarbonation reactions as they went. According to Stern *et al.* (in press) and Ferry (1992), very large amounts of an isotopically light, H_2O -rich fluid moved from the noncalcareous formations to the east and west of the Waits River Formation into the cores of two large antiforms in the Waits River Formation. These authors also believe that the fluid was further focused around the granitic plutons that intrude the axes of these two antiforms, of which the Knox Mountain pluton (Figure 7.2) is the major example. The above conclusions are based on extensive petrologic work by Ferry (1992) on the metacarbonate rocks of the Waits River Formation and extensive carbon and oxygen isotope work by Stern *et al.* (in press) on the carbonate fraction of the Waits River Formation at a variety of metamorphic grades. Those authors did not analyze the $\delta^{18}\text{O}$ of any samples of the bulk silicate fraction of the Waits River Formation, however, so the present study has a great deal of pertinence to their conclusions.

In the discussion below, a calcareous rock is defined as one containing more than fifty per cent carbonate. The Waits River Formation samples have a mean bulk silicate

$\delta^{18}\text{O}$ of +17.7. Four samples from the noncalcareous Gile Mountain Formation were also analyzed. These samples have a mean bulk silicate $\delta^{18}\text{O}$ of +13.9. One sample from the Gile Mountain Formation (166) has a bulk silicate $\delta^{18}\text{O}$ of +17.0, but this sample is unique in that it was collected from the sillimanite zone close to the contact with the Waits River Formation. The location of this sample in a minor fold on the flank of the Willoughby-Chester antiform means that it is bounded on three sides by the Waits River Formation. It also lies closer to the zone of very high fluid flux mapped by Ferry (1992) than any other Gile Mountain sample in this work, and it can be readily inferred that this high temperature locality also represented a local high in fluid flux. Communication with high- ^{18}O fluid that circulated from the adjacent Waits River Formation was presumably responsible for the high bulk silicate $\delta^{18}\text{O}$ of this particular sample. When this high- ^{18}O sample is excluded, the mean bulk silicate $\delta^{18}\text{O}$ for the Gile Mountain Formation is only +12.7.

Three samples of the Waits River Formation were collected from the southeast part of the quadrangle at the contact with the Gile Mountain Formation; they are embedded in a very tight fold surrounded on three sides by the Gile Mountain Formation. The bulk silicate $\delta^{18}\text{O}$ values of these samples (148, 151, 152) are lower than the rest of the analyzed samples of the Waits River Formation, suggesting exchange with lower- ^{18}O fluid derived from the Gile Mountain Formation, the reverse of the situation outlined above. If these 3 light samples are excluded, the mean bulk silicate $\delta^{18}\text{O}$ for the Waits River Formation is +18.1, which is 5.4 per mil heavier than the mean bulk silicate $\delta^{18}\text{O}$ for the Gile Mountain Formation.

Figure 7.8 shows data from the present work indicating that there has been a net

loss of isotopically heavy oxygen from the higher-grade calcareous metasediments of the Waits River Formation with increasing metamorphic grade, as well as a decrease in the difference between the coexisting carbonate and the silicate $\delta^{18}\text{O}$ values in a single sample. In contrast to the work of Stern et al. (in press), who showed that the values of $\delta^{18}\text{O}$ carbonate at grades higher than the biotite grade in the same outcrop seldom showed more than a one per mil variation, several "outcrop pairs" of bulk silicate $\delta^{18}\text{O}$ values from samples collected from different parts of a single outcrop in this work typically show a 1.4 to 1.8 per mil variation, indicating either less thorough equilibration and homogenization of $^{18}\text{O}/^{16}\text{O}$ between the bulk silicate and the postulated metamorphic-hydrothermal fluid, or that the bulk silicate fraction is more heterogeneous than the carbonate fraction. Both possibilities probably have some validity.

Stern et al. (in press) analyzed 20 samples of carbonate from the Waits River Formation in the St. Johnsbury Quadrangle. They delineated a zone of ^{18}O depletion ($\delta^{18}\text{O} < +18$) around the margins of the Knox Mountain pluton (Figure 7.2), but elsewhere in the quadrangle their carbonate $\delta^{18}\text{O}$ values ranged from +18 to +21. Our 12 carbonate samples cover a similar range of $\delta^{18}\text{O}$, except for the aforementioned samples 151 and 152 from the tight fold in the southeast part of the quadrangle that are adjacent to, and surrounded by, the low- ^{18}O Gile Mountain Formation. Like the coexisting bulk silicate fraction mentioned above, the carbonate $\delta^{18}\text{O}$ values of these samples are strongly depleted in ^{18}O , with $\delta^{18}\text{O} = +15.8$ and $+15.6$, lower than any values reported by Stern et al. from this area. It seems clear that these Waits River carbonates, like their coexisting silicates, were depleted in ^{18}O because of their proximity to the low- ^{18}O fluids that circulated from the Gile Mountain Formation into the Waits

River Formation. Similar conclusions were reached by Stern *et al.* (in press) on carbonates analyzed from the western and eastern margins of the Waits River Formation farther south in Vermont, where this formation is in contact with the Gile Mountain Formation and other pelitic schists.

According to Stern *et al.* (in press), temperatures of metamorphism in the metacarbonate rocks in the St. Johnsbury Quadrangle ranged from 530°C to 575°C. According to the petrologic data of Ferry (1992), the Waits River Formation consists of mostly quartz and calcite. The equilibrium quartz-calcite fractionation factor is less than 1 per mil at 530°C to 575°C (Clayton and Kieffer, 1991), and at equilibrium $\delta^{18}\text{O}_{\text{quartz}} > \delta^{18}\text{O}_{\text{calcite}}$ at all temperatures. For many garnet grade and higher samples of the Waits River Formation $\delta^{18}\text{O}_{\text{carbonate}} > \delta^{18}\text{O}_{\text{bulk silicate}}$, which is impossible at equilibrium for such quartz-rich assemblages. Obviously, many of these samples did not retain the equilibrium isotopic signature that would be expected at the temperatures of peak metamorphism. Either equilibrium was never attained or there has been significant retrograde exchange of carbonate with an external fluid. These possibilities will be discussed further in the following section.

Bulk silicate $\delta^{18}\text{O}$ ranges from +16 to +20 in the garnet zone and higher grade Waits River Formation samples. Assuming the bulk silicate fraction was in oxygen isotopic equilibrium with a water-rich fluid at 530°C to 575°C, the $\delta^{18}\text{O}$ of the fluid would be about +13 to +19 for an open system. This is similar to the range in bulk silicate $\delta^{18}\text{O}$ for unmetamorphosed Central Appalachian sedimentary rocks (see Chapter 5). Figures 7.4 and 7.5 both suggest that the bulk silicate $\delta^{18}\text{O}$ values of calcareous-facies metasedimentary rocks initially increased with increasing metamorphic grade, but

that at garnet grade and higher these values slightly decreased. An increasing fluid-flux ratio with higher metamorphic grade could cause such an effect, compatible with the calculations of Ferry (1992), who showed that fluid flux increased with increasing metamorphic grade in the Waits River Formation.

A question which nags at us in all this discussion is: What is the range of $\delta^{18}\text{O}$ of bulk silicate for fine-grained, unmetamorphosed sedimentary rocks containing more than 50% carbonate? Is it the same as for carbonate-poor rocks, for which we have plenty of adequate statistical data? Or is it more like the very high $\delta^{18}\text{O}$ value of the single calcilutite sample analyzed from Tennessee in Chapter 5 (sample 138 with bulk silicate $\delta^{18}\text{O} = +21.7$)? Calcilutites in Utah/Arizona also typically have higher bulk silicate $\delta^{18}\text{O}$ than analogous sedimentary rocks containing smaller amounts of carbonate. No comparable data exist for sandstones, but the available data indicate that sandstones containing less than 50% carbonate do not differ significantly in bulk silicate $\delta^{18}\text{O}$ from sandstones with little or no carbonate. However, this might *a priori* be expected for sedimentary rocks containing sand-size detrital quartz, which would be much less readily exchanged than the very fine-grained clay minerals. In any event, for this work it does not answer the question with regard to the bulk silicate $\delta^{18}\text{O}$ values of marls and calcilutites.

This question is important because a metamorphosed marl or calcilutite with bulk silicate $\delta^{18}\text{O}$ of +18 or higher would imply a distinct upward shift in $\delta^{18}\text{O}$ with increasing metamorphic grade if its calcareous sedimentary protolith had a $\delta^{18}\text{O}$ similar to that of noncalcareous Central Appalachian shales and sandstones. If the original pre-metamorphic bulk silicate material of the protolith were already enriched in ^{18}O , this

isotopic shift might be minor or non-existent. However, arguing in favor of a distinct upward ^{18}O shift is the fact that in Figure 7.5 we purposely excluded from the data set all samples of the Waits River formation containing more than 50% carbonate, and putting these data-points back in the figure does not change any of the $^{18}\text{O}/^{16}\text{O}$ relationships of the metamorphic rocks shown on Figure 7.5.

Other remaining unanswered questions in comparing the relatively low carbonate samples of the Waits River Formation schists to the Central Appalachian shales and sandstones are: (1) How have the $^{18}\text{O}/^{16}\text{O}$ relationships been affected by the amounts of carbonate that have been lost from the Waits River protolith by dissolution and devolatilization reactions? (2) How has the diagenetic/metamorphic fluid changed in $\delta^{18}\text{O}$ as a result of the proximity to, and exchange with, this carbonate-rich formation? (3) How has exchange with this fluid influenced the $\delta^{18}\text{O}$ values of the minerals produced by the diagenetic/metamorphic reactions? Though beyond the scope of this study and that of Stern *et al.* (in press), detailed answers to these questions are obviously very important and should be the subject of further work. Differences in the bulk silicate $\delta^{18}\text{O}$ of the protolith particularly would have a major bearing on estimates of the fluid flux calculated from the isotopic data.

7.4 Oxygen isotope studies of metasedimentary rocks from western Vermont

Sixteen samples were analyzed from western Vermont, nine from the Lincoln Mountain Quadrangle in the west-central part of the state. These nine samples range in metamorphic grade from biotite to garnet to chloritoid-kyanite. Previous work by Taylor *et al.* (1963) on mineral separates from this quadrangle indicated equilibration during regional metamorphism with a widespread fluid of relatively constant $\delta^{18}\text{O}$ value. The

bulk silicate data from the present study are in general agreement with the conclusions of Taylor *et al.* (1963). Seven of the samples from the carbonate-poor, terrigenous-facies metasedimentary rocks of this large area in west-central Vermont have uniform bulk silicate $\delta^{18}\text{O}$ values that vary from +11.4 to +13.7, with a mean value of +12.8, which is similar to the mean for the Gile Mountain Formation in east-central Vermont, and more than 5 per mil lighter than the mean for the calcareous Waits River Formation. These samples are from three different sedimentary formations, the Underhill and Pinnacle Formations and the Cheshire Quartzite. Only an amphibolitic greenstone (metabasalt) with a $\delta^{18}\text{O} = +7.1$ and the carbonate-bearing Vt55 schist with $\delta^{18}\text{O} = +14.4$, which was singled out above as being somewhat peculiar, lie outside this relatively restricted $\delta^{18}\text{O}$ range.

The other samples from western Vermont include only relatively low-grade samples from the biotite and chlorite zones. These 7 samples include a wide range in lithologies from the Dunham Dolomite, the Pawlett Formation, St. Catherine's Formation, the Moosalamoo Phyllite, and another sample of the Cheshire Quartzite. Excluding the Moosalamoo Phyllite, $\delta^{18}\text{O}$ values of these samples divide nicely into two groups, a high- ^{18}O group of 4 samples that contain 20% to 65% carbonate, and a low- ^{18}O group of 2 samples that contain no carbonate. The mean $\delta^{18}\text{O}$ values of these two groups are +19.4 and +13.5, respectively. Thus, except for the high- ^{18}O Moosalamoo Phyllite, all of the samples from western Vermont display $^{18}\text{O}/^{16}\text{O}$ relationships very similar to those established above in the St. Johnsbury Quadrangle. The bulk silicate $\delta^{18}\text{O}$ values of the terrigenous-facies samples are consistently about 5 to 6 per mil lower than those of the carbonate facies.

These data from western Vermont thus strongly support the observation from the $^{18}\text{O}/^{16}\text{O}$ data of the St. Johnsbury Quadrangle that a different set of oxygen isotopic dynamics dominate in the metamorphism of calcareous versus noncalcareous sediments. If exchange with a pervasive H_2O -rich fluid is responsible for the general lowering of bulk silicate $\delta^{18}\text{O}$ in noncalcareous sedimentary rocks during metamorphism, what dynamics are different in calcareous sedimentary rocks? One possibility is that calcareous sedimentary rocks at some stage in their metamorphic history act as an aquitard and diminish the fluid/rock ratio. Another possibility is that the fluid/rock ratio is similar for calcareous and noncalcareous sedimentary rocks, but that because the carbonate-rich protolith starts out with much higher overall $^{18}\text{O}/^{16}\text{O}$ ratios, even though the $\delta^{18}\text{O}$ values of both formations are lowered by similar amounts during metamorphism, the calcareous formations preserve the signature of this overall higher initial $\delta^{18}\text{O}$ value. Both possibilities appear to have validity in different circumstances. Regarding the bulk silicate oxygen isotopic ratio the problem then becomes how to discern the contrasting effects of internal oxygen isotopic equilibration within the calcareous metasedimentary formation and ^{18}O depletion due to exchange with an externally derived, pervasive fluid. These problems are addressed below.

7.5 Relationships between bulk silicate $\delta^{18}\text{O}$ and carbonate $\delta^{18}\text{O}$ in sedimentary and metasedimentary rocks

A significant correlation ($r=0.85$) exists between bulk silicate $\delta^{18}\text{O}$ and coexisting carbonate $\delta^{18}\text{O}$ for the Northern Appalachian metasedimentary rocks analyzed in this study (Figure 7.10). This correlation supports the hypothesis that even though complete isotopic equilibrium was either not attained or not "frozen in" for most of these samples,

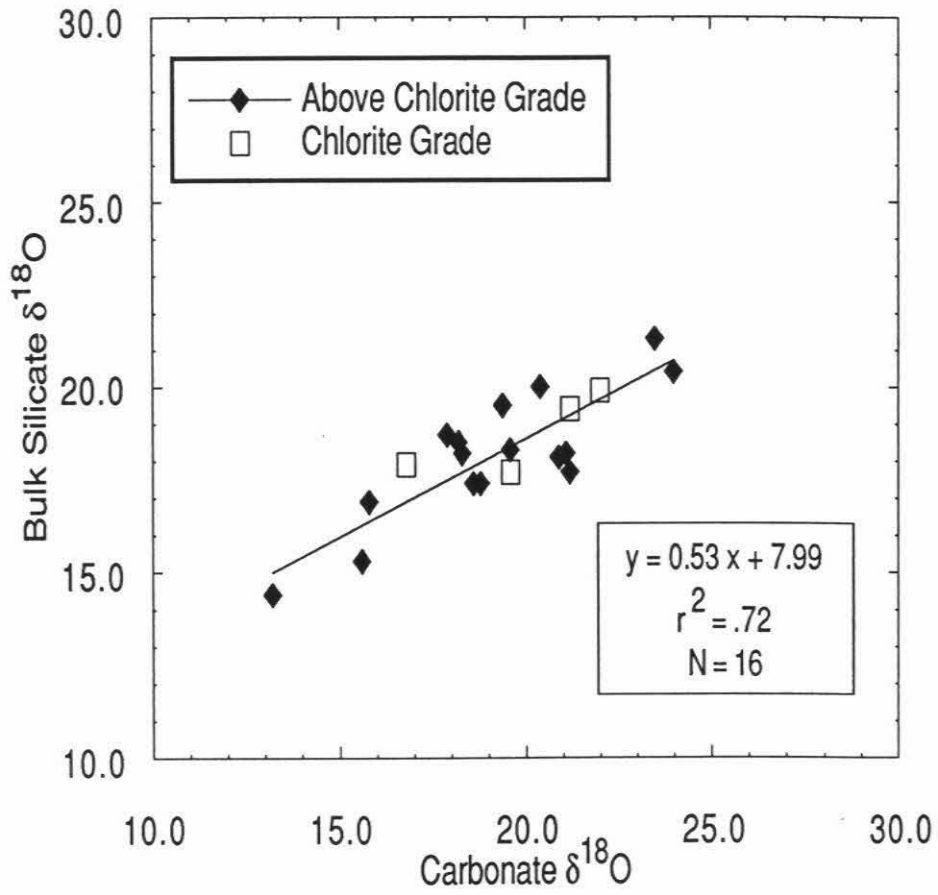
Figure 7.10

Plot of bulk silicate $\delta^{18}\text{O}$ versus carbonate $\delta^{18}\text{O}$ for Northern Appalachian metamorphic rocks in this study. The linear regression line shown is for the 16 biotite zone and higher grade samples, calculated after Fisher et al. (1970): $y = 0.53 x + 7.99$; $r = 0.85$ (this is significant at $P < 0.01$). A regression line for the 4 chlorite zone samples (not shown) is: $y = 0.39 x + 10.90$; $r = 0.83$.

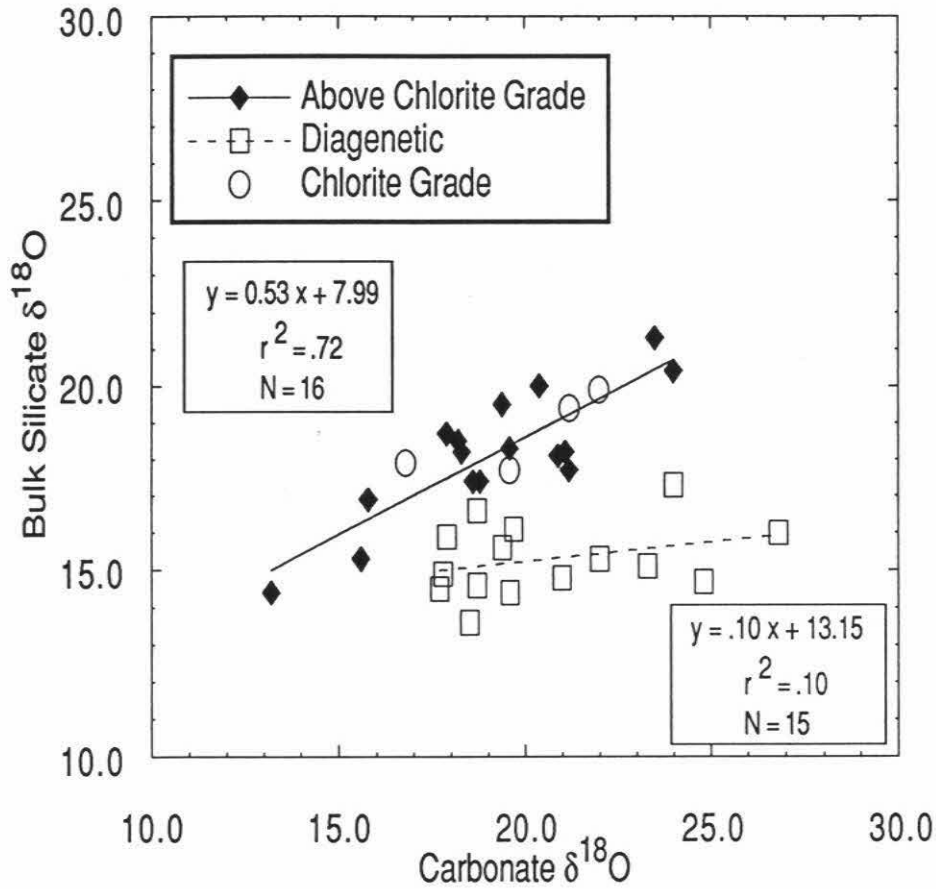
Figure 7.11

Plot of bulk silicate $\delta^{18}\text{O}$ versus carbonate $\delta^{18}\text{O}$ for Appalachian metamorphic rocks in this study. In addition to the linear regression line for samples above biotite grade from Figure 7.10 (solid line) a linear regression line for the 15 Central Appalachian sedimentary rocks from Chapter 5 is also shown (dashed line):
 $y = 0.10 x + 13.15$; $r = 0.31$.

Bulk silicate $\delta^{18}\text{O}$ vs. Carbonate $\delta^{18}\text{O}$
for Northern Appalachian
Metamorphic Rocks: This Study



Bulk silicate $\delta^{18}\text{O}$ vs. Carbonate $\delta^{18}\text{O}$
for Appalachian Sedimentary
and Metamorphic Rocks: This Study



there was nevertheless very considerable exchange between the carbonate oxygen and the bulk silicate oxygen in these calcareous metasediments (which are principally from the Waits River Formation). In Figure 7.11, bulk silicate $\delta^{18}\text{O}$ and carbonate $\delta^{18}\text{O}$ of Northern Appalachian metasedimentary rocks are compared with those of Central Appalachian sedimentary rocks. The slope of the regression line drawn through the Central Appalachian sedimentary rocks is nowhere near as steep as the slope of a regression line drawn through the Northern Appalachian metasediments (0.10 as compared to 0.53). Also, because of scatter in the data points on Figure 7.11, the correlation of bulk silicate $\delta^{18}\text{O}$ with carbonate $\delta^{18}\text{O}$ is probably not statistically significant for the Central Appalachian sedimentary rocks ($r=0.31$). It is clear that the slope of the regression line should increase with increasing diagenesis and metamorphism, due to a closer approach to equilibrium of the carbonate and silicate fractions. All other factors being equal (which, because of mineralogical variations, they are not!), this slope would be expected to approach 1.0 if complete isotopic equilibrium were attained at some uniform temperature.

Figure 7.12 compares data from the Texas Coastal Plain (Yeh and Savin, 1977) with metasedimentary rocks from the Northern Appalachians. The slope for these data ($m=0.37$) is intermediate to that of the Central Appalachian sedimentary rocks and that of the Northern Appalachian metasedimentary rocks. The Texas Coastal Plain samples are all shales of similar lithology and similar silicate mineralogy that have undergone diagenesis over a limited range of temperatures from 44°C to 169°C (Yeh and Savin, 1977). The very uniform original silicate mineralogy and lithology of these samples probably explains the unusually high correlation coefficient ($r=0.98$) observed for these

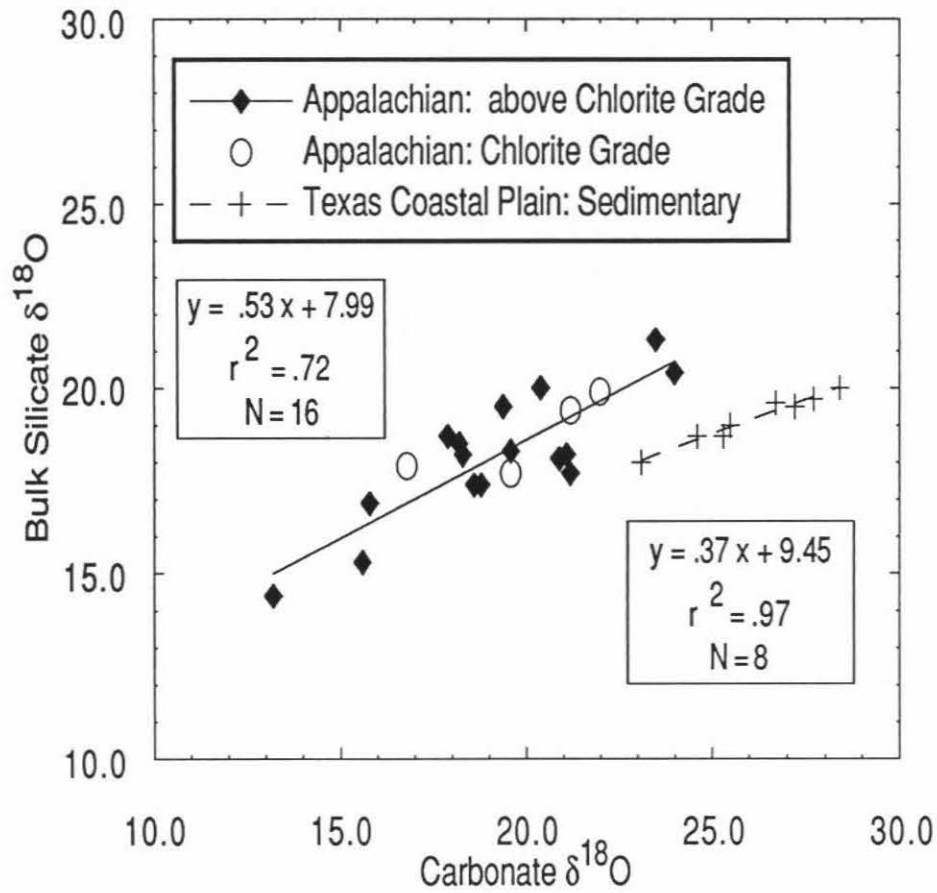
Figure 7.12

Plot of bulk silicate $\delta^{18}\text{O}$ versus carbonate $\delta^{18}\text{O}$ for Northern Appalachian samples in this study and Texas Coastal Plain shales from Yeh and Savin (1977). The linear regression line from Figure 7.10 is shown for samples above biotite grade, and another regression line is shown for the 8 samples of Texas Coastal Plain sediments: $y = 0.37x + 9.45$; $r = 0.98$; this is significant at $P < 0.01$.

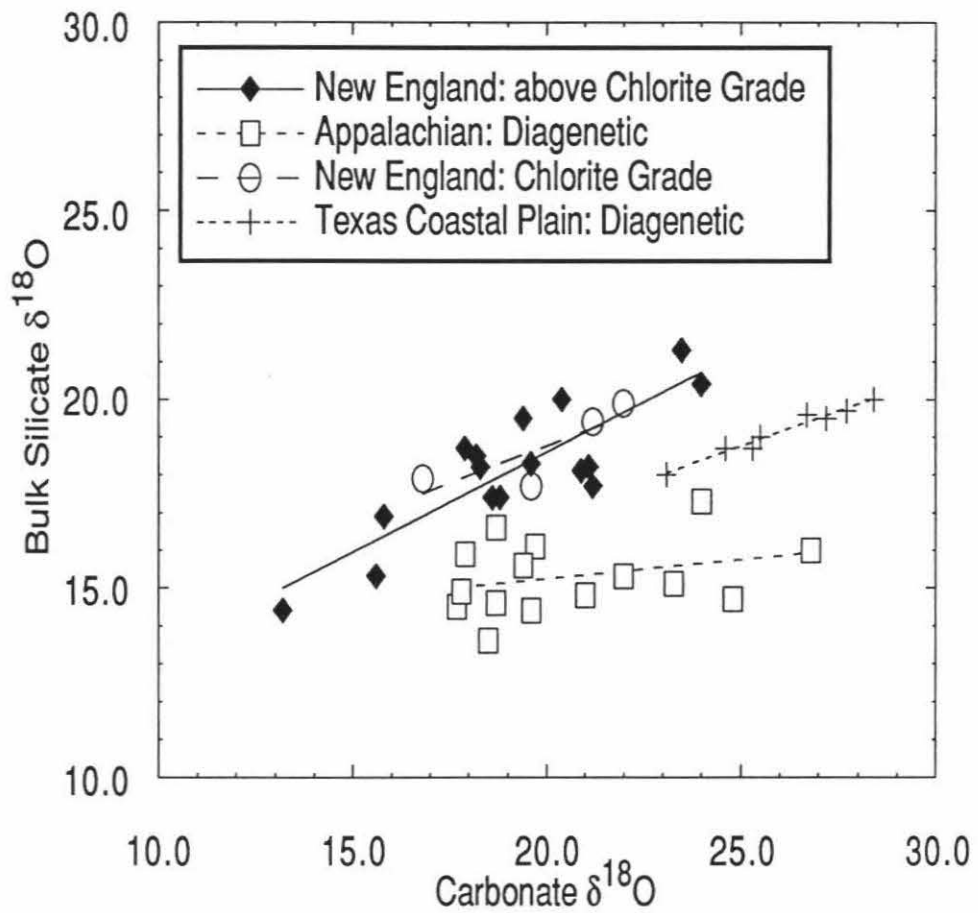
Figure 7.13

Plot of bulk silicate $\delta^{18}\text{O}$ versus carbonate $\delta^{18}\text{O}$ for sedimentary and metamorphic rocks from the Appalachians (this study) and the Texas Coastal Plain (Yeh and Savin, 1977). The four linear regressions from Figures 7.10, 7.11 and 7.12 are also shown.

Bulk silicate $\delta^{18}\text{O}$ vs. Carbonate $\delta^{18}\text{O}$
for Northern Appalachians
and Texas Coastal Plain



Bulk silicate $\delta^{18}\text{O}$ vs. Carbonate $\delta^{18}\text{O}$
for Sedimentary and Metamorphic Rocks:
Appalachians and Texas Coastal Plain



Texas Coastal Plain sediments, when the isotopic data are plotted as bulk silicate $\delta^{18}\text{O}$ versus carbonate $\delta^{18}\text{O}$. The $\delta^{18}\text{O}$ values of both parts of these rocks decrease with increasing temperature in a simple, monotonic fashion. In these Texas Coastal Plain sediments, there is also a significant decrease in weight per cent carbonate with increasing temperature.

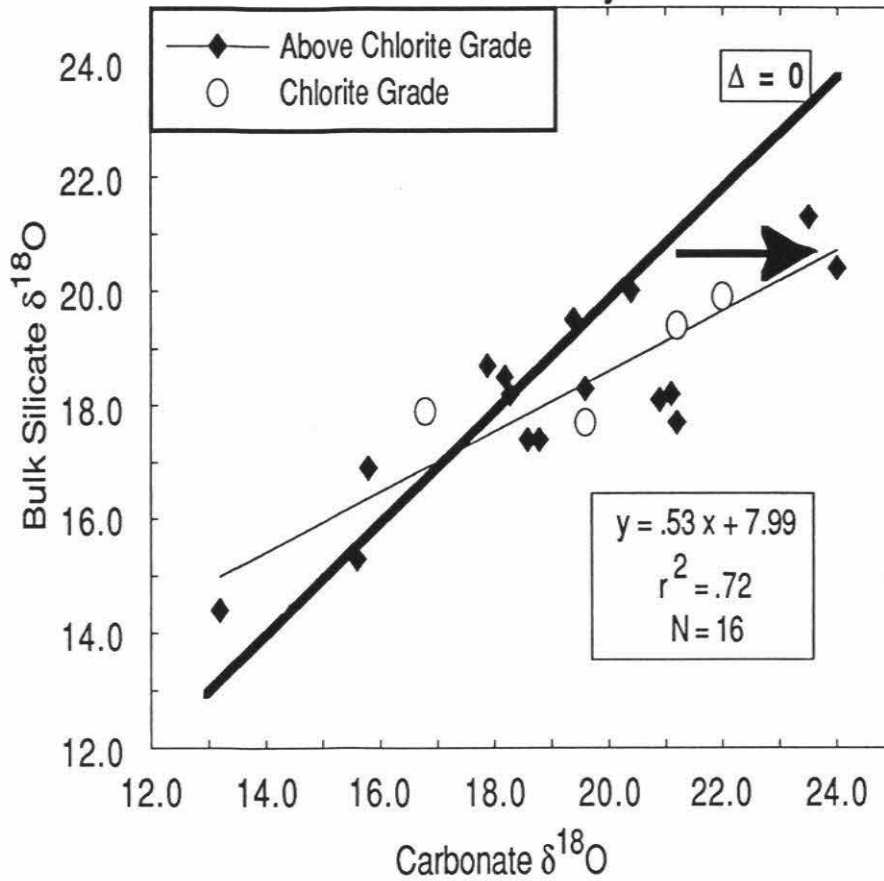
Figure 7.13 compares Central Appalachian sedimentary rocks, Texas Coastal Plain sediments, Northern Appalachian metasedimentary rocks, and Northern Appalachian chlorite-grade metasediments. The slopes of the regression lines through each set of data points decrease in the following order: Northern Appalachian metasedimentary > Northern Appalachian chlorite grade > Texas Coastal Plain > Central Appalachian sedimentary. If the coexisting carbonate and bulk silicate oxygen were in isotopic equilibrium with each other in a closed system at very high temperatures, the $\delta^{18}\text{O}$ values would plot along the 45° line with slope 1 where bulk silicate $\delta^{18}\text{O} = \text{carbonate } \delta^{18}\text{O}$. If there were no isotope exchange between the bulk silicate material and the coexisting carbonate, and if the carbonate alone exchanged during diagenesis with an external fluid (as is reasonable because calcite exchanges orders of magnitude faster with aqueous fluids than does quartz), then a slope near zero might be expected. For example, assuming that the data from the Central Appalachians are typical of unmetamorphosed sediments (Figure 7.11), a progression from a slope of near zero to a slope of one might be encountered as the system was heated up and metamorphosed, thereby approaching isotopic equilibrium.

What information do these $\delta^{18}\text{O}$ bulk silicate— $\delta^{18}\text{O}$ carbonate plots contain on the role of fluid in metamorphism? Figure 7.14 compares bulk silicate $\delta^{18}\text{O}$ and carbonate

Figure 7.14

Plot of bulk silicate $\delta^{18}\text{O}$ versus carbonate $\delta^{18}\text{O}$ for Appalachian metamorphic rocks in this study. The heavy solid line represents $\Delta=0$ (*i.e.*, zero $^{18}\text{O}/^{16}\text{O}$ fractionation between coexisting carbonate and silicate). The linear regression for 16 samples above chlorite grade is also shown from Figure 7.10. The arrow represents the direction that the samples would be shifted from the $\Delta=0$ line, assuming (1) open-system fluid-rock exchange; (2) that the bulk silicate is dominantly quartz; (3) a temperature gradient varying from low temperature at the upper right to high temperature at the lower left; and (4) that the bulk silicate $\delta^{18}\text{O}$ remains roughly constant, with most of the isotopic shift occurring in the more easily exchanged carbonate.

**Bulk silicate $\delta^{18}\text{O}$ vs. Carbonate $\delta^{18}\text{O}$
for Northern Appalachian
Metamorphic Rocks:
This Study**



$\delta^{18}\text{O}$ of calcareous samples of chlorite grade and higher from the Northern Appalachians. A heavy line representing $\Delta=0$ is drawn on the graph for reference, where Δ is the isotopic fractionation (difference between carbonate $\delta^{18}\text{O}$ and bulk silicate $\delta^{18}\text{O}$). At equilibrium at infinite temperature, this fractionation is zero for all minerals. Lines of constant temperature will be lines of equal fractionation at constant composition and will be parallel to $\Delta=0$, with the Δ -values increasing with decreasing temperature. The linear regression for the Northern Appalachian data is clearly not parallel to $\Delta=0$, nor would it be expected to be, because of the wide range of metamorphic grade of these samples. This regression line distinctly cuts across lines of constant temperature. So do the regression lines for the Central Appalachians and for the Texas Gulf sediments. It is extremely unlikely that more than a few of these samples represent equilibrium assemblages. If this were the case, then other factors being equal, the higher-temperature rocks would lie closer to the $\Delta=0$ line and the lower-temperature rocks would lie farther away, which in fact they do in a general way. However, the 4 chlorite-grade samples are of lower metamorphic grade than the other Northern Appalachian samples, and they clearly do not follow this systematic pattern on Figure 7.14. Also, the bulk silicate fractions of most of these samples are dominated by quartz, so at equilibrium the data points should be above and to the left of the $\Delta = 0$ line; most of them plot below and to the right of this line.

The most likely explanation of most of the data in Figure 7.14 is oxygen isotopic disequilibrium between the carbonate and silicate fractions of each sample. However, this cannot be a random disequilibrium, because of this striking correlations that exist. For example, if the samples plotted on Figure 7.15 had at one time all been equilibrium

Figure 7.15

Plot of bulk silicate $\delta^{18}\text{O}$ versus carbonate $\delta^{18}\text{O}$ showing hypothetical trajectories that would be followed during closed-system heating of a sedimentary rock containing variable amounts of carbonate and bulk silicate. The vertical arrow labeled $>99\%$ indicates the trajectory of a rock containing more than 99% carbonate. The other two arrows labeled 50% and $>1\%$, respectively, indicate analogous closed-system trajectories for rocks that contain 50% carbonate and 50% silicate, or rocks that contain less than 1% carbonate and more than 99% bulk silicate.

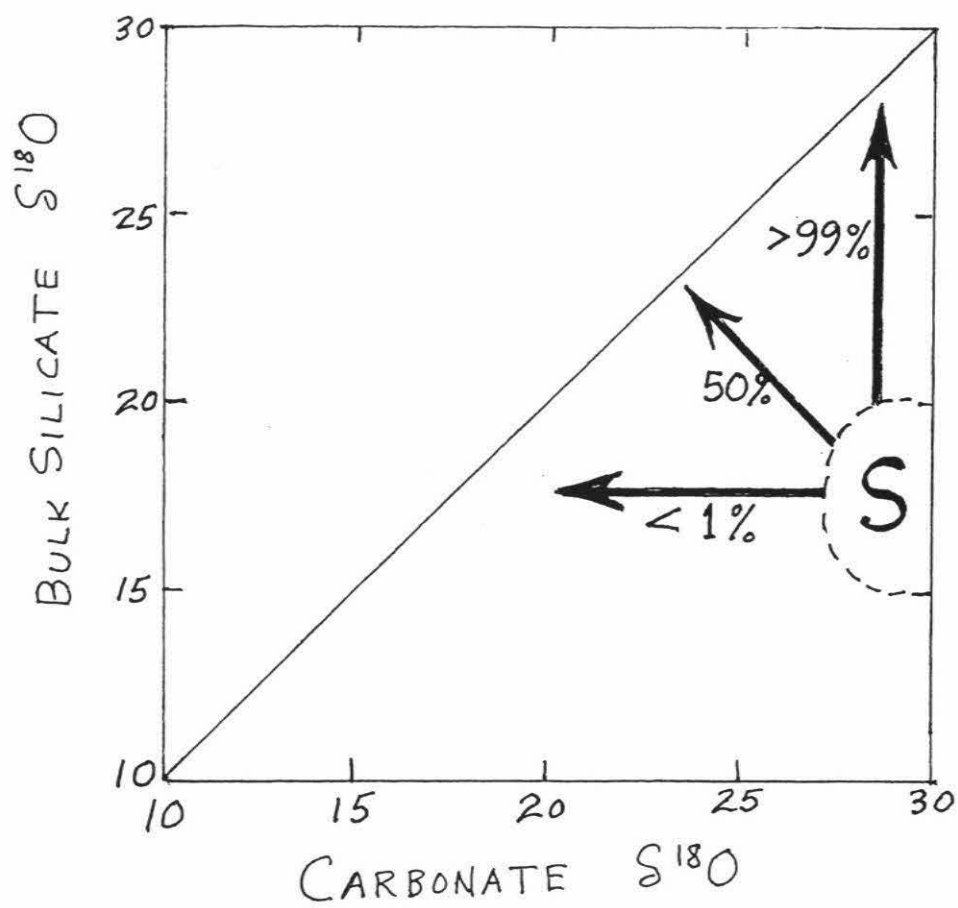
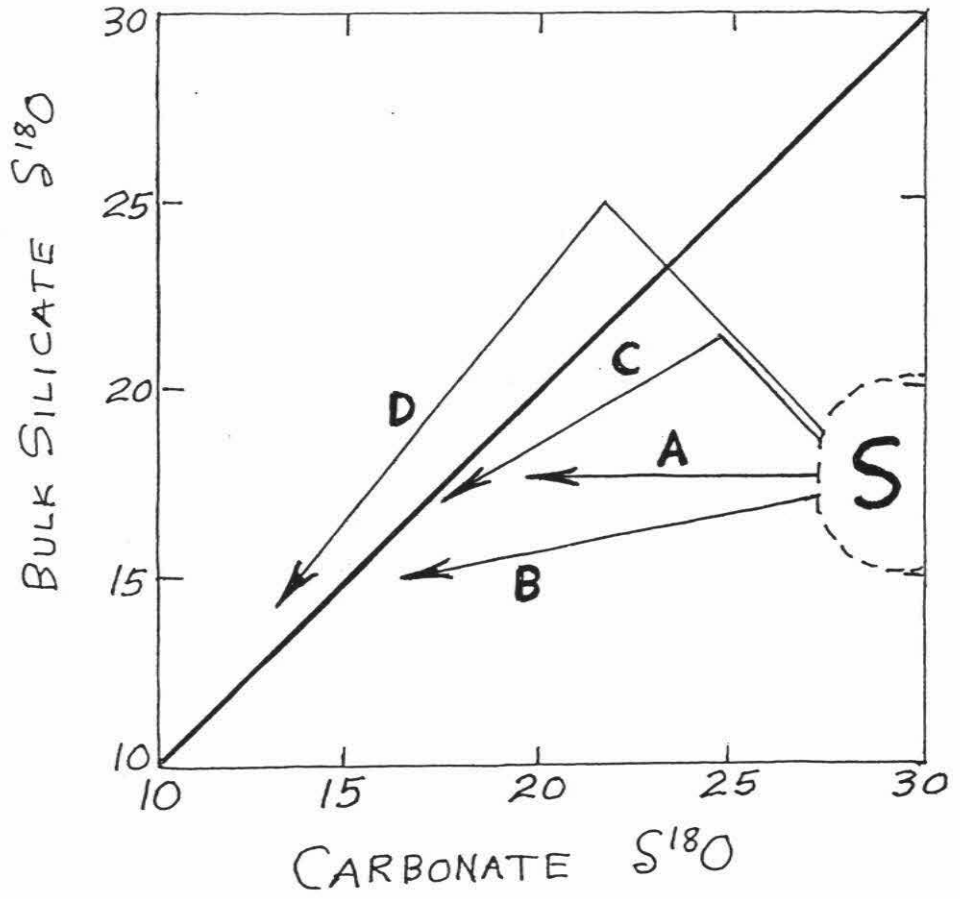


Figure 7.16

Plot of bulk silicate $\delta^{18}\text{O}$ versus carbonate $\delta^{18}\text{O}$ showing hypothetical trajectories that would be followed during open-system hydrothermal metamorphism of a sedimentary rock containing either variable amounts of carbonate and bulk silicate, or following different paths of metamorphism and aqueous fluid-rock interaction, or both (see text). The horizontal arrow labeled A shows the trajectory to be followed by a rock if only the carbonate minerals are exchanging with such a fluid (*e.g.*, a fluid that is in exchange equilibrium with an adjacent lower- ^{18}O silicate rock). Arrow B indicates a hypothetical trajectory of a rock that might be followed if both the carbonate and the silicate are exchanging with an external fluid over a range of temperatures. Arrow C indicates a hypothetical trajectory of a rock initially containing about 50% carbonate and 50% silicate that first undergoes closed-system exchange during diagenesis (see Figure 7.15), and which subsequently shifts to another trajectory as a result of an attempt to reach equilibrium between both the carbonate and the silicate fractions and an external reservoir of aqueous fluid at high temperatures. The open-system portion of path C could represent either partial equilibration with this hydrothermal fluid or complete equilibration at varying fluid-rock ratios (with greater extent of equilibration or higher fluid/rock ratio pushing the sample farther along the trajectory downward and to the left). Path D starts out in the same fashion as outlined above for Path C but undergoes more severe heating or recrystallization, sufficient that the bulk silicate and carbonate thoroughly equilibrate with one another during the closed-system part of the event; only then does the system become open to fluid/rock exchange with a much lower- ^{18}O external fluid, at which point it follows a series of equilibrium stages at successively higher temperatures, finally equilibrating with the large reservoir of aqueous fluid at the peak metamorphic temperature.



assemblages (*e.g.*, at the peak temperature of metamorphism), then the data points would have had to undergo a systematic ^{18}O shift to the right, as shown by the large arrow on the diagram. This shift would have to be much larger for the higher- ^{18}O , lower-temperature samples than for the lower- ^{18}O (higher-temperature) samples. In other words, the carbonate fraction would be preferentially shifted toward higher $\delta^{18}\text{O}$ values during retrograde exchange with some kind of external fluid, and this shift would have to be systematic enough to produce a linear array of non-equilibrium data points. Such a scenario does not seem likely, as there is no obvious reason why the retrograde exchange of the carbonate should stop along the plotted regression line. However, retrograde effects such as this cannot be totally ruled out, because of the notorious ease with which carbonates are known to exchange with aqueous fluids at elevated temperatures, much more easily than most silicates, particularly quartz. Arguing against this are the data of Stern *et al.*, (in press) who have shown that the oxygen isotope and carbon isotope systematics of the Waits River Formation are clearly correlated with prograde metamorphic effects, not retrograde. Also, retrogradation should be evidenced by observing $\delta^{18}\text{O}$ inhomogeneities in the carbonates on an outcrop scale, particularly along veins and fractures, and Stern *et al.* (in press) not only did not observe such effects, they presented evidence that individual outcrops were very homogeneous in both $\delta^{18}\text{O}$ and $\delta^{13}\text{C}$.

Figures 7.15 and 7.16 were prepared for discussion purposes only, in order to quantitatively address some of the problems raised above. The area labelled "S" on the right-hand side of these two figures represents the general range of $\delta^{18}\text{O}$ carbonate and bulk silicate $\delta^{18}\text{O}$ in unmetamorphosed sediments, prior to burial and diagenesis. These carbonate values are based on literally thousands of studies in the geochemical literature on $^{18}\text{O}/^{16}\text{O}$ relationships in carbonate rocks, while the values for the bulk silicate fraction

are mainly from the data in this work and other references quoted in Chapter 3.

On Figure 7.15, which represents closed-system systematics, the upward pointing arrow labeled >99% represents the exchange trajectory that would be followed during metamorphism or diagenesis of rocks that are more than 99% carbonate and <1% silicate. The horizontal arrow represents the closed-system exchange trajectory that would be followed under similar conditions for rocks that contain less than 1% carbonate. The arrow drawn at a 45° angle perpendicular to the diagonal line that represents zero $^{18}\text{O}/^{16}\text{O}$ fractionation is the closed-system trajectory for samples containing 50% carbonate oxygen and 50% silicate oxygen. These closed-system trajectories shown on Figure 7.15 are but 3 out of a whole family of trajectories that would fan out in the quadrant from <1% carbonate to >99% carbonate, depending on the mineralogical composition of the rock. They represent essentially fluid-absent conditions, or conditions where the pore fluid is completely restricted to the rock unit in question. These trajectories are determined solely by material balance, assuming that when the samples are heated they undergo internal isotopic exchange in the direction of equilibrium; they are independent of any other variables, including temperature, isotopic composition of the water, etc., etc. These trajectories can cross the 45° $\Delta=0$ fractionation line if the bulk silicate material is a quartz-rich assemblage.

On Figure 7.16, which represents only a minuscule fraction of the actual number of open-system exchange possibilities, 4 hypothetical arrows are drawn to illustrate different scenarios. Arrow A shows the horizontal trajectory that would be followed if the easily-exchanged carbonate minerals interact with an externally-derived fluid while the relatively inert (quartz-rich) silicate assemblage does not. Arrow B shows the trajectory of a rock in which both the silicate and the carbonate are exchanging, but in which the carbonate is exchanging much faster than the silicate material. This system

is trying to reach equilibrium with a large reservoir of external aqueous fluid at a temperature where the final equilibrium assemblage would have a carbonate $\delta^{18}\text{O}$ of about +13 and bulk silicate $\delta^{18}\text{O}$ of about +14, as might be characteristic of a quartz-rich silicate assemblage at high metamorphic grades (*e.g.*, sample 180).

Arrow C indicates a hypothetical trajectory that would be followed by a rock initially containing about 50% silicate and 50% carbonate, first under closed-system conditions (*i.e.*, see Figure 7.15) and then under open-system conditions in which the system tries to reach a similar final equilibrium state as Arrow B. Finally, Arrow D starts out just as does Arrow C, but the closed-system part of the trajectory goes well across the $45^\circ \Delta = \text{O}$ line and reaches equilibrium at a low metamorphic grade before open-system conditions are imposed. The system then begins to equilibrate with a large amount of aqueous fluid of uniform $\delta^{18}\text{O}$ value, passing through a prograde metamorphic path in continuous equilibrium with this fluid at successively higher temperatures, finally ending up at about the same equilibrium isotopic compositions as those being approached by Arrows B and C.

Figure 7.17 shows the same data from Figure 7.10 except that the higher-grade (above chlorite zone) samples are separated into two groups based on carbonate content. These envelopes on Figure 7.17 mimic the hypothetical closed-system trajectories shown on Figure 7.15, in that the actual data points of Figure 7.17 plot in roughly the positions expected for the arrows of varying per cent carbonate shown on Figure 7.15. This suggests that the basic reason for the distribution of data-points on Figure 7.17 is that these systems tried to approach closed-system equilibrium, but that they only went part way toward equilibrium before being interrupted. This interruption could have been a transformation to open-system conditions as postulated for arrow C on Figure 7.16, where these various systems are trying to reach equilibrium with a large amount of

aqueous fluid of uniform $\delta^{18}\text{O}$ that would be in equilibrium with an assemblage having bulk silicate $\delta^{18}\text{O} \approx +14$ and carbonate $\delta^{18}\text{O} \approx +13$. The carbonate-rich assemblages would retain higher $\delta^{18}\text{O}$ values than the silicate-rich assemblages even if the fluid-rock ratio were the same for both, because at a given fluid-rock ratio or per cent shift in $\delta^{18}\text{O}$, the ^{18}O -rich carbonate assemblages have much farther to go than do the silicates. Thus the data points on Figure 7.17 may represent a "partial exchange line" between a low-grade (diagenetic?) end member that has basically undergone only closed-system exchange, and another end member that has undergone much more thorough equilibration at a much higher temperature with a large volume of aqueous pore fluid. Except that it is happening at much lower temperatures (50° - 150°C) this same scenario also probably applies to the Texas Gulf Coastal Plain sediments (Yeh and Savin, 1977).

There is no evidence in this work that path D on Figure 7.16 was ever approached in any of the carbonate-rich rocks. The oxygen isotope systematics of the open-system "leg" of path D have been thoroughly discussed by Clayton and Epstein (1958), particularly as they apply to coexisting quartz and calcite, and none of the carbonate-rich samples in this work seem to have reached isotopic equilibrium (of if they did, all vestiges of such an event have been wiped out by later retrograde effects). However, paths A, B and C all conceivably could have applications to the rocks analyzed in the present study, and in part, some sort of trajectory like path C seem to be required for the carbonate-rich rocks. For example a mixture of open-system paths A and B could explain much of the data for the Central Appalachian sediments shown on Figures 7.11 and 7.13.

Why should the carbonate-rich rocks behave so differently from the carbonate-poor or carbonate-absent rocks? This is a matter of speculation with so little data, but the following scenario seems plausible based on previous work on the isotope systematics

Figure 7.17

Plot of bulk silicate $\delta^{18}\text{O}$ versus $\delta^{18}\text{O}$ for the same data shown in Figure 7.10 but delineating two group of samples, one containing more than 40% carbonate and the other less than 15% carbonate.

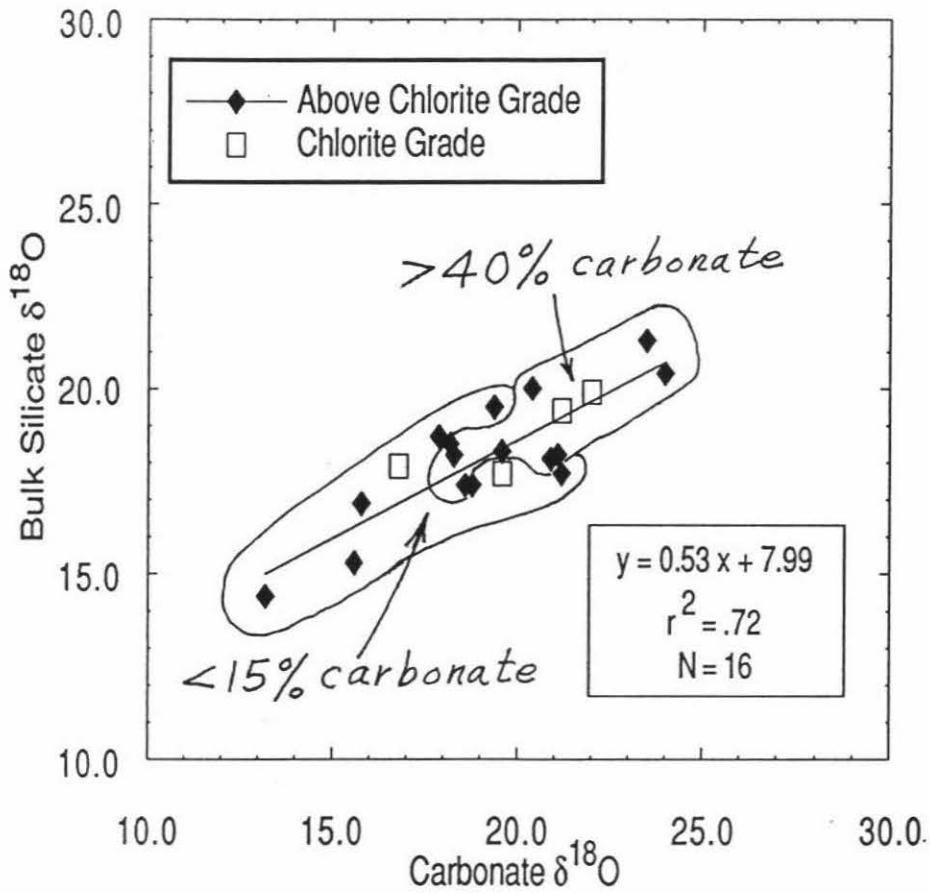
Figure 7.18

Plot of whole rock $\delta^{18}\text{O}$ versus per cent carbonate for Northern Appalachian samples in this study. The correclation is significant at the 0.01 probability level.

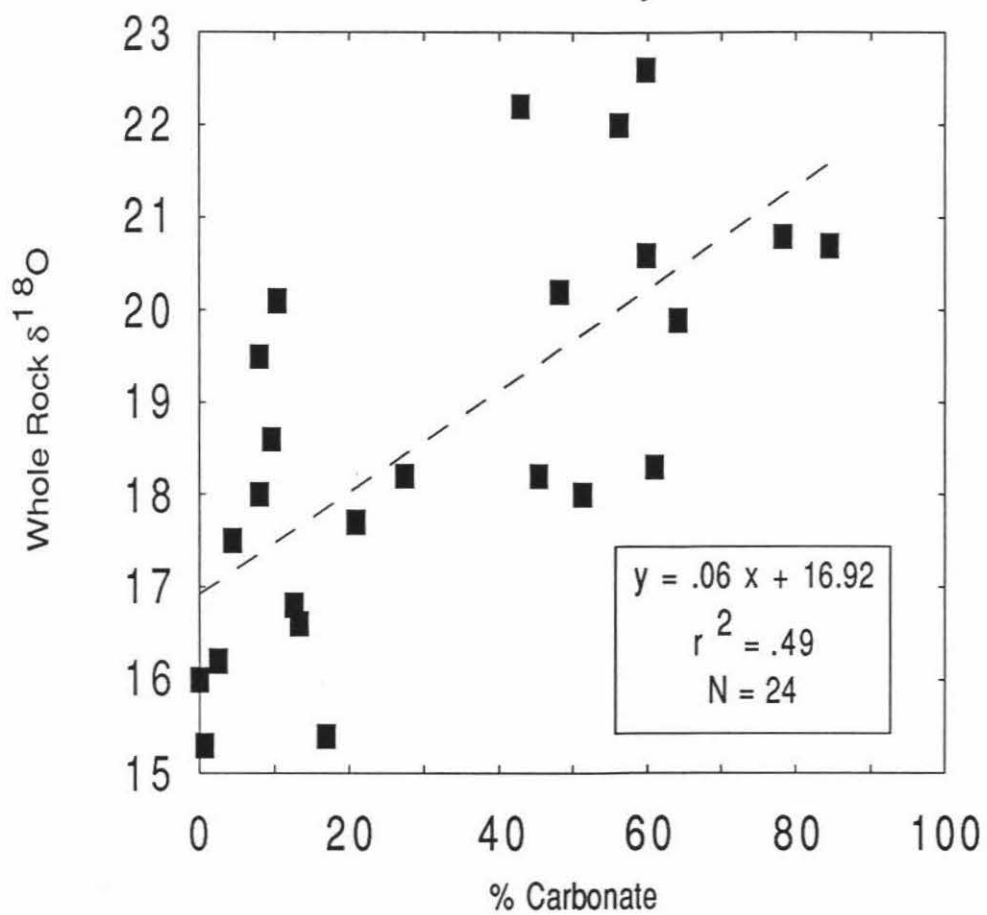
Figure 7.19

Plot of $\delta^{18}\text{O}$ carbonate versus $\delta^{13}\text{C}$ carbonate for Northern Appalachian metasedimentary rocks in this study. The correlation is significant at the 0.01 probability level.

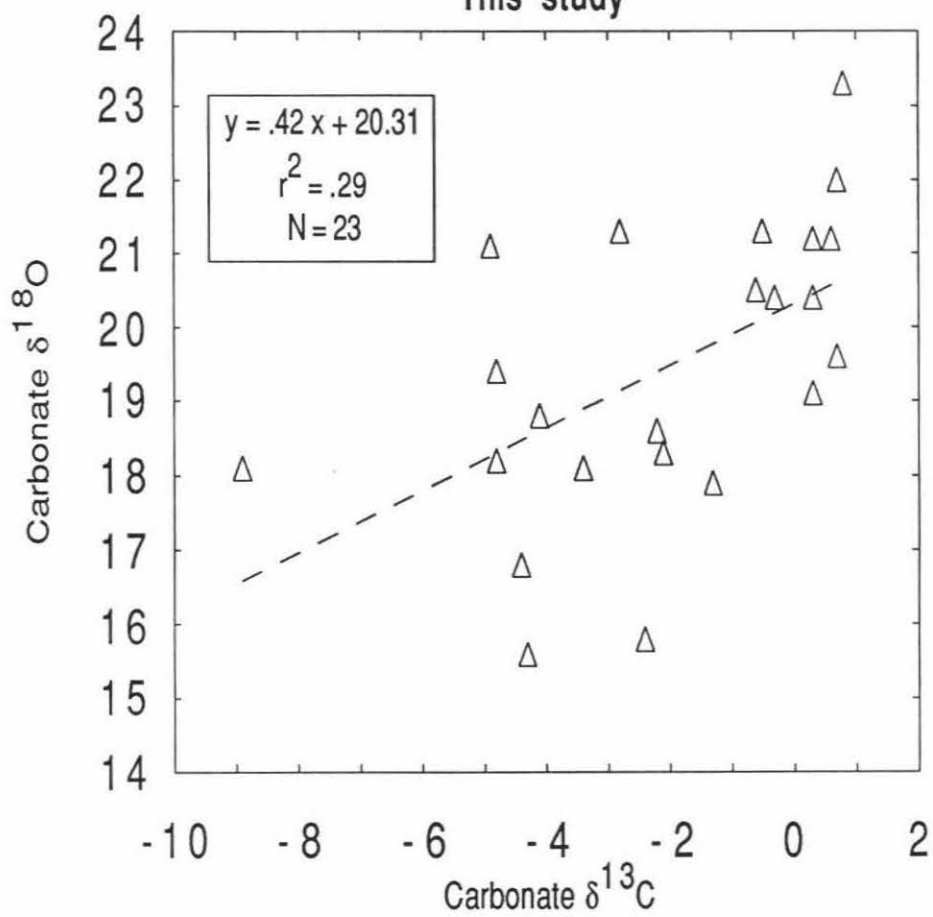
Bulk silicate $\delta^{18}\text{O}$ vs. Carbonate $\delta^{18}\text{O}$
for Northern Appalachian
Metamorphic Rocks: This Study



Whole Rock $\delta^{18}\text{O}$ vs Percent Carbonate
for Northern Appalachian Samples:
This Study



$\delta^{18}\text{O}$ Carbonate vs $\delta^{13}\text{C}$ Carbonate
for Northern Appalachian
Metasedimentary Rocks:
This study



of carbonate rocks in metamorphic and hydrothermal environments (*e.g.*, Rye *et al.*, 1976; Valley, 1986). Carbonate rocks recrystallize very easily. Therefore, during deformation, even at relatively low temperatures, they behave plastically, whereas adjacent silicate rocks are subject to fracturing through brittle failure. When this happens, the carbonates become essentially impermeable to metamorphic-hydrothermal fluids, while these interbedded silicate layers remain permeable because fluids can penetrate the fractures that continue to form during deformation. This essentially fluid-absent situation in the low-grade deformed carbonates would promote movement along the closed-system portion of path C on Figure 7.16, and it could also explain a lack of attainment of complete isotopic equilibrium..

For pure carbonate layers, the conditions outlined above may prevail to the highest grades of regional metamorphism. However, for impure carbonates like the Waits River Formation, something dramatically different may occur. These rocks begin to undergo decarbonation at some stage in the prograde metamorphic path. This "opens up" the carbonate unit to external fluids as the porosity and permeability change, as a result of reactions between the silicates and the carbonates, with consequent evolution of both CO₂ and H₂O. Thus at some stage in the prograde history the carbonate unit may change from a closed-system to an open-system scenario, just as predicted by path C. During the "dry" closed-system path isotopic equilibrium may not be fully attained between coexisting carbonate and silicate, as seems to be required by the data. There is an approach to isotopic equilibrium during this stage, but there is no evidence in the data on Figure 7.17 that complete isotopic equilibrium was ever attained at low metamorphic grades. However, after the system changes to open-system conditions there is a much greater likelihood of a close approach to equilibrium, both between the coexisting silicate and the carbonate and with the large reservoir of external aqueous

fluid. Much more work will be required to test the above model of metamorphic-hydrothermal infiltration of impure carbonate rocks.

Figure 7.18 shows a significant correlation between whole rock $\delta^{18}\text{O}$ content and per cent carbonate for the metamorphic rocks studied in this research ($r=0.7$). These correlations in Figure 7.18 are analogous to those shown in Figure 7.17 in the sense that lower $\delta^{18}\text{O}$ values of both carbonate and silicate are correlated with smaller amounts of carbonate in the samples. Thus, the arguments given above also apply to the correlations shown in Figure 7.18. If closed-system effects involving only small amounts of aqueous fluid were important, the high- ^{18}O carbonate would be expected to control the bulk silicate $\delta^{18}\text{O}$ of the system for all carbonate-rich samples, and this definitely seems to be the case. Exchange with this carbonate would result in an isotopically heavy silicate fraction as it tries to reach isotopic equilibrium with the carbonate fraction.

When $\delta^{18}\text{O}$ of carbonate is plotted against $\delta^{13}\text{C}$ of carbonate, there is a significant low correlation ($r=0.54$) for these two isotopes. Stern *et al.* (in press) observed a similar type of correlation in their study of 302 samples of the Waits River Formation collected throughout eastern Vermont. Although Stern *et al.* (in press) did not come to any firm conclusion about these correlated ^{18}O and ^{13}C depletions, it is likely that a combination of three factors may have been important: (1) original sedimentary protolith differences, with $\delta^{18}\text{O}$ and $\delta^{13}\text{C}$ both being lower in samples affected by meteoric ground-water diagenesis; (2) exchange with low- ^{13}C graphite at high temperatures during the metamorphic-hydrothermal event; and (3) decarbonation reactions, which are known to produce correlated ^{18}O and ^{13}C depletions. All of these factors also might tend to be correlated with per cent carbonate, as rocks with smaller amounts of carbonate would be expected to be most susceptible to (1) and (2), whereas (3) by itself produces a reduction in the amount of carbonate in the rock.

7.6 Conclusions

Noncalcareous Northern Appalachian metasedimentary rocks show a decrease in bulk silicate $\delta^{18}\text{O}$ with increasing metamorphic grade. This is interpreted to be the result of exchange with an isotopically light aqueous fluid at increasing temperature. Calcareous Northern Appalachian sedimentary rocks show much higher bulk silicate $\delta^{18}\text{O}$ values than the noncalcareous samples, but they also show a decrease in bulk silicate $\delta^{18}\text{O}$ at garnet grade and higher as compared to their calcareous equivalents at biotite grade and lower. Further work on the bulk silicate $\delta^{18}\text{O}$ values of sandy limestones is needed to determine if there is an initial increase in bulk silicate $\delta^{18}\text{O}$ at very low grade.

Using Central Appalachian terrigenous miogeosynclinal sedimentary rocks as our best estimates of sedimentary protoliths of Northern Appalachian metasediments, we conclude that such rocks typically have been depleted in ^{18}O by about 2 per mil during regional metamorphism. In those rocks that contain significant carbonate (>2%) but excluding those with more than 50% carbonate, there is an overall increase in bulk silicate $\delta^{18}\text{O}$ of 5 to 6 per mil as compared to the nearby noncalcareous metasedimentary rocks. Therefore, since these different rocks were metamorphosed over a similar range of temperatures, there is either a difference in fluid flux (*i.e.*, fluid-rock ratio) for calcareous metasediments versus noncalcareous metasediments, or a difference in the $\delta^{18}\text{O}$ of the fluid, or both. We have presented arguments that these kinds of contrasting differences in both fluid-rock ratio and isotopic composition are to be expected in carbonate rocks, because of their vastly different permeabilities under varying conditions of deformation and metamorphic grade.

Ferry (1992) and Stern *et al.* (in press) cite evidence for pervasive exchange of the Waits River Formation rocks with an isotopically "light" aqueous fluid throughout the length of Vermont, and including the St. Johnsbury Quadrangle, where most of the

data from the present study were obtained. Bulk silicate data from the St. Johnsbury Quadrangle in this study suggest that an isotopically heavy fluid ($\delta^{18}\text{O} = +16$ to $+20$) equilibrated with the silicate fraction of the Waits River Formation. These high $\delta^{18}\text{O}$ values are clearly controlled by the local reservoir of high- ^{18}O material that makes up the Waits River Formation. Thus, even though significant amounts of lower- ^{18}O external fluid penetrated this formation, as required by the data of Ferry (1992) and Stern *et al.* (in press), these amounts were well short of the quantity needed to lower the $\delta^{18}\text{O}$ of the Waits River Formation down to the values exhibited by the adjacent Gile Mountain Formation. Nevertheless, these kinds and amounts of aqueous fluid seem adequate to explain most of the isotopic data obtained in the present study.

CHAPTER 8

Summary and Conclusions

This research has addressed the question of the range and variation of whole-rock $\delta^{18}\text{O}$ in terrigenous sedimentary rocks such as shales, siltstones, and sandstones as a function of such factors as lithology, depositional environment, source region, geologic age, and post-depositional diagenetic changes. Using these data, it was then possible to evaluate the role of diagenesis and metamorphism in altering the whole rock $\delta^{18}\text{O}$ values of large masses of these terrigenous sedimentary rocks.

Previous data from the literature were compared with the new data obtained in this study on the Paleozoic and Mesozoic shelf sediments of the Colorado Plateau, the Paleozoic geosynclinal sediments of the Ouachita Mountains, and particularly the geosynclinal sediments of the Central Appalachian Mountains. A few summary diagrams were prepared to illustrate some of the major conclusions of this study (Figures 8.1, 8.2, 8.3 and 8.4). In terms of depositional environment, pelagic sediments show the largest range in $\delta^{18}\text{O}$. In the pelagic environments very ^{18}O -rich sediments are formed biogenically and authigenically from sea water, and ^{18}O -poor sediments may form from hydrothermal alteration of basalts. The limited data available for eugeosynclinal sediments suggest that they have lower $\delta^{18}\text{O}$ than most other marine sediments (Figures 8.2 and 8.3). This is probably due to a lack of weathering, rapid erosion, and a higher volcanogenic component in these sediments, as well as to metamorphic-hydrothermal changes at high pressures during burial metamorphism.

Marine terrigenous sediments typically show a higher mean bulk silicate $\delta^{18}\text{O}$ than nonmarine sediments (Figures 8.1 and 8.2). This is most likely due to the involvement of isotopically light meteoric water in the diagenesis of nonmarine sediments.

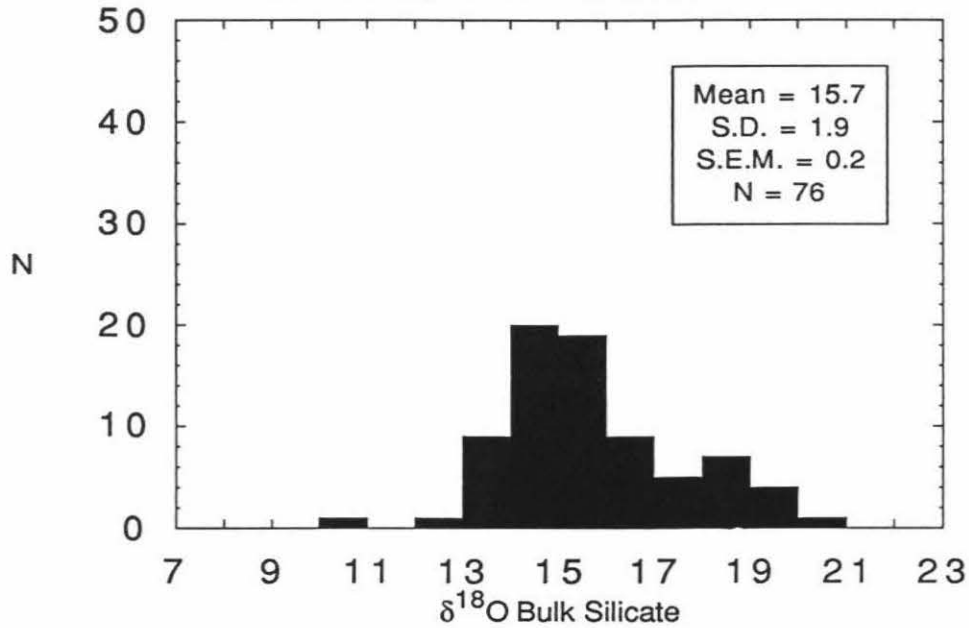
Figure 8.1

Two histograms comparing the bulk silicate $\delta^{18}\text{O}$ of marine and nonmarine samples from the literature and this study. The upper histogram is a compilation of the silicate $\delta^{18}\text{O}$ of all marine samples in this study and in the literature review. The lower histogram is a compilation of the bulk silicate $\delta^{18}\text{O}$ of all nonmarine samples in this study and the literature review. The mean bulk silicate $\delta^{18}\text{O}$ is significantly lower for the nonmarine samples.

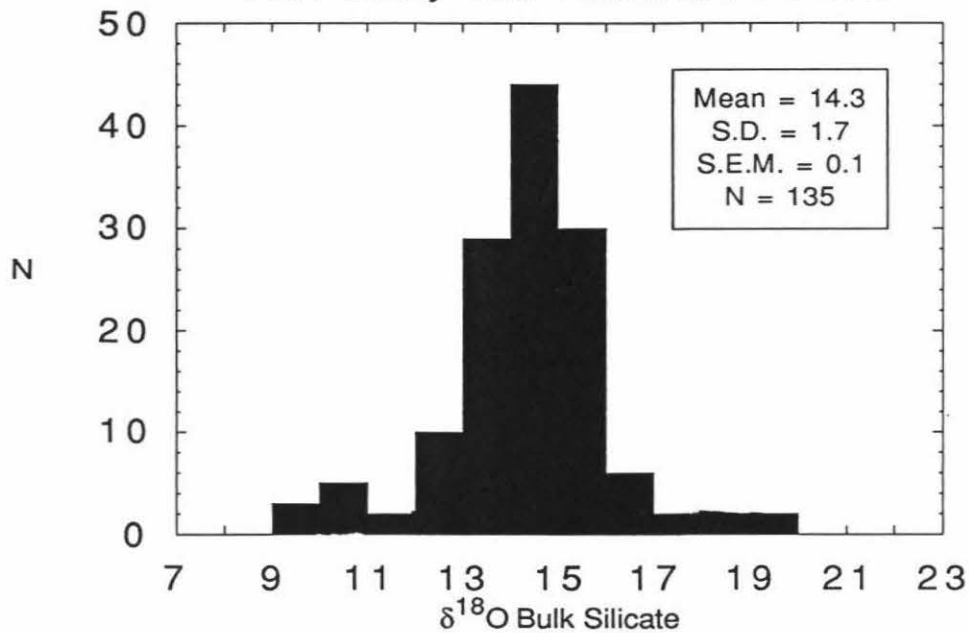
Figure 8.2

Two histograms comparing the bulk silicate $\delta^{18}\text{O}$ of all marine samples (upper histogram) with all nonmarine samples (lower histogram) analyzed in this study. Note the significantly decreased dispersion of the bulk silicate $\delta^{18}\text{O}$ values as compared to the larger data set in Figure 8.1. The mean bulk silicate $\delta^{18}\text{O}$ of marine samples in this data set is also significantly higher than that for the nonmarine samples, but the difference is smaller than for the larger data set in Figure 8.1 (0.7 versus 1.4 per mil).

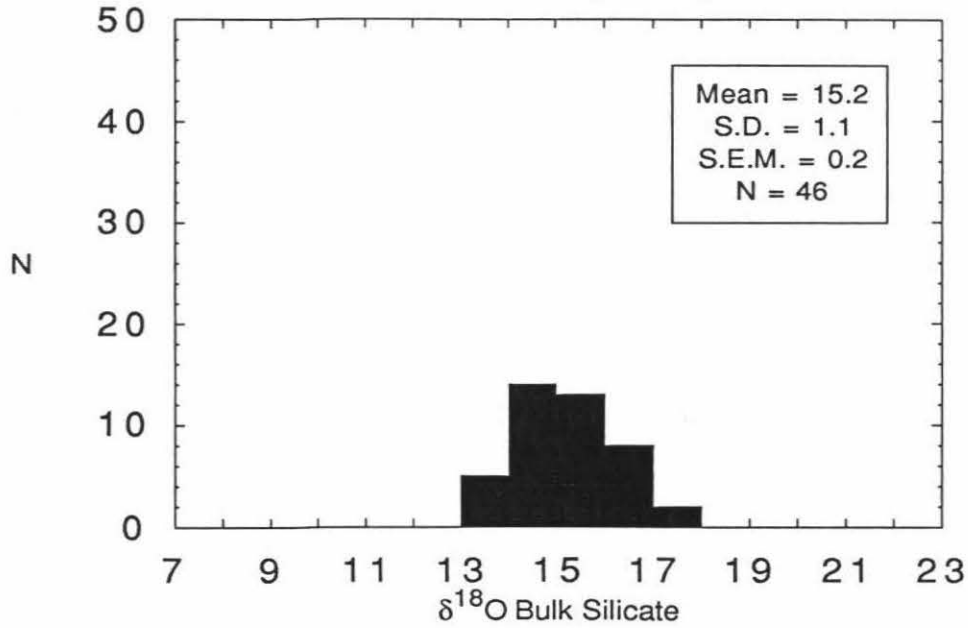
$\delta^{18}\text{O}$ Bulk Silicate
All Marine Samples:
This Study and Literature Review



$\delta^{18}\text{O}$ Bulk Silicate
All Non-Marine Samples:
This Study and Literature Review



$\delta^{18}\text{O}$ Bulk Silicate
All Marine Samples:
This Study Only



$\delta^{18}\text{O}$ Bulk Silicate
All Non-Marine Samples:
This Study Only

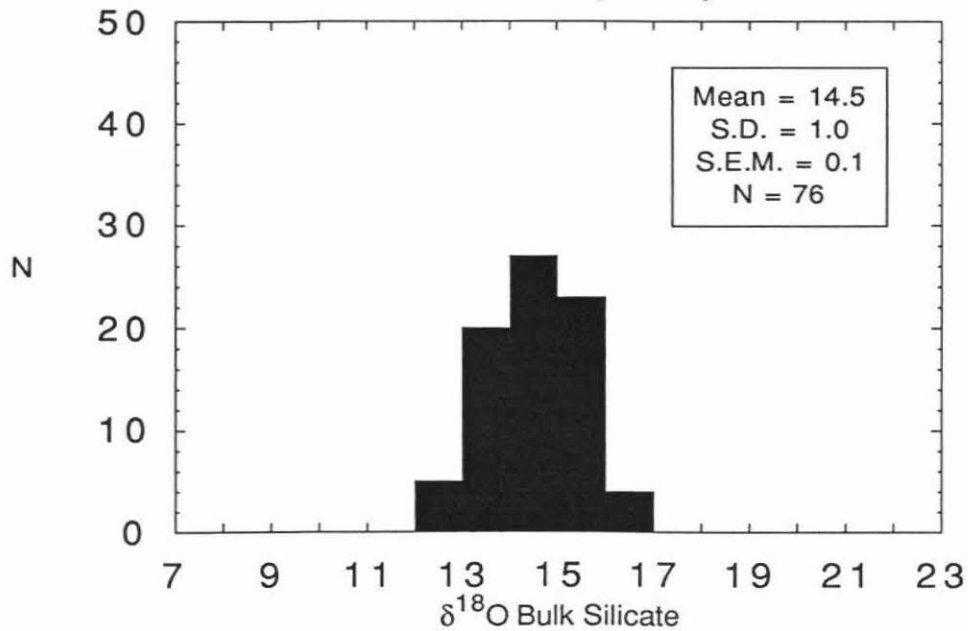


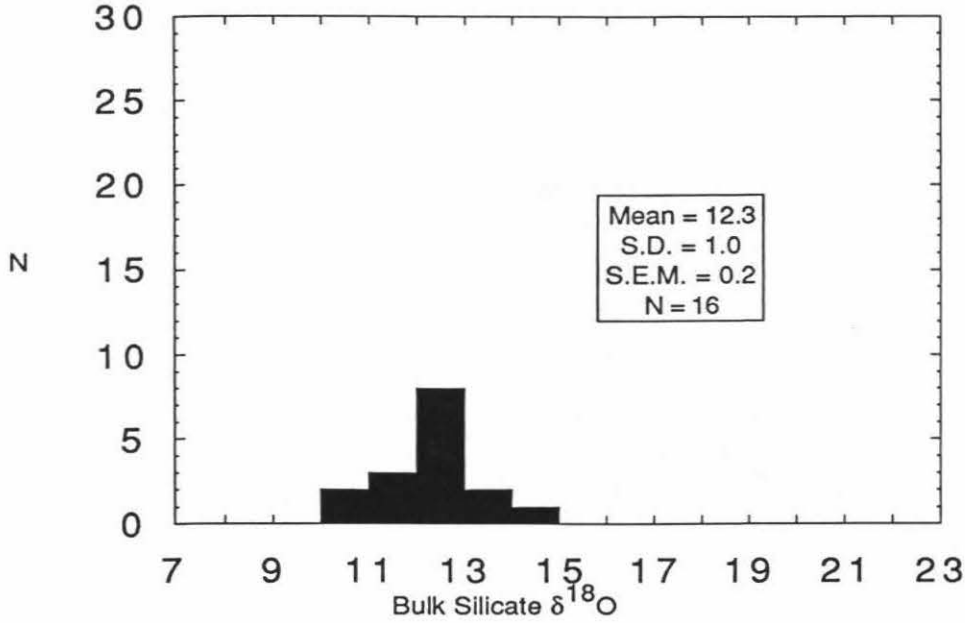
Figure 8.3

Two histograms comparing the bulk silicate $\delta^{18}\text{O}$ of greywackes and shales from a eugeosynclinal environment (the Franciscan Formation of the California Coast Ranges) based on analyses by Magaritz and Taylor (1976). Although one group of the eugeosynclinal shales is relatively high in ^{18}O , the mean bulk silicate $\delta^{18}\text{O}$ is lower for both eugeosynclinal greywackes and shales as compared to the marine sandstones and shales studied in this work, most of which are from miogeosynclinal regions of the Central Appalachians and the Ouachita Mountains (Compare Figures 8.2 and 8.3.)

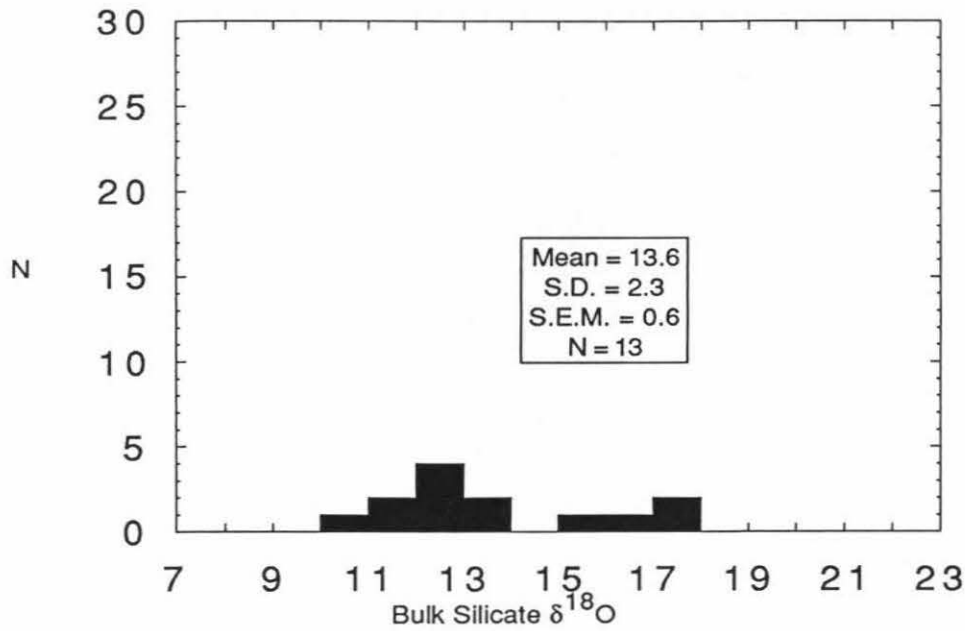
Figure 8.4

Two histograms comparing all available bulk silicate $\delta^{18}\text{O}$ values for sandstones and shales in this study and the literature.

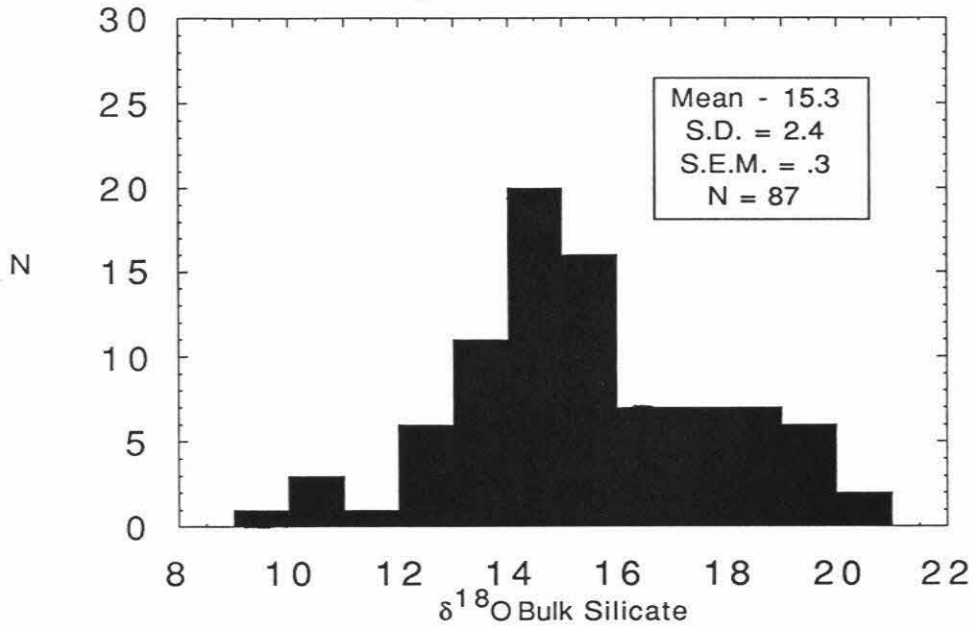
Bulk Silicate $\delta^{18}\text{O}$ Distribution Greywackes



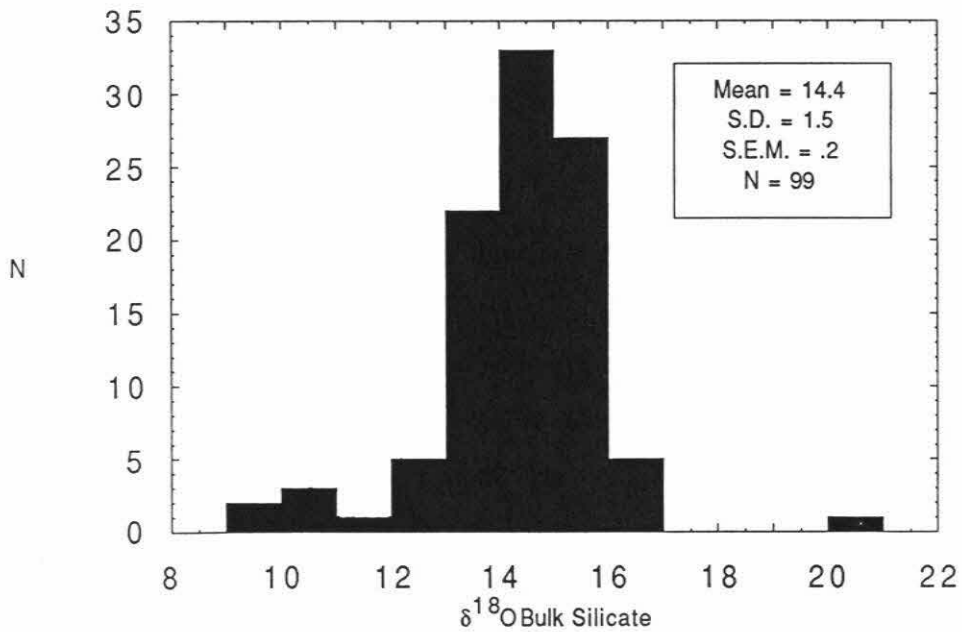
Bulk Silicate $\delta^{18}\text{O}$ Distribution Eugeosynclinal Shales



Bulk Silicate $\delta^{18}\text{O}$
All Shale Samples:
This Study and Literature Review



Bulk Silicate $\delta^{18}\text{O}$
All Sandstone Samples:
This Study and Literature Review



Shales are isotopically heavier than sandstones in most cases (Figure 8.4). This is largely due to the abundance of ^{18}O -rich clay minerals in shales relative to sandstones. Chert and carbonate can also cause shales to be isotopically heavy. The presence of a significant feldspar component can also cause shales to be lighter in ^{18}O . However, in the case of the terrigenous miogeosynclinal sediments of the Central Appalachians, the shales and siltstones were found to be very similar in ^{18}O to the sandstones, independent of geologic age. Diagenetic alteration of the clay minerals in shales can shift their bulk silicate $\delta^{18}\text{O}$ to lighter values, and it is believed that this is one of the main reasons why the Central Appalachian shales and sandstones have relatively similar oxygen isotopic compositions.

Terrigenous sedimentary rocks of the Central Appalachians show a remarkably homogeneous bulk silicate $\delta^{18}\text{O}$. In addition to the diagenetic effects described above, a critical factor in this homogeneity probably is the homogeneity of the source material, most of which was derived from a tectonic sourceland to the east. Another critical factor is the mixing process that produced isotopic homogenization of sediment on the scale of the entire Central Appalachian basin. A continental margin which experienced three major episodes of uplift, erosion, and deposition -- especially the re-erosion and re-deposition of previous sediments from a similar sourceland -- greatly facilitated this homogenization.

Terrigenous sedimentary rocks of the Colorado Plateau show a regional trend in bulk silicate $\delta^{18}\text{O}$. This is interpreted to be the result of incomplete mixing of sediment from at least two isotopically distinct sources. A low- $\delta^{18}\text{O}$ source from the craton to the northeast, and a high- $\delta^{18}\text{O}$ source from the Cordilleran miogeosyncline to the southwest.

As a result of this incomplete mixing, there is a somewhat larger dispersion in bulk silicate $\delta^{18}\text{O}$ in the Colorado Plateau as compared to the Central Appalachians. Sandstones of the Colorado Plateau are somewhat lighter isotopically than those of the Central Appalachians when the two bentonite-containing samples are excluded from the Colorado Plateau samples. This is attributed to the greater maturity of the sediment in the Colorado Plateau as evidenced by the abundance of quartz arenites and feldspathic arenites in the Colorado Plateau region as compared to the preponderance of lithic arenites in the Central Appalachians.

Sandstones of the Ouachita Mountains apparently experienced less sediment mixing than the Central Appalachians and they also show greater dispersion of bulk silicate $\delta^{18}\text{O}$ values. While the geologic setting of the Ouachita Mountains is a matter of debate, they almost certainly did not undergo the same degree of sediment recycling that was experienced by the Central Appalachians during three major Paleozoic orogenies. The mean bulk silicate $\delta^{18}\text{O}$ of the Ouachita Mountain sandstones is nevertheless only 0.2 per mil heavier than that for the Central Appalachian sandstones, which would not be inconsistent with an isotopically similar sediment source for both convergent margins. The hypothesized western miogeosynclinal source for the Colorado Plateau region is also quite similar to these two regions in bulk silicate $\delta^{18}\text{O}$.

As mentioned above, pelagic sediments have the greatest range in $\delta^{18}\text{O}$ of all the sedimentary environments discussed. Unique conditions allow for the deposition of materials with extreme $\delta^{18}\text{O}$ values, such as siliceous oozes, calcareous oozes, iron and manganese oxides, and hydrothermally altered clay minerals. Pelagic sediments from these diverse sources do not usually experience the type of extensive mixing phenomena

active at continental margins such as the Central Appalachians.

These mixing phenomena, which are largely a result of tectonic processes, can also obliterate variations in source $\delta^{18}\text{O}$ with geologic time. This may explain why there are no overall correlations of $\delta^{18}\text{O}$ with geologic age in the regions studied and why there are some correlations of geologic age with $\delta^{18}\text{O}$ for the relatively undisturbed pelagic sediments. The exception to this is the Central Appalachian siltstones which may be fortuitously correlated with age because of the general correlation of conodont alteration index with age.

This study has shown that burial diagenesis can play a role in the oxygen isotopic homogenization of sediments. The most evident effects of this process are in the Paleozoic siltstones and shales of the Central Appalachians, which apparently underwent ^{18}O depletion when they were subjected to temperatures of burial diagenesis up to 300°C . A significant correlation of siltstone and shale bulk silicate $\delta^{18}\text{O}$ with conodont color alteration index was also found in the Central Appalachians. A significant correlation was also found between mean vitrinite reflectance and the difference between shale and sandstone bulk silicate $\delta^{18}\text{O}$ for shale-sandstone pairs in a reconnaissance study of the Ouachita Mountains. The correlations with conodont color alteration index and with vitrinite reflectance are attributed to changes in bulk silicate $\delta^{18}\text{O}$ due to diagenetic alteration. Linear regressions of bulk silicate $\delta^{18}\text{O}$ with conodont color alteration index in the Central Appalachians suggest that the bulk silicate $\delta^{18}\text{O}$ of fine-grained terrigenous sedimentary rocks can be lowered by 2.5 to 4.0 per mil during diagenesis.

Terrigenous-facies miogeosynclinal sediments predominantly have bulk-silicate $\delta^{18}\text{O}$ values of +14 to +16, and thus appear to be more uniform in $\delta^{18}\text{O}$ than was

heretofore thought; such rocks therefore can be used as a baseline marker to monitor bulk changes in the $\delta^{18}\text{O}$ of these kinds of rocks during regional metamorphism. A reconnaissance survey of Northern Appalachian metasedimentary rocks showed a significant decrease in the mean bulk silicate $\delta^{18}\text{O}$ of noncalcareous metasedimentary rocks with increasing metamorphic grade. These metasedimentary rocks have distinctly lower $\delta^{18}\text{O}$ values than the great bulk of the geosynclinal sedimentary rocks from the Central Appalachians studied in this work. This is interpreted to be the result of exchange with large quantities of an isotopically light aqueous fluid at increasing temperatures during prograde metamorphism.

Northern Appalachian carbonate-facies metasedimentary rocks are overall about 5-6 per mil higher in bulk silicate $\delta^{18}\text{O}$ compared to terrigenous-facies metasedimentary rocks in the same area. This difference is preserved at all metamorphic grades and is attributed to the large interbedded high- ^{18}O reservoir of carbonate in these formations. These carbonate-facies rocks also show a decrease in whole rock $\delta^{18}\text{O}$ at garnet grade and higher as compared to their biotite-grade and chlorite-grade equivalents. However, the most clear-cut decrease in ^{18}O occurs at the margins of these formations, adjacent to the terrigenous-facies rocks. The coexisting carbonate and bulk silicate of metamorphosed sedimentary rocks in general do not preserve equilibrium $\delta^{18}\text{O}$ values, even though these values are significantly correlated. Further study is needed to determine if there is an initial increase in bulk silicate $\delta^{18}\text{O}$ of these carbonate-facies rocks at low metamorphic grade and to understand how the role of fluid differs in the diagenesis and metamorphism of the bulk silicate material in calcareous sedimentary rocks as compared to that of terrigenous sedimentary rocks.

REFERENCES

- Aagaard, P., Egeberg, P.K., and Smalley, C.P., 1989. Diagenetic reactions in Leg 104 sediments inferred from isotope and major element chemistry of interstitial waters: In: Edholm, O., Thiede, J. *et al.* (eds), Proceedings of the Ocean Drilling Program. *Scientific Results*, v. **104**, pp. 273-279.
- Anderson, T.F., and Lawrence, J.R., 1976. Stable isotope investigations of sediments, basalts, and authigenic phases from Leg 35 cores: In: Hollister, C.D., Craddock, C. *et al.* (eds), *Initial Reports of the Deep Sea Drilling Project*, v. **35**, U.S. Government Printing Office, Washington, D.C., pp. 497-505.
- Arkle, T., Jr., Beissel, D.R., Larese, R.E., and others, 1979. The Mississippian and Pennsylvanian (Carboniferous) Systems in West Virginia and Maryland, *U.S. Geological Survey Professional Paper 1110-D*, U.S. Government Printing Office, Washington, D.C., p. 35.
- Auramtchev, L., 1985. Carte Geologie du Quebec, Direction General de L'Exploration geologique et minerale.
- Ayalon, A. and Longstaffe, F.J., 1988. Oxygen isotope studies of diagenesis and pore-water evolution in the western Canada sedimentary basin: Evidence from the Upper Cretaceous Basal Belly River Sandstone, Alberta: *Journal of Sedimentary Petrology*, v. **58**, pp. 489-505.
- Baars, D.L., 1987. Paleozoic rocks of Canyonlands Country: In: Campbell, J.A. (ed), *Geology of Cataract Canyon and Vicinity*. Guidebook of the Four Corners Geological Society, Durango, Colorado, pp. 11-16.
- Babaei, A., Viele, G.W., 1992. 2-Decked nature of the Ouachita Mountains, Arkansas. *Geology*, v. **20(11)**, pp. 995-998.
- Baertchi I, P., and Silverman, S.R., 1951. The determination of relative abundances of the oxygen isotopes in silicate rocks: *Geochimica et Cosmochimica Acta*, v. **1**, pp. 317-328.
- Barnett, D.E. and Chamberlain, C.P., 1991. Relative scales of thermal- and fluid infiltration-driven metamorphism in fold nappes, New England, U.S.A.: *American Mineralogist*, v. **76**, pp. 713-727.
- Barrett, T.J., Jarvis, I., Longstaffe, F.J., Farquhar, R., 1988. Geochemical Aspects of Hydrothermal Sediments in the Eastern Pacific Ocean: An Update: *Canadian Mineralogist*, v. **26**, pp. 841-858.

- Barrett, T.J., Friedrichsen, H., and Fleet, A.J., 1983. Elemental and stable isotopic composition of some metalliferous and pelagic sediments from the Galapagos Mounds Area, Deep Sea Drilling Project Leg 70: In: Honnorez, J., Von Herzen, R.P., *et al.*, *Initial Reports of the Deep Sea Drilling Project*, v. 70, U.S. Government Printing Office, Washington, D.C., pp. 315-323.
- Baumgartner, L.P., and Ferry, J.M., 1991. A model for coupled fluid-flow and mixed-volatile mineral reactions with applications to regional metamorphism: *Contributions to Mineralogy and Petrology*, v. 106, pp. 273-285.
- Beaumont, C., Quinlan, G., and Hamilton, J., 1988. Orogeny and stratigraphy: numerical models of the Paleozoic in the eastern interior of North America: *Tectonics*, v. 7, pp. 389-416.
- Bennison, A.P., 1986. Geologic highway map of the Mid-Continent Region: American Association of Petroleum Geologists, Tulsa, Oklahoma.
- Berg, T.M., 1980. Geologic Map of Pennsylvania: Pennsylvania Bureau of Topographic and Geologic Survey.
- Bickle, M.J., Wickham, S.M., Chapman, H.J., Taylor, H.P., Jr., 1988. A strontium, neodymium and oxygen isotope study of the hydrothermal metamorphism and crustal anatexis in the Trois Seigneurs Massif, Pyrenees, France. *Contributions to Mineralogy and Petrology*, v. 100, pp. 399-417
- Blakey, R.C., 1989. Triassic and Jurassic geology of the southern Colorado Plateau: In: Jenny, J.P., and Reynolds, S.J. (eds), *Geologic Evolution of Arizona: Arizona Geological Society Digest Number 17*, Tuscon, Arizona, pp. 369-396.
- Blakey, R.C., and Knepp, R., 1989. Pennsylvanian and Permian geology of Arizona. In: Jenny, J.P., and Reynolds, S.J. (eds), *Geologic Evolution of Arizona: Arizona Geological Society Digest Number 17*, Tuscon, Arizona, pp. 313-347.
- Blakey, R.C., and Gubitosa, R., 1983. Late Triassic paleogeography and depositional history of the Chinle Formation, southern Utah and northern Arizona: In: Reynolds, M.W., and Dolly, E.D. (eds), *Mesozoic Paleogeography of the West-Central United States, Rocky Mountain Paleogeography Symposium 2: Rocky Mountain Section of the Society of Economic Paleontologists and Mineralogists*, Denver, Colorado, pp. 57-76.
- Blakey, R.C., 1980. Pennsylvanian and Early Permian paleogeography, southern Colorado Plateau and vicinity: In: Fouch, T.D., and Magathan, E.R. (eds), *Paleozoic Paleogeography of the West-Central United States*, Society of Economic Paleontologists and Mineralogists, Rocky Mountain Section, Denver, Colorado, pp. 239-257.

- Blakey, R.C., 1979, Lower Permian Stratigraphy of the southern Colorado Plateau: In: Baars, D.L. (ed), *Permianland*, Four Corners Geological Society Guidebook, 9th Field Conference, Durango, Colorado, pp. 115 - 129.
- Bray, C.J., Spooner, E.T.C., and Longstaffe, F.J., 1988. Unconformity-related uranium mineralization, Mclean Deposits, North Saskatchewan, Canada: hydrogen and oxygen isotope geochemistry: *Canadian Mineralogist*, v. **26**, pp. 249-268.
- Butts, C., 1933. Geologic map of the Appalachian Valley of Virginia with explanatory text: *Virginia Geological Survey Bulletin*, v. **42**.
- Cadigan, R.A., and Stewart, J.H., 1972. Petrology of the Triassic Moenkopi Formation and related strata in the Colorado Plateau Region, *U.S. Geological Survey Professional Paper 692*, U.S. Government Printing Office, Washington, D.C., p. 70.
- Cady, W.M., 1960. Stratigraphic and geotectonic relationships in northern Vermont and southern Quebec: *Geological Society of America Bulletin*, v. **71**, pp. 531-576.
- Cady, W.M., 1968. The lateral transition from the miogeosynclinal to the eugeosynclinal zone in northwest New England and adjacent Quebec. In: Zen, E., White, S.W., Hadley, J.B., and Thompson, J.B., Jr., (eds), *Studies of Appalachian Geology: Northern and Maritime*, Interscience Publishers, New York, pp. 151-161.
- Cady, W.M., Albee, A.L., Murphy, J.F., 1962. Bedrock geology of the Lincoln Mountain Quadrangle, Vermont, U.S. Geological Survey Quadrangle Map GQ-164.
- Calver, J.L., 1963. Geologic map of Virginia: Division of Mineral Resources, Charlottesville, Virginia.
- Cardwell, D.H., Erwin, R.B., Woodward, H.P., 1986. Geologic Map of West Virginia: West Virginia Geological and Economic Survey.
- Chamberlain, C.P., Ferry, J.M., Rumble, D., III, 1990. The effect of net-transfer reactions on the isotopic composition of minerals: *Contributions to Mineralogy and Petrology*, v. **105**, pp. 322-336.

- Chamberlain, C.P., and Rumble, D., III, 1989. The influence of fluids on the thermal history of a metamorphic terrain: New Hampshire, USA: In: Daly, J.S., Cliff, R.A., Yardley, B.W.D. (eds), *Evolution of Metamorphic Belts. Geological Society Special Publication No. 43*, Blackwell Scientific Publications, Oxford, England, pp. 203-213.
- Chamberlain, C.P., and Rumble, D., III, 1988. Thermal anomalies in a Regional metamorphic terrane: an isotopic study of the role of fluids: *Journal of Petrology*, v. **29**, pp. 1215-1232.
- Christman, R.A., and Secor, D.T., Jr., 1961. Geology of the Camel's Hump Quadrangle, Vermont: *Vermont Geological Survey Bulletin 15*, p. 70.
- Churchman, G.J., Clayton, R.N., Sridhar, K., and Jackson, M.L., 1976. Oxygen isotopic composition of aerosol size quartz in shales. Univ. Wis., Madison, Wis., United States, Univ. Chic., United States. *Jour. Geophys. Res.*, 81 v. **3**, pp. 381-386.
- Clayton, R.N., O'Neil, J.R., Mayeda, T.K., 1972a. Oxygen isotope exchange between quartz and water: *Journal of Geophysical Research*, V. **77**, pp. 3057-3067.
- Clayton, R.N., Rex, R.W., Syers, J.K., Jackson, M.L., 1972b. Oxygen isotope abundances in quartz from Pacific pelagic sediments, *Journal of Geophysical Research*, v. **77**, pp. 3907-3913.
- Clayton, R.N., Friedman, I., Graf, D.L., Mayeda, T.K., Meents, W.F., and Shimp, N.F. 1966. The origin of saline formation waters--(Pt.) 1, Isotopic composition. *Jour. Geophys. Res.*, V. **71**, no. 16, pp. 3869-3882.
- Clayton, R.N. and Epstein, S. 1958. The relationship between $^{18}\text{O}/^{16}\text{O}$ ratios in coexisting quartz, carbonate, and iron oxides from various geological deposits. *Joru. Geology*, v. **66**, no. 4, pp. 352-373.
- Cleaves, E.T., Edwards, J.E., Jr., Glaser, J.D., 1968. Geologic Map of Maryland, Maryland Geological Survey.
- Compton, R.R., 1960. Contact metamorphism in Santa Rosa Range, Nevada: *Bulletin of the Geological Society of America*, v. **71**, pp. 1383-1416.
- Cotter, E., 1983. Shelf, paralic, and fluvial environments and eustatic sea-level fluctuation in the origin of the Tuscarora formation (Lower Silurian) of central Pennsylvania, *Journal of Sedimentary Petrology*, v. **53**, pp. 25-49.
- Craig, H., 1961, Standard for reporting concentrations of deuterium and oxygen-18 in natural waters: *Science*, v. **133**, pp. 1833-1834.

- Craig, H., 1957. Isotopic standards for mass-spectrometric analysis of carbon dioxide: *Geochimica et Cosmochimica Acta*, v. **12**, pp. 133-149.
- Craig, L.C., and Shawe, D.R., 1975. Jurassic rocks of East-Central Utah: In: Fasset, J.E. (ed), *Canyonlands Country. A guidebook of the Four Corners Geological Society*, Durango, Colorado, pp. 157-166.
- David, J., Gariépy, C., Philippe, S., 1991. Lower paleozoic tholeiitic dykes from central New Brunswick: possible evidence for the early opening of an ensialic Taconian back-arc: *Canadian Journal of Earth Sciences*, v. **28**, pp. 1444-1454.
- Davis, M.W., and Ehrlich, R., 1974. Late Paleozoic crustal composition and dynamics in the Southeastern United States: *Geological Society of America Special Paper 148*, Bolder, Colorado, pp. 171-185.
- Decker, C.E., 1952. Stratigraphic significance of the Athens shale: *American Association of Petroleum Geologists Bulletin*, v. **36**, pp. 1-145.
- Degens, E.G., and Epstein, S., 1962. Relationship between coexisting $^{18}\text{O}/^{16}\text{O}$ ratios on coexisting carbonates, cherts, and diatomites: *American Association of Petroleum Geologists Bulletin*, v. **46**, pp. 534-542.
- Doll, C.G., 1961. Centennial Geologic Map of Vermont: Vermont Geological Survey, Montpelier, Vermont.
- Doll, C.G., Cady, W.M., Thompson, J.B., Billings, M.P., 1961. Centennial geologic map of Vermont. 1:250,000, Vermont Geological Society.
- Donohoe, H.V., Jr., and Grantham, R.G., 1989. Geologic highway map of Nova Scotia, second edition: *Atlantic Geoscience Society, Special Publication Number 1*, Halifax, Nova Scotia.
- Douglas, R.G., and Savin, S.M., 1975. Oxygen and carbon isotope analyses of Tertiary and Cretaceous microfossils from the Shatsky Rise and other sites in the North Pacific Ocean: In: Larson, R.L., and Moberly, R. et al. (eds), *Initial Reports of the Deep Sea Drilling Project*, v. **32**, U.S. Government Printing Office, Washington, D.C., pp. 509-520.
- Douglas, R.G., Savin, S.M. 1973. Oxygen and carbon isotope analyses of Cretaceous and Tertiary foraminifera from the central North Pacific: In: Winterer, E.L., Ewing, J.I. et al. (eds), *Initial Reports of the Deep Sea Drilling Project*, v. **17**, U.S. Government Printing Office, Washington, D.C., pp. 591-605.

- Duba, D., and William-Jones, A.E., 1983. Studies of burial metamorphism in the post-Taconic stage of the Appalachian orogen, southwestern Gaspe: *Canadian Journal of Earth Sciences*, v. **20**, pp. 1152-1158.
- Dugion, M.T., and Dine, J.R., 1987. Water resources of Frederick County, Maryland: *Maryland Geological Survey Bulletin 33*, p. 106.
- Dulong, F.T., and Cecil, C.B., 1989. Stratigraphic variation in bulk sample mineralogy of Pennsylvanian underclays from the central Appalachian basin: Coal and Hydrocarbon resources of North America, v. **2**, *American Geophysical Union*, Washington D.C., pp. 112-118.
- Dutton, S.P., and Land, L.S., 1988. Cementation and burial history of a low-permeability quartzarenite, Lower Cretaceous Travis Peak Formation, East Texas: *Geochimica et Cosmochimica Acta*, v. **100**, pp. 1271-1282.
- Dymond, J., Corliss, J.B., Heath, G.R., Field, E.J., Veeh, H.H., 1973. Origin of metalliferous sediments from the Pacific Ocean: *Geological Society of America Bulletin*, v. **84**, pp. 3355-3372.
- Dyni, J.R., Milton, C., Jr., Cashion, W.B., Jr., 1985. The saline facies of the upper part of the Green River Formation near Duschene, Utah: in Picard, M. D. (ed), *Geology and Energy Resources*, Uinta Basin of Utah, Utah Geological Association, Salt Lake City, Utah, pp. 51-60.
- Eaton, J.G., 1991. Biostratigraphic framework for the Upper Cretaceous rocks of the Kaiporowitz Plateau, southern Utah: In: Nations, J.D., and Eaton, J.G. (eds), Stratigraphy, depositional environments, and sedimentary tectonics of the Western Margin, Cretaceous Interior Seaway, *Geological Society of America Special Paper 260*, pp. 47-64.
- Egeberg, P.K., Aagaard, P., And Smalley, P.C., 1990. Major element and oxygen isotope studies of interstitial waters: ODP Leg 113: In: Barker, P.F., and Kennet, J.P. et al. (eds), *Proceedings of the Ocean Drilling Program*, v. **113**, pp. 135-146.
- Elliot, W.C., and Aronson, J.L., 1990, *Geological Society of America Abstracts*, v. **22**, p. A62.
- Epstein, A.G., Epstein, J.B., and Harris, L.D., 1977. Conodont color alteration - an index to organic metamorphism: *Geological Survey Professional Paper 995*, United States Government Printing Office, Washington D.C., p. 27.
- Epstein, S., Buchsbaum, R, Lowenstam, H.A., and Urey, H.C., 1951. Carbonate-water isotopic temperature scale. *Gol. Soc. America Bull.*, v. **62**, pp. 417-425.

- Eslinger, E.V., and Savin, S.M., 1973. Oxygen isotope geothermometry of the burial metamorphic rocks of the Precambrian Belt Supergroup: *Geological Society of America Bulletin*, v. **84**, pp. 2449-2560.
- Eslinger, E.V., and Yeh, H-W, 1986. Oxygen and hydrogen isotope geochemistry of Cretaceous bentonites and shales from the Disturbed Belt, Montana: *Geochimica et Cosmochimica Acta* v. **50**, pp. 59-68.
- Ferguson, Laing, and Fyffe, L.R., 1985. Geologic highway map of New Brunswick and Prince Edward Island: *Atlantic Geoscience Society, Special Publication Number 2*.
- Ferry, J.M., 1992. Regional metamorphism of the Waits River Formation, Eastern Vermont: Delineation of a new hydrothermal system. *Journal of Petrology*, v. **33**. pp. 45-94.
- Ferry, J.M., 1988a. Contrasting mechanisms of fluid flow through adjacent stratigraphic units during regional metamorphism, south-central Maine, USA: *Contributions to Mineralogy and Petrology*, v. **98**, pp. 1-12.
- Ferry, J.M., 1988b. Infiltration-driven metamorphism in northern New England, USA: *Journal of Petrology*, v. **29**, pp. 1121-1159.
- Ferry, J.M., 1987. Metamorphic hydrology at 13-km depth and 400-550° C: *American Mineralogist*, v. **72**, pp. 39-58.
- Ferry, J.M., 1986. Infiltration of aqueous fluid and high fluid: rock ratios during greenschist facies metamorphism: a reply: *Journal of Petrology*, v. **27**, pp. 695-714.
- Ferry, J.M., 1984. A biotite isograd in south-central Maine, USA: mineral reactions, fluid transfer, and heat transfer: *Journal of Petrology*, v. **25**, pp. 871-893.
- Ferry, J.M., 1983. Regional metamorphism of the Vassalboro Formation, south-central Maine, USA: A case study of the role of fluid in metamorphic petrogenesis: *Journal of the Geological Society of London*, v. **140**, pp. 551-576.
- Finlayson, C.P., Barnes, R.H., Colvin, J.M., Jr., Luther, E.T., 1964. Geologic Map and Mineral Resources Summary of the Chatanooga Quadrangle, Tennessee, Tennessee Geological Division, Nashville, Tennessee.
- Fisher, R.S. and Land, L.S., 1986, Diagenetic history of Eocene Wilcox sandstones, south-central Texas, *Geochimica et Cosmochimica Acta*, v. **50**, pp. 551-561.

- Fisher, G.W., and Karabinos, P., 1980. Stratigraphic sequence of the Gile Mountain and Waits River Formations near Ryalton, Vermont. *Geol Soc. Am. Bull.*, v. **91**, pp. 282-286.
- Fisher, D.W., Isachsen, Y.W., Rickard, L.V., 1970. Geologic Map of New York, New York State Museum and Science Service Map and Chart Series Number 15.
- Fleck, R.J., and Criss, R.E., 1985, Strontium and oxygen isotope variations in Mesozoic and Tertiary plutons of central Idaho: *Contributions to Mineralogy and Petrology*, v. **90**, pp. 291-308.
- Folk, R.L., Andrews, P.B., and Lewis, D.W., 1970, Detrital sedimentary rock classification and nomenclature for use in New Zealand: *New Zealand Journal of Geology and Geophysics*, v. **13**, pp. 937-968.
- Folk, R.L., 1960, Petrography and origin of the Tuscarora, Rose Hill, and Keefer Formations, Lower and Middle Silurian of eastern West Virginia: *Journal of Sedimentary Petrology*, v. **30**, pp. 1-58.
- Friedman, G.M., Sanders, J.E., 1978, Principles of Sedimentology, John Wiley and Sons, New York.
- Gallagher, R.A., Parks, J.M., 1983, Depositional environments of the Loyalhanna Member of the Mauch Chunk Formation, north-central Pennsylvania: *Geological Society of America Abstracts with Programs*, v. **15**, n. 3, pp. 127.
- Garlick, D.G., 1974, The stable isotopes of oxygen, carbon, and hydrogen in the marine environment. In: Goldberg, E.D. (ed), *The Sea*, v. **5 Marine Chemistry**, John Wiley and Sons, New York, pp. 393-425.
- Garlick, C.D. and Epstein, S., 1967, Oxygen isotope ratios in coexisting minerals of regionally metamorphosed rocks: *Geochimica et Cosmochimica Acta*, v. **31**, pp. 181-214.
- Goldstein, A., Jr., and Reno, D.H., 1952, Petrography and metamorphism of sediments of Ouachita facies: *Bulletin of the Association of American Petroleum Geologists*, v. **36**, pp. 2275-2290.
- Gray, D.R., Gregory, R.T., and Durney, D.W., 1991. Rock-buffered fluid-rock interaction in deformed quartz-rich turbidite sequences, Eastern Australia. *J. Geo. R. Sol.*, v. **96**, (NB12), pp. 9681-9704.

- Gregory, R.T. and Criss, R.E., 1986, Isotopic exchange in open and closed systems: In: Valley, J.W., Taylor, H.P., Jr., and O'Neil, J.R. (eds), *Stable Isotopes in High Temperature Geological Processes, Reviews in Mineralogy*, v. 16, Mineralogical Society of America, Washington, D.C., pp. 91-128.
- Gregory, R.T., and Taylor, H.P., Jr., 1981, An oxygen isotope profile in a section of the Cretaceous oceanic crust, Somal Ophiolite, Oman: Evidence for $d^{18}O$ buffering of the oceans by deep (> 5 km) seawater-hydrothermal circulation at mid-ocean ridges, *Journal of Geophysical Research*, v. 86, pp. 2737-2755.
- Guthrie, J. M., Houseknecht, D. W. , Johns, W. D., 1986. Relationships among vitrinite reflectance, illite crystallinity, and organic geochemistry in Carboniferous strata, Ouachita Mountains, Oklahoma and Arkansas. *American Association of Petroleum Geologists Bulletin*, v. 70, pp. 26-33.
- Hackman, R.J., and Wyant, D.G., 1973. Geology, structure, and uranium deposits of the Escalante Quadrangle, Utah and Arizona, Miscellaneous geological map investigations map I-744: U.S. Geological Survey, Washington, D.C.
- Hall, L.M., 1959. The Geology of the St. Johnsbury Quadrangle, Vermont and New Hampshire, Vermont Geological Survey Bulletin 13, p. 105.
- Hardeman, W.D., 1966. Geologic Map of Tennessee, Tennessee Division of Geology, Nashville, Tennessee.
- Hatch, N.L. 1988a. Some revisions to the stratigraphy and structure of the Connecticut Valley Trough, eastern Vermont. *Am. J. Science*, v. 288, pp. 1041-1059.
- Hatch, N.L. 1988b. New evidence for faulting along the "Monroe line", eastern Vermont and westernmost New Hampshire. *Am. J. Science*, v. 288, pp. 1-18.
- Hatcher, R.D., Thomas, W.A., Viele, G.W. (eds), The Appalachian-Ouachita Orogen in the United States, The geology of North America. v. F-2: *Geological Society of America*, Boulder, Colorado, p. 767.
- Haynes, D.D., Vogel, J.D., and Wyant, D.G., 1972. Geology, structure, and uranium deposits of the Cortez Quadrangle, Colorado, and Utah, Miscellaneous geological map investigations map I-629: U.S. Geological Survey, Washington, D.C.
- Hein, J.R., Yeh, H-W, Alexander, E., 1979. Origin of iron-rich montmorillonite from the manganese nodule belt of the North Equatorial Pacific: *Geochimica et Cosmochimica Acta*, v. 27, pp. 185-194.

- Hintze, L.F., 1988. Geologic history of Utah, A field guide to Utah's rocks: Brigham Young University Geology Studies, *Special Publications 7*, Provo, Utah.
- Hintze, L.F., 1984. Geologic highway map of Utah: Department of Geology, Brigham Young University, University Geology Studies Special Publication Number 3, Provo, Utah.
- Hintze, L.F., 1963. Geologic map of Southwest Utah: Department of Geology, Brigham Young University, Provo, Utah.
- Hoffman, R.B., 1984. Depositional environment and regional correlation of the Ridgely Member of the Old Port Formation: *Geological Society of America Abstracts with Programs*, v. **16**, n. 1, p. 24.
- Hoque, M.U., 1968. Sedimentologic and paleocurrent study of Mauch Chunk sandstones (Mississippian), south-central and western Pennsylvania: *American Association of Petroleum Geologists Bulletin*, v. **52**, pp. 246-263.
- Hosterman, J. W., and Whitlow, S.I., 1983. Clay mineralogy of Devonian shales in the Appalachian Basin, Geological Survey Professional Paper 1298, U.S. Government Printing Office, Washington D.C., p. 31.
- Houseknecht, D.W., and Matthews, S.M., 1985. Thermal maturity of Carboniferous strata, Ouachita Mountains: *American Association of Petroleum Geologists Bulletin*, v. **69**, pp. 335-345.
- Hower, J., Eslinger, E.V., Hower, M., and Perry, E.A., 1976. The mechanism of burial metamorphism of argillaceous sediments: 1. Mineralogical and chemical evidence: *Geological Society of America Bulletin*, v. **87**, pp. 725-737.
- Hueber, F.S., Bothner, W.A., Hatch, N.L., Finney, S.C., and Aleinikoww, J.N. 1990. Devonian plants from southern Quebec and northern New Hampshire and the age of the Connecticut valley trough. *Am J Science*, v. **290**, pp. 360-395.
- Hummel, J.M., 1969. Anatomy of a gas field - clay basin Dagget County, Utah. In: Lindsay J.B., (ed.), *Geologic Guidebook of the Unita Mountains*. Intermountain Association of Geologists, Salt Lake City, Utah, p. 123.
- Jado, A.R., 1980. Paleogeographic interpretation of Permian units in northwest Colorado and northeast Utah: In: Fouch, T.D., and Magathan, E.R. (eds), *Paleozoic Paleogeography of the West-Central United States*, Society of Economic Paleontologists and Mineralogists, Rocky Mountain Section, Denver, Colorado, pp. 293-304.

- Johansen, S.J., 1988. Origins of upper Paleozoic quartzose sandstones, American southwest: *Sedimentary Geology*, v. **56**, pp. 153-166.
- Jones, D.L., and Knauth L.P., 1979, Oxygen isotopic and petrographic evidence relevant to the origin of the Arkansas Novaculite: *Journal of Sedimentary Petrology*, v. **49**, pp. 581-598.
- Kay, M. 1951. North American Geosynclines. Geological Society of America Memo, no. 48, p. 143.
- Knauth, L.P., 1973. Oxygen and hydrogen isotope ratios in cherts and related rocks. Doctoral dissertation, California Institute of Technology, Pasadena, California.
- Keith, M.L., Weber, J.N., 1964. Carbon and oxygen isotopic composition of selected limestones and fossils. *Geochim. et Cosmochim. Acta.*, v. **28**, no. 11, pp. 1787-1816.
- Keller, W.D., Stone, C.G., and Hoersch, A.L., 1985. Textures of Paleozoic chert and novaculite in the Ouchita Mountains of Arkansas and Oklahoma and their geologic significance: *Geological Society of America Bulletin*, v. **96**, pp. 1353-1363.
- Keperfle, R.C., 1977. Stratigraphy, petrology, and depositional environment of the Kenwood Siltstone Member, Borden Formation, (Mississippian) Kentucky and Indiana: United States Geological Survey Professional Paper 1007, p. 49.
- Keppie, J.D., 1989. Northern Appalachian terranes and their accretionary history In Dallmeyer, R.D. (ed), *Terranes in the Circum-Atlantic Paleozoic Origins*, Geological Society of America Special Paper 230, pp. 159-192.
- Keppie, J.D., 1982. Tectonic map of the province of Nova Scotia: Geologic Survey of Canada, Department of Mines and Energy.
- Keppie, J. D., 1979. Geologic map of the province of Nova Scotia: Geologic Survey of Canada, Nova Scotia Department of Mines and Energy.
- Keith, M.L. and Weber, J.N. 1964. Carbon and oxygen isotopic composition of selected limestone and fossils. *Geochim. et Cosmochim. Acta.* v. **28**, no. 11, pp. 1787-1816.
- Knauth, L.P., and Lowe, D.R., 1978. Oxygen isotope geochemistry of cherts from the Onverwacht Group (3.4 billion years), Transvaal, South Africa, with implications for secular variations in the isotopic compositions of cherts: *Earth and Planetary Science Letters*, v. **41**, pp. 209-222.

- Knauth, L.P., and Epstein, S., 1976. Hydrogen and oxygen isotope ratios in nodular and bedded cherts: *Geochimica and Cosmochimica Acta*, v. 40, pp. 1095-1108.
- Koemel, M.J., 1986. Post-Mississippian paleotectonic, stratigraphic, and diagenetic history of the Weber Sandstone in the Rangely Field Area, Colorado In: J.A. Peterson, Paleotectonics and sedimentation in the Rocky Mountain Region, United States, *American Association of Petroleum Geologists Memoir 41*, U.S. Geological Survey, Billings, Montana, pp. 371-396.
- Kolodny, Y., and Epstein, S., 1976. Stable isotope geochemistry of deep sea cherts: *Geochimica and Cosmochimica Acta*, v. 40, pp. 1195-1209.
- Krieger, M.H., 1958. Geologic map of Yavapai County, Arizona, Arizona Bureau of Mines, University of Arizona, Tuscon, Arizona.
- Kubler, B., 1968, Évaluation quantitative du métamorphisme par la cristallinité de l'illite; état des progrès réalisés dernières années: *Bulletin du centre de Recherches de Pau*, v. 2, pp. 385-397.
- Lajoie, J., Lesperence, P.J., and Beland, J., 1968. Silurian stratigraphy and paleogeography of Matapedia-Temiscouta region, Quebec: *American Association of Petroleum Geologists Bulletin*, v. 52, pp. 615-640.
- Land, L.S., 1984. Frio sandstone diagenesis, Texas Gulf Coast: a regional isotopic study: In: Surdam, R.C., and MacDonald, D.A. (eds), *Clastic Diagenesis*, *American Association of Petroleum Geologists Memoir 37*, pp. 47-62.
- Land, L.S., and Fisher, R.S., 1987. Wilcox sandstone diagenesis, Texas Gulf Coast: a regional isotopic comparison with the Frio Formation: In: Marshall, J.D. (ed), *Diagenesis of Sedimentary Sequences. Geological Society Special Publication Number 36*, pp. 219-235.
- Land, L.S., and Dutton, S.P., 1978. Cementation of a Pennsylvanian deltaic sandstone: isotopic data. *Journal of Sedimentary Petrology*, v. 48, pp. 1167-1176.
- Lawrence, J.R., 1973. Interstitial water studies, Leg 15 - stable oxygen and carbon isotope variations in water, carbonates, and silicates from the Venezuela Basin (Site 149) and the Aves Rise (Site 148): In: Heezen, B.C., MacGregor, I.D., et al.. *Initial Reports of the Deep Sea Drilling Project*, v. 20, U.S. Government Printing Office, Washington, D.C., pp. 891-899.

- Lawrence, J.R., 1974. Stable oxygen and carbon isotope variations in the pore waters, carbonates, and silicates, Sites 225 and 228, Red Sea: In: Whitmarsh, R.B., Weser, O.E., Ross, D.A., et al., *Initial Reports of the Deep Sea Drilling Project*, v. 23, U.S. Government Printing Office, Washington, D.C., pp. 891-899.
- Lawrence, J.R., 1970. $^{18}\text{O}/^{16}\text{O}$ and D/H ratios of soils, weathering zones, and clay deposits: Ph. D. Thesis, California Institute of Technology, Pasadena, CA, p. 263.
- Lawrence, J.R., Drever, J.I., Anderson, T.F., Brueckner, H.K., 1979. Importance of alteration of volcanic material in the sediments of Deep Sea Drilling Site 323: chemistry, $^{18}\text{O}/^{16}\text{O}$, and $^{87}\text{Sr}/^{86}\text{Sr}$: *Geochimica et Cosmochimica Acta*, v. 43, pp. 573-588.
- Lawrence, J.R., and Taylor, H.P., Jr., 1972. Hydrogen and oxygen isotope systematics in weathering profiles: *Geochimica et Cosmochimica Acta*, v. 36, pp. 1377-1303.
- Lawrence, J.R., and Taylor, H.P., Jr., 1971. Deuterium and oxygen-18 correlation: Clay minerals and hydroxides in Quaternary soils compared to meteoric waters: *Geochimica et Cosmochimica Acta*, v. 35, pp. 993-1003.
- Lee, M., Aronson, J.L., and Savin, S.M., 1989. Timing and conditions of Permian Rotliegende Sandstone diagenesis, southern North Sea: K/R and oxygen isotopic data: *American Association of Petroleum Geologists Bulletin*, v. 73, pp. 195-215.
- Lee, M. and Savin, S.M., 1985. Isolation of diagenetic overgrowths on quartz sand grains for oxygen isotopic analysis: *Geochimica et Cosmochimica Acta*, v. 49, pp. 497-501.
- Longstaffe, F.J., and Ayalon, A., 1990. Hydrogen-isotope geochemistry of diagenetic clay minerals from Cretaceous sandstones, Alberta, Canada: evidence for exchange: *Applied Geochemistry*, v. 5, pp. 657-668.
- Longstaffe, F.J., and Ayalon, A., 1987. Oxygen isotope studies of clastic diagenesis in the Lower Cretaceous Viking Formation, Alberta: implications for the role of meteoric water: In: Marshall, J.D. (ed), *Diagenesis of Sedimentary Sequences*, *Geological Society Special Publication Number 36*, pp. 277-296.
- Longstaffe, F.J., 1987a. Stable isotope studies of diagenetic processes, In: Kyser, T.K. (ed), *Short Course in Stable Isotope Geochemistry of Low Temperature Fluids*, *Mineralogical Association of Canada*, Saskatoon, Canada, v. 13, pp. 187-257.

- Longstaffe, F.J., 1987b. Mineralogical and oxygen-isotope studies of clastic diagenesis: implications for fluid flow in sedimentary basins, In: Hitchon, B. (ed), *Hydrogeology of Sedimentary Basins, Third Annual Canadian/American Conference on Hydrogeology*, National Water Well Association, Banff, Alberta, Canada.
- Longstaffe, F.J., 1986a. Diagenesis 4. Stable isotope studies of diagenesis in clastic rocks: *Geoscience Canada*, v. 10, pp. 43-58.
- Longstaffe, F.J., 1986b. Oxygen isotope studies of diagenesis in the basal Belly River sandstone, Pembina I-Pool, Alberta: *Journal of Sedimentary Petrology*, v. 56, pp. 78-88.
- Longstaffe, F.J., 1984. The role of meteoric water in the diagenesis of shallow sandstones: Stable isotope studies of the Milk River aquifer and gas pool: In: Surdam, R.C., and MacDonald, D.A. (eds), *Clastic Diagenesis, American Association of Petroleum Geologists Memoir 37*, pp. 81-98.
- Longstaffe, F.J., Cerny, P., and Muehlenbachs, K., 1981. Oxygen-isotope geochemistry of the granitoid rocks in the Winnipeg River Pegmatite District, southeastern Manitoba: *Canadian Mineralogist*, v. 19, pp. 195-294.
- Longstaffe, F.J., Smith, T.E., and Muehlenbachs, K., 1980. Oxygen isotope evidence for the genesis of Upper Paleozoic granitoids from southwestern Nova Scotia: *Canadian Journal of Earth Sciences*, v. 17, pp. 132-141.
- Longstaffe, F.J., and Schwarcz, H.P., 1977. $^{18}\text{O}/^{16}\text{O}$ of Archean clastic metasedimentary rocks: a petrogenetic indicator for Archean gneisses?: *Geochimica et Cosmochimica Acta*, v. 41, pp. 1330-1312.
- Lowe, D.R., 1985. Ouachita Trough: Part of a Cambrian failed rift system: *Geology*, v. 13, pp. 790-793.
- Lundegard, P.D., and Trevena, A.S., 1990. Sandstone diagenesis in the Pattani Basin (Gulf of Thailand): history of water-rock interaction and comparison with the Gulf of Mexico: *Applied Geochemistry*, v. 5, pp. 669-685.
- Mack, G. H., 1985. Provenance of the Middle Ordovician Blount clastic wedge, Georgia and Tennessee: *Geology*, v 13, pp. 299-302.
- Magaritz, M. and Taylor, H.P., Jr., 1986. Oxygen 18/Oxygen 16 and D/H studies of plutonic granitic metamorphic rocks across the Cordilleran batholiths of southern British Columbia: *Journal of Geophysical Research*, v. 91, pp. 2193-2217.

- Magaritz, M., and Taylor, H.P., Jr., 1976. Oxygen, hydrogen, and carbon isotope studies of the Franciscan formation, Coast Ranges, California: *Geochimica et Cosochemica Acta*, v. **40**, pp. 215-234.
- Marzolf, J.E., 1988. Controls on late Paleozoic and early Mesozoic eolian deposition of the western United States: *Sedimentary Geology*, v. **56**, pp. 167-191.
- Matthews, A., and Kolodny, Y., 1978. Oxygen isotope fractionation in decarbonation metamorphism: the Mottled Zone event: *Earth and Planetary Science Letters*, v. **39**, pp. 179-192.
- McCaig, A.M., Wickham, S.M., Taylor, H.P., Jr., 1990. Deep fluid circulation in alpine shear zones, Pyrenees, France: field and oxygen isotope studies: *Contribution to Mineralogy and Petrology*, v. **106**, pp. 41-60.
- McCrea, J.M., 1950. On the isotopic chemistry of carbonates and a paleotemperature scale: *Chemical Physics*, v. **18**, pp. 849-857.
- McDowell, R.C., Grabowski, J., Jr., Moore, S.L., 1981. Geologic Map of Kentucky: Kentucky Geological Survey.
- McDowell, R.J., 1986. Depositional environments of the upper Chemung and lower Hampshire Formations of east-central West Virginia as determined from subsurface and outcrop data: *Geological Society of America Abstracts with Programs*, v. **18**, n.3, p. 254.
- McKerrow, W.S., and Ziegler, A.M., 1971. The lower Silurian paleogeography of New Brunswick and adjacent areas: *Journal of Geology*, v. **79**, pp. 635-646.
- Meckel, L.D., 1970. Paleozoic alluvial deposition in the central Appalachians: a summary: In: Fisher, G.W., Pettijohn, F.J., Reed, J.C., Jr., Weaver, K.N., *Studies of Appalachian Geology: Central and Southern*, John Wiley and Sons, New York, pp. 49-68.
- Meckel, L.D., 1967. Origin of Pottsville conglomerates (Pennsylvanian) in the central Appalachians: *Geological Society of America Bulletin*, v. **78**, pp. 223-258.
- Milliken, K.L., Land, L.S., Loucks, R.G., 1981. History of burial diagenesis determined from isotopic geochemistry, Frio Formation, Brazoria County, Texas: *American Association of Petroleum Geologists Bulletin*, v. **65**, pp. 1397-1413.
- Miser, H. D., 1954. Geologic map of Oklahoma: United States Geological Survey, Washington, D.C.

- Miser, H.D., 1943. Quartz veins in the Ouachita Mountains of Arkansas and Oklahoma: *Economic Geology*, v. 38, pp. 91-114.
- Molenaar, C.M., 1983. Major depositional cycles and regional correlations in Upper Cretaceous rocks, southern Colorado Plateau and adjacent areas. In: Reynolds, M.W., and Dolly, E.D. (eds), *Mesozoic Paleogeography of the West-Central United States, Rocky Mountain Paleogeography Symposium 2: Rocky Mountain Section of the Society of Economic Paleontologists and Mineralogists*, Denver, Colorado, pp. 201-224.
- Moore, R.T., 1972. Geology of the Virgin and Beaverdam Mountains, Arizona: *Arizona Bureau of Mines Bulletin 186*, University of Arizona, Tucson, Arizona, p. 98.
- Mora, C.I., and Valley, J.W., 1989. Halogen-rich scapolite and biotite: implications for metamorphic fluid-rock interaction: *American Mineralogist*, v. 74, pp. 721-737.
- Morris, R.C., Proctor, K.E., and Koch, M.R., 1979. Petrology and diagenesis of deep-water sandstones, Ouachita Mountains, Arkansas and Oklahoma In: Scholle, P.A., and Schluger, P.R., eds., *Aspects of Diagenesis: Society of Economic Paleontologists and Mineralogists Special Paper 26*, pp. 263-279.
- Muehlenbachs, K. 1987. Oxygen isotope exchange during weathering and low temperature alteration: In: Kyser, T.K. (ed), *Short Course in Stable Isotope Geochemistry of Low Temperature Fluids, Mineralogical Association of Canada*, Saskatoon, Canada, v. 13. pp. 162-186.
- Muehlenbachs, K., 1986. Alteration of the oceanic crust and the ^{18}O history of seawater: In: Valley, J.W., Taylor, H.P., Jr., and O'Neil, J.R. (eds), *Stable Isotopes in High Temperature Geological Processes, Reviews in Mineralogy*, Mineralogical Society of America, Washington, D.C., v. 16, pp. 424-443.
- Muehlenbachs, K. and Clayton, R.N., 1976. Oxygen isotope composition of the oceanic crust and its bearing on seawater: *Journal of Geophysical Research*, v. 81, pp. 4365-4369.
- Nabelek, P.I. 1991. Stable isotope monitors. *Reviews in Mineralogy*. v. 26, pp. 395-435.
- Nabelek, P.I., Labotka, T.C., O'Neil, J.R., Papike, J.J., 1984. Contrasting fluid/rock interaction between the Notch Peak granitic intrusion and argillites and limestones in western Utah: evidence from stable isotopes and phase assemblages: *Contributions to Mineralogy and Petrology*, v. 86, pp. 25-34.

- Nesbitt, B.E., and Muehlenbachs, K., 1991. Stable isotopic constraints on the nature of the syntectonic fluid regime of the Canadian Cordillera: *Geophysical Research Letters*, v. **18**, pp. 963-966.
- Nesbitt, B.E., and Muehlenbachs, K., 1989. Origins and movement of fluids during deformation and metamorphism in the Canadian Cordillera: *Science*, v. **245**, pp. 733-736.
- Niem, A.R., 1977. Mississippian pyroclastic flow and ash-fall deposits in the deep-marine Ouachita flysch basin, Oklahoma and Arkansas: *Geological Society of America Bulletin*, v. **88**, pp. 49-61.
- Odell, M.S., 1970. Geology of the Eagle Rock, Strom, Oriskany, and Salisbury Quadrangles, Virginia: Virginia Division of Mineral Resources Report of Investigations 24, plate 3.
- Oetking, P., 1967. Geologic highway map of the Southern Rocky Mountain Region: American Association of Petroleum Geologists, Tulsa, Oklahoma.
- Ogunyomi, O., Hesse, R., Heroux, Y., 1980. Pre-orogenic and synorogenic diagenesis and anchimetamorphism in the lower paleozoic continental margin sequences of the northern Appalachians in and around Quebec City, Canada: *Bulletin of Canadian Petroleum Geology*, v. **28**, pp. 559-577.
- O'Neil, J.R., 1986. Terminology and Standards, Appendix: In: Valley, J.W., Taylor, H.P., Jr., and O'Neil, J.R. (eds), Stable Isotopes in High Temperature Geological Processes, *Reviews in Mineralogy*, v. **16**, Mineralogical Society of America, Washington, D.C., pp. 561-570.
- Osberg, P.H., 1978. Synthesis of the northeastern Appalachians, U. S. A.: *Geologic Survey of Canada Paper 78-13*, pp. 137-143.
- Osberg, P.H., Tull, J.F., Robinson, P., Hon, R., and Butler, J.R., 1989. The Acadian orogen. In: Hatcher, R.D., Jr., Thomas, W.A. and Viele, G.W. (eds.). The Appalachian-Ouachita Orogen in the United States. *The Geology of North America*, F-2, pp. 179-232.
- Pavlidis, L., 1968. Stratigraphic and facies relationships of the Cary's Mills Formation of Ordovician and Silurian age, northeast Maine: *U.S. Geological Survey Bulletin 1264*, U.S. Government Printing Office, Washington, D.C., p. 44.
- Pavlidis, L., Griscom, A., Kane, M.F., 1965. Geology of the Bridgewater Quadrangle, Aroostook County, Maine: *U.S. Geological Survey Bulletin 1206*, U.S. Government Printing Office, Washington, D.C., p. 72.

- Pelletier, B.R., 1958. Pocono paleocurrents in Pennsylvania and Maryland: *Geological Society of America Bulletin*, v. **69**, pp. 1033-1064.
- Perry, E.C., 1967. The oxygen isotope chemistry of ancient cherts: *Earth and Planetary Science Letters*, v. **3**, pp. 62-66.
- Perry, E.C., Jr., Tan, F.C., and Morey, G.B., 1973. Geology and stable isotope geochemistry of the Biwabik Iron Formation, Northern Minnesota: *Economic Geology*, v. **68**, pp. 1110-1125.
- Perry, E.C., and Tan, F.C., 1972. Significance of oxygen and carbon isotope variations in early Precambrian cherts and carbonate rocks of southern Africa: *Geological Society of America Bulletin*, v. **83**, pp. 647-664.
- Pettijohn, F.J., 1975. *Sedimentary Rocks*, Third edition, Harper and Row, Publishers, San Francisco, pp. 628.
- Pettijohn, F.J., 1963. Chemical composition of sandstones - excluding carbonate and volcanic sands: In: Fleischer, M. (ed), *Data of Geochemistry*, sixth edition, *Geological Survey Professional Paper 440-S*, U.S. Government Printing Office, Washington D.C., pp. S1-S21.
- Pierce, H. W., 1989. Correlation problems of Pennsylvanian-Permian strata of the Colorado Plateau of Arizona: In: Jenny, J.P., and Reynolds, S.J. (eds), *Geologic Evolution of Arizona: Arizona Geological Society Digest Number 17*, Tuscon, Arizona, pp. 349-368.
- Potter, R.P, Hamilton, J.B., Davies, J.L., 1979. *Geologic map of New Brunswick*, second edition, Department of Natural Resources, New Brunswick.
- Reading, H.G., 1978. *Sedimentary Environments and Facies*, Elsevier Publishers, New York, pp. 557.
- Renfro, H.B., and Feray, Dan E., 1970. *Geologic highway map of the Mid-Atlantic Region*: American Association of Petroleum Geologists, Tulsa, Oklahoma.
- Reynolds, S.J., 1988. *Geologic map of Arizona*: United States Geological Survey, Map Number 26, Washington, D.C.
- Rice, C.L., Sable, E.G., Dever, G.R., Jr., Kehn, T.M., 1979. The Mississippian and Pennsylvanian (Carboniferous) Systems in the United States - Kentucky: United States Geological Survey Professional Paper 1110-F, pp. 32.
- Rickard, L.V., and Fisher, D.W., 1970. *Geologic Map of New York*: New York Geological Survey.

- Ruitenbergh, A.A., Fyffe, L.R., McCutcheon, S.R., St. Peter, C.J., Irrinki, R.R., and Venugopal, D.V., 1977. Evolution of pre-carboniferous tectonostratigraphic zones in the New Brunswick Appalachians: *Geoscience Canada*, v. 4, pp. 171-181.
- Rumble, D., III, 1989. Evidences of fluid flow during regional metamorphism: *European Journal of Mineralogy*, v. 1, pp. 731-737.
- Rumble, D., III, 1978. Mineralogy, petrology, and oxygen isotopic geochemistry of the Clough Formation, Black Mountain, western New Hampshire, U.S.A.: *Journal of Petrology*, v. 19, pp. 317-340.
- Rye, D.M., and Williams, N., 1981. Studies of the base metal sulfide deposits at McArthur River, Northern Territory, Australia: III. The stable isotope geochemistry of the H.Y.C., Ridge and Cooley Deposits: *Economic Geology*, v. 76, pp. 1-26.
- Rye, R.O., Schuiling, R.D., Rye, D.M., Jansen, J.B.H., 1976. Carbon, hydrogen, and oxygen isotope studies of the regional metamorphic complex at Naxos, Greece: *Geochimica et Cosmochimica Acta*, v. 40, pp. 1031-1049.
- Rye, R.O., 1966. The carbon, hydrogen, and oxygen isotopic composition of the hydrothermal fluids responsible for the lead-zinc deposits at Providencia, Zacatecas, Mexico: *Economic Geology*, v. 61, pp. 1399-1427.
- St. Julien, P., and Hubert, C., 1975. Evolution of the Taconic orogen in the Quebec Appalachians: *American Journal of Science*, v. 275A, pp. 337-362.
- Savin, S.M., 1980. Oxygen and hydrogen isotope effects in low-temperature mineral-water interactions, In: Fritz, A.P., and Fontes, J., Ch (eds), *Handbook of Environmental Isotope Geochemistry*, v. 1, pp. 283-327.
- Savin, S. M., 1967. Oxygen and hydrogen isotope ratios in sedimentary rocks and minerals: Ph. D. Thesis, California Institute of Technology, Pasadena, CA, p. 220.
- Savin, S.M., and Epstein, S., 1970a. The oxygen and hydrogen isotope geochemistry of clay minerals: *Geochimica et Cosmochimica Acta*, v. 34, pp. 25-42.
- Savin, S.M., and Epstein, S., 1970b. The oxygen and hydrogen isotope geochemistry of ocean sediments and shales: *Geochimica et Cosmochimica Acta*: v. 34, pp. 43-63.

- Savin, S.M., and Epstein, S., 1970c. The oxygen isotopic compositions of coarse grained sedimentary rocks and minerals: *Geochimica et Cosmochimica Acta*, v. **34**, pp. 323-329.
- Savin, S.M., and Yeh, H-W, 1981. Stable isotopes in ocean sediments, In: Emiliani, C. (ed), *The Sea, The Oceanic Lithosphere*, v. **7**, John Wiley and Sons, New York, pp. 1521-1554.
- Schedl, A., McCabe, C., Montanez, I.P., Fullager, P.D., Valley, J.W., 1992. Alleghenian regional diagenesis: a response to the migration of modified metamorphic fluids derived from beneath the Blue Ridge-Piedmont Thrust Sheet: *Journal of Geology*, v. **100**, pp. 339-352.
- Schenk, P.E., 1978. Synthesis of the Canadian Appalachians: *Geologic Survey of Canada Paper 78-13*, pp. 111-136.
- Scotford, D.M., 1951. Structure of the Sugarloaf Mountain area, Maryland, as a key to Piedmont stratigraphy: *Geological Society of America Bulletin*, v. **62**, pp. 45-76.
- Sevon, W.D., 1985. Nonmarine facies of the middle and late Devonian Catskill coastal alluvial plain: In: Woodrow, D.L., and Sevon, W.D., *The Catskill Delta, Geological Society of America Special Paper 201*, pp. 79 - 90.
- Sharma, T., and Clayton, R.N., 1965. Measurement of $^{18}\text{O}/^{16}\text{O}$ ratios of total oxygen from carbonates: *Geochimica et Cosmochimica Acta*, v. **29**, pp. 1347-1353.
- Sheppard, S.M.F., 1986. Characterization and isotopic variations in natural waters, In: Valley, J.W., Taylor, H.P., Jr., and O'Neil, J.R. (eds), *Stable Isotopes in High Temperature Geological Processes, Reviews in Mineralogy*, v. **16**, Mineralogical Society of America, Washington, D.C., pp. 165-184.
- Sheppard, S.M.F., and Schwarcz, H.P., 1970. Fractionation of carbon and oxygen isotopes and magnesium between coexisting metamorphic calcite and dolomite: *Contributions to Mineralogy and Petrology*, v. **26**, pp. 161-198.
- Shieh, Y-N, 1978,. Oxygen isotope studies of rocks across the Grenville Front near Val d'Or, Quebec (Abstract): *Transactions, American Geophysical Union*, v. **59**, p. 407.
- Shieh, Y-N, and Schwarcz, H.P., 1978. The oxygen isotope composition of the surface crystalline rocks of the Canadian Shield: *Canadian Journal of Earth Sciences*, v. **15**, pp. 1773-1782.

- Shieh, Y. N., and Taylor, H.P., Jr., 1969. Oxygen and hydrogen isotope studies of contact metamorphism in the Santa Rosa Range, Nevada and other areas: *Contributions to Mineralogy and Petrology*, v. 20, pp. 306-356.
- Shumaker, R.C., 1967. Bedrock geology of the Pawlett Quadrangle: Part I central and western Portions: *Vermont Geological Survey Bulletin 30*, p. 98
- Siever, R., 1959. Petrology and geochemistry of silica cementation in some Pennsylvanian sandstones: In: Ireland, H. A. (ed), *Silica in Sediments, Society of Economic Paleontologists and Mineralogists Special Publication Number 7*, Tulsa, Oklahoma, pp. 55-79.
- Silverman, S.R., 1951. The isotope geology of oxygen: *Geochimica et Cosmochimica Acta*, v. 2, pp. 26-42.
- Sloss, L.L. (ed), 1988. Sedimentary Cover - North American Craton: U.S., The geology of North America, v. D-2: Geological Society of America, Boulder, Colorado, p. 506.
- Solomon, G.C., 1989. An $^{18}\text{O}/^{16}\text{O}$ study of Mesozoic and Early Tertiary granitic batholiths of the southwestern North American Cordillera: Ph.D. Thesis, California Institute of Technology, Pasadena, California, p. 514.
- Solomon, G.C., and Taylor, H.P., 1989. Isotopic evidence for the origin of Mesozoic and Cenozoic granitic pluton in the Northern Great-Basin. *Geology*, v. 17(7), pp. 591-594.
- Spear, F.S., and Harrison, T.M. 1989. Geochronologic studies in central New England I; evidence for pre-Acadian metamorphism in eastern Vermont. *Geology*, v. 17, pp. 181-184.
- Stern, L.A., Chamberlain, C.P., Barnett, D.E., and Ferry, M. (in preparation). Stable isotopic evidence for regional-scale fluid migration in a Barrovian metamorphic terrane, Vermont, U.S.A.
- Stern, L.A., 1991. Stable isotopic constraints on regional-scale fluid migration in a Barrovian metamorphic terrane, Vermont, USA. MS Thesis, Dartmouth College.
- Stewart, J.H., Poole, F.G., Wilson, R.F., 1972a. Stratigraphy and origin of the Chinle Formation and related Upper Triassic strata in the Colorado Plateau Region, *U.S. Geological Survey Professional Paper 690*, U.S. Government Printing Office, Washington, D.C., p. 336.

- Stewart, J.H., Poole, F.G., Wilson, R.F., 1972b. Stratigraphy and origin of the Triassic Moenkopi Formation and related strata in the Colorado Plateau Region, U.S. *Geological Survey Professional Paper 691*, U.S. Government Printing Office, Washington, D.C., p. 195.
- Stille, H., 1940. Eiführung in den Bau Nordamerikas, Bontrager, Berlin, p. 717.
- Suchecky, R.K., and Land, L.S., 1983. Isotopic geochemistry of burial-metamorphosed volcanogenic sediments, Great Valley sequence, northern California: *Geochimica et Cosmochimica Acta*, v. **47**, pp. 1487-1499.
- Sutter, J.F., Ratcliffe, A.M., Mukasa, S.B., 1985. $^{40}\text{Ar}/^{39}\text{Ar}$ and K-Ar data bearing on the metamorphic and tectonic history of western New England: *Geological Society of America Bulletin*, v. **96**, pp. 123-146.
- Taylor, F.C., 1969. Geology of the Annapolis - St. Mary's Bay map area, Nova Scotia: *Geological Survey of Canada Memoir 358*, p. 65.
- Taylor, F.C., and Schiller, E.A., 1966. Metamorphism of the Meguma Group of Nova Scotia: *Canadian Journal of Earth Sciences*, v. **3**, pp. 959-974.
- Taylor, H.P., Jr. and Silver, L.T., 1978. Oxygen isotope relationships in plutonic igneous rocks of the Penninsular Ranges batholith, southern and Baja California. In: Short Papers of the 4th International Conference on Geochronology, Cosmochronology, and Isotope Geology, (R. E. Zartman, ed.). U.S. Geological Survey Open File Report 78-701, pp. 423-426
- Taylor, H.P., Jr., Albee, A.L., Epstein, S., 1963. $^{18}\text{O}/^{16}\text{O}$ ratios of coexisting minerals in three assemblages of kyanite-zone pelitic schist: *Journal of Geology*, v. **71**, pp. 513-522.
- Taylor, H.P., Jr., and Epstein, S., 1962a. Oxygen isotope studies on the origin of tektites: *Journal of Geophysical Research*, v. **67**, pp. 4485-4490.
- Taylor, H.P., Jr., and Epstein, S., 1962b. Relationship between $\text{O}^{18}/\text{O}^{16}$ ratios in coexisting minerals of igneous and metamorphic rocks, Part 2. Application to petrologic problems: *Geological Society of America Bulletin*, v. **73**, pp. 675-694.
- Teichmüller, M., 1987. Organic material and very low grade metamorphism. In: Frey, M. (ed), *Low Temperature Metamorphism*, Chapman and Hall, New York, pp. 114-161.
- Thompson, A.B., 1983. Fluid-absent metamorphism: *Journal of the Geological Society of London*, v. **140**, pp. 533-547.

- Thompson, J.B., Jr., and Norton, S.A., 1968. Paleozoic regional metamorphism in New England and adjacent areas. In: Zen, E-an, White, W.S., Hadley J.B. and Thompson, J.B., Jr. (eds.). *Studies in Appalachian Geology: Northern and Maritime*. New York: Interscience, pp. 319-327.
- Thompson, J.B., Jr., Robinson, P., Clifford, T.N., and Trask, N.F. 1968. Nappes and gneiss domes in west-central New England. *ibid.* pp. 203-218.
- Tilley, B.J., and Longstaffe, F.J., 1989. Diagenesis and evolution of porewaters in the Alberta Deep Basin: the Falher Member and Cadomin Formation: *Geochimica et Cosmochimica Acta*, v. **53**, pp. 2529-2546.
- Tourtelot, H.A., 1979. Black shale-its deposition and diagenesis: *Clays and Clay Minerals*, v. **27**, pp. 313-321.
- Truesdell, A.H., 1974. Oxygen isotope activities and correlations in aqueous salt solutions of elevated temperatures - consequences for isotope geochemistry. *Earth and Planetary Science Letters*, v. **23**, pp. 387-396.
- Turi, B. and Taylor, H.P., 1971. An oxygen and hydrogen isotope study of a granodiorite pluton from the Southern California batholith: *Geochimica et Cosmochimica Acta*, v. **35**, pp. 383-406.
- Valley, J.W., 1986. Stable isotope geochemistry of metamorphic rocks: In: Valley, J.W., Taylor, H.P., Jr., and O'Neil, J.R. (eds), *Stable Isotopes in High Temperature Geological Processes*, *Reviews in Mineralogy*, v. **16**, Mineralogical Society of America, Washington, D.C., pp. 445-459.
- Valley, J.W., Bohlen, S.R., Essene, E.J., and Lamb, W., 1990. Metamorphism in the Adirondacks: II. The role of fluids: *Journal of Petrology*, v. **31**, pp. 555-596.
- Valley, J.W. and O'Neil, J.R., 1984. Fluid heterogeneity during granulite facies metamorphism in the Adirondacks: stable isotope evidence: *Contributions to Mineralogy and Petrology*, v. **85**, pp. 158-173.
- Veizer, J., and Hoefs, J., 1976. The nature of $^{18}\text{O}/^{16}\text{O}$ and $^{13}\text{C}/^{12}\text{C}$ secular trends in sedimentary carbonate rocks: *Geochimica and Cosmochimica Acta*, v. **40**, pp. 1387-1395.
- Vrolijk, P., Chambers, S.R., Gieskes, J.M., and O'Neil, J.R., 1990. Stable isotope ratios of interstitial fluids from the Northern Barbados accretionary prism, ODP Leg 110: In: Moore, J.C., Mascle, A. *et al.*, (eds), *Proceedings of the Ocean Drilling Program, Scientific Results*, v. **110**, pp. 189-205.

- Walker, R.G., and Harms, J.C., 1971. The "Catskill Delta": a prograding muddy shoreline in central Pennsylvania: *Journal of Geology*, v. 79, pp. 281-299.
- Wallace, C.H., Crittenden, M.P., 1969. The stratigraphy, depositional environment and correlation of the Precambrian Uinta Mountain Group, Western Uinta Mountains, Utah: Lindsay, J.B. (ed), *Geologic Guidebook of the Uinta Mountains*, Intermountain Association of Geologists, Salt Lake City, Utah, pp. 125-141.
- Walther, J.V., 1990. Fluid dynamics during progressive regional metamorphism: In: Geophysics Study Committee, Commission on Geosciences, Environment, and Resources, National Research Council (eds), *Studies in Geophysics: The Role of Fluids in Crustal Processes*, National Academy Press, Washington, D.C., pp. 64-71.
- Weaver, C.E., 1989. *Clays, Muds, and Shales*, Elsevier Publishers B.V., New York, p. 819.
- Weaver, C.E., Eslinger, E.V., and Yeh, H.W., 1984. Oxygen isotopes, In: Weaver, C.E. and Associates, *Shale-Slate Metamorphism in Southern Appalachians*, Elsevier Science Publishing Company, Inc., New York, pp.142-152.
- Wickham, J., Roeder, E., and Briggs, G., 1976. Plate tectonics models for the Ouachita fold belt: *Geology*, v. 4, pp. 173-176.
- Wickham, S.M. and Taylor, H.P., 1990. Hydrothermal systems associated with regional metamorphism and crustal anatexis: example from the Pyrenes, France: In: Geophysics Study Committee, Commission on Geosciences, Environment, and Resources, National Research Council (eds), *Studies in Geophysics: The Role of Fluids in Crustal Processes*, National Academy Press, Washington, D.C., pp. 96-112.
- Wickham, S.M. and Taylor, H.P., 1987. Stable isotope constraints on the origin and depth of penetration of hydrothermal fluids associated with Hercynian regional metamorphism and crustal anatexis in the Pyrenees: *Contributions to Mineralogy and Petrology*, v. 95, pp. 225-268.
- Wickham, S.M. and Taylor, H.P., 1985. Stable isotopic evidence for large-scale seawater infiltration in a regional metamorphic terrane; the Trois Seigneurs Massif, Pyrenees, France: *Contributions to Mineralogy and Petrology*, v. 91, pp. 122-137.
- Williams, H., Appalachian orogen in Canada: *Canadian Journal of Earth Sciences*, v. 16, pp. 792-807.

- Williams, P.L., and Hackman, R.J., 1971. Geology, structure, and uranium deposits of the Salina Quadrangle, Utah, Miscellaneous geological map investigations map I-591: U.S. Geological Survey, Washington, D.C.
- Wilson, E.D., and Moore, R.T., 1969. Geologic map of Arizona: U.S. Geological Survey, Washington, D.C.
- Wilson, E.D., and Moore, R.T., 1959. Geologic map of Mohave County, Arizona: Arizona Bureau of Mines, University of Arizona, Tucson, Arizona.
- Wilson, R.L., 1989. Geologic Map and Mineral Resources Summary of the East Chatanooga Quadrangle, Tennessee: Tennessee Geological Division, Nashville, Tennessee.
- Wilson, R.L., 1986. Geologic Map and Mineral Resources Summary of the Ooltewah Quadrangle, Tennessee: Tennessee Geological Division, Nashville, Tennessee.
- Wilson, R.L.C., 1966. Silica diagenesis in Upper Jurassic limestones of Southern England: *Journal of Sedimentary Petrology*, v. 36, pp. 1036-1049.
- Wood, B.J., and Graham, C.M., 1986. Infiltration of aqueous fluid and high fluid-rock ratios during greenschist facies metamorphism: A discussion: *Journal of Petrology*, v. 27, pp. 751-761.
- Wood, B. J., and Walther, J.V., 1986. Fluid flow during metamorphism and its implications for fluid-rock ratios: In: Walther, J.V. and Wood, B.J. (eds), Fluid Rock Interactions During Metamorphism, Springer-Verlag, New York, pp. 89-108.
- Woodland, B.G., 1965. Geology of the Burke Quadrangle, Vermont: *Vermont Geological Survey Bulletin* 28, p. 151.
- Yeakel, L.S., 1962. Tuscarora, Juniata, and Bald Eagle paleocurrents and paleogeography in the central Appalachians: *Geological Society of America Bulletin*, v. 73, pp. 1515-1540.
- Yeh, H.W, Savin, S.M., 1977. Mechanism of burial metamorphism of argillaceous sediments: 3. O-isotope evidence: *Geological Society of America Bulletin*, v. 88, pp. 1321-1330.
- Yeh, H.W, and Epstein, S., 1976. The extent of oxygen isotope exchange between clay minerals and sea water: *Geochimica et Cosmochimica Acta*, v. 40, pp. 743-748.

- Zen, E., 1968. Nature of the Ordovician orogeny in the Taconic area. In: Zen, E., White, W.S., Hadley, J.B., and Thompson, J.B., Jr. (eds), *Studies in Appalachian Geology: Northern and Maritime*, Interscience Publishers, New York, pp. 129-139.
- Zen, E., 1960. Time and space relations of the Taconic rocks in western Vermont and eastern New York (abstract), *Geological Society of America Bulletin*, v. **71**, p. 2009.